2018
Atomic, Molecular, and Optical Sciences Research PI Meeting

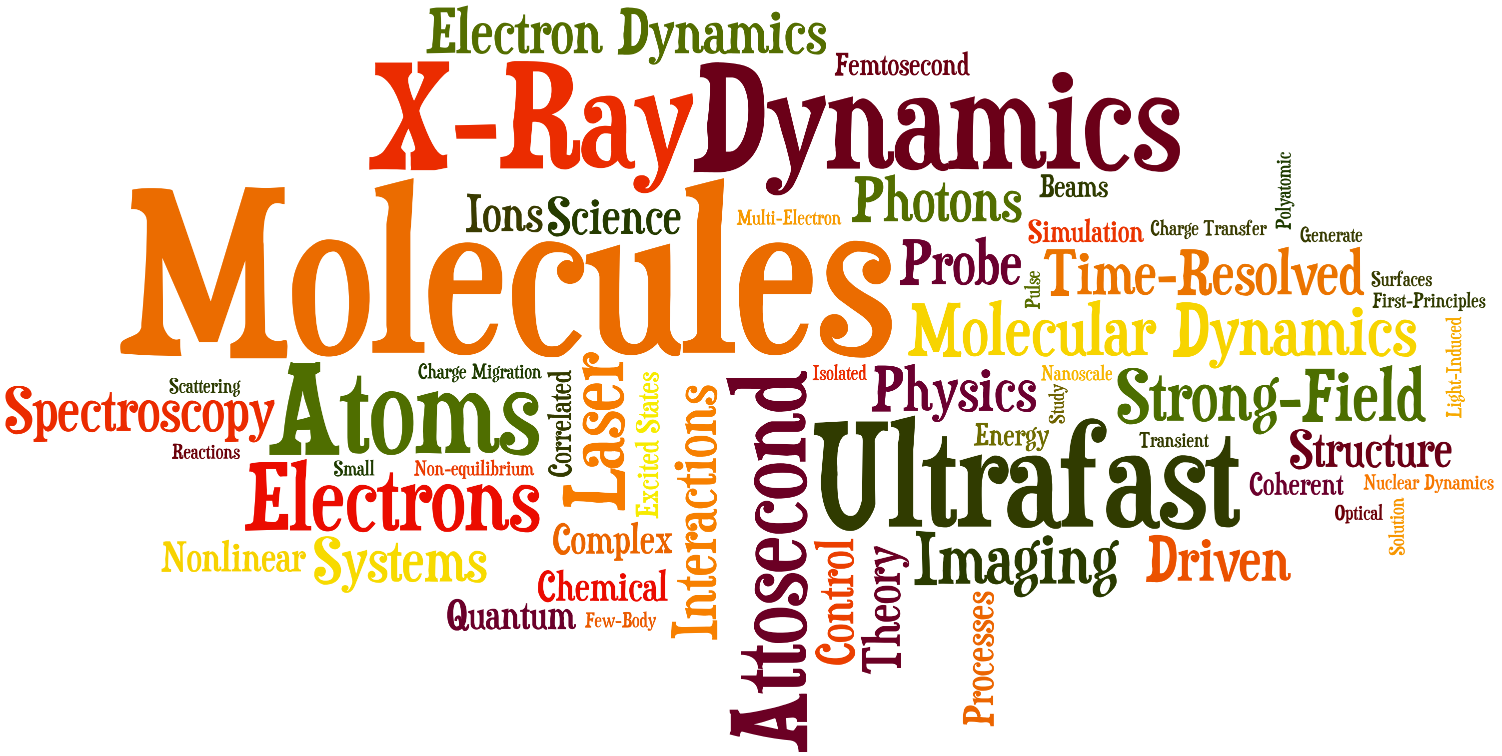

Gaithersburg Marriott Washingtonian Center
Gaithersburg, Maryland
October 22-24, 2018

U.S. DEPARTMENT OF ENERGY | Office of Science

Office of Basic Energy Sciences
Chemical Sciences, Geosciences & Biosciences Division

Page is intentionally blank.

Program and Abstracts

2018
Atomic, Molecular, and Optical Sciences Research PI Meeting

Gaithersburg Marriott Washingtonian Center
Gaithersburg, Maryland
October 22–24, 2018

Chemical Sciences, Geosciences, and Biosciences Division
Office of Basic Energy Sciences
Office of Science
U.S. Department of Energy

Cover Graphics: The input for the Wordle (http://www.wordle.net) cover art is based on the titles of the abstracts for this year's meeting. The font is "Duality."

The research grants and contracts described in this document are supported by the U.S. DOE Office of Science, Office of Basic Energy Sciences, Chemical Sciences, Geosciences and Biosciences Division.

Page is intentionally blank.

FOREWORD

This volume summarizes the 38th annual Research Meeting of the Atomic, Molecular and Optical Sciences (AMOS) Program sponsored by the U. S. Department of Energy (DOE), Office of Basic Energy Sciences (BES), and comprises descriptions of the current research sponsored by the AMOS program. The participants of this meeting include the DOE laboratory and university principal investigators (PIs) within the BES AMOS Program. The purpose is to facilitate scientific interchange among the PIs and to promote a sense of program identity.

The BES AMOS program is vigorous and innovative, and enjoys strong support within the Department of Energy. This is due entirely to our scientists, the outstanding research they perform, and the relevance of this research to DOE missions. The AMOS community continues to explore new scientific frontiers relevant to the DOE mission and the strategic challenges facing our nation and the world.

We are deeply indebted to the members of the scientific community who have contributed their valuable time toward the review of proposals and programs, either by electronic review of grant applications, panel reviews, or on-site reviews of our multi-PI programs. These thorough and thoughtful reviews are central to the continued vitality of the AMOS program.

We are privileged to serve in the management of this research program. In performing these tasks, we learn from the achievements and share the excitement of the research of the scientists and students whose work is summarized in the abstracts published on the following pages.

Many thanks to the staff of the Oak Ridge Institute for Science and Education (ORISE), in particular Connie Lansdon and Tim Ledford, and to the Gaithersburg Marriott Washingtonian Center for assisting with the meeting. We also thank Gwen Johnson and Teresa Crocket in BES for their indispensable behind-the-scenes efforts in support of the BES/AMOS program.

Thomas B. Settersten
Jeffrey L. Krause
Chemical Sciences, Geosciences, and Biosciences Division
Office of Basic Energy Sciences
Office of Science
U.S. Department of Energy

Page is intentionally blank.

AGENDA

2018 Atomic, Molecular and Optical Sciences Research PI Meeting

Office of Basic Energy Sciences
U. S. Department of Energy
Gaithersburg Marriott Washingtonian Center, Gaithersburg, Maryland
October 22–24, 2018

Monday, October 22

7:30 am	**** Breakfast (Salon E) ****
	All presentations are in Salons A–D
8:15 am	*BES/CSGB Update and Outlook* **Bruce C. Garrett**, CSGB Division Director
8:45 am	*Welcome and Introductory Remarks* **Thomas B. Settersten**, AMOS Program Manager
Session I	Chair: **Nora Berrah**, University of Connecticut
9:00 am	*Tracking Inner- and Outer-Shell Electron Dynamics with Ultrafast X-rays* **Linda Young**, Argonne National Laboratory
9:30 am	*Electronic Excited States from Non-Orthogonal Configuration Interaction: Valence and Core Excitations, and Strong Correlations* **Martin Head-Gordon**, Lawrence Berkeley National Laboratory
10:00 am	**** Break ****
Session II	Chair: **Cosmin Blaga**, Kansas State University
10:30 am	*Attosecond Electron Dynamics* **James P. Cryan**, SLAC National Accelerator Laboratory
11:00 am	*Nonlinear and Multidimensional Spectroscopy with Attosecond XUV Pulses* **Daniel M. Neumark**, Lawrence Berkeley National Laboratory
11:30 am	*Nonlinear X-ray Optics* **Matthias Fuchs**, University of Nebraska
12:00 pm	**** Working Lunch (Salon E) ****
1:30 pm	*Discussion Session: LCLS-II Overview and Time-resolved AMO Instrument* **Robert Schoenlein**, LCLS Deputy for Science, SLAC National Accelerator Laboratory **Peter Walter**, Beamline Scientist, SLAC National Accelerator Laboratory
3:00 – 4:00 pm	Free/Discussion Time

Session III Chair: **Michael Chini**, University of Central Florida

4:00 pm *Imaging Ultrafast Electronic and Nuclear Dynamics in Molecules*
Daniel Rolles, Kansas State University

4:30 pm *Photon and Electron Driven Processes in Complex Molecular Systems and Molecules in Complex Environments*
Thorsten Weber, Lawrence Berkeley National Laboratory

5:00 pm *Atomic Precision Studies of Catalyst Photochemistry using Transient X-ray Absorption*
Amy A. Cordones-Hahn, SLAC National Accelerator Laboratory

5:30 pm *Ultrafast Dynamics of Molecules on Surfaces Studied with Time-Resolved XUV Photoelectron Spectroscopy*
Thomas K. Allison, Stony Brook University

6:00 pm **** Working Dinner (Salon E) ****

7:00 pm **** Reception (No Host, Lobby Lounge) ****

Tuesday, October 23

7:30 am **** Breakfast (Salon E) ****

Session IV Chair: **Loren Greenman**, Kansas State University

8:30 am *First Principles Dynamics and Ultrafast Diffraction*
Todd J. Martinez, SLAC National Accelerator Laboratory

9:00 am *Imaging Structural Dynamics in Isolated Molecules with Ultrafast Electron Diffraction*
Martin Centurion, University of Nebraska

9:30 am *Investigating Ultrafast Photochemistry with Soft X-ray Spectroscopy and Electron Diffraction*
Thomas J.A. Wolf, SLAC National Accelerator Laboratory

10:00 am **** Break ****

Session V Chair: **Taisia Gorkhover**, SLAC National Accelerator Laboratory

10:30 am *Dynamical Electron Vortices in Attosecond Double Photoionization of the Hydrogen Molecule*
Anthony F. Starace, University of Nebraska

11:00 am *Probing Non-Equilibrium Charge Dynamics: 3D Two-electron Angular Streaking*
Wen Li, Wayne State University

11:30 am *Probing Non-equilibrium Charge Dynamics: Modeling Angular Dependent Ionization Rates*
H. Bernhard Schlegel, Wayne State University

12:00 pm **** Working Lunch (Salon E) ****
1:00 – 4:00 pm Free/Discussion Time

Session VI Chair: **Carlos A. Trallero**, University of Connecticut

4:00 pm *Ultrafast Coherent Non-equilibrium Charge Dynamics in Molecules*
Françoise Remacle, University of Liège

4:30 pm *Evidence of Roaming Chemical Reactions in Strong Laser Fields*
Marcos Dantus, Michigan State University

5:00 pm *Combining High Level Ab Initio Calculations with Laser Control of Molecular Dynamics*
Spiridoula Matsika, Temple University

5:30 pm *Controlling Rotations of Asymmetric Top Molecules: Methods and Applications*
Vinod Kumarappan, Kansas State University

6:00 pm **** Dinner (on your own) ****
7:00 pm **** Reception (No Host, Lobby Lounge) ****

Wednesday, October 24

7:30 am **** Breakfast (Salon E) ****

Session VII Chair: **Anne Marie March**, Argonne National Laboratory

8:30 am *Attosecond, Imaging and Ultrafast X-ray Science*
Louis F. DiMauro, Ohio State University

9:00 am *Transient Absorption and Reshaping of Ultrafast Radiation*
Mette Gaarde, Louisiana State University

9:30 am *Physics of Correlated Systems*
Chris H. Greene, Purdue University

10:00 am **** Break ****

10:30 am *Strong-Field Dynamics of Few-body Atomic and Molecular Systems*
Brett D. Esry, Kansas State University

11:00 am *Quantum Dynamics Probed by Coherent Soft X-Rays*
Henry C. Kapteyn, University of Colorado

11:30 am *Closing Remarks*
Thomas B. Settersten, DOE BES

Adjourn

Page is intentionally blank.

TABLE OF CONTENTS

Laboratory Research Summaries (by Institution)

Argonne National Laboratory

J.R. Macdonald Laboratory

Lawrence Berkeley National Laboratory

SLAC National Accelerator Laboratory

University Research Summaries (by PI)

AMO Physics at Argonne National Laboratory

Gilles Doumy, Phay Ho, Anne Marie March, Stephen Southworth,
Linda Young, (Christoph Bostedt[†])
Chemical Sciences and Engineering Division
Argonne National Laboratory, Argonne, IL 60439
[†]*present address Paul Scherrer Institute and EPFL*
gdoumy@aps.anl.gov, pho@anl.gov, amarch@anl.gov,
southworth@anl.gov, young@anl.gov

1 Overview

The Argonne AMO physics program explores the frontiers of x-ray physics as enabled by accelerator-based light sources, and, in so doing, lays the foundation for ultrafast x-ray applications in other scientific domains. We utilize the novel properties of accelerator-based coherent x-ray sources, primarily the Advanced Photon Source (APS) synchrotron at Argonne and the Linac Coherent Light Source (LCLS) x-ray free-electron laser (XFEL) at SLAC in concert with ultrafast lasers, to create exotic and/or non-equilibrium states and to probe their rapidly evolving properties with atomic-scale spatial and temporal resolution. The experimental work is supported and complemented by theoretical developments, often taking advantage of massively parallel codes developed for the MIRA supercomputer at the Argonne Leadership Computing Facility (ALCF).

The program is structured in three complementary subtasks. The first subtask aims at a quantitative and predictive understanding of x-ray interactions with matter in the high-intensity limit. Here we explore new atomistic imaging approaches enabled by the most intense femtosecond x-ray pulses. We build upon our knowledge base of the response of atomic and small molecular systems to examine nanometer-sized samples and the resulting complex phenomena that impact single-shot imaging of single particles. Our computational code developments using the MIRA supercomputer uncover unusual phenomena associated with transient resonant excitation and provide guidance for optimal conditions for serial single shot coherent x-ray imaging of nanoscale samples.

In the second subtask we strive to understand and control the trajectory of ultrafast inner-shell excitations in molecular systems. We build upon our deep knowledge base of studying inner-shell phenomena in the energy domain and use ultrashort x-ray pulses from free-electron laser sources to explore new types of inner-shell spectroscopies in the time domain - e.g. x-ray pump/x-ray probe photoelectron spectroscopy to observe time-evolving chemical shifts and stimulated x-ray Raman spectroscopies to create localized electronic excitations which are then probed in a variety of ways to study the evolving charge densities.

The third subtask focuses on understanding molecular dynamics in condensed phases at the atomic, molecular and electronic level. Here we use XFELs to access the femtosecond timescale and the APS for picosecond phenomena. Within this subtask we have developed uniquely sensitive high-repetition-rate methods to measure electronic and geometric changes of photo-excited molecules in solution in chemically relevant systems at the APS. Recent developments have improved the efficiency of x-ray emission spectroscopy more than 500-fold and the high statistics inherent with high-repetition-rate studies have allowed the implementation of “time-slicing” techniques which give a $\sim$10-fold improvement in time resolution.

2 X-ray Physics at the Intensity Frontier

2.1 Fundamental processes for x-ray imaging applications

P. J. Ho, C. Bostedt, L. Young, S. H. Southworth, C. Knight[1], A. Rudenko[2], D. Rolles[2], S.-K. Son[3], R. Santra[3,18], J. Hajdu[4], F. Maja[4], and other collaborators

Project Scope: The unprecedented intensity of XFELs enables exploration of a new frontier of light-matter interactions and the associated applications of imaging structure and chemical dynamics. We aim at an predictive understanding of the fundamental processes induced by intense x-ray pulses through a combined experimental and theoretical approach in systems of increasing complexity from atoms to molecules to clusters.

Recent Progress: In the high-intensity x-ray regime, where the saturation fluence for single-photon absorption is exceeded, early experiments at LCLS established that multiphoton x-ray ionization via sequential single photon absorption is the dominant interaction [42] but that "hidden" inner-shell resonances [43] and the atomic environment [44] can vastly alter the inner shell ionization dynamics. To expand our fundamental understanding of multiphoton x-ray physics and the role of hidden resonances, we have carried out a series of theoretical studies using the Monte-Carlo rate equation approach. From these studies, we have revealed the roles of atomic and inner-shell resonances for the production of high-charge states in Ar, Kr and Xe [45, 46]. With these systematic calculations, we uncovered a new mechanism called "preservation of inner-shell vacancy" that enhances high-charge state production in intense, short pulses and identified hot spots (in photon energy and fluence) for enhanced x-ray ionization in heavy elements.

Building on the knowledge gained from these earlier studies, we developed the Monte-Carlo /Molecular Dynamics (MC/MD) method [9] to investigate intense-field dynamics in nanoscale systems. The MC/MD approach incorporates all multiphoton ionization features of isolated atoms [42, 43, 45], namely photoionization, Auger, fluorescence, elastic scattering and Compton scattering. To account for the effects of the cluster environment, electron collision dynamics as well as electron-ion recombination processes are included. In this hybrid MC/MD method, all these electronic processes are treated as quantum transitions, whereas the motion of the ionized electrons/ions/atoms are evaluated through classical molecular dynamics. The MC/MD code is highly parallel and has been shown to achieve good scalability on the MIRA, a massively parallel supercomputer at ALCF. Using this fully atomistic approach we examined the physics of coherent x-ray diffraction imaging of nanosized particles with intense XFEL pulses [8]. Our results point out the optimal pulse conditions needed for achieving 3-Å resolution with a 10-nm inorganic cluster and the importance of both the electron and nuclear dynamics even for few femtosecond pulses.

Last year, we carried out a combined computational and experimental study to investigate ultrafast diffractive imaging of sucrose clusters which are often used as benchmark organic samples. For this study, the MC/MD method was extended to treat resonant scattering processes; that is the scattering response is modelled by complex atomic form factors and includes the effect of absorption. Our computational study reproduces the experimental data and reveals that transient electronic resonances driven by non-linear x-ray interactions can be dominant in ultrafast imaging applications (see Fig. 1). When pulses have durations that are multiple times the inner-shell lifetime, transient resonances greatly enhance the light-induced damage. In contrast, for short pulses comparable to the inner-shell lifetime, transient electronic configurations can be exploited to increase the scattering response and elemental contrast. Our study demonstrates the

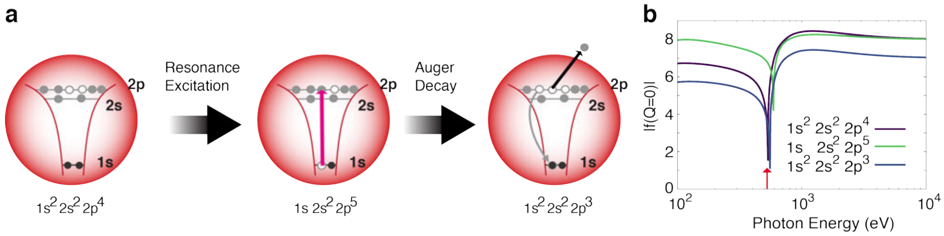

Figure 1: Effect of transient resonances in the water window. (a) At 530 eV, resonance-mediated pathways lead to enhanced ionization in oxygen atoms. (b) Calculated amplitudes of the atomic form factor of oxygen atoms and ions with different electronic configurations. The vertical red arrow indicates 530 eV.

complexity of the imaging process due to the rapidly changing transient electronic structures in XFEL experiments and shows how computational models allow optimization of the parameters for ultrafast imaging experiments.

Future Plans: We plan to exploit transient resonances to achieve elemental contrast for single-particle imaging in heterogeneous systems, starting from simple core-shell systems to complex catalytic relevant nanoparticles. Understanding x-ray induced electron and nuclear dynamics in these heterogeneous particles is important as they typically contain mixtures of high- and low-Z elements. Therefore these particles have inherently localized x-ray ionization hot spots.

2.2 Ultrafast imaging of electron and nuclear dynamics in clusters and nanoparticles

C. Bostedt, Y. Kumagai, P. J. Ho, G. Doumy, A. Al-Haddad, L. Young, T. Gorkhover[5], O. Gessner[6], A. Vilesov[7], T. Fennel[8], A. Rudenko[2], M. Kling[9], D. Rupp[10], T. Möller[10], and other collaborators

Project Scope: Single-shot imaging with intense x-ray pulses from XFELs opens the opportunity to probe the non-equilibrium electronic and nuclear dynamics in nanometer-sized samples with femtosecond time and Angstrom spatial resolution. We combine experiments and theory to investigate the correlation between x-ray ionization and ultrafast imaging with single-pulse, x-ray pump / x-ray probe approaches.

Recent Progress: Electronic excitation is closely coupled to nuclear response and structural changes. For any sample in strong fields, the ionization and electron redistribution within the sample leads to strong changes in its interatomic potential energy landscape. In finite, nanoscale systems these sudden changes can lead to a strong structural response that competes with nanoparticle expansion and disintegration dynamics.

Over the past years we have developed experimental methods [12, 14] for ultrafast imaging as well as coincident imaging and spectroscopy for imaging high-resolution structure and studying electronic and nuclear dynamics in clusters [7, 16, 47, 48] and superfluid helium droplets [5, 11, 49, 50]. We have performed the first femtosecond time-resolved coherent x-ray diffractive imaging experiments at LCLS that captures ultrafast surface melting of Xe cluster in intense optical fields [1] and anisotropic expansion of doped helium droplets in intense optical fields. Also, we developed a method to obtain in-flight X-ray Fourier holograms of biological test particles using single Xe clusters as reference scatterers in the gas phase [13].

In order to gain insight into the surprising ultrafast cluster compression upon massive parallel ionization [2], we continue to develop novel x-ray/x-ray pump/probe methods to study transient nuclear dynamics upon strong electronic excitation in nanocrystals with Angstrom spatial resolution. As a common problem in imaging, the interpretation of the x-ray diffraction images has been hindered due to the fact that the initial state, size and orientation of the sample was not characterized. A complete characterization of the sample can yield a dramatically better insight into physical processes. To aid the experimental efforts, we have expanded the capability of the MC/MD method to examine the fundamental interactions and optimal pulse conditions for x-ray/x-ray pump/probe experiments. Guided by the theoretical results, we performed two-color hard x-ray scattering experiments with well separated energies and well characterized arrival times at the SACLA free-electron laser. The first x-ray pulse characterized the size of each van der Waals nanocrystal as well as induced the x-ray ionization and expansion processes. The second x-ray pulse probed the nuclear dynamics following the ionization pulse. Using the same Bragg reflection from two different color x-ray pulses yields unprecedented information about the nanoparticle lattice response upon ionization that was not accessible in previous experiments [2].

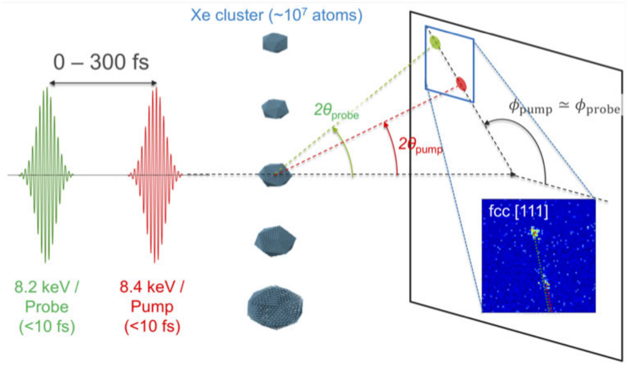

Figure 2: Tracking ultrafast x-ray induced dynamics of Xe clusters using the same Bragg reflection from two different color x-ray pulses with 0 to 300 fs time delays.

Future Plans: Our ongoing and future efforts are targeted at understanding the x-ray induced electron dynamics during the ultrafast imaging process. Exploiting the broad bandwidth and sub-femtosecond capability of the XLEAP operation mode at LCLS, we will experimentally investigate the resonant and non-resonant imaging processes on femtosecond time scales. Theoretically we will continue to develop and use our Monte-Carlo/Molecular Dynamics calculations for systems with heavier (Xe) elements under realistic experimental pulse conditions. Xe is of particular interest as it has been the system of choice for ultrafast x-ray scattering experiments. Our parallelized MC/MD codes are able to model the large number of electronic states and transitions involved in experiments on Xe clusters.

2.3 X-ray imaging using higher-order correlations

P. J. Ho, Y. Kumagai, L. Young, C. Bostedt, C. Knight[1], and other collaborators

Project Scope: Coherent diffractive imaging (CDI) with XFEL pulses holds the promise to probe structure [15] and follow dynamics of non-periodic entities with atomic resolution. However, this approach remains challenging due to the need to acquire a large number of images for reconstruction and the neccessary pulse conditions for limiting sample damage during the pulse [8] are still not available. We aim to explore the potential of x-ray correlation methods as a high-resolution structural and dynamical probe by investigating the higher-order correlations associated with the fluorescence spectrum and speckle patterns from illuminated samples.

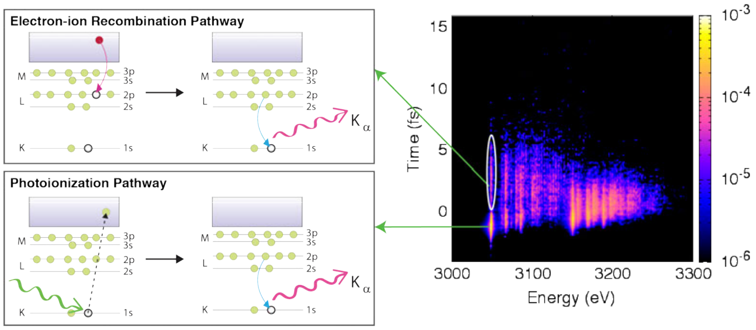

Figure 3: Fluorescence processes and spectra of an Ar cluster exposed to intense, 2-fs x-ray pulses. Two Kα fluorescence pathways from electron-ion recombination and photoionization and their emission times.

Recent Progress: In CDI, a coherent x-ray pulse produces the observed fringes in the diffraction patterns from a sample. These fringes are the result of the interference between the amplitudes of scattered light from atoms located within the sample. It is worth noting that the interference effect is not limited to the amplitude of the light. Hanbury Brown and Twiss demonstrated an interference effect between two light intensities [51]. In fact, using the correlation between two different points on Sirius, which is a random/thermal light source, they determined its angular size. Classen and coworkers [52] proposed to use the Hanbury Brown and Twiss effect for molecular imaging. Here, by treating the heavy atoms as random light emitters, they suggest that the intensity correlation from the inner-shell fluorescence of the heavy atoms can be exploited for retrieving high-resolution structural information.

Motivated by the work by Classen and coworkers [52], we theoretically examined the fluorescence spectrum of a nanocluster from XFEL pulses with our MC/MD method [8]. As a first step, using Ar clusters as a prototype, we focused on fluorescence processes in intense x-ray fields. We found that non-linear x-ray absorption leads to a high-degree of ionization and creates a dense electron environment within the sample on the femtosecond timescale. Already during the pulse, electron-ion recombination and massive electron rearrangement begin to transform the exposed cluster into core-shell structure (neutral core and highly charged shell). These ultrafast processes produce x-ray emission profiles in an extended sample that are very different from the atomic profile. Most notably, in addition to the direct photoionization pathways, electron-ion recombination processes provide additional pathways to reach the same fluorescence channels and gives rise to higher K_α and K_α^h yields in clusters [9]. Depending on the fluorescence channels involved, the presence of the recombination pathway leads to extended fluorescence emission time beyond the lifetime of the core-excited states. We show that the K_α^h emission line can be a good candidate for incoherent imaging as it has relatively short emission time (a few femtosecond) compared to the x-ray induced distortion time [8]. A manuscript reporting this new result will be submitted soon.

Future Plans: We plan to explore further the use of intensity correlations of the fluorescence spectrum for high-resolution structure determination. Due to the elemental specificity of fluorescence lines, we will investigate fluorescence processes of catalytic nanoparticles exposed to intense XFEL pulses and the feasibility for achieving atomic and elemental resolution. Multi-t, multi-q x-ray scattering correlations may also be used to study solvation dynamics at the APS.

3 Ultrafast Inner-Shell Induced Molecular Dynamics

3.1 Using time-resolved photoelectron spectroscopy to follow the electronic and nuclear relaxation of a molecular core-hole state

S. H. Southworth, A. Al-Haddad, G. Doumy, M. Bucher, P. J. Ho, A. M. March, L. Young, C. Bostedt, A. Picón[11], S. T. Pratt[12], R. Sheppard[12], T. Gorkhover[5], J. Cryan[5], A. Lutman[5], A. Marinelli[5], T. Maxwell[5] and other collaborators

Project Scope: Inner-shell spectroscopy yields element and even site specific electronic information. The core-hole states produced by x-ray absorption decay by Auger electron emission, x-ray fluorescence, and ion fragmentation. Understanding the electronic and nuclear motions that are triggered by x-ray absorption in small molecules is key to applying inner-shell spectroscopies to complex systems. Electron, photon, ion, and coincidence spectroscopies yield insight into decay pathways of core holes produced by absorbing synchrotron x-rays [53]. However, the intense, femtosecond x-ray pulses generated at free-electron lasers offer the opportunity to trigger and follow electronic and nuclear motions in time using pump-probe methods. Both optical-pump/x-ray-probe [54] and x-ray-pump/x-ray-probe experiments [18, 19] on small molecules have been performed. Methods have been developed at the LCLS to control the temporal and geometric properties of the electron bunches that radiate within the undulators in order to generate multiple x-ray pulses with adjustable colors, pulse durations, and time delays [55–57]. We seek to exploit these capabilities for time-dependent, site-specific experiments on inner-shell dynamics.

Recent Progress: The concept of "chemical shift" of inner-shell binding energies is well known from x-ray photoelectron spectroscopy (XPS) [58]. While the binding energies of core electrons are mainly determined by their electrostatic interactions with the nearby nucleus, the binding potential can be modified by the shielding effects of other electrons. The binding energy increases (decreases) if valence electron charge is reduced (increased). A well-known example is ethyl trifluoroacetate ($CF_3CO_2CH_2CH_3$) in which the four C sites have distinct 1s binding energies spread over 8 eV [59]. We recently studied the site-selective ion fragmentation of this molecule [28] as described in the following progress report. We have also exploited the chemical shift concept in a two-color x-ray-pump/x-ray-probe experiment on CO molecules at the LCLS. The "fresh slice" method [57] was used to generate two x-ray pulses at 534 and 524 eV, each with 2-3 eV bandwidths, $\sim$10 fs durations, and adjustable time delay between -20 to 40 fs. Referring to Fig. 4, the first pulse excites the O 1s $\rightarrow \pi^*$ resonance at 534 eV and the 524-eV pulse ejects a C 1s electron that is recorded with a photoelectron spectrometer. The photoelectron experiences a time-dependent chemical shift as the molecular core-hole state decays electronically to participator and spectator Auger final states [60]. Most of those states are unstable and will dissociate into neutral and ionic atomic fragments [61] which further modifies the chemical shift. To follow the chemical shifts in time, we recorded C 1s photoelectron spectra at delays of -20, 0, 5, 10, 15, 20, 35, and 40 fs. For each pair of pump and probe pulses, images from the X-band RF transverse deflector (XTCAV) [62], electron orbits and energies were analyzed to extract information on the photon energies, pulse intensities, pulse durations and time delays. In addition, ion time-of-flight spectra of CO recorded downstream of the photoelectron spectrometer confirmed that pump photon energies were on the 534-eV resonance.

To interpret the measured photoelectron spectra, comparisons are made with calculated chemical shifts that include the resonant Auger decay and ion fragmentation steps. Theoretical models of core-hole decays have usually treated the static case, but this experiment and future studies using femtosecond x rays require a time-dependent theory. We have developed a time-dependent Schrödinger equation approach for molecular core-hole dynamics [25]. With our formalism we can

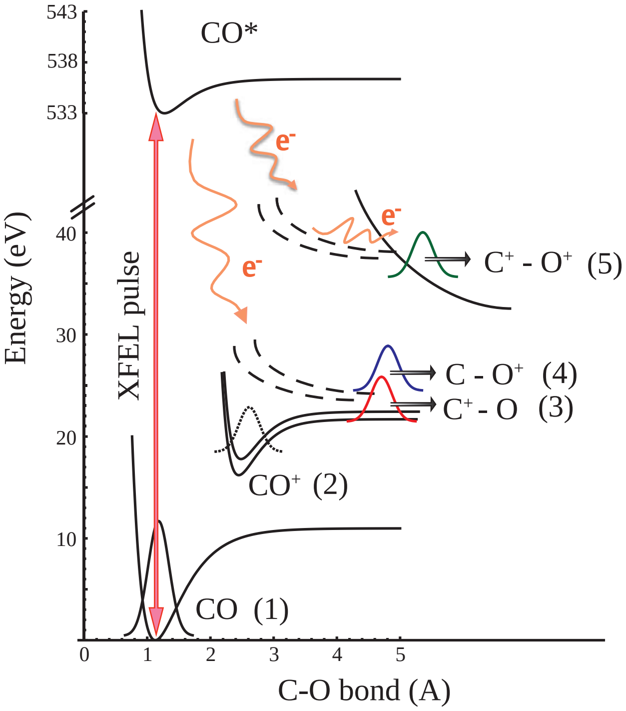

Figure 4: A 534-eV pump pulse excites the O 1s → π^* resonant core-hole state in CO and relaxes to participator and spectator Auger final states. Most of those states are unstable to dissociation to neutral and ionic atomic fragments. A 524-eV probe pulse ejects a C 1s electron after a delay between -20 to 40 fs.

follow electronic relaxation during Auger decay and nuclear relaxation processes on their natural femtosecond time scales. Our theoretical time-dependent approach is flexible but also fully integrated in a quantum chemistry code in order to calculate the required electronic and nuclear properties. We will be able to calculate the continuum orbitals and the corresponding transition elements involving those orbitals, such as Auger or photoionization transitions, as we have already demonstrated for the atomic case [21].

Future Plans: We will continue to exploit new capabilities at FELs to generate fs x-rays for studies of inner-shell excitation and decay dynamics in both small and complex molecules. In an upcoming LCLS experiment, stimulated x-ray Raman processes in metallo-porphyrins will be studied using an x-ray-pump/optical-probe technique. We also anticipate using ∼1 fs x rays to pump and probe molecules while Auger decays are in progress. This capability, along with high repetition rates, will significantly enhance investigations of inner-shell dynamics.

3.2 Rapid core-hole delocalization and site-specific photochemistry

L. Young, S. H. Southworth, G. Doumy, C. Bostedt, S. L. Sorensen[13], B. Oostenrijk[13], M. Simon[14], M. Patanen[15], L. Inhester[3], S.-K. Son[3], R. Santra[3,17] and other collaborators

Project Scope: Earlier work in our group investigated the femtosecond molecular response to site-specific inner-shell excitation in simple diatomic and triatomic systems with x-ray pump/x-ray probe techniques with recoil ion spectroscopy as a probe [18,19] or with photoelectron spectroscopy [as described above]. Here we extend this theme to more complex molecules, where an initially localized inner-shell hole can be created in several distinct chemical environments. Rapid delocalization of the initially created core hole, via e.g. Auger decay, can limit the site-specificity of chemical bond breakage. A model system in which to study the rapid hole delocalization and its effects on the chemical environment is the "ESCA" molecule, where the concept of chemical shift, as discussed above, was showcased [63]. A first step is understanding the decay mechanisms following inner-shell excitation.

Recent Progress:

The ethyl trifluoroacetate molecule is a perfect example where the concept of site-selective inner-shell molecular photofragmentation may be examined; 1s hole creation on a specific carbon atom may be easily distinguished by the well-separated photoelectron signature (see Fig. 5) which may be detected in coincidence with fragment ion momenta. One might expect such site-selective behavior if the fragmentation occurred on a timescale shorter than the initial-site hole delocalization via, e.g. Auger decay. We experimentally examined the propensity for site-selectivity using photoelectron-photoion-photoion coincidence spectroscopy using excitation at a photon energy well above the carbon K-edge where the photoabsorption cross-section was comparable for each of the four environmentally distinct carbon sites. The ability to record momentum distributions of photoion-photoion coincidences allowed determination of the fragmentation mechanism. We found that here, as in many cases, fragmentation of molecules upon inner-shell ionization was not very specific with respect to the initially localized ionization site. While often this finding has been interpreted in terms of an equilibration of internal energy into vibrational degrees of freedom after Auger decay, our *ab initio* calculations yield additional chemical insight. How does the molecule fragment? Which bonds break first? For all four carbon ionization sites, the Auger decay weakens the same bonds and transfers the two charges to opposite ends of the molecule, which leads to a rapid dissociation into three fragments, followed by further fragmentation steps. The lack of site specificity is attributed to the character of the dicationic electronic states after Auger decay rather than a fast equilibration of internal energy that is often assumed, as described in our recent publication [28]

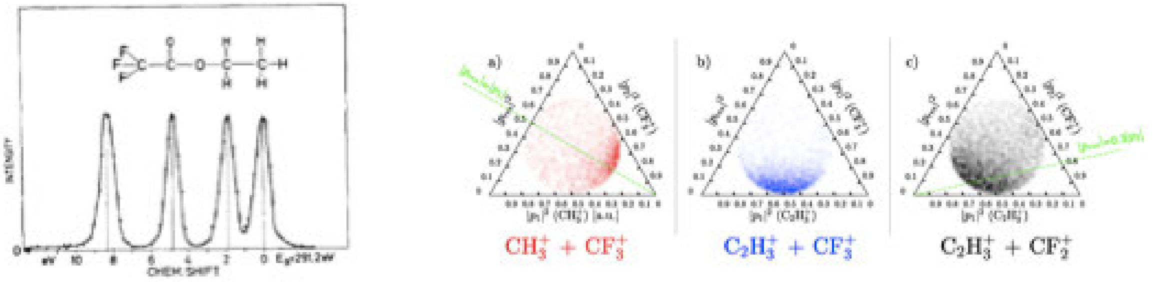

$CH_3^+ + CF_3^+$ $C_2H_3^+ + CF_3^+$ $C_2H_3^+ + CF_2^+$

Figure 5: Left: The original C 1s photoelectron spectrum from ethyl-trifluoroacetate taken with Al Kα radiation [64]. Right: Fragmentation patterns arising from 1s ionization of any of the four distinct carbon atoms in ethyl trifluoroacetate. Dalitz plots of momentum sharing between two fragment pairs and the residual momentum coincident with one carbon inner-shell photoelectron for any of the ionization sites: (a) $CH_3^+ + CF_3^+$, (b) $C_2H_3^+ + CF_3^+$, and (c) $C_2H_3^+ + CF_2^+$.The initial breakup channel is shown in (b) with equal momentum sharing between $C_2H_3^+$ and CF_3^+ to leave a CO_2 neutral molecule [28].

.

Future Plans: Armed with the knowledge of the dominant dissociation mechanism and the careful study of the ground state photoelectron spectrum in this model system [59], it may be possible to use x-ray pump/x-ray probe time-resolved photoelectron spectroscopy gain insight into ultrafast charge migration and charge delocalization that occur during the core-hole decay process.

3.3 Stimulated X-ray Raman Spectroscopy

G. Doumy, A. Al-Haddad, P. J. Ho, Y. Kumagai, A.M. March, S.H. Southworth, L. Young, C. Bostedt, J. Cryan[5], and other collaborators

Project Scope: The high intensities afforded by ultrashort x-ray pulses available at XFELs have created the opportunity to explore the behavior of matter undergoing non-linear interaction with x-ray fields [65]. In analogy with optical techniques, the opportunity to greatly enhance the sensitivity of some spectroscopic techniques through stimulated emission or scattering has started to be explored [20, 66, 67].

Recent Progress: The recent progress towards generating sub-femtosecond pulses (e.g. the XLEAP project at LCLS) is in particular spurring new attempts to use a single short pulse with large enough bandwidth capable of providing both necessary photon energies for excitation and stimulated emission in a time significantly shorter than the natural decay dominated by Auger electron emission.

The element selectivity afforded by x-ray radiation is expected to both provide local probes and a means to produce localized valence excitations or coherences, the time evolution of which could then be probed, ideally with another localized probe. Challenges to realize these ideas are many, starting from the competition from linear photoionization and rapid decay of core excited states. At this point, while stimulated emission has been demonstrated, both in the soft and hard x-ray region, stimulated Raman scattering, leaving the molecule in a valence excited state, is still elusive. Several schemes have been proposed to detect the neutral excited states that should be produced, including using UV photoemission. We proposed to use optical transient absorption as a probe of the localized excitation at the copper center of Cu-based porphyrin in the gas phase. For this study, we will operate near the Cu 2p to 3d resonance in order to increase the cross section for the Raman process, and take advantage of the well characterized optical properties of both valence excited and valence ionized Cu porphyrins (in particular, any ionized species will exhibit a blue shift in absorption, while the neutral excited states exhibit a red shift). Care has to be taken to minimize sample ionization by using a moderate focus spot ($\approx 100\mu\text{m}^2$), but with the expected 500 as pulses, the fraction of Raman excited molecules could reach 5 %, safely above the detection limit using self-referenced white light optical probing. The current lack of direct diagnostics of the attosecond pulse duration is a limiting factor, but we will have the ability to measure the photon energy spectrum on a shot by shot basis, which is thought to be good proxy for evaluating the behavior of the XLEAP process.

Future Plans: Although LCLS is shutting down this year, the much higher repetition rate at the upcoming LCLS-II and the new soft x-ray beamline at Swiss-FEL that are expected to produce very intense attosecond pulses that will provide much improved conditions to study stimulated processes. We will also examine the effect of ultra-high intensity x rays on the propagation through dense targets.

3.4 Femtosecond profiling of shaped x-ray pulses

G. Doumy, A. Al-Haddad, C. Bostedt, M. Hoffman[5], A. Cavalieri[3,16], J. Cryan[5], and other collaborators

Project scope: Ever improving accelerator modes allow manipulation of temporal and spectral characteristics of x-ray pulses at free-electron lasers, but require shot to shot characterization, ideally on or near target. One of the most promising ways uses so-called optical streaking, where a strong laser field is used to encode temporal characteristics (e.g. pulse duration, delays...) into the energy of detected electrons [68, 69].

Recent Progress: The most direct application was demonstrated in a published paper, Ref. [29]. Using THz radiation, the pulse envelope and in particular a two-pulse mode was characterized temporally, including measuring on a shot to shot basis the timing jitter between the x-ray pulse and the THz field with a sub 10-fs precision (see Fig. 6).

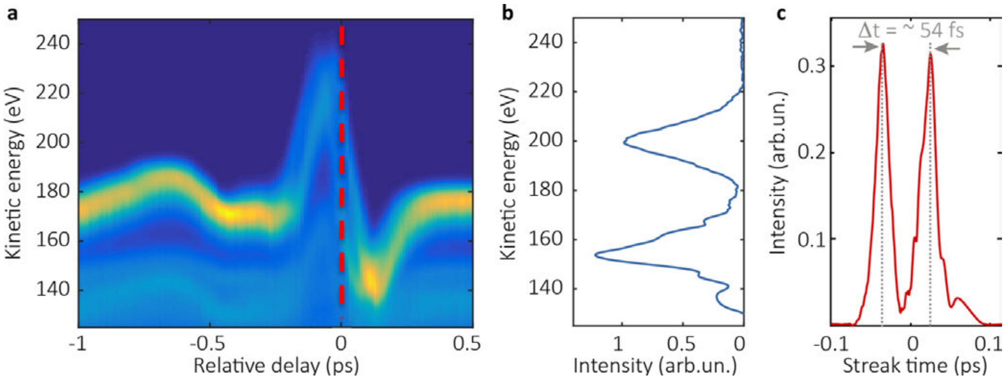

Figure 6: Optical streaking with THz fields at XFELs, illustrating the ability to characterize a two-pulse configuration. a) Spectrogram of streaked electron energy from Ne atoms ionized by 1100eV light. The double structure due to the two-pulse configuration is obvious, as well as the shape of the vector potential from the THz field. b) Optimum time resolution occurs at the maximum slope of the vector potential, as shown in this single shot example. c) Reconstruction of the tw-pulse profile, with a 54fs delay between the two pulses. (from Ref. [29])

In addition, using a more sophisticated measurement apparatus, it is possible to perform so-called self-referenced temporal measurements, where on a shot-to-shot basis, one is able to measure precisely the delay between the x-ray pulse(s) and the streaking field, even in the mid-IR region. This allows first to measure precisely short pulse durations (<10fs), and provides the means to temporally characterize electron dynamics following interaction with the initial x-ray pulse. The setup relies on the combination of two electron spectrometers detecting streaked electrons experiencing different optical Gouy phase along the focus of the streaking field, and was successfully implemented earlier this year.

Future Plans: All upcoming soft x-ray XFEL beamlines will include streaking capabilities. Diagnostics of the pulse properties, especially at high repetition rate, are very challenging, but laser streaking is one method with the potential to provide such information shot-to-shot.

4 X-ray Probes of Photo-excited Dynamics in Solution

4.1 Dynamics and coherence in strong-field ionized water

L. Young, G. Doumy, S.H. Southworth, Y. Kumagai, A. Al Haddad, M.-F. Tu, A. M. March, P. Ho, C. Bostedt, Z.-H. Loh[17], J. E. Rubensson[4], L. Kjellson[4], R. Santra[3,18], C. Arnold[3], R. Welsch[3], L. Inhester[3], W. Schlotter[5], and other collaborators

Project Scope: Time-resolved x-ray spectroscopies in the water window provide a powerful and unique probe for understanding valence hole dynamics, electronic coherence and proton transfer in liquid water. Such elementary processes are of fundamental importance as the initiators of radiation damage in condensed matter systems [70, 71].

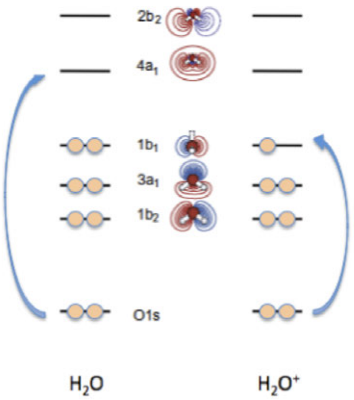

Figure 7: Schematic of the soft x-ray absorption-based signature for an ionized water molecule, H_2O^+, compared to neutral water. A prominent new resonance appears, red-shifted by the 8-eV HOMO-LUMO gap, for the H_2O^+.

Recent Progress: Although understanding the birth and fate of an excess electron in liquid water created by ionization has been the subject of longstanding scientific inquiry [72], surprisingly its partner, the initially created cation H_2O^+, remains undetected due to its femtosecond lifetime and unclear spectroscopic signature in the UV/VIS region [73]. Our calculations demonstrate a clear signature for this and other relevant species, in the soft x-ray regime (see Figure 7), thus providing a handle on electronic and chemical dynamics that extends to the earliest timescales and inform our experimental effort. We used strong-field ionization in water to impulsively eject an electron along the field polarization axis to a radius of ≈ 35 Å. The ejected electron ultimately equilibrates in a spherical solvent cavity of $\sim$3 Å in an s-like ground state within ~ 1 ps. How does this occur? Earlier studies of this process used an optical probe at 800 nm to monitor the hydrated electron and revealed surprising polarization oscillations on the tens-of-femtosecond timescale [74]. How are these hydrated electron polarization oscillations correlated with localized hole dynamics in the residual ion? Is the modulation of the polarization anisotropy due to charge density oscillations between oxygen centers, as hypothesized, or to something else? We studied the elementary dynamics of the valence hole following strong-field ionization of liquid water using transient absorption based spectroscopies at the SXR endstation at LCLS. A 2μm flat-sheet liquid jet system was developed and used for simultaneous time-resolved soft x-ray transmission, fluorescence and emission spectroscopy. In an optical-pump/x-ray probe configuration, we found signatures and followed the kinetics of the elusive H_2O^+ species and its subsequent reaction product OH in the three detection channels. Moreover, modifications of the pre-edge structure, due to the injected electron were observed! Theoretical calculations using a QM/MM (quantum mechanics/molecular mechanics) treatment of a multi-molecule water cluster predict rapid oscillations of the valence hole absorption and are being refined.

Future Plans: While the detection of the elusive H_2O^+ species and its subsequent elementary proton transfer reaction kinetics is a considerable achievement, the time resolution available was insufficient to detect the theoretically predicted polarization oscillations. We plan improvements of the pump/probe time-stamping accuracy to sub-20 femtoseconds, as would be possible with a co-located time-tool, high-statistics emission spectroscopy, and extended x-ray absorption fine structure measurements to further our ability to observe and understand elementary reactions in liquid water.

4.2 Tracking solution phase photoinduced reactions with sub-pulse duration temporal resolution: implementation of synchrotron time-slicing

A. M. March, G. Doumy, A. Al-Haddad, M.-F. Tu, Y. Kumagai, S. H. Southworth, L. Young, C. Bostedt, W. Gawelda[19], G. Vanko[20], Z. Nemeth[20], N. Govind[21], J. Uhlig[13]

Scope: Over the past several years our group has built up laser-pump, hard-X-ray-probe capabilities combining both X-ray absorption and X-ray emission spectroscopies at the Advanced Photon Source for studies of photophysical and photochemical reactions in solutions [33, 38, 40, 41, 75–80]. We can probe a very large range of timescales, from ∼100 ps dictated by the X-ray pulse duration to the microsecond regime or longer utilizing a pump, probe, probe, probe . . . scheme. We are exploring ways to improve our temporal resolution to capture events occurring on the ≈10 ps timescale, beginning with a time-slicing technique where a short laser pulse is scanned within the X-ray pulse temporal envelope (see Fig. 8). Such sub-pulse duration temporal resolution is important for bridging the gap between the femtosecond regime accessible at XFEL and synchrotron studies and for taking full advantage of the higher-brightness, but longer duration, X-ray pulses that will be provided by the upcoming upgrade of the Advanced Photon Source.

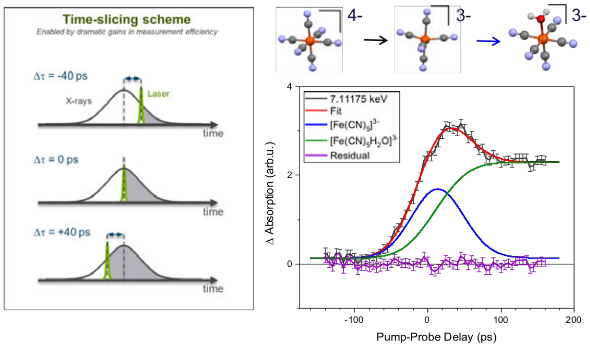

Figure 8: Time-slicing scheme along with delay scan data capturing the pentacoordinated intermediate species in the photoaquation reaction of $[Fe(CN)_6]^{4-}$.

Recent Progress: We have applied the time-slicing technique to the study of aqueous $[Fe(CN)_6]^{4-}$, a model FeII complex that undergoes a photoaquation reaction when excited by UV light [81]. Investigation of the specific mechanism by which the ligand exchange occurs has been undertaken only recently where DFT, 2D UV and tansient visible and IR spectroscopy results were used to formulate a proposed model; photoexcitation leads to fast CN- dissociation, leaving behind a $[\mathrm{Fe(CN)_5}]^{3-}$ fragment in a triplet square pyramidal geometry that then geometrically rearranges, in 3-4 ps, to the lowest triplet trigonal bipyrimidal state from which aquation occurs in $\sim$20 ps producing $[\mathrm{Fe(CN)_5H_2O}]^{3-}$ [82]. TR-XANES at the Fe K-edge provides a direct probe of the structurally different species and can be used to test the proposed mechanism. We collected a set of pump-probe delay scans at different incident x-ray energies and then used a global fit to extract the kinetics details (see Fig. 8 for one such scan and its decomposition), finding good agreement with the existence of a $\sim$20ps-lived intermediate. We will reconstruct the spectrum of this intermediate using a set of TR-XANES spectra taken at different pump-probe delays. Comparison with QM/MM calculations that take explicit account of the solvent, presently being carried out, should validate the geometry of the transient species. These single photon absorption results will help inform interpretation of our previous work on the multiphoton absorption of this complex as well as shorter timescale studies carried out at SACLA.

Future Plans: We will apply the time-slicing technique using both TR-XAS and TR-XES (see 4.3) to study a series of Fe carbene complexes designed to have extended charge transfer state lifetimes [83, 84]. This, combined with pump, pump, probe and sculpted pump pulse techniques, will allow us to understand the interplay of charge transfer and ligand field states in these systems and gain insight into how such dynamics might be controlled.

4.3 Efficient time-resolved x-ray emission spectroscopy using pink beam at the APS

G. Doumy, M.-F. Tu, A. Al-Haddad, A. M. March, S. H. Southworth, Y. Kumagai, L. Young, C. Bostedt, D. Walko[22], A. Di Chiara[22], L. Assoufid[22]

Scope: We extended our high-repetition-rate laser pump/ x-ray probe techniques by taking advantage of the large flux available in the polychromatic output of a synchrotron undulator for time-resolved, non-resonant x-ray emission spectroscopy. By increasing the experimental output by more than two orders of magnitude, much better sensitivity for core-to-core emission is achieved, and access to the chemically sensitive valence-to-core region becomes practical.

Recent Progress: X-ray emission spectroscopy (XES) probes occupied orbitals (core or valence) through radiative decay to inner-shell holes. In non-resonant XES, the incident energy of the x-ray photon responsible for hole creation is not critical, provided it is above the ionization energy (above the absorption edge). Therefore, using the full first harmonic radiation from an undulator source (so-called pink beam) instead of monochromatic beam is a route to dramatically increase the XES signal. We have developed at Sector 7 of the APS a pink-beam microfocus capability at full repetition rate of the synchrotron. A water-cooled harmonic rejection mirror, and water-cooled beryllium Compound Refractive Lenses (CRLs) [30] are used to produce a small x-ray spot (see Fig. 9). As expected from ray tracing simulations, the x-ray focal spot is elliptical due to the source properties but fully compatible with high-repetition rate laser excitation using our fast liquid jet. The laser spot shape on sample was matched by using a cylindrical-lens based telescope before the final focusing optic.

Our first demonstration experiment used the well-known spin-cross over iron complex $[\mathrm{Fe(bpy)_3}]^{2+}$, which following light excitation undergoes a low-spin to high-spin conversion. Using a dispersive XES spectrometer in the von Hamos geometry, we obtained high quality transient signals for dilute

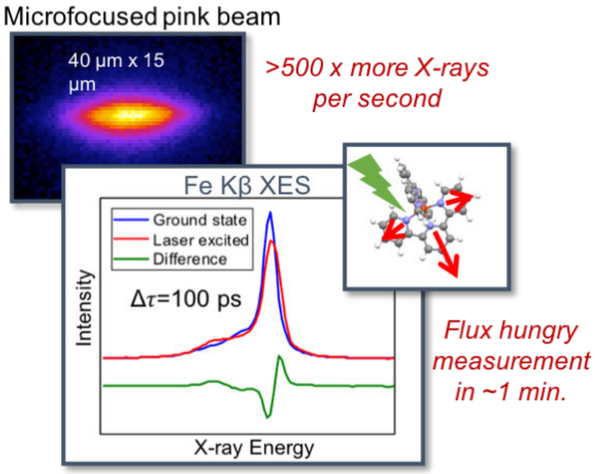

Figure 9: Time resolved Kβ measurement on $[\mathrm{Fe(bpy)_3}]^{2+}$ excited by 355 nm light, using pink beam centered at 8 keV. Top: Focused x-ray spot using CRLs at 7ID-B.

samples ($\approx$ 1mM) in the Kβ region in minutes instead of hours (see Fig.9), and easily measured a high quality valence-to-core signal.

Future Plans: The ability to measure transients in the Kβ region so efficiently opens the possibility to use it as a feedback measurement when exploring the manipulation of the output of photochemical reactions using sculpted laser pulses. In addition, it can also be used in "time-slicing" conditions (see 4.2). With the APS-U upgrade of the synchrotron, a new spectroscopy beamline will provide easy switching between monochromatic beam and pink beam using a multi-layer monochromator, allowing for optimized pump-probe measurements of both XAS and XES in a single experimental beamtime.

4.4 Probing transient molecular dynamics in solution

A. M. March, G. Doumy, S. H. Southworth, A. Al-Haddad, M.-F. Tu, Y. Kumagai, L. Young, C. Bostedt, A. Cordones-Hahn,[5] J. Uhlig[13], C. Elles[23], J. Blakemore[23], M. Mara[24], K. Raymond[24], C. Milne[25], T. Penfold[26], R. Van der Veen[27], M. Chergui[28]

Scope: Our combined setup for high-repetition rate time-resolved x-ray absorption and x-ray emission spectroscopies is able to efficiently collect small transient signals, and the quick data acquisition allows for exploring several samples/conditions in a single beamtime. As such, it has attracted several collaborations, on problems related to molecular complexes used for photosensitizers or photocatalysts.

Recent Progress: The first new project, with a group at Lund University, uses combined XAS and non-resonant XES to characterize the excited states' geometric and electronic structures of a new class of Fe-based photosensitizers that exhibit remarkably long-lived (tens to hundreds of picoseconds) charge transfer states. The potential of replacing high cost ruthenium by abundant iron is of great interest. The competition after photoexcitation between metal-centered excited states and the charge-transfer states is crucial to the behavior of these photosensitizers, and is most directly studied using XAS and XES. As such, these complexes will greatly gain from use of the pink beam capability.

The second new project, with groups at the University of Kansas, aims at getting a better understanding of the behavior of a series of Mn-based CO_2 reduction catalysts that have the form $Mn(CO)_3(bpy)Br$, with substituted 2,2-bipyridyl (bpy) ligands that tune the activity and stability of the complexes. They offer a promising alternative to the toxic and expensive rhenium tricarbonyl complexes that have been shown to be efficient and stable CO_2 reduction catalysts. Unfortunately, they suffer from photodegradation under even moderate irradiation with visible light that must be overcome for applications. TR-XAS studies demonstrated a large transient signal strength (around 50%) and complex spectral changes as a function of pump-probe delay, consistent with the model involving first a ligand loss and then diffusion controlled bimolecular reactions occurring on the nanosecond and microsecond timescale.

The third new project, with a group from the University of California Berkeley, intends to identify the mechanism for energy transfer in a class of Europium(III)-based photoluminescent complexes. These complexes aim at exploiting the long-lived emission in the visible/near-IR spectrum of trivalent lanthanide complexes by using a sensitizer ligand, which efficiently absorbs a photon and excites the lanthanide ion by energy transfer. The mechanism for this energy transfer is still debated, and it remains a mystery as to why some very similar complexes exhibit very different quantum efficiencies. X-ray spectroscopies represent the only viable way to interrogate directly the rare-earth center. We have performed time-resolved XAS and HERFD-XAS at the Eu(III) L_3-edge following UV excitation, and preliminary results indicate that the energy transfer predominantly stems from so-called Dexter charge exchange from the ligand triplet state, and occurs over a few hundreds of picoseconds.

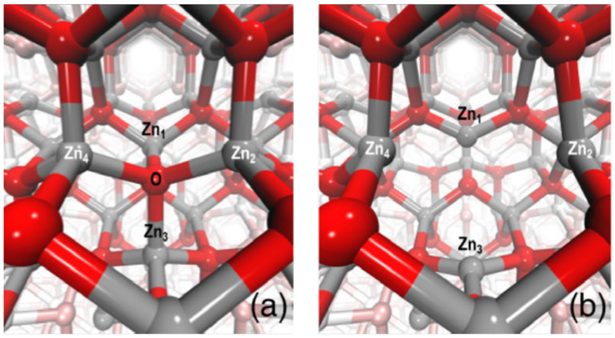

Figure 10: Trap structure: (a) Schematic of the ZnO structure without the oxygen vacancy (b) Distortion around the hole trap (doubly positively charged oxygen vacancy). Figure from Ref. [41]

In addition, several other collaborations are ongoing. With a group from SLAC, a class of Ni-based photocatalysts for hydrogen evolution is studied using TR-XAS, which gives insights into the influence of the ligand on the charge transfer mechanisms. With a group from the Paul Scherrer Institute, final results on the identification of hole trapping sites in ZnO nanaparticles following UV excitation were published [41] (see Fig. 10). With a group from University of Illinois, we studied the charge transfer properties of quantum dot heterostructures using TR-XAS at multiple edges, probing both shells of the heterostructure (ZnTe/CdSe). First results strongly suggest hole localization at Zn sites, but the study is complicated by the lattice heating occurring due to laser absorption. Finally, with a group from EPFL, we studied charge carrier dynamics in inorganic lead halide perovskites (specifically $CsPbBr_3$) with TR-XAS. First indications confirm the hypothesis of polaron formation at the Br center and establish that both electron and hole are following the same dynamics. High resolution fluorescence (HERFD) at the Pb edge also allowed capturing the opening of new channels for absorption after photoexcitation which were obscured otherwise.

Future Plans: We will continue to explore those collaborative studies since they are a natural fit for our time resolved setup at 7ID-D. Follow up studies could happen at XFELS.

5 Affiliations of collaborators

[1]Argonne Leadership Computing Facility, Argonne National Laboratory, Argonne, IL
[2]Kansas State University, Manhattan, KS
[3]Center for Free-Electron Laser Science, DESY, Hamburg, Germany
[4]Uppsala University, Sweden
[5]SLAC National Accelerator Laboratory, Menlo Park, CA
[6]Lawrence Berkeley National Laboratory, Berkeley, CA
[7]University of Southern California, Los Angeles, CA
[8]Universität Rostock, Germany
[9]Ludwig Maximilian Universität München, Germany
[10]Technische Universität Berlin, Germany
[11]Universidad Autónoma de Madrid, Spain
[12]Chemical Sciences and Engineering Division, Argonne National Laboratory, Argonne, IL
[13]Lund University, Lund, Sweden
[14]Université Pierre et Marie Curie, Paris, France
[15]University of Oulu, Oulu, Finland
[16]Max Planck Institute for the Structure and Dynamics of Matter, Hamburg, Germany
[17]Nanyang Technological University, Singapore
[18]Deutsches Elektronen-Synchrotron (DESY), Hamburg, Germany
[19]European XFEL, Hamburg, Germany
[20]Wigner Research Centre for Physics, Hungarian Academy Sciences, Budapest, Hungary
[21]Pacific Northwest Natioanl Laboratory, Richland, WA
[22]X-Ray Science Division, Argonne National Laboratory, Argonne, IL
[23]University of Kansas, Lawrence, KS
[24]University of California Berkeley, Berkeley, CA
[25]Paul Scherrer Institute, Villigen, Switzerland
[26]Newcastle University, Newcastle, UK
[27]University of Illinois Urbana-Champaign, Champaign, IL
[28]Ecole Polytechnique Federale de Lausanne, Lausanne, Switzerland

References

Peer-Reviewed Publications Resulting from Subtask 1 (2016-2018)

[1] T. Gorkhover, S. Schorb, R. Coffee, M. Adolph, L. Foucar, D. Rupp, A. Aquila, J. D. Bozek, S. W. Epp, B. Erk, L. Gumprecht, L. Holmegaard, A. Hartmann, R. Hartmann, G. Hauser, P. Holl, A. Hömke, N. Kimmel, K.-U. Kühnel, P. Johnsson, M. Messerschmidt, C. Reich, A. Rouzée, B. Rudek, C. Schmidt, J. Schulz, H. Soltau, S. Stern, G. Weidenspointner, B. White, J. Küpper, L. Strüder, I. Schlichting, J. Ullrich, D. Rolles, A. Rudenko, T. Möller, and C. Bostedt, "Femtosecond and nanometer visualisation of structural dynamics in superheated nanoparticles," Nature Photonics **10**, 93 (2016).

[2] K. R. Ferguson, M. Bucher, T. Gorkhover, S. Boutet, H. Fukuzawa, J. E. Koglin, Y. Kumagai, A. Lutman, A. Marinelli, M. Messerschmidt, K. Nagaya, J. Turner, K. Ueda, G. J. Williams, P. H. Bucksbaum, and C. Bostedt, "Transient lattice compression in the solid-to-plasma transition," Science Advances **2**, 1500837 (2016).

[3] C. Bostedt, S. Boutet, D. M. Fritz, Z. Huang, H. J. Lee, H. T. Lemke, A. Robert, W. F. Schlotter, J. J. Turner, and G. J. Williams, “The Linac Coherent Light Source: The First Five Years,” Rev. Mod. Phys. **88**, 015007 (2016).

[4] L. Flückiger, D. Rupp, M. Adolph, T. Gorkhover, M. Krikunova, M. Müller, T. Oelze, Y. Ovcharenko, M. Sauppe, S. Schorb, C. Bostedt, S. Düsterer, M. Harmand, H. Redlin, R. Treusch, T. Möller, “Time-resolved x-ray imaging of a laser-induced nanoplasma and its neutral residuals,” New J. Phys. **18**, 043017 (2016).

[5] C.F. Jones, C. Bernando, R.M.P. Tanyag, C. Bacellar, K.R. Ferguson, L.F. Gomez, D. Anielski, A. Belkacem, R. Boll, J.D. Bozek, S. Carron, J. Cryan, L. Englert, S.W. Epp, B. Erk, L. Foucar, R. Hartmann, D. Neumark, D. Rolles, A. Rudenko, K.R. Siefermann, F. Weise, B. Rudek, F.P. Sturm, J. Ullrich, C. Bostedt, O. Gessner, A.F. Vilesov, “Coupled motion of Xe clusters and quantum vortices in He nanodroplets,” Phys. Rev. B **93**, 180510 (2016).

[6] R. Boll, B. Erk, R. Coffee, S. Trippel, T. Kierspel, C. Bomme, J.D. Bozek, M. Burkett, S. Carron, K.R. Ferguson, L. Foucar, J. Kpper, T. Marchenko, C. Miron, M. Patanen, T. Osipov, S. Schorb, M. Simon, M. Swiggers, S. Techert, K. Ueda, C. Bostedt, D. Rolles, A. Rudenko, “Charge transfer in dissociating iodomethane and fluoromethane molecules ionized by intense femtosecond X-ray pulses,” Struc. Dyn. **3**, 043207 (2016).

[7] D. Rupp, L. Flückiger, M. Adolph, T. Gorkhover,M. Krikunova, J.P. Muüller, M. Muüller, T. Oelze, Y. Ovcharenko, B. Röben, M. Sauppe, S. Schorb, D. Wolter, R. Mitzner, M. Wöstmann, S. Roling, M. Harmand, R. Treusch, M. Arbeiter, T. Fennel, C. Bostedt, and T. Möller, “Observation of recombination-enhanced surface expansion of clusters in intense soft x-ray laser pulses”, Phys. Rev. Lett., **117**, 153401 (2016).

[8] Phay J. Ho, Chris Knight, Miklos Tegze, Gyula Faigel, C. Bostedt, and L. Young, “Atomistic 3D coherent X-ray imaging of non-biological systems,” Phys. Rev. A **94**, 063823 (2016).

[9] Phay J. Ho, and Chris Knight, “Large-scale atomistic calculations of cluster in intense x-ray pulses,” J. Phys. B: At. Mol. Opt. Phys. **50**, 104003 (2017).

[10] A. Rudenko, L. Inhester, K. Hanasaki, X. Li, S. J. Robatjazi, B. Erk, R. Boll, K. Toyota, Y. Hao, O. Vendrell, C. Bomme, E. Savelyev, B. Rudek, L. Foucar, S. H. Southworth, C.S. Lehmann, B. Kraessig, T. Marchenko, M. Simon, K. Ueda, K. R. Ferguson, M. Bucher, T. Gorkhover, S. Carron, R. Alonso-Mori, J. E. Koglin, J. Correa, G. J. Williams, S. Boutet, L. Young, C. Bostedt, S.-K. Son, R. Santra, D. Rolles, “Femtosecond response of polyatomic molecules to ultra-intense hard X-rays,” Nature **546**, 129 (2017).

[11] E. C. Bernando, R.M.P. Tanyag, C. Jones, C. Bacellar, M. Bucher, K.R. Ferguson, D. Rupp, M.P. Ziemkiewicz, L.F. Gomez, A.S. Chatterley, T. Gorkhover, M. Mller, J. Bozek, S. Carron, J. Kwok, S.L. Butler, T. Möller, C. Bostedt, O. Gessner, and A.F. Vilesov, “Shapes of rotating superfluid helium nanodroplets,” Phys. Rev. B **95**, 064510 (2017).

[12] T. Osipov, C. Bostedt, J. C. Castagna, K. R. Ferguson, M. Bucher, S. C. Montero, M. L. Swiggers, R. Obaid, D. Rolles, A. Rudenko, J. D. Bozek, N. Berrah, “The LAMP instrument at the Linac Coherent Light Source free-electron laser,” Review of Scientific Instruments **89**, 035112 (2018)

[13] T. Gorkhover, A. Ulmer, K. Ferguson, M. Bucher, F. Maia, J. Bielecki, T. Ekeberg, M.F. Hantke, B.J. Daurer, C. Nettelblad, J. Andreasson, A. Barty, P. Bruza, S. Carron, D. Hasse, J. Krzywinski, D.S.D. Larsson, A. Morgan, K. Mühlig, M. Müller, K. Okamoto, A. Pietrini, D. Rupp, M. Sauppe, Gijs van der Schot, M. Seibert, J.A. Sellberg, M. Svenda, M. Swiggers, N. Timneanu, D. Westphal, G. Williams, A. Zani, H.N. Chapman, G. Faigel, T. Möller, J. Hajdu, C. Bostedt, “Femtosecond X-ray Fourier holography imaging of free-flying nanoparticles”, Nature Photonics **12**, 150153 (2018).

[14] M. Sauppe, D. Rompotis, B. Erk, S. Bari, T. Bischoff, R. Boll, C. Bomme, C. Bostedt, S. Dörner,S. Düsterer, T. Feigl, L. Flückiger, T. Gorkhover, K. Kolatzki, B. Langbehn, N. Monserud, E. Müller, Jan P. Müller, C. Passow, D. Ramm, D. Rolles, K. Schubert, L. Schwob, B. Senfftleben, R. Treusch, A. Ulmer, H. Weigelt, J. Zimbalski, J. Zimmermann, T. Möller and D. Rupp,“XUV double-pulses with femtosecond to 650 ps separation from a multilayer-mirror-based split-and-delay unit at FLASH,” J. Synchrotron Rad. **25**, 15171528 (2018).

[15] I. V. Lundholm, J. A. Sellberg, T. Ekeberg, Max F. Hantke, K. Okamoto, G. van der Schot, J. Andreasson, A. Barty, J. Bielecki, P. Bruza, M. Bucher, S. Carron, B. J. Daurer, K. Ferguson, D. Hasse, J. Krzywinski, D. S. D. Larsson, A. Morgan, Kerstin Mühlig,Maria Müller, C. Nettelblad, A. Pietrini, H. K. N. Reddy, D. Rupp, M. Sauppe, M. Seibert, M. Svenda, M. Swiggers, N. Timneanu, A. Ulmer, D. Westphal, G. Williams, A. Zani, G. Faigel, H. N.Chapman, T. Möller, C. Bostedt, J. Hajdu, T. Gorkhover, and F. R. N. C. Maia,“Considerations for three-dimensional image reconstruction from experimental data in coherent diffractive imaging,” IUCrJ **5**, 531541 (2018).

[16] Y. Kumagai, H. Fukuzawa, K. Motomura, D. Iablonskyi, K. Nagaya, S. Wada, Y. Ito, T. Takanashi, Y. Sakakibara, D. You, T. Nishiyama, K. Asa, Y. Sato,T. Umemoto, K. Kariyazono, E. Kukk, K. Kooser, C. Nicolas, C. Miron, T. Asavei, L. Neagu, M. S. Schffler, G. Kastirke, X. Liu, S. Owada, T. Katayama, T. Togashi, K. Tono, M. Yabashi, N. V. Golubev, K. Gokhberg, L. S. Cederbaum, A. I. Kuleff, and K. Ueda, “Following the Birth of a Nanoplasma Produced by an Ultrashort Hard-X-Ray Laser in Xenon Clusters”, Phys. Rev. X **8**, 031034 (2018).

[17] B. Rudek, K. Toyota, L. Foucar, B. Erk, R. Boll, C. Bomme, J. Correa, S. Carron, S. Boutet, G. J. Williams,

K. R. Ferguson, R. Alonso-Mori, J. E. Koglin, T. Gorkhover, M. Bucher, C. S. Lehmann, B. Krässig, S. H. Southworth, L. Young, C. Bostedt, K. Ueda, T. Marchenko, M. Simon, Z. Jurek, R. Santra, A. Rudenko, S-K. Son, and D. Rolles, "Relativistic and resonant effects in the ionization of heavy atoms by ultra-intense hard X-rays,"Nature Communications, accepted (2018).

Peer-Reviewed Publications Resulting from Subtask 2 (2016-2018)

[18] A. Picón, C. S. Lehmann, C. Bostedt, A. Rudenko, A. Marinelli, T. Osipov, D. Rolles, N. Berrah, C. Bomme, M. Bucher, G. Doumy, B. Erk, K. Ferguson, T. Gorkhover, P. J. Ho, E. P. Kanter, B. Krässig, J. Krzywinski, A. A. Lutman, A. M. March, D. Moonshiram, D. Ray, L. Young, S. T. Pratt, and S. H. Southworth, "Hetero-site-specific ultrafast intramolecular dynamics," Nature Comm. **7**, 11652 (2016).

[19] C. S. Lehmann, A. Picón, C. Bostedt, A. Rudenko, A. Marinelli, D. Moonshiram, T. Osipov, D. Rolles, N. Berrah, C. Bomme, M. Bucher, G. Doumy, B. Erk, K. Ferguson, T. Gorkhover, P. J. Ho, E. P. Kanter, B. Krässig, J. Krzywinski, A. A. Lutman, A. M. March, D. Ray, L. Young, S. T. Pratt, and S. H. Southworth, "Ultrafast measurements of molecular nuclear dynamics using two x-ray pulses," Phys. Rev. A **94**, 013426 (2016).

[20] V. Kimberg, A. Sanchez-Gonzalez, L. Mercadier, C. Weninger, A. Lutman, D. Ratner, R. Coffee, M. Bucher, M. Mucke, M. Agaker, C. Sathe, C. Bostedt, J. Nordgren, J.-E. Rubensson and N. Rohringer, "Stimulated X-ray Raman scattering a critical assessment of the building block of nonlinear X-ray spectroscopy," Faraday Disc., **194**, 305 (2016).

[21] R. Sullivan, J. Jia, A. Vázquez-Mayagoitia, and A. Picón, "Normal Auger processes with ultrashort x-ray pulses in neon," Phys. Rev. A **94**, 043421 (2016).

[22] L. Rego, J. San Roman, A. Picón, L. Plaja, C. Hernandez-Garcia, "Nonperturbative Twist in the Generation of Extreme-Ultraviolet Vortex Beams," Phys. Rev. Lett. **117**, 163202 (2016).

[23] T. J. A. Wolf, R. H. Myhre, J. P. Cryan, S. Coriani, R. J. Squibb, A. Battistoni, N. Berrah, C. Bostedt, P. Bucksbaum, G. Coslovich, R. Feifel, K. J. Gaffney, J. Grilj, T. J. Martinez, S. Miyabe, S. P. Moeller, M. Mucke, A. Natan, R. Obaid, T. Osipov, O. Plekan, S. Wang, H. Koch, M. Gühr, "Probing ultrafast $\pi\pi^*/n\pi^*$ internal conversion in organic chromophores via K-edge resonant absorption," Nature Communications **8**, 29 (2017).

[24] T. J. A. Wolf, F. Holzmeier, I. Wagner, N. Berrah, C. Bostedt, J. Bozek, P. Bucksbaum, R. Coffee, J. Cryan, J. Farrell, R. Feifel, T.J. Martinez, B. McFarland, M. Mucke, S. Nandi, F. Tarantellio, I. Fischer, M. Gühr, "Observing Femtosecond Fragmentation Using Ultrafast X-ray-Induced Auger Spectra," Appl. Sci. **7**, 681 (2017).

[25] A. Picón, "Time-dependent Schrödinger equation for molecular core-hole dynamics," Phys. Rev. A **95**, 0233401 (2017).

[26] A. Sanchez-Gonzalez, P. Micaelli, C. Olivier, T. R. Barillot, M. Ilchen, A.A. Lutman, A. Marinelli, T. Maxwell, A. Achner, M. Agaker, N. Berrah, C. Bostedt, J. D. Bozek, J. Buck, P. H. Bucksbaum, S. Carron Montero, B. Cooper, J. P. Cryan, M. Dong, R. Feifel, L. J. Frasinski, H. Fukuzawa, A. Galler, G. Hartmann, N. Hartmann, W. Helml, A. S. Johnson, A. Knie, A. O. Lindahl, J. Liu, K. Motomura, M. Mucke, C. O'Grady, J-E Rubensson, E. R. Simpson, R. J. Squibb, C. Sathe, K. Ueda, M. Vacher, D. J. Walke, V. Zhaunerchyk, R. N. Coffee, J. P. Marangos, "Accurate prediction of X-ray pulse properties from a free-electron laser using machine learning," Nature Communications **8**, 15461 (2017).

[27] L. Young, K. Ueda, M Gühr, P.H. Bucksbaum, M. Simon, S. Mukamel, N. Rohringer, K. Prince, C. Masciovecchio, M. Meyer, A. Rudenko, D. Rolles, C. Bostedt, M. Fuchs, D. Reis, R. Santra, H. Kapteyn, M. Murnane, H. Ibrahim, Franois Légaré, M. Vrakking, M. Isinger, D. Kroon, M. Gisselbrecht, A. L'Huillier, H. J. Wörner and S. R. Leone,"Roadmap on Ultrafast X-ray Atomic and Molecular Physics," J. Phys. B., **51** 032003 (2018).

[28] L. Inhester, B. Oostenrijk, M. Patanen, E. Kokkenen, S.H. Southworth, C. Bostedt, O. Travnikova, T. Marchenko, S.-K. Son, R. Santra, M. Simon, L. Young, and S. L. Sorenson, "Chemical understanding of the limited site-specificity in molecular inner-shell photofragmentation," J. Phys. Chem. Lett. **9**, 1156 (2018).

[29] M. C. Hoffmann, I. Grguras, C. Behrens, C. Bostedt, J. Bozek, H. Bromberger, R. Coffee, J. T. Costello, L. F. DiMauro, Y. Ding, G. Doumy, W. Helml, M. Ilchen, R. Kienberger, S. Lee, A. R. Maier, T. Mazza, M. Meyer, M. Messerschmidt, S. Schorb, W. Schweinberger, K. Zhang, A. L. Cavalieri, "Femtosecond profiling of shaped x-ray pulses," New J. Phys. **20**, 033008 (2018).

Peer-Reviewed Publications Resulting from Subtask 3 (2016-2018)

[30] E. M. Dufresne, R. W. Dunford, E. P. Kanter, Y. Gao, S. Moon, D. A. Walko, and X. Zhang, "Pink-beam focusing with a one-dimensional compound refractive lens," J. Synchrotron Rad. **23**, 1082 (2016).

[31] D.A. Walko, B.W. Adams, G. Doumy, E.M. Dufresne, Y. Li, A.M. March, A.R. Sandy, J. Wang, H. Wen, and Y. Zhu, "Developments in Time-Resolved X-ray Research at APS Beamline 7ID," 12th International Conference on Synchrotron Radiation Instrumentation, AIP Conf. Proc., **1741**, 030048 (2016).

[32] Y. Gao, R. Harder, S. Southworth, J. Guest, N. Scherer, Z. Yan, L. Ocola, M. Pelton, and L. Young, "Bragg diffraction from sub-micron particles isolated by optical tweezers," AIP Conf. Proc. **1741**, 050010 (2016).

[33] D. Moonshiram, C. Gimbert-Suriñach, A. Guda, A. Picon, C.S. Lehmann, X. Zhang, G. Doumy, A.M. March,

J. Benet-Buchholz, A. Soldatov, A. Llobet, and S.H. Southworth "Tracking the Structural and Electronic Configurations of a Cobalt Proton Reduction Catalyst in Water," J. Am. Chem. Soc. **138**, 10586 (2016).

[34] D. Moonshiram, A. Guda, L. Kohler, A. Picon, S. Guda, C.S. Lehmann, X. Zhang, S.H. Southworth, and K.L. Mulfort, "Mechanistic Evaluation of a Nickel Proton Reduction Catalyst Using Time-Resolved X-ray Absorption Spectroscopy," J. Phys. Chem. C **120**, 20049-20057 (2016).

[35] C. Suriñach, D. Moonshiram, L. Francas, N. Planas, F. Bozoglian, A. Guda, L. Mognon, I. Lopez, C.J. Cramer, L. Gagliardi, and A. Llobet, "Structural and Spectroscopic Characterization of Reaction Intermediates involved in a Dinuclear Co-Hbpp Water Oxidation Catalyst", J. Am. Chem. Soc. **138**, 15291 (2016).

[36] D. Moonshiram, Y. Pineda-Galvan, D. Erdman, M. Palenik. R. Thummel, and Y. Pushkar, "Uncovering the role of oxygen atom transfer in Ru-based catalytic water oxidation," J. Am. Chem. Soc. **138**, 15605 (2016).

[37] J. Creus, R. Matheu, I. Penafiel , D. Moonshiram, J. Benet-Buchholtz, J. Garcia-Anton, X. Sala, C. Godard, and A. Llobet, "A Million Turnover Molecular Anode for Catalytic Water Oxidation", Angew. Chem. Int. Ed. **55**, 15382 (2016).

[38] A. M. March, T. A. Assefa, C. Boemer, C. Bressler, A. Britz, M. Diez, G. Doumy, A. Galler, M. Harder, D. Khakhulin, Z. Németh, M. Pápai, S. Schulz, S. H. Southworth, H. Yavas, L. Young, W. Gawelda, G. Vankó, "Probing transient valence orbital changes with picosecond valence-to-core X-ray emission spectroscopy," J. Phys. Chem. C, **121**, 2620 (2017).

[39] D. Moonshiram, A. Picón, A. Vazquez-Mayagoitia, X. Zhang, M.-F. Tu, P. Garrido-Barros, J.-P. Mahy, F. Avenier, and A. Aukauloo, "Elucidating light-induced charge accumulation in an artificial analogue of methane monooxygenase enzymes using time-resolved X-ray absorption spectroscopy," Chem. Commun. **53**, 2725 (2017).

[40] M. Ross, A. Andersen, Z.W. Fox, Y. Zhang, K. Hong, J.-H. Lee, A. Cordones, A. M. March, G. Doumy, S. H. Southworth, M. A. Marcus, R. W. Schoenlein, S. Mukamel, N. Govind, M. Khalil, "Comprehensive Experimental and Computational Spectroscopic Study of Hexacyanoferrate Complexes in Water: From Infrared to X-ray Wavelengths," J. Phys. Chem. B **122**, 5075-5086 (2018).

[41] T. J. Penfold, J. Szlachetko, F. G. Santomauro, A. Britz, W. Gawelda, G. Doumy, A. M. March, S. H. Southworth, J. Rittmann, R. Abela, M. Chergui and C. J. Milne, "Revealing hole trapping in zinc oxide nanoparticles by time-resolved X-ray spectroscopy," Nature Communications **9**, 478 (2018).

Other cited references

[42] L. Young, E. P. Kanter, B. Krässig, Y. Li, A. M. March, S. T. Pratt, R. Santra, S. H. Southworth, N. Rohringer, L. F. DiMauro, G. Doumy, C. A. Roedig, N. Berrah, L. Fang, M. Hoener, P. H. Bucksbaum, J. P. Cryan, S. Ghimire, J. M. Glownia, D. A. Reis, J. D. Bozek, C. Bostedt, and M. Messerschmidt, "Femtosecond electronic response of atoms to ultra-intense x-rays," Nature **466**, 56 (2010).

[43] E. P. Kanter, B. Krässig, Y. Li, A. M. March, P. Ho, N. Rohringer, R. Santra, S. H. Southworth, L. F. DiMauro, G. Doumy, C. A. Roedig, N. Berrah, L. Fang, M. Hoener, P. H. Bucksbaum, S. Ghimire, D. A. Reis, J. D. Bozek, C. Bostedt, M. Messerschmidt, and L. Young, "Unveiling and driving hidden resonances with high-fluence, high-intensity x-ray pulses," Phys. Rev. Lett. **107**, 233001 (2011).

[44] S. Schorb, D. Rupp, M. L. Swiggers, R. N. Coffee, M. Messerschmidt, G. Williams, J. D. Bozek, S.-I. Wada, O. Kornilov, T. Möller, and C. Bostedt, "Size-dependent ultrafast ionization dynamics of nanoscale samples in intense femtosecond x-ray free-electron-laser pulses," Phys. Rev. Lett. **108**, 233401 (2012).

[45] P. J. Ho, C. Bostedt, S. Schorb, and L. Young, "Theoretical tracking of resonance-enhanced multiple ionization pathways in x-ray free-electron laser pulses," Phys. Rev. Lett. **113**, 253001 (2014).

[46] P. J. Ho, E. P. Kanter, and L. Young, "Resonance-mediated atomic ionization dynamics induced by ultraintense x-ray pulses,"Phys. Rev. A **92**, 063430 (2015).

[47] T. Gorkhover, M. Adolph, D. Rupp, S. Schorb, S. W. Epp, B. Erk, L. Foucar, R. Hartmann, N. Kimmel, K.-U. Kühnel, D. Rolles, B. Rudek, A. Rudenko, R. Andritschke, A. Aquila, J.D. Bozek, N. Coppola, T. Erke, F. Filsinger,11 H. Gorke, H. Graafsma, L. Gumprecht, G. Hauser, S. Herrmann, H. Hirsemann, A. Ho mke, P. Holl, C. Kaiser, F. Krasniqi, J.-H. Meyer, M. Matysek, M. Messerschmidt, D. Miessner, B. Nilsson, D. Pietschner, G. Potdevin, C. Reich, G. Schaller, C. Schmidt, F. Schopper, C.D. Schröter, J. Schulz, H. Soltau, G. Weidenspointner, I. Schlichting, L. Strüder, J. Ullrich, T. Möller, and C. Bostedt, "Nanoplasma dynamics of single large xenon clusters irradiated with superintense x-ray pulses from the Linac Coherent Light Source free-electron laser," Phys Rev Lett. **108**, 245005 (2012).

[48] C. Bostedt, E. Eremina, D. Rupp, M. Adolph, H. Thomas, M. Hoener, A. R. B. de Castro, J. Tiggesbumker, K.-H. Meiwes-Broer, T. Laarmann, H. Wabnitz, E. Plönjes, R. Treusch, J. R. Schneider, and T. Möller, "Ultrafast X-Ray Scattering of Xenon Nanoparticles: Imaging Transient States of Matter," Phys. Rev. Lett. **108**, 093401 (2012).

[49] R.M.P. Tanyag, C. Bernando, C.F. Jones, C. Bacellar, K.R. Ferguson, D. Anielski, R. Boll, S. Carron, J.P. Cryan, L. Englert, S.W. Epp, B. Erk, L. Foucar, L.F. Gomez, R. Hartmann, D.M. Neumark, D. Rolles, B. Rudek, A. Rudenko, K. R. Siefermann, J. Ullrich, F. Weise, C. Bostedt, O. Gessner, and A. Vilesov, "X-ray

coherent diffractive imaging by immersion in nanodroplets," Struc. Dyn. **2**, 051102 (2015).

[50] L. F. Gomez, K. R. Ferguson, J. P. Cryan, C. Bacellar, R. M. P. Tanyag, C. Jones, S. Schorb, D. Anielski, A. Belkacem, C. Bernando, R. Boll, J. Bozek, S. Carron, G. Chen, T. Delmas, L. Englert, S. W. Epp, B. Erk, L. Foucar, R Hartmann, A. Hexemer, M. Huth, J. Kwok, S. R. Leone, J. H. S. Ma, F. R. N. C. Maia, E. Malmerberg, S. Marchesini, D. M. Neumark, B. Poon, J. Prell, D. Rolles, B. Rudek, A. Rudenko, M. Seifrid, K. R. Siefermann, F. P. Sturm, M. Swiggers, J. Ullrich, F. Weise, P. Zwart, C. Bostedt, O. Gessner and A. F. Vilesov, "Shapes and vorticities of superfluid helium nanodroplets," Science **345**, 907 (2014).

[51] R. Hanbury Brown and R. Q. Twiss, "Correlation between Photons in two Coherent Beams of Light," Nature **177**, 27 (1956).

[52] A. Classen, K. Ayyer, H. N. Chapman, R. Röhlsberger and J. von Zanthier "Incoherent Diffractive Imaging via Intensity Correlations of Hard X Rays," Phys. Rev. Lett. **119**, 053401 (2017).

[53] R. W. Dunford, S. H. Southworth, D. Ray, E. P. Kanter, B. Krässig, L. Young, D. A. Arms, E. M. Dufresne, D. A. Walko, O. Vendrell, S.-K. Son, and R. Santra, "Evidence for interatomic Coulombic decay in Xe K-shell-vacancy decay of XeF_2," Phys. Rev. A **86**, 033401 (2012).

[54] B. Erk, R. Boll, S. Trippel, D. Anielski, L. Foucar, B. Rudek, S. W. Epp, R. Coffee, S. Carron, S. Schorb, K. R. Ferguson, M. Swiggers, J. D. Bozek, M. Simon, T. Marchenko, J. Küpper, I. Schlichting, J. Ullrich, C. Bostedt, D. Rolles, and A. Rudenko, "Imaging charge transfer in iodomethane upon x-ray photoabsorption," Science **345**, 288 (2014).

[55] A. A. Lutman, R. Coffee, Y. Ding, Z. Huang, J. Krzywinski, T. Maxwell, M. Messerschmidt, and H.-D. Nuhn, "Experimental demonstration of femtosecond two-color x-ray free-electron lasers," Phys. Rev. Lett. **110**, 134801 (2013).

[56] A. Marinelli, D. Ratner, A. A. Lutman, J. Turner, J. Welch, F.-J. Decker, H. Loos, C. Behrens, S. Gilevich, A. A. Miahnahri, S. Vetter, T. J. Maxwell, Y. Ding, R. Coffee, S. Wakatsuki, and Z. Huang, "High-intensity double-pulse X-ray free-electron laser," Nat. Commun. **6**, 6369 (2015).

[57] A. A. Lutman, T. J. Maxwell, J. P. MacArthur, M. W. Guetg, N. Berrah, R. N. Coffee, Y. Ding, Z. Huang, A. Marinelli, S. Moeller, and J. C. U. Zemella, "Fresh-slice multicolour X-ray free-electron lasers," Nat. Photon. **10** 745 (2016).

[58] K. Siegbahn, C. Nordling, A. Fahlman, R. Nordberg, K. Hamrin, J. Hedman, G. Johansson, T. Bergmark, S.-E Karlsson, I. Lindgren, B. Lindberg, "ESCA, Atomic, Molecular and Solid State Structure Studied by Means of Electron Spectroscopy," Almqvist and Wiksells, Uppsala, 1967.

[59] O. Travnikova, K. J. B, M. Patanen, J. Söderström, C. Miron, L. J. Sæthre, N. Mårtensson, and S. Svensson, "The ESCA molecule–Historical remarks and new results," J. Electron Spectrosco. Relat. Phenom. **185**, 191 (2012).

[60] M. N. Piancastelli, M. Neeb, A. Kivimäki, B. Kempgens, H. M. Köpper, K. Maier, A. M. Bradshaw, and R. F. Fink, "Vibrationally resolved 1s $\rightarrow 2\pi$ decay spectra of CO at the C and O K-edges: experiment and theory," J. Phys. B **30**, 5677 (1997).

[61] A. P. Hitchcock, P. Lablanquie, P. Morin, E. Lizon, A. Lugrin, M. Simon, P. Thiry, and I. Nenner, "Ionic fragmentation of K-shell excited and ionized CO," Phys. Rev. A **37**, 2448 (1988).

[62] C. Behrens, F.-J. Decker, Y. Ding, V. A. Dolgashev, J. Frisch, Z. Huang, P. Krejcik, H. Loos, A. Lutman, T. J. Maxwell, J. Turner, J. Wang, M.-H. Wang, J. Welch, and J. Wu, "Few-femtosecond time-resolved measurements of X-ray free-electron lasers," Nat. Commun. **5**, 3762 (2014).

[63] K. Siegbahn, "Electron Spectroscopy for Atoms, Molecules, and Condensed Matter,"Rev. Mod. Phys. **54**, 709728 (1982).

[64] U. Gelius, E. Basilier, S. Svensson, T. Bergmark and K. Siegbahn, "A High Resolution ESCA Instrument with X-ray Monochromator For Gases and Solids,"J. Elec.Spec. Rel. Pheno. **2**, 405-434 (1974).

[65] S. Mukamel, D. Healion, Y. Zhang and J. Biggs, "Multidimensional attosecond resonant x-ray spectroscopy of molecules: lessons from the optical regime," Annu. Rev. Phys. Chem.., **64**, 101 (2013).

[66] T. Kroll, C. Weninger, R. Alonso-Mori, D. Sokaras, D. Zhu, L. Mercadier, V.P. Majety, A. Marinelli, A. Lutman, M. W. Guetg, F.-J. Decker, S. Boutet, A. Aquila, J. Koglin, J. Koralek, D. P. DePonte, J. Kern, F. D. Fuller, E. Pastor, T. Fransson, Y. Zhang, J. Yano, V. K. Yachandra, N. Rohringer, and U. Bergmann, "Stimulated X-Ray Emission Spectroscopy in Transition Metal Complexes," Phys. Rev. Lett., **120**, 133203 (2018).

[67] S. Schreck, M Beye, J. A. Sellberg, T. McQueen, H. Laksmono, B. Kennedy, S. Eckert, D. Schlesinger, D. Nordlund, H. Ogasawara, R.G. Sierra, V.H. Segtnan, K. Kubicek, W. F. Schlotter, G. L. Dakovski, S. P. Moeller, U. Bergmann, S. Techert, L. G. M. Pettersson, P. Wernet, M. J. Bogan, Y. Harada, A. R. Nilsson and A. Fohlisch, "Reabsorption of soft x-ray emission at high x-ray free-electron laser fluences," Phys. Rev. Lett., **113**, 153002 (2014).

[68] W. Helml, A. R. Maier, W. Schweinberger, I. Grguras, P. Radcliffe, G. Doumy, C. Roedig, J. Gagnon, M. Messerschmidt,S. Schorb, C. Bostedt, and F. Grüner, L. F. DiMauro, D. Cubaynes, J. D. Bozek, Th. Tschentscher, J.T. Costello, M. Meyer, R. Coffee, S. Düsterer, A.L. Cavalieri, R. Kienberger, "Measuring the temporal structure of

few-femtosecond free-electron laser X-ray pulses directly in the time domain," Nat. Photon., **8**, 950 (2014).

[69] S. Duesterer, P. Radcliffe, C. Bostedt, J. Bozek, A. L. Cavalieri, R. Coffee, J. T. Costello, D. Cubaynes, L. F. DiMauro, Y. Ding, G. Doumy, F. Grner, W. Helml, W. Schweinberger, R. Kienberger, A. R. Maier, M. Messerschmidt, V. Richardson, C. Roedig, T. Tschentscher and M. Meyer,"Femtosecond x-ray pulse length characterization at the Linac Coherent Light Source free-electron laser" New J. of Phys., **13**, 093024 (2011).

[70] B. C. Garrett, D. Dixon *et al.* "Role of Water in Electron-Initiated Processes and Radical Chemistry: Issues and Scientific Advances", Chem. Rev. **105**, 355 - 389 (2005).

[71] E. Alizadeh, T. M. Orlando, L. Sanche, "Biomolecular damage induced by ionizing radiation: the direct and indirect effects of low-energy electrons on DNA," Annu. Rev. Phys. Chem. **66**, 379398 (2015).

[72] J. M. Herbert, M. P. Coons, "The Hydrated Electron, "Annu. Rev. Phys. Chem. **68**, 447472 (2017)

[73] O. Marsalek, C. G. Elles, P. A. Pieniazek, E. Pluhaov, J. VandeVondele, S. E. Bradforth, and P. Jungwirth, "Chasing charge localization and chemical reactivity following photoionization in liquid water," J. Chem. Phys. **135**, 224510 (2011).

[74] J. Li, Z. Nie, Y. Y. Zheng, S. Dong and Z.-H. Loh, "Elementary electron and ion dynamics in ionized liquid water," J. Phys. Chem. Lett. **4**, 3698 (2013).

[75] G. Vankó, A. Bordage, M. Pápai, K. Haldrup, P. Glatzel, A. M. March, G. Doumy, A. Britz, A. Galler, T. Assefa, D. Cabaret, A. Juhin, T. B. van Driel, K. S. Kjær, A. Dohn, K. B. Møller, H. T. Lemke, E. Gallo, M. Rovezzi, Z. Németh, E. Rozsályi, T. Rozgonyi, J. Uhlig, V. Sundström, M. M. Nielsen, L. Young, S. H. Southworth, C. Bressler, and W. Gawelda, "Detailed characterization of a nanosecond-lived excited state: x-ray and theoretical investigation of the quintet state in photoexcited $[\mathrm{Fe(terpy)_2}]^{2+}$, J. Phys. Chem C **119**, 5888 (2015).

[76] A. M. March, T. A. Assefa, C. Bressler, G. Doumy, A. Galler, W. Gawelda, E. P. Kanter, Z. Németh, M. Pápai, S. H. Southworth, L. Young, and G. Vankó, Feasibility of valence-to-core x-ray emission spectroscopy for tracking transient species," J. Phys. Chem. C **119**, 14571 (2015).

[77] C. Bressler, W. Gawelda, A. Galler, M. M. Nielsen, V. Sundström, G. Doumy, A. M. March, S. H. Southworth, L. Young, and G. Vankó, "Solvation dynamics monitored by combined X-ray spectroscopies and scattering: photoinduced spin transition in aqueous $[\mathrm{Fe(bpy)_3}]^{2+}$," Faraday Discuss. **171**, 169 (2014).

[78] G. Vankó, A. Bordage, P. Glatzel, E. Gallo, M. Rovezzi, W. Gawelda, A. Galler, C. Bressler, G. Doumy, A. M. March, E. P. Kanter, L. Young, S. H. Southworth, S. E. Canton, J. Uhlig, V. Sundström, K. Haldrup, T. B. van Driel, M. M. Nielsen, K. S. Kjaer, and H. T. Lemke, "Spin-state studies with XES and RIXS: From static to ultrafast," J. Electron Spectrosc. Relat. Phenom. **188**, 166 (2013).

[79] K. Haldrup, G. Vankó, W. Gawelda, A. Galller, G. Doumy, A. M. March, E. P. Kanter, A. Bordage, H. Dohn, T. B. van Driel, K. S. Kjaer, H. T. Lemke, S. Canton, J. Uhlig, V. Sundström, L. Young, S. H. Southworth, M. M. Nielsen, and C. Bressler, "3. Guest-host interactions investigated by time-resolved x-ray spectroscopies and scattering at MHz rates: solvation dynamics and photoinduced spin transition in aqueous $\mathrm{Fe(bipy)}_3^{2+}$," J. Phys. Chem. A **116**, 9878 (2012).

[80] A. M. March, A. Stickrath, G. Doumy, E. P. Kanter, B. Krässig, S. H. Southworth, K. Attenkofer, C. A. Kurtz, L. X. Chen, and L. Young, "Development of high-repetition-rate laser pump/x-ray probe methodologies for synchrotron facilities," Rev. Sci. Instrum. **82**, 073110 (2011).

[81] M. Shirom, G. Stein, "Excited state chemistry of the ferrocyanide ion in aqueous solution. II. Photoaquation," J. Chem. Phys., **55**, 3379 (1971).

[82] M. Reinhard, G. Auböck, N. A. Besley, I. P. Clark, G. M. Greetham, M. W. D. Hanson-Heine, R. Horvath, T. S. Murphy, T. J. Penfold, M. Towrie, M. W. George, M. Chergui, "Photoaquation Mechanism of Hexacyanoferrate(II) Ions: Ultrafast 2D UV and Transient Visible and IR Spectroscopies," J. Am. Chem. Soc. **139**, 7335 (2017).

[83] T. C. B. Harlang, Y. Liu, O. Gordivska, L. A. Fredin, C. S. Ponseca Jr, P. Huang, P. Chábera, K. S. Kjaer, H. Mateos, J. Uhlig, R. Lomoth, R. Wallenberg, S. Styring, P. Persson, V. Sundstr om, K. Wärnmark, "Iron sensitizer converts light to electrons with 92% yield," Nat. Chem. **7**, 883 (2015).

[84] W. Zhang, K Kjaer, R. Alonso-Mori, U. Bergmann, M. Chollet, L. Fredin, R. Hadt, R. Hartsock, T. Harlang, T. Kroll, K. Kubicek, H. Lemke, H. Liang, Y. Liu, M. Nielsen, P. Persson, J. Robinson, E. Solomon, Z. Sun, D. Sokaras, T. vanDriel, T-S Weng, D. Zhu, K. Warnmark. V. Sundstrom and K. Gaffney "Manipulating charge transfer excited state relaxation and spin crossover in iron coordination complexes with ligand substitution," Chem. Sci. **8**, 515 (2017).

Page is intentionally blank.

J.R. Macdonald Laboratory Overview

The J.R. Macdonald Laboratory (JRML) focuses on the interaction of intense laser pulses with matter for the purpose of understanding and even controlling the resulting ultrafast dynamics. The timescales involved range from attoseconds, necessary for studying electronic motion in matter, to femtoseconds and picoseconds for molecular vibration and rotation, respectively. We continue to harness the expertise within the Lab to further our progress in both understanding and control. The synergy afforded by the close interaction of theory and experiment within the Lab serves as a significant multiplier for this effort. To achieve our goals, we are advancing theoretical modeling and computational approaches as well as experimental techniques, such as particle imaging (COLTRIMS, VMI, etc.), molecular alignment, and high-harmonic generation.

Most of our research projects are associated with either "Strong-field and attosecond science" or "Correlated dynamics". These themes serve as broad outlines only, as the boundary between them is not always well defined. Similarly, in many cases it is hard to distinguish between improving theoretical and experimental "tools" and the resulting science discovery. A few examples are briefly mentioned below, while further details are provided in the individual abstracts of the PIs: I. Ben-Itzhak, C. Blaga, B.D. Esry, V. Kumarappan, C.D. Lin, D. Rolles, A. Rudenko, and U. Thumm.

Strong-field and attosecond science: Attosecond science is motivated by the idea of observing electronic motion in atoms and molecules on its natural timescale. The retrieval of information, such as laser-pulse or atomic-dipole phase, from attosecond streaking experiments is one of the challenges addressed by theorists, who also suggested new methods to enhance high-harmonic generation (HHG). In fact, we have recently experimentally demonstrated HHG enhancement by ω-2ω and ω-3ω driving fields following one of their suggestions. Angle-resolved HHG spectroscopy of ethylene enabled the retrieval of the phase and amplitude of each harmonic. Strong-field ionization studies were carried out on atoms and molecules from mid-infrared to X-ray regimes. Those include angle-resolved strong-field ionization studies of CO_2, and pump-probe studies of small polyatomic molecules, like CH_3I. On another front, we continued the effort to develop a general framework for characterizing and predicting—without computation—the dependence of strong-field processes on parameters of the laser.

Correlated dynamics: The correlated dynamics of the electrons in He during double ionization and shakeup were explored theoretically. Methods for controlling the motion of heavy particles in small molecules continue to be developed. Ionization calculations of the benchmark H_2^+ molecule have been extended to very large internuclear distances revealing unexpected rate oscillations, which explain our experimental observation of enhanced ionization of highly stretched HD^+ and Ar_2^+. Work in the Lab has been extended to anion molecular beams, while novel methods for improving solutions of the time-dependent Schrödinger equation were developed and tested, expanding the applicability of such calculations to more complex systems. Imaging the time evolution of the geometry of polyatomic molecules during light-induced fragmentation have been pursued. Intramolecular charge transfer and dissociation have been explored employing similar pump-probe techniques. We have proposed and demonstrated a systematic method for analyzing three-body breakup momentum imaging data that enables separation of sequential breakup from concerted fragmentation.

A significant fraction of JRML research is done in collaboration with others, either at JRML or elsewhere. For example, M. Dantus from Michigan State University, E. Wells from Augustana University and R.R. Lucchese from Lawrence Berkeley National Laboratory benefit from data measured at JRML. Similarly, some of us conduct experiments at free electron lasers, such as LCLS and FLASH, and at other facilities. Our group is well connected through such collaborations with many AMO groups across the world (ALS, ANL, Århus, BNL, FLASH, Univ. of Frankfurt, ICFO Barcelona, Univ. of Jena, LBNL, LCLS, Max-Born Institute – Berlin, Max-Planck Institutes for Quantum Optics and Kernphysik, the Ohio State Univ., PULSE-SLAC, and others).

Finally, it is worth mentioning the laser facilities available to researchers at JRML. Our high-repetition rate laser, PULSAR, and the high-power, tunable, long-wavelength laser, HITS, are the main laser systems, while the old workhorse laser, KLS, is still yielding high-quality results. On the personnel side, Cosmin Blaga, from the Ohio State University, has recently taken the position vacated by C. Trallero's departure a year ago, and he plans to employ mid-IR pulses to influence strong-field ionization and fragmentation of molecules. The new AMO theorist that was hired as part of our department-expansion plan, Loren Greenman, is an expert on structure and dynamics in complex molecules. He has recently obtained separate DOE support for XFEL studies as part of a collaboration with Artem, Daniel, and Robin Santra. Moreover, Loren and his group have already begun collaborating with other members of the JRML group. Combining the theoretical and experimental expertise within the Lab with our large spectrum of laser and imaging capabilities continues to produce exciting physics.

Structure and Dynamics of Atoms, Ions, Molecules, and Surfaces: Molecular Dynamics with Ion and Laser Beams

Itzik Ben-Itzhak, J. R. Macdonald Laboratory, Physics Department, Kansas State University,
Manhattan, KS 66506; ibi@phys.ksu.edu

Project Scope: *The goal of this part of the JRML program is to study and control molecular dynamics under the influence of ultrashort intense laser pulses. To this end, we typically study molecular ion beams and have a close collaboration between theory and experiment.*[i]

Pump-probe studies of fragmentation of fast HD^+ and Ar_2^+ beams

Ben Berry, M. Zohrabi, T. Severt, Bethany Jochim, P. Feizollah, Kanaka Raju P., K.D. Carnes,
Y. Yu, B.D. Esry, and I. Ben-Itzhak

Our first-of-its-kind NIR-pump–NIR-probe measurements on a few-keV HD^+ beam target revealed an unexpected enhancement of ionization at large internuclear separation. In such measurements the first pulse initiates dissociation of the molecular ion, while the second ionizes it. The ionization yield of the dissociating wave packet is enhanced at about 24 and 200 fs, as shown in Fig. 1.

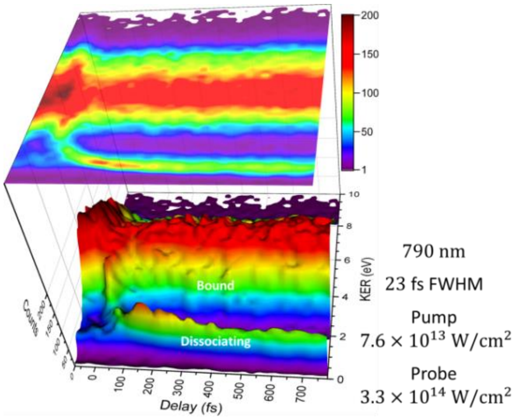

Figure 1. Measured ionization yield of HD^+ ($H^+ + D^+$) as a function of KER and pump-probe delay.

According to classical estimates, these correspond to internuclear distances of about 15 and 60 a.u., respectively. The enhancement around 15 a.u. is consistent with previous work (see, e.g., Refs. [1-3]). In contrast, the enhancement at large internuclear separation is surprising as the interaction between the ionic and atomic fragments is extremely weak. Recently, Esry and co-workers have shown that this enhancement is due to two-center interference [4].

To verify that this large-*R* enhanced ionization is, in fact, a general phenomenon, we recently conducted similar pump-probe measurements on Ar_2^+. Here, too, enhanced ionization is observed at large delays centered around 300 fs, estimated to correspond to R~17 a.u. The potentials are flat beyond about 9.5 a.u.

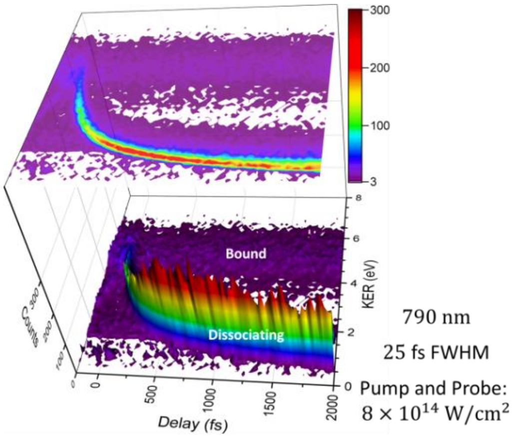

Figure 2. Measured ionization yield of Ar_2^+ ($Ar^+ + Ar^+$) as a function of KER and pump-probe delay.

The Ar_2^+ data, shown in Fig. 2, provided an additional surprise: ionization of the bound vibrational states is strongly suppressed relative to ionization of the dissociating wavepacket, especially when contrasted with the HD^+ data in Fig. 1. These recent findings are still under investigation.

Native frames: Separating sequential and concerted three-body fragmentation

T. Severt, J. Rajput, B. Berry, B. Jochim, P. Feizollah, B. Kaderiya, M. Zohrabi, U. Ablikim, F. Ziaee,
Kanaka Raju P., D. Rolles, A. Rudenko, K. D. Carnes, B. D. Esry, and I. Ben-Itzhak

Separating concerted breakup from sequential fragmentation of polyatomic molecules is a long-standing experimental goal. We have recently demonstrated a powerful method to analyze three-body breakup momentum-imaging data that allows us to systematically distinguish sequential fragmentation events if the intermediate molecule rotates long enough in the fragmentation plane (see Pub. [14] and references therein). Moreover, this method allows us to "recover" the sequential-fragmentation events that are masked by competing processes.

Since this first demonstration, which used OCS^{3+} fragmentation into $O^+ + C^+ + S^+$ via CO^{2+} or CS^{2+} intermediate molecules, we have been exploring the limitations of the method and its applicability to other molecules. For example, implications of identical fragments on the analysis method have been explored using CO_2 and CO_2^+ targets, which are ionized and breakup into $O^+ + C^+ + O^+$.

In another case we identified sequential breakup in pump-probe studies of CH_2I_2 led by Rudenko's group. We identified and separated sequential breakup via $CH_2I^{2+} + I^+$ leading to the $CH_2^+ + I^+ + I^+$ final products. In addition, we have shown that sequential breakup via I_2^{2+} + CH_2^+ with the intermediate I_2^{2+} rotating in the fragmentation plane does not occur. More importantly, our analysis is done "frame by frame" enabling the production of a molecular movie of each process, sequential or concerted, separately. This will enhance our ability to visualize the time evolution of some molecular processes.

Finally, we have implemented our analysis method on single photon double ionization data acquired through our ALS collaboration[ii]. Specifically, we identified and separated sequential fragmentation of the water dication leading to $O + H^+ + H^+$ via $OH^+ + H^+$, as shown in Fig. 3. The identical H^+ fragments were arbitrarily labeled (blue and red) and treated as the correct and incorrect sequential pathways. As both choices lead to a uniform $N(\theta_{OH,H})$ distribution, the correct sequential order is identified by the KER_{OH} in the second step which is predicted to be below about 2.4 eV. Note that we are able to analyze the electrons associated uniquely with this sequential fragmentation, and it does not exhibit any sign of autoionization.

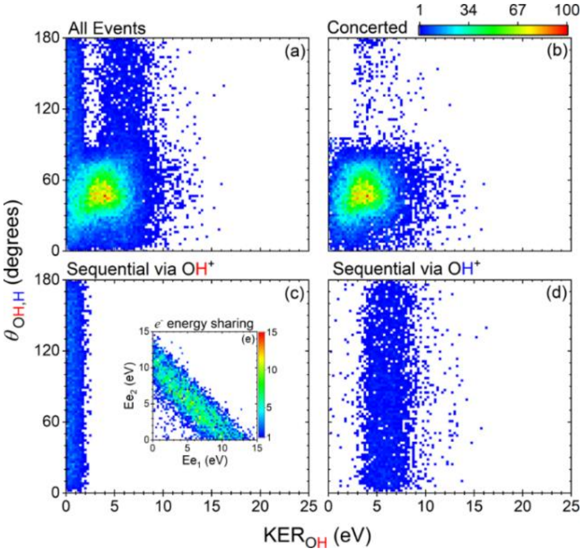

Figure 3. Channel separation of $H_2O^{2+} \rightarrow H^+ + H^+ + O$ fragmentation, where "All" denotes all channels together, while "Concerted," "Sequential via OH^+," and "Sequential via OH^+," refer to the separate breakup channels, respectively (see text). (a-d). The inset shows the energy sharing diagram for the two electrons associated with the sequential breakup via OH^+.

Strong field photodetachment of F_2^-

B. Berry, B. Jochim, T. Severt, P. Feizollah, Kanaka Raju P., K.D. Carnes, B.D. Esry, and I. Ben-Itzhak

Our studies include anion beams, like F_2^-, measured with a coincidence 3D-momentum imaging technique.

In this work we focused on photodetachment of F_2^- in a strong field. More specifically, we looked at the relative importance of the "sequential-photodetachment" mechanism proposed by Hultgren and Kiyan [6], in their interpretation of the photoelectron spectra produced by a strong field. This mechanism involves photodetachment of the F^- fragment after dissociation of the F_2^-.

The measurement of F_2^- dissociation into $F^- + F$ simultaneously with dissociative (F + F) and non-dissociative (F_2) photodetachment, allows us to determine that photodetachment of the F^- fragment long after dissociation is not the dominant process [8].

The main dissociation pathway, X $^2\Sigma_u^+ \rightarrow {}^2\Sigma_g^+$ for both 790- and 395-nm photons, is shown in Fig. 4.

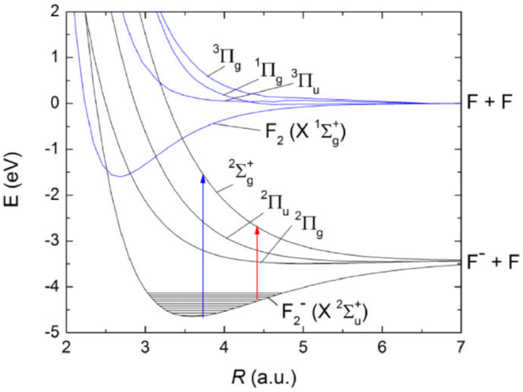

Figure 4. F_2^- (black) and F_2 (blue) potentials adapted from Refs. [7, 8]. The red and blue arrows represent the 790-nm and 395-nm photon energies, respectively, and illustrate the dominant photodissociation path.

The measured KER distribution of the F + F channel, shown in Fig. 5, extends to much lower KER than that of the F^- + F dissociation products. Moreover, it does not match the KER distribution of dissociation as one would expect if photodetachment occurs after the dissociating fragments reach their asymptotic velocities. This indicates that other mechanisms play a key role in the formation of F + F.

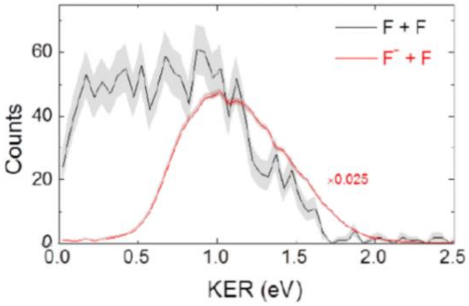

Figure 5. Measured KER distribution of dissociative photodetachment (black line) for 790-nm, 25-fs, and 5×10^{13}-W/cm^2 pulses. The corresponding dissociation KER (red line) is scaled to match roughly the high-KER tail, to indicate the range in which sequential photodetachment is expected to contribute.

References

1. T. Zuo and A.D. Bandrauk, Phys. Rev. A **52**, R2511 (1995)
2. G.N. Gibson *et al.*, Phys. Rev. Lett. **79**, 2022 (1997)
3. Th. Ergler *et al.*, Phys. Rev. Lett. **95**, 093001 (2005)
4. Y. Yu, Ph.D. thesis, Kansas State Univ. (2018)
5. Ben Berry, Ph.D. thesis, Kansas State Univ. (2017)
6. H. Hultgren and I.Y. Kiyan, Phys. Rev. A **84**, 015401 (2011)
7. J.G. Dojahn, E.C.M. Chen, and W.E. Wentworth, J. Phys. Chem. **100**, 9649 (1996)
8. I.A. Delyagina, D.B. Kokh, and A.M. Pravilov, Opt. and Spectr. **94**, 170 (2003)

Future plans: We will continue to probe molecular-ion beams in a strong laser field, specifically exploring challenging two-color, pump-probe and CEP-dependence experiments. We will carry on our studies of more complex systems, including simple polyatomic molecules focusing on three-body breakup, as well as isomerization processes.

Peer-Reviewed Publications Resulting from this Project (2016-2018)

17. “Dissociation dynamics of the water dication following one-photon double ionization II: Experiment”, D. Reedy, J.B. Williams, B. Gaire, A. Gatton, M. Weller, T. Bauer, K. Henrichs, Ph. Burzynski, B. Berry, Z. Streeter, J. Sartor, I. Ben-Itzhak, T. Jahnke, R. Dörner, Th. Weber, and A.L. Landers, Phys. Rev. A – accepted.

16. “Signatures of quantum interference in the valence photoionization of CF_4”, K.A. Larsen, C. Trevisan, R. Lucchese, S. Heck, W. Iskandar, E. Champenois, A. Gatton, R. Moshammer, R. Strom, T. Severt, B. Jochim, D. Reedy, M. Weller, A. Landers, J.B. Williams, I. Ben-Itzhak, R. Dörner, D. Slaughter, C.W. McCurdy, Th. Weber, and T.N. Rescigno, Phys. Chem. Chem. Phys. **20**, 21075 (2018).

15. “State-selective dissociation dynamics of oxygen molecular ion studied with single-harmonic pump and infrared probe pulses”, Y. Malakar, F. Wilhelm, D. Trabert, Kanaka Raju P., X. Li, W.L. Pearson, W. Cao, B. Kaderyia, I. Ben-Itzhak, and A. Rudenko, Phys. Rev. A **98**, 013418 (2018).

14. “Native frames: Disentangling sequential from concerted three-body fragmentation”, Jyoti Rajput, T. Severt, B. Berry, B. Jochim, P. Feizollah, B. Kaderiya, M. Zohrabi, U. Ablikim, F. Ziaee, Kanaka-Raju P., D. Rolles, A. Rudenko, K.D. Carnes, B.D. Esry, and I. Ben-Itzhak, Phys. Rev. Lett. **120**, 103001 (2018).
Highlighted in Physics Today – online story: *Three-body fragmentation in a new frame by Johanna L. Miller*

13. “Non-unique and non-uniform mapping in few-body Coulomb-explosion imaging”, A.M. Sayler, E. Eckner, J. McKenna, B.D. Esry, K.D. Carnes, I. Ben-Itzhak, and G.G. Paulus, Phys. Rev. A **97**, 033412 (2018).
Selected for PRA Kaleidoscope Images: https://journals.aps.org/pra/kaleidoscope/pra/97/3/033412 March 2018

12. “Single-shot carrier-envelope-phase tagging using an *f*-2*f* interferometer and a phase meter: a comparison”, Xiaoming Ren, A.M. Summers, Kanaka-Raju P., A. Vajdi, V. Makhija, C.W. Fehrenbach, N.G. Kling, K.J. Betsch, Z. Wang, M.F. Kling, K.D. Carnes, I. Ben-Itzhak, C. Trallero-Herrero, and V. Kumarappan, J. of Optics **19**, 124017 (2017).
11. “Three-dimensional momentum imaging of dissociation in flight of metastable molecules”, Bethany Jochim, Reid Erdwien, Y. Malakar, T. Severt, Ben Berry, Peyman Feizollah, Jyoti Rajput, B. Kaderiya, W.L. Pearson, K.D. Carnes, A. Rudenko, and I. Ben-Itzhak – New J. Phys. **19**, 103006 (2017).
10. “Phase- and intensity-dependence of ultrafast dynamics in hydrocarbon molecules in few-cycle laser fields”, M. Kübel, C. Burger, R. Siemering, Nora G. Kling, B. Bergues, A.S. Alnaser, I. Ben-Itzhak, R. Moshammer, R. de Vivie-Riedle, and M.F. Kling, **115**, 1835 (2017) – Bandrauk special issue.
9. “Mechanisms and time-resolved dynamics for trihydrogen cation (H_3^+) formation from organic molecules in strong laser fields”, Nagitha Ekanayake, Muath Nairat, Balram Kaderiya, Peyman Feizollah, Bethany Jochim, Travis Severt, Ben Berry, Kanaka Raju P., Kevin D. Carnes, Shashank Pathak, Daniel Rolles, Artem Rudenko, Itzik Ben-Itzhak, Christopher A. Mancuso, B. Scott Fales, James E. Jackson, Benjamin G. Levine, and Marcos Dantus, Scientific Reports **7**, 4703 (2017).
8. “The importance of Rydberg orbitals in dissociative ionization of small hydrocarbon molecules in intense few-cycle laser pulses”, Bethany Jochim, R. Siemering, M. Zohrabi, A. Voznyuk, J.B. Mahowald, D.G. Schmitz, K.J. Betsch, Ben Berry, T. Severt, Nora G. Kling, T.G. Burwitz, U. Ablikim, K.D. Carnes, M.F. Kling, I. Ben-Itzhak, E. Wells, and R. de Vivie-Riedle, Scientific Reports **7**, 4441 (2017).
7. “Unambiguous observation of F-atom core-hole localization in CF_4 through body-frame photoelectron angular distributions”, C.W. McCurdy, T.N. Rescigno, C.S. Trevisan, R.R. Lucchese, B. Gaire, A. Menssen, M.S. Schöffler, A. Gatton, J. Neff, P.M. Stammer, J. Rist, S. Eckart, B. Berry, T. Severt, J. Sartor, A. Moradmand, T. Jahnke, A.L. Landers, J.B. Williams, I. Ben-Itzhak, R. Dörner, A. Belkacem, and Th. Weber, Phys. Rev. A **95**, 011401(R) (2017) – Rapid Communication.
   Selected for PRA Kaleidoscope: http://journals.aps.org/pra/kaleidoscope/pra/95/1/011401 January 2017.
6. “A comprehensive study of Interatomic Coulombic Decay in argon dimers: Extracting *R*-dependent absolute decay rates from the experiment”, J. Rist, T. Miteva, B. Gaire, H. Sann, F. Trinter, M. Keiling, N. Gehrken, A. Moradmand, B. Berry, M. Zohrabi, M. Kunitski, I. Ben-Itzhak, A. Belkacem, T. Weber, A.L. Landers, M. Schöffler, J.B. Williams, P. Kolorenč, K. Gokhberg, T. Jahnke, and R. Dörner, Chem. Phys. **482**, 185 (2017) – Special issue on ICD
5. “Transition from SAMO to Rydberg state ionization in C_{60} in femtosecond laser fields”, H. Li, B. Mignolet, Z. Wang, K.J. Betsch, K.D. Carnes, I. Ben-Itzhak, C.L. Cocke, F. Remacle, and M.F. Kling, J. Phys. Chem. Lett. **7**, 4677 (2016).
4. “Bond-rearrangement and ionization mechanisms in the photo-double-ionization of simple hydrocarbons (C_2H_4, C_2H_3F, and 1,1-$C_2H_2F_2$) near and above threshold”, B. Gaire, A. Gatton, F. Wiegandt, J. Neff, C. Janke, S. Zeller, D. Reedy, J. Rajput, I. Ben-Itzhak, A.L. Landers, A. Belkacem, and Th. Weber, Phys. Rev. A **94**, 033412 (2016).
3. “Complete characterization of single-cycle double-ionization of argon from the non-sequential to the sequential ionization regime”, M. Kübel, C. Burger, Nora G. Kling, T. Pischke, Lucas Beaufore, I. Ben-Itzhak, G.G. Paulus, J. Ullrich, T. Pfeifer, R. Moshammer, M. F. Kling, and B. Bergues, Phys. Rev. A **93**, 053422 (2016).
2. “Steering proton migration in hydrocarbons using intense few-cycle laser fields”, M. Kübel, R. Siemering, C. Burger, Nora G. Kling, H. Li, A.S. Alnaser, B. Bergues, S. Zherebtsov, A.M. Azzeer, I. Ben-Itzhak, R. Moshammer, R. de Vivie-Riedle, and M.F. Kling, Phys. Rev. Lett. **116**, 193001 (2016).
1. “Molecular frame photoelectron angular distributions for core ionization of ethane, carbon tetrafluoride and 1,1-difluoroethylene”, A. Menssen, C.S. Trevisan, M.S. Schöffler., T. Jahnke, I. Bocharova, F. Sturm, N. Gehrken, B. Gaire, H. Gassert, S. Zeller, J. Voigtsberger, A. Kuhlins, F. Trinter, A. Gatton, J. Sartor, D. Reedy, C. Nook, B. Berry, M. Zohrabi, A. Kalinin, I. Ben-Itzhak, A. Belkacem, R. Dörner, T. Weber, A.L. Landers, T.N. Rescigno, C.W. McCurdy, and J.B. Williams, J. Phys. B **49**, 055203 (2016).

---

[i] In addition to the close collaboration with the theory group of *Brett Esry*, some of our studies are done in collaboration with others at JRML and elsewhere.

[ii] Collaboration with the experimentalists: R. Dörner, T. Jahnke A.L. Landers, R. Moshammer, D. Reedy, D. Slaughter, Th. Weber, J.B. Williams, the theorists: R.R. Lucchese, C.W. McCurdy, T.N. Rescigno, C.S. Trevisan and others.

Strong Field Molecular Excitation and Ionization with Midinfrared Laser Drivers: The Role of Molecular Vibrations

Cosmin Ioan Blaga
J. R. Macdonald Laboratory, Physics Department, Kansas State University,
Manhattan, KS, 66506
blaga@phys.ksu.edu

Project Scope

The scope of this new JRML project is to investigate the role played by molecular resonances in strong field physics, with emphasis on excitation and ionization.

The intensities required to ionize molecules depend upon the ionization potential, IP, of each target. For most molecules, the intensity range of interest is ~10-100 TW/cm^2. As vibrational resonances lie in the midinfrared region, the ionization takes place in the strong field limit, i.e., tunneling [1]. For example, the over the barrier saturation intensity of iodomethane (CH_3I, with IP = 9.54 eV) – a widely studied molecule in the literature and at JRML – is estimated to be I_{sat} = 33 TW/cm^2. At this intensity, for a laser driver resonant with the C-H stretch mode centered at ~3.3 µm, the Keldysh parameter is $\gamma = 0.38$, deep in the tunneling regime.

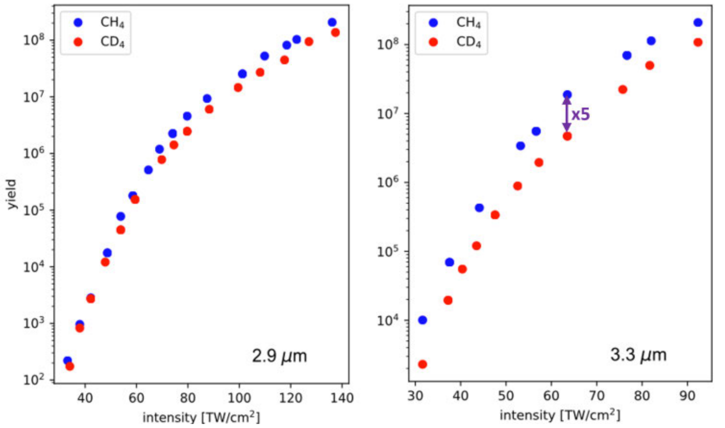

Figure 1: Strong field ionization rates of methane isotopes as a function of intensity. **Left** – At 2.9 µm, both CH_4 (blue) and CD_4 (red) are vibrationally nonresonant and display identical ionization rates. **Right** – At 3.3 µm, the resonantly excited CH_4 (blue) has an ionization rate 4-5 times higher than the still nonresonant CD_4 (red).

Molecular tunneling theory [1] assumes electronic transitions are virtually instantaneous when compared to typical vibrational periods, thus justifying the use of vertical ionization potentials. Under this assumption, strong field ionization with vibrational resonant pulses can be modeled using vertical ionization rates averaged over ground state vibrational distributions. On resonance, broad vibrational distributions extend to large internuclear distances and lead to significant ionization rate increases since vertical ionization potentials usually decrease with distance. An exploratory experiment recently performed while at Ohio State and illustrated in Figure 1 confirmed this prediction in the case of methane when the 100 fs mid-infrared pulses were resonant with the C-H stretch mode. These preliminary investigations also revealed rich fragmentation dynamics at vibrationally resonant wavelengths that included enhanced dehydrogenation, deprotonation and C-C fragmentation pathways.

Tunable midinfrared sources that are both intense and broadband can efficiently deposit significant laser energy into molecular degrees of freedom via direct vibrational excitation. This project aims to understand in detail this process and its role in ionization, excitation and molecular nuclear dynamics.

Recent Progress

This project started September 2018. We are currently in the design phase for the multidetector time of flight apparatus and the two midinfrared optical parametric amplifiers that will be installed at JRM Laboratory on the 1 kHz, 20 mJ/pulse, Ti:Sapphire HITS laser and the 10 kHz, 1.7 mJ/pulse, Ti:Sapphire PULSAR laser.

Future Plans

The first phase of this project consists of developing the necessary intense, tunable midinfrared capabilities at JRM. Using startup funds, two multistage optical parametric amplifiers pumped by JRML's existing Ti:Sapphire sources (PULSAR and HITS, respectively) and seeded by white light continuum generation will allow us to generate 2.8-4.2 µm pulses delivering intensities exceeding 1 PW/cm^2. These new sources are ideal to study the role of the C-H stretch vibrational resonance present in organic compounds.

The second phase of the project will be dedicated to understanding the role played by molecular vibrations in fundamental strong field processes like ionization, excitation, alignment and fragmentation. Mass and 2D photoelectron spectroscopy as well as complete coincidence detection techniques with fragmentation channel sensitivity for neutral and/or ion targets as a function of laser parameters will allow as to test the limits of molecular tunneling theories and if necessary, provide experimental data for improving theoretical models. The proposed work will assist other JRML projects as it is designed to investigate fundamental processes in the same targets of interest (CH_3I, CH_2I_2 and C_2H_2).

The last phase of the project is aimed at applied studies. Using isotopic substitutions, we propose to control energy deposition with site specificity to control fragmentation pathways via wavelength tuning. For example, at 3.3 µm energy deposition in D_3C-CHD-CD_3 and D_3C-CD_2-CD_2H takes place in the center or the edge of the hydrocarbon chain, respectively. Experiments with time-delayed bichromatic fields targeting different roto-vibrational manifolds are also envisioned.

References

[1] Tong, X. M., Zhao, Z. X. and Lin, C-D., *Theory of Molecular Tunneling Ionization*, Phys. Rev. A **66**, 033402 (2002).

Peer-reviewed publications resulting from this project (2016-2018)

No publications to report; PI joined the AMOS project September, 2018.

Strong-field dynamics of few-body atomic and molecular systems

B.D. Esry
J. R. Macdonald Laboratory, Kansas State University, Manhattan, KS 66506
`esry@phys.ksu.edu`

Project Scope

My group's efforts are focused on developing novel analytical and numerical tools to more efficiently and more generally treat atoms and molecules in strong laser fields. Our goal is to advance the state-of-the-art to enable increasingly complicated processes and systems to be treated in an *ab initio* manner. We specialize in treating few-body systems with minimal approximations, using the results to validate general analytic approaches. Moreover, with more effective tools for such systems, we are able to explore a broader range of physical phenomena and can more realistically contemplate quantitative comparisons with experiment for these highly non-perturbative processes.

Time-dependent perturbation-theory propagator

Recent progress

Surprisingly, when the literature is surveyed, needs are assessed, and costs are tallied, it is clear that even after decades of effort there is a compelling need to improve the numerical solution of the strong-field time-dependent Schrödinger equation (TDSE). In particular, even though it is often possible to make nearly any scheme work by throwing sufficient resources at it, there is a real need for an efficient, accurate approach. While we have explored conventional routes to this end, we have also tried some unconventional ones with the hope of finding a disruptive solution.

One promising such approach is, surprisingly, time-dependent perturbation theory (TDPT). Despite the fact that the strong-field ionization problem is often described as nonperturbative, it can be solved by using high-enough-order TDPT. This possibility is typically discarded since the sums over intermediate states required are daunting. Nevertheless, TDPT offers a number of advantages.

Foremost is the independence of the nth-order component ψ_n on the perturbation parameter ϵ. Consequently, ψ at *any* ϵ can be constructed as

$$\psi(t) = \sum_n \epsilon^n \psi_n(t), \tag{1}$$

from which any observable can also be computed at any ϵ. Since ϵ is the field strength for strong-field ionization, the intensity averaging necessary to compare with experiment — which normally requires 100–150 intensities [R1] — can be done analytically. This is significant only if the ψ_n can be calculated at a cost much less than calculating 100–150 intensities conventionally. Being a project in progress, the answer to this question is still not known, although we do have reasons to believe it is possible.

One important aspect of our approach is that we solve the differential version of TDPT,

$$i\frac{\partial}{\partial t}\psi_n = H_0\psi_n + V\psi_{n-1}, \tag{2}$$

where $H{=}H_0{+}\epsilon V$ is the total Hamiltonian. We thus avoid sums over intermediate states and can bring to bear the same kinds of numerical schemes normally used for the TDSE — with some advantages. Care must, however, be taken since errors tend to accumulate in Eq. (2). Nevertheless, we have been able to solve to relatively high order for a one-dimensional soft-Coulomb test problem. Eighth-order results are shown in Fig. 1, and we have solved as high as 24th order.

This expansion suggests a number of interesting computational possibilities. For instance, a calculation can be stopped at a given order, then restarted so long as $\psi_{n_{\max}}(t)$ was saved. More ψ_n could then be added to treat higher intensities — without rerunning the whole calculation. Another potential efficiency is offered by symmetry since a given ψ_n only needs the subset of symmetries accessible at that order. Importantly, this expansion is applicable to any system so that the savings could be realized in any strong-field problem.

The potential runtime savings alone are motivation enough to pursue this idea, but it offers other intriguing possibilities as well. For example, having the ψ_n would provide valuable physical insight into the multiphoton pathways involved. The movie of the nth-order wavepackets in a molecule, for example, could be very illuminating.

Future plans

To be useful for NIR or MIR fields, we must demonstrate that we can go to much higher orders — likely in the hundreds — both in terms of accuracy and efficiency. Unfortunately, in our efforts to date, we have identified an issue complicating such a high-order calculation. Specifically, the power series for $\psi(t)$ in Eq. (1) is an alternating series with terms whose magnitude can grow very large. We can thus only calculate up to the order at which the cancellation inherent in such a series eliminates more significant digits than our accuracy goal allows. The simplest solution, increasing the number of significant digits in the calculation beyond the double precision format we are using, carries too large of a performance penalty. We are therefore examining resummation techniques and other alternative strategies. Should these efforts prove unfruitful, we believe that our TDPT approach will still be helpful for few-photon processes in complex systems.

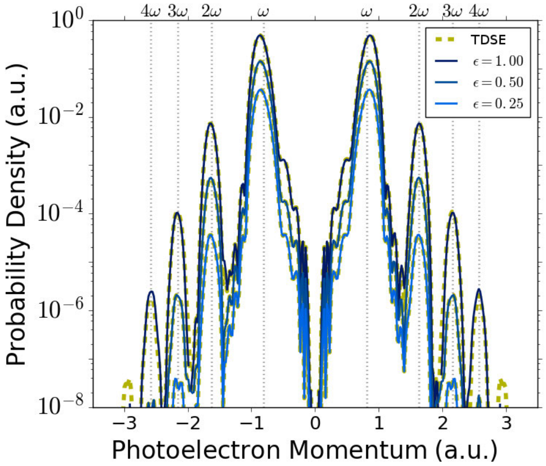

Figure 1: Comparison of the photoionization momentum distribution for a soft-Coulomb potential using TDPT and using a conventional TDSE solver showing ATI peaks. A $\sin^2$, 46-nm, 3-cycle pulse with peak intensity $8.75\epsilon^2\times10^{15}$ W/cm^2 was used. A single 8th-order TDPT calculation gives all intensities $\epsilon<1$, while separate TDSE calculations were required.

Comparing coherent control via two-color fields and the carrier-envelope phase

Recent Progress

In a new application of our parametric-state expansion [R2, R3], we investigate coherent control of strong-field processes via two common schemes: varying the delay between two colors in a laser field and varying the carrier-envelope phase (CEP) of a single few-cycle laser pulse. With our analysis, we rigorously demonstrate the many similarities between these schemes as well as show, in a very general way, that two-color control will essentially always surpass CEP control.

We can analyze both schemes with the same formalism by writing the vector potential for the laser field in the dipole approximation as

$$\boldsymbol{\mathcal{A}}(t) = \hat{\mathbf{z}} \sum_j \mathcal{A}_j e^{(-t/\tau_j)^2} \sin(\omega_j t + \varphi_j), \qquad (3)$$

with ω_j the central frequency for each color. Thus, for CEP control there is a single pulse, while for two-color pulses, j=1,2, and we typically take φ_1=0 and φ_2=$-\omega_2\tau$. Note that this analysis does assume that the pulse envelopes are independent of φ_j.

Since the laser field is periodic in φ_j, the Hamiltonian is as well. Therefore, the system's wave function must also be periodic in φ_j, which we can ensure by expanding it in a Fourier series — thereby making the φ_j dependence explicit and the Fourier coefficients ψ_j independent of φ_j. This, in turn, allows us to derive the φ_j dependence of any observable. In particular, we can write the momentum distribution of a system fragmenting into two pieces following the pulses as

$$\frac{\partial^2 P}{\partial E \partial \theta_k} = \sum A^*_{n_1' n_2' J'}(E) A_{n_1 n_2 J}(E) \times Y_{J'0}(\theta_k) Y_{J0}(\theta_k) e^{i(n_1-n_1')\varphi_1} e^{i(n_2-n_2')\varphi_2}. \qquad (4)$$

In addition to the explicit φ_j dependence, this expression also separates the angle and energy dependence. Moreover, all of the details of the particular system under study are contained in the amplitudes

$$A_{n_1 n_2 J}(E) = \sqrt{2\pi}(-i)^J e^{i\delta_J} \langle EJ | F_{n_1 n_2 J}(t_f) \rangle \qquad (5)$$

where $F_{n_1 n_2 J}(t_f)$ is the radial wave function at the final time.

Equation (4) shows that the momentum distribution will display φ_j dependence only if two or more pathways — *i.e.*, combinations of (n_1, n_2, J) — differing in their values of n_j are non-zero at the same momentum (energy and angle). Of course, this is just the interference expected in coherent control. The picture is completed by the identification of n_j as the net number of photons of color ω_j absorbed or emitted in the field [R2, R3]. The amplitudes $A_{n_1 n_2 J}(E)$ are thus the amplitudes for absorbing n_j photons of energy ω_j resulting in a final energy of E and angular momentum J — the "photon-pathway" amplitudes for conciseness.

For these control schemes, two observables are often considered: the energy-dependent yield and the spatial asymmetry. More specifically, the φ_j dependence of the yield is most conveniently shown through the relative yield

$$\mathcal{Y}(E) = \frac{dP}{dE}\left\langle\frac{dP}{dE}\right\rangle_{\varphi_j}^{-1}. \tag{6}$$

Similarly, the normalized spatial asymmetry is convenient

$$\bar{\mathcal{A}}(E) = \left[\frac{dP_{\text{up}}}{dE} - \frac{dP_{\text{down}}}{dE}\right]\left\langle\frac{dP}{dE}\right\rangle_{\varphi_j}^{-1}. \tag{7}$$

The denominator in each case is the φ_j-averaged value to ensure all control-parameter dependence is from the numerator to simplify the interpretation.

In order to have φ_j dependence in $\mathcal{Y}(E)$, we must have two interfering photon pathways that end with the same J. The canonical example of this is the Brumer-Shapiro ω-3ω scheme sketched for strong-field dissociation of HeH$^+$ in Fig. 2. In this case, the control is exercised over the 3ω peak.

The scenario shown in Fig. 2(b) gives the maximum contrast since the two interfering amplitudes are chosen to be equal in magnitude at every energy. This is accomplished by independently tuning the intensities and durations of the ω and 3ω pulses.

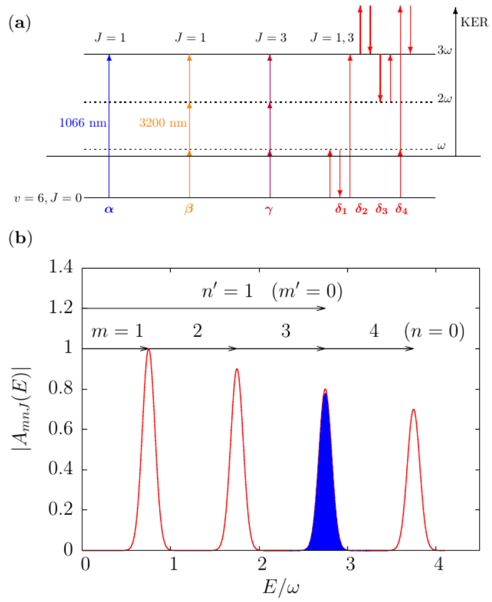

Figure 2: (a) Scheme for two-color control of the yield of the 3ω peak in strong-field dissociation of HeH$^+$ by 3.2-μm light. (b) A lowest-order perturbation theory depiction of $|A_{n_1 n_2 J}(E)|$ for pathways α (blue shading) and β (solid red lines).

The sketch analogous to Fig. 2(b) for CEP control looks similar. But, with only a single central frequency ω, interference at a particular energy relies on the overlap of different photon peaks. This interference is possible only when the individual peaks are very broad — as they are for few-cycle (and shorter) pulses. However, the interference always occurs in the tails of the peaks so that maximum contrast is only possible at a single energy. For CEP effects in the yield, pathways differing by an even number of photons must interfere [R3]. This requires a pulse bandwidth on the order of ω or very high intensities — which explains why producing significant CEP effects in the yield are challenging.

The yield as a function of energy and control parameter for both schemes as calculated from solutions of the time-dependent Schrödinger equation is shown in Figs. 3(b) and 3(d). It is clear that the contrast (or control) is much larger in the two-color case. This

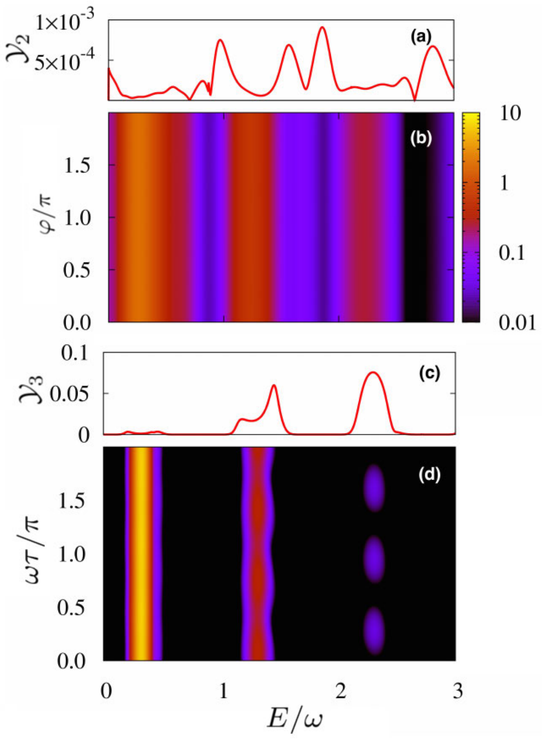

Figure 3: Control over the yield of strong-field dissociation of HeH$^+$($v = 6, J = 0$). (a) The relative amplitude $\mathcal{Y}_2$ of the π-periodic CEP-dependent oscillation in the KER spectrum, and (b) KER spectrum as a function of CEP. (c) The relative amplitude $\mathcal{Y}_3$ of the $2\pi/3$-periodic delay-dependent oscillation in the KER spectrum, and (d) the KER spectrum as a function of the two-color relative phase.

fact is quantified in Figs. 3(a) and 3(c) based on the parametric-state analysis. Specifically, carrying through that analysis gives

$$\mathcal{Y}(E) = 1 + \mathcal{Y}_3(E)\cos[3\omega\tau + \Phi_3(E)] + \ldots \tag{8}$$

for the two-color yield with $\Phi_3(E)$ a system- and energy-dependent phase. Similarly, for CEP control,

$$\mathcal{Y}(E) = 1 + \mathcal{Y}_2(E)\cos[2\varphi + \Phi_2(E)] + \ldots \tag{9}$$

The quantities $\mathcal{Y}_3$ and $\mathcal{Y}_2$ thus characterize the magnitude of the control.

Numerical results from the time-dependent Schrödinger equation for the spatial asymmetry (shown in Fig. 4) further support the conclusion that two-color control — ω-2ω in this case — is more effective than CEP control.

Future Plans

We believe that the parametric-state expansion is a useful tool for understanding strong-field control and its dependence on the control parameters as well as for deriving explicit expressions and making general predictions. This example served to illustrate its utility while also clarifying the relative merits of these two control schemes in a very general way. We plan to follow up with application of the parametric-state expansion to other examples. By doing so, we hope to convince others in the community that it is indeed a useful picture that they might profitably employ.

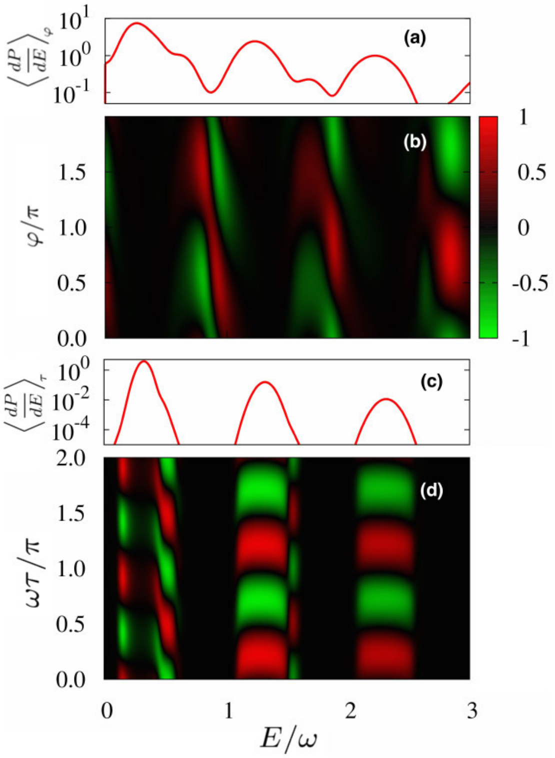

Figure 4: Control over the spatial asymmetry of strong-field dissociation of HeH$^+$($v = 6, J = 0$). (a) CEP-averaged KER spectrum, and (b) normalized spatial asymmetry as a function of CEP. (c) Delay-averaged KER spectrum, and (d) normalized spatial asymmetry as a function of two-color phase.

References

[R1] T. Morishita, Z. Chen, S. Watanabe, and C. D. Lin, Phys. Rev. A **75**, 023407 (2007).

[R2] V. Roudnev and B. D. Esry, Phys. Rev. Lett. **99**, 220406 (2007).

[R3] J. J. Hua and B. D. Esry, J. Phys. B **42**, 085601 (2009).

Peer-reviewed publications resulting from this project (2016–2018)

[P1] Y. Yu, S. Zeng, J. V. Hernández, Y. Wang, and B. D. Esry, "Influence of the initial angular distribution on strong-field molecular dissociation," Phys. Rev. A **94**, 023423 (2016).

[P2] D. Ursrey and B. D. Esry, "Using the carrier-envelope phase to control strong-field dissociation of HeH$^+$ at midinfrared wavelengths," Phys. Rev. A **96**, 063409 (2017).

[P3] J. Rajput, T. Severt, B. Berry, B. Jochim, P. Feizollah, B. Kaderiya, M. Zohrabi, U. Ablikim, F. Ziaee, Kanaka Raju P., D. Rolles, A. Rudenko, K. D. Carnes, B. D. Esry, and I. Ben-Itzhak, "Native frames: disentangling sequential from concerted three-body fragmentation," Phys. Rev. Lett. **120**, 103001 (2018).

[P4] A. M. Sayler, E. Eckner, J. McKenna, B. D. Esry, K. D. Carnes, I. Ben-Itzhak, and G. G. Paulus, "Nonunique and nonuniform mapping in few-body coulomb-explosion imaging," Phys. Rev. A **97**, 033412 (2018).

[P5] Y. Yu and B. D. Esry, "An optimized absorbing potential for ultrafast, strong-field problems," J. Phys. B **51**, 095601 (2018).

Controlling rotations of asymmetric top molecules: methods and applications

Vinod Kumarappan
James R. Macdonald Laboratory, Department of Physics
Kansas State University, Manhattan, KS 66506
vinod@phys.ksu.edu

Program Scope

The goal of this program is to improve molecular alignment methods, especially for asymmetric top molecules, and then use well-aligned molecules for further experiments in ultrafast molecular physics. We use multi-pulse sequences for 1D alignment and orientation, and for 3D alignment of molecules. Our main focus now is to further develop our method for extracting orientation-resolved information from rotational wavepacket dynamics, particularly for asymmetric top molecules. We are particularly interested in applying this method to obtain molecular frame photo-ion and photoelectron angular distributions, and to extract the complex dipole responsible for high-harmonic generation.

Recent Progress

In the past few years we have shown that the rotational wave packet dynamics induced by impulsive alignment of a molecule can be exploited to obtain the orientation dependence of probe-driven processes as well as the time evolution of the molecular axis distribution. Briefly, the angle-dependence of the measured signal is expressed as an expansion in a Wigner function basis, and the delay-dependent signal as a convolution of the time-dependent molecular axis distribution and the angle dependence of the probe process. The algorithm uses TDSE calculations of the rotational wavepacket and linear regression to deconvolve the two functions. In the case of asymmetric top molecules, this method (which we call Orientation Resolution from Rotational Coherence Spectroscopy, or ORRCS) can extract the dependence of probe-driven processes as a function of the two Euler angles that are necessary to specify the orientation of the molecule relative to a linearly polarized field. In many cases — non-dissociative ionization by an ultrashort laser pulse, for instance—this method is unique in this capability. ORRCS is also the only method available for determining the full 2D rotational wavepacket dynamics in asymmetric tops. We are currently using this method to study angle-resolved strong field ionization in asymmetric tops and developing new measurement techniques based on ORRCS. These include the analysis of momentum distributions of ions and electrons, and extracting the phase and amplitude of high order harmonics. Some examples are discussed below.

Strong-field fragmentation of CO_2

The axial recoil approximation is often used in the study of molecular fragmentation dynamics, but there is usually no experimental means for validating the approximation. Validation would require measurement of the molecular axis distribution independent of the measurement of the momentum distribution. In collaboration with Daniel Rolles and Tom Weinacht, we measured the delay dependence of the momentum distribution of CO^+ and O^+ produced from CO_2 by an 785 nm pulse at 10^{15} W/cm^2 with a VMI spectrometer and a Tpx3Cam detector.The peak alignment obtained was $\langle\cos^2\theta\rangle = 0.86$. The pump and probe pulse were both linearly polarized in the plane of detector,

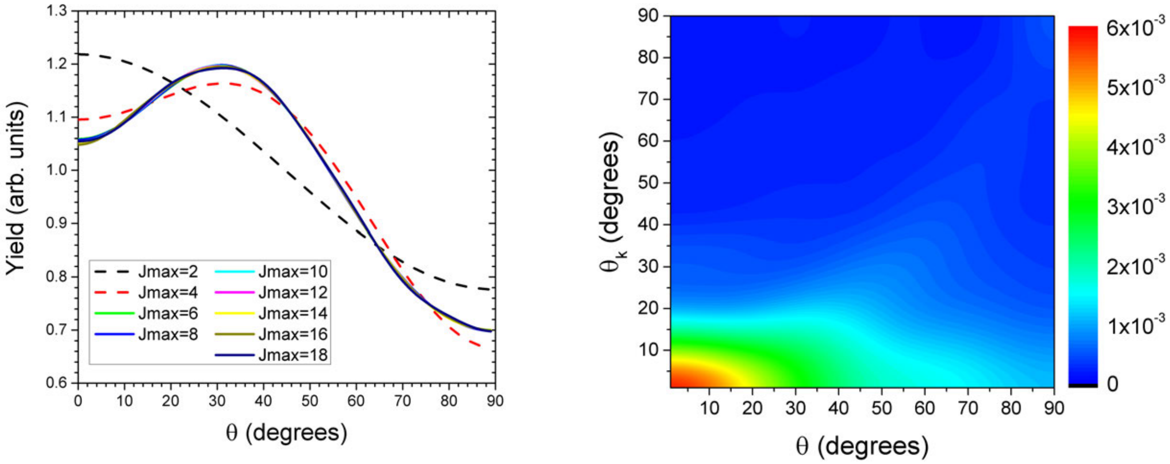

Figure 1: (Left) The dependence of the $CO_2 \longrightarrow CO^+ + O^+$ channel on the angle between the laser polarization vector and the molecular axis, extracted from the delay dependence of the yield of CO^+ in this channel. The fit converges with $J \leq 6$; higher order terms up to $J = 18$ can be fit but do not change the angle dependence. (Right) 2D distribution function for CO^+ to be ejected at angle θ_k from a molecule at θ. The plot clearly shows that axial recoil is a poor approximation for this channel.

and the 2D momentum distribution measured at each delay was decomposed into gaussian and Legendre polynomial bases for the magnitude of the momentum and the polar angle, respectively. The coefficients obtained from this decomposition were fitted to the delay-dependent moments of the molecular axis distribution using the ORRCS algorithm. From these fits we obtained both the angle-dependence of the yield of this fragmentation channel, and the probability distribution for a molecular at angle θ relative to the laser polarization vector to fragment with an asymptotic momentum along θ_k. Both are shown in Fig. 1. The left panel shows that the molecule is most likely to fragment into the $CO_2 \longrightarrow CO^+ + O^+$ channel when at an angle of about 35°, and that the fragments are preferentially ejected along the laser polarization vector (that is, near $\theta_k = 0$) irrespective of their orientation in the absence of the probe pulse. Measurements of this kind directly quantify the applicability of the axial recoil approximation.

Since the Tpx3Cam detector measured all the ions simultaneously, the momentum distribution of the O^+ under identical conditions is also available. The same analysis repeated for this ion yielded results consistent with that obtained from CO^+.

Molecular frame photoelectron angular distributions

Photoelectron momentum distributions measured using a VMI spectrometer in the axially symmetric configuration, in which the laser polarization vector defines an axis of symmetry parallel to the plane of the detector, can also be analyzed in the same manner as ion momentum distributions. The fits to the momentum distributions yield time-dependent asymmetry parameters, which are no longer limited by averaging over an isotropic distribution of molecules, and reflect the dependence of the photoelectron angular distribution on the orientation of the molecules in space. We measured the photoelectron VMI spectrum from multiphoton ionization of SO_2 by 266 nm pulses. The molecules were cooled to ~2 K, and aligned using a 150 fs, 800 nm pulse at $\sim 10^{13}$ W/cm^2. The VMI spectrum and the delay dependence of the anisotropy parameter β_2 are shown in Fig. 2. We were also able to determine the delay dependence of β_4 and β_6 (which is small and noisy). Marceau

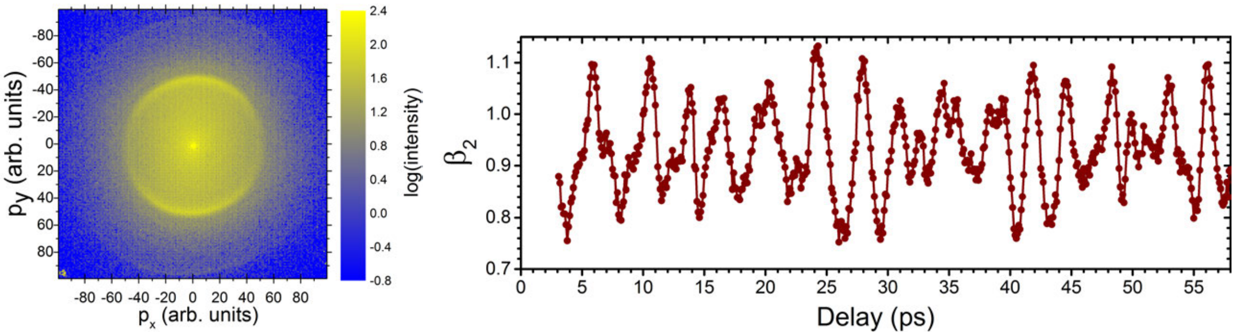

Figure 2: (Left) VMI spectrum of photoelectrons from three-photon ionization of SO_2 by 266 nm pulses. The ring at ~ 50 pixels radius is at ~ 1.6 eV. (Right) The delay dependence of the second order asymmetry parameter β_2 for the 1.6 eV peak as a function of delay between the 800 nm alignment pulse and the 266 nm pulse.

et al. [2] have recently shown that complex photoionization dipole matrix elements can be obtained from such delay dependent data. We are attempting to apply similar techniques to asymmetric top molecules.

Angle-resolved HHG dipole in ethylene

High harmonic spectroscopy from aligned molecules can be used to measure differential photoionization cross-sections. As an example, our measurements of HHG from strongly aligned N_2 showed both a shape resonance and a Cooper in the photoionization cross section of the molecule [3]. But our measurements did not determine the phase of the HHG dipole, although in that case phase-determination was not critical. In general, because the measured HHG spectrum depends on the angle-dependence of the phase, the determination of HHG dipole phase is required. For asymmetric top molecules, it would be also be necessary to determine both amplitude and phase of the HHG dipole as a function of orientation of the molecules in space.

Such measurements have been made by Spector *et al.* [4] on HHG from SO_2, although their analysis was limited to the second order axis distribution moments (that is, to $\cos^2\theta$'s for the three molecular axes). Using ORRCS, we can improve the angular resolution of the measurements and cover the entire space of relevant angles (the polar angle θ and the rotation of the molecule around its own axis, χ). We generated high harmonics in jet-cooled ethylene with 30 fs, 795 nm pulses. The molecules were first aligned with a 130 fs, 795 nm pulse, and the HHG driver was delayed with respect to the alignment pulse up to 75 ps. Using the measured harmonic spectrum from harmonic orders 9 to 25, a phase retrieval algorithm, and the calculated molecular axis distribution as a function of time, we were able to extract both the amplitude and phase of the harmonics as a function of the molecule's orientation in space. Since ethylene is an asymmetric top molecule and the HHG driver was linearly polarized, the molecular orientation is described by two Euler angles. A model based on the strong filed approximation shows that lower order harmonics have features that have contributions from multiple orbitals, but this model is inadequate for the higher order harmonics. Further theoretical analysis of the data is ongoing.

This project involved a collaboration with Salvatore Stagira, Caterina Vozzi (Polytecnico Milano), Varun Makhija (University of Ottawa), Paul Hockett and Michael Spanner (NRC, Ottawa).

Future plans

The ORRCS method provides uniquely detailed access to the orientation dependence of ultrafast photo-induced processes. We will continue to measure photoelectrons and photoions using a VMI spectrometer with goal of understanding photo-induced excitation and fragmentation processes in small polyatomic molecules. For ion measurements, we plan to use the Tpx3Cam detector to measure VMI spectra without axial symmetry in the molecular axis distribution by using elliptically polarized pump pulses. Due to the ∼5 ns time resolution of the detector, we can measure 3D momentum distributions of ions without have to slice the images. Such measurements will allow us to complete molecular frame ion angular distributions (including the azimuthal angle, which is averaged over in axially symmetric measurements). In collaboration with Cosmin Blaga, we plan to measure the angle-dependence of strong-field ionization using mid-IR lasers, including cases where the laser wavelength coincides with vibrational resonances. This information would be helpful for using LIED to measure molecular structure.

Peer-Reviewed Publications Resulting from this Project (2016-2018):

[P1] Artem Rudenko, Varun Makhija, Aram Vajdi, Thorsten Ergler, Markus Schuerholz, Rajesh K Kushawaha, Robert Moshammer, Joachim Ullrich, and Vinod Kumapparan, “Strong-field-induced wave packet dynamics in carbon dioxide molecule”, Faraday Discuss., 194, 463-478, (2016).

[P2] Utuq Ablikim, Cédric Bomme, Hui Xiong, Evgeny Savelyev, Razib Obaid, Balram Kaderiya, Sven Augustin, Kirsten Schnorr, Ileana Dumitriu, Timur Osipov, René Bilodeau, David Kilcoyne, Vinod Kumarappan, Artem Rudenko, Nora Berrah, Daniel Rolles “Identification of absolute geometries of *cis* and *trans* molecular isomers by Coulomb Explosion Imaging”, Scientific Reports 6, 38202 (2016).

[P3] Jan Troß, Xiaoming Ren, Varun Makhija, Sudipta Mondal, Vinod Kumarappan, and Carlos A. Trallero-Herrero, “N_2 HOMO-1 orbital cross section revealed through high-order-harmonic generation”, Phys. Rev. A 95, 033419 (2017).

[P4] Ren, X., Summers, A. M., Kanaka Raju, P., Vajdi, A., Makhija, V., Fehrenbach, C. W., Kling, N. G., Betsch, K. J., Wang, Z., Kling, M. F., Carnes, K. D., Ben-Itzhak, I., Trallero-Herrero, C. and Kumarappan, V., “Single-shot carrier-envelope-phase tagging using an f-2f interferometer and a phase meter: a comparison”, Journal of Optics, 19, 124017 (2017).

References:

[1] A. Zhao *et al.*, Rev. Sci. Inst. 88, 113104 (2017).
[2] C. Marceau *et al.*, Phys. Rev. Lett. 119, 083401 (2017).
[3] X. Ren, *et al.*, Phys. Rev. A 88, 043421 (2013).
[4] L. S. Spector *et al.* Nat. Commun. 5, 3190 (2014).

Strong field rescattering physics and attosecond physics

C. D. Lin
J. R. Macdonald Laboratory, Kansas State University
Manhattan, KS 66506
e-mail: cdlin@phys.ksu.edu

Program Scope:

We investigated the interaction of ultrafast intense lasers and attosecond pulses with atoms and molecules. The most notable accomplishment in the past grant period is the ongoing development of a new method to retrieve the phase of broadband isolated attosecond pulses. We believe that the reported attosecond pulse durations in the water window region in the literature are incorrect. We also identified non-conventional phase matching method for enhancing and extending harmonics cutoff energies and new mechanism for generating harmonics in CO_2 that would produce abnormal attosecond pulse trains. Our plan for further studies is also discussed.

1. A new method of retrieving broadband single attosecond pulses in the water-window region

Recent progress

In 2017, we developed a PROBP method for retrieving attosecond pulses which have spectral bandwidth in the order of 100 eV. In the same year, using 1850 nm mid-infrared lasers, three experimental groups (ETH, UCF, and ICFO) reported high-order harmonics in the water-window region. Using the same streaking technique, two groups reported that they have generated isolated attosecond pulses (IAP) with pulse duration of 53 as and 43 as, respectively, while another group claimed that they only know the pulse is shorter than 225 as.

The conventional method of retrieving the pulse duration of an IAP is to determine its spectral phase since the amplitude of the IAP in the energy domain is easily retrieved from the IAP-alone photoelectron spectra. If the spectral bandwidth is of the order of 10 eV or so, the so-called FROG-CRAB method may be used. When the bandwidth extends to about 100 eV, the condition of narrow bandwidth used in the FROG-CRAB method is not valid. We removed this limitation by developing the PROBP method for such pulses, but we found later that PROBP cannot be efficiently extended to even shorter pulses where the spectral bandwidth is about 250 eV. The new retrieval method PROBP or the competing method (called VTGPA) all converge very slowly, taking tens of thousands of iterations, and there is no way to know if the results are indeed converged to the correct answer. We thus set to finding new retrieval method for calibrating ultra-broadband pulses.

Attosecond pulses are shortest when the pulse is nearly transform-limited. The 53as and 43 as pulses reported in the experiments are all very close to be transform-limited. To “prove” that the retrieved result is correct, the retrieved pulse is often used to generate the streaking spectra to compare with the observed spectra. The agreement is mostly un-convincing. The retrieved pulse is also near the transform-limited. It is difficult to believe that the pulse has no chirp over such a broad spectral range when it is well-known that harmonics generated in strong fields always produce pulses that have chirps, especially the chirp has not been compensated

For broadband pulses, we have found that the streaking spectra are very insensitive to the spectral phase of the IAP. We have found that the autocorrelation of the streaking spectra reveals much more sensitive dependence on the spectral phase. The latter is a plot of S (τ_1, τ_2) where τ is the time delay between the two pulses. If the IAP is nearly transform-limited, S is very close to rectangular shape within each optical cycle of the Mid-IR. If the spectral phase of the IAP has larger chirps, then S is skewed and deviates from a square.

Ongoing projects and future plan

We have extensively examined the autocorrelation S for many different IAPs theoretically. We have been able to show that the shape is rather insensitive to the intensity of the laser and the photoionization transition dipole matrix element. The contrast of S becomes weaker as the IR intensity is decreased. Thus it disfavors the PROOF method for phase retrieval in general since it requires the IR intensity be small. Furthermore, we have also tested that it is easier to find the spectral phase by fitting the auto-correlation S than fitting the streaking spectra. For pulses with small chirps we have found that convergence can be achieved within a few hundred iterations, which compares very favorably to the tens of thousands generations used in previous methods.

We have tested our new method for phase retrieval successfully for attosecond pulses that have spectral width of about 100 eV. For broadband pulses of spectral width close to 250 eV, we can retrieve accurately the spectral phase easily for linear-chirp pulses, but challenges remain for those pulses that have large chirp (or large variation of spectral phase). In fact, we have found examples of pulses that have very different temporal characters but nearly identical spectral characters generate nearly identical streaking spectra and auto-correlation pattern. For more complex pulses with large chirp, in fact, one may not be able to find a unique solution. We will be continuing this project in the coming year to fine tune the method and then use it to test experimental data if we can get the data from experimental groups.

2. Selective highlights in Strong field physics

Recent Progress and future plan

We continue to carry out strong field rescattering physics studies in the last year. Only two notable projects are mentioned here.

(A) Unexpected deep minimum in the harmonic spectra generated using mid-infrared laser pulses in CO_2

In 2011, deep minima in the harmonic spectra in CO_2 were reported by Vozzi et al [Nature Physics 7, 822 (2011)] at 60 eV using mid-IR lasers with wavelength from 1.4 to 1.7 microns. The deep minimum was two to three orders in comparison to the typical one order minima observed in most harmonic spectra. The position of the minimum was found to be independent of the wavelength and laser intensity. Such deep minima have never been observed in any other HHG experiments. Minima in the HHG spectra have been known for a long time. When the photoionization transition dipole has a minimum (often called Cooper minimum) from a given molecular orbital, the minimum would occur also in the HHG spectra. Such minima would not change with the laser intensity nor on the wavelength of the laser. The other type of minimum would occur if more than one molecular orbital contributing to the HHG spectra. Interference of the transition dipoles from them would also produce a minimum but the position of such a minimum would change with laser intensity and wavelength. The deep minimum in CO_2 at 60 eV observed by Vozzi et al is not the standard Cooper minimum since it is too deep. In our recent analysis, we found that the minimum appears only when CO_2 are weakly aligned, for $\langle\cos^2\theta\rangle$ about 0.4. We have since confirmed that the minimum would fade out if the degree of alignment is deviating from this value. Thus, the deep minimum is a macroscopic effect, due to the destructive interference of harmonic emissions from the ensemble of rotationally distributed CO_2.

We have further identified that such deep minimum can also be observed if one varies the angle between the alignment pulse and the harmonics generating pulse for each alignment distribution with <$\cos^2 \theta$> near 0.4. This unique deep minimum feature in the harmonic spectra means that the resulting attosecond pulse trains are made of a series of bursts at every half optical cycle, but each burst is split into two, with temporal separation of about a few tens of attoseconds. The generation of such pulse trains and their possible applications will be further examined.

(B). Unconventional phase matching for enhancing harmonic generation at high laser intensities

In applications it is desirable to have harmonics at higher fluxes and higher photon energies. Experiments on HHG have progressed far in the last two decades, but the harmonics available today for applications are still constrained by both factors. Waveform synthesis may increase the efficiency of harmonics generated by each atom, but limitations of phase matching is a key factor. By increasing laser intensity and/or gas pressure, phase mis-match comes into play such that harmonics cannot be built up and the emergence of copious free electrons would reduce the intensity of the incident laser pulse. In a joint theory and experiment effort, we have found that a new phase matching window opens at high laser intensity. The new mechanism is called defocusing-assisted phase matching (DAPM). In DAPM, the high-intensity laser at the beginning generates much higher harmonics to achieve higher harmonic cutoff and higher yields. The DAPM then kicks in later to coherently adding up the harmonics, thus achieving higher cutoff harmonics and higher yields. The new phase matching is accomplished by compensating the defocusing of the beam by the free electrons with the rapidly decreasing atomic dipole phase as the laser intensity is decreased. Experimentally, using 800 nm lasers and Ar target, it has been experimentally demonstrated that the cutoff can be extended from the typically 50 eV to 75 eV [A8]. To reach such conditions, the length of the gas cell, the gas pressure and the incident laser intensity have to be properly adjusted. Extensive simulations have been shown to explain how phase matching is achieved. Simulations have shown that the method can be extended to longer wavelengths lasers such as 1500 nm. Experimental verification is underway in our collaborator's laboratory.

3. Notable events in the last grant period

A. Publication of a textbook entitled " *Attosecond and Strong Field Physics- Principle and Applications*" by C. D. Lin, Anh Thu Le, Cheng Jin and Hui Wei, **Cambridge University Press**, June 2018.

B. Publication of a book chapter " *Elements of structure retrieval in ultrafast electron and laser-induced electron diffraction from aligned polyatomic molecules*", by Anh Thu Le, Martin Centurion and C. D. Lin, in the book "*Attosecond Molecular Dynamics*", edited by Marc Vrakking and Franck Lepine, by **Royal Society of Chemistry**, September, 2018**.**

4. Published Papers (2017- 2018)

A1. Anh Thu Le, Martin Centurion and C. D. Lin, "Elements of structure retrieval in ultrafast electron and laser-induced electron diffraction from aligned polyatomic molecules", Book Chapter in Attosecond molecular dynamics, edited by Franck Lepine and Marc Vrakking. **Royal Society of Chemistry.**

A2. Tobias Kroh, et al., "Enhanced high-harmonic generation up to the soft X-ray region driven by mid-infrared pulses mixed with their third harmonic", **Optics Express** 26, 16955 (2018)

A3. Shicheng Jiang, Jigen Chen, Hui Wei, Chao Yu, Ruifeng Lu and C. D. Lin " The role of transition dipole amplitude and phase on the generation of odd and even high-order harmonics in crystals", **Phys. Rev. Lett.** 120, 253201 (2018).

A4. Cheng Jin and C. D. Lin, "Control of soft X-ray high harmonic spectrum by using two-color laser pulses", **Photonic Research** 6, 000434 (2018).

A5. C D Lin, Anh-Thu Le, Cheng Jin and Hui Wei, "Elements of the quantitative rescattering Theory", **J. Phys. B51**, 104001 (2018).

A6. Shan Xue, Hongchuan Du, Bitao Hu, C. D. Lin, and Anh-Thu Le, " Following coherent multichannel nuclear wave packets in pump-probe studies of O_2 with ultrashort laser pulses, " **Phys. Rev.** A97, 043409 (2018)

A7. Zhangjin Chen, X. Li, O. Zatsarinny, K. Bartschat, "Ratios of double to single ionization of He and Ne by strong 400-nm laser pulses using the quantitative rescattering theory", **Phys. Rev**. A97, 013425 (2018).

A8. Hung-Wei Sun, Pei-Chi Huang, Yi-Hsuan Tzeng, Jen-Ting Huang, C. D. Lin, Cheng Jin, and Ming-Chang Chen, "Extended phase matching of high harmonic generation by plasma-induced defocusing", **Optica**, 8, 976 (2017).

A9. Xu Wang, Anh-Thu Le, Zhaoyan Zhou, Hui Wei and C D Lin, "Theory of retrieving orientation-resolved molecular information using time-domain rotational coherence spectroscopy", **Phys. Rev**. A96, 023424 (2017).

A10. Cheng Jin, Kyung-Han Hong and C D Lin, "Macroscopic scaling of high-order harmonics generated by two-color optimized waveforms in a hollow waveguide", **Phys. Rev**. A96, 013422 (2017).

A11. Zhaoyan Zhou, Xu Wang, Zhangjin Chen and C. D. Lin, "Retrieval of parameters of few-cycle laser pulses from high-energy photoelectron spectra of atoms by a genetic algorithm", **Phys. Rev**. A95, 063411 (2017).

A12. Xi Zhao, Hui Wei, Yan Wu, and C.D. Lin, "A new phase retrieval algorithm for characterization of broadband single attosecond pulses," **Phys. Rev**. A95 , 043407 (2017).

A13. Zhaoyan Zhou, Xu Wang, and C. D. Lin, "Analysis of THz generation through the asymmetry of photoelectron angular distribution', **Phys. Rev**. A 95, 033418 (2017).

A14. Van-Hung Hoang, Van-Hoang Le, C. D. Lin, and Anh-Thu Le, "Retrieval of target structure from laser-induced photoelectrons by few-cycle bicircular laser fields, **Phys. Rev**. A95, 031402(R) (2017).

A15. Van-Hung Hoang, Song-Feng Zhao, Van-Hoang Le, and Anh-Thu Le, " Influence of permanent dipole and dynamic core-electron polarization on tunneling ionization of polar molecules", **Phys. Rev**. A95, 023407 (2017)

[Additional 15 publications from 2016 are not listed here.]

Imaging Ultrafast Electronic and Nuclear Dynamics in Polyatomic Molecules

Daniel Rolles
J.R. Macdonald Laboratory, Physics Department, Kansas State University,
Manhattan, KS 66506, rolles@phys.ksu.edu

Program Scope: *This program focuses on imaging nuclear and electronic dynamics during photochemical reactions by means of femtosecond pump-probe experiments with laboratory-based laser sources and free-electron lasers, complemented by experiments with 3rd generation synchrotrons. The aim of these experiments is to study exemplary reactions in gas-phase molecules with the goal of clarifying their reaction mechanisms and pathways.*

Recent Progress: As in previous years, my research primarily consisted of projects that linked experiments with our laboratory laser sources at the J.R. Macdonald Lab (JRML) with larger-scale efforts at the free-electron lasers FLASH and LCLS and the ALS synchrotron radiation facility. For example, we studied the dissociation dynamics of various halogenated hydrocarbons upon photoexcitation in the ultraviolet (UV) as well as intramolecular charge transfer in dissociating molecules via pump-probe experiments at JRML and at FLASH [*Amini2017, Savelyev2017, Fisher2018, Amini2018, Brausse2018, Allum2018*]. We also investigated multiphoton ionization of atoms and molecules from the long-wave infrared to the X-ray regime [*Rudenko2017, Rudek2018, Wilson2018*]. Furthermore, based on our COLTRIMS coincidence expertise at JRML and experiments we had previous performed at the ALS, we contributed significantly to an in-house beamtime at LCLS in January 2018, where we demonstrated the feasibility of electron-ion-ion coincidence experiments with FELs as a strategic milestone for similar experiments planned for LCLS-II.

(i) Dissociation and intramolecular charge transfer probed by femtosecond pump-probe experiments, *F. Ziaee, K. Borne, B. Kaderiya, S. Pathak, Kanaka Raju P., I. Ben-Itzhak, A. Rudenko, D. Rolles, R. Boll*[1]*, B. Erk*[1]*, J. Küpper*[1]*, K. Amini*[2]*, F. Allum*[2]*, M. Burt*[2]*, M. Brouard*[2]*, A. Rouzee*[3]*, T. Marchenko*[4]*, M. Simon*[4]*, H. Stapelfeldt*[5]*, N. Berrah*[6]*, A. Nomerotski*[7] *et al.;* [1]*DESY, Hamburg, Germany;* [2]*Oxford University, UK;* [3]*Max-Born-Institut, Berlin, Germany;* [4]*UPMC/CNRS, Paris, France;* [5]*Arhus University, Denmark;* [6]*University of Connecticut;*[7]*Brookhaven National Lab.*

In several experimental campaigns at the FLASH free-electron laser, we generalized our work on ultrafast intramolecular charge transfer, which we initially performed at LCLS with a near-infrared pump pulse to dissociate CH_3I molecules and with a soft X-ray probe pulse that predominantly ionized the iodine 3d level, to a number of other molecules and other pump and probe wavelengths [*Savelyev2017, Fisher2018, Amini2018, Brausse2018*]. Our results demonstrate that charge transfer is ubiquitous in dissociating molecules, and that it can be probed using ionization of both deep inner-shells in the soft X-ray regime as well as of the most shallow inner-shell levels in the XUV. In all of these cases, we confirmed that within the temporal resolution of the experiments, the charge transfer process is well-described by the over-the-barrier model that we employed in our original publication [*Erk2014*].

In parallel to the FEL experiment, we used the same experimental setup at FLASH [*Erk2018*] to perform UV-NIR pump-probe experiments studying the UV-induced photodissociation of CH_3I, CH_2IBr, and CH_2ICl [*Burt2017, Allum2018*]. These experiments as well as the above-mentioned FEL experiments employed novel time-stamping cameras developed by our collaborators at Oxford University (PImMS; Mark Brouard group) and Brookhaven National Lab (TimepixCam; Andrei Nomerotski group), which allow simultaneous velocity map imaging of all ionic fragments with different mass-to-charge ratio, thereby significantly reducing the measurement times and also allowing for covariance analysis, e.g., to extract angular correlations between fragments.

Complementing our studies at FLASH, which were done in a non-coincident mode (due to the low FEL and laser repetition rate of 10 Hz) and with rather long UV pulse durations (>100 fs), we continued to develop a new setup at JRML for UV-NIR pump-probe experiments, which combines sub-50-fs UV pulses and sub-25-fs NIR pulses generated by our 10 kHz PULSAR laser system with our COLTRIMS coincidence momentum imaging capabilities (see Fig. 1). In the last year, we have performed several experiments with this setup, which are currently under analysis.

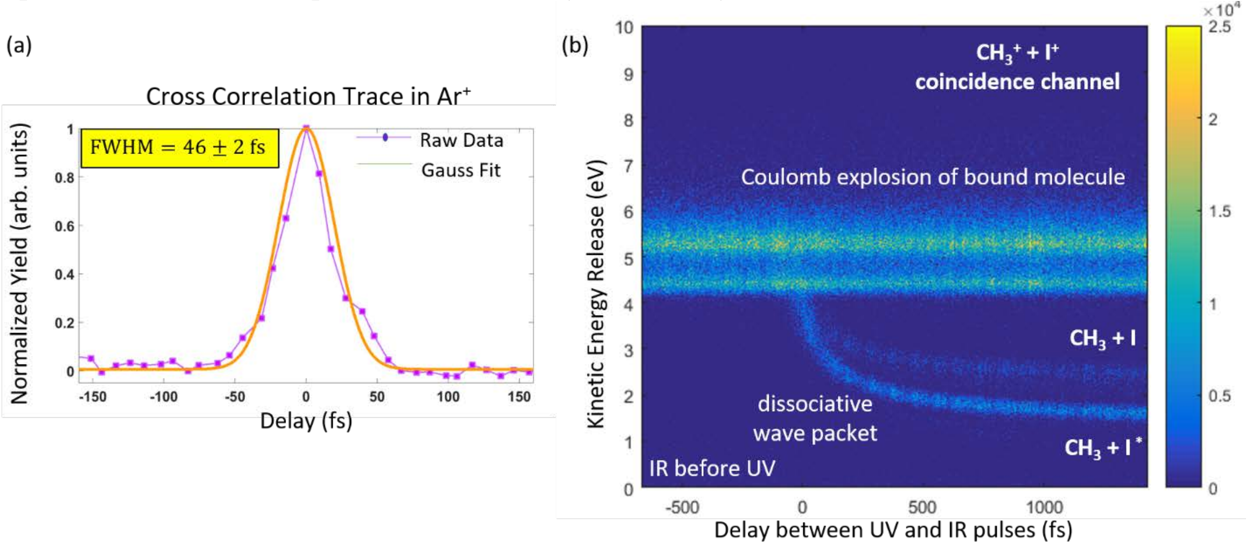

Figure 1: *(a) Cross correlation between the UV and NIR pulses in our new pump-probe setup at JRML measured in COLTRIMS. (b) Preliminary experimental data for the kinetic energy release of the* $CH_3^+ + I^+$ *coincidence channel measured after NIR-induced Coulomb explosion of dissociating* CH_3I*.*

(ii) Multiphoton ionization of atoms and molecules from the long-wave infrared to the X-ray regime, *A. Summers, D. Wilson, S.J. Robatjazi, X. Li, A. Rudenko, and D. Rolles, B. Rudek*[1]*, R. Boll*[1]*, B. Erk*[1]*, K. Toyota*[1]*, S.-K. Son*[1]*, R. Santra*[1]*, L. Young*[2]*, S. Southworth*[2]*, S. Boutet*[3]*, C. Trallero*[4] *et al.;* [1]*DESY, Hamburg, Germany;* [2]*Argonne National Lab;* [3]*SLAC;* [4]*University of Connecticut.*

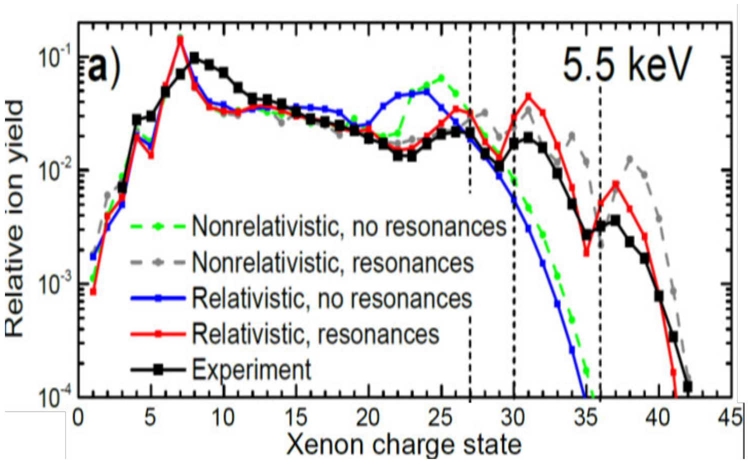

Figure 2: *Multiphoton ionization of Xe atoms by ultra-intense (2x10*^{19} *W/cm*^{2}*), 30-fs hard X-ray pulses at 5.5 keV photon energy. The experimental charge state distributions (black) are compared to calculations carried out with and without consideration of relativistic effects and resonances, which are marked by the dashed lines [Rudek2018].*

We have extended our work on the hard X-ray multiphoton ionization of molecules at ultra-high intensities [*Rudenko2017*], which we reported last year, to atomic ionization of high-Z elements such as xenon under similar conditions. In close collaboration with the theory group of Robin Santra at DESY, we showed that the interplay of relativistic and resonant effects leads to prominent structures in the experimentally observed charge state distributions (see Fig. 2), which reflect resonant positions of relativistically shifted electronic levels of highly charged ions created during the X-ray pulse [*Rudek2018*]. Our results further elucidate the interaction of high-intensity X-rays with matter and provide, for example, a basis for accurate modeling of radiation damage in hard X-ray imaging experiments on targets with high-Z constituents. At the opposite end of the spectrum, we have used a new source for intense, few-cycle pulses in the long-wave infrared (5 – 8 µm), which we have developed at JRML in collaboration with Carlos Trallero from U Conn, to investigate strong-field ionization of atoms in the pure tunneling regime [*Wilson2018*].

(iii) Electron-ion-ion coincidence experiments at LCLS, *X. Li, A. Rudenko, D. Rolles P. Walter*[1], *J.Cryan*[1], *R. Boll*[2], *A. Knie*[3] *et al.;* [1]*SLAC;* [2]*DESY, Hamburg, Germany;* [3]*Uni Kassel, Germany.*

We have participated in an in-house experiment at LCLS in January 2018 (PI Walter) with the goal of exploring the technical requirements for electron-ion-ion coincidence experiments with XFELs. During the experiment, we recorded the photoelectron spectrum of molecular nitrogen upon multiphoton ionization at 500 eV photon energy in coincidence with both fragment ions. By selecting only those events where an electron was detected in coincidence with a specific pair of ions that must stem from multiphoton ionization, we can enhance specific spectral features such as ionic photolines and signatures of double-core holes, which are barely visible in the non-coincident spectra. Our preliminary data thus clearly demonstrates the feasibility of electron-ion-ion coincidence experiments at LCLS, albeit with limited statistics due to the current repetition rate of 120 Hz. Furthermore, it has yielded important information on the experimental conditions needed for such experiments at LCLS-II.

Future Plans: We will use our UV-NIR pump-probe and coincidence capabilities at JRML to study more complex photo-induced isomerization reactions such as ring-opening of cyclic hydrocarbons as well as the internuclear-distance and angle dependence of strong-field ionization in dissociating molecules. We are also planning to extend our strong-field ionization studies in the LWIR to molecules and to investigate, in particular, the role of vibrational resonances on the strong-field ionization process. Due to the shutdown of LCLS for the planned upgrade to LCLS II, our FEL activities for the upcoming year will mainly concentrate on FLASH and, in particular, the European XFEL, where we are currently participating in the commissioning of the end-station for "small quantum systems" (a.k.a. AMO), and have submitted several proposals for the first user beamtime cycle in late 2018 and early 2019.

References:

D. J. Wilson, A. M. Summers, S. Zigo, B. Davis, S.-J. Robatjazi, J. Powell, D. Rolles, A. Rudenko, C. A. Trallero-Herrero, *An intense, few-cycle source in the long-wave infrared*, submitted to Scientific Reports (2018).

Peer-Reviewed Publications Resulting from this Project in the Last Three Years (2016-2018):

1. F. Allum, …, A. Rudenko, …, F. Ziaee, M. Brouard, T. Marchenko, D. Rolles, *Coulomb explosion imaging of CH_3I and CH_2ClI photodissociation dynamics*, J. Chem. Phys., in press (2018).
2. B. Rudek, …, R. Santra, A. Rudenko, S.-K. Son, and D. Rolles, *Relativistic and resonant effects in the ionization of heavy atoms by ultra-intense hard X-rays*, Nature Communications, in press (2018).
3. R. Forbes, ..., D. Rolles, ..., J. G. Underwood, D.M.P. Holland, *Photoionization of the iodine 3d, 4s, and 4p orbitals in methyl iodide*, J. Chem. Phys., in press (2018).
4. R. Forbes, ..., D. Rolles, ..., J. G. Underwood, D.M.P. Holland, *Auger electron angular distributions following excitation or ionization of the I 3d level in methyl iodide*, J. Chem. Phys., J. Chem. Phys. **149**, 094304 (2018).
5. M. Sauppe, …, D. Rolles, ..., T. Möller, D. Rupp, *XUV double-pulses with femtosecond to 650 picoseconds separation from a multilayer mirror based split-and-delay unit at FLASH*, J. Synchr. Rad. **25**, 1517-1528 (2018).
6. B. Erk, …, D. Rolles, *CAMP@FLASH - An End-Station for Imaging, Electron- and Ion-Spectroscopy, and Pump-Probe Experiments at the FLASH Free-Electron Laser*, J. Synchr. Rad. **25**, 1529-1540 (2018).

7. D. Rolles, R. Boll, B. Erk, D. Rompotis, B. Manschwetus, *An Experimental Protocol for Femtosecond NIR/UV-XUV Pump-Probe Experiments with Free-Electron Lasers*, Journal of Visualized Experiments, in press (2018).
8. T. Kierspel, …, D. Rolles, …, J Küpper, *Photophysics of indole upon x-ray absorption*, Phys. Chem. Chem. Phys. **20**, 20205 – 20216 (2018).
9. J. Rajput, T. Severt, B. Berry, B. Jochim, P. Feizollah, B. Kaderiya, M. Zohrabi, U. Ablikim, F. Ziaee, Kanaka Raju P., D. Rolles, A. Rudenko, K.D. Carnes, B.D. Esry, and I. Ben-Itzhak, *Native frames: Disentangling sequential from concerted three-body fragmentation*, Phys. Rev. Lett. **120**, 103001 (2018).
10. T. Osipov, ..., D. Rolles, A. Rudenko, J. D. Bozek, N Berrah, *The LAMP Instrument at the Linac Coherent Light Source Free-Electron Laser*, Rev. Sci. Intr. **89**, 035112 (2018).
11. L. Young, …, A. Rudenko, D. Rolles, …, *Roadmap of Ultrafast X-ray Atomic and Molecular Physics*, J. Phys. B: At. Mol. Opt. Phys. **51**, 032003 (2018).
12. K. Amini, …, A. Rudenko, … D. Rolles, R. Boll, *Photodissociation of Aligned CH_3I and $C_6H_3F_2I$ Molecules probed with Time-Resolved Coulomb Explosion Imaging by Site-Selective Extreme Ultraviolet Ionization*, Struct. Dyn. **5**, 014301 (2018).
13. F. Brauβe, …, A. Rudenko, …, A. Rouzée, D. Rolles, *Time-resolved inner-shell photoelectron spectroscopy: From a bound molecule to an isolated atom*, Phys. Rev. A **97**, 043429 (2018).
14. M. Fisher-Levine, R. Boll, F. Ziaee, …, A. Nomerotski, D. Rolles, *Time-resolved ion imaging at free-electron lasers using TimepixCam*, J. Synchr. Rad. **25**, 336-345 (2018).
15. A. Rudenko, …, D. Rolles, *Femtosecond response of polyatomic molecules to ultra-intense hard X-rays*, Nature **546**, 129-132 (2017).
16. N. Ekanayake, …, D. Rolles, A. Rudenko, I. Ben-Itzhak, …, M. Dantus, *Mechanisms and time-resolved dynamics for trihydrogen cation (H_3^+) formation from organic molecules in strong laser fields*, Scientific Reports **7**, 4703 (2017).
17. U. Ablikim, …, A. Rudenko, N. Berrah, D. Rolles, *Isomer-Dependent Fragmentation Dynamics of Inner-Shell Photoionized Difluoroiodobenzene,* Phys. Chem. Chem. Phys. **19**, 13419 (2017).
18. M. Burt, …, A. Rudenko, F. Ziaee, M. Brouard, D. Rolles, *Coulomb-explosion imaging of concurrent CH_2BrI photodissociation dynamics*, Phys. Rev. A **96**, 043415 (2017).
19. K. Amini, …, A. Rudenko, …, D. Rolles, *Alignment, Orientation, and Coulomb Explosion of Difluoroiodobenzene Studied with the Pixel Imaging Mass Spectrometry (PImMS) Camera*, J. Chem. Phys. **147**, 013933 (2017).
20. E. Savelyev, …, N. Berrah, …, A. Rudenko, D. Rolles, *Jitter-Correction for IR/UV-XUV Pump-Probe Experiments at the FLASH Free-Electron Laser*, New J. Phys. **19**, 043009 (2017).
21. I. Dumitriu, …, D. Rolles, …, N. Berrah, *Inner-Shell Photodetachment from Ni^-: A giant Feshbach resonance*, Phys. Rev. A **96**, 023405 (2017).
22. H. Xiong, … , D. Rolles, N. Berrah, *Soft X-ray induced ionization and fragmentation dynamics of $Sc_3N@C_{80}$ investigated using an ion-ion coincidence momentum imaging technique,* Phys. Phys. A 96, 033408 (2017).
23. U. Ablikim, …, V. Kumarapan, A. Rudenko, N. Berrah, D. Rolles, *Separation of cis and trans geometric isomers by Coulomb Explosion Imaging*, Scientific Reports **6**, 38202 (2016).
24. J. Rothhardt, ..., D. Rolles, *High-repetition-rate and high-photon-flux 70 eV high-harmonic source for coincidence ion imaging of gas-phase molecules*, Optics Express **24**, 18133-18147 (2016).
25. A. Picon, …, A. Rudenko, …, D. Rolles, …, S. H. Southworth, *Hetero-site-specific ultrafast intramolecular dynamics*, Nat. Commun. **7**, 11652 (2016).
26. T. Gorkhover, …, D. Rolles, A. Rudenko, T. Möller, C. Bostedt, *Femtosecond and nanometer visualization of structural dynamics in superheated nanoparticles*, Nature Photon. **10**, 93-97 (2016).
27. R. Boll, …, D. Rolles, A. Rudenko, *Charge transfer in dissociating iodomethane and fluoromethane molecules ionized by intense femtosecond X-ray pulses*, Struct. Dyn. **3**, 043207 (2016).
28. C. S. Lehmann, …, A. Rudenko, …, D. Rolles, …, S. H. Southworth, *Ultrafast x-ray-induced nuclear dynamics in diatomic molecules using femtosecond x-ray-pump – x-ray-probe spectroscopy*, Phys. Rev. A **94**, 013426 (2016).
29. C. F. Jones, …, D. Rolles, A. Rudenko, …, C. Bostedt, O. Gessner, A.F. Vilesov, *Coupled motion of Xe clusters and quantum vortices in He nanodroplets*, Phys. Rev. B **93**, 180510(R) (2016).

Imaging Light-Induced Dynamics of Small Quantum Systems: From Infrared to Hard X-ray Domain

Artem Rudenko

J. R. Macdonald Laboratory, Department of Physics, Kansas State University, Manhattan, KS 66506

rudenko@phys.ksu.edu

Program Scope: The main goals of this research are (i) to understand basic physics of (non-linear) light-matter interactions in a broad span of wavelengths, from terahertz and infrared to XUV and x-ray domains, and (ii) to apply the knowledge gained for real-time imaging of ultrafast photo-induced reactions. These goals are being pursued using both, lab-based laser and high-harmonic sources, and external free-electron laser (FEL) facilities. The program aims at studying light-induced phenomena in systems of increasing complexity, from isolated atoms to small and mid-size molecules. In particular, it focuses at understanding multiple ionization processes in atoms and molecules, multidimensional imaging of light-induced molecular wave packets, structural rearrangement reactions and charge dynamics, and developing new strong-field and X-ray imaging schemes.

Recent Progress:

1. Experiments at XFELs: parameter dependence of X-ray - matter interactions in hard X-ray domain

(in collaboration with D. Rolles, Argonne National Lab group, and theory division at CFEL, Hamburg)

Within the last couple of years, our main efforts in XFEL-based research focused at studying interaction of atoms and molecules with ultra-intense hard X-rays. This regime is crucially important for many XFEL imaging applications that require angstrom wavelengths and extreme intensities (> 10^{20} W/cm^2) to reach atomic resolution. At LCLS. we have recently demonstrated that an isolated atom can be charged to extreme levels (such as Xe^{48+}), and that in molecules with single heavy atom constituent the ionization can be further enhanced, fuelled by the recurrent electron transfer to the multiply ionized heavy atom from its molecular partners [10]. This behaviour is in stark contrast with the earlier results obtained in soft X-ray domain (see [3] and references therein) and for weaker hard X-rays at SACLA [6,7], where the total charge in the molecular system was roughly equal to the charge of an isolated atom with similar absorption cross section. Within the last year, our efforts focused on more quantitative understanding of atomic and molecular response to extremely intense X-ray pulses and, in particular, on its dependence on the key XFEL parameters. For atoms, we have studied the wavelength dependence of X-ray ionization between 5.5 and 8.3 keV. Our combined experimental and theoretical analyses have shown that, depending on the wavelength, the interplay between relativistic and resonant effects must be considered in order to understand the formation of atomic charge state distributions (CSD) [25]. However, for a given fluence these effects become less important above certain photon energy, such that for the conditions of our experiment [10] (8.3 keV, ~2x10^{19} W/cm^2), a quantitative agreement between theory and experiment can be achieved without taking them into account.

Our further effort focused on understanding how molecular ionization and fragmentation dynamics depend on XFEL pulse energy and pulse duration, which are crucial parameters for designing imaging experiments. We have observed that the experimental CSD of iodine ions for CH_3I at 8.3 keV is, as expected, very sensitive to the pulse energy, and shows only rather weak dependence on the X-ray pulse duration. However, as illustrated in Fig. 1, the situation is different if we consider the fragment kinetic energy distributions (KED), which represent a sensitive gauge for the timing of molecular fragmentation. For a given iodine charge state, the KEDs obtained for a fixed pulse duration but at different pulse energies are essentially identical (top raw in Fig. 1), whereas for the fixed pulse energy they sensitively depend on the pulse duration (bottom raw in Fig. 1), with the shortest pulse yielding the most energetic fragments. The later pattern can be qualitatively understood considering that

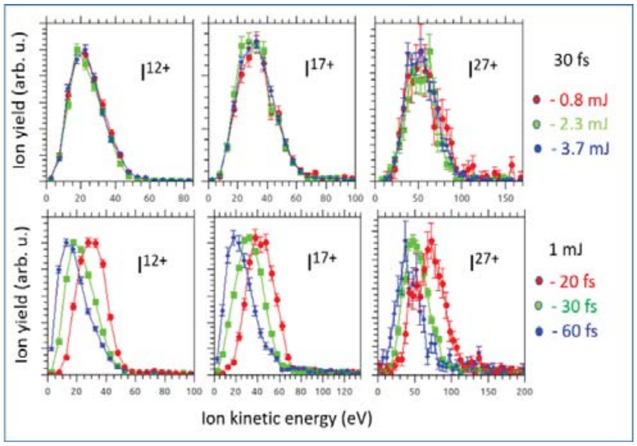

Figure 1. Kinetic energy distribution of iodine ions resulting from CH_3I fragmentation by an 8.3 keV X-ray pulses at LCLS. Top: fixed pulse duration, varying pulse energy. Bottom: fixed pulse energy, varying pulse duration.

within the shorter pulse molecular fragments have less time to propagate away from each other during the pulse, resulting in smaller internuclear separations and, thus, larger Coulomb explosion energies for a given charge state. The independence of the KED on the pulse energy is less intuitive, and indicates that a given charge state is typically produced at the same time after the first X-ray absorption. This originates from a combination of two effects, both related to the depletion of the target for the later steps of the multi-photon absorption sequence. Once a certain charge state is reached during the pulse, at high pulse energy it is likely to be further ionized by absorbing additional photon(s), reaching more than 40 charges at the iodine atom. The events ending up in a lower charge state are thus either produced in the outer region of the X-ray beam focus, or later in the pulse, where further photoabsorption becomes unlikely. These qualitative considerations are in good accord with quantitative predictions by the XMOLECULE code developed by R. Santra's group at CFEL [10].

2. Channel-selective and energy-resolved Fourier analysis of molecular wavepackets in strong-field ionization

(in collaboration with V. Kumarappan, D. Rolles, I. Ben-Itzhak and A.-T. Le)

Understanding strong-field ionization (SFI) mechanisms is an essential step for attosecond pulse generation and provides a basis for imaging molecular dynamics via HHG spectroscopy. During the last year, we have continued our studies to characterize different stages of SFI and fragmentation of molecules in pump-probe experiments, extending them to larger polyatomic systems. Following our recent study on CO_2, where we showed how delay-dependent fragment yields and their Fourier analysis can reveal the structure of strong-field-induced vibrational wavepackets in different electronic states as well as electronic wavepacket motion resulting from the fine-structure splitting [1], we extend the advanced version of this experimental technique to CH_3I, one of the prototypical systems for ultrafast photochemistry. We create a molecular wavepacket by irradiating the molecule with an 800-nm, 25-fs laser pulse, and probe it by ionization (single or double), dissociative ionization (DI), or Coulomb explosion (CE) induced by the delayed, identical pulse. Some illustrative results of this experiment are presented in Fig. 2. The left panels of Fig. 2 show the low-energy part of the delay-dependent KED of I^+ and CH_3^+. These plots contain the fragments resulting from DI in a singly charged final state (i.e., they have an undetected neutral partner). For I^+ fragments, a clear oscillatory structure reflecting molecular vibrations can be observed. For CH_3^+, traces of an oscillatory motion are clearly distinguishable only in the higher energy part of the spectrum (above 0.3 eV). To understand this behavior, we plot the Fourier transforms (FTs) of the I^+ and CH_3^+ yields as a function of their KE in the right panels of Fig. 3.2. In both cases, the Fourier spectrum exhibits a pronounced line centered at 533 cm^{-1} corresponding to the frequency of C-I stretching vibration in the ground electronic state of neutral CH_3I. Analyzing the relative phases of DI fragments and the parent ion, we conclude that off-resonant two photon Raman scattering is a dominant mechanism for vibrational excitation in the neutral molecule.

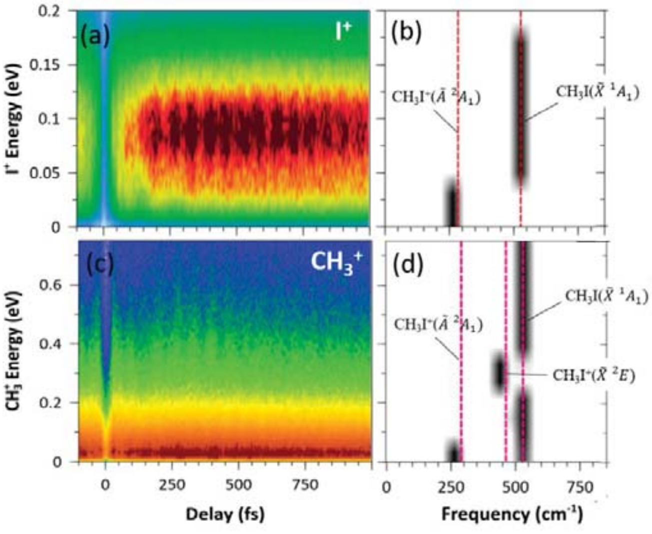

Figure 2. Left panels: Delay-dependent KE distributions of (a) I_+ and (c) CH_3^+. Right panels: KE-resolved FTs of the delay-dependent (b) I^+ and (d) CH_3^+ yields. For each energy bin, the Fourier power spectrum is normalized to its maximum value to reveal the dominant frequency at a given KE.

The FT in the region of the lowest KE for both I^+ and CH_3^+ exhibits a pronounced feature close to the C-I stretching frequency in the first excited state of CH_3I^+ (A), indicating a significant population of this state by the pump pulse. From the A state, the lowest repulsive PESs resulting in I^+ and CH_3^+ are both accessible with a single probe photon, resulting in very low KE of the corresponding fragments. C-I stretching vibrations in the A state also dominate the delay-dependent CE signal observed in this experiment.

At the intensities of the pump and probe pulses used here ($1.7 \cdot 10^{14}$ W/cm^2), we do not observe any signature of vibrational motion in the ground (X) state of CH3I in the I+ or the CE signal. However, it does appear in the FT of the CH3 + yields, dominating the power signal at the KE close to 0.3 eV [Fig. 3.2(d)]. Overall, the relatively weak contribution of the ionic ground state to the observed delay dependence is likely due to the similar geometries of the neutral and ionic ground states.

3. Imaging transient molecular geometries in the light-induced fragmentation of polyatomic systems

(in collaboration with D. Rolles and I. Ben-Itzhak)

Mapping transient molecular configurations and reaction intermediates in light-driven processes is one of the central topics for strong-field physics and ultrafast photochemistry. Time-resolved momentum imaging of molecular fragments provides a powerful experimental tool to address this task. We have continued developing the experimental schemes and data analysis methods needed to make this technique an efficient tool for a broad range of photochemical applications. We illustrate this approach using laser-induced fragmentation of CH_2ICl molecules. The dynamics triggered by the pump pulse (in this case 800 nm, ~$2x10^{14}$ W/cm^2) are probed with a second, more intense 800 nm pulse , resulting in multiple ionization and CE. For this illustration, we select the final state with three singly charged fragments. While there are many possible observables characterizing the three-body breakup, for the present analysis we consider the yield of $CH_2^+ + I^+ + Cl^+$ channel as a function of the KER of all three ions and the angle Θ between the measured momentum vectors of the two halogens (see Fig. 3). This representation constitutes an intuitive way of creating snapshots of a "molecular movie" visualizing the spatio-temporal evolution of a photo-induced reaction. We particularly focus on the scheme allowing one to separate the events corresponding to the transient ICl formation and its subsequent breakup. For this, we sort all the "movie frames" according to the sum energy of the I^+ and Cl^+ fragments. The events containing the intermediate ICl or ICl^+ molecule should yield a significant, non-zero CE energy of these two fragments for any delay. In Fig. 3 the three-particle break-up maps integrated over all pump-probe delays from 0 to 1400 fs are shown for large (a) and small (b) $I^+ + Cl^+$ sum energies, as well as for all events (c). In Fig. 3(a), for high I+ and Cl+ sum KE, a dissociating band propagating towards 180º (i.e., back-to-back emission of I^+ and Cl^+) can be observed, visualizing the molecular halogen formation and elimination. In contrast, in Fig. 3(b), showing events with I^+ and Cl^+ KE below 4 eV, a broad distribution spreading over a large angular range can be observed. These events reflect other dissociation channels (e.g., CH_2I+Cl or CH_2Cl+I, where either fragment can be singly charged). The region where the ICl elimination channel(s) can be clearly identified is labeled 3 in the delay-integrated map containing all events in Fig. 3(c). The region marked 1 reflects the fragmentation of bound CH_2ICl. Interestingly, at all delays the fragmentation maps also contain a significant fraction of events at high KER but at larger angles (region 2 in Fig. 3(c)). Preliminary analysis employing "native frames" approach developed in [18] shows that these events originate from long-lived metastable molecular ions decaying long after both pulses.

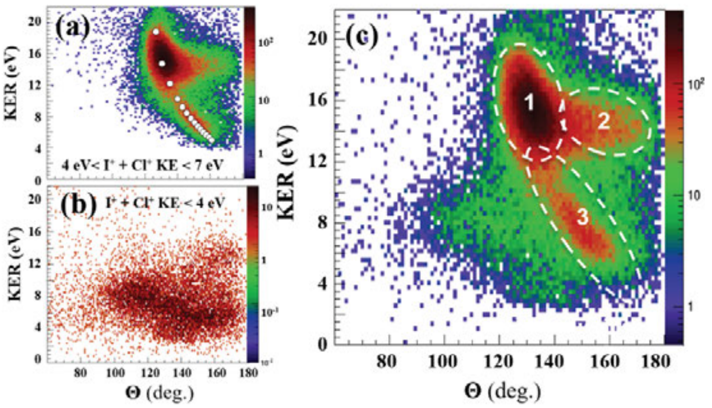

Figure 3. The delay-integrated yields of a three-body fragmentation channel as a function of KER and Θ for events with I^++Cl^+ KE (a) between 4 and 7 eV, (b) below 4 eV, and (c) for all events. White circles in (a) depict the result of the CE simulation of ICl formation.

Future Plans: We plan to continue research activities in all three areas outlined above. The efforts in the experiments using intense, ultrafast X-rays will focus on understanding the response of larger polyatomic systems (like iodobenzene or even larger), on the effect of self-seeded pulses, and on developing schemes for multi-particle ion-electron coincidence schemes for high repetition-rate LCLS-II. The first step in the latter direction was recently made during the in-house LCLS experiment (led by P. Walter), where we succeeded in conducting ion-ion-electron coincidence measurement on two-photon fragmentation of N_2. For studies of molecular wave packets we plan to complement the studies of the SFI-generated wave packets by similar measurements for a single-photon XUV-induced dynamics (using the configuration similar to the one employed in [24]). We will also employ a new electron-ion coincidence momentum imaging setup recently developed at the JRML for studies of dynamics triggered by valence- or inner-shell XUV absorption. Finally, for time-resolved 3D imaging of transient molecular configuration we plan to employ 5 fs pump and probe pulses, which will allow us to visualize the initial bond breaking, bond formation and their relation to different vibrational modes. At the same time, we would perform similar experiments on halomethanes employing ~20-30 fs UV pulse as a pump, which would yield information on several open questions in UV-driven photochemistry in those systems.

Peer-Reviewed Publications Resulting from this Project (2016-2018):

[1] A. Rudenko, V. Makhija, A. Vajdi, Th. Ergler, M. Schuerholz, R. Moshammer, J. Ullrich, V. Kumapparan, *Strong-field-induced wave packet dynamics in carbon dioxide molecule,* Faraday Discussions, **194**, 493 (2016).

[2] T. Gorkhover, …, D. Rolles, A. Rudenko, T. Möller, C. Bostedt, *Femtosecond and nanometre visualization of structural dynamics in superheated nanoparticles,* Nature Photonics **10**, 93 (2016).

[3] R. Boll, …, C. Bostedt, D. Rolles, A. Rudenko, *Charge transfer in dissociating iodomethane and fluoromethane molecules ionized by intense femtosecond X-ray pulses,* Structural Dynamics **3**, 043207 (2016).

[4] A. Picón, C.S. Lehmann, C. Bostedt, A. Rudenko, A. Marinelli, T. Osipov, D. Rolles, N. Berrah, C. Bomme, M. Bucher, G. Doumy, B. Erk, K.R. Ferguson, T. Gorkhover, P.J. Ho, E.P. Kanter, B. Krässig, J. Krzywinski, A.A. Lutman, A.M. March, D. Moonshiram, D. Ray, L. Young, S.T. Pratt, S.H. Southworth, *Hetero-site-specific X-ray pump-probe spectroscopy for femtosecond intramolecular dynamics,* Nature Communications **7**, 11652 (2016).

[5] C.S. Lehmann, A. Picón, C. Bostedt, A. Rudenko, A. Marinelli, D. Moonshiram, T. Osipov, D. Rolles, N. Berrah, C. Bomme, M. Bucher, G. Doumy, B. Erk, K.R. Ferguson, T. Gorkhover, PJ Ho, E.P. Kanter, B. Krässig, J. Krzywinski, A.A. Lutman, A.M. March, D. Ray, L. Young, S.T. Pratt, S.H. Southworth, *Ultrafast x-ray-induced nuclear dynamics in diatomic molecules using femtosecond x-ray-pump–x-ray-probe spectroscopy,* Phys. Rev. A **94**, 013426 (2016).

[6] K. Nagaya, K. Motomura, E. Kukk, …, A. Rudenko, .., K. Ueda, *Ultrafast Dynamics of a Nucleobase Analogue Illuminated by a Short Intense X-ray Free Electron Laser Pulse,* Phys. Rev. X **6**, 021035 (2016).

[7] K. Nagaya, K. Motomura, E. Kukk, …, A. Rudenko, …, K. Ueda, *Femtosecond charge and molecular dynamics of I-containing organic molecules induced by intense X-ray free-electron laser pulses*, Faraday Discussions **194**, 537 (2016).

[8] C. F. Jones, …, D. Rolles, A. Rudenko, …, C. Bostedt, O. Gessner, A.F. Vilesov, *Coupled motion of Xe clusters and quantum vortices in He nanodroplets*, Phys. Rev. B **93**, 180510(R) (2016).

[9] U. Ablikim, C. Bomme, H. Xiong, E. Savelyev, R. Obaid, B. Kaderiya, S. Augustin, K. Schnorr, I. Dumitriu, T. Osipov, R. Bilodeau, D. Kilcoyne, V. Kumarappan, A. Rudenko, N. Berrah, D. Rolles, *Separation of cis and trans geometric isomers by Coulomb Explosion Imaging* Scientific Reports **6**, 38202 (2016).

[10] A. Rudenko, L. Inhester, K. Hanasaki, X. Li, S. J. Robatjazi, …, L. Young, Ch. Bostedt, S.-K. Son, R. Santra and D. Rolles, *Femtosecond response of polyatomic molecules to ultra-intense hard X-rays*, Nature **546**, 129 (2017).

[11] N. Ekanayake, M. Nairat, B. Kaderiya, P. Feizollah, B. Jochim, T. Severt, B. Berry, Kanaka Raju P., K. D. Carnes, S. Pathak, D. Rolles, A. Rudenko, I. Ben-Itzhak, C. A. Mancuso, B. S. Fales, J. E. Jackson, B. G. Levine and M. Dantus, *Mechanisms and time-resolved dynamics for trihydrogen cation (H_3^+) formation from organic molecules in strong laser fields,* Scientific Reports **7**, 4703 (2017).

[12] U. Ablikim, C. Bomme, E. Savelyev, H. Xiong, R. Kushawaha, R. Boll, K. Amini, T. Osipov, D. Kilcoyne, A. Rudenko, N. Berrah and D. Rolles*, Isomer-Dependent Fragmentation Dynamics of Inner-Shell Photoionized Difluoroiodobenzene,* Phys. Chem. Chem. Phys. **19**, 13419 (2017).

[13] K. Amini, R. Boll, A. Lauer, …, A. Rudenko, …, D. Rolles, *Alignment, Orientation, and Coulomb Explosion of Difluoroiodobenzene Studied with the Pixel Imaging Mass Spectrometry (PImMS) Camera* J. Chem. Phys. **147**, 013933 (2017).

[14] E. Savelyev, …, A. Rudenko, D. Rolles, *Jitter-Correction for IR/UV-XUV Pump-Probe Experiments at the FLASH Free-Electron Laser*, New J. Phys. **19**, 043009 (2017).

[15] T. Takanashi, …, A. Rudenko, …,K. Ueda, *Ultrafast coulomb explosion dynamics of the diiodomethane molecule induced by an X-ray free-electron laser pulse, Phys. Chem. Chem. Phys.* **19,** 19707 (2017).

[16]" B. Jochim, R. Erdwien, T. Severt, B. Berry, P. Feizollah, J. Rajput, Y. Malakar, B. Kaderiya, W.L. Pearson, K. Carnes, A. Rudenko and I. Ben-Itzhak, *Three-dimensional momentum imaging of dissociation in flight of metastable molecular ions, New J. Phys*., **19**, 103006 (2017).

[17] M. Burt, …, A. Rudenko, …, D. Rolles,, *Coulomb-explosion imaging of concurrent CH_2BrI photodissociation dynamics*, Phys. Rev. A **96**, 043415 (2017).

[18] J. Rajput, T. Severt, B. Berry, B. Jochim, P. Feizollah, B. Kaderiya, M. Zohrabi, U. Ablikim, F. Ziaee, Kanaka Raju P., D. Rolles, A. Rudenko, K.D. Carnes, B.D. Esry, and I. Ben-Itzhak, *Native frames: Disentangling sequential from concerted three-body fragmentation*, Phys. Rev. Lett. **120**, 103001 (2018).

[19] T. Osipov, Ch. Bostedt, J.-C. Castagna, K.R. Ferguson, M. Bucher, S. Montero, M. Swiggers, R. Obaid, D. Rolles, A. Rudenko, J. D. Bozek, N Berrah, *The LAMP Instrument at the Linac Coherent Light Source Free-Electron Laser*, Rev. Sci. Intr. **89**, 035112 (2018).

[20] L. Young, A. Rudenko, D. Rolles, C. Bostedt, …, S. R. Leone, *Roadmap of Ultrafast X-ray Atomic and Molecular Physics*, J. Phys. B: At. Mol. Opt. Phys. **51**, 032003 (2018).

[21] K. Amini, …, A. Rudenko, …, D. Rolles, and R. Boll, *Photodissociation of Aligned CH_3I and $C_6H_3F_2I$ Molecules probed with Time-Resolved Coulomb Explosion Imaging by Site-Selective Extreme Ultraviolet Ionization*, Struct. Dyn. **5**, 014301 (2018).

[22] F. Brauße, …, A. Rudenko, …, D. Rolles,, *Time-resolved inner-shell photoelectron spectroscopy: From a bound molecule to an isolated atom*, Phys. Rev. A **97**, 043429 (2018).

[23] B. Erk, ..., A. Rudenko, … D. Rolles, *CAMP@FLASH - An End-Station for Imaging, Electron- and Ion-Spectroscopy, and Pump-Probe Experiments at the FLASH Free-Electron Laser*, J. Synchr. Rad., **25**, 1529 (2018).

[24] Y. Malakar, F. Wilhelm, D. Trabert, Kanaka Raju P., X. Li, W. L. Pearson, W. Cao, B. Kaderiya, I. Ben-Itzhak, and A. Rudenko, *State-selective dissociation dynamics of an oxygen molecular ion studied with single-harmonic pump and infrared-probe pulses*, Rhys. Rev. A **98**, 013418 (2018).

[25] B. Rudek, …, R. Santra, A. Rudenko, S.-K. Son, and D.Rolles, *Relativistic and resonant effects in the ionization of heavy atoms by ultra-intense hard X-rays*, Nature Communications, accepted (2018).

[26] F. Allum, …, A. Rudenko, …, F. Ziaee, M. Brouard, T. Marchenko, D. Rolles, *Coulomb explosion imaging of CH_3I and CH_2ClI photodissociation dynamics*, J. Chem. Phys., accepted (2018).

Structure and Dynamics of Atoms, Ions, Molecules and Surfaces

Uwe Thumm
J.R. Macdonald Laboratory, Kansas State University, Manhattan, KS 66506, thumm@phys.ksu.edu

A. Shake-up and double-ionization dynamics of He

Project scope: To examine, with atomic resolution in time, correlation effects, photoexcitation, and photoemission mechanisms during the ionization of atoms and diatomic molecules in intense short XUV pulses.

Recent progress: Solving the TDSE *ab initio* within a fully dimensional finite-element discrete-variable representation scheme [R1-R4] for few-photon double ionization (DI), we calculated XUV DI yields from $1s2s\,^1S$ and $1s2s\,^1P$ excited He atoms. For $1s2s\,^1S$ initial states and 78 eV, 2.12 fs XUV pulses with 5×10^{14} W/cm^2 peak intensity, we revealed two different pathways to single-photon DI by analyzing joint photoelectron energy and angle distributions: **(i)** photoabsorption by the K-shell electron followed by L-shell emission (favoring a 136^O angular difference between the emitted photoelectrons) and **(ii)** photoabsorption by the L-shell electron followed by K-shell emission (occurring predominantly at an angular difference of 65^O (Fig.1) [R3].

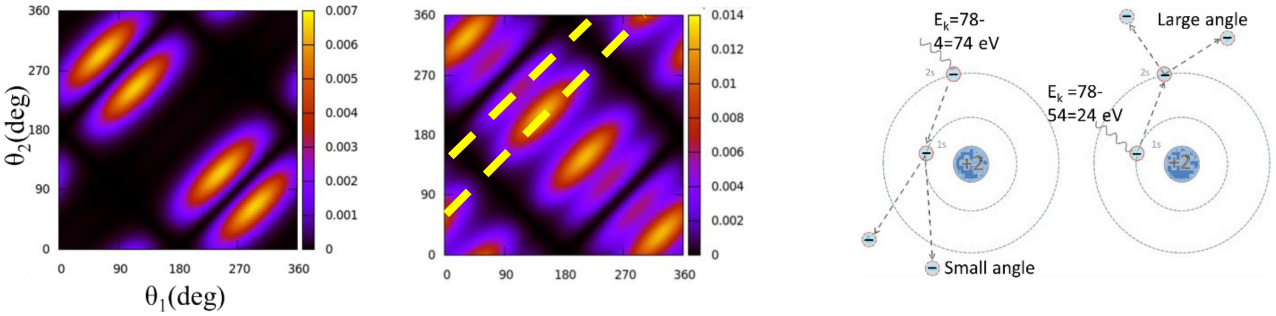

Fig. 1: Joint angular distributions for the DI of He from the ground state (left) and $1s2s\,^1S$ excited state (center) at equal energy sharing and for coplanar emission geometry. For DI from the excited state additional peaks occur at angular differences of 65^O and 136^O due to two distinct double emission mechanisms (right) [R3].

Future plans: We plan to extend these studies to laser-assisted DI with variable delay between ultrashort XUV and IR pulses in order to resolve in time the correlated two-electron dynamics. Specifically, we intend to perform time-resolved two-active-electron calculations [R1] for DI and shake-up ionization of He and of He-isoelectronic atoms and ions for **(i)** streaked [1-3, R5, R6] and **(ii)** interferometric [4-7] photoemission.

B. Time-resolved photoelectron spectroscopy

Project scope: To numerically model and understand streaked and interferometric XUV photoelectron emission and Auger decay in XUV pump – IR probe experiments with **(i)** atoms and molecules, and to **(ii)** quantitatively assess the fidelity at which material properties and the collective electronic dynamics in atoms, molecules, and solids can be imaged in streaked photoemission and RABITT spectra.

Recent progress: We continued to develop and improve quantum-mechanical simulations for streaked and side-banded photoemission from atomically flat surfaces by single attosecond XUV pulses and XUV attosecond pulse trains into the electric field of phase-coherent assisting delayed fs IR pulses [4-7]. In order to reproduce recently measured RABITT (reconstruction of attosecond beating by interference of two-photon transitions) spectra, we found it necessary to **(i)** refine our modeling of the target electronic structure within a tight-binding approach [5], **(ii)** include the Fresnel-reflection of the IR pulse at the surface [4-5, 7], and **(iii)** account for large XUV-pulse-induced secondary-electron and IR-pulse-induced above-threshold-ionization (ATI) background contributions [7].

Example 1: Interferometric photoemission from Cu(111). Based on a quantum-mechanical model for photoelectron emission by an XUV attosecond pulse train from the *d* band of a Cu (111) surface into a delayed assisting IR laser pulse, we calculated two-pathway two-photon interferograms as functions of the photoelectron energy and pulse delay [4, 5]. Comparing our calculated RABITT spectra and phases with experimental data [R7], we find that our localized-orbital initial-state expansion and inclusion of the potential-step at the surface in the final state provide spectra in good agreement with the measurements (Figs. 2a-d). In addition, our model explains the measured temporal broadening of sidebands and the narrowing of high-harmonic peaks in the photoemission spectrum as due to distinct four-IR-photon-interference pathways [5]. We find the Cu(111) RABITT energy profile to be robust with regard to variations of most simulation parameters. We identified the potential-step height U_0 in the calculation of the photoelectron final state as the most critical parameter. Adjustment (within reasonable limits) of U_0 in the final state noticeably improves the agreement with the experiment and emphasizes the sensitivity of the RABITT spectra on the electron-emission dynamics near solid surfaces. An IR-skin-depth increase (decrease) visibly increases (decreases) the sideband yields relative to high-harmonic yields. Mean-free-path effects on the energy profile are moderate. The most favorable comparison with the experimental energy profile we achieved by matching the Sturmian basis-orbital asymptotic decay to the central 3*d*-band binding energy. Our RABITT phases are strongly affected by the inclusion of the Fresnel-reflected IR pulse and are in reasonable agreement with experimental data and classical simulations (Fig. 2e) [5, R7].

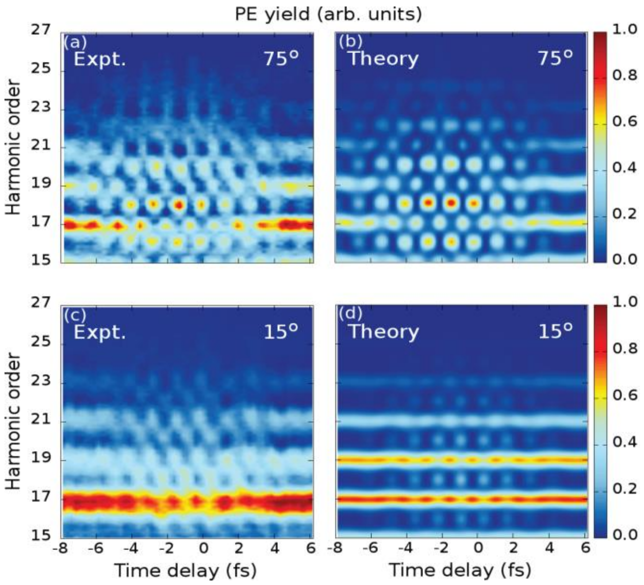

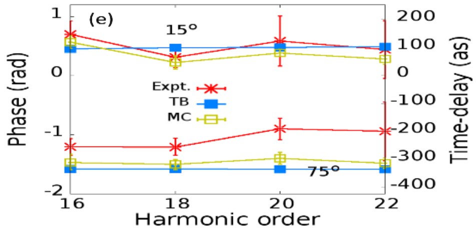

Fig. 2: RABITT interferograms for (a,b) 75^{O} and (c,d) 15^{O} pulse incidence relative to the surface normal, normalized separately. (a,c) Experiment [R7]. (b,d) Theory [5]. Photoelectrons are emitted in the pulse-reflection plane and detected at (a,b) -30^{O} and (c,d) 15^{O} relative to the surface normal. (e) RABITT phases extracted from our calculated spectra in (b) and (d) in comparison with the experimental and classically simulated results (MC) [R7].

Example 2: Time-resolved photoemission from Ag(111) and Au(111). Photoelectron emission from solid surfaces induced by attosecond pulse trains into the electric field of delayed (IR) pulses allows the surface-specific observation of energy-resolved electronic phase accumulations and photoemission delays. We quantum-mechanically modeled interferometric photoemission spectra from the (111) surfaces of Au and Ag [7].

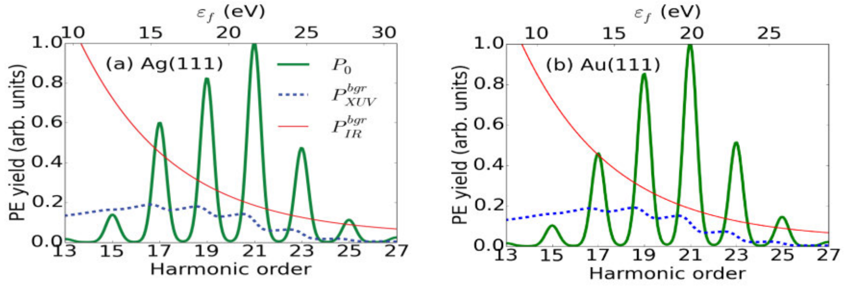

Fig. 3: Normalized background of secondary electrons P^{bgr}_{XUV}, above-threshold electrons P^{bgr}_{IR}, and the interferometric electron yield P_0 without background contributions from (a) Ag(111) and (b) Au(111) surfaces.

We adjusted open parameters of our model to energy-resolved photoelectron spectra recently measured at a synchrotron light source [R8]. We observe dominant contributions to the photoelectron yield from secondary electrons and find smaller background contributions from the Au(111) than from the Ag(111) surface, in qualitative agreement with Au having a larger work function than Ag (Fig.3). Including XUV secondary-electron and IR ATI background contributions, our simulations are in fair agreement with experimental RABITT spectra from Ag(111) and Au(111) surfaces [R9]. We find that all RABITT phases are strongly affected by Fresnel reflection of the IR pulse at the surface (Fig. 4).

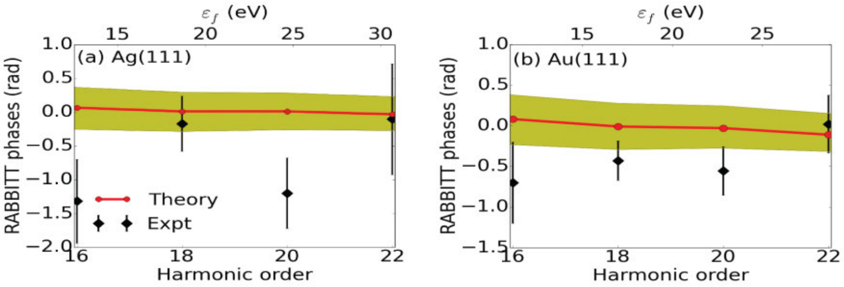

Fig. 4: RABITT phases for (a) Ag(111) and (b) Au(111) surfaces. The experimental phases are adapted from [R9] (black markers with error bars). The yellow bands show phases obtained by varying the onset of the IR electric field from the image plane to two layers inside the solid. Interpolation lines are added to guide the eye.

Example 3: Electric field imaging with atomic spatiotemporal resolution. We developed a model to simulate streaked photoemission from metal nanospheres by sampling over classical photoelectron trajectories [8]. Our calculations comprise a sequence of four steps: (1) XUV excitation, (2) electron transport inside the target, (3) electron escape from the surface, and (4) propagation to the photoelectron detector. Our numerical applications to streaked photoemission spectra from gold nanospheres of 5 and 50 nm radius reveal effects of the **(i)** nanoparticle's dielectric response to the electric field of the streaking laser pulse, **(ii)** relative contributions of photoelectron release from different locations on the surface and inside the nanoparticle, and **(iii)** contributions of photoemission from the Fermi level only versus emission from the entire occupied conduction band [2]. Based on this classical trajectory-sampling model, we suggested a method for reconstructing inhomogeneous time-dependent nanoplasmonic fields with nm spatial and sub-fs temporal resolution from streaked photoemission spectra. Applying this imaging scheme to Au nanospheres, we demonstrated the accurate spatiotemporal reconstruction of the plasmonic near-field distribution in comparison with the directly Mie-theory calculated plasmonic field [S1].

Within an independently developed quantum mechanical model, we calculated streaked photoemission spectra from Au, Ag, and Cu nanoparticles [1, 2] and propose a scheme for the reconstruction of plasmonic fields near isolated nanoparticles from streaked photoelectron spectra [3]. We numerically demonstrated and analyzed the accurate imaging of the IR-streaking-pulse-induced transient plasmonic fields at the surface of gold nanospheres and nanoshells with sub-fs temporal and sub-nm spatial resolution. The numerical reconstruction shows excellent agreement between the electric field distributions predicted within Mie theory and reconstructed from streaked spectra [3].

Future plans: **(i)** The significant differences of the measured [R9] and our calculated [7] Ag(111) RABITT phases for different sideband orders remains to be explained. As our model includes the influence of the surface electronic structure on the *final* photoelectron state in a rudimentary way, assuming a sharp potential-energy decline at the surface and free-electron dispersion, its inability to reproduce the observed phase oscillations may be seen as evidence for relevant final-state photoelectron-surface interactions not included in our simulation. We therefore intend to refine our representation of the photoelectron – final state interaction, including band-structure effects. **(ii)** We intend to combine our efforts described in sections A and B with the goal of addressing shake-up and shake-off ionization of He, He – isoelectronic targets, and H_2 in fully correlated two-electron calculations [R1-R4] of streaked and interferometric photoelectron spectra. **(iii)** We intend to combine our classical trajectory with a quantum-mechanical surface-flux ("virtual detection") approach [R10, R11] for simulating photoelectron momentum distributions, employing the surface-flux scheme at the edge of 3-dimensional numerical grid and classically propagating from there to asymptotic distances. We plan to apply this hybrid approach to the photoemission imaging of chiral light pulses for atomic targets [R12].

Peer-reviewed publications resulting from this project (2016-2018)

[1] *Retrieving plasmonic near-field information: a quantum-mechanical model for streaking photoelectron spectroscopy of gold nanospheres*, J. Li, E. Saydanzad, and U. Thumm, Phys. Rev. A **94**, 051401(R) (2016).

[2] *Attosecond time-resolved streaked photoelectron spectroscopy of transition-metal nanospheres*, J. Li, E. Saydanzad, and U. Thumm, Phys. Rev. A **95**, 043423 (2017).

[3] *Imaging plasmonic fields near Au nanospheres with spatiotemporal* resolution, J. Li, E. Saydanzad, and U. Thumm, Phys. Rev. Lett. **120**, 223903 (2018).

[4] *Comparative time-resolved photoemission from Cu(100) and Cu(111) surfaces*, M. Ambrosio and U. Thumm, Phys. Rev. A **94**, 063424 (2016).

[5] *Electronic structure effects in spatiotemporally resolved photoemission interferograms of copper surfaces*, M. J. Ambrosio and U. Thumm, Phys. Rev. A. **96**, 051403(R) (2017).

[6] *Distinguishing attosecond electron-electron scattering and screening in transition metal*, C. Chen, Z. Tao, A. Carr, P. Matyba, T. Szilvási, S. Emmerich, M. Piecuch, M. Keller, D. Zusin, S. Eich, M Rollinger, W. You, S. Mathias, U. Thumm, M. Mavrikakis, M. Aeschlimann, P. M. Oppeneer, H. Kapteyn, and M. Murnane, Proc. Natl. Acad. Sci. **114**, E5300 (2017).

[7] *Energy-resolved attosecond interferometric photoemission from Ag(111) and Au(111) surfaces*, M. J. Ambrosio and U. Thumm, Phys. Rev. A **97**, 043431 (2018).

[8] *Characterization of nanoplasmonic fields in time-resolved photoemission: a classical trajectory approach applied to gold nanospheres*, E. Saydanzad, J. Li, and U. Thumm, Phys. Rev. A **95**, 053406 (2017).

Submitted manuscripts resulting from this project

[S1] *Spatiotemporal imaging plasmonic fields near metallic nanoparticles beyond the diffraction limit*, E. Saydanzad, J. Li, and U. Thumm, New. J. Phys., submitted.

[S2] *Film-thickness dependent attosecond streaking time delays for photoemission from magnesium surfaces*, Q. Liao, K. Liu, M. Qin, P. Lu, and U. Thumm, Phys. Rev. A, submitted.

References ([R1-R6, R11] acknowledge previous DOE support)

[R1] *A criterion for distinguishing sequential from non-sequential contributions to two-photon double ionization of helium in ultrashort XUV pulses*, A. Liu and U. Thumm, Phys. Rev. Lett. **115**, 183002 (2015).

[R2] *Laser-assisted XUV double ionization of helium: energy-sharing dependence of joint angular distributions*, A. Liu and U. Thumm, Phys. Rev. A **91**, 043416 (2015).

[R3] Correlation dynamics in double photoionization of excited helium atom by a single ultrashort XUV pulse, A. Liu, D. Ding, and U. Thumm, J. Phys.: Conf. Ser. **875**, 022012 (2017).

[R4] *Laser-assisted XUV few-photon double ionization of helium: joint angular distributions*, A. Liu and U. Thumm, Phys. Rev. A **89**, 063423 (2014).

[R5] *Attosecond physics: attosecond streaking spectroscopy of atoms and solids*, U. Thumm, Q. Liao, E. M. Bothschafter, F. Süßmann, M. F. Kling, R. Kienberger, in: *Photonics: scientific foundations, technology and applications*, Vol. **1**: *Fundamentals of photonics and physics*, D. L. Andrew (ed.), Chapter XIII, (Wiley & Sons, New Jersey 2015).

[R6] *Attosecond time-resolved streaked photoemission from Mg-covered W(110) surfaces*, Q. Liao and U. Thumm, Phys. Rev. A **92**, 031401(R) (2015).

[R7] *Light-Matter Interaction at Surfaces in the Spatiotemporal Limit of Macroscopic Models,* M. Lucchini, L.Castiglioni, L. Kasmi, P. Kliuiev, A. Ludwig, M. Greif, J. Osterwalder, M. Hengsberger, L. Gallmann, and U. Keller, Phys. Rev. Lett. **115**, 137401 (2015).

[R8] *Angle resolved Photoemission from Ag and Au single crystals: Final state lifetimes in the attosecond range*, F. Roth, T. Arion, H. Kaser, A. Gottwald, and W. Eberhardt, J. Electron Spectrosc. Relat. Phenom. **224**, 84 (2018).

[R9] *Energy-dependent photoemission from noble metal surfaces by attosecond interferometry,* R. Locher, L. Castiglioni, M. Lucchini, M. Greif, L. Gallmann, J. Osterwalder, M. Hengsberger, and U. Keller, Optica **2**, 405 (2015).

[R10] *On the computation of momentum distributions within wave packet propagation calculations*, B. Feuerstein, U. Thumm, J. Phys. B **36**, 707 (2003).

[R11] *Virtual detector theory for strong-field atomic ionization*, X. Wang , J. Tian, J. H. Eberly, J. Phys. B 51, 084002 (2018).

[R12] Attosecond recorder of the polarization state of Light, Á. Jiménez-Galán, G. Dixit, S. Patchkovskii, O. Smirnova, F. Morales, and M. Ivanov, Nat. Commun., DOI: 10.1038/s41467-018-03167-2 (2018).

Atomic, Molecular and Optical Sciences at the Lawrence Berkeley National Laboratory

C. William McCurdy (PI), Co-Investigators: Oliver Gessner, Robert R. Lucchese, Martin Head-Gordon, Stephen R. Leone, Daniel M. Neumark, Thomas N. Rescigno, Daniel S. Slaughter, Thorsten Weber

Chemical Sciences Division, Lawrence Berkeley National Laboratory, Berkeley, CA 94720
CWMcCurdy@lbl.gov, OGessner@lbl.gov, RLucchese@lbl.gov, MHead-Gordon@lbl.gov, SRLeone@lbl.gov, DMNeumark@lbl.gov, TNRescigno@lbl.gov, DSSlaughter@lbl.gov, TWeber@lbl.gov

Project Scope: The AMOS Program at LBNL seeks to answer fundamental questions in atomic, molecular and chemical sciences that are central to the mission of the DOE Office of Science, Division of Basic Energy Sciences. The essential strategy is to apply a broad span of existing and currently emerging tools such as synchrotron radiation, lasers, laboratory-based extreme ultraviolet sources, and low-energy electron beams together with state-of-the-art experimental techniques including momentum imaging, coincidence techniques, electron and X-ray absorption spectroscopy, scattering, and transient absorption, in combination with the development of advanced theoretical methodologies, to studies across a broad range of time scales and systems. This approach provides new insights into the chemistry and physics of the fundamental interactions that drive key chemical processes in simple molecules, complex molecular systems and molecules in complex environments. The current emphasis of the program is in three major areas with important connections and overlap: time-resolved studies of charge dynamics involving molecules in the gas phase, in the condensed phase and at interfaces using a combination of attosecond to picosecond X-rays and laser pulses; inner-shell photo-ionization and multiple-ionization and dissociation dynamics of small molecules; and low-energy electron impact and dissociative electron attachment of molecules. The theory component of the program focuses on the development of new methods for solving, from first-principles, the equations that govern complex molecular and multi-electron processes that play a key role in these systems. The theory and experimental parts of the program are closely coupled. They are designed to work together to tackle problems of scale that are inaccessible without a strong and continuous collaboration and interaction.

The Atomic, Molecular and Optical Sciences Program at LBNL consists of three subtasks:

1. **Photon and Electron Driven Processes in Atoms and Small Molecules**
2. **Photon and Electron Driven Processes in Complex Molecular Systems and Molecules in Complex Environments**
3. **First-principles Theory of Dynamics and Electronic Structure**

The co-investigators participate in multiple subtasks, collaborating and using common techniques in studies in which experiment and theory are tightly integrated.

Subtask 1: Photon and Electron Driven Processes in Atoms and Small Molecules

S. R. Leone, R. R. Lucchese, C. W. McCurdy, D. M. Neumark, T. N. Rescigno, D. S. Slaughter, Th. Weber

Attosecond Dynamics (Leone, Neumark)

The attosecond dynamics subgroup aims to elucidate ultrashort time processes associated with extreme ultraviolet (XUV) electronically excited states and core level transitions of gas-phase atoms and small molecules. To access excited-state dynamics directly in the time domain, coherences initiated by attosecond XUV pulses produced by high harmonic generation are probed by delayed few-cycle near-infrared (NIR) pulses. Collinear beam geometries result in rich, time-dependent spectra complicated by overlapping spectral effects from multiple NIR-induced processes, precluding quantitative measurements in complex systems. To disentangle these effects, this subgroup works to transpose nonlinear wave-mixing techniques originally developed for optical, infrared, and radiofrequency spectroscopies into the XUV regime. A noncollinear beam geometry between the XUV and NIR pulses capitalizes on the wavevector phase matching inherent to wave-mixing processes to spatially isolate features depending on the nonlinear susceptibility, $\chi^{(n)}$. Examining these signals as a function of XUV-NIR delay has already provided background-free measurements of wavepacket dynamics in long-lived Rydberg states of atomic [Cao et al., *Phys. Rev. A*. **94**, 053846 (2016)] and diatomic [Cao et al., *Phys. Rev. A* **97,** 023401 (2018)] systems. The implementation of a second, independently-delayed noncollinear NIR arm enhances the versatility of the technique, allowing for the characterization of a poorly characterized dark state inaccessible by other techniques [Warrick et al., *Faraday Discuss.* (2018)].

Recent Progress: Initial time-dependent wave-mixing experiments focused primarily on the NIR-induced coupling of long-lived states through ladder-type and, with the addition of the second NIR arm, V(Λ)-type pathways. Time-evolution of the so-obtained emissions show quantum beat oscillations due to interferences between emitted wave-mixing fields. Although analyses of the quantum beat oscillations permit precise study of wavepacket dynamics, they prevent the investigation of individual states composing the wavepacket. Recent work has focused on developing a multidimensional spectroscopy method in the XUV to extract state-specific lifetimes from four wave-mixing emissions.

By combining a noncollinear three-beam geometry (one XUV and two NIR) with a spatial light modulator-based pulse shaper in one of the NIR arms, different components of XUV wave-mixing signals are separated on a new NIR energy axis, forming a 2D spectrum [Marroux et al, *Science Advances*, (2018) submitted]. In Fig. 1-1a, the 2D spectrum of argon's Rydberg states located below the first ionization potential is acquired by delaying one NIR pulse by 200 fs after pulse overlap to probe the time evolution of *np* dark states. The spectrum was formed by modulating the amplitude and phase of a narrow-band portion of the NIR spectrum and plotting the XUV emission spectrum as a function of the central frequency of the narrow band modulation. The spectrum is composed of discrete peaks for which the NIR energy corresponds to the energy difference between the final n*s*/n'*d* state from which the emission occurs and the dark n*p* state. This technique not only provides sub-10 meV frequency resolution, but it also preserves the sub-6 fs time resolution of the 1D experiment. To compare the information given by 1D and 2D experiments, time traces obtained in each experiment are shown in Fig. 1-1b and 1c respectively. The time trace of the 1D measurement has strong oscillations due to quantum beats. The 2D peak time evolution in Fig 1-1c has no quantum beats, as expected, and therefore the time evolution supports the dynamics of a single eigenstate. This is the first implementation of multidimensional spectroscopy in the XUV and its future applications in quickly evolving, large systems will yield useful insights into highly excited state dynamics that so far have been difficult to study with available techniques.

At short timescales, the dynamics of nonlinear signal generation become significant to the accuracy of lifetime measurements. To probe these dynamics, a sub-femtosecond XUV pulse train and two time-coincident NIR pulses interact with a medium of helium gas to produce up to five orders of wave-mixing features from the 1s*np* Rydberg states and NIR-induced dressed states, called light induced states (LISs). The detection method employed for these experiments allows for the time domain characteristics of each of these orders to be measured simultaneously and reveals delays associated with the emergence of higher order signals. At the energy of the long-lived 4p state, delays of 3 ± 1 fs between the first and second orders and 4 ± 1 fs between the first and third orders are observed. For the dressed state features, second and third order diffraction features emerge at 1.5 ± 0.6 fs and 2.4 ± 0.6 fs later than the first order, respectively. Furthermore, the delays result in less pronounced AC Stark shifting of the higher-order transient LIS features. These results are validated theoretically through macroscopic coupled Schrödinger-Maxwell calculations performed by collaborators Mette Gaarde and Ken Schafer at Louisiana State University (LSU) and can be attributed to the accumulation of an AC Stark phase grating over the NIR pulse duration due to the noncollinear beam geometry. As the phase grating accumulates, higher order signals are diffracted more efficiently, delaying the emergence of higher order signals and attenuating the energy shifts observed for higher order LIS features. As nonlinear methods are extended into the attosecond regime, the observed higher-order signal generation times may have considerable implications for the temporal signatures of dynamic processes.

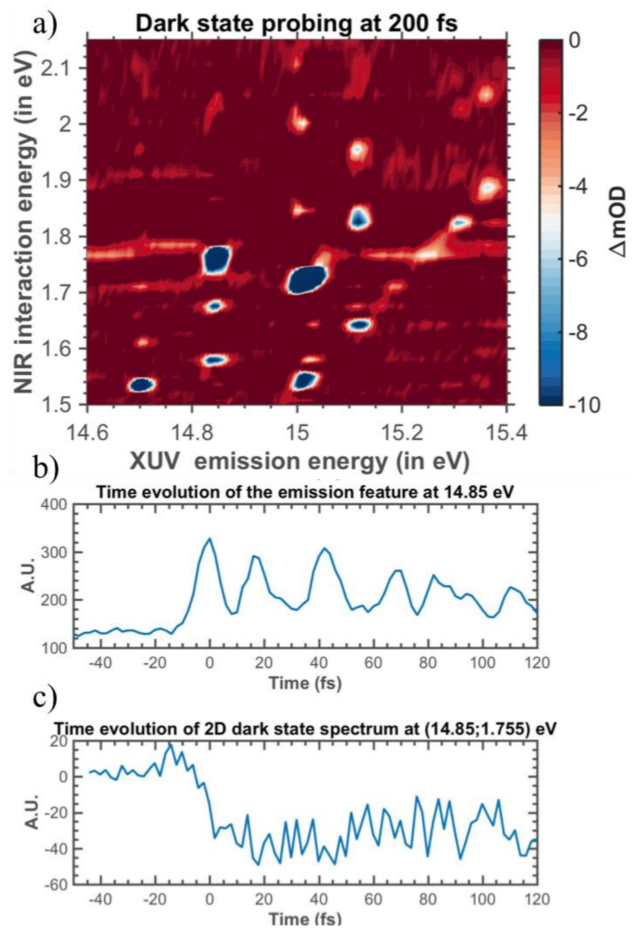

Figure 1-1: Multidimensional spectroscopy in the XUV. (a) The 2D spectrum of argon's long-lived Rydberg states showing the emitted XUV signal as a function of NIR frequency. (b) Quantum beating is observed in the time dependence of the feature at 14.85 eV in the 1D spectrum, indicating contributions from multiple *np* states. (c) The time dependence of the 2D spectrum feature at (14.85 eV; 1.755 eV) shows no beating, and therefore originates from only one *np* state.

Future Plans: These advances provide the foundations necessary for eigenstate dynamics measurements on electronic timescales. Enabled by the recent installation of a commercial stretched fiber, future work will focus on extending these background-free wave-mixing and multidimensional techniques to more complex systems with faster underlying dynamics. Initial target systems include the inner valence excitations of argon, core excited states of methyl iodide, and valence excited states of water vapor. In argon, the 3s3p^{6}np excited states exhibit lifetimes on the order of 20 - 100 fs due to autoionization. However, the time dependence of wave-mixing signals from these states are not expected to be state-specific due to the large number of allowed V-type coupling pathways. This system therefore provides an excellent opportunity to utilize a pulse shaping apparatus to eliminate interfering pathways and recover the ultrafast lifetime of a single target state, demonstrating the specificity of the developed nonlinear techniques on short timescales.

This technique can also be extended to more complex, molecular systems. Preliminary transient absorption measurements on the iodine $6pe \leftarrow 4d_{5/2;3/2}$ core excited states of methyl iodide at ~55 eV yield lifetimes on the order of 5 fs, suggesting a dominant decay mechanism governed by electronic, rather than nuclear, dynamics. To validate this result, the lifetimes of these transitions in the CH_3I molecule can be directly compared to equivalent transitions in the iodine atom. In water, an excited state wavepacket in the $^2B_2$ state located around 16 eV is predicted to relax into the $^2A_2$ via a conical intersection in approximately 7 fs, but the exact energetic location of the crossing and rate of passage are not well known [Reutt et al., *J. Chem. Phys,* **85** (1986)]. Lifetime measurements from quantum beating of different vibrational levels in the $^2B_2$ ion core will identify this conical intersection and provide more information about its dynamics. By effectively employing wave-mixing signals for ultrafast measurements, these experiments represent substantive progress toward the extension of versatile and highly specific nonlinear techniques into the XUV regime with attosecond pulses.

Determination of Interatomic Potentials of Small van der Waals and Covalent Bound Systems by Wave Function Imaging (Weber)

Recent Progress: We used our COLTRIMS technique as a direct method to measure the interatomic potential energy curve of diatomic systems. We were able to measure the squares of the vibrational wave functions of H_2, He_2, Ne_2, and Ar_2 [S. Zeller et al., *Phys. Rev. Lett.*, (2018), accepted]. This was achieved by inverting a fundamental relationship: According to the Schrödinger equation, a given bound state wave function Ψ(R) of a two-particle system determines the full functional dependence of the interaction potential V(R) between the particles. By employing an ionization process which is independent of the internuclear distance of the diatomic system, or which has a well-known dependency, the square of its wave function can hence be imaged. The wave function, along with the binding energy of the system, can subsequently be used for a retrieval of the interaction potential V(R) by inverting the Schrödinger equation. The kinetic energy release (KER) ~ 1/R is measured using the COLTRIMS reaction microscope. By recording a large number of Coulomb explosion events, we obtain the distribution of internuclear distances R. Accordingly, this distribution represents a direct measurement of the square of the vibrational wave function $|\Psi(R)|^2$. The results for the hydrogen molecule are presented in Fig. 1-2 as an example.

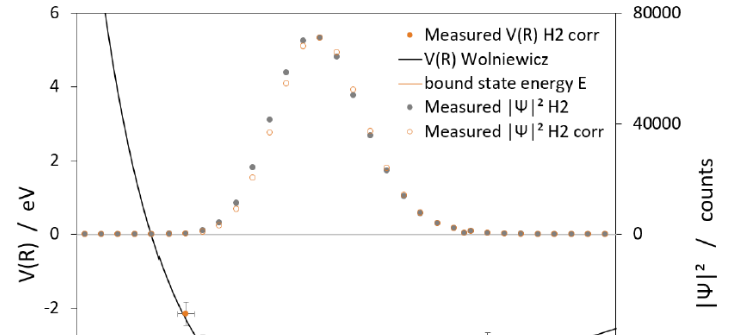

Figure 1-2: Measured potential energy curve of H_2 after single photon double ionization with 160 eV. Experimental data (orange dots) is shown in comparison with a calculation by Wolniewicz et al. (black line). Correcting the measured distance distribution (grey dots) according to the R-dependence of the ionization probability results in the measured square of the wave function $|\Psi|^2$ (open dots).

Our elegant approach does not rely on complex scattering experiments or spectroscopic transitions. While the accuracy of our method is not yet competitive with accuracies attained by established techniques, it allows, in principle, for direct access to the shape of the potential for the full range of internuclear distances R. No theoretical assumptions about the shape of the potential are required. Furthermore, the current approach allows for the most direct determination of the zero-point vibrational energy.

Imaging the Square of the Correlated Two-electron Wave Function of a Molecule (Weber)

Recent Progress: We applied our COLTRIMS imaging scheme at the ALS to directly visualize correlations between electrons by coincident detection of the reaction fragments after high energy photo-fragmentation. We examined the H_2 two-electron wave function in which electron-electron correlation beyond the mean-field level is prominent [M. Waitz et al., *Nat. Commun.* **8:2266**, 1-8 (2017)]. Our approach allows us to visualize the square of the H_2 correlated two-electron wave function by projecting the initial two-electron wave function onto products of different H_2^+ (bound) molecular orbitals (B) and a plane wave (A). In doing so, one can thus determine if and how the density distribution of one electron changes upon changing the region of phase space in which one detects the other, correlated, electron. Experimentally, in the ionization step, one of the electrons is mapped onto a detector, and simultaneously the quantum state of the second electron is determined by coincident detection of the fragments. The angular distribution of electron A depends strongly on the properties of electron B as seen in Fig. 1-3, which shows electron A under the condition that electron B is detected in the $2p\sigma_u$ and $2s\sigma_g$ states of H_2^+. Upon this change in the selection of electron B, the maxima in the angular distribution of electron A become minima and vice versa. This approach can in principle be extended to molecules with more than two electrons. This depends on the shape of the potential energy surfaces, which determines to which extent different ionic states can be separated by the kinetic energy of the fragments. Combined with coincidence detection, this technique opens the door to image correlations in electronic wave functions. In combination with ultrafast two pulse techniques, such correlation imaging offers the promise to make movies of the time evolution of electron correlations in molecules.

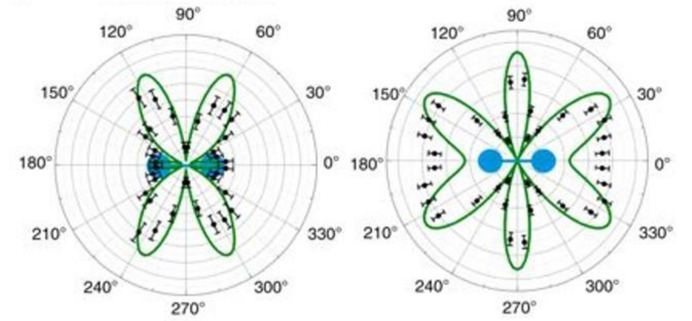

Figure 1-3: Experimental and theoretical MFPADs for electron A (symbols and green line, respectively) obtained after photoionization with photons of an energy of 400 eV for electron B measured in coincidence in the $2p\sigma_u$ (left) and $2s\sigma_g$ (right) states of H_2^+.

Revealing the Role of Electron-Electron Correlations by Mapping the Dissociation of Highly Excited D_2^+ using Ultrashort XUV Pulses (Weber)

Recent Progress: We have used perfectly synchronized ultrashort high-harmonic XUV and IR pulses to respectively ionize the D_2 molecule and map the dissociation dynamics of a highly excited D_2^+ molecular ion [L. Martin et al., *Phys. Rev. A* **97**, 062508 (2018)]. Moreover, we have used synchrotron radiation from the ALS and electron-ion coincidence imaging to perform highly differential single-ionization measurements to reveal electron correlation effects in the molecular frame photoelectron angular distributions MFPADs (not shown here). The time dependent relative KER yield for each molecular orientation in Fig. 1-4 is a consequence of different probabilities for single ionization into the D_2^+ $2s\sigma_g$ and $2p\pi_u$ states. The higher asymptotic value of the KER for the parallel case is the result of the larger population of the D_2^+ $2s\sigma_g$ state, which lies higher in energy than the D_2^+ $2p\pi_u$ state in the Franck Condon region. As advanced theory reveals, none of these features would be observed in the absence of electron-electron correlation. Due to the highly correlated nature of this process, it conveys that the mapping of the rapid XUV-induced dissociation dynamics shows up in the form of a coherent superposition of several electronic states. Ultimately, electron-electron correlation is responsible for changes in the relative population of these states due to changes in the polarization direction of the incoming light, thus leading to a certain degree of control of the D^+ yields under the combined action of the XUV and the IR pulses.

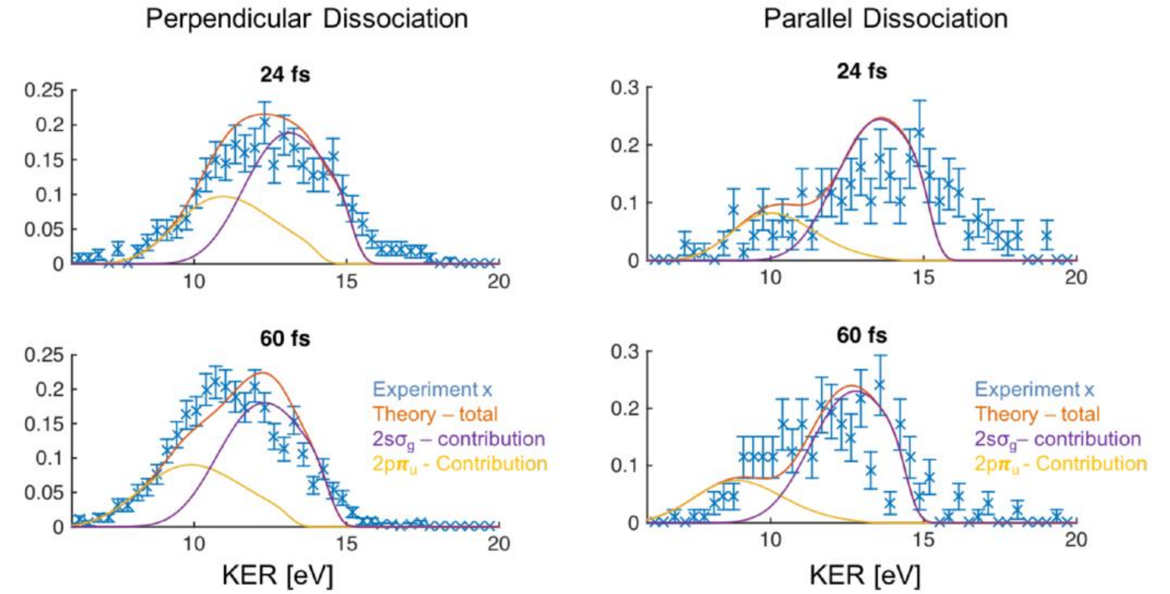

Figure 1-4: (left column) KER of Coulomb-exploding D_2 molecule at 24 fs and 60 fs delays for the perpendicular dissociation. Experimental (with error bars) and theoretical data (full orange line). Violet and yellow lines: truncated models including only a single path, through the $2s\sigma_g$ (violet line) or through the $2p\pi_u$ states (yellow line). The theory shows that the $2s\sigma_g$ contribution is the largest. (right column) Same for the parallel dissociation.

Time-Resolved Molecular Reaction Pathways of Electronically Excited Gases (Slaughter, Weber, Lucchese, McCurdy, Rescigno)

Recent Progress: The dynamics of dissociation and isomerization in excited electronic states of neutral molecules were recently investigated in detail by time-resolved photoelectron and photoion momentum imaging spectroscopy, employing a tabletop extreme ultraviolet (XUV) laser system with spectrally-selectable pump-probe schemes [E.G. Champenois et al., *J. Chem. Phys.* **144**, 014303 (2016); T.W. Wright et al., *Phys. Rev. A* **95**, 023412 (2017), F.P. Sturm et al., *Phys. Rev. A* **95**, 012501 (2016); P. Ranitovic et al., *Phys. Rev. A* **98**, 013410 (2018)].

Future Plans: We are currently extending the capabilities of the high harmonics system to enable high harmonic generation (HHG) from 400 nm pulses to produce 9.3 eV, 15.5 eV, and higher odd harmonics of 400nm. Recent measurements using the 50 Hz HHG beamline show that the photon yield above 15 eV with f200 (6-meter focus) in a Krypton gas cell may be high enough for XUV-XUV and XUV-visible pump-probe photoelectron and photoion coincidence experiments. When compared to a near-infrared driving pulse, the visible fundamental wavelength for HHG brings a unique combination of improved spectral isolation between odd harmonics and higher HHG efficiency in the vacuum ultraviolet. This new system will enable the detailed investigation of excited electronic states in fundamental polyatomic molecules OCS and NH_3, and enable us to explore the hydrogen elimination dynamics driven by VUV photons in small hydrocarbons such as ethane.

Investigation of Electron-Ion Retroaction in the Dissociative Ionization of H_2^+ in the Presence of an IR Laser Field (Weber, Slaughter)

Future Plans: In a recent test experiment we investigated the effect of a low energy electron retroacting back to the dissociating H_2^+ target in the presence of a moderate laser IR field (1062 nm, $3{\cdot}10^{11}$ W/cm^2). While we found no indications for Light Induced Conical Intersections (LICIs) in this XUV+IR scheme (not shown here), we see that the asymmetry in the MFPAD, induced by the transient field of the photoelectron, which was ejected by single photon XUV ionization leaving an H_2^+ ion behind and which was sufficient to preferentially localize the bound electron at one side of the molecular ion [M. Waitz et al., *Phys. Rev. Lett.* **116**, 043001 (2016)], persists for XUV energies above and below the dissociation threshold for overlapped pulses as well as for pulse delays as long as 136 ps (see Fig. 1-5). We will verify this surprising result and hope to quantitatively explain this effect in the near future.

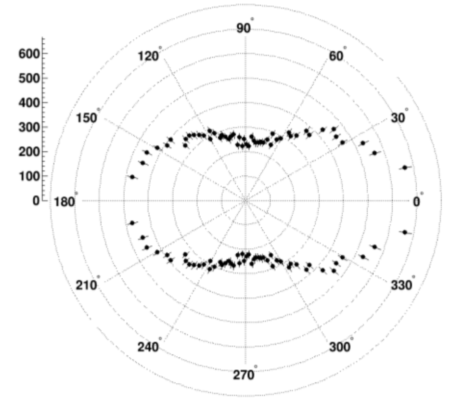

Figure 1-5: MFPADs for XUV (17.9 eV) and IR (1.2 eV) pulses after single photo ionization and dissociation of H_2 for a delay of 136 ps. The proton always goes to the right.

Single Photo Double Ionization of Small Polyatomic Molecules: Reaction Pathways for Hydrogen Elimination in H_2O and NH_3 (Weber, Slaughter, Lucchese, McCurdy, Rescigno)

Recent Progress: We recently conducted initial test experiments on the single photo double ionization (PDI) of H_2O and NH_3 molecules, where we focused on the nuclear dynamics after two and three body breakup. Together with theory [Z.L. Streeter et al., *Phys. Rev. A*, (2018), accepted] we could identify eight active states in the PDI of H_2O, distinguish between prompt and indirect ionization mechanisms, and extract dissociation angles as well as branching ratios [D. Reedy et al., *Phys. Rev. A*, (2018), accepted]. Moreover, we could clearly see failures of the axial recoil approximation. We recently made progress on the investigation of the PDI of NH_3.

PDI of NH_3 results in rich fragmentation dynamics that cannot be measured in detail by the ion fragment detection alone. Similarly, significant challenges are presented for *ab initio* theoretical methods to determine electronic structural changes over multiple dissociation coordinates. Two-electron and two-proton kinetic energy correlation maps were measured at the Advanced Light Source using the COLTRIMS technique, allowing the characterization of the different dynamics in four electronic states, each producing two protons. In these measurements, the neutral fragment(s) (NH or N + H) were not measured, however the center of mass of the NH system is determined from the proton momenta, since the total momentum of the photoionized system is conserved. MCSCF calculations from our theory group (C.W. McCurdy, R.R. Lucchese et al.) of the potential energy surfaces of the ammonia dication reveal several conical intersections that facilitate the complex interaction of these states. Molecular plane proton momentum distributions (see Fig. 1-6) of the $(2a_1^{-1}, 3a_1^{-1})\ {}^1A_1$ and $(1e^{-2})\ {}^3A_2$ states suggest prompt dissociation, with the proton angular distributions exhibiting very small deviations from the equilibrium bond angles of the ground electron state of NH_3. On the other hand, the $(1e^{-2})\ {}^1A_1$ proton momenta appear to dissociate to wider angles, with significant coupling between the proton kinetic energy and its dissociation angle in the molecular frame. The $(1e^{-2})\ {}^1E$ state is dissimilar to the A_1 and A_2 states, in that momentum is shared unequally between the two protons, suggesting a sequential breakup process.

Future Plans: In the past we were able to conduct kinematically complete experiments for diatomic molecules only. With our recent work on the nuclear dynamics of H_2O and NH_3 we are now in the excellent position to break new frontiers, i.e. fully describe the photo induced break-up of a polyatomic molecule for the very first time in order to study electron-electron correlation and simultaneous electron-nuclei interactions. In the next step we hence seek to measure the two emitted electrons in coincidence with the nuclei of the three body breakup of the PDI of H_2O as well as NH_3 and capture the complete break-up dynamics in full dimensionality.

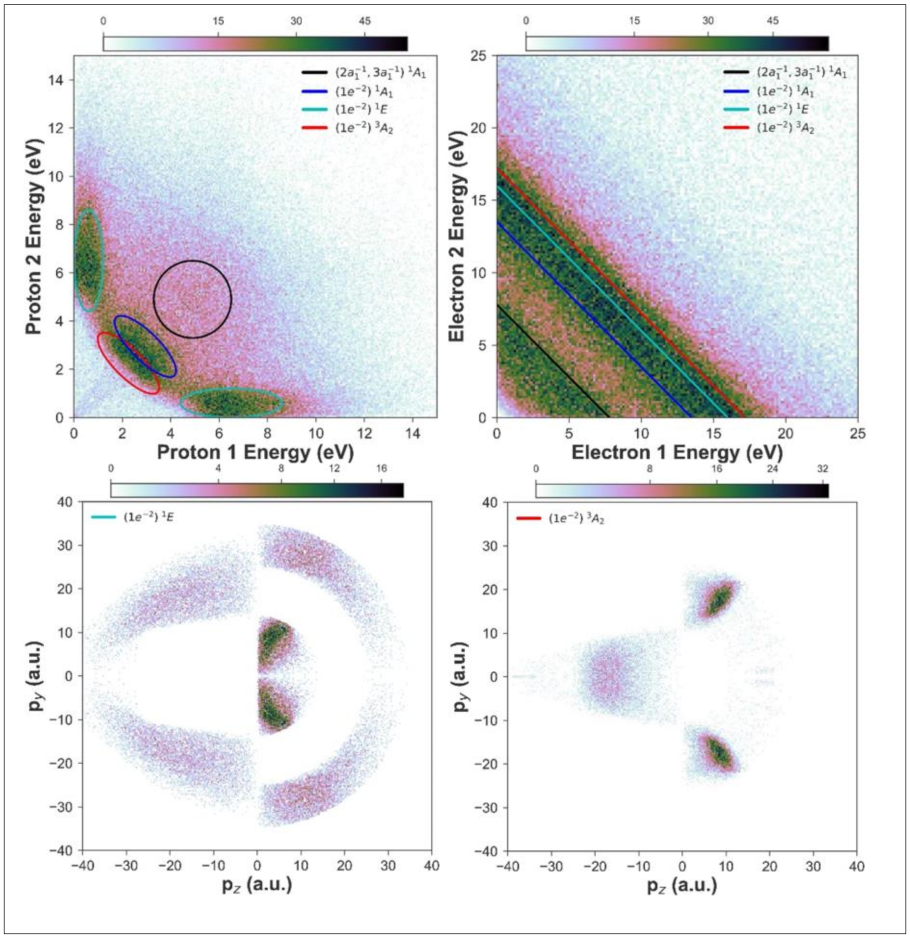

Figure 1-6: (Upper-left) H^+ kinetic energy map for photo double ionization of ammonia by 61.5 eV photons. Each state is identified by its momentum signature and connected event-by-event to the electron-electron kinetic energy map (shown upper-right). Molecular plane momentum distributions for the $1e^{-2}\ ^1E$ state (lower-left) and $1e^{-2}\ ^3A_2$ state (lower-right). The proton momenta are defined as $p_z > 0$, while the inferred N-H momenta are $p_z < 0$. The intensity color scale is the fragment yield in arbitrary units. Contributions from the following electronic states are indicated in the energy maps: $(2a_1^{-1}, 3a_1^{-1})\ ^1A_1$ (black), $(1e^{-2})\ ^1A_1$ (blue), $(1e^{-2})\ ^1E$ (cyan), and $(1e^{-2})\ ^3A_2$ (red).

Subtask 2: Photon and Electron Driven Processes in Complex Molecular Systems and Molecules in Complex Environments

A. Belkacem, O. Gessner, M. Head-Gordon, S. R. Leone, R. R. Lucchese, C. W. McCurdy,
D. M. Neumark, T. N. Rescigno, D. S. Slaughter, Th. Weber

Tracing Inter-Coulombic Decay of Carbon Dioxide and Oxygen Dimers after Valence Photo Ionization (Weber, Slaughter, Lucchese, McCurdy)

Studying Inter-Coulombic Decay (ICD) processes is important for our understanding of fundamental ionization mechanisms in photochemistry and is of multidisciplinary relevance especially in weakly bound matter, e.g. biological systems. This is because the ejected low energy electrons accompanying the ICD process are prone to induce biological damage such as DNA (double) strand breaks. Moreover, the radical cationic fragments can react with surrounding molecules, causing further damage in biological systems via secondary reactions. ICD has been studied in great detail in atomic dimers [Rist et al., *Chem. Phys.* **482**, 185–191, (2017)] and by resonant Auger decay after core excitation of molecular dimers. ICD after direct inner valence ionization of molecular clusters remains, so far, widely unexplored, and we hence set out to trace ICD in the symmetric breakup of CO_2 and O_2 dimers.

It is important to point out that the fragmentation into e.g. the $(CO_2)^+ + (CO_2)^+$ channel after photo double ionization can result not only from a one-site single ionization/excitation process like in ICD, but also from two competing double ionization processes. A two-site double ionization, wherein one electron is removed from each molecule of the dimer, leads to direct Coulomb explosion, while a one-site double ionization populates $(CO_2)^{2+}$ - CO_2 non-dissociative molecular states. The latter transient states relax in a second step through radiative charge transfer, i.e. charge transfer accompanied by radiative emission, or via charge transfer at direct crossings towards the same dissociative states like the two-site double ionization $(CO_2)^+ + (CO_2)^+$ events.

Recent Progress: In this work, the competition between one-site dissociation and two-site fragmentation of carbon dioxide dimers and oxygen dimers has been investigated via single photon double ionization (PDI) of inner valence electrons with the COLTRIMS technique at the Advanced Light Source (ALS). The highly differential triple and quadruple coincidence experiments we performed provide us with powerful observables like KER measurements, electron-ion and electron-electron energy correlation maps, as well as lab frame angular distributions, relative electron-electron emission angles, and Recoil Frame Photoelectron Angular Distributions (RFPADs) to investigate the PDI of small molecular dimers in great detail (see Fig. 2-1). Their generation and interpretation are however very challenging due to statistical shortcomings that stem from the low cluster target density of around 1.5%. Nevertheless, we could narrow down the cluster geometry and ionization mechanisms at play for XUV radiation damage of those fundamental cluster targets [Iskandar et al., *Phys. Rev. A*, (2018), *to be submitted*].

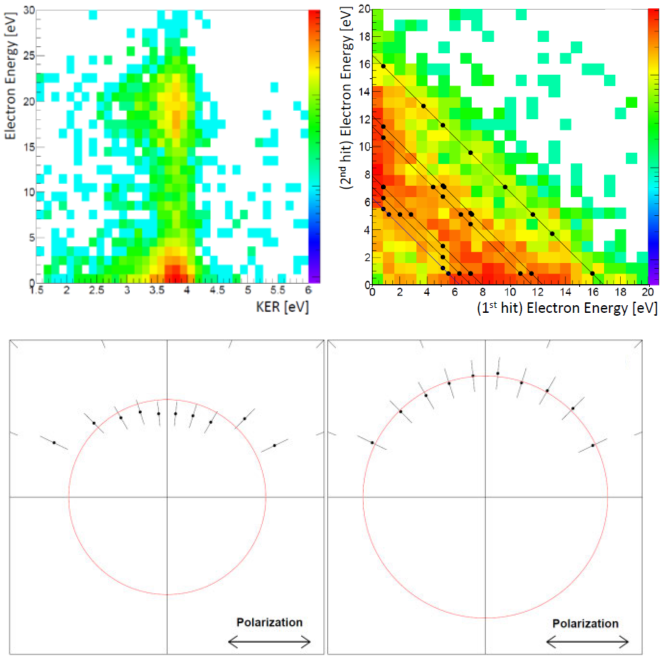

Figure 2-1: Top row: (left) Kinetic energy of the emitted electrons versus the KER of the CO_2 dimer for PDI with a photon energy of 55 eV. (right) Electron energy correlation map of PDI of O_2 dimers showing one electron energy as a function of the energy distribution of the second electron for a photon energy of 46 eV. The estimated energy maps of the emitted electrons for Coulomb explosion and radiative charge transfer (diagonal black lines) and ICD (black dots) processes are overlaid. Bottom row: Angular distribution of the high energy electron (left) and low energy electron (right) with respect to the polarization axis (horizontal) of the PDI of O_2 dimers for a photon energy of 46 eV.

We found that the direct dissociation or auto-ionization of CO_2^{+*} on a single site of a CO_2 dimer is strongly suppressed due to fast relaxation of the dimer via ICD. The symmetric ionic breakup ICD of the small cluster, which involves two sites of the dimer, is almost a thousand times more prominent than the autoionization of one site after XUV absorption. The KER of the dissociating ions enables us to pinpoint the internuclear distance at the time of fragmentation and allows us to deduce the geometry of the dimers as slipped parallel /--/ (60º, 60º, 0º) by comparison with calculated intermolecular distances from the literature. Measuring the kinetic energies of the emitted photoelectrons and the ICD electrons and comparing them to estimates, based on the well-known monomer states, enabled us to coarsely identify the contributing electronic states in the ICD process.

For the investigation of the PDI of the O_2 dimer we applied the same approach. The KER measurements reveal a preferred |--| (90º, 90º, 0º) structure of the cluster target. The electron angular distributions with respect to the polarization axis look very similar to the PDI of CO_2 dimers. In both cases we see a signature of a two-step process, emitting a photo electron preferentially along the polarization direction, and an isotropically emitted low energy ICD electron (Fig. 2-1). However, for the PDI of the O_2 dimer, the electron-electron energy correlation map (Fig. 2-1) and the relative emission angle between the two electrons also showed contributions from knock-out processes (not shown).

Ultrafast Dynamics in Photoexcited Nitrobenzene (Belkacem, Lucchese, McCurdy, Rescigno, Slaughter, Weber)

Recent Progress: We have recently implemented a new ultrafast technique, Ultrafast Transient Polarization Spectroscopy (UTPS), to probe the 3^{rd}-order nonlinear response of excited electronic states in neutral molecules. One goal of this project is to establish a highly sensitive probe of transient systems without a resonant or ionizing probe pulse. In the present implementation, an ultrafast Ti:sapphire laser system provides a 260 nm UV pump pulse to access a low-lying excited electronic state manifold, as well as a moderately strong 780 nm drive pulse and a weaker 780 nm probe pulse to monitor the excited state dynamics by homodyne and heterodyne detection (Fig. 2-2(a)). A chopper modulates the UV beam with a reference pattern for phase-sensitive detection of the excited state signal. The probe beam crosses the drive beam at a small angle inside the sample and the polarization of the drive pulse is tilted by 45° with respect to the probe. After passing through the sample, the spatially separated probe beam encounters a polarizer that is aligned perpendicular to the original probe polarization axis. For heterodyne detection, a quarter-wave plate is placed in the probe beam before the sample (producing an out-of-phase local oscillator), to probe the pump-induced birefringence of the target, or a polarizer is allowed to leak a small component of the original probe polarization to the detector (producing an in-phase local oscillator) to probe the pump-induced dichroism. The detected signals provide a relative measurement of specific elements of the 3^{rd}-order susceptibility of the excited state.

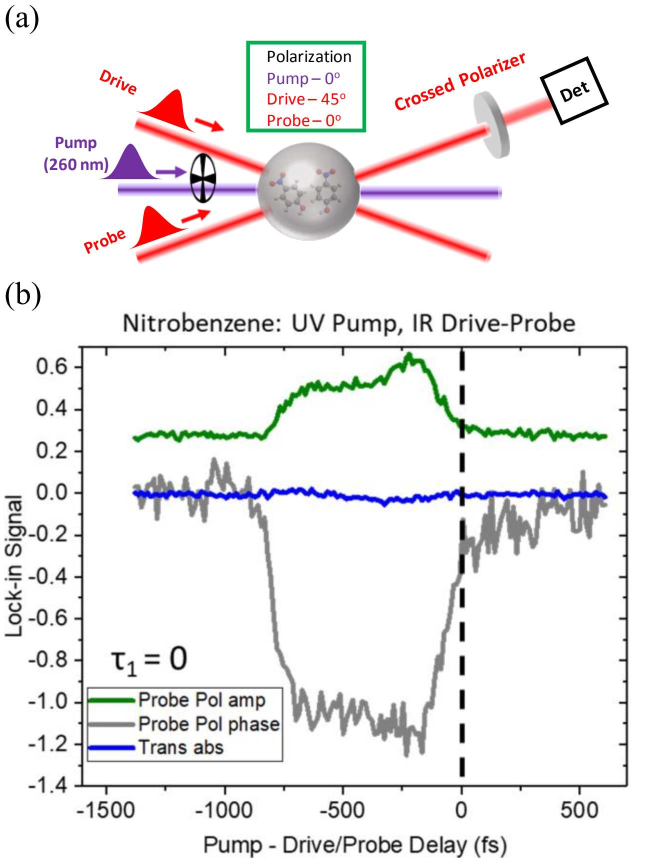

Figure 2-2: (a) Schematic of ultrafast transient polarization spectroscopy experimental geometry. (b) Preliminary results for nitrobenzene, showing the transient polarization signal (amplitude in green and phase in grey), and the much smaller 800 nm transient absorption signal collected in the same experiment. The drive-probe delay is fixed at 0 fs and the pump pulse is early at positive delays. Vertical scale is in arbitrary units.

One major advantage of this approach is that it is virtually background-free, enabling up to 3 orders of magnitude higher sensitivity than the signal intensity changes in transient absorption experiments. Since the optically induced birefringence and dichroism depend on the third-order susceptibility of the excited sample (and therefore the electronic configuration of the excited state), the probe signal modulations can be associated with the instantaneous electronic structure of the excited system. Preliminary results on liquid nitrobenzene exhibit a clear transient signal of the electronic excitation populated by the UV pump pulse, suggesting electronic dynamics following multi-photon NIR and/or UV excitation that recovers within ~1 ps (Fig. 2-2(b)). In this homodyne measurement, a polarization signal, which is the amplitude or phase shift in the polarization component orthogonal to the incident probe polarization, is observed for negative time delays. The time-dependence corresponds to the pump pulse arriving a few to 800 fs after the drive and probe pulses, which are time-overlapped for this measurement. This may be a signature of an intermediate electronic excited state that is excited by two or more photons from the 780 nm drive and probe pulses, interacting with the resonant 260 nm pump pulse.

Future Plans: The sensitivity of UTPS to different excitation schemes and the underlying processes will be investigated using wavelength-tunable pulses derived from an optical parametric amplifier. UTPS is a uniquely sensitive and versatile probe of transient electronic dynamics in molecules and complex molecular systems. The early development of UTPS is performed with tabletop UV and near-IR pulses using liquid samples, to facilitate rapid experimental measurements while exploring the capabilities of the technique. Future efforts will be directed towards detailed investigation of fundamental dynamics in highly-excited molecules using vacuum ultraviolet and extreme ultraviolet pump pulses. UTPS will be further developed to complement our ongoing efforts on photoelectron and photoion momentum imaging spectroscopy [E. G. Champenois et al., *J. Chem. Phys*., **144**, 014303 (2016); T.W. Wright et al., *Phys. Rev. A*, **95**, 023412 (2017); F.P. Sturm et al., *Phys. Rev. A*, **95**, 012501 (2016); P. Ranitovic et al., *Phys. Rev. A* **98**, 013410 (2018)] to access more detailed information on excited state dynamics in relatively complex molecules such as nitrobenzene, and molecules within a chemical environment.

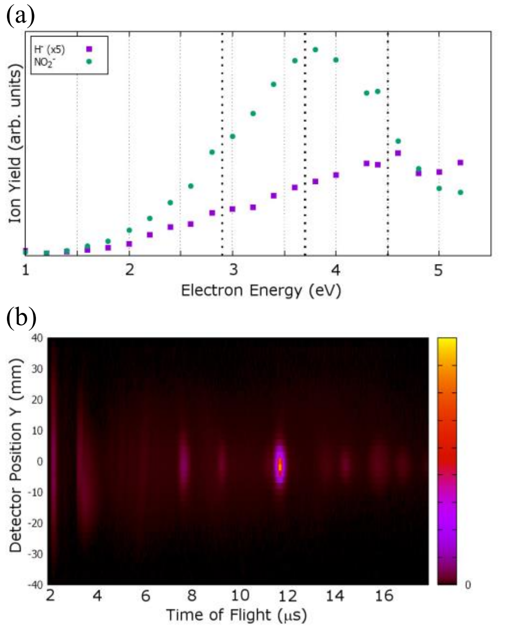

Figure 2-3: (a) H$^-$ and NO$_2^-$ fragment yields as a function of electron energy for DEA to nitrobenzene. Vertical dashed lines indicate resonance central energies measured by A. Modelli and M. Venuti (2001, *Int. J. Mass Spectrometry* 205 7–16). (b) Time of flight vs. position spectrum for 4.5 eV electron attachment to nitrobenzene, where each peak represents a different anion fragment and the vertical extent of each peaks represents the relative momentum spread along the momentum coordinate co-linear with the incident electron. The intensity scale is the anion yield in arbitrary units.

Dynamics of Dissociative Electron Attachment to Gas Phase Nitrobenzene and Ortho-nitrophenol

(Belkacem, Lucchese, McCurdy, Rescigno, Slaughter, Weber)

Recent Progress: Nitroaromatic molecules exhibit strong electron acceptor properties due to the inductive effect of the NO$_2$ functional group and to low-energy unoccupied π* orbitals. These properties may have some role in the unusual low-energy resonance structures in resonant electron scattering from nitrobenzene and o-nitrophenol, including narrow features that may be due to low-energy core-excited resonances [A. Modelli and M. Venuti, *Int. J. Mass*

Spectrometry **205** (2001)]. Whether or not these resonances play any role in the electron-driven chemistry of these systems is unclear, which motivates an investigation of the dynamics of resonant dissociative electron attachment (DEA) in nitrobenzene and o-nitrophenol. Collaborating with A. Moradmand (California State University, Maritime), we have performed a preliminary study of the characteristic kinetic energy release in each anion fragment, for DEA at low incident electron energies from 1 eV to 5 eV, in nitrobenzene (Fig. 2-3). Preliminary results exhibit remarkably low kinetic energy release in the two most dominant fragments, H^- and NO_2^-, over one or more broad resonances from 2 eV to 5 eV incident electron energy.

Future Plans: Laboratory-frame angular distributions of the recoiling anion fragments will be examined for DEA to nitrobenzene and o-nitrophenol to investigate any asymmetry with respect to the incident electron momentum. The combined experimental and theoretical methods developed for simpler molecules [D.S. Slaughter et al., *J. Phys. B* **49**, 222001 (2016)] will be extended to understand these larger systems having relatively complex electronic structure. Electronic structure calculations will be performed to determine possible electronic configurations of the lowest-energy excited anions of nitrobenzene and o-nitrophenol, to develop an understanding of the dynamics that lead to the final state momenta measured in the present momentum imaging experiments.

Ultrafast XUV and X-ray Absorption Studies of Photoinduced Dynamics in Organic Molecules (Gessner, Neumark, Leone, Head-Gordon)

In this effort, laboratory-based ultrafast transient XUV/X-ray absorption (TXA) spectroscopy techniques are developed and applied to probe unimolecular reaction dynamics from the perspectives of well-defined reporter atoms. Experiments are complemented by high-level *ab initio* calculations of inner-shell transitions.

Recent Progress: Using an experimental setup on UC Berkeley campus, a femtosecond time-resolved TXA study of 267 nm induced radical formation in dimethyl disulfide (DMDS, $CH_3S_2CH_3$) was performed (Fig. 2-4). Previous studies using other techniques reported partly conflicting results with either S-S bond or C-S bond scission, resulting in the formation of two methylthiyl (CH_3S)

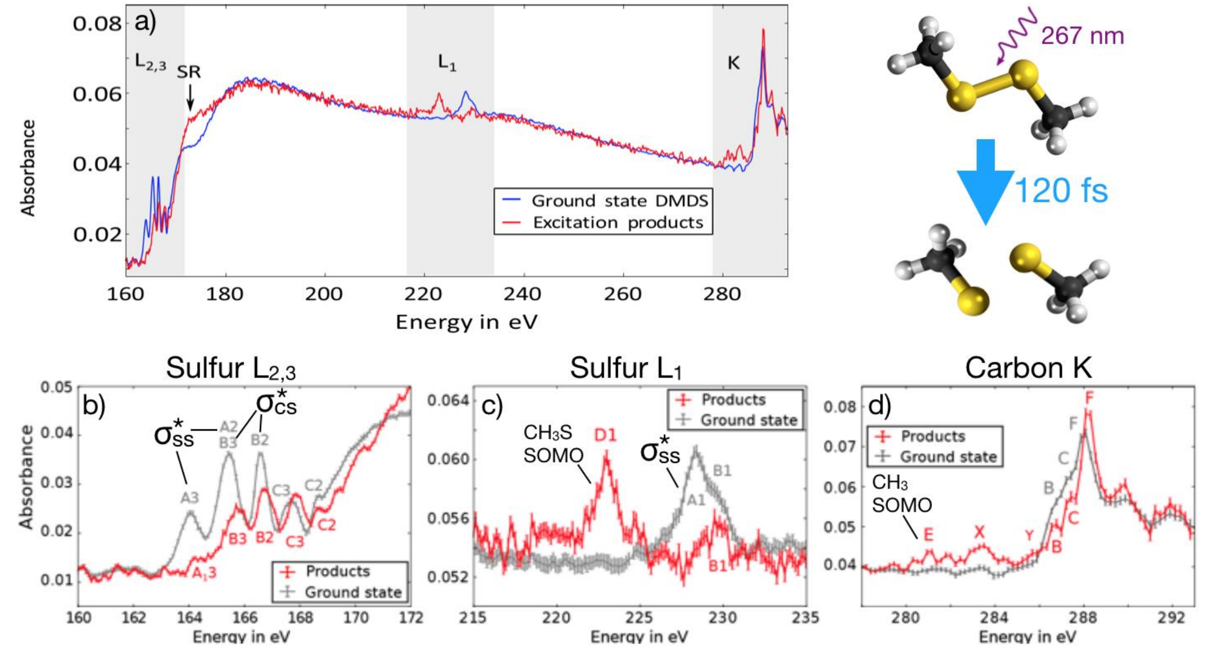

Figure 2-4: UV-induced radical formation in dimethyl disulfide studied by ultrafast broadband transient X-ray absorption. Dynamics are probed simultaneously at the sulfur $L_{2,3}$-, sulfur L_1-, and carbon K-edges. Ground state spectra are shown in blue and grey, product spectra in red.

radicals or one methyl (CH_3) and one methylperthiyl (CH_3S_2) radical, respectively. The high-order harmonic generation (HHG) based TXA setup provides a photon energy bandwidth of ~140 eV, enabling simultaneous probing of the UV-induced dynamics at the sulfur $L_{2,3}$-, sulfur L_1-, and carbon K-edges under identical experimental conditions (Fig. 2-4a). The experiments are interpreted with the aid of high-level *ab initio* descriptions of both valence- and core-excitations (see Subtask 3). The study provides clear evidence that the predominant reaction channel is rapid dissociation of the molecule into two methylthiyl radicals by scission of the S-S bond on a timescale of ~120 fs. This is supported, in particular, by a strong suppression of S2p→σ^*_{SS} and S2s→σ^*_{SS} resonance peaks and the emergence of a S2s→CH_3S-SOMO resonance (Fig. 2-4b,c). Albeit, some methyl radical production is also indicated by a small peak associated with C1s→CH_3-SOMO transitions (Fig. 2-4d). The work has been submitted for publication [Schnorr et al., *J. Am. Chem. Soc*., (submitted)].

At LBNL, a new laser system has been installed to support the AMOS TXA and helium nanodroplet (see below) efforts. First experiments on UV-induced dissociation of bromoform molecules ($CHBr_3$) have been conducted, employing Br 3d inner-shell transitions to monitor the dissociation from the perspective of a departing Br atom. The analysis of the data and complementary *ab initio* calculations are ongoing.

Future Plans: The LBNL based setup currently operates below ~100 eV photon energy. After completing a series of experiments on halogenated hydrocarbons, the available photon energy range will be extended beyond the sulfur L- and, ultimately, carbon K-edges using a long wavelength driver HHG scheme. This will enable a larger range of experiments on sulfur-containing compounds, which are of particular interest for biology, atmospheric chemistry, and industrial applications.

Future XFEL light sources such as LCLS II will provide unique opportunities for TXA studies in energy and intensity regimes not available via HHG. Therefore, members of the LBNL AMOS program are among the main drivers toward identifying opportunities to implement TXA capabilities in the early stages of LCLS II.

Ultrafast X-ray Studies of Interfacial Charge-transfer Dynamics (Gessner)

This effort employs synchrotron- and X-ray free-electron laser (XFEL) based time-resolved X-ray spectroscopy techniques to study the flow of energy and charge during photoinduced interfacial dynamics. The goal is to achieve an atomic-level understanding of the electronic dynamics that underlie novel concepts for molecular electronics and light harvesting technologies.

Recent Progress: Photo-induced energy and charge transfer dynamics in planar heterojunctions made of copper-phthalocyanine (CuPc) donor and C_{60} acceptor domains have been studied by picosecond time-resolved X-ray photoelectron spectroscopy (TRXPS) at the Advanced Light Source (ALS) (Fig. 2-5). The

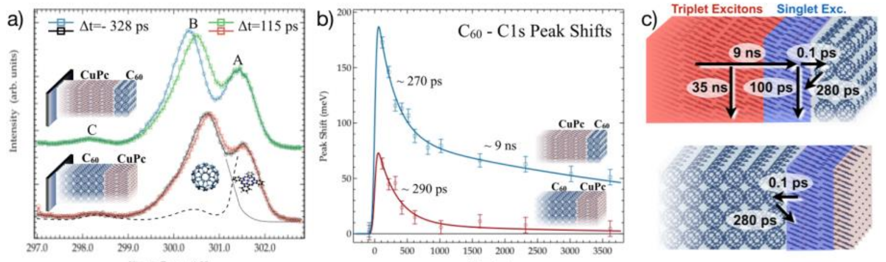

Figure 2-5: Disentangling the roles of singlet and triplet excitons to interfacial charge transfer in an organic heterojunction. a),b) Picosecond time-resolved XPS after optical excitation of two bilayer configurations of CuPc and C_{60} with either 2 ML C_{60} atop a multilayer of CuPc (upper curves) or vice versa (lower curves). The measurements reveal a predominant role of triplet excitons, accessed via fast intersystem crossing from initially excited singlet states, to interfacial charge transfer. See text for details.

experiment provides direct access to the triplet exciton diffusivity and diffusion length within a multilayer CuPc phase, as well as the relative charge generation efficiency for triplet and singlet donor excitons via exciton splitting at the donor-acceptor interface. Contrary to common belief, ultrafast intersystem crossing from the initially excited singlet excitons to triplet excitons is not a loss channel but the long-lived triplet excitons contribute to a significantly larger extent to the time-integrated interfacial charge than the short-lived singlet excitons. The work has been submitted for publication [Roth et al., *Phys. Rev. Lett.,* submitted]. Most recently, studies on the CuPc/C_{60} system have been extended to the femtosecond domain at the FLASH XFEL. The analysis of this experiment is ongoing.

Electron injection dynamics of N3 chromophores attached to nanoporous ZnO substrates were probed by picosecond TRXPS using both the C1 s photoline of the N3 molecules as well as the Zn 3d photoline of the substrate. Clear differences are observed including a time-delayed response of the Zn 3d compared to the C1 s signal. The results are being analyzed in the context of coupled electron injection and delocalization dynamics at the molecule-semiconductor interface.

TRXPS studies of interfacial charge dynamics at the ALS are complemented by picosecond time-resolved XAS studies employing a recently developed mobile TRXAS technique [Neppl et al., *Faraday Discuss*. **194**, 659 (2016)]. A series of experiments has probed the relative impact of electronic and lattice dynamics to the TRXAS signals of photoinduced dynamics in semiconductor substrates. The analysis of these data is ongoing.

Future Plans: In addition to the ALS-based picosecond time-resolved XPS and XAS experiments, more femtosecond time-domain experiments are being proposed to be conducted at the FLASH XFEL. These will both complement the ALS based experiments toward shorter timescales as well as serve as preparation for future interfacial charge dynamics investigations at next generation XFELs such as European XFEL and LCLS-II. The pulse structure of the latter will be particularly well suited for TRXPS studies using the techniques developed at the ALS.

Ultrafast Dynamics in Helium Nanodroplets (Gessner, Neumark)

This effort employs HHG-driven photoelectron imaging and XFEL-based X-ray coherent diffractive imaging to study ultrafast electronic and nuclear dynamics in pure and doped helium nanodroplets.

Recent Progress: Analysis of a recent LCLS experiment to image nanoplasma dynamics in strong-field ionized helium nanodroplets and corresponding dynamics simulations have been completed (Fig. 2-6). The measurements reveal that an anisotropic, ~20 nm wide surface region is established within ≈100 fs, in qualitative agreement with recent theoretical predictions [Peltz et al., *Phys. Rev. Lett.* **113**, 133401 (2014)]. On longer ~picosecond timescales, however, the width of this region remains largely constant while the dense plasma core shrinks at average rates of ≈140 nm/ps along and ≈70 nm/ps perpendicular to the laser polarization. These dynamics are rather surprising and are not captured by previous plasma expansion models. The work has been submitted for publication [Bacellar et al., *Nat. Phys.* (submitted)].

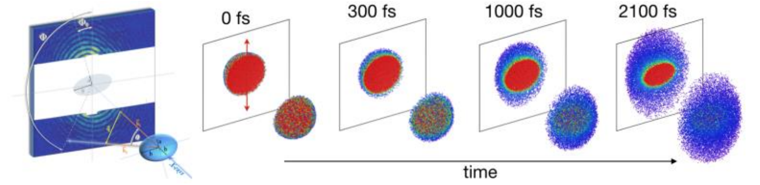

Figure 2-6: Anisotropic evolution of a strong-field ionization induced nanoplasma derived from a femtosecond time-resolved X-ray coherent scattering experiment at LCLS.

The HHG-based photoelectron imaging activity has been hampered by a series of hardware failures including, in particular, the driving laser that eventually needed to be replaced (see TXA activity above). The setup is currently being prepared for operation with the new laser system.

Future Plans: Future studies will focus more strongly on dynamics involving dopants within the helium host matrix. In their superfluid ground state, ^{4}He droplets equilibrate at a temperature of ~0.4 K and constitute one of the most homogeneous matrices available to study, for example, charge transfer dynamics and inter-molecular interactions by "freezing out" molecular constellations not observable at higher temperatures. The latter technique will be tested in an upcoming LCLS beam time that will employ ultrafast X-ray coherent diffractive imaging to compare atomic and molecular aggregation in both ^{4}He and ^{3}He matrices. Laboratory-based studies will focus on host-dopant energy- and charge-transfer processes that will be probed by femtosecond time-resolved photoelectron imaging using a newly developed 400 nm driver HHG scheme. Experiments will be complemented by first principles calculations on coupled electronic-nuclear dynamics in electronically excited, heterogeneous clusters as discussed in Subtask 3.

Subtask 3: First-Principles Theory of Dynamics and Electronic Structure

M. Head-Gordon, C. W. McCurdy, R. R. Lucchese, T. N. Rescigno

Double Photionization of Water by One Photon (McCurdy, Lucchese, Rescigno)

Recent Progress: We have undertaken a major new effort to calculate and observe the angular dependence in the body frame of one-photon double photoionization of water. This will be the first such observation and *ab initio* calculation of this process for a polyatomic molecule. We completed the first step in this project, which was to unravel the dissociation dynamics of the nine states of the water dication produced by removing two electrons from the highest three occupied orbitals of neutral water in the process $H_2O\ +\ h\nu \longrightarrow H_2O^{++} + 2e^- \longrightarrow O + 2H^+ + 2e^-$. We computed the relevant H_2O^{++} potential surfaces, and calculated ensembles of classical trajectories to compare with ALS experiments by the LBNL AMOS group that observed the protons. The theory reproduces the dynamics for dissociation of all eight states observed in the experiment, allowing their unambiguous identification in coincidence measurements, as shown in Fig. 3-1. In several ionization channels axial-recoil dissociation dynamics allow easy identification of the molecular orientation. Even in cases where axial recoil breaks down, and the H_2O^{++} dication scissors to eject two protons towards the side of the molecule opposite the original OH bonds, our calculations potentially allow the identification of molecular plane in a four-particle coincidence detection of both electrons and both protons. This work, appearing in two papers [Streeter et al., *Phys. Rev. A*, (accepted) and Reedy et al., *Phys Rev A* (accepted)] opens the way for the measurement of the triple differential cross section (TDCS) for the correlated angular dependence of the two electrons in the molecular frame.

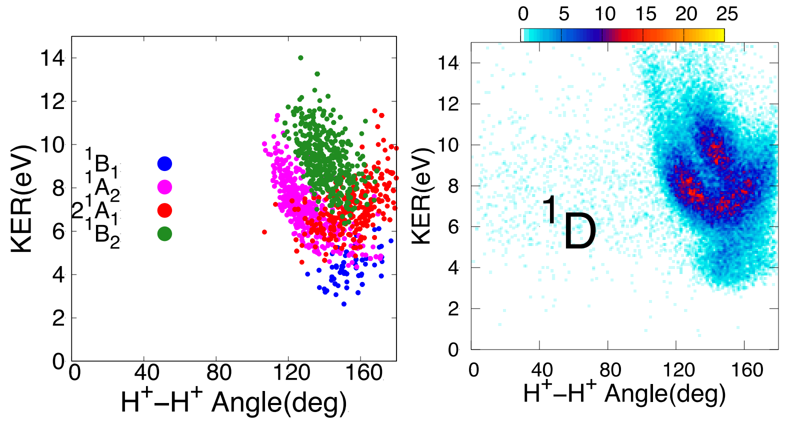

Figure 3-1: Classical trajectories on the four states that dissociate H_2O^{++} to $O(^1D) + 2\ H^+$ compared with ALS experimental momentum image (right) unambiguously identifying the electronic states observed in the experiment.

Future Plans: We will calculate the TDCS for double photoionization of water by one photon using our finite element discrete variable representation coupled with exterior complex scaling in time independent calculations that treat two active electrons, freezing the rest in Hartree-Fock orbitals. We solve the driven Schrödinger equation, $(E_0 + \hbar\omega - H)\Psi sc = \mu\Phi_0$, in which the right hand side is the dipole operator times the initial state, in a single center expansion and extract the TDCS from Ψsc as we have done in our previous work on double photoionization of H_2. These large supercomputer calculations are in process, and we are making multiple improvements to the computational algorithms we previously applied to double photoionization of H_2 to make it possible to solve this challenging problem. New coincidence data has been taken at the ALS from which the TDCS will be extracted, and these comparisons will be the first of their kind on a polyatomic molecule. This work is being done in collaboration with Prof. Frank Yip (California State University, Maritime).

One-Photon Double Photoionization as a Probe of Initial State Correlation (McCurdy, Lucchese, Rescigno)

Future Plans: It has long been asserted that one-photon double ionization is exquisitely sensitive to correlation both in the initial electronic state of the neutral molecule and in the final doubly ionized state describing the departure of the electrons. However there has never been a systematic and quantitative test of what these experiments tell us about correlation in the neutral target molecule. We have undertaken systematic study in which the initial state is built up by the addition of uniquely defined terms in its expansion in natural orbitals that diagonalize the one-electron density matrix, while treating final state correlation essentially exactly for each different resulting approximation to the initial state. We do this by solving the driven Schrödinger equation mentioned above essentially exactly, but adding terms in the natural orbital expansion of the right hand side one at a time in order of decreasing natural orbital occupation. Our preliminary results on double photoionization of the two electron systems He, H^- and H_2 have been profoundly surprising. The molecular case is dramatically more sensitive to correlation in the bond than either atomic case, even though by most measures the hydrogen anion, H^-, is substantially more correlated than H_2. As shown in Fig. 3-2, for some orientations relative to the polarization vector, the TDCS in the molecular case has a completely wrong shape and magnitude until natural orbital configurations with occupations greater than 10^{-5} are included. This analysis suggests that double photoionization of water will be particularly sensitive to correlation in the description of OH bonds for particular directions of polarization.

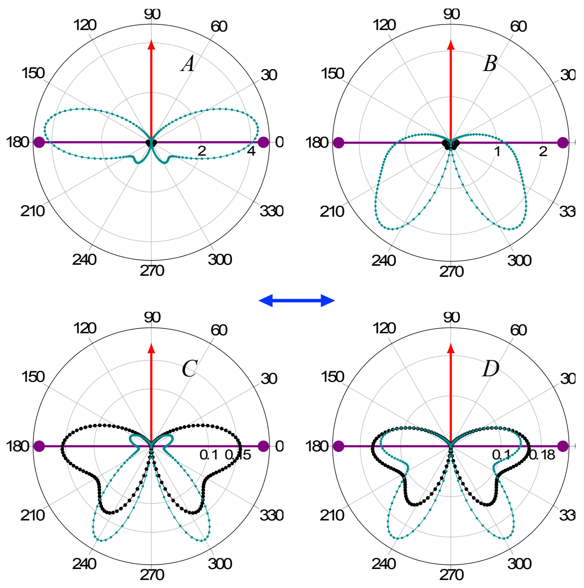

(blue) as correlating contributions are added to the initial state. A: $1\sigma_g$, B: A+$1\sigma_u$ + $1\pi_u$, C: B + $2\sigma_g$ (all occupations > 10^{-4}), D: first 15 natural orbital terms. Black in all panels is converged result which is an order of magnitude smaller than the partially correlated results in panels A and B.

Valence Photoionization of CF_4 (Lucchese, McCurdy, Rescigno)

Recent Progress: We have completed a joint theoretical/experimental study of valence photoionization of CF_4. This molecule shows striking resonance effects, when observed in the body-frame, that have not been previously observed. In a highly symmetric molecule with degenerate valence orbitals, it is possible to find resonance states of different orbital symmetry that couple to the same total symmetry and that can therefore interact. If such resonance states are narrow yet sufficiently close in energy, this can lead to strong coupling effects. Our calculations, done in collaboration with Prof. Cynthia Trevisan (California State University, Maritime), showed that such is the case with CF_4 - a molecule of high symmetry, unstable parent ion states, and massive enough to support narrow shape resonances close to threshold. In the case of photoionization from the valence HOMO-1 $4t_2$ orbital, interference between overlapping a_1 and t_2 resonances leads to a reversal in shape of the recoil-frame photoelectron angular distribution over a narrow range in energy as shown in Fig. 3-3. Our study was published this year in PCCP.

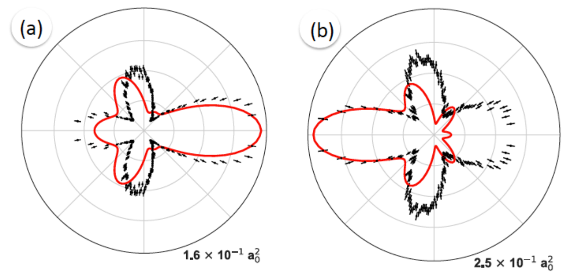

Figure 3-3: RFPADs for photoionization from the $4t_2$ orbital of CF_4 at photoelectron energies of (a) 3.2 eV and (b) 4.3 eV, showing a striking reversal in shape.

Core-Hole Localization in CCl_4 (McCurdy, Lucchese, Rescigno)

Future Plans: Our study of F $1s^{-1}$ ionization in CF_4 [McCurdy et al., *Phys. Rev. A* **95**, 011401(R) (2017)] showed that Molecular Frame Photoelectron Angular Distributions (MFPADs) computed with a hole localized on one of the four spatially equivalent F atoms closely matched the measured angular distributions for high kinetic energy release when fluorine is detected as F^+ in dissociation after Auger decay. We showed that the physics underlying the breakup dynamics derives from the Ne-like valence structure of the dissociating F $(1s^{-1})$ core-excited atom. We plan to examine whether similar effects can be found in chlorine core ionization of CCl_4. While the chlorine 2s and 2p core orbital IPs in CCl_4 are both in an energy range accessible for study at the ALS, it is found that only ionization from the 2p orbital results in fragmentation to the two-body CCl_3^+ + Cl^+ channel following Auger decay. All-electron calculations on such a large molecule will be challenging, but will answer some important questions. It will be interesting to see if a Cl-2p hole, which can be distributed over three spatially inequivalent orbitals on each of four equivalent atoms obscures any observable hole localization effects.

Overset Grid Based Complex Kohn Method for Electron-Polyatomic Molecule and Ion Scattering (Lucchese, McCurdy)

Recent Progress: We have developed a new computational implementation of the complex Kohn variational method that describes the scattered (or ionized) electrons on "overset grids" that combine local spherical grids centered on each atom, with one centered at the middle of the molecule and reaching to the asymptotic region that overlaps all the smaller grids. Using a discrete variable representation in each subgrid we have implemented and tested the method on single-channel static-exchange calculations on small molecules, and described the method in Greenman et al. [*Phys. Rev. A* **96** 052706 (2017)]. The new approach combines aspects of the Complex Kohn method used for decades at LBNL and advantages of the Schwinger variational method developed for electron-molecule scattering by Lucchese to allow the accurate treatment of electronic collision problems at higher energies without any approximation of exchange interactions.

Future Plans: We are developing a photoionization capability using the overset-grid method that has the same rapid convergence properties described for electron scattering from neutral molecules in our first publication on this approach. It has been tested on small molecules in the static-exchange approximation, proving that we can now properly apply Coulomb boundary conditions in this approach. We are now developing the capability to hold the scattering solution orthogonal to any orbitals occupied in all configurations that contribute to a correlated target wave function. This is the first step to completing a general multi-channel implementation of the overset grid method for polyatomic molecules that will eventually replace our current core computational capability for electronic collisions and photoionization of polyatomics. The planned theoretical and computational developments will ultimately produce a modern, easy-to-use, and general electron-molecule collision code, parallelized with OpenMPI that will be made available to other users and will support experiments on dissociative electron attachment and molecular photoionization.

K-shell Photodetachment of C_n^- Ions (Rescigno)

Recent Progress: It is well known that K-shell photodetachment of the simplest carbon anion, C^-, is characterized by a prominent shape resonance (1s→2p) close to threshold. Carbon can also form linear chains whose anions are all bound. Recent K-shell photodetachment experiments at the ALS by N. Berrah and coworkers have shown that the shape resonance seen in C^- persists in the carbon anion chains, but that the resonance splits into multiple peaks in the heavier anions. In collaboration with Nicolas Douguet (U. Central Florida) and Samantha Fonseca (Rollins College), a detailed theoretical study of K-shell photodetachment of C_2^- and C_3^- was carried out, showing that the number of resonance peaks observed is related to the number of inequivalent C (1s) sites in the anion. Our calculated results, shown in Fig. 3-4 are in good agreement with experiment. We are preparing a manuscript with Berrah and coworkers for publication, reporting both theory and experiment.

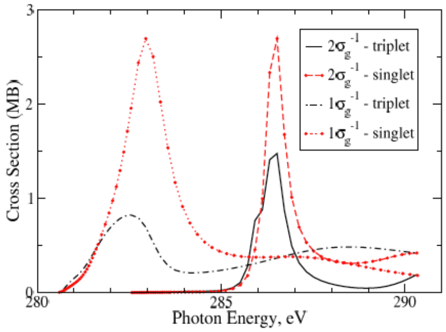

Figure 3-4: Calculated cross section for $^2\Sigma_g^+ \rightarrow {}^2\Sigma_u^+$ K-shell photodetachment of C_3^-, showing contributions of individual final channels.

Multichannel Theory of Conversion of Resonances to Bound States in Coulomb Potentials (Lucchese, Rescigno, McCurdy)

Recent Progress: A central concept of collision theory is the idea that bound states can become metastable states with finite lifetimes (scattering resonances) and vice versa as the strength of the interaction potential is varied. This phenomenon is well known in electron-molecule scattering, where it provides the mechanism for dissociative attachment of electrons to molecules and dissociative recombination (DR) of electrons to molecular cations.

In the case of scattering potentials which behave asymptotically as attractive Coulomb potentials, a pole of the S matrix in the fourth quadrant of the complex k plane that is associated with a scattering resonance, ***does not become a pole corresponding to a bound state*** which is created as the short range part of the potential is made more attractive. However, we have shown that it is paired exactly with a zero in the first quadrant that modifies the Rydberg series at negative energy.

We have developed an S-matrix version of quantum defect theory that relates the motion of the poles and zeros of the S-matrix to the quantum defects of Rydberg series and extended it to multi-channel problems. For a system with an asymptotic attractive Coulomb potential we can define a multichannel quantum defect matrix **M** in terms of the short-range **S** matrix as

$$\mathbf{M}^{-1} = \left(\mathbf{1} - \mathbf{Q}\right)^{\frac{1}{2}} \left(\mathbf{S}^{\mathrm{SR}}\right)^{-1} \left(\mathbf{1} - \mathbf{Q}\right)^{\frac{1}{2}} + \mathbf{Q} \qquad (1)$$

where **Q** is defined as $(\mathbf{Q})_{i,j} = \delta_{i,j} \exp(-2\pi/k_i)$. When applied to a single channel case, this reduces to an M-matrix that is related to the quantum defect, μ, through $M(k) = \exp[i2\pi\mu(k)]$.We can see that when all channels are open and when, $\mathrm{Re}(2\pi/k_i) \gg 1$ that is when k is close to the real axis and not too large, then **M** and $\mathbf{S}^{\mathrm{SR}}$ will be the same. When all channels are closed and the k_i are pure imaginary along the positive imaginary axis, **S** has a series of poles corresponding to the bound states, while the $\mathbf{M}$ is a smooth function from which the bound states can be obtained from the condition

$$\det\left(\mathbf{1} - \mathbf{QM}\right) = 0 \qquad (2)$$

At real energies, $\mathbf{M}$ is unitary over both open and closed channels in contrast to $\mathbf{S}$, which is only unitary over the sub-matrix containing all of the open channels, $\mathbf{S}_{\mathrm{OO}}$. Thus $\mathbf{M}$ can be modeled in terms of a real symmetric matrix $\mathbf{K}$ using the form

$$\mathbf{M} = (1 + i\mathbf{K})(1 - i\mathbf{K})^{-1} \qquad (3)$$

When there are some open and some closed channels, the open channel $\mathbf{S}$-matrix, $\mathbf{S}_{\mathrm{OO}}$, can have resonances due to poles at scattering energies with negative imaginary parts and there will be zeros in the determinant of the $\mathbf{S}_{\mathrm{OO}}$ matrix at energies corresponding to the complex conjugates of the energies of the poles. If the pole is due to a Feshbach resonance caused by a nearly bound state in one of the closed channels, then the full $\mathbf{M}$ matrix will be smooth. However, one can also consider the $\mathbf{M}_{\mathrm{OO}}$ matrix generated by only the open channels in the $\mathbf{S}$ matrix, i.e. from using only $\mathbf{S}_{\mathrm{OO}}$ in Eq. (1). In that case, $\mathbf{M}_{\mathrm{OO}}$, will also have the same poles and zeros in its determinant, but as the system is modified to pull the resonance states below the last threshold, the zero in the first quadrant of the complex k plane will move up towards the positive imaginary axis and the resonance pole will move down the negative imaginary k-axis, not becoming a bound state.

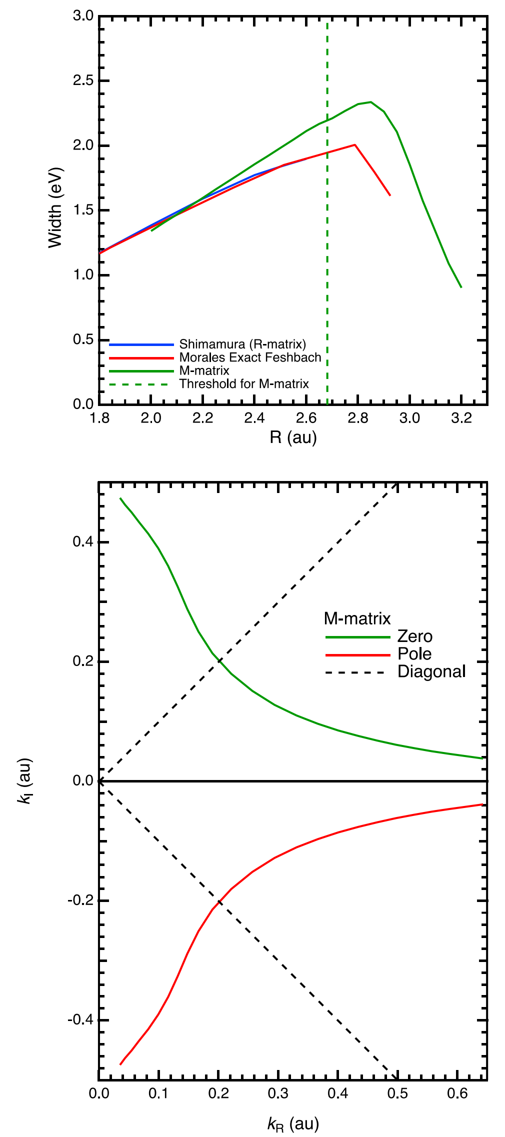

Figure 3-5: Results for the resonance in $^1\Sigma_g^+$ in e-H_2^+ scattering. Top panel: width as a function of R compared to the results Shimamura et al. and Morales et al. Lower panel trajectory of the zero/pole in the complex k plane for varying R.

As an example, consider the case of the e-H_2^+ system in the $^1\Sigma_g^+$ symmetry. For bond lengths of $R < 2.6$ bohr there is a low-energy scattering resonance in this symmetry [I. Shimamura et al., *Phys. Rev. A* **41**, 3545 (1990); F. Morales et al., *Phys. Rev. A* **73**, 014702 (2006)]. For longer bond lengths the resonance disappears but a strong perturbation appears in the Rydberg series below threshold. We studied this problem using a three channel description. For a range of R values, we computed both the $\mathbf{S}$-matrix for energies above the threshold for the ionization of H_2 to the ground state of H_2^+ and also the s and d Rydberg series below the ionization threshold.

For each R, a 3×3 $\mathbf{K}$-matrix was then obtained by first transforming it to an $\mathbf{M}$-matrix using Eq. (3), then the bound Rydberg series were fit using Eq. (2) and simultaneously, at positive energies, the $\mathbf{S}$-matrix was obtained using the inverse relationship of Eq. (1) and the $\mathbf{S}_{\mathrm{OO}}$ part was fit to the computed scattering matrices. The zeros of the open channel part of the analytically continued **M**-matrix were then obtained as a function of *R*. The resulting values of the resonance widths are given on the top panel of Fig. 3-5 and the corresponding zero/pole trajectories of $\mathbf{M}_{OO}$ are given in the complex momentum plane in the bottom panel of Fig. 3-5. The pole/zero trajectories behave in the same manner as we found in the one-channel case with the resonance scattering pole **not** being converted into a bound state pole.

Molecular Frame Photoelectron Angular Distributions in Two-Photon XUV+IR Experiments (Lucchese, McCurdy)

Future Plans: Molecular frame photoelectron angular distributions (MFPADs) from one-photon ionization can be used to determine the relative phases of the different partial waves excited at fixed photon energies. This type of experiment however cannot measure the energy dependence of the phases, which for energies near a resonance can yield information about Wigner time delays associated with such resonances. In two-photon XUV+IR experiments, where the XUV light is produced by high-harmonic generation (HHG) and the IR light is the same as was used in the HHG, it is possible to have photoionization of a target system by the XUV light at the odd harmonics of the IR light, and through the absorption or emission of a second IR photon produce sidebands at the even harmonics of the IR light. Using this process one can then determine the relative phases of the XUV transitions at odd harmonics by measuring the intensity of the sidebands produced by two interfering paths (XUV_{2n-1}+IR and XUV_{2n+1}-IR) as a function of the relative phases of the IR and HHG light [P. Hockett, *J. Phys. B*, **50**, 154002 (2017)].

We will derive the expression for the full MFPAD for the two-photon process. This will provide the appropriate expression for the analysis of such experiments where the state being produced in the target molecule is dissociative so that angle-resolved photoelectron-photoion coincidence measurements can determine the MFPAD for the two-photon process. We will assume that the first step is the photoionization of the molecule by the XUV photon, governed by one-photon matrix elements [R. R. Lucchese et al., *Phys.Rev. A* **65**, 020702 (2002)]. The IR absorption will then occur between two continuum states which we will treat using an asymptotic approximation [D. Baykusheva and H. J. Wörner, *J. Chem. Phys.* **146**, 124306 (2017)]. These expressions will then allow us to predict how the phase variation with energy depends on the direction of emission of the photoelectron. Additionally, we will be able to determine the extent to which the underlying one-photon ionization phase is modified by the phase contributions of the continuum-continuum interaction and, as a consequence, the possibility for such experiments to measure the Wigner time delay as a function of emission direction in the one-electron process.

Non-orthogonal Single Excitation CI for Core Excitations (Head-Gordon)

Recent Progress: The core hole in a core-excited state leads to significant valence orbital relaxation (contraction, primarily) that is natural to capture within a non-orthogonal CI (NOCI) treatment. For this purpose we have recently defined and implemented the non-orthogonal configuration interaction singles (NOCIS) method for calculating core-excited states of closed-shell molecules [Oosterbaan et al., *J. Chem. Phys.* **149**, 044116 (2018)]. NOCIS is a black-box variant of NOCI (that in itself makes NOCIS a very rare variant of NOCI), which uses *A* different core-ionized determinants for a molecule with *A* atoms of a given element to form single substitutions. NOCIS is a variational, spin-pure, size-consistent *ab initio* method that dramatically improves on standard CIS (see Fig. 3-6) by capturing essential orbital relaxation effects, in addition to essential configuration interaction. To demonstrate feasibility, we have applied it to the calculation of core-excitations involving the K-edge of C, N, O, F in a range of small molecules and demonstrate that it vastly out-performs standard CIS and TDDFT using ground state functionals. Its performance is competitive with DFT-based methods using short-range-corrected functionals that are adapted for computing core spectra. With further development, NOCIS may be a very valuable computational tool for calculating core excitations in medium-sized molecules.

Molecule	Experiment	CIS	Δ-SCF	NOCIS
C_2H_2 C(1s)	285.9[56]	16.68	9.97	1.26
H_2CO C(1s)	286[58]	20.29	4.94	2.01
HCN C(1s)	286.37[63]	17.07	2.77	1.71
CO C(1s)	287.4[61]	19.14	-0.34	1.70
CH_3OH C(1s)	287.92[62]	17.15	0.70	1.07
CH_4 C(1s)	288.1[57]	14.68	-1.17	-0.83
CO_2 C(1s)	290.8[59]	18.56	3.90	2.12

Figure 3-6: *Ab initio* calculations K-edge spectra of several small molecules using the newly developed NOCIS method, as well as standard CIS and Δ–SCF. Errors for each of the three methods are given in eV. NOCIS is a dramatic improvement over CIS, and is a major improvement over Δ–SCF for cases with equivalent nuclei such as C_2H_2.

Future Plans: The initial version of NOCIS is restricted to closed shell molecules. We intend to extend the theory to permit treatment of core excitations via NOCIS in open shell species, as needed to enable collaborations within the program (e.g. see DMDS example, with Gessner and Leone above). We are also very interested in the inclusion of spin-orbit coupling to enable the treatment of the L-edge in third row elements. Additionally, NOCIS includes only essential electron correlations, and it is therefore of much interest to us to consider suitable strategies for including dynamical electron correlation effects. One possibility is to adapt the NOCI-MP2 approach discussed below.

Calculations of Core Excitation Spectra in Dimethyl Disulfide (DMDS) (Head-Gordon)

Recent Progress: We have performed calculations of core excitations in CH_3SSCH_3 (DMDS) to complement the time-resolved experimental measurements of Leone and Gessner that follow its photodissociation after absorption of 267nm radiation, as described in Subtask 1. Using the extended second order algebraic diagrammatic construction (ADC-2X), with core-valence separation, we evaluated C K-edge and S L-edge core excitations in DMDS itself, as well as the potential photoproducts, CH_3S, CH_3, and CH_3SS. The calculations were in generally satisfactory agreement with the experimental observations, and supported an interpretation of the experiments in which CH_3S fragments were the dominant photoproduct.

Second Order Correction to Non-orthogonal CI (NOCI-MP2) (Head-Gordon)

Recent Progress: We have developed [Yost et al., *J. Chem. Theory Comput.* **14**, (2018)] an efficient implementation of the perturb-then-diagonalize non-orthogonal configuration interaction method with second order Møller-Plesset perturbation theory (NOCI-MP2). Relative to other low scaling multireference perturbation theories, NOCI-MP2 often requires a much smaller active space because of the use of non-orthogonal reference configurations. Reworking the NOCI-MP2 equations with the resolution of the identity (RI) approximation enables the method to have the same memory requirements and computational scaling as single reference RI-MP2. The working equations are extended to include single substitutions as required when the reference determinants do not satisfy the Hartree-Fock equations. In addition to implementing and validating the algorithm, we have applied NOCI-MP2 to the binding energy and charge resonance energy in dication and monocation π dimers (see Fig. 3-7), \as well as di-diamantane ethane, and hexaphenyl ethane. We have also addressed the problem of defining suitable non-orthogonal configurations in these systems by using absolutely localized molecular orbitals (ALMOs), as solutions to the self-consistent field for molecular interactions (SCF-MI) equations corresponding to covalent and ionic determinants. Agreement with experimental information where available, and other multi-reference methods, is satisfactory, with the use of an 0.3 a.u. level shift to guard against large MP2 amplitudes. For di-

diamantane ethane and hexaphenyl ethane, large dispersion forces help stabilize the molecules despite the steric repulsion. By contrast, in the case of hexaphenyl ethane, the energy penalty from the geometric distortion of the fragments significantly weakens the bond.

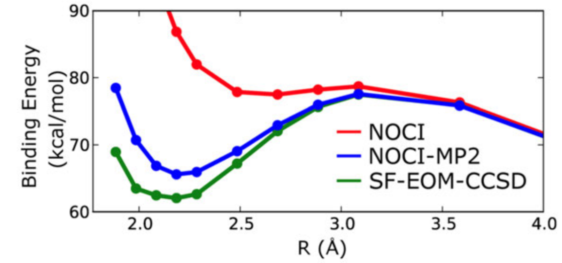

Figure 3-7: Calculations using the newly developed NOCI-MP2 method for the "anti-electrostatic" complex between two ethylene cations. This complex is bound together by a weak biradicaloid bond augmented by dispersion interactions. NOCI itself does not capture dispersion, while NOCI-MP2, using ionic and covalent references is in quite good agreement with a reference SF-EOM-CCSD calculation.

Future Plans: The NOCI-MP2 framework appears very promising for efficiently and accurately treating dynamic correlation in excited states of molecules and molecular clusters. We intend to explore several interesting extensions that will broaden its applicability and improve its robustness. We intend to generalize NOCI-MP2 to correct reference functions that are obtained from the spin-flip (SF) version of NOCI. This extension is interesting because SF-NOCI is the closest we have to a black-box approach to the NOCI method. It is also interesting because the NOCI-MP2 theory will need to be modified to ensure that spin-multiplet degeneracies which are present in SF-NOCI are preserved after the NOCI-MP2 correction. Straightforward application of the existing theory does not satisfy this condition. We are also interested in trying to improve the present somewhat heuristic use of level shifts to ensure that the method does not suffer from intruder states. This suggests that development and testing of more sophisticated regularization methods could be valuable.

Simulations of Helium Clusters in Excited States (Head-Gordon)

Recent Progress: The newly developed ALMO-CIS+CT method has been applied to model the size-dependence of helium cluster spectra, up to systems of 300 helium atoms [Ge et al., *J. Chem. Phys.* **146**, 044111 (2017)]. To correctly simulate the clusters, path integrals were applied to the nuclear motion, at a temperature of 3K (above the superfluid transition), and spherical boundary conditions were employed to establish a droplet-vapor equilibrium. The results, some of which are shown in Fig. 3-8, illustrate several interesting features. First, the size-dependence of the width of the 2p band (21.2 to 22.0 eV) emerges nicely from the simulations, in qualitative agreement with experiments. Second, signatures of the droplet versus dense gas can be established by removing the attractive part of the potential, and comparing the spectra simulated using different cutoff radii (giving different gas densities in the gas case, and different fractions of gas versus droplet atoms in the droplet-vapor equilibrium case). The dense gas simulation shows narrower bandwidth, and that bandwidth depends strongly on the gas density, while the droplet spectrum is as shown in the figure.

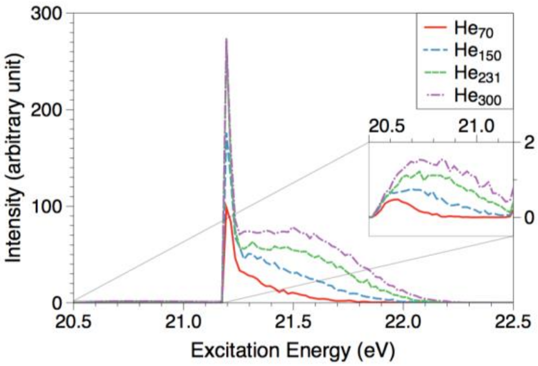

Figure 3-8: *Ab initio* calculations of the size-dependence of helium cluster excitation spectra, calculated using the newly developed ALMO-CIS+CT treatment of the electrons, together with path-integral treatment of nuclear motion.

Resonances Using Quantum Chemistry Methods (Head-Gordon, McCurdy)

Recent Progress: In contrast to scattering methods, the goal is to harness appropriately generalized versions of the powerful tools of bound state quantum chemistry. Examples include techniques such as complex absorbing potentials (CAPs), complex basis functions (CBFs), or stabilizing potentials. Under a one-off DOE SciDAC grant that recently ended, we (Head-Gordon and McCurdy) have implemented the CBF method in a modern quantum chemistry program exploiting object-oriented tools including the new SCF package developed under the support of this program. Efficient algorithms for the complex two-electron matrix elements were developed, and applied to the simple static exchange (SE) model, non-Hermitian Hartree-Fock (NH-HF), MP2 and we have completed equation-of-motion coupled cluster theory with single and double substitutions (EOM-EA-CCSD). EOM-EA-CCSD with CBFs is quite accurate (within 0.2 eV) for a range of shape resonances and the $1s2s^2$ Feshbach resonance in He^-. Additionally, an accurate and efficient analytic continuation (AC) method was very recently developed that uses a series of Hermitian bound state quantum chemistry calculations performed with stabilizing potentials to determine (the lowest) shape resonance. New appropriate continued fraction (CF) forms were determined for the Pade approximant, and a new formally justifiable stabilizing potential was introduced for the analytic continuation, defining what we term the CFAC method. This approach was used with HF and CCSD(T) methods.

Computational Analysis of Excimers and Exciplexes (Head-Gordon)

Recent progress: Experimental studies of excited states of clusters, such as the helium clusters, and related systems studied experimentally by Gessner motivate further developments in electronic structure theory. Whilst computational methodology has made tremendous advances in providing calculations of excited states in molecules, there is a corresponding challenge in analyzing those computational results that is as yet incompletely addressed. We would like to unravel the origin of red or blue shifts relative to the monomer or the origin of changes in the character in the state. The answers to these questions require quantifying the contributions from resonance, charge-transfer, etc., to excimer and/or exciplex binding. For this purpose, we have developed two versions of an energy decomposition analysis (EDA) scheme for understanding intermolecular interactions in delocalized exciplexes [Ge et al., *J. Chem. Phys.* **148**, 064105 (2018)], and excimers [Ge et al., *J. Chem. Theory Comput.* (in press) (2018)]. In the EDA procedure, excited states are treated with linear response theory such as configuration interaction singles (CIS) or time-dependent density functional theory (TDDFT), and absolutely localized molecular orbitals (ALMOs) are used to define the intermediate frozen, excitonic coupling, and polarized states. The excited state intermolecular interaction energy is thereby separated into frozen, excitonic splitting, polarization and charge transfer (CT) contributions. The role of CT is illustrated in Fig. 3-9. The excitonic splitting term describes the delocalization effect as two or more degenerate local excitations couple with each other, which is often an important binding force in excimers. A maximum overlap state-tracking procedure is introduced to connect the initial fragment excitations to the constrained intermediate states, and finally to the

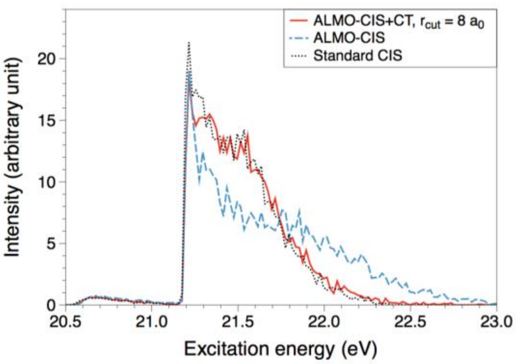

Figure 3-9: The effect of charge-transfer (CT) on the 2s and 2p excitation spectra of He clusters. The new analysis tools separate CT effects from excitonic mixing, polarization, and frozen interactions. In He clusters, CT stabilizes states at the blue edge of the 2p band.

unconstrained delocalized states of the complex. We have applied the EDA scheme to several excimer systems, including the He_2* and Ne_2 noble gas excimers, the doubly hydrogen-bonded 2-pyridone dimer, and the aromatic benzene and perylene excimers. We gained useful insights into the role each term is playing in the formation of these excimers, and the resulting method may also be useful for understanding a range of other complexes in excited states.

Future Plans: We are interested in applications of this approach to understand the effect of clustering and environment on problems such as dopants in helium clusters, and excited states of other complexes that are of interest in the program. We are also interested in extending the theory to permit analysis of intra-molecular effects analogous to the intermolecular contributions treated at present.

Peer-Reviewed Publications Resulting from this Program 2016–2018

1. Borja, L. J.; Zürch, M.; Pemmaraju, C. D.; Schultze, M.; Ramasesha, K.; Gandman, A.; Prell, J. S.; Prendergast, D.; Neumark, D. M.; Leone, S. R., Extreme Ultraviolet Transient Absorption of Solids from Femtosecond to Attosecond Timescales. *J. Opt. Soc. Am. B* **2016,** *33*, 000C57. **DOI**: 10.1364/JOSAB.33.000C57
2. Cao, W.; Warrick, E. R.; Fidler, A.; Leone, S. R.; Neumark, D. M., Near-resonant Four-wave Mixing of Attosecond Extreme-ultraviolet Pulses with Near-Infrared Pulses in Neon: Detection of Electronic Coherences. *Phys. Rev. A* **2016,** *94* (2). **DOI**: 10.1103/PhysRevA.94.021802
3. Cao, W.; Warrick, E. R.; Fidler, A.; Neumark, D. M.; Leone, S. R., Noncollinear Wave Mixing of Attosecond Xuv and Few-Cycle Optical Laser Pulses in Gas-Phase Atoms: Toward Multidimensional Spectroscopy Involving Xuv Excitations. *Phys. Rev. A* **2016,** *94* (5), 053846. **DOI**: 10.1103/PhysRevA.94.053846
4. Cao, W.; Warrick, E. R.; Neumark, D. M.; Leone, S. R., Attosecond Transient Absorption of Argon Atoms in the Vacuum Ultraviolet Region: Line Energy Shifts Versus Coherent Population Transfer. *New Journal of Physics* **2016,** *18* (1), 013041. **DOI**: 10.1088/1367-2630/18/1/013041
5. Champenois, E. G.; Shivaram, N. H.; Wright, T. W.; Yang, C.-S.; Belkacem, A., Involvement Of A Low-Lying Rydberg State In The Ultrafast Relaxation Dynamics Of Ethylene. *J. Chem. Phys.* **2016,** *144* (1), 014303 **DOI**: 10.1063/1.4939220
6. Chang, Z.; Corkum, P. B.; Leone, S. R., Attosecond Optics and Technology: Progress to Date and Future Prospects. *J. Opt. Soc. Am. B* **2016,** *33*, 1081–1097. **DOI**: 10.1364/JOSAB.33.001081
7. Chatterley, A. S.; Lackner, F.; Neumark, D. M.; Leone, S. R.; Gessner, O., Tracking Dissociation Dynamics of Strong-Field Ionized 1,2-Dibromoethane With Femtosecond Xuv Transient Absorption Spectroscopy. *Phys. Chem. Chem. Phys.* **2016,** *18*, 14644-14653. **DOI**: 10.1039/C6CP02598F
8. Chatterley, A. S.; Lackner, F.; Pemmaraju, C. D.; Neumark, D. M.; Leone, S. R.; Gessner, O., Dissociation Dynamics and Electronic Structures of Highly Excited Ferrocenium Ions Studied by Femtosecond XUV Absorption Spectroscopy. *J. Phys. Chem. A* **2016,** *120* (48), 9509-9518. **DOI**: 10.1021/acs.jpca.6b09724
9. Gaire, B.; Gatton, A.; Wiegandt, F.; Neff, J.; Janke, C.; Zeller, S.; Reedy, D.; Rajput, J.; Ben-Itzhak, I.; Landers, A. L.; Belkacem, A.; Weber, T., Bond-Rearrangement And Ionization Mechanisms In The Photo-Double-Ionization Of Simple Hydrocarbons (C_2H_4 , C_2H_3F and $1,1{-}C_2H_2F_2$) Near And Above Threshold. *Phys. Rev. A* **2016,** *94* (3). **DOI**: 10.1103/PhysRevA.94.033412
10. Gessner, O.; Gühr, M., Monitoring Ultrafast Chemical Dynamics by Time-Domain X-ray Photo- and Auger-Electron Spectroscopy. *Acc. Chem. Res.* **2016,** *49*, 138-145. **DOI**: 10.1021/acs.accounts.5b00361
11. Jones, C. F.; Bernando, C.; Tanyag, R. M. P.; Bacellar, C.; Ferguson, K. R.; Gomez, L. F.; Anielski, D.; Belkacem, A.; Boll, R.; Bozek, J.; Carron, S.; Cryan, J.; Englert, L.; Epp, S. W.; Erk, B.; Foucar, L.; Hartmann, R.; Neumark, D. M.; Rolles, D.; Rudenko, A.; Siefermann, K. R.; Weise, F.; Rudek, B.; Sturm, F. P.; Ullrich, J.; Bostedt, C.; Gessner, O.; Vilesov, A. F., Coupled Motion Of Xe Clusters And Quantum Vortices In He Nanodroplets.

Phys. Rev. B **2016,** *93* (18), 180510(R). **DOI**: 10.1103/PhysRevB.93.180510

12. Jones, J., R.; Rouet, F.-H.; Lawler, K. V.; Vecharynski, E.; Ibrahim, K. Z.; Williams, S.; Abeln, B.; Yang, C.; McCurdy, C. W.; Haxton, D. J.; Xiaoye, S. L.; Rescigno, T. N., An Efficient Basis Set Representation for Calculating Electrons in Molecules. *Mol. Phys.* **2016,** *114*, 2014. **DOI**: 10.1080/00268976.2016.1176262
13. Lackner, F.; Chatterley, A. S.; Pemmaraju, C. D.; Closser, K. D.; Prendergast, D.; Neumark, D. M.; Leone, S. R.; Gessner, O., Direct Observation Of Ring-Opening Dynamics In Strong-Field Ionized Selenophene Using Femtosecond Inner-Shell Absorption Spectroscopy. *J. Chem. Phys.* **2016,** *145* (23), 234313. **DOI**: 10.1063/1.4972258
14. Larsen, K. A.; Cryan, J. P.; Shivaram, N.; Champenois, E. G.; Wright, T. W.; Ray, D.; Kostko, O.; Ahmed, M.; Belkacem, A.; Slaughter, D. S., VUV and XUV Reflectance of Optically Coated Mirrors for Selection of High Harmonics. *Optics Express* **2016,** *24*, 18209–18216. **DOI**: 10.1364/OE.24.018209
15. Lehtola, S.; Head-Gordon, M.; Jonsson, H., Complex Orbitals, Multiple Local Minima, and Symmetry Breaking in Perdew-Zunger Self-Interaction Corrected Density Functional Theory Calculations. *J. Chem. Theor. Comput.* **2016,** *12*, 3195–3207. **DOI**: 10.1021/acs.jctc.6b00347
16. Leone, S. R.; Neumark, D. M., Attosecond Science in Atomic, Molecular, and Condensed Matter Physics. *Faraday Discuss.* **2016,** *194*, 15–39. **DOI**: 10.1039/C6FD00174B
17. Li, X.; Haxton, D. J.; Gaarde, M. B.; Schafer, K. J.; McCurdy, C. W., Direct Extraction of Intense-Field-Induced Polarization in the Continuum on the Attosecond Time Scale from Transient Absorption. *Phys. Rev. A* **2016,** *93* (2), 023401. **DOI**: 10.1103/PhysRevA.93.023401
18. López-Domínguez, J. A.; Lucchese, R. R., Effects Of Molecular Rotation After Ionization And Prior To Fragmentation On Observed Recoil-Frame Photoelectron Angular Distributions In The Dissociative Photoionization Of Nonlinear Molecules. *Phys. Rev. A* **2016,** *93* (3), 033421. **DOI**: 10.1103/PhysRevA.93.033421
19. Menssen, A.; Trevisan, C. S.; Schöffler, M. S.; Jahnke, T.; Bocharova, I.; Sturm, F.; Gehrken, N.; Gaire, B.; Gassert, H.; Zeller, S.; Voigtsberger, J.; Kuhlins, A.; Trinter, F.; Gatton, A.; Sartor, J.; Reedy, D.; Nook, C.; Berry, B.; Zohrabi, M.; Kalinin, A.; Ben-Itzhak, I.; Belkacem, A.; Dörner, R.; Weber, T.; Landers, A. L.; Rescigno, T. N.; McCurdy, C. W.; Williams, J. B., Molecular Frame Photoelectron Angular Distributions For Core Ionization Of Ethane, Carbon Tetrafluoride And 1,1-Difluoroethylene. *J. Phys. B: At. Mol. Phys. Opt.* **2016,** *49* (5), 055203. **DOI**: 10.1088/0953-4075/49/5/055203
20. Neppl, S.; Mahl, J.; Tremsin, A. S.; Rude, B.; Qiao, R.; Yang, W.; Guo, J.; Gessner, O., Towards Efficient Time-Resolved X-ray Absorption Studies Of Electron Dynamics At Photocatalytic Interfaces. *Faraday Discuss.* **2016,** *194*, 659-682. **DOI**: 10.1039/C6FD00125D
21. Ramasesha, K.; Leone, S. R.; Neumark, D. M., Real-Time Probing of Electron Dynamics Using Attosecond Time-Resolved Spectroscopy. *Annu. Rev. Phys. Chem.* **2016,** *67*, 41–63. **DOI**: 10.1146/annurev-physchem-040215-112025
22. Rescigno, T. N.; Trevisan, C. S.; Orel, A. E.; Slaughter, D. S.; Adaniya, H.; Belkacem, A.; Weyland, M.; Dorn, A.; McCurdy, C. W., Dynamics Of Dissociative Electron Attachment To Ammonia. *Phys. Rev. A* **2016,** *93* (5), 052704. **DOI**: 10.1103/PhysRevA.93.052704
23. Shivaram, N.; Champenois, E.; Cryan, J.; Wright, T.; Wingard, T.; Belkacem, A., Focal Overlap

Gating in Velocity Map Imaging to Achieve High Signal-to-Noise Ratio in Photoion Pump-Probe Experiments. *Appl. Phys. Lett.* **2016,** *109*. **DOI**: 10.1063/1.4972343

24. Slaughter, D. S.; Belkacem, A.; McCurdy, C. W.; Rescigno, T. N.; Haxton, D. J., Ion-Momentum Imaging Of Dissociative Attachment Of Electrons To Molecules. *J. Phys. B: At. Mol. Phys. Opt.* **2016,** *49* (22), 222001. **DOI**: 10.1088/0953-4075/49/22/222001
25. Sturm, F. P.; Wright, T. W.; Ray, D.; Zalyubovskaya, I.; Shivaram, N.; Slaughter, D. S.; Ranitovic, P.; Belkacem, A.; Weber, T., Time Resolved 3D Momentum Imaging Of Ultrafast Dynamics By Coherent VUV-XUV Radiation. *Rev. Sci. Instrum.* **2016,** *87*, 063110. **DOI**: 10.1063/1.4953441
26. Waitz, M.; Aslitürk, D.; Wechselberger, N.; Gill, H. K.; Rist, J.; Wiegandt, F.; Goihl, C.; Kastirke, G.; Weller, M.; Bauer, T.; Metz, D.; Sturm, F. P.; Voigtsberger, J.; Zeller, S.; Trinter, F.; Schiwietz, G.; Weber, T.; Williams, J. B.; Schöffler, M. S.; Schmidt, L. P. H.; Jahnke, T.; Dörner, R., Electron Localization in Dissociating H_2^+ by Retroaction of a Photoelectron onto Its Source. *Phys. Rev. Lett.* **2016,** *116* (4). **DOI**: 10.1103/PhysRevLett.116.043001
27. Waitz, M.; Metz, D.; Lower, J.; Schober, C.; Keiling, M.; Pitzer, M.; Mertens, K.; Martins, M.; Viefhaus, J.; Klumpp, S.; Weber, T.; Schmidt-Böcking, H.; Schmidt, L. P. H.; Morales, F.; Miyabe, S.; Rescigno, T. N.; McCurdy, C. W.; Martín, F.; Williams, J. B.; Schöffler, M. S.; Jahnke, T.; Dörner, R., Two-Particle Interference of Electron Pairs on a Molecular Level. *Phys. Rev. Lett.* **2016,** *117* (8). **DOI**: 10.1103/PhysRevLett.117.083002
28. Warrick, E. R.; Cao, W.; Neumark, D. M.; Leone, S. R., Probing the Dynamics of Rydberg and Valence States of Molecular Nitrogen with Attosecond Transient Absorption Spectroscopy. *J. Phys. Chem. A* **2016,** *120* (19), 3165-3174. **DOI**: 10.1021/acs.jpca.5b11570
29. White, A. F.; Heide, C. J.; Saalfrank, P.; Head-Gordon, M.; Luppi, E., Computation of High-Harmonic Generation Spectra of the Hydrogen Molecule using Time-Dependent Configuration-Interaction. *Mol. Phys.* **2016,** *114*, 947–956. **DOI**: 10.1080/00268976.2015.1119900
30. Wilson, B. P.; Fulfer, K. D.; Mondal, S.; Ren, X.; Tross, J.; Poliakoff, E. D.; Jose, J.; Le, A.-T.; Lucchese, R. R.; Trallero-Herrero, C., High Order Harmonic Generation from SF_6: Deconvolution of Macroscopic Effects. *J. Chem. Phys.* **2016,** *145* (22), 224305. **DOI**: 10.1063/1.4971244
31. Yip, F. L.; Rescigno, T. N.; McCurdy, C. W., Fully Differential Single-Photon Double Photoionization of Atomic Magnesium. *Phys. Rev. A* **2016,** *94* (6), 063414. **DOI**: 10.1103/PhysRevA.94.063414
32. Bernando, C.; Tanyag, R. M. P.; Jones, C.; Bacellar, C.; Bucher, M.; Ferguson, K. R.; Rupp, D.; Ziemkiewicz, M.; Gomez, L. F.; Chatterley, A. S.; Gorkhover, T.; Mueller, M.; Bozek, J.; Carron, S.; Kwok, J.; Butler, S. L.; Moeller, T.; Bostedt, C.; Gessner, O.; Vilesov, A. F., Shapes of Rotating Superfluid Helium Nanodroplets. *Phys. Rev. B* **2017,** *95* (6), 064510. **DOI**: 10.1103/PhysRevB.95.064510
33. Ge, Q.; Mao, Y.; White, A. F.; Epifanovsky, E.; Closser, K. D.; Head-Gordon, M., Simulating the Absorption Spectra of Helium Clusters (N = 70, 150, 231, 300) Using a Charge Transfer Correction to Superposition of Fragment Single Excitations. *J. Chem. Phys.* **2017,** *146* (4), 044111. **DOI**: 10.1063/1.4973611
34. Greenman, L.; Lucchese, R. R.; McCurdy, C. W., Variational Treatment of Electron-Polyatomic-Molecule Scattering Calculations Using Adaptive Overset Grids. *Phys. Rev. A*

2017, *96* (5), 052706. **DOI**: 10.1103/PhysRevA.96.052706

35. Greenman, L.; Whaley, K. B.; Haxton, D. J.; McCurdy, C. W., Optimized Pulses for Raman Excitation Through the Continuum: Verification Using the Multiconfigurational Time-Dependent Hartree-Fock Method. *Phys. Rev. A* **2017,** *96* (1), 013411. **DOI**: 10.1103/PhysRevA.96.013411
36. Ito, Y.; Carranza, R.; Okunishi, M.; Lucchese, R. R.; Ueda, K., Extraction of Geometrical Structure of Ethylene Molecules by Laser-induced Electron Diffraction Combined with *ab initio* Scattering Calculations. *Phys. Rev. A* **2017,** *96* (5), 053414. **DOI**: 10.1103/PhysRevA.96.053414
37. Liao, C.-T.; Li, X.; Haxton, D. J.; Rescigno, T. N.; Lucchese, R. R.; McCurdy, C. W.; Sandhu, A., Probing Autoionizing States of Molecular Oxygen with Xuv Transient Absorption: Electronic Symmetry Dependent Lineshapes and Laser Induced Modification. *Phys. Rev. A* **2017,** *95* (4), 043427. **DOI**: 10.1103/PhysRevA.95.043427
38. McCurdy, C. W.; Rescigno, T. N.; Trevisan, C. S.; Lucchese, R. R.; Gaire, B.; Menssen, A.; Schöffler, M. S.; Gatton, A.; Neff, J.; Stammer, P. M.; Rist, J.; Eckart, S.; Berry, B.; Severt, T.; Sartor, J.; Moradmand, A.; Jahnke, T.; Landers, A. L.; Williams, J. B.; Ben-Itzhak, I.; Dörner, R.; Belkacem, A.; Weber, T., Unambiguous Observation of F-atom Core-hole Localization in CF_4 through Body-Frame Photoelectron Angular Distributions. *Phys. Rev. A* **2017,** *95* (1), 011401. **DOI**: 10.1103/PhysRevA.95.011401
39. Ochmann, M.; von Ahnen, I.; Cordones, A. A.; Hussain, A.; Lee, J. H.; Hong, K.; Adamczyk, K.; Vendrell, O.; Kim, T. K.; Schoenlein, R. W.; Huse, N., Light-Induced Radical Formation and Isomerization of an Aromatic Thiol In Solution Followed By Time-Resolved X-ray Absorption Spectroscopy at The Sulfur K-Edge. *J. Am. Chem. Soc.* **2017,** *139* (13), 4797-4804. **DOI**: 10.1021/jacs.6b12992
40. Rist, J.; Gaire, B.; Sann, H.; Keiling, M.; Gehrken, N.; Moradmand, A.; Kunitski, M.; Ben-Itzhak, I.; Belkacem, A.; Weber, T.; Berry, B.; Zohrabi, M.; Trinter, F.; Landers, A. L.; Schoeffler, M.; Williams, J. B.; Miteva, T.; Kolorenc, P.; Gokhberg, K.; Jahnke, T.; Doerner, R., A Comprehensive Study Of Interatomic Coulombic Decay In Argon Dimers: Extracting R-Dependent Absolute Decay Rates From The Experiment. *Chem. Phys.* **2017,** *482* (SI), 185-191. **DOI**: 10.1016/j.chemphys.2016.09.024
41. Sturm, F. P.; Tong, X. M.; Palacios, A.; Wright, T. W.; Zalyubovskaya, I.; Ray, D.; Shivaram, N.; Martin, F.; Belkacem, A.; Ranitovic, P.; Weber, T., Mapping and Controlling Ultrafast Dynamics of Highly Excited H_2 Molecules by Attosecond VUV Radiation. *Phys. Rev. A* **2017,** *95* (1), 012501. **DOI**: 10.1103/PhysRevA.95.012501
42. Waitz, M.; Bello, R. Y.; Metz, D.; Lower, J.; Trinter, F.; Schober, C.; Keiling, M.; Lenz, U.; Pitzer, M.; Mertens, K.; Martins, M.; Viefhaus, J.; Klumpp, S.; Weber, T.; Schmidt, L. P. H.; Williams, J. B.; Schöffler, M. S.; Serov, V. V.; Kheifets, A. S.; Argenti, L.; Palacios, A.; Martín, F.; Jahnke, T.; Dörner, R., Imaging the Square of the Correlated Two-electron Wave Function of a Hydrogen Molecule. *Nat. Commun.* **2017,** *8*, 2266 **DOI**: 10.1038/s41467-017-02437-9
43. Warrick, E. R.; Bækhøj, J. E.; Cao, W.; Fidler, A. P.; Jensen, F.; Madsen; Leone, S. R.; Neumark, D. M., Attosecond Transient Absorption Spectroscopy Of Molecular Nitrogen: Vibrational Coherences in the b' ^{1}Σ_{u}^{+} State. *Chem. Phys. Lett.* **2017,** *683*, 408-415. **DOI**: 10.1016/j.cplett.2017.02.013
44. Weber, T.; Foucar, L.; Jahnke, T.; Schoeffler, M.; Schmidt, L.; Prior, M.; Doerner, R., The

Hydrogen Molecule under the Reaction Microscope: Single Photon Double Ionization at maximum Cross Section and Threshold (Doubly Differential Cross Sections). *J. Phys. B: At. Mol. Phys. Opt.* **2017,** *50* (16), 164002 **DOI**: 10.1088/1361-6455/aa7e3b

45. White, A. F.; Epifanovsky, E.; McCurdy, C. W.; Head-Gordon, M., Second order Moller-Plesset and coupled cluster singles and doubles methods with complex basis functions for resonances in electron-molecule scattering. *J. Chem. Phys.* **2017,** *146* (23), 234107. **DOI**: 10.1063/1.4986950
46. White, A. F.; Head-Gordon, M.; McCurdy, C. W., Stabilizing Potentials in Bound State Analytic Continuation Methods for Electronic Resonances in Polyatomic Molecules. *J. Chem. Phys.* **2017,** *146*, 044112. **DOI**: 10.1063/1.4974761
47. Wright, T. W.; Champenois, E. G.; Cryan, J. P.; Shivaram, N.; Yang, C.-S.; Belkacem, A., Ultrafast Dynamics Of The Lowest-Lying Neutral States In Carbon Dioxide. *Phys. Rev. A* **2017,** *95*, 023412. **DOI**: 10.1103/PhysRevA.95.023412
48. Cao, W.; Warrick, E. R.; Fidler, A.; Leone, S. R.; Neumark, D. M., Excited-state Vibronic Wave-packet Dynamics in H_2 Probed by XUV Transient Four-wave Mixing. *Phys. Rev. A* **2018,** *97* (2), 023401. **DOI**: 10.1103/PhysRevA.97.023401
49. Ge, Q.; Head-Gordon, M., Energy Decomposition Analysis for Excimers using Absolutely Localized Molecular Orbitals within Time-Dependent Density Functional Theory and Configuration Interaction with Single Excitations. *J. Chem. Theory Comput.* **2018,** *in press*. **DOI**: 10.1021/acs.jctc.8b0053
50. Ge, Q.; Mao, Y.; Head-Gordon, M., Energy Decomposition Analysis for Exciplexes using Absolutely Localized Molecular Orbitals. *J. Chem. Phys.* **2018,** *148* (6), 064105. **DOI**: 10.1063/1.5017510
51. Hoshino, M.; Kato, H.; Kuze, N.; Tanaka, H.; Fukuzawa, H.; Ueda, K.; Lucchese, R. R., Changes in Site-specific Shape Resonances in Nitrogen K-Shell Photoionization Of N_2O Induced by Vibrational Excitation. *J. Phys. B: Atomic, Molecular and Optical Physics* **2018,** *51* (6), 065402. **DOI**: 10.1088/1361-6455/aaaeb3
52. Hvizdos, D.; Vana, M.; Houfek, K.; Greene, C. H.; Rescigno, T. N.; McCurdy, C. W.; Curık, R., Dissociative Recombination by Frame Transformation to Siegert Pseudostates: A Comparison with a Numerically Solvable Model. *Phys. Rev. A* **2018,** *97* (2), 022704. **DOI**: 10.1103/PhysRevA.97.022704
53. Kraus, P. M.; Zürch, M.; Cushing, S. K.; Neumark, D. M.; Leone, S. R., The Ultrafast X-ray Spectroscopic Revolution in Chemical Dynamics. *Nat. Rev. Chem.* **2018,** *2* (6), 82-94. **DOI**: 10.1038/s41570-018-0008-8
54. Larsen, K.; Trevisan, C.; Lucchese, R.; Heck, S.; Iskandar, W.; Champenois, E.; Gatton, A.; Moshammer, R.; Strom, R.; Severt, T.; Jochim, B.; Reedy, D.; Weller, M.; Landers, A.; Williams, J. B.; Ben-Itzhak, I.; Dörner, R.; Slaughter, D.; McCurdy, C. W.; Weber, T.; Rescigno, T. N., Resonance Signatures in the Body-frame Valence Photoionization of CF_4. *Phys. Chem. Chem. Phys.* **2018,** *20* (32), 21075-21084 **DOI**: 10.1039/C8CP03637C
55. Martin, L.; Bello, R. Y.; Hogle, C. W.; Palacios, A.; Tong, X. M.; Sanz-Vicario, J. L.; Jahnke, T.; Schöffler, M.; Dörner, R.; Weber, T.; Martín, F.; Kapteyn, H. C.; Murnane, M. M.; Ranitovic, P., Revealing the Role of Electron-Electron Correlations by Mapping Dissociation of Highly Excited D_2+ using Ultrashort XUV Pulses. *Phys. Rev. A* **2018,** *97*

(6), 062508. **DOI**: 10.1103/PhysRevA.97.062508

56. Oosterbaan, K. J.; White, A. F.; Head-Gordon, M., Non-orthogonal Configuration Interaction with Single Substitutions for the Calculation of Core-Excited States. *J. Chem. Phys.* **2018,** *149* (4), 044116. **DOI**: 10.1063/1.5023051
57. Ranitovic, P.; Sturm, F. P.; Tong, X. M.; Wright, T. W.; Ray, D.; Zalyubovskya, I.; Shivaram, N.; Slaughter, D. S.; Belkacem, A.; Weber, T., Attosecond Coherent Control of Oxygen Dissociation by XUV-IR Laser Fields Using Three-Dimensional Momentum Imaging. *Phys. Rev. A* **2018,** *98* (1), 013410. **DOI**: 10.1103/PhysRevA.98.013410
58. Reedy, D.; Williams, J. B.; Gaire, B.; Gatton, A.; Weller, M.; Menssen, A.; Bauer, T.; Henrichs, K.; Burzynski, P.; Berry, B.; Streeter, Z. L.; Sartor, J.; Ben-Itzhak, I.; Jahnke, T.; Doerner, R.; Weber, T.; Landers, A. L., Dissociation Dynamics of the Water Dication Following One-photon Double Ionization II: Experiment. *Phys. Rev. A* **2018**. **DOI**: Accepted 7 September 2018
59. Streeter, Z. L.; Yip, F. L.; Rescigno, T. N.; Lucchese, R. R.; Gervais, B.; McCurdy, C. W., Dissociation Dynamics of the Water Dication Following One-photon Double Ionization I: Theory. *Phys. Rev. A* **2018**. **DOI**: Accepted 7 September 2018
60. Warrick, E. R.; Fidler, A. P.; Cao, W.; Bloch, E.; Neumark, D. M.; Leone, S. R., Multiple Pulse Coherent Dynamics and Wave Packet Control of the N_2 a'' $^1\Sigma_g^+$ Dark State by Attosecond Four Wave Mixing. *Faraday Discuss.* **2018**. **DOI**: 10.1039/C8FD00074C
61. Yost, S. R.; Head-Gordon, M., Efficient Implementation of NOCI-MP2 using the Resolution of the Identity Approximation with Application to Charged Dimers and Long C-C Bonds in Ethane Derivatives. *J. Chem. Theory Comput.* **2018**. **DOI**: 10.1021/acs.jctc.8b00697
62. Young, L.; Ueda, K.; Gühr, M.; Bucksbaum, P. H.; Simon, M.; Mukamel, S.; Rohringer, N.; Prince, K. C.; Masciovecchio, C.; Meyer, M.; Rudenko, A.; Rolles, D.; Bostedt, C.; Fuchs, M.; Reis, D. A.; Santra, R.; Kapteyn, H.; Murnane, M.; Ibrahim, H.; Légaré, F.; Vrakking, M.; Isinger, M.; Kroon, D.; Gisselbrecht, M.; L'Huillier, A.; Wörner, H. J.; Leone, S. R., Roadmap for Ultrafast X-ray Atomic and Molecular Physics. *J. Phys. B: At. Mol. Opt. Phys.* **2018,** *51* (3), 032003. **DOI**: 10.1088/1361-6455/aa9735
63. Zeller, S.; Kunitski, M.; Voigtsberger, J.; Waitz, M.; Trinter, F.; Eckart, S.; Kalinin, A.; Czasch, A.; Schmidt, L. P. H.; Weber, T.; Schöffler, M.; Jahnke, T.; Dörner, R., Determination of the He-He, Ne-Ne, Ar-Ar, and H_2 Interaction Potential by Wave Function Imaging. *Phys. Rev. Lett.* **2018,** *121* (083002). **DOI**: 10.1103/PhysRevLett.121.083002

PULSE Ultrafast Chemical Science

P.H. Bucksbaum, D.A. Reis, K. Gaffney, T. Heinz, T. Martinez, T. Wolf, A. Natan, J. Cryan, S. Ghimire, A. Cordones-Hahn, T. Gorkhover, SLAC National Accelerator Laboratory, 2575 Sand Hill Rd. MS 59, Menlo Park, CA 94025. Email michelley@slac.stanford.edu

Project Scope:

The PULSE Ultrafast Chemical Science program focuses on ultrafast chemical physics research at SLAC that is enabled by SLAC's x-ray and relativistic electron facilities, including LCLS, SSRL, Ultrafast Electron Diffraction (UED) and in the future, LCLS-II. Our research at SLAC makes optimal use of these unique tools for fundamental discoveries and new insights in ultrafast science. The two distinguishing advantages of this program are the on-site presence of the LCLS; and our connection to Stanford University. These help to keep us competitive on an international level.

The Ultrafast Chemical Science program has connections to many of the themes in the current BESAC Transformation Opportunities. We have particular emphasis on the transformation opportunities of "Imaging Matter across Scales", "Harnessing Coherence in Light and Matter". We also have high relevance to the Grand Challenges in the areas of "Energy and Information on the Nanoscale" and "Control at the Level of Electrons."

Imaging matter across scales: The nanoscale in space and the femtoscale in time. Microscopy at its most essential level in both space and time is paramount to the BES mission to control matter. Non-periodic nano-structures and ultrafast timescales dominate the workings of biology and chemistry. To understand and control function we therefore must first observe structure and motion on these scales.

X-ray lasers are revolutionary sources of short wavelength coherent radiation for investigations on the nanoscale, and ultrafast electrons or High Harmonics complement this new capability. PULSE subtasks are devoted to developing science using time-resolved imaging techniques at x-ray free electron lasers, (NPI and SPC subtask) ultrafst electron diffraction facilities (EIM subtask) and with laboratory sources (ATO and SFA subtasks).

Much of chemistry happens at the femtosecond scale, and it is necessary to develop new methods to simultaneously achieve this level of temporal resolution with simultaneous chemical and structural sensitivity. FEL and laser-based sources of x-ray and extreme ultraviolet radiation afford the opportunity for atomic specificity combined with femtosecond resolution. To realize this opportunity, pump-probe spectroscopy at visible and infrared wavelengths must be extended to the soft and hard x-ray range, and to new sources such as FELs. Much of our efforts are devoted to developing new methods and advancing ultrafast science in this area, including impulsive stimulated Raman and other nonlinear x-ray scattering methods.

Energy and Information: The architecture of light conversion chemistry. Light from the sun is the primary source of energy on earth, and so we are exploring light conversion to electron motion and then to chemical bonds. Some molecules are particularly adept at this conversion and we would like to understand how they work. For example, how does non-adiabatic dynamics affect the process of photocatalysis within coordination complexes and similar materials.

Energy conversion is initiated by charge separation, and we know that the charge distribution of the electron and hole, as well as the presence of low-energy ligand field excited states greatly influence the lifetime of optically generated charge transfer excited states. The detailed mechanism for the excited state quenching remains unclear. New methods of linear and nonlinear spectroscopy, and especially x-ray spectroscopy involving short-pulse FELs, can help provide the answer.

An equally important problem is the protection of some chemical bonds, particularly in biology, from destruction in the presence of ultraviolet sunlight. Photoprotection is also an ultrafast process involving charge transfer, and so these new techniques such as ultrafast x-ray absorption and Auger emission can show how critical bonds are protected.

The incorporation of theory within this FWP is critical for rapid progress in light conversion chemistry, and helps us to focus our efforts in areas of greatest impact.

Harnessing coherence on the eV scale in time, space, and field strength. This is the fundamental scale that determines structure and dynamics of electrons in molecules, and motivates advances in sub-femtosecond time-resolution and Angstrom spatial resolution in theory and experiments. To achieve an adequate view of the molecular realm with at this level, we must interrogate atoms with fields comparable to Coulomb binding fields and even beyond this, and on time scales set by the fundamental energy splittings in atoms.

One method to reach this scale is through nonlinear frequency conversion, known as high harmonic generation (HHG). We now have sources of attosecond pulsed vacuum ultraviolet radiation based on HHG, and are beginning to use them to develop new spectroscopies that can detect the motion of electrons within molecules.

We are particularly interested in the response of atoms to ultrastrong fields, from infrared to x-rays. Issues here range from mechanisms for enhanced ionization of infrared light, to new discoveries in nonlinear x-ray Compton scattering, to our most recent first test of nonlinear nuclear photoabsorption using the strongest available focused x-ray fields. New theoretical approaches are also required for this, and we are tackling these as well.

LCLS is also capable of sub-femtosecond or few femtosecond pulses, and these have the unique property of wavelengths short enough to reach the most deeply bound electrons in first through third row atoms. We can use LCLS to image the strong-field electronic response during HHG in solids at the atomic-scale in length and time, and to explore nonlinear x-ray Compton scattering and other coherent multi-x-ray processes as a means to achieve simultaneous chemical and structural sensitivity. Through the use of novel methods such as low bunch charge, double-slotted spoilers, enhanced SASE, strong laser fields, and novel data sorting methods, as well as future methods such as self-seeding, we will incorporate LCLS fully as a tool for sub-femtosecond spectroscopy.

Recent Progress:

Our Ultrafast Chemical Science programs are described fully in the abstracts for those subtasks, which follow this overview.

Awards and Prizes: Awards and prizes for scientists in this program included David Reis' elevation to Fellow in the Optical Society, and the LCLS Young Investigator Award for Tais Gorkhover. Gorkhover also received a DOE Early Career Award.

Management Structure: This Ultrafast Chemical Science research program resides within the Chemical Science Division within the SLAC Energy Sciences Directorate. The current ES ALD is Tony Heinz. Jo-Anne Hewett is the Acting Associate Laboratory Director for the Science Directorate.

Space allocations: Most of our research activities take place in laboratories in SLAC Building 40a. SLAC currently provides office space for our research groups, and also allocates approximately 8000 square feet to research laboratories and a computer room for this FWP. The co-location of most of our program within Building 40 and 40a is a distinct advantage, but is not entirely sufficient for the space requirements of this program, and so we also perform some of this research in PULSE Institute space within the Varian Physics Lab and the Keck Chemistry Lab on the Stanford campus (approximately 1000 square feet, including offices and labs, in each building).

Connections to other units within the SLAC organizational structure: Close collaborations are maintained with the Science R&D Division within the LCLS Directorate; the Materials Science Division (SIMES) within the Science Directorate; SSRL; and the SUNCAT Center within our own Chemical Sciences Division, as shown in figure 4.1. Our location near these facilities and research organizations at SLAC greatly aids collaboration.

Other important connections: The PIs have affiliations with other Stanford University research and academic units: All members of this FWP are members of the Stanford PULSE Institute, and several are affiliated with the SIMES Institute, Bio-X, the Ginzton Laboratory, and the Departments of Chemistry, Physics, and Applied Physics.

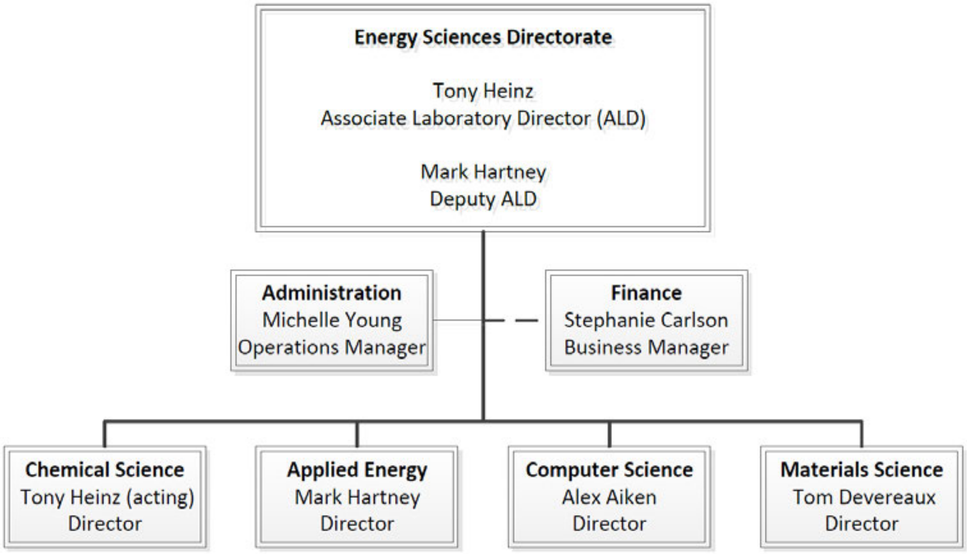

Figure 1. Partial organization chart for SLAC, showing the relation of the Chemical Science Division where this PULSE FWP sits to other units with close research ties.

We also have collaborative connections to other outside research labs, including DESY, the Lawrence Berkeley Laboratory, the Center for Free Electron Lasers (CFEL) in Hamburg, and BES funded groups at the University of Michigan, the Ohio State University, the University of Connecticut, Louisiana State University, Weizmann Institute, and Northwestern University.

Knowledge transfer to LCLS and LCLS-II: Transfer of knowledge to and from LCLS and LCLS-II is extremely fluid and critical to our success. Much of our research creates benefits for the x-ray laser facilities by providing new research methods and research results, and in addition there are several more direct transfers of our research product to help LCLS:

- We continue to help to commission several LCLS-II instruments and setup space. Particularly noteworthy are:
    - We are helping to design, build, and commission attosecond streak capabilities for the XLEAP attosecond pulse initiative, which is scheduled for its first trial this fall.
    - We have secured LDRD funding to build and commission experimental instruments that can use the LCLS-II prototype 100 kHz OPCPA for attosecond x-ray transient absorption.
- Some of our graduate students provide user support through to LCLS users, particularly in cooperation with CXI, AMO, and the Laser Division, and they receive salary supplements for this work. This activity has been endorsed by review panels and is supported by the Associate Laboratory Directors and the SLAC Director.
- Several of our postdocs and students have transferred to permanent staff positions at LCLS.
- Several LCLS Scientists and Staff have become members of the PULSE Institute, and this provides a connection to the larger research community of Stanford.
- Some LCLS Instrument Scientists have a direct connection to the research activities of this FWP. In the previous year this included collaborations with XPP, AMO, and CXI scientists.

- PULSE has helped LCLS to institute a Graduate Fellowship program, and PULSE manages several LCLS graduate student campus appointments.
- PULSE conducts an annual Ultrafast X-ray Summer School to train students and postdocs about LCLS science opportunities.

Advisory committee: The SLAC Science Policy Committee advises SLAC and the Stanford Provost on all science activities at the laboratory. Neither the SLAC Chemical Sciences Division nor the SLAC Science Directorate has their own standing science advisory committee at present. The PULSE External Advisory Board advises us on our DOE activities. This board meets annually and reports to the PULSE Director and to the Stanford Dean of Research. The reports are also forwarded to the SLAC Director, the ALD for Science, and to the SLAC Science Policy Committee.

Educational programs and outreach activities: We have an active outreach and visitors program supported by Stanford through the PULSE Institute. In this past year visitors have included Massimo Alterelli, Keith Nelson, and Peter Hommelhof.

PULSE continues to serve the larger ultrafast community with our annual Ultrafast X-ray Summer School. This school, which was founded by the PIs of this FWP in 2007, continues to be a main mechanism for expanding the research community interested in using x-ray free electron lasers for their research. The twelfth annual UXSS was at SLAC in Summer, 2018.

Future Plans:

We are currently working with SLAC and our Advisory Committee to plan utilization of a new laboratory building, the Arillaga Science Center, which is nearing completion adjacent to the PULSE laboratories. We would especially like to use this new space to create space for joint activities with scientists at LCLS and LCLS-II.

Subtasks and allocations, and future plans: Seven key personnel are responsible for six subtasks, which represent six different areas of expertise:

1. UTS: Ultrafast Theory and Simulation (Martinez)
2. ATO: Attoscience (Cryan, Bucksbaum)
3. SPC: Solution Phase Chemistry (Cordones-Hahn, Gaffney)
4. NPI: Non-periodic X-ray Imaging (Natan)
5. SFA: Strong Field AMO Physics (Bucksbaum, Natan)
6. NLX: Nonlinear X-ray Science (Reis, Ghimire)
7. EDN: Electron Dynamics on the Nanoscale (Heinz)
8. EIM: Excitations in Molecules (Wolf)

Tais Gorkhover (EC, Panofsky)

The most significant change this year has been the success of Panofsky Fellow Tais Gorkhover in developing a new program with an Early Career award. We anticipate adding her to the FWP in the future as her career progresses. In addition, Shambhu Ghimire is completing his last year of his Early Career Award, and has been invited to submit a proposal for a new subtask for our upcoming renewal.

Support operations (finance, HR, safety, purchasing, travel) are directed by the Associate Laboratory Director for Energy Sciences, and the Chemical Sciences Director staff. They provide oversight and delegate the work to appropriate offices in the SLAC Operations Directorate or to the staff of the Stanford PULSE Institute.

UTS: Ultrafast Theory and Simulation (Todd J. Martínez, PI), SLAC National Accelerator Laboratory, 2575 Sand Hill Road, Menlo Park, CA, 94025, toddmtz@slac.stanford.edu

Program Scope: This program is focused on developing and applying new methods for describing molecular dynamics on electronically excited states, as well as the interaction of molecules with radiation fields. We continue to develop and apply the *ab initio* multiple spawning (AIMS) method that solves the electronic and nuclear Schrodinger equations simultaneously from first principles, including the treatment of cases where the Born-Oppenheimer approximation breaks down (e.g. around conical intersections where two or more electronic states are exactly degenerate). We are working to extend this methodology to incorporate the effects of novel pump and probe pulses using high energy photons, including those obtained from modern x-ray sources such as LCLS. We are also extending these approaches to predict and interpret diffraction signals from ultrafast electron and X-ray experiments. Primary application areas include understanding the behavior of molecular excited states in paradigmatic phenomena such as light-induced isomerization, excited state proton transfer, and excitation energy transfer.

Recent Progress

Femtosecond time-resolved photoelectron spectroscopy (TRPES) of butadiene: In a close collaboration with experimentalists (Stolow, U Ottawa), we have studied the femtosecond photodynamics of trans-butadiene, the smallest conjugated polyene and long a paradigm for cis-trans isomerization. Through simulation results, we were able to show that the experiment had observed the elusive transition from the bright B state to the dark A state (as seen by the delayed appearance of the two-photon ionized signal for photoelectron kinetic energy greater than 1.5eV in Figure 1). The electronic structure (computed simultaneously with the nonadiabatic dynamics) was computed with multireference perturbation theory, which includes dynamic electron correlation and is expected to be quite accurate. Indeed, the simulated and experimental TRPES are in excellent agreement, as shown in Figure 1. (Boguslavskiy, et al. J. Chem. Phys. 2018; Glover, et al. J. Chem. Phys. 2018)

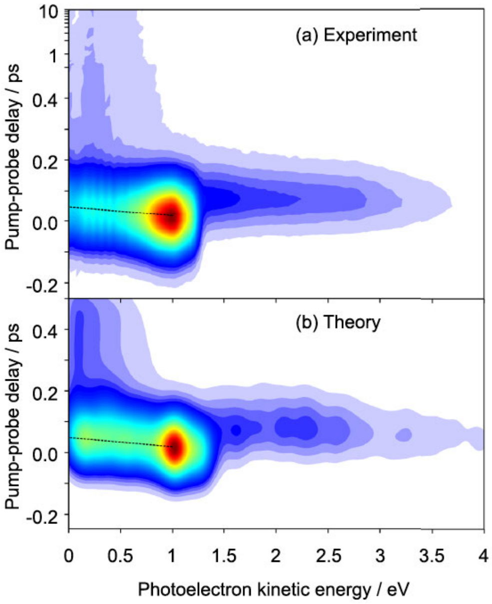

Figure 1. Comparison of experimental (top) and simulated (bottom) TRPES spectra for trans-butadiene. Simulations use AIMS with MS-CASPT2 for potential energy surfaces and couplings.

Ultrafast Electron Diffraction of CF_3I and Cyclohexadiene Ring-Opening: We have initiated numerous collaborations with the ultrafast electron diffraction team centered at SLAC. Two recent cases involved femtosecond diffraction of photoexcited CF_3I and cyclohexadiene (CHD). AIMS modeling of CF_3I indicated that one might be able to observe wavepacket splitting after two-photon absorption. Indeed, this signal was present in the diffraction data, as shown below in Figure 2. (Yang, et al. Science 2018). This work showed that complex dynamics including wavepacket splitting due to nonadiabatic transitions could be observed with UED. The simulation and the experiment are in excellent agreement and the simulation provides detailed information about the electronic state character involved at different points in time. Application of a ridge finding algorithm to the experimental data highlights the wavepacket trajectory, and enhances the comparison of theory and experiment.

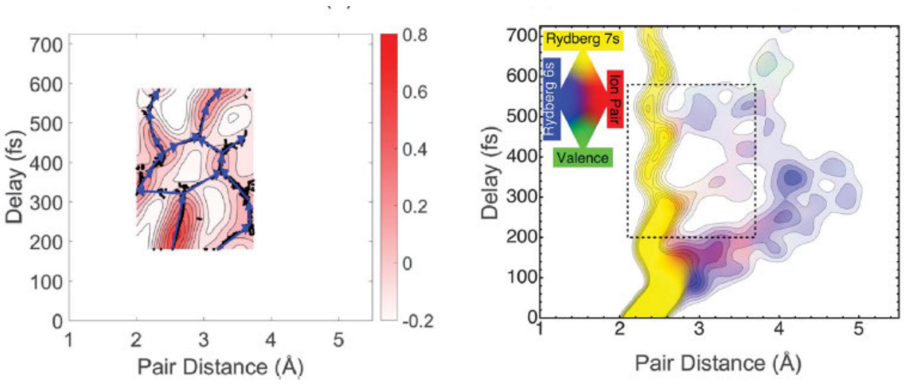

Figure 2. Comparison of experimental (left) and simulated (right) ultrafast electron diffraction data (in pair distance space) for CF_3I after two-photon photoexcitation to the 7s Rydberg state. A nonadiabatic transition to the 6s Rydberg state mediated by an ion pair state is visible at 100 fs in the simulated data. The region in dotted lines in the right panel corresponds to the rectangular region in the left panel.

Efficient Calculation of Diffraction Signals Directly from Ab Initio Molecular Dynamics: The usual interpretation of diffraction experiments relies on the independent atom model (IAM) which posits that the electron density can be written as a sum of spherical atomic densities. This is clearly sufficient to extract nuclear dynamics (i.e. to make “molecular movies”), but it cannot provide any information about the evolving electron density. We have explored the possibility of computing scattering signals directly from electronic densities computed in AIMS – this opens the door to simultaneous measurement of nuclear motion and electronic transitions. We developed an efficient graphical processing unit (GPU)-accelerated scattering code which can compute diffraction signals from ab initio electron densities for molecules with more than 10 atoms in a few seconds. This enables the routine computation of diffraction patterns beyond the IAM. In Figure 3, we compare the results of full ab initio X-ray scattering from an AIMS simulation of ethylene photoexcited to the 3s Rydberg state with an IAM analysis of the same excited state dynamics simulation. This simulation predicts that X-ray diffraction can observe the electronic density for this case of a Rydberg excitation, mandating analysis with full ab initio scattering.

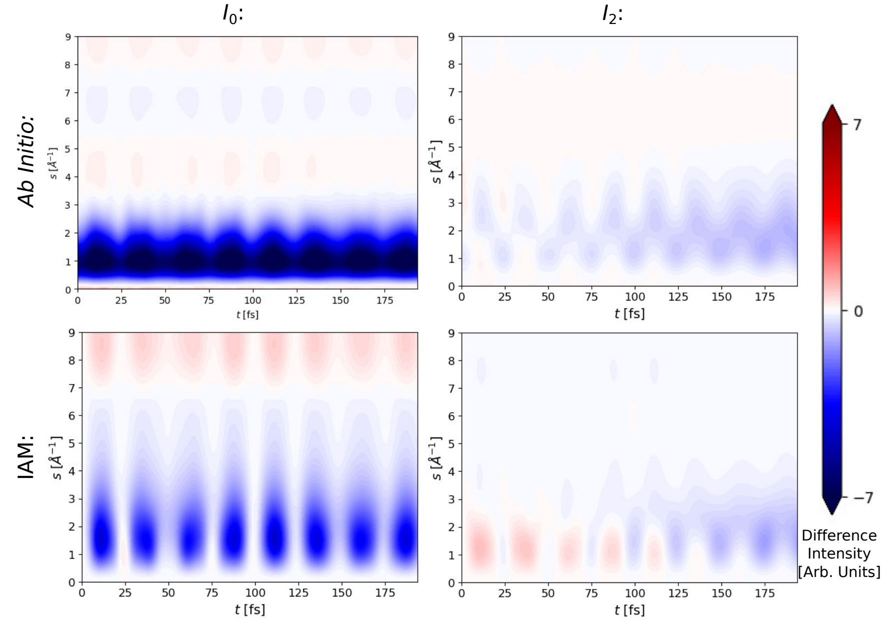

Figure 3. Comparison of full ab initio X-ray scattering and IAM analysis (both zeroth and second moments) for photoexcitation of ethylene to the 3s Rydberg state. The difference in the signal shows that experimental visualization of the electronic density may be possible for this molecule.

Future Plans

Over the next year, we will explore a number of possible molecules where either X-ray or electron diffraction might be able to observe both nuclear and electronic dynamics, leveraging the newly developed full ab initio scattering analysis code. We will also continue the development of generalized ab initio multiple spawning (GAIMS) which can simulate both internal conversion and intersystem crossing. We will apply this to excited state dynamics of metal complexes like $Fe(CO)_5$.

References

Wolf, T. J. A., D. M. Sanchez, J. Yang, R. M. Parrish, J. P. F. Nunes, M. Centurion, R. Coffee, J. P. Cryan, M. Guehr, K. Hegazy, A. Kirrander, R. K. Li, J. Ruddock, X. Shen, T. Veccione, S. P. Weathersby, P. M. Weber, K. Wilkin, H. Yong, Q. Zheng, X. J. Wang, M. P. Minitti, T. J. Martínez, Imaging the Photochemical Ring-Opening of 1,3-Cyclohexadiene by Ultrafast Electron Diffraction, in preparation for submission to Nature Chemistry.

Parrish, R. M. and T. J. Martínez, Ab Initio Computation of Rotationally-Averaged Pump-Probe X-Ray and Electron Diffraction Signals, in preparation for submission to J. Chem. Theo. Comp.

Peer-Reviewed Publications Resulting from this Project (2016-2018)

Curchod, B. F. E., A. Sisto, and T. J. Martínez. (2016). Ab Initio Multiple Spawning Photochemical Dynamics of DMABN Using GPUs. J. Phys. Chem. A 121:265.

Liu, L., J. Liu and T. J. Martínez. (2016). Dynamical Correlation Effects on Photoisomerization: Ab Initio Multiple Spawning Dynamics with MS-CASPT2 for a Model trans-Protonated Schiff Base. J. Phys. Chem. B 120:1940.

Snyder, Jr., J. W., B. F. E. Curchod, and T. J. Martínez. (2016). GPU-Accelerated State-Averaged Complete Active Space Self-Consistent Field Interfaced with Ab Initio Multiple Spawning Unravels the Photodynamics of Provitamin D3. J. Phys. Chem. Lett. 7:2444.

Filatov, M., T. J. Martínez and K. S. Kim. (2016). Using the GVB Ansatz to develop ensemble DFT method for describing multiple strongly correlated electron pairs. Phys. Chem. Chem. Phys. 18:21040.

Filatov, M., F. Liu, K. S. Kim, and T. J. Martínez. (2016). Self-consistent implementation of ensemble density functional theory method for multiple strongly correlated electron pairs. J. Chem. Phys. 145:244104.

Curchod, B. F. E., C. Rauer, P. Marquetand, L. Gonzalez, and T. J. Martínez. (2016). Communication: GAIMS-Generalized Ab Initio Multiple Spawning for both internal conversion and intersystem crossing processes. J. Chem. Phys. 144:101102.

Mignolet, B., B. F. E. Curchod, and T. J. Martínez. (2016). Rich Athermal Ground-State Chemistry Triggered by Dynamics through a Conical Intersection. Ang. Chem. Int. Ed. 55:14993.

Mignolet, B., B. F. E. Curchod, and T. J. Martínez. (2016). Communication: XFAIMS-eXternal Field Ab Initio Multiple Spawning for electron-nuclear dynamics triggered by short laser pulses. J. Chem. Phys. 145:191104.

Li, Z., L. Inhester, C. Liekhuas-Schmaltz, B. F. E. Curchod, J. W. Snyder, Jr., N. Medvedev, J. Cryan, T. Osipov, S. Pabst, O. Vendrell, P. Bucksbaum, and T. J. Martínez. (2017). Ultrafast isomerization in acetylene dication after carbon K-shell isomerization. Nat. Comm. 8:453.

Kjonstad, E. F., R. H. Myhre, T. J. Martínez and H. Koch. (2017). Crossing conditions in coupled cluster theory. J. Chem. Phys. 147:164105.

Filatov, M., F. Liu, and T. J. Martínez. (2017). Analytical derivatives of the individual state energies in ensemble density functional theory method. I. General formalism. J. Chem. Phys. 147:034113.

Li, X., R. M. Parrish, F. Liu, S. I. L. Kokkila Schumacher, and T. J. Martínez. (2017). An Ab Initio Exciton Model Including Charge-Transfer Excited States. (2017). J. Chem. Theo. Comp. 13:3493.

Nabo, L. J., J. M. H. Olsen, T. J. Martínez, and J. Kongsted. (2017). The Quality of the Embedding Potential is Decisive for Minimal Quantum Region Size in Embedding Calculations: The Case of the Green Fluorescent Protein. J. Chem. Theo. Comp. 13:6230.

Martínez, T. J. (2017). Ab Initio Reactive Computer Aided Molecular Design. Acc. Chem. Res. 50:652.

Sisto, A., C. Stross, M. W. van der Kamp, M. O'Connor, S. McIntosh-Smith, G. T. Johnson, E. G. Hohenstein, F. R. Manby, D. R. Glowacki, and T. J. Martínez. (2017). Atomistic non-adiabatic dynamics of the LH2 complex with a GPU-accelerated ab initio exciton model. Phys. Chem. Chem. Phys. 19:14924.

Filatov, M., T. J. Martínez and K. S. Kim. (2017). Description of ground and excited electronic states by ensemble density functional method with extended active space. J. Chem. Phys. 147:064104.

Lefrancois, D., D. Tuna, T. J. Martínez, A. Dreuw. (2017) The Spin-Flip Variant of the Algebraic Diagrammatic Construction Yields the Correct Topology of S1/S0 Conical Intersections. J. Chem. Theo. Comp. 13:4436.

Wolf, T. J. A., F. Holzmeier, I. Wagner, N. Berrah, C. Bostedt, J. Bozek, P. Bucksbaum, R. Coffee, J. Cryan, J. Farrell, R. Feifel, T. J. Martínez, B. McFarland, M. Mucke, S. Nandi, F. Tarantelli, I. Fischer, M. Guehr. (2017). Observing Femtosecond Fragmentation Using Ultrafast X-ray-Induced Auger Spectra. Appl. Sci. 7:681.

Wolf, T. J. A., R. H. Myhre, J. P. Cryan, S. Coriani, R. J. Squibb, A. Battistoni, N. Berrah, C. Bostedt, P. Bucksbaum, G. Coslovich, R. Feifel, K. J. Gaffney, J. Grilj, T. J. Martínez, S. Miyabe, S. P. Moeller, M. Mucke, A. Natan, R. Obaid, T. Osipov, O. Plekan, S. Wang, H. Koch, and M. Guehr. (2017). Probing ultrafast pipi*/npi* internal conversion in organic chromophores via K-edge resonant absorption. Nat. Comm. 8:29.

Curchod, B. F. E. and T. J. Martínez, (2018). Ab Initio Nonadiabatic Quantum Molecular Dynamics. Chem. Rev. 118:3305.

Boguslavskiy, A. E., O. Schalk, N. Gador, W. J. Glover, T. Mori, T. Schultz, M. S. Schuurman, T. J. Martínez and A. Stolow. (2018). Excited state non-adiabatic dynamics of the smallest polyene, trans 1,3-butadiene. I. Time-resolved photoelectron-photoion coincidence spectroscopy. J. Chem. Phys. 148:164302.

Glover, W. J., T. Mori, M. S. Schurrman, A. E. Boguslavskiy, O. Schalk, A. Stolow, and T. J. Martínez. (2018). Excited state non-adiaabtic dynamics of the smallest polyene, trans 1,3-butadiene. II. Ab initio multiple spawning simulations. J. Chem. Phys. 148:164303.

Yang, J., X. Zhu, T. J. A. wolf, Z. Li, J. P. F. Nunes, R. Coffee, J. P. Cryan, M. Guehr, K. Hegazy, T. F. Heinz, K. Jobe, R. Li, X. Shen, T. Veccione, S. Weathersby, K. J. Wilkin, C. Yoneda, Q. Zheng, T. J. Martínez, M. Centurion, and X. Wang. (2018). Imaging CF3I conical intersection and photodissociation dynamics with ultrafast electron diffraction. Science 361:64.

Li, T. E., A. Nitzan, M. Sukharev, T. Martínez, H.-T. Chen, and J. E. Subotnik. (2018). Mixed quantum-classical electrodynamics: Understanding spontaneous decay and zero-point energy. Phys. Rev. A. 97:032105.

Sachse, T., T. J. Martínez, B. Dietzek, and M. Presselt. (2018). A Program for Automatically Predicting Supramolecular Aggregates and Its Application to Urea and Porphin. J. Comp. Chem. 39:763.

Hollas, D., L. Sistik, E. G. Hohenstein, T. J. Martínez, and P. Slavicek. (2018). Nonadiabatic Ab Initio Molecular Dynamics with Floating Occupation Molecular Orbital-Complete Active Space Configuration Interaction Method. J. Chem. Theo. Comp. 14:339.

ATO: Attosecond Science

PIs: James Cryan and Phil Bucksbaum
jcryan@slac.stanford.edu, phb@slac.stanford.edu
Stanford PULSE Institute, SLAC National Accelerator Laboratory
2575 Sand Hill Rd. Menlo Park, CA 94025

Project Scope: All photochemical transformations are initially driven by electron motion. Thus in order to more fully understand photon driven chemistry, we would like to track the evolution of electrons on their intrinsic timescale. For isolated molecules in the gas phase, this natural timescale is in the attosecond domain.

The ATO task is focused on understanding how coherent superpositions of electronic states evolve in time, and how these superpositions couple to other degrees of freedom in the molecular system. Moreover, the ability to measure real-time information of electron dynamics on attosecond timescales leads to a number of open-ended questions. For example, the nature of the information that is encoded in attosecond measurements, and how this information can be retrieved from the measurement, is still an active field of study.

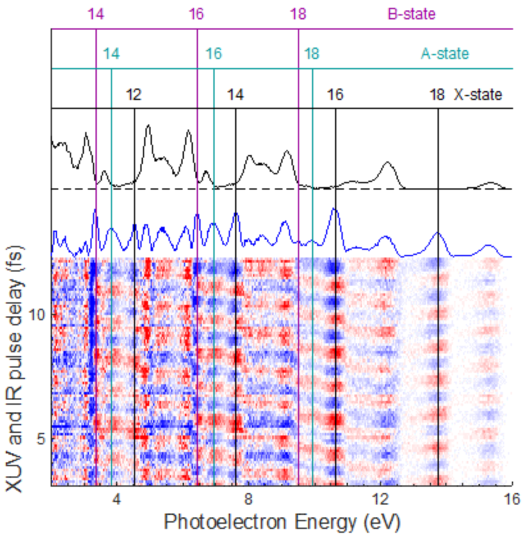

Figure 1 - Measured photoelectron kinetic energy spectrum from CO_2 exposed to an attosecond pulse train (top, black line). The colored axes show the expected energetic position of electrons for the different cationic states of CO_2. The lower panel shows the yield of photoelectrons as the delay between the IR and XUV pulses is changed. The time-averaged spectrum has been subtracted to increase the contrast. The middle plot (blue line) shows the amplitude of the 2ω oscillation as a function of photoelectron kinetic energy, demonstrating well resolved side-band peaks for the *X*, *A*, and *B* states of the CO_2 cation.

Recent Progress: One of the current research focuses of the ATO task is to understand the effect of the molecular potential on the dynamics of photoionization. To this end, we employ the well-known RABBITT technique to measure so-called photoionization delay associated with molecular photoionization[1], [2]. The RABBITT technique has been used to resolve ionization dynamics in a number of different atomic systems. The application of the RABBITT technique to systems that lack spherical symmetry, i.e. molecular systems, is more challenging. Molecular targets often have multiple accessible cationic states, which lead to substantial overlap of features in the photoelectron spectra (see Fig 1). In addition, the partial-wave expansion of the outgoing photoelectron wavepacket can contain a large number of contributions, all of which add coherently, a challenge not typically encountered in atomic targets. In order to focus the effect of the molecular potential, we reference our molecular RABBITT measurements to atomic systems with similar ionization potentials. We have collected RABITT traces for a number of molecular systems (CO_2, H_2, and NO). The CO_2 data, shown in Fig. 1, clearly demonstrates the characteristic 2ω oscillation of the electron yield with XUV-IR delay [1]. We observe well-resolved peaks in the amplitude of the 2ω oscillation (middle trace in Fig. 1), which align with the expected energetic positions of the harmonic sidebands for the various final cationic states of CO_2. Interleaving scans of a krypton reference gas we are able to remove measurement-induced contributions to the phases of these oscillations, and retrieve the molecular photoionization time delays, shown in Fig. 2. The *X*-state shows minimal delays consistent with low-order partial waves. Both the *A* and *B* cationic continua show much longer delay times for the low energy electrons. This is consistent with higher-order partial waves for the outgoing electron and the existence of a σ_g shape resonance just above threshold for these channels

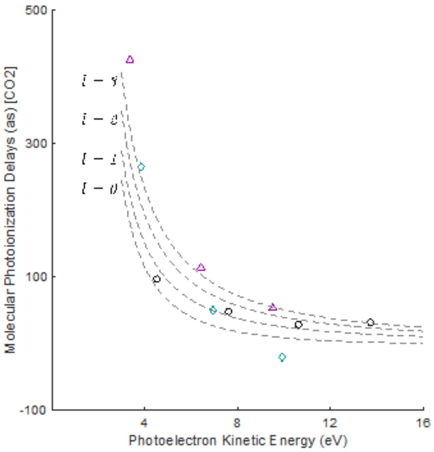

Figure 2 - Extracted molecular photo-ionization delays for the *X* (black), *A* (teal), and *B* (magenta) final states of the CO_2 cation. The dashed curves show the calculated values of the laser-assisted photoionization delays in atomic hydrogen.

The H_2 data we have collected is referenced to argon scans in a manner similar as the CO_2 data. In the case of H_2, we can resolve the vibrational structure of the H_2^+ cation, and are able to extract delay variations across the vibrational states. For the higher energy photoelectrons, there appears to be no variation in molecular photoionization time delays across vibration states, however near threshold, we see strong variations, which we will compare with the result of indirect measurements reported by Nabekawa *et al.* [3].

Another focal point of the ATO task is the development of high pulse energy, isolated attosecond pulses to be used to study electronic dynamics in molecular systems. We have been pursuing this goal both in the laboratory and at the free electron laser (FEL) facility at LCLS. Through an on-going collaboration lead by Agostino Marinelli, we have developed an electron bunch shaping method based on the ESASE technique [4]. This technique is being implemented at LCLS through the XLEAP project. Through the ATO task we have been developing research ideas based on the angular streaking technique which was recently demonstrated at LCLS by Hartmann and Helml [5]. We developed a new methodology for analyzing angular streaking data [6]. Our algorithm exploits the phase dependent energy modulation of a photoelectron ionized in the presence of a strong laser field. The energy modulation due to a circularly polarized laser field is manifest strongly in the angle-resolved photoelectron momentum distribution, as shown in the upper panel of Fig. 3, allowing for complete reconstruction of the temporal and spectral profile of an attosecond burst**.**

In FY18 we were granted LCLS User beamtime for first experiments with the new sub-femtosecond operation mode. In this experiment, we exploited the large coherent bandwidth afforded by the ESASE technique to investigate the feasibility of impulsive stimulated electronic Raman scattering (ISERS) as a method for creating excited-state electronic wavepackets. X-ray wavelengths are particularly interesting for driving ISERS since the x-rays interact most strongly with the core electrons. This means that the superposition of neutral excited states produced by x-ray stimulated Raman scattering (SXRS) will initially be highly localizied near a particular atomic-site of the molecular system [7].

Our experiment was sensitive to electronically excited neutral molecules produced by interaction with the x-ray pulse. The goal was to measure the excited state population variation as a function of the x-ray pulse energy and central photon energy. Analysis is currently underway and we intend to use this dataset to validate models for ISERS driven electronic population transfer, which we have been developing in collaboration with Daniel Haxton. We will validate Haxton's Multiconfiguration Time-Dependent Hartree Fock (MCTDHF) approach for calculating excited state populations, and to develop simple models that have substantial less computational cost.

Future Plans:

In the coming year, we have many continuing projects which we hope to complete. Firstly, we have two beamtimes at LCLS in the first quarter of FY19. The purpose of this beamtime is to make diagnostic measurements of the ESASE performance using the angular streaking technique. Then we plan to use the same setup to directly measure the Auger process in molecular systems in the time domain. We will also finish the analysis of data hoping to find signatures of impulsive Raman scattering in molecular systems.

During the LCLS shutdown, we intend to use velocity map imaging (VMI) spectrometers borrowed from LCLS to make momentum resolved measurements of photoionzation time delays via the angular streaking technique described above. All of the measurements described above are done in an angle-integrated measurement on unaligned ensembles. We will use molecular alignment with VMI spectroscopy to attempt measurements of photoionization time delays in the molecular frame.

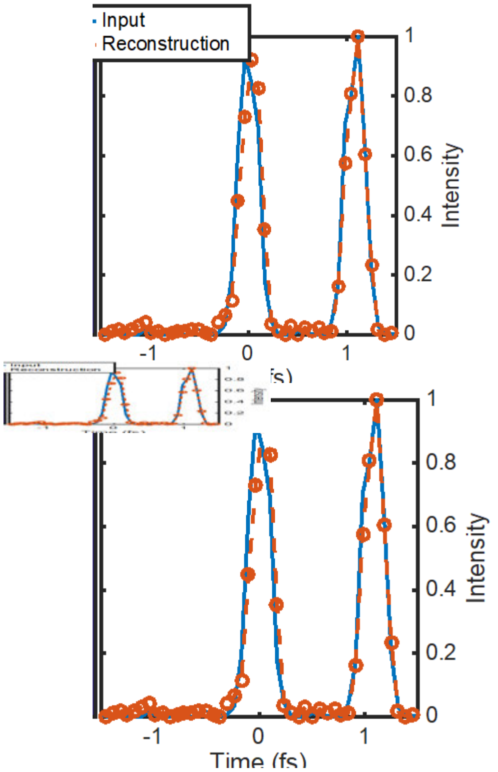

Figure 3 - Reconstruction of an electron wavepacket (EWP) with the angular streaking technique. The top panel shows a calculation of the streaked photoelectron momentum distribution from two 0.3 fs EWPs separated by 1.1 fs. The streaking laser is co-propagating with the x-ray pulse, and circularly polarized with a central wavelength of 1300 nm. The lower panel shows the temporal profile of the input laser pulse and the retrieved result using our reconstruction algorithm.

References and preprints:

[1] P. M. Paul *et al.*, “Observation of a Train of Attosecond Pulses from High Harmonic Generation,” *Science*, vol. 292, no. 5522, pp. 1689–1692, Jun. 2001.

[2] J. M. Dahlström, A. L’Huillier, and A. Maquet, “Introduction to attosecond delays in photoionization,” *J. Phys. B At. Mol. Opt. Phys.*, vol. 45, no. 18, p. 183001, 2012.

[3] Y. Nabekawa *et al.*, “Settling time of a vibrational wavepacket in ionization,” *Nat. Commun.*, vol. 6, Sep. 2015.

[4] A. A. Zholents, “Method of an enhanced self-amplified spontaneous emission for x-ray free electron lasers,” *Phys. Rev. Spec. Top. - Accel. Beams*, vol. 8, no. 4, p. 040701, Apr. 2005.

[5] N. Hartmann *et al.*, “Attosecond time–energy structure of X-ray free-electron laser pulses,” *Nat. Photonics*, vol. 12, no. 4, pp. 215–220, Apr. 2018.

[6] S. Li *et al.*, “Characterizing isolated attosecond pulses with angular streaking,” *Opt. Express*, vol. 26, no. 4, pp. 4531–4547, Feb. 2018.

[7] J. D. Biggs, Y. Zhang, D. Healion, and S. Mukamel, “Watching energy transfer in metalloporphyrin heterodimers using stimulated X-ray Raman spectroscopy,” *Proc. Natl. Acad. Sci.*, vol. 110, no. 39, pp. 15597–15601, Sep. 2013.

[preprint] Matthew R Ware, Philip H Bucksbaum, James P Cryan, Daniel J Haxton, "The attosecond regime of impulsive stimulated electronic Raman excitation." arXiv preprint arXiv:1610.01190 (2016).

[preprint] James P Cryan, Matthew R Ware, Daniel J Haxton, "Optimizing impulsive X-ray Raman scattering for population transfer in atomic systems." arXiv preprint arXiv:1609.04175 (2016).

Peer-Reviewed Publications Resulting from this Project (2016-2018):

1. Jie Yang, Xiaolei Zhu, Thomas JA Wolf, Zheng Li, J Pedro F Nunes, Ryan Coffee, James P Cryan, Markus Gühr, Kareem Hegazy, Tony F Heinz, Keith Jobe, Renkai Li, Xiaozhe Shen, Theodore Veccione, Stephen Weathersby, Kyle J Wilkin, Charles Yoneda, Qiang Zheng, Todd J Martinez, Martin Centurion, Xijie Wang, "Imaging CF3I conical intersection and photodissociation dynamics with ultrafast electron diffraction." Science **631**, 64-67 (2018)
2. Siqi Li, Zhaoheng Guo, Ryan N Coffee, Kareem Hegazy, Zhirong Huang, Adi Natan, Timur Osipov, Dipanwita Ray, Agostino Marinelli, James P Cryan, "Characterizing isolated attosecond pulses with angular streaking." Optics Express **26** 4531-4547 (2018).
3. Zheng Li, Ludger Inhester, Chelsea Liekhus-Schmaltz, Basile FE Curchod, James W Snyder, Nikita Medvedev, James Cryan, Timur Osipov, Stefan Pabst, Oriol Vendrell, Phil Bucksbaum, Todd J Martinez, "Ultrafast isomerization in acetylene dication after carbon K-shell ionization." Nature Communications **8**,453 (2017)
4. Thomas JA Wolf, Fabian Holzmeier, Isabella Wagner, Nora Berrah, Christoph Bostedt, John Bozek, Phil Bucksbaum, Ryan Coffee, James Cryan, Joe Farrell, Raimund Feifel, Todd J Martinez, Brian McFarland, Melanie Mucke, Saikat Nandi, Francesco Tarantelli, Ingo Fischer, Markus Gühr, "Observing Femtosecond Fragmentation Using Ultrafast X-ray-Induced Auger Spectra." Applied Sciences **7**, 681 (2017).
5. TJA Wolf, Rolf H Myhre, JP Cryan, Sonia Coriani, RJ Squibb, Andrea Battistoni, Nora Berrah, Christoph Bostedt, Phil Bucksbaum, Giacomo Coslovich, Raimund Feifel, KJ Gaffney, Jakob Grilj, Todd J Martinez, Shungo Miyabe, Stefan P Moeller, Melanie Mucke, Adi Natan, Razid Obaid, Timur Osipov, Oksana Plekan, Song Wang, Henrik Koch, Markus Gühr. "Probing ultrafast ππ*/nπ* internal conversion in organic chromophores via K-edge resonant absorption." Nature Communications **8**, 29 (2017).
6. JM Glownia, A Natan, JP Cryan, R Hartsock, M Kozina, MP Minitti, S Nelson, J Robinson, T Sato, T van Driel, G Welch, C Weninger, D Zhu, PH Bucksbaum, "Self-referenced coherent diffraction X-ray movie of Ångstrom-and femtosecond-scale atomic motion" Physical Review Letters **117**, 153003 (2016).
7. Chelsea Liekhus-Schmaltz, Gregory A McCracken, Andreas Kaldun, James P Cryan, and Philip H Bucksbaum 2016. "Coherent control using kinetic energy and the geometric phase of a conical intersection." The Journal of Chemical Physics **145** 144304 (2016).

SPC: Solution Phase Chemistry (Kelly Gaffney (PI), Amy Cordones-Hahn (co-PI)), SLAC National Accelerator Laboratory, 2575 Sand Hill Road, Menlo Park, CA, 94025, gaffney@slac.stanford.edu, acordon@slac.stanford.edu

Program Scope

Harnessing the strong optical absorption and photocatalytic activity of inorganic complexes depends on our ability to control fundamental physical and chemical phenomena associated with the non-adiabatic dynamics of electronic excited states. Internal conversion and intersystem crossing events governed by non-adiabatic interactions between electronic states critically influence the electronic excited state chemistry. Conventional wisdom predicts dynamics to occur with a hierarchy of time scales – vibrational energy redistribution followed first by internal conversion, and then by intersystem crossing. Contrary to conventional wisdom, ultrafast time-domain studies have shown that spin-state transitions can compete with spin-conserving electronic state transitions and both types of electronic-state transitions can occur on the time scale of vibrational energy redistribution.

There is a clear need for a new conceptual framework that can supplant the conventional wisdom for understanding electronic excited-state dynamics. The incisive observation of the electronic excited state dynamics is an essential step towards this objective. To achieve this experimental objective, the Solution Phase Chemistry (SPC) sub-task focuses on the application of ultrafast x-ray methods to the study of electronic excited state dynamics of inorganic molecules in complex chemical environments. More specifically, we endeavor to:

- Identify how excited state electron and spin density distributions control non-radiative relaxation with time resolution measurements, simple ligand exchange reactions, and simulation.
- Determine the importance of site-specific interactions between solvent and solute in electronic excited-state relaxation with ultrafast time-resolved measurements and molecular simulation.

Achieving these scientific objectives also requires development of ultrafast x-ray methods. Our previous research has emphasized the development of simultaneous hard x-ray diffuse scattering (XDS) and x-ray emission spectroscopy (XES) as probes of charge, spin, and metal-ligand bonding dynamics in electronic excited states. We currently focus on methods that will be transformed by LCLS-II, in particular soft x-ray Resonant Inelastic X-ray Scattering (RIXS) as a probe of metal-ligand covalency in electronic excited states, and the extension of ultrafast electron diffraction (UED) to solution phase dynamics.

Recent Progress

Controlling MLCT excited state lifetimes in 3d coordination complexes **(Biasin 2016; Kjaer 2017; Lemke 2017; Liang 2017; Mara 2017; Zhang 2017; Kjaer 2018a; Kjaer 2018b):** Cost effective use of light to direct chemical catalysis necessitates the use of photocatalysts derived from abundant materials, but the majority of inorganic artificial photosynthetic materials have been based on rare 4*d* and 5*d* transition metals. Replacing ruthenium dyes with iso-electronic iron dyes has been a long standing target for solar energy applications, but to date the ultrafast spin crossover dynamics have inhibited the usefulness of iron dyes.

Understanding the non-radiative relaxation mechanisms of electronic excited state requires a detailed characterization of multiple electronic excited state potential energy surfaces, the nuclear motions that access degeneracies between surfaces, and how the distinct levels couple with one another. Given the complexity of the phenomena, a coordinated effort including experiment, synthesis, theory, and simulation increases the rate of progress. Our development and application of femtosecond resolution x-ray spectroscopic probes of charge and spin dynamics in electronic excited states puts us in an excellent position to investigate the mechanism and rate of charge transfer excited state relaxation in transition metal complexes. Our research has made significant progress in two complementary directions:

- The development application of novel ultrafast x-ray methods to the investigation of internal conversion and intersystem crossing mechanisms in molecular systems well characterized by ultrafast optical methods. This includes solution phase studies of $[Fe(2,2\text{-bipyridine})_3]^{2+}$, $Fe(CO)_5$, and cytochrome C.
- Joint ultrafast optical and x-ray studies of charge transfer excited state relaxation in a series of mixed ligand complexes $[Fe(L)_{3\text{-}N}(CN)_{2N}]^{2\text{-}3N}$, where L is a series of polypridyl ligands. The interplay between chemical synthesis and ultrafast measurements has enabled us to investigate the impact of metal-ligand covalency, as well as ligand field strength and symmetry, on the rate and mechanism of internal conversion and intersystem crossing in 3*d* transition metal complexes.

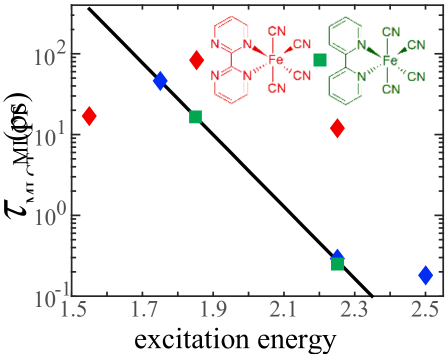

Figure 1: Dependence of the MLCT lifetime as a function of the MLCT absorption energy, where the absorption energy is modified with polypyridyl ligand exchange and changes in solvent. For the bipyrimidine containing complex (red diamond), the MLCT lifetime shows very weak absorption energy dependence, indicating a distinct relaxation mechanism for this complex compared to the other polypyridyl complexes and bringing into question whether simple ligand substitution is sufficient to control MLCT lifetime.

Our most recent investigations of $[Fe(bpy)_3]^{2+}$ and cytochrome C have demonstrated the power of ultrafast x-ray absorption, x-ray emission, and x-ray scattering studies to acquire a mechanistic characterization of non-adiabatic internal conversion and intersystem crossing in 3*d* transition metal complexes.(Lemke 2017; Mara 2017; Kjaer 2018b) We have also made significant progress on the $[Fe(L)_{3\text{-}N}(CN)_{2N}]^{2\text{-}3N}$ mixed ligand series, where L is a polypridyl ligand.(Kjaer 2017; Zhang 2017; Kjaer 2018a) These studies have increased MLCT lifetimes by a factor of 400, compared to $[Fe(bpy)_3]^{2+}$. The MLCT lifetime, however, does not follow a simple exponential dependence on the optical absorption energy (Fig. 1). This demonstrates the relaxation mechanism changes as a function of ligand composition.

Site-specific solvation and coordination dynamics in model photo-catalysts studied with X-ray diffuse scattering and spectroscopy **(Biasin 2016; van Driel 2016; Biasin 2018; Kjaer 2018a; Koroidov, 2018):** The site-specific interaction of solvent and reactants with metal centers in electronically excited molecules controls many photocatalytic reactions. Femtosecond resolution x-ray scattering provides a means of measuring the site-specific solvation and coordination dynamics of photocatalysts (van Driel 2016). Our recent work in this direction extends these studies beyond model systems to applied photocatalysts and applies multi-edge x-ray absorption spectroscopy (XAS) to resolve catalyst electronic structure and determine photochemical reaction outcomes. These studies have focused a class of Ni-centered hydrogen evolving catalysts with redox-active ligands. These ‘non-innocent’ ligands are commonly employed with first row transition metals, where the role of the ligand is to prevent uncommon oxidation or coordination states of the metal by storing charge or bonding reactants on the ligand. Multi-edge XAS allows us to map the extended orbital and charge distributions over both metal and ligand atomic sites for these highly covalent complexes. Soft and tender x-ray absorption at the Ni L-edge and S K-edge were used to identify ligand-dependent changes in the distribution of the electron accepting orbitals that participate in catalysis (Fig. 2, left), thus yielding insight to the reaction mechanisms for this class of catalyst (Koroidov, 2018). Time-resolved hard x-ray absorption at the Ni K-edge was also used to track the photochemical reaction products formed for a Ni pyridinethiolate catalyst (Fig. 2, right). Although the excited state lifetime of the catalyst is short (few ps), we observe photoreduction by electron transfer from the surrounding solvent. A secondary reaction product is also observed and assigned to the hydrogenated catalyst that is formed by proton abstraction from water.

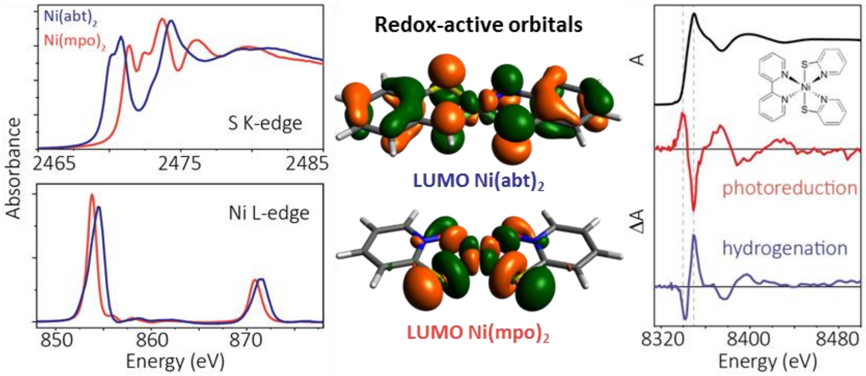

Figure 2: Ni L-edge and S K-edge XAS of two Ni-centered catalysts (left) reveal the ligand-dependent differences in metal-ligand covalency of their redox active orbitals (center). Transient Ni K-edge XAS tracks the photochemical changes in redox state and structure (left).

Future Plans

Planning for future science opportunities enabled by LCLS-II and UED **(Kunnus 2016a; Kunnus 2016b; Kunnus 2016c; Yang 2016a; Yang 2016b; Titus 2017; Wolf 2017; Cordones 2018; Jay 2018; Koralek 2018; Norell 2018)**

Femtosecond resolution RIXS: Soft x-ray spectroscopy measurements provide a powerful approach of characterizing metal-ligand bonding and covalency. These measurements have also demonstrated the clear connection between catalytic activity of molecular catalysts and the metal-ligand covalency of the catalyst. The SPC sub-task has been committed to developing ultrafast soft x-ray RIXS measurements at 3*d* metal L-edges and ligand K-edges to characterize the metal-ligand covalency of charge transfer excited states, how this covalency influences relaxation dynamics, and the catalytic activity and mechanisms of charge transfer excited states. This effort has focused on the LMCT dynamics of $[Fe(CN)_6]^{3-}$, an archetypical strong field ligand complex and has the SPC sub-task well prepared for the transformative science opportunities enabled by the increased repetition rate of LCLS-II.

Liquid jet developments for RIXS and ultrafast electron diffraction measurements: Due to the large soft x-ray absorption cross-section of dense solvent environments, ultrathin free-flowing liquid jets are an important technical development required for solution-phase soft x-ray spectroscopy at LCLS-II. We have recently implemented such sub-micron vacuum-compatible jets developed by the LCLS Sample Delivery Group for soft x-ray absorption spectroscopy (Koralek 2018). The Fe L-edge absorption spectrum was measured for an aqueous solution of $K_3Fe(CN)_6$ in transmission mode, through a liquid jet ~600 nm thick. This successful demonstration of ultra-thin liquid jets paves the way for soft x-ray solution-phase science at LCLS-II. Ultrafast electron diffraction (UED) measurements have similar sample thickness requires to eliminate multiple scattering signals that make signal analysis intractable. We are also involved in the development of a liquid jet chamber for UED measurements that will complement the ultrafast x-ray scattering studies of solution phase samples we have utilized at LCLS.

Tender X-ray Spectroscopy: Access to the tender x-ray energy range of ~2-5 keV will be enabled by LCLS-II. This new capability will provide spectroscopic access to a new range of elements and transitions relevant to solar energy applications. For example, the valence orbitals of the second row transition metals, which frequently demonstrate high efficiencies for photoredox chemistry and catalysis, can be probed in this energy range. Spectroscopic access to lighter elements, such as S and P, will also be enabled. In preparation for this new capability, we have collaborated on experiments using time-resolved tender x-ray absorption spectroscopy to resolve the photoisomerization mechanism of a ruthenium sulfoxide complex (Cordones, 2018). Access to both the Ru L-edge and S K-edge enabled tracking of the excited state electronic configuration (Ru edge) and ligand bonding configuration (S K-edge) in real-time. A detailed mechanism, highlighting the importance of metal-centered excited states, was resolved.

References

Kjaer, K. S., T. B. van Driel, T. C. B. Harlang, et al. (2018b). Finding Intersections between Electronic Excited State Potential Energy Surfaces with Simultaneous Ultrafast X-ray Scattering and Spectroscopy. Submitted.

Koroidov, S., K. Hong, K. S. Kjaer, et al. (2018) Probing the Electron Accepting Orbitals of Ni-Centered Hydrogen Evolution Catalysts with Non-Innocent Ligands by Ni L-Edge and S K-Edge X-Ray Absorption. Submitted.

Peer-Reviewed Publications Resulting from this Project (2016-2018)

Biasin, E., T. B. van Driel, K. S. Kjaer, et al. (2016). Femtosecond X-Ray Scattering Study of Ultrafast Photoinduced Structural Dynamics in Solvated $[Co(terpy)_2]^{2+}$. Phys. Rev. Lett. 117: 013002.

Biasin, E., T. B. van Driel, G. Levi, et al. (2018). Anisotropy enhanced X-ray scattering from solvated transition metal complexes. J. Synchrotron Radiat. 25: 306.

Cordones, A. A., J. H. Lee, K. Hong, et al. (2018). Transient metal-centered states mediate isomerization of a photochromic rutheniumsulfoxide complex. Nature Comm. 9: 1989.

Jay, R. M., J. Norell, S. Eckert, et al. (2018). Disentangling Transient Charge Density and Metal-Ligand Covalency in Photoexcited Ferricyanide with Femtosecond Resonant Inelastic Soft X-ray Scattering. J. Phys. Chem. Lett. 9: 3538.

Kjaer, K. S., K. Kunnus, T. C. B. Harlang, et al. (2018a). Solvent control of charge transfer excited state relaxation pathways in $[Fe(2,2\text{'-bipyridine})(CN)_4]^{2-}$. Phys. Chem. Chem. Phys. 20: 4238.

Kjaer, K. S., Z. Wenkai, R. Alonso-Mori, et al. (2017). Ligand manipulation of charge transfer excited state relaxation and spin crossover in $[Fe(2,2\text{'-bipyridine})_2(CN)_2]$. Struct. Dyna. 4: 044030

Koralek, J. D., J. B. Kim, P. Bruza, et al. (2018). Generation and characterization of ultrathin free-flowing liquid sheets. Nature Comm. 9.

Kunnus, K., I. Josefsson, I. Rajkovic, et al. (2016a). Anti-Stokes Resonant X-ray Raman Scattering for atom specific and excited state selective dynamics. New J. Phys. 18: 103011.

Kunnus, K., I. Josefsson, I. Rajkovic, et al. (2016b). Identification of the dominant photochemical pathways and mechanistic insights to the ultrafast ligand exchange of $Fe(CO)_5$ to $Fe(CO)_4EtOH$. Struct. Dyna. 3: 043204.

Kunnus, K., W. K. Zhang, M. G. Delcey, et al. (2016c). Viewing the Valence Electronic Structure of Ferric and Ferrous Hexacyanide in Solution from the Fe and Cyanide Perspectives. J. Phys. Chem. B 120: 7182.

Lemke, H., K. S. Kjær, R. W. Hartsock, et al. (2017). Coherent structural trapping through wave packet dispersion during photoinduced spin state switching. Nature Comm. 8: 15342.

Liang, H. W., T. Kroll, D. Nordlund, et al. (2017). Charge and Spin-State Characterization of Cobalt Bis(o-dioxolene) Valence Tautomers Using Co Kβ X-ray Emission and L-Edge X-ray Absorption Spectroscopies. Inorg. Chem. 56: 737.

Mara, M. W., R. G. Hadt, M. E. Reinhard, et al. (2017). Metalloprotein entatic control of ligand-metal bonds quantified by ultrafast x-ray spectroscopy. Science 356: 1276.

Norell, J., R. M. Jay, M. Hantschmann, et al. (2018). Fingerprints of electronic, spin and structural dynamics from resonant inelastic soft X-ray scattering in transient photo-chemical species. Phys. Chem. Chem. Phys. 20: 7243.

Titus, C. J., M. L. Baker, S. J. Lee, et al. (2017). L-edge spectroscopy of dilute, radiation-sensitive systems using a transition-edge-sensor array. J. Chem. Phys. 147.

van Driel, T. B., K. S. Kjær, R. W. Hartsock, et al. (2016). Atomistic characterization of the active-site solvation dynamics of a model photocatalyst. Nature Comm. 7: 13678.

Wolf, T. J. A., R. H. Myhre, J. P. Cryan, et al. (2017). Probing ultrafast $\pi\pi^*$ / $n\pi^*$ internal conversion in organic chromophores via K-edge resonant absorption. Nature Comm. 8: 29.

Yang, J., M. Guehr, T. Vecchione, et al. (2016a). Femtosecond Gas Phase Electron Diffraction with MeV Electrons. Faraday Discuss. 194: 563.

Yang, J., M. Guehr, T. Vecchione, et al. (2016b). Diffractive imaging of a rotational wavepacket in nitrogen molecules with femtosecond megaelectronvolt electron pulses. Nature Comm. 7: 11232.

Zhang, W., K. S. Kjaer, R. Alonso-Mori, et al. (2017). Manipulating charge transfer excited state relaxation and spin crossover in iron coordination complexes with ligand substitution. Chem. Sci. 8: 515.

NPI: Ultrafast X-ray Imaging of Molecules

Principal investigators: Adi Natan, Phil Bucksbaum
Stanford PULSE Institute, SLAC National Accelerator Laboratory
2575 Sand Hill Rd. Menlo Park, CA 94025
phb@slac.stanford.edu, natan@slac.stanford.edu

Staff and students: Matthew Ware, ***Collaborators:*** James Cryan, Thomas Wolf, Rob Parrish, Mike Glownia (LCLS)

Project scope:

The NPI program studies the nature of time-resolved short wavelength scattering on photoexcited molecular systems. We explore ways to image quantum dynamics de-novo using experimental and computational approaches with the aim to produce molecular movies of structural dynamics of systems of increased complexity in the sub-angstrom and femtosecond scales. We have implemented signal decomposition analysis to image different physical mechanism of excited systems such as electronic population transfer, vibrational motion, dissociation, rotational dephasing and Raman transitions in a diatomic system. We have extended or efforts to polyatomic systems and dynamics of a driven diatomic systems in a solvent environment.

Recent Progress:

Imaging complex photodissociation of transition metal complex: An understanding at the atomic level of how transition-metal complexes catalyze reactions, and in particular, the role of the short-lived and reactive intermediate states involved is of great importance for future control of photocatalytic hydrogen production and selective carbon–hydrogen bond activation. The photo-physics governing the formation of intermediate complexes such as $Fe(CO)_4$ has received a lot of attention, often focusing on the reaction pathways and molecular structures of these transient species. We are led an LCLS beam time in October 2017 aiming to capture a molecular movie of the photo-physics of CO loss from the transition metal carbonyl complex $Fe(CO)_5$ as well as further dissociations to the intermediate complex. We excited $Fe(CO)_5$ with an ultrashort UV pulse (266nm) and probed with a delayed hard X-ray pulse. The ultrafast dynamics of such excitation is complex, involves multiple states and is extremely hard to calculate using the state-of-the-art tools. We set to understand to what level the short-term coherence and anisotropy play a role in the onset of the CO loss mechanism of such system. We have evidence for very short-lived anisotropy at the pulses overlap and have measured the primary dissociation via CO loss. We also have evidence that subsequent molecular dissociation (CO loss) takes place ~1.6-1.8 ps and 4-5ps later with corresponding slower kinetic energies and a broader temporal distribution. Analysis in ongoing. We are collaborating with the Martinez group to establish a way to calculate the dynamics of such a system. While such calculations are challenging, we have identified a fast (<100 fs) dissociation channel at the molecules equatorial plane and slow (~400 fs) dissociation that also involves the axial molecular plane. Such observations support an asymmetry in the photo physics of the molecule that can manifest in the signal anisotropy. We are also collaborating with Thomas Wolf and have very recently used the ultrafast electron diffraction (UED) capability at SLAC to be able to obtain higher resolution for the average bond distances and gain more insight into the intermediate complexes following dissociation.

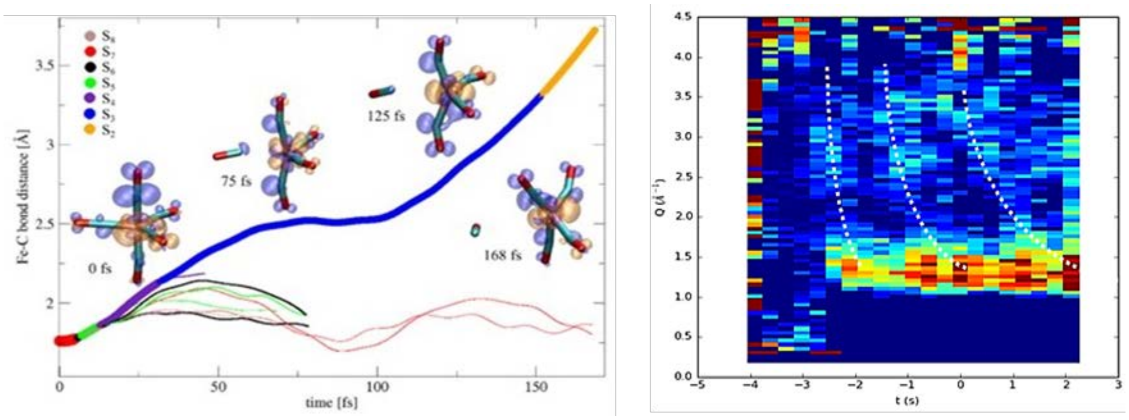

Fig 1 *(Left) Ab-initio multiple spawning calculation of Fe-C bond lengths as function of time following a UV excitation of $Fe(CO)_5$ using TDDFT for the electronic structure. As the dynamics evolves more trajectories are spawned and the population is distributed between them. The population's magnitude is represented by the thickness of the lines, and different line colors encode the singlet excited state these trajectories are populating. (Right) Measured radial distribution as function of delay (in ps) of $Fe(CO)_5$ for a specific excitation intensity, dashed lines were added to point to dissociation signals.*

Imaging coherently controlled dynamics: One of the most successful coherent control approaches in the time domain is the Tannor-Rice pump-dump scheme. In this scheme we steer an excited wavepacket into a specific state by coinciding a delayed dump pulse with a proper timed evolution of wavepacket that was born when a pump pulse excites the molecule into a particular Franck Condon region. Experimental demonstrations of this control has been performed by several groups via non-linear spectroscopy. Here, we offer a direct imaging approach of such a punp-dump experiment where we probe the excited charge density of a pump-dump scheme with a delayed X-ray probe pulse. As a result, we have access to the entire dynamics including additional states that participate as a result of time reversed dump-pump sequences. We used 520 nm to pump population from the X to the B state in diatomic Iodine vapor, and a delayed 800nm pulse to dump the population back to the X state at a larger internuclear separation. We used the Legendre decomposition approach that have developed to filter the dumped population and saw how the control scheme was effective at the proper timing of the wavepacket evolution near the outer turning point of the B state. We have also mapped a secondary channel where the 800nm dump pulse acts as a pump pulse from the ground X-state to the A-state. We further developed a Fourier decomposition in the temporal delay domain to retrieve physical parameters and efficiency of such processes as well as dissociation. (see next section).

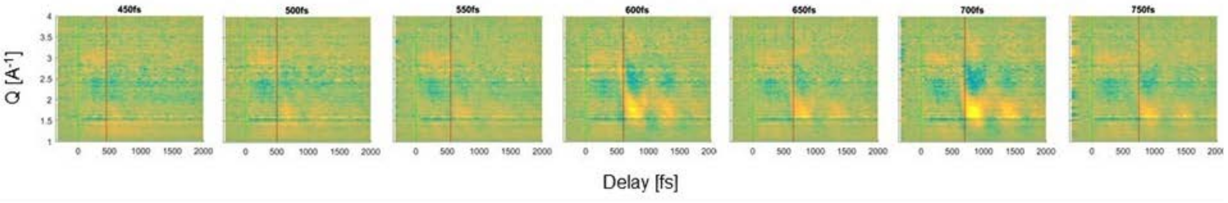

Fig 2*: Each subplot shows the momentum map as function of X-ray probe delay for different dump pulse delays as noted in the subplot titles and by the red vertical line. Note the strong onset of signal around 600fs and 700fs, corresponding to the favorable resonant coupling condition of the 800nm dump pulse to the ground state that takes place when the excited wave packet is near the outer turning point.*

Fourier Transform inelastic X-ray scattering for gas phase targets: We have extended the Fourier-transform inelastic x-ray (FTIX) scattering technique to the gas phase, enabling identification of harmonic, anharmonic, and dissociative motion. This technique was successfully used in the past to obtain dispersion curves for solids to high precision, and here we apply it to analyze the anharmonic vibrations and dissociations of molecular iodine that was measured in our previous work. This approach allows us to obtain a dispersion plot for the system under study and facilitates the retrieval of physical observables without the need to invert the scattering data. We demonstrate the ability to measure the dissociation velocity and vibrational excitation on molecular iodine in high precision.

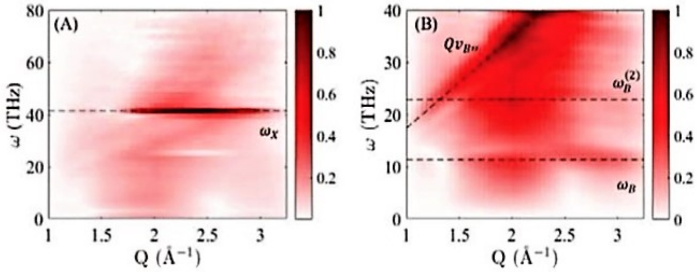

***Fig 3** the FT-IXS spectra (radially integrated scattering) at two wavelengths measured across a 3 ps delay range. (A) Exciting with 800 nm, we observe a single beat frequency at the fundamental of the X state around 40.5 THz. (B) Exciting with 520 nm, we observe the dissociation along the $Qv_{B''}$ dashed line, the slope of which yield the dissociation velocity of ~17.4 A/ps. In addition, we observe the fundamental vibrational mode and it's first overtone at 11.4 and 22.8 THz.*

Understanding ultrafast dynamics of simple systems in solvents: In June 2017 and August 2018, we studied at SACLA coherent diffraction from diatomic Iodine molecules in different solvents (ethanol and cyclohexane) in order to image molecular motion in the condensed phase using wide angle x-ray scattering. We have also developed molecular dynamics simulations with Rob Parrish to investigate the role of the solvent cage on the photo absorption process and the following dynamics, and how anisotropy can be used to study these dynamics. We show that under the experimental conditions used, iodine dissociates ballistically between 2.6 and 5 Ang in the first 150 fs of the interaction. Then it rapidly slows down and relaxes into a new bond distance where vibration motion is completely damped. We are in the process of analyzing the data form the experiment as well as modeling the angle resolved cage dynamics to obtain an effective image of iodine in methanol, and the mechanical propertied of the solvent solute interaction. The analysis is ongoing from the last experiment.

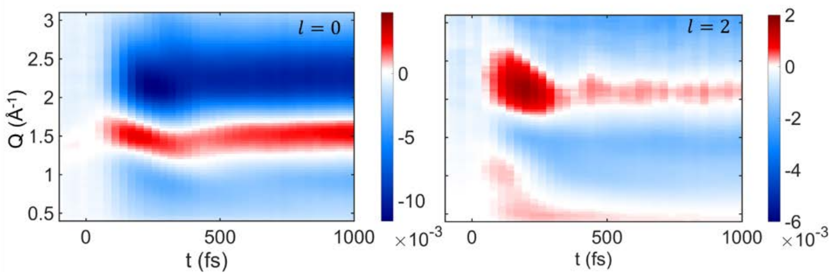

Fig 4: Measured radial and 2nd order Legendre distributions as function of delay of Iodine in methanol.

Complete Mapping of femtosecond dynamics in I_2: In February 2018, we revisited I_2 in LCLS where we systematically mapped the dynamics pumping with tunable light from 480 to 600 nm, elucidating the relative weight and position of different dipole allowed transitions. Analysis in ongoing,

Future Plan:

Polyatomic molecules and aligned ensembles: While the current Legendre decomposition approach proved successful for diatomic systems, it is not optimal for larger systems or aligned ensembles where complex angular distributions take place. We plan to study triatomic systems such as two channel dissociation in aligned CS_2 and aperiodic coherent rotational dynamics in the asymmetric top SO_2. Extending our efforts to polyatomic systems will advance the understanding of the connection between coherence and function in complex systems, a subject that is only just emerging within the scientific community. **Double blind holography in an orthogonal projection space**: We will continue to develop an holographic approach that makes use of the results we obtained, namely, to measure separately the autocorrelation of two excited states via lower order basis projection, and their cross-correlation following coherent population mixing via higher order basis projection, thus obtaining the amplitude and phase of the total wavepacket. This a new way of thinking about holography in functional space rather than in position space or time, which allows in principle to apply a protocol similar to double blind Fourier holography. We propose to use aligned CS_2, where a 200 nm photon will excite to both $S(^1D)$ and $S(^3P)$ quasi-bound channels, creating a coherent beat with time period of 80 fs that decays in about 500 fs, with several vibration periods are also taking place. Because the geometry changes during the excitation, the initial nuclear motion proceeds along the bending and symmetric stretch coordinates. **Toward imaging electronic motion in molecules:** We have contributed to the development of a method to allow single shot attosecond X-ray pulse full characterization using angular streaking of laser driven photoelectrons. In the future, this method will allow single shot characterization of the phase and amplitude two attosecond hard x-rays pulses, opening the way to develop new imaging modalities where the relative phase of the two x-ray pulses is important for reconstruction of electronic motion of excited systems.

References and material under review

Ware M., Glownia J. M., Natan A., Cryan J., and Bucksbaum P. (2018), to appear in Phil. Trans. R. Soc. A.

Ware M., Glownia J. M., Natan A., Cryan J., and Bucksbaum P. (2018), Fourier-transform inelastic x-ray scattering: A new kind of gas-phase vibrational spectroscopy, in Conference on Lasers and Electro-Optics, OSA Terchnical Digest (online) (Optical Society of America, 2018), paper FM4F.5.

Natan A., Ware, M., A., Glownia, J., Cryan, & Backsbaum, P. H., Seeing an electronic transition using ultrafast x-ray diffraction. In preparation.

“Filming non-adiabatic population transfer with x-ray diffraction”, MR Ware, JM Glownia, JP Cryan, R Hartsock, A Natan, PH Bucksbaum, arXiv:1708.03847, Physical review A (under review)

“Simultaneous x-ray imaging of A and B state dynamics in iodine at the LCLS”, M Ware, A Natan, J Cryan, P Bucksbaum, J Glownia,, Bulletin of the American Physical Society, (2017)

Publications Resulting from this Project (Project start date: 10/2016)

“Filming nuclear dynamics of iodine using x-ray diffraction at the LCLS”, M Ware, A Natan, J Glownia, J Cryan, P Bucksbaum, Bulletin of the American Physical Society (2017)

“Glownia et al. Reply”, JM Glownia, et-al Physical Review Letters 119 (6), 069302 (2017)

“Self-referenced coherent diffraction X-ray movie of Ångstrom-and femtosecond-scale atomic motion” JM Glownia, et-al, Physical review letters 117 (15), 153003 (2017)

SFA: Strong Field AMO Physics

PIs: Phil Bucksbaum and Adi Natan
Stanford PULSE Institute, SLAC National Accelerator Laboratory
2575 Sand Hill Rd. Menlo Park, CA 94025
phb@slac.stanford.edu, natan@slac.stanford.edu

Participants: *Phil Bucksbaum, Adi Natan, Anna Wang, Matt Ware, Andy Kaldun, James Cryan, David Reis*

Project Scope

The Strong Field AMO task investigates the dynamics, and control of atoms and molecules in externally applied strong coherent electromagnetic fields, from optical to x-ray frequencies. X-ray free electron lasers are a source of some of the strongest electromagnetic fields available, up to kilovolts per Angstrom. We study strong-field excitation of external and internal quantum coherences in molecules to gain a deeper understanding of strong-field ionization and field-induced changes in symmetry and topology as well as strong-field quantum control.

This year we experienced significant turnover in this group. Andreas Kaldun has returned to Germany to take up an opportunity in industry. Anna Wang has elected to join the ATO group rather than continue her work on SFA analysis of our results in H2O. A new postdoc and new graduate student will join this group this fall. Meanwhile, ongoing work with significant new results include a new experimental measurement of the relative time delays of tunnel-ionized electrons with different vector momenta; cusps in strong-field dissociation; a second attempt to verify previous preliminary results about nonlinear x-ray absorption for a nuclear transition; and further analysis of strong-field phonemena in x-ray scattering.

Recent Progress

Attosecond time-resolved photoelectron holography: For the past few years we have been developing methods to investigate the attosecond scale dynamics associated with strong-field tunneling. We have employed interferometric techniques to directly measure the energy-dependent tunneling delays.. The tunneling process is the starting point for other strong field effects as well,, such as high harmonic generation (HHG), strong-field rescattering (so-called laser-induced electron diffraction) as well as collective multiple ionization. A key feature of all of these distinct phenomena is that they evolve during a single optical cycle, and therefore extracting their time evolution generally requires spectral phase measurements, such as harmonic phase-dependent referencing.

This year we made significant additional progress, together with collaborators in Germany (Vrakking) and Israel (Dudovich), to apply attosecond photoelectron holography to time-resolve the tunneling process, a variant on our earlier work.

Previously we added a weak sub-harmonic ($\omega/2$) field to a strong fundamental field, and employed a method similar to RABBITT attosecond pulse measurements to characterize the energy-dependent attosecond delays of tunnel electrons. This was done by observing the phase-dependence of the interference between two above-threshold ionization paths to the same final energy, where the lower-energy peak absorbs one additional sub-harmonic photon while the higher-energy peak emits one.

In this new method, we add a weak second harmonic (2ω) field to the strong fundamental laser field, and view the combined system using momentum-resolved velocity-map imaging (VMI). This is a holographic method which allows us to reconstruct the momentum-dependent ionization times of photoelectrons with precision down to ten attoseconds, again by measuring the phase dependence of two-path interference.

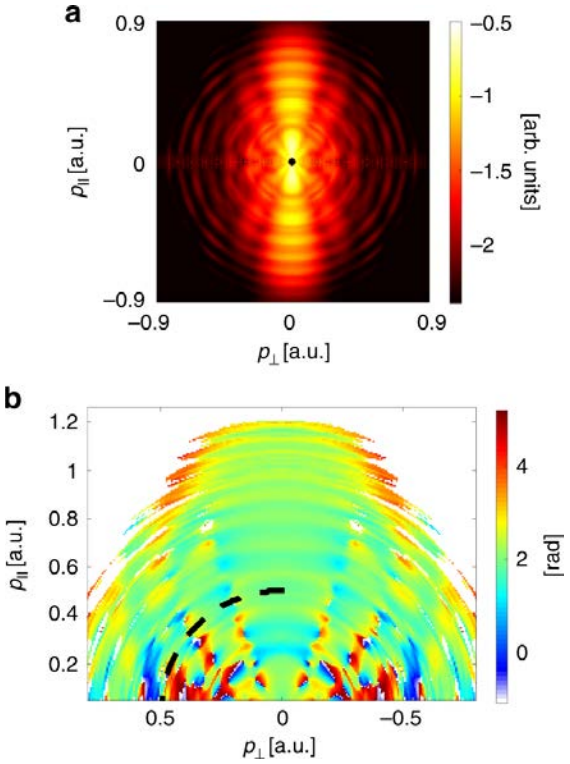

Figures from our recent publication in Nature Communications, showing electron holographic images created by mixing a weak 2ω field with a strong field at frequency ω. The top image shows the photoelectron momentum distribution in Ar obtained from the VMI using only the field at frequency ω. In the lower plot we show the phase extracted from the interferometric measurement. The relative ionization times of different locations in this space can be extracted by the dispersion with respect to energy.

Experimental Observation of Cusp Catastrophes in Strong Field Dissociation. Wave singularities such as diffraction cusps have universal features that can be described in catastrophe theory. An important example for matter waves is the quantum rotor under the influence of an intense impulsive torque. This leads to transient angular focusing of the wave function, which is a well-known means to achieve transient molecular alignment in such systems. After the angle cusp is formed, the wave function continues to evolve and a wavefront fold is created with rainbow like angular structure.

We have observed this kind of cusp catastrophe in angle-resolved dissociation of the H2 molecular cation. A sharp peak in the photodissociation angle is observed following interaction with a 30 fs laser pulse with a peak intensity of $0.4 \times 10^{14}\ W/cm^2$. The vector momentum of both fragments was measured, which enables reconstruction of both the KER and the angle of the interatomic axis with respect to the laser polarization that produced the torque.

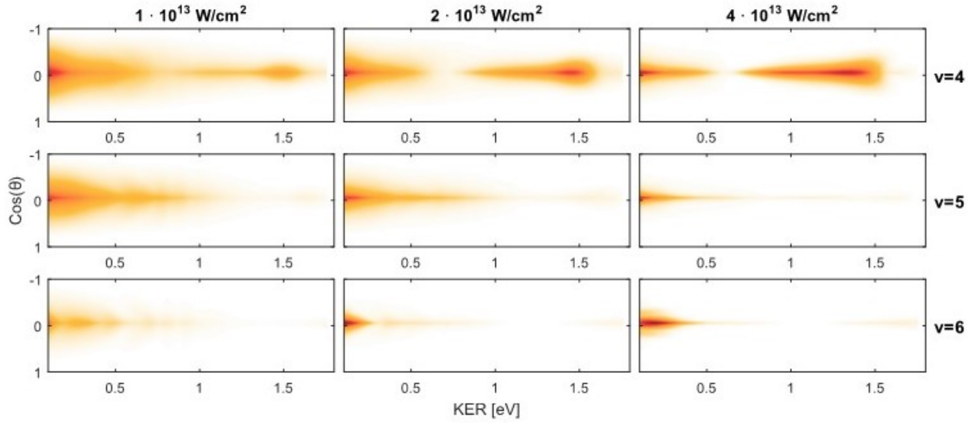

Calculated kinetic energy releases and $cos(\theta)$ maps of H_2^+ dissociation for different pulse intensities, using the v=4,5,6, J=0 initial vibration states. As intensity increases, angular focusing of the dissociation fragments is increased, and the cusp that is created by these low vibration levels extends to a broad KER range.

Momentum Imaging using photoelectrons: We have developed some new techniques to observe above-threshold ionization momentum distributions to display signatures of both molecular and electronic structure on of the molecules (H2O, N2, O2, H2) and in rare gas atoms. These data contain a wealth of information about the strong-field ionization process, which we continued to analyze this year through a combination of simulations and imaging filter methods. Current work includes the following:

- Analysis of the strong intensity dependence of time delays in strong-field ionization measured by electron interferometry. The primary finding is that near the threshold intensity for strong-field ionization, the low-order ATI electrons appear to experience delays of up to 100 attoseconds in ionization. Such temporal behavior is hypothesized to be due to the importance of Stark-induced Freeman resonances, which temporarily store the electrons in Rydberg states.
- Analysis of the quantum interference due to rescattering of strong-field-ionized electrons, to uncover features such as the angular dependence of strong-field ionization, and the motion that is induced by the ionization process, particularly in molecules containing light atomic constituents such as H2O.
- Low-energy structures clearly show double-excitation induced by field ioninzation that leaves the cat- ion in an excited state.

SFA collaborations with other tasks: We have continued a collaboration with the NPI task on x-ray imaging of gas-phase molecules to uncover strong-field aspects of molecular interactions that can be viewed with x rays. An important example is stimulated Raman redistribution, where x-ray scattering reveals both vibrational and electronic excitations. New double-FFT methods $(S(Q,t) \rightarrow S(R,\omega))$ show directly how vibrational modes are spatially localized following impulsive excitation.

Future Plans

A new student and new postdoc will be joining this task this fall. We plan to update our workhorse electron VMI apparatus to create a more flexible platform for the study of fully-resolved strong-field ionization electrons and electron rescattering from quantum systems. We are particularly interested in adding the capability of molecular alignment to our system. Science goals for this include laser-induced electron diffraction from small molecules. An alternative approach that we could also explore is strong-field ionization studies on one- or two-dimensional materials, such as those studied in the Heinz group.

We are preparing to be early users of a 100 Khz, 1mJ, 30 fs, 1.5 microns wavelength system that is being build in an adjoining laboratory by LCLS. Strong field nonlinear spectroscopy methods could be initiated here that would help directly with the development of nonlinear methods using strong XUV and x-ray pulses from LCLS; and using strong interfering fields in aligned molecules

Finally, we are also collaborating with ATO and the XLEAP initiative at SLAC in development of a new VMI setup that will use momentum streaking to encode the properties of an attosecond x-ray pulse in the angle resolved photoelectrons.

Peer-Reviewed Publications Resulting from this Project (2016-2018)

Porat, G., *et al.*, Attosecond Time-Resolved Photoelectron Holography, *Nature Communications* **9**, 2805 (2018).

Young, L., *et al.*, Roadmap of Ultrafast X-Ray Atomic and Molecular Physics, *Journal of Physics B: Atomic, Molecular and Optical Physics* **51**, 032003 (2018)

Zipp, L. J., Natan, A. & Bucksbaum, P. H. Imaging the breakdown of molecular-frame dynamics through rotational uncoupling. *Physical Review A* **95,** 061403 (2017).

Natan, A. *et al.* Observation of Quantum Interferences via Light-Induced Conical Intersections in Diatomic Molecules. *Physical Review Letters* **116,** (2016).

Wolf, T. J. A. *et al.* Probing ultrafast ππ*/nπ* internal conversion in organic chromophores via K-edge resonant absorption. *Nature Communications* **8,** (2017).

Wolf, T. *et al.* Observing Femtosecond Fragmentation Using Ultrafast X-ray-Induced Auger Spectra. *Applied Sciences* **7,** 681 (2017).

Sanchez-Gonzalez, A. *et al.* Accurate prediction of X-ray pulse properties from a free-electron laser using machine learning. *Nature Communications* **8,** 15461 (2017).

Glownia, J. M. *et al.* Glownia *et al.* Reply: *Physical Review Letters* **119,** (2017).

Tenney, I. F., Artamonov, M., Seideman, T. & Bucksbaum, P. H. Collisional decoherence and rotational quasirevivals in asymmetric-top molecules. *Physical Review A* **93,** (2016).

Marinelli, A. *et al.* Optical Shaping of X-Ray Free-Electron Lasers. *Physical Review Letters* **116,** (2016).

Lutman, A. A. *et al.* Fresh-slice multicolour X-ray free-electron lasers. *Nature Photonics* **10,** 745–750 (2016).

Lutman, A. A. *et al.* Polarization control in an X-ray free-electron laser. *Nature Photonics* **10,** 468–472 (2016).

Kroll, T. *et al.* X-ray absorption spectroscopy using a self-seeded soft X-ray free-electron laser. *Optics Express* **24,** 22469 (2016).

Hartmann, G. *et al.* Circular dichroism measurements at an x-ray free-electron laser with polarization control. *Review of Scientific Instruments* **87,** 083113 (2016).

Gorkhover, T. *et al.* Femtosecond and nanometre visualization of structural dynamics in superheated nanoparticles. *Nature Photonics* **10,** 93–97 (2016).

Glownia, J. M. *et al.* Self-Referenced Coherent Diffraction X-Ray Movie of Ångstrom- and Femtosecond-Scale Atomic Motion. *Physical Review Letters* **117,** (2016).

NLX: Nonlinear X-ray Science

David A. Reis*, Shambhu Ghimire
Stanford PULSE Institute, SLAC National Accelerator Laboratory,
Menlo Park, CA 94025 *dreis@slac.stanford.edu

Project Scope:

In the NLX *program, we are focused on the nonlinear optics of short-wavelength, ultrafast coherent radiation***.** We seek to understand strong-field and multi-photon interactions and exploit them to probe electronic structure at the atomic-scale in space and time. We are interested in fundamental interactions, with a primary focus on coherent non-sequential processes such as wave-mixing and two-photon Compton scattering using hard x rays. In the upcoming funding period, we propose experiments on x-ray and optical wave-mixing to image the strong-field- driven attosecond electronic dynamics responsible for solid-state high-harmonic generation. We will also explore the bound-state contribution to two-photon Compton scattering. The new scattering mechanism holds promise as a nonlinear photons-in/photon-out method of achieving simultaneous chemical specificity and atomic-scale structure in low Z materials. Our program is synergistic with other strong-field investigations in PULSE and makes use of the unprecedented intensities at hard x-ray wavelengths of LCLS and SACLA free-electron lasers. The results could have a profound impact on future light sources such as the LCLS-II.

Progress Report

Non-sequential two-photon interactions at x-ray wavelengths became possible with the advent of the LCLS free-electron laser. Much of the focus in this program has been the exploration of fundamental nonlinear x-ray interactions and their use for measurements of chemical and materials dynamics. However, we have also historically studied fundamentals of strong-field high-harmonics generation (HHG) in solids. Much of the DOE supported portion of that work has been collaborative with Shambhu Ghimire's early career award and will thus be described elsewhere in this program. Additionally, first measurements on 2D HHG in atomically thin semiconductors were in collaboration with Heinz's Tony subtask.

Our emphasis in NLX has thus been primarily on nonlinear optics in the hard x-ray regime, where the interaction of multiple photons is expected to give simultaneous and near instantaneous atomic-scale structural and spectroscopic information. Within the AMOS program, we have made several seminal advances in x-ray nonlinear optics, including first measurements of phased-matched x-ray second harmonic generation in diamond, x-ray and optical wave-mixing (diamond), and anomalous nonlinear Compton scattering (beryllium) on LCLS as well as two-photon K-shell absorption (zirconium) on the SACLA FEL

In the past year, we have completed several additional beamtimes on LCLS and SACLA aimed at a better understanding of these phenomena, and the limits to the free-electron nonlinearities for non-resonant excitation. This is important, since far from resonance, the linear x-ray matter interaction can be well approximated by the scattering off a collection of free-electrons. However, the x-ray nonlinearities are nominally extremely weak, especially off resonant. Here we find that models that treat the solid as a collection of free-electrons are successful at describing both the x-ray second-harmonic generation and the (optically modulated) x-ray susceptibility in x-ray–optical sum frequency generation. We are utilizing this to try and understand the solid-state HHG process from an atomic-scale perspective. Such experiments are largely linear in the x-ray intensity but nonetheless require the extreme brightness and short pulses of the X-ray FEL. Here an active area of research has been the theory of x-ray scattering from laser-excited systems. In the context of atomic-scale probes of HHG, Daria Gorelova in Robin Santra's group has recently formulated the problem in terms of a Floquet formalism that allows one to calculate the scattering strength, and determine the regime under which it can be considered as scattering from the instantaneous charges and current densities (submitted. 2018).

However, as we have reported previously, we found that in nonlinear two-photon Compton scattering, the free-electron model breaks down spectacularly. The spectrum shows an anomalously large broadening and redshift as compared to both the free-electron theory and to the simultaneously measured linear scattering from the weak residual FEL second harmonic generated by the undulators. Our observations are incompatible with kinematics for the ground state electron distribution in the usual impulse approximation (IA). These anomalies are consistent with a novel nonlinear scattering mechanism involving bound-state electrons, despite an X-ray energy of approximately two orders of magnitude above the 1*s* binding energy. We have recently extended our original measurements to significantly *larger* red-shift and *smaller* scattering angles; however, recent theoretical work (responding to referee reports) with Robin Santra's group predict no such anomalies from the single atom, two-photon absorption, single photon emission, suggesting an even more exotic mechanism must be at play.

We have also searched for evidence of two-photon excitation of the nuclear resonance in ^{57}Fe in a series of measurements at LCLS and SACLA. This transition is extremely narrow (~5neV) and is commonly used for chemical, biological and increasingly quantum optics applications. Sources of the nuclear florescence are weak and available from both natural radioactive decay products, as well as from coherent nuclear forward scattering using synchrotron excitation. Apart from the fundamental interest, nonlinear excitation of the nucleus could in principle more efficiently pump the nuclear by converting broadband radiation. Here we have explored both the degenerate and electronically-resonant (electronically-bridged) two-color channels. Preliminary results indicate that we will only be able to set a lower limit for the effective nonlinear cross-section in these two cases, despite having intense x-ray FEL pulses. Theoretical support on this project is provided by the Palffy group in Heidelberg, where preliminary but detailed calculations are consistent with a null result. Despite this, we do see an enormously single-photon resonantly enhanced two-photon scattering into a higher energy photon, that is independent of isotope and thus presumed to be purely electronic in nature. The effective cross-section appears to be orders of magnitude (>5) higher than in Be, such that we can excite it at much lower intensities. The mechanism is still under exploration, but bodes well for future multiple color x-ray experiments, aimed at combining structure and spectroscopy (including soft + hard x-ray at the LCLS-II TXI end station).

Future Plans:

Significant effort is ongoing to analyze the results of recent beamtimes at LCLS and SACLA. This includes completing the analysis on recent transient grating and x-ray pump x-ray probe experiments as well as more complete measurements on x-ray second harmonic generation and two-photon Compton scattering in Be. We continue to pursue nonlinear x-ray optical mixing, resonant two-photon scattering and two-photon Mossbauer. Future measurements are aimed at a better understanding of novel x-ray matter interactions and development of novel spectroscopies based thereon. For example, upcoming experiments at SACLA in December are aimed at measuring the near-field nonlinear response of GaAs with atomic precision. Nonlinear x-ray interactions will become ever more important for LCLS-II and in particular LCLS-II-HE, and we are also exploring possible ways to make use of other multi-color/multi-pulse interactions.

Peer-Reviewed Publications Resulting from this Project (2016-2018)

[1] S. Ghimire and D. A. Reis, High Harmonics from Solids, *Nature Physics*, In press, 2018. (Collaborative with Ghimire ECA)

[2] Y. S. You, E. Cunningham, D. A. Reis, and S. Ghimire. Probing periodic potential of crystals via strong-field re-scattering. Journal of Physics B: Atomic, Molecular and Optical Physics, 51(11):114002, 2018. (Collaborative with Ghimire ECA)

[3] M. Fuchs and D. A. Reis. Hard x-ray nonlinear optics, in L. Young, K. Ueda, M. Gühr, P. H. Bucksbaum, M. Simon, S. Mukamel, N. Rohringer, K. C. Prince, C. Masciovecchio, M. Meyer, A. Rudenko, D. Rolles, C. Bostedt, M. Fuchs, D. A. Reis, R. Santra, H. Kapteyn, M. Murnane, H. Ibrahim, F. L´egar´e, M. Vrakking, M. Isinger, D. Kroon, M. Gisselbrecht, A. L'Huillier, H. J. Wörner, and S. R. Leone. Roadmap of ultrafast x-ray atomic and molecular physics. Journal of Physics B: Atomic, Molecular and Optical Physics, 51(3):032003, 2018.

[4] M. Wu, Y. You, S. Ghimire, D. A. Reis, D. A. Browne, K. J. Schafer, and M. B. Gaarde. Orientation dependence of temporal and spectral properties of high-order harmonics in solids. Phys. Rev. A, 96:063412, 2017.

[5] Y. S. You, D. A. Reis, and S. Ghimire. Anisotropic high-harmonic generation in bulk crystals. *Nature Physics*, **13**:345–349, 2017 (collaborative with Ghimire ECA).

[6] S. Ghimire, M. Fuchs, J. B. Hastings, S. Herrmann, Y. Inubushi, J. Pines, S. Shwartz, M. Yabashi, and D. A. Reis. Nonsequential two-photon absorption from the K shell in solid zirconium. *Physical Review. A*, **94**, 043418, 2016.

[7] G. Ndabashimiye, S. Ghimire, M. Wu, D. A. Browne, K. J. Schafer, M. B. Gaarde, and D. A. Reis. Solid-state harmonics beyond the atomic limit. *Nature*, **534**, 520, 2016.

Page is intentionally blank.

Electron Dynamics on the Nanoscale

Tony F. Heinz, PI
SLAC National Accelerator Laboratory, 2575 Sand Hill Road, Menlo Park, CA 94025
Email: theinz@slac.stanford.edu

Project Scope

This component of the SLAC research program examines the dynamics of electron motion and electronically excited states in nanostructures. The research currently focuses on electrons in atomically thin two-dimensional (2D) layers of van-der-Waals crystals and heterostructures, using transition metal dichalcogenide semiconductors as model systems. The investigations make use of complementary spectroscopic techniques to probe radiative and non-radiative relaxation pathways after photoexcitation, including the role of Coulomb interactions and vibrational coupling as manifest in exciton formation, exciton-exciton and exciton-carrier interactions, intervalley scattering, and exciton radiative decay. The role of the external environment in modifying the electronic states and their dynamics is also a focus of attention, as are heterostructures composed of atomically thin 2D van der Waals layers combined with other 2D layers and with 0D structures. 2D van der Waals layers, with their lack of chemical reactivity, can be combined in a wide variety of structures simply by mechanical assembly to provide a set of customizable systems in which to investigate underlying principles of excited-state dynamics.

Recent Progress

A focus of research in this program has been the elucidation of the nature and dynamics of excited states in atomically thin transition metal dichalcogenide layers in the class of MX_2 (M = Mo, W and X = S, Se, Te). These systems provide models for the behavior of electrons in two-dimensional (2D) semiconducting van-der-Waals layers, which are prototypes for laterally delocalized electronic states with strong vertical localization. The systems have attracted great interest because of their strong and anomalous excitonic interactions, their strong spin-orbit interactions, as well as the possibility of accessing the valley degree of freedom through their valley circular dichroism and of constructing diverse heterostructures from multiple layers.

Recent efforts have examined the influence of the environment of a given monolayer on electronic excited states and their dynamics. Here we briefly summarize two advances. One involves the role of a second layer in the crystallographic bilayer in altering exciton dynamics; the second involves studying the significant influence of the dielectric screening of the environment induced by stacked external layers on the excited states of a monolayer. Additional activities within this project, including contributions to ultrafast excited-states dynamics of dissociating molecules probed by ultrafast electron diffraction and electronic dynamics in bulk semiconductors, are not explicitly presented.

Influence of layer thickness on exciton dynamics in photoexcited in WS_2

Exciton-phonon scattering in semiconducting TMDCs, the interaction of the optically excited states with lattice vibrations, is the dominant dephasing mechanism for high-quality monolayers at room temperature. In addition to defining exciton coherence lifetimes, such exciton-phonon scattering also strongly influences exciton motion and diffusion. The conclusion that exciton-phonon interactions are the most important contribution to exciton dephasing has been reached in this research program through a combination of experimental and (collaborative) theoretical investigations. For the band-edge direct (A) exciton, time-resolved measurements indicate that the intrinsic radiative relaxation rate is ~ 1/ps and makes only a modest contribution to the observed (~ 30 – 50 meV) exciton linewidth at room temperature. The strong temperature dependence of the exciton linewidth and its thermally activated behavior also indicate a phonon scattering mechanism, a conclusion in quantitative agreement with theoretical studies.

In recent investigations, we have examined how exciton dephasing in monolayer WS_2 changes when probing excitons in crystallographic bilayers of the semiconductor. For the case of the monolayer, the A exciton corresponds to a feature at (or near) the band edge, without any states lying significantly lower in energy. For the AB stacked crystallographic bilayer, the material becomes an indirect semiconductor, with the A exciton now lying hundreds of meV above the (indirect) band gap (left panel of Fig. 1). The question that then arises is how this significant change in electronic structure alters the exciton scattering/dephasing rate. We have addressed this question through systematic measurements of the temperature-dependent A exciton linewidth in mono- and bilayer WS_2 and theoretical studies performed by our collaborators at the Technical University of Berlin and at Chalmers University.

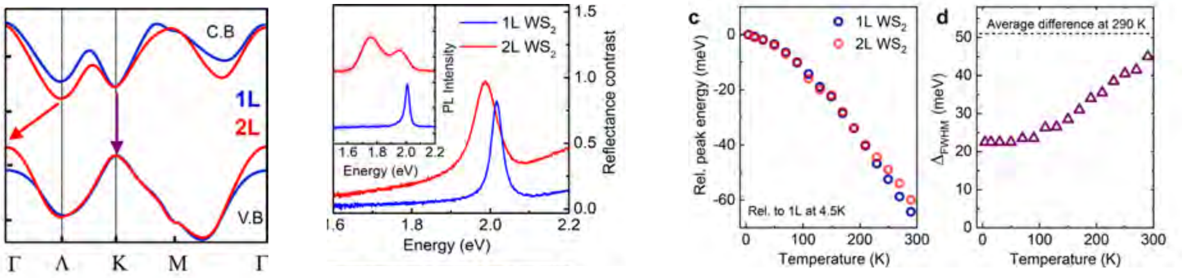

Fig. 1: (left) Calculated band structure of single (1L) and bilayer (2L) WS_2. The purple vertical arrow corresponds to the A exciton transition, which is at the band edge for 1L and remains a direct transition at nearly the same energy for 2L. The red slanting arrow corresponds to the indirect optical transition at the 2L band edge. (center) Optical spectra of the A exciton in 1L WS_2 and 2L WS_2 as obtained in a reflection contrast (absorption) measurement. Note the much larger linewidth of the A exciton for the 2L system compared to the 1L case. The inset shows the corresponding photoluminescence spectra. The much lower emission energy in the 2L case corresponds to the indirect gap. (right) The two panels show comparison of the A exciton feature in the mono- and bilayer as a function of the temperature. The spectral shift for the two systems with temperature is essential identical; however, the bilayer has a consistently larger linewidth, but with a difference that is activated with temperature

As indicated in Fig. 1, the linewidth of the A exciton in the bilayer (2L) sample approximately twice that of the monolayer at room temperature. As the temperature decreases, but exciton lines become sharper, but there remains a significant difference in linewidth between the 2L exciton and the 1L exciton, as shown in the rightmost panel in Fig. 1.

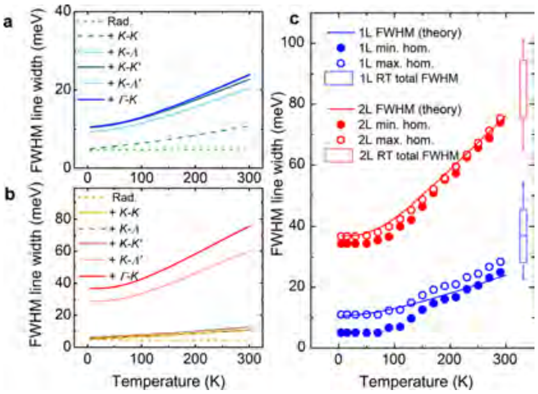

Fig. 2: Results for the temperature dependence A exciton linewidth in monolayer (1L) and bilayer (2L) WS_2. The theory (left) shows the cumulative contribution with the inclusion of the indicated scattering channel. The comparison with experiment (right) includes experimental data with different limits on the inferred homogeneous linewidth based on statistics of linewidth to infer inhomogeneous broadening in the samples. Good overall agreement between experiment and theory is obtained.

Theoretical analysis of the temperature dependent linewidth indicates that exciton-phonon scattering dominates dephasing also in the bilayer. The significant increase in the linewidth (decrease in phase coherence time) is the consequence of the opening of new scattering channels, such as hole scattering to the valence band maximum of the bilayer at the Γ-point. The contribution of radiative broadening to the observed linewidths remains small. In addition, the scattering channels operative in the monolayer are modified because of energy shifts in the bands. This also contributes to the enhanced scattering rate for the bilayer. The relative contributions calculated for different allowed exciton-phonon scattering process, assuming that scattering involves only either the electron or hole, are shown in Fig. 2 as function of temperature. Also included is the relatively small calculated radiative broadening. A comparison with experimental linewidths shows good agreement, both in terms of the absolute magnitude and the temperature dependence. These measurements highlight the importance of exciton-phonon scattering in determining the exciton dephasing rate and dynamics. The study also reveals the strong dependence on the interlayer interactions (comparing 1L to 2L) for the excited-state dynamics.

Interactions of 2D semiconducting layers with the surrounding dielectric media: Coulomb engineering

The interactions of a monolayer semiconductor with the surrounding dielectric material (of a different chemical composition) was also investigated. The aim of the study was to determine how screening of the many-body (carrier-carrier) interactions external layers influenced the energy of the excited states. The possibility of strong renormalization of energy levels by external dielectric media was foreseen based on the very strong Coulomb interactions between carriers exhibited in these materials. This is highlighted by the fact that the monolayer TMDC semiconductors exhibit exciton binding energies in the range of 100’s of meV, which are expected to be strongly modified by the presence of surrounding media given the thickness of the semiconductor layer of just a few Angstroms.

To investigate this phenomenon, we applied spectroscopy to determine the Rydberg series of lowest-lying and excited A exciton states in a monolayer WS_2 in the presence of different dielectric environments. This was accomplished by constructing diverse heterostructures involving WS_2. This process allowed us to determine shifts induced in the exciton spectrum and, by extrapolation in the quasi-particle band gap, by the surrounding media. While the shifts in the ground exciton state were relatively small (10’s of meV), the higher-lying exciton states shifted by more than 100 meV in the presence of an adjoining graphene layer and the inferred quasi-particle (electrical) band gap. Fig. 3 shows the spectroscopic data underlying these observations.

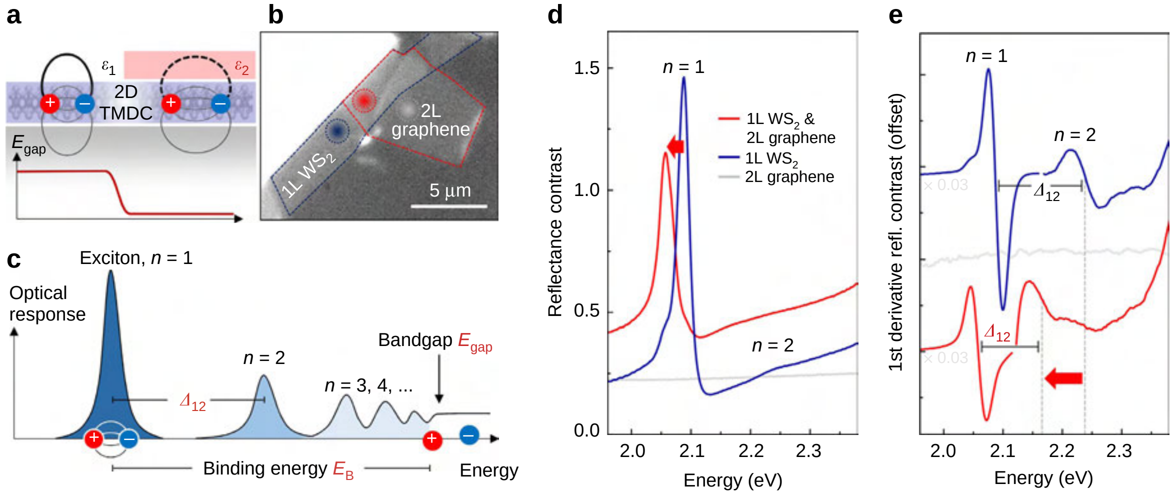

Fig. 3: Investigations of the influence of surrounding dielectric media on the excited states and band gap of a monolayer of the 2D semiconductor WS_2. The scheme of the experiment is shown at the left and spectroscopic results for the ground and first excited-state excitonic transitions are shown in the right panels.

These results show the possibility of modifying not only the excitonic states of a 2D semiconductor, but also of controlling the layer's quasi-particle band gap simply by the choice of the external media. This concept, which can be termed Coulomb engineering, has potential for a new approach to band gap engineering and lateral patterning of 2D semiconductors.

Future Plans

In the coming period of time, we plan to extend the investigations of excited-state dynamics in 2D systems described above from bilayers of a single material to examine the case of interlayer charge transfer in 2D heterostructures comprised of two different 2D semiconductor layers, particularly in materials with staggered band alignment where rapid electron-hole separation and the formation of an interlayer exciton is expected. These issues can be addressed using ultrafast pump-probe spectroscopy, with polarization dependent measurements allowing one to determine the rates of valley and spin dependent processes. We also wish to explore the degree of spatial localization of the band and exciton renormalization processes induced by an external dielectric layer of defined lateral extent.

Peer-Reviewed Publications Resulting from this Project (2016-2018)

1. A. Raja, M. Selig, G. Berghäuser, J. Yu, H. M. Hill, A. F. Rigosi, L. E. Brus, A. Knorr, T. F. Heinz, E. Malic, and A. Chernikov, "Enhancement of exciton-phonon scattering from monolayer to bilayer WS_2," *Nano Lett.* (2018) 10.1021/acs.nanolett.8b01793
2. J. K. Kim. X. Shi, M. J. Jeong, J. Park, H. S. Han, S. H. Kim, Y. Guo, T. F. Heinz, S. Fan, C.-L. Lee, J. H. Park, and X. Zheng, "Enhancing Mo:$BiVO_4$ Solar Water Splitting with Patterned Au Nanospheres by Plasmon-Induced Energy Transfer," *Adv. Eng. Mater*. **8**, 1701765 (2018).
3. G. Wang, A. Chernikov, M. M. Glazov, T. F. Heinz, X. Marie, T. Amand, and B. Urbaszek, "Colloquium: Excitons in atomically thin transition metal dichalcogenides," *Rev. Mod. Phys.* **90**, 021001 (2018).
4. C. Jin, E. Y. Ma, O. Karni, E. C. Regan, F. Wang, and T. F. Heinz, "Ultrafast dynamics in van der Waals heterostructures," *Nature Nanotech.* (accepted).
5. J. Yang, X. Zhu, T. J. A. Wolf, Z. Li, J. P. F. Nunes, R. Coffee, J. P. Cryan, M. Gühr, K. Hegazy, T. F. Heinz, K. Jobe, R. Li, X, Shen, T. Veccione, S. Weathersby, K. J. Wilkin, C. Yoneda, Q. Zheng, T. J. Martinez, M. Centurion, and X. Wang "Imaging CF_3I conical intersection and photodissociation dynamics with ultrafast electron diffraction," *Science* **361**, 64-67 (2018).
6. C. Ruppert, A. Chernikov, H. M. Hill, A. Rigosi, and T. F. Heinz, "The Role of Electronic and Phononic Excitation in the Optical Response of Monolayer WS_2," *Nano Lett.* **17**, 644-651 (2017).
7. X.-X. Zhang, T. Cao, Z. Lu, Y.-C. Lin, F. Zhang, Y. Wang, Z. Li, J. Hone, J. A. Robinson, D. Smirnov, S. G. Louie, T. F. Heinz, "Magnetic brightening and control of dark excitons in monolayer WSe_2," *Nature Nanotech*. **12**, 883–888 (2017).
8. O. Yaffe, Y. Guo, L. Z. Tan, D. A. Egger, T. Hull, C. C. Stoumpos, F. Zheng, T. F. Heinz, L. Kronik, M. G. Kanatzidis, J. S. Owen, A. M. Rappe, M. A. Pimenta, and L. E. Brus, "Local Polar Fluctuations in Lead Halide Perovskite Crystals," *Phys. Rev. Lett.* **118**, 136001 (2017).
9. C. Schüller, T. Korn, C. Nuckolls, J. Hone, L. E. Brus, T. F. Heinz, D. R. Reichman, and A. Chernikov, "Coulomb engineering of the bandgap in 2D materials," *Nature Commun.* **8**, 15251 (2017).
10. Raja, A. Montoya-Castillo, J. Zultak, X. X. Zhang, Z. Ye, C. Roquelet, D. A. Chenet, A. M. van der Zande, P. Huang, S. Jockusch, J. Hone, D. R. Reichman, L. E. Brus and T. F. Heinz, "Energy transfer from quantum dots to graphene and MoS_2: absorption versus screening," *Nano Lett.* **16**, 2328 (2016).
11. M. Selig, G. Berghuser, A. Raja, P. Nagler, C. Schuller, T. F. Heinz, T. Korn, A. Chernikov, E. Malic, and A. Knorr. "Excitonic linewidth and coherence lifetime in monolayer transition metal dichalcogenides," *Nature Commun.* **7**, 13279 (2016).

EIM: Excited States in Isolated Molecules

Thomas Wolf and Markus Guehr
SLAC National Accelerator Laboratory, 2575 Sand Hill Road, Menlo Park, CA 94025

thomas.wolf@slac.stanford.edu

Project Scope

Our interest is the investigation of elementary chemical processes in isolated molecules on their natural time scale of femtoseconds and picoseconds. We are especially interested in non-Born-Oppenheimer approximation (non-BOA) dynamics, because of its importance for light harvesting, atmospheric chemistry and DNA nucleobases photoprotection. For this purpose, we use time resolved spectroscopy with extreme ultraviolet (EUV) light from laboratory-based high harmonic generation (HHG) and soft x-rays (SXR) from the Linac Coherent Light Source (LCLS). Those techniques allow a site and element specific access to non-BOA dynamics. We complement spectroscopic investigation methods with gas phase ultrafast electron diffraction (UED).

Recent Progress

We have undertaken extensive studies of ultrafast gas phase photochemistry at the megaelectronvolt ultrafast electron diffraction (UED) facility at SLAC. The study on the ultrafast photodissociation of trifluoromethyliodide of our collaboration including the EIM, attosecond science (ATO), and ultrafast theory and simulation (UTS) subtasks of the PULSE FWP and Martin Centurion's group was recently published in Science (see peer-reviewed publications). Additionally, we have now a high level of understanding of the UED signatures obtained for the ultrafast photoinduced ring-opening reaction in 1,3-cyclohexadiene (CHD). Upon photoexcitation, CHD relaxes in an electronically excited state along a bond dissociation degree of freedom (see Fig. 1, left). It returns through a conical intersection on the bond dissociation coordinate back to the ground state. The photoproduct 1,3,5-hexatriene (HT) is a chain of three conjugated double bonds i.e. the reaction transforms a ring of two double bonds and four single bonds into a chain of three single bonds and three double bonds. HT exhibits three structural isomers with low isomerization barriers. Isomerization takes place by rotations of the terminal double bonds around the single bonds connecting them to the central double bond.

We are able to resolve the structural dynamics involved in the ring-opening for the first time both on the level of single atomic distances and the femtosecond timescale. The nuclear wavepacket encounters the conical intersection (80 ± 40) fs after leaving the Franck-Condon region of the photoexcited state. After return to the ground state, we observe a substantial acceleration of the nuclear wavepacket towards the isomer minima of the photoproduct 1,3,5-hexatriene (HT) by the strongly repulsive ground state potential along the ring-opening coordinate. Initially, the majority of the photoabsorbed excess energy is, therefore, dissipated into this degree of freedom.

After the ring-opening, the degree of freedom transforms into the rotation of the terminal double bonds of HT, which connect the different HT isomer minima. The kinetic energy stored in this rotation is considerably larger than the low isomerization barriers. We, therefore, observe a quasi-free, coherent rotation leading to a fully stretched configuration of HT 0.25 ps after photoexcitation. We observe a subsequent return of the molecule into a more entangled shape followed by a coherent revival of the stretched configuration (see Fig. 1, right). In collaboration with the UTS subtask we were able to simulate time-dependent diffraction and atomic pair distribution functions based on ab-initio wavepacket dynamics calculations. We find quantitative agreement between experimental and simulated datasets.

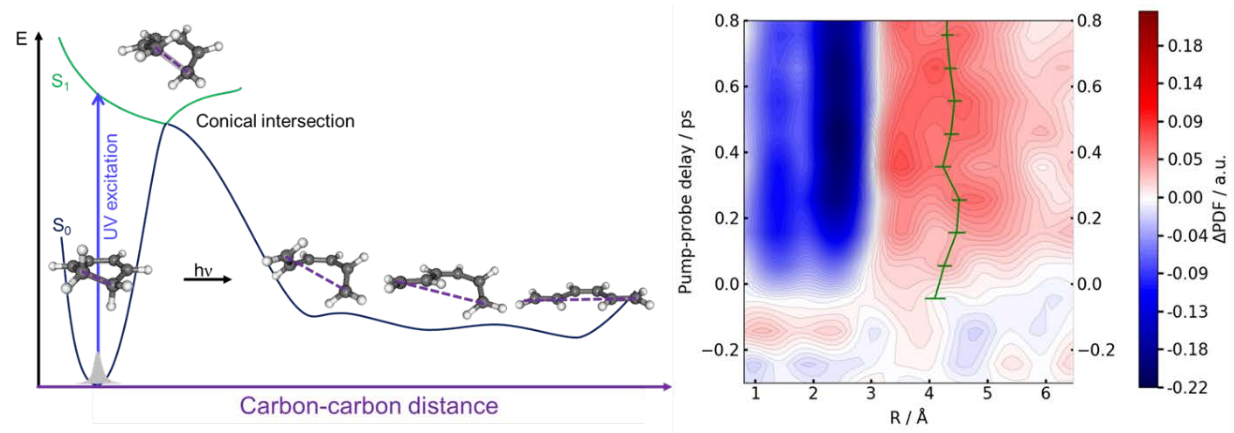

Figure 1 left: One-dimensional scheme of the photoinduced ring-opening reaction coordinate. Photoexcited 1,3-cyclohexadiene (CHD) evolves along a gradient in the excited state elongating the carbon-carbon distance highlighted in purple. It encounters a conical intersection with the ground state. After return to the ground state, it evolves along a steep gradien towards several isomer minima of the photoproduct 1,3,5-hexatriene (HT). The isomer minima are connected via rotations of the terminal double bonds around the bonds connecting them to the central double bond with low barriers. Right: Right: Time-dependent difference pair distribution functions ΔPDF) from ultrafast electron diffraction. The two negative peaks at 1.4 Å and 2.4 Å refer to atomic distances in CHD, which change substantially during the ring-opening. The positive contribution beyond 3 Å originates from the changed carbon-carbon distance in the photoproduct. The green line marks the time-dependent center of mass of the positive contributions. We observe coherent oscillations, which we can assign with the help of *ab-initio* simulations to quasi-free rotations of the termina double bonds in HT.

We were working in a collaboration between the UTS and ATO subtasks, Xijie Wang, and the groups of Martin Centurion and Thomas Weinacht on improvements of the gas phase UED setup and a 6 months long experimental run. The improvements allow us to investigate a considerably higher variety of samples. In a series of new experiments at the UED facility we have investigated two additional photochemical reactions, the ring-opening of α-phellandrene and the NO abstraction reaction in nitrobenzene. We are currently analyzing these new experimental datasets.

Future Plans

We plan on analyzing and publishing the datasets from the most recent UED run during the next year. Furthermore, we plan to conduct experimental studies of the samples we have investigated by UED using ultrafast VUV photoelectron spectroscopy and soft x-ray spectroscopy methods. These experiments will provide the missing complementary information about the dynamics in the electronic part of the molecular wavefunction to the structural dynamics observables from UED. Specifically, we plan to perform investigations of the sample nitrobenzene with the gas phase time-resolved absorption spectroscopy technique we have recently demonstrated at the example of the nucleobase thymine.

Peer-Reviewed Publications Resulting from this Project (2016-2018)

Femtosecond gas phase electron diffraction with MeV electrons
J. Yang, M. Guehr, T. Vecchione, M. S. Robinson, R. Li, N. Hartmann, X. Shen, R. Coffee, J. Corbett, A. Fry, K. Gaffney, T. Gorkhover, C. Hast, K. Jobe, I. Makasyuk, A. Reid, J. S. Robinson, S. Vetter, F. Wang, S. Weathersby, C. Yoneda, M. Centurion, X. Wang, Faraday Discuss. 194, 563 (2016).

Monitoring Ultrafast Chemical Dynamics by Time-Domain X-ray Photo- and Auger-Electron Spectroscopy
O. Gessner and M. Gühr, Acc. Chem. Res. 49, 138 (2016).

Diffractive imaging of a rotational wavepacket in nitrogen molecules with femtosecond megaelectronvolt electron pulses `
J. Yang, M. Guehr, T. Vecchione, M. S. Robinson, R. Li, N. Hartmann, X. Shen, R. Coffee, J. Corbett, A. Fry, K. Gaffney, T. Gorkhover, C. Hast, K. Jobe, I. Makasyuk, A. Reid, J. S. Robinson, S. Vetter, F. Wang, S. Weathersby, C. Yoneda, M. Centurion, X. Wang, Nature Comm. 7, 11232 (2016).

Diffractive Imaging of Coherent Nuclear Motion in Isolated Molecules
J. Yang, M. Guehr, X. Shen, R. Li, T. Vecchione, R. Coffee, J. Corbett, A. Fry, N. Hartmann, C. Hast, K. Hegazy, K. Jobe, I. Makasyuk, J. Robinson, M. S. Robinson, S. Vetter, S. Weathersby, C. Yoneda, X. Wang, M. Centurion, Phys. Rev. Lett. 115, 173002 (2016).

The Role of Super-Atom Molecular Orbitals in Doped Fullerenes in a Femtosecond Intense Laser Field
H. Xiong, B. Mignolet, L. Fang, T. Osipov, T. J. A. Wolf, E. Sistrunk, M. Gühr, F. Remacle, N. Berrah Sci. Rep. 7, 121 (2017).

Emitter–site selective photoelectron circular dichroism of trifluoromethyloxirane
M. Ilchen, G. Hartmann, P. Rupprecht, A. N. Artemyev, R. N. Coffee, Z. Li, H. Ohldag, H. Ogasawara, T. Osipov, D. Ray, Ph. Schmidt, T. J. A. Wolf, A. Ehresmann, S. Moeller, A. Knie, Ph. V. Demekhin Phys. Rev. A 95, 053423 (2017).

Probing ultrafast ππ*/nπ* internal conversion in organic chromophores via K-edge resonant absorption
T. J. A. Wolf, R. H. Myhre, J. P. Cryan, S. Coriani, R. J. Squibb, A. Battistoni, N. Berrah, C. Bostedt, P. Bucksbaum, G. Coslovich, R. Feifel, K. J. Gaffney, J. Grilj, T. J. Martinez, S. Miyabe, S. P. Moeller, M. Mucke, A. Natan, R. Obaid, T. Osipov, O. Plekan, S. Wang, H. Koch, M. Gühr, Nature Comm., 8, 29 (2017).

Observing Femtosecond Fragmentation Using Ultrafast X-ray-Induced Auger Spectra
T. J. A. Wolf, F. Holzmeier, I. Wagner, N. Berrah, C. Bostedt, J. Bozek, P. Bucksbaum, R. Coffee, J. Cryan, J. Farrell, R. Feifel, T. J. Martinez, B. McFarland, M. Mucke, S. Nandi, F. Tarantelli, I. Fischer, M. Gühr, Appl. Sci. 7, 681 (2017).

Soft-x-ray-induced ionization and fragmentation dynamics of Sc3N@C80 investigated using an ion-ion-coincidence momentum-imaging technique
H. Xiong, R. Obaid, L. Fang, C. Bomme, N. G. Kling, U. Ablikim, V. Petrovic, C. E. Liekhus-Schmaltz, H. Li, R. C. Bilodeau, T. Wolf, T. Osipov, D. Rolles, N. Berrah, Phys. Rev. A 96, 033408 (2017).

Time-resolved photoelectron spectroscopy of nitrobenzene and its aldehydes
O. Schalk, D. Townsend, T. J.A. Wolf, D. M.P. Holland, A. E. Boguslavskiy, M. Szöri, A. Stolow, Chem. Phys. Lett., 691, 379 (2018).

A theoretical and experimental benchmark study of core-excited states in nitrogen
R. H. Myhre, T. J. A. Wolf, L. Cheng, S. Nandi, S. Coriani, M. Gühr, H. Koch, J. Chem. Phys, 148, 064106 (2018).

Fragmentation of endohedral fullerene $Ho_3N@C_{80}$ in an intense femtosecond near-infrared laser field
H. Xiong, L. Fang, N. G. Kling, T. J. A. Wolf, E. Sistrunk, R. Obaid, M. Gühr, N. Berrah, Phys. Rev. A, 96, 023419 (2018).

Imaging CF3I conical intersection and photodissociation dynamics by ultrafast electron diffraction
J. Yang, X. Zhu, T. J. A. Wolf, Z. Li, J. P. F. Nunes, R. Coffee, J. Cryan, M. Gühr, K. Hegazy, T. F. Heinz, K. Jobe, R. Li, X. Shen, T. Veccione, S. Weathersby, K. J. Wilkin, C. Yoneda, Q. Zheng, T. J. Martinez, M. Centurion, X. Wang, Science, *361*, 64 (2018).

Normal and Resonant Auger Spectroscopy of Isocyanic Acid HNCO
F. Holzmeier, T. J. A. Wolf, C. Gienger, I. Wagner, J. Bozek, S. Nandi, C. Nicolas, I. Fischer, M. Gühr, R. F. Fink, J. Chem. Phys., *149*, 034308 (2018).

A tilted pulse-front setup for femtosecond transient grating spectroscopy in highly non-collinear geometries
A. Battistoni, H. A. Dürr, M. Gühr, T. J. A. Wolf, J. Opt., *20*, 095501 (2018).

Roadmap of ultrafast x-ray atomic and molecular physics
L.Young, K. Ueda, M. Gühr, P. H. Bucksbaum, M. Simon, S. Mukamel, N. Rohringer, K. C Prince, C. Masciovecchio, M. Meyer, A. Rudenko, D. Rolles, C. Bostedt, M. Fuchs, D. A. Reis, R. Santra, H. Kapteyn, M. Murnane, H. Ibrahim, F. Légaré, M. Vrakking, M. Isinger, D. Kroon, M. Gisselbrecht, A. L'Huillier, H. J. Wörner and S. R. Leone, J. Phys. B, *51*, 032003 (2018).

Early Career: Strongly-driven attosecond electron-dynamics in periodic media

Shambhu Ghimire, SLAC National Accelerator Laboratory
2575 Sand Hill Rd, Menlo Park, CA, 94025
shambhu@slac.stanford.edu

Scope of the program

High-order harmonic generation (HHG) in isolated atoms and molecules has been the basis for attosecond science and technology. High-order harmonics are also observed from bulk crystals subjected to strong mid-infrared laser fields [Ghimire2010] and since then there is growing interest in understanding and exploiting underlying microscopic dynamics. In the condensed phase, field-driven the electron is never far from the core therefore the strong field approximation is not valid without Coulomb correction. Consequently, the well-studied three-step re-collision model of the gas phase becomes questionable in describing microscopic electronic processes in dense media. In dense, periodic media there are two potentially competing mechanisms; radiation from intraband non-linear current and the emission from interband polarization, and there is an escalated debate in the community in determining their relative roles. Main fundamental questions we are trying to address in this program are: (i) could harmonics be the atomic-scale probe of generating medium similar to the gas phase, (ii) how does the time-domain profiles of harmonics look like and would that information be useful to resolve the ongoing debate and (iii) what is the role of medium and long range periodicity of the crystal in generating harmonics?

Recent Progress

1. Real-space electron trajectory approach probes atomic-scale structures in bulk crystals: In the gas phase, high-harmonics have been utilized to probe the electronic orbital structure of molecules [Itatani2004]. Here, we extend that approach to the condensed phase systems. We use a real-space electron trajectory model [You2017c], which considers the conduction band motion of strong-field driven electron. In MgO crystals, 2p orbital of O and 3s orbital of Mg have dominant contributions in the highest valance band and the lowest conduction bands respectively. So, we consider atomic-like picture and assume that tunnel ionization begins from the O sites in each unit cell. In this model, strong (weak) high-harmonic emission occurs when the electron trajectories connect (miss) the nearest neighbor O and Mg atomic sites.

In the experiments, we rotate the crystal with respect to laser polarization direction as shown in figure 1a). Figure 1b) shows charge density distribution around ion cores in (111) cut MgO calculated with density functional theory using quantum espresso package. In figure 1c), we use blue solid line to show the angular distribution of calculated high-harmonic yield considering the location and size of atoms in b). The dotted line is the measured angular distribution of 17th order harmonic. For (111) cut orientation, experiments and theory agree reasonably well. Some discrepancies on angular widths were observed along (110), where we had to consider quantum diffusion of electron wave-packet as this orientation has larger inter-atomic distances [You2018]. Our analysis shows that the process of HHG could be utilized to measure atomic-scale structure of the source material. Our approach is essentially a coherent electron diffraction method, where we use the material's own electrons instead of using external electron or x-ray beam. Our results are published in the special issue of 25-years of re-collision physics.

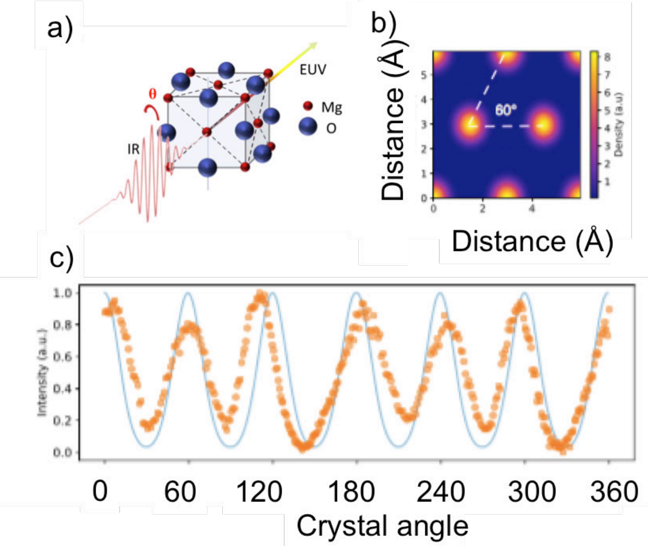

Figure 1 a) Experimental setup to study crystal orientation dependent strong-field response in MgO crystals. **b)** Calculated charge density distribution along (111) plane. **c)** Solid line is calculated angular distribution of high-harmonics from real-space trajectory model using the charge distribution from b). Dotted line is measured harmonic signal (17th order) as a function of the angle between crystal planes and laser polarization direction.

2. Reporting recent progress in the area of HHG:

We reviewed recent progress in HHG and the manuscript has been accepted by Nature Physics [Ghimire2018b]. Our review surveys main experimental efforts aimed at understanding the microscopic mechanism of solid-state HHG in terms of what it can tell us about the electronic structure of the source materials, how it can be used to probe driven ultrafast dynamics, and what are its prospects for novel, compact short-wavelength light sources. In HHG from gases, the high-energy cutoff scales quadratically with the wavelength and peak field strength of the laser pulse, and it depends only weakly on the target material through the ionization potential. Therefore, much of the efforts towards high-energy cutoff extension are focused on using a longer wavelength pump, and gas-phase HHG has reached the soft-x-ray wavelength range. In contrast, high-energy cutoff in solid-state-HHG scales linearly to the peak field and high-harmonic spectrum depends strongly on the electronic band structure of target material [Ghimire2010]. Strong materials dependence has been evident from our recent studies in rare gas solids [Ndabashimiye2016], crystalline and amorphous quartz [You2017a], and single crystal MgO [You2017b]. Therefore, high-harmonic spectroscopy has already shown the potential to emerge as an all-optical, tabletop approach to probe both passive and active electronic structure of source materials. In terms of active electronic structure, high-order harmonics could in principle present an unprecedented temporal resolution because of their sub-cycle scale emission characteristics. Nonetheless, solid-state HHG has also reached the XUV photon range and therefore a new approach in attosecond metrology is emerging. Figure 2 shows

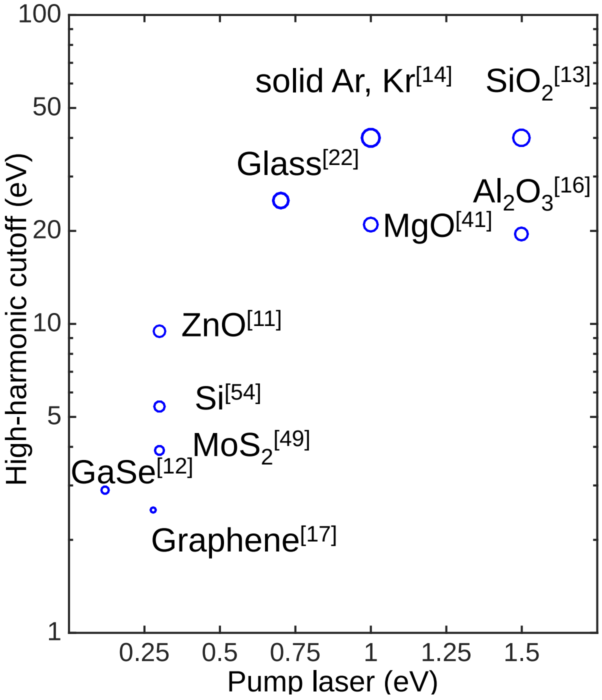

Figure 2: A survey of major experimental efforts in the area of HHG (2010 to 2018), adapted from Ref [Ghimire2018a]

the wide range of source materials, pump laser wavelengths, and reported approximate high-harmonic cutoff energies. It can be seen that narrow band-gap materials are suitable for pumps in terahertz and mid-infrared wavelength range while wide band-gap dielectrics can be pumped by strong near infrared lasers without sample damage. Notable experimental results are the observation of XUV harmonics from crystalline SiO_2 pumped by 1.5 cycle ~800 nm laser pulses of intensity ~16 TW/cm^2 and from frozen Ar and Kr, pumped by ~50 fs, ~1300 nm pulses of peak intensities ~26 TW/cm^2.

Planned Research

We will use real-space electron trajectory model and perform multidimensional high-harmonic spectroscopy. We can use laser parameters such as wavelength, polarization, and impurity states in the target material to control the real-space electron trajectories. An interesting target could be the mixed rare gas solid, where the relative concentration of different entities can be controlled. Such controlled experiments will allow us to understand the details of microscopic processes in strongly driven dense optical media. Additional challenges of high-density solid target are the self-action effects such as self-phase modulation to the pump laser [Ghimire2012]. We plan to tackle this problem by taking advantage of the reflection geometry [vampa2018]. In collaboration with NLX-subtask of Chemical Science FWP, we are conducting strong field laser pump and x-ray diffraction experiments at the LCLS and SACLA. These experiments (in absence of jitter between x rays and optical) will provide element specific view of charge migration processes in dense optical media. We are also working closely with XLEAP team at the LCLS to take advantage of attosecond pulses at the LCLS. Similarly, in collaboration with Atto-subtask of Chemical Sciences FWP, we are considering attosecond streaking and RABBITT type of experiments using solid-state HHG.

Publications

1. [Ghimire2018a] Shambhu Ghimire and David Reis "*Review: high-order harmonic generation from solids*", accepted, Nature Physics
2. [Ghimire2018b] Shambhu Ghimire, "*Locking the waveform with a quartz crystal*" NATURE PHOTONICS 12 (5), 256-257, 2018
3. [You2018] YongSing You, Eric Cunningham, David Reis and Shambhu Ghimire, "*Probing periodic potential of the crystal via strong-field re-scattering*", J. Phys. B: At. Mol. Opt. Phys. 51, 114002, 2018
4. [Vampa2018] Giulio Vampa, YongSing You, Hanzhe Liu, Shambhu Ghimire, and David Reis, "*Observation of backward high-harmonic emission from solids*" Optics express 26 (9), 12210-12218, 2018 (ECA not lead)
5. [Wu2018] Mengxi Wu, YongSing You, Shambhu Ghimire, David Reis, DA Browne, Kenneth J Schafer, and Mette Gaarde, "*Orientation dependence of temporal and spectral properties of high-order harmonics in solids*", Physical Review A 96 (6), 063412, 2018 (ECA not lead)

6. [You2017a] Yong Sing You, Yanchun Yin, Yi Wu, Fengjiang Zhuang, Andrew Chew, Xiaoming Ren, Shima Gholam-Mirzaei, Michael Chini, Zenghu Chang, and Shambhu Ghimire, "*High-harmonic generation in amorphous solids*", Nature Communications 8:724, 2017
7. [You2017b] Yong Sing You, Mengxi Wu, Yanchun Yin, Andrew Chew, Xiaoming Ren, Shima Gholam-Mirzaei, Dana A. Browne, Michael Chini, Zenghu Chang, Keneth J. Schafer, Mette B. Gaarde and Shambhu Ghimire, "*Laser waveform control of extreme ultraviolet high harmonic generation in solids*", Optics Letters 42, 9, (2017)
8. [You2017c] Yong Sing You, David A. Reis, and Shambhu Ghimire, "*Anisotropic high harmonic generation in bulk crystals*", Nature Physics 13, 345-349, (2017)
9. [Liu2017] Hanzhe Liu, Yilei Li, Yong Sing You, Shambhu Ghimire, Tony F. Heinz, and David A. Reis, "*Observation of high harmonics from an atomically thin semiconductor*", Nature Physics 13, 262, 2017 (ECA not lead)
10. [Ndabashimiye2016] Georges Ndabashimiye, Shambhu Ghimire, Mengxi Wu, Dana A. Browne, Kenneth J. Schafer, Mette B. Gaarde, David A. Reis "*Solid-state harmonics beyond the atomic limit*", Nature 534, 520, (2016)

References

[Ghimire2010] Ghimire, S. *et al.* "*Observation of high-order harmonic generation in a bulk crystal*" Nat. Phys. **7,** 138–141 (2011)

[Ghimire2012] Ghimire, S. *et al.* "*Generation and propagation of high-order harmonics in crystals*" Phys. Rev. A **85,** 043836 (2012)

[Itatani2004] "*Tomographic imaging of molecular orbitals*", Nature 432, 867-871 (2004)

Early Career: Time-resolved imaging of non-equilibrium electron dynamics with novel X-ray holographic approaches

Tais Gorkhover, Panofsky fellow
Stanford PULSE Institute,
SLAC National Acceleratory Laboratory,
Menlo Park, CA 94025

Project scope:

The ability to follow transient structural changes is essential for understanding and controlling non-equilibrium phenomena such as catalytic reactions, ultrafast phase transitions, and energy transfer from light to matter. These processes often evolve from a complex interplay between rapid electronic and nuclear motions at the nanoscale, which are hardly accessible with conventional microscopic methods. State-of-the-art imaging tools often require long exposure times to achieve high spatial resolution and thus, their sensitivity to short-lived phenomena is limited. Ultrafast spectroscopic methods can provide valuable information about transient states, but the signal ambiguity often increases with the complexity and heterogeneity of the sample. The capabilities offered by current and next-generation X-ray laser facilities, such as the Linac Coherent Light Source (LCLS) and its successor, LCLS II, offer the potential to directly visualize ultrafast dynamics with high spatial and temporal resolutions. This research program will develop and apply novel ultrafast X-ray diffraction imaging approaches that exploit these cutting-edge X-ray sources to advance the fundamental understanding of non-equilibrium processes in complex nanoscale systems.

Future Plans:

Coherent X-ray diffraction imaging (CDI) is a very promising route to visualize the electronic and nuclear movement at the nanoscale with unprecedented resolution [1]. First LCLS studies on model-systems demonstrated that ultrafast X-ray CDI can successfully resolve laser-induced structural changes with sub-nanometer precision and femtosecond time resolution in single nanoparticles [2]. The first part of this proposal will explore the potential of CDI to direct image subtle dynamics of the electronic structure preceding the nuclear response. We will develop a novel soft X-ray/XUV interferometric holography approach based on recent advancements in X-ray holography [3]. This method aims to increase sensitivity to light-induced changes in the valence electron density of metal nanoparticles and has the potential to resolve light-induced collective electron oscillations with sub-cycle and sub-nanometer resolutions.

In the second part of the proposal, we will use a new ground-breaking instrumentation such as aberration-corrected Be-lenses which can provide 70 nm small X-ray FEL foci [4]. Our aim is to image the structure of catalytically relevant metal nanoparticles within a single femtosecond short exposure with sub-nanometer spatial resolution. The capability to image nanocatalysts with high spatial resolution during the onset of the reaction will lead to deeper understanding of the initiation of catalytic processes. In the third part, this proposal will explore the potential of novel ultrafast X-ray imaging methods beyond CDI.

Overall, the scope of this proposal is directed towards the long-term advancement of science using BES facilities such as LCLS and LCLS-II. Innovative techniques demonstrated and developed at large scale facilities will have the greatest impact on our society if they can spark new useful advancements in table-top experiments. Thus, significant parts of this proposal will focus on implementing and exploring the potential of bench-top versions of several projects described above.

References:

[1] Aquila,A., et al., "The linac coherent light source single particle imaging road map.", *Structur. Dynam.* **2.4** (2015): 041701

[2] Gorkhover,T., et al., "Femtosecond and nanometre visualization of structural dynamics in superheated nanoparticles.", *Nat. Phot.* **10** (2016): 93

[3] Gorkhover,T., et al., "Femtosecond X-ray Fourier holography imaging of free-flying nanoparticles.", *Nat. Phot.* **12**.**3** (2018): 150

[4] Seiboth,F., et al., "Perfect X-ray focusing via fitting corrective glasses to aberrated optics." *Nat. Comm.* **8** (2017): 14623

Peer-Reviewed Publications Resulting from this Project (Project start 09/2018):

No publications to report.

Early Career: Ultrafast Dynamics of Molecules on Surfaces Studied with Time-Resolved XUV Photoelectron Spectroscopy

Thomas K. Allison
Departments of Chemistry and Physics
Stony Brook University, Stony Brook, NY 11794-3400
email: thomas.allison@stonybrook.edu

Program Scope

The capture and storage of solar energy involves the separation and steering of electrons and holes created by the absorption of light. In dye-sensitized solar cells and organic photovoltaics, electrons are injected from a photo-excited molecule into a semiconductor. In heterogeneous photo-catalysis, excitation of the electrons in a solid can cause reactions on the surface, storing the photon's energy in chemical bonds. In both cases, the dynamics of charge separation and subsequent reactions are complex and often involve multiple intermediate states. The main objective of this work is to provide important fundamental insight into these dynamics using time-resolved photoelectron spectroscopy to track the motion of electrons, holes, and nuclei at molecule/surface interfaces. An ancillary objective is also developing the required instrumentation.

Recent Progress

Photoemission spectroscopy using synchrotron radiation is one of the most important methods for establishing relationships between structural and electronic properties at surfaces, with core and valence level shifts providing information about charge transfer, electronic screening, and the geometrical structure of molecules at surfaces. The quasi-CW nature of synchrotron radiation ($\sim$100 ps pulses at MHz repetition rates), which produces few photoelectrons per pulse, is essential for surface experiments where electrons emerge from a small volume of space at the surface, and space charge/image charge effects can blur and shift the photoelectron spectrum.

Many attempts to extend XUV photoemission spectroscopy to the ultrafast time domain using either high-order harmonic generation (HHG) from femtosecond lasers or x-ray pulses from free electron lasers have encountered severe limitations due to either space-charge effects, low photon flux, or limited tuning range. For pump/probe experiments, data-rate limitations are particularly stark for several reasons. First is that pump excitation adds additional dimensions to the data set. At a minimum, data should be recorded at several pump-probe delays and pump fluences, and there are also the parameters of pump wavelength and polarization. Second is that the signal of interest is inherently small, since only a fraction of the sample's electrons are excited by the pump. Combined, these two factors result in the need for orders of magnitude more data than ground state studies done at synchrotrons, but space charge limits the data rate to be orders of magnitude lower. Experiments have then been almost exclusively restricted to strongly excited samples using absorbed fluences on the order ~ 1 mJ/cm^2, such that laser excitation produces changes to the EDC visible on a *linear* scale. In addition to probing different physics than can be accessed in the low-fluence regime [1], at high fluences ultrashort pump pulses also produce many electrons through multiphoton processes which add to the space-charge problem [2], and pump-induced space charge can also have a non-trivial dependence on the pump-probe delay, making space charge effects difficult to separate from the dynamics of interest [3].

The ideal XUV light source for extending photoemission techniques to the time domain would have the flux and multi-MHz repetition rate of a synchrotron, but with ultrashort pulse durations. Many groups around the world have been working towards this goal using a variety of platforms.

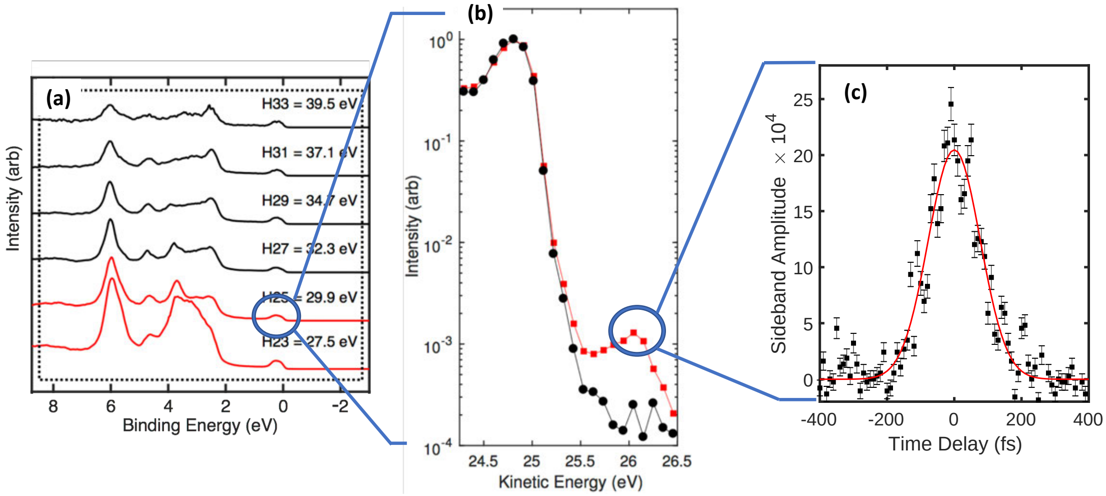

Figure 1: **Laser-assisted photoeffect** a) Photoelectron spectra of a clean Au (111) surface taken at different photon energies. b) A zoom-in near the Fermi edge spectrum using the 25th harmonic ($h\nu = 29.9$ eV). The black curve is taken with only XUV light only. A dynamic range of 10^4 for the small amplitude surface state is obtained in only a few minutes of integration time despite the inefficient single-channel analyzer. The red curve is taken with an additional 1.035 μm laser field with a peak intensity of 1.3×10^9 W/cm^2, producing a LAPE sideband. c) Sideband amplitude as a function of pump/probe delay. The 180 fs cross correlation width is dominated by the NIR pulse duration of > 155 fs, giving an upper limit for the XUV pulse duration of 93 fs. Complete details in [4].

At Stony Brook, we have been working to develop this ideal light source using cavity-enhanced high-harmonic generation and now have achieved a setup with sufficient flux, tuning range, and (most important) reliability to enable challenging surface science experiments at the endstation. We have summarized the details and the performance of the instrument in two papers acknowledging DOE support [4, 5]. In January 2018, we published a seven page SPIE proceedings (technically a conference proceeding, although peer reviewed to some extent) providing many technical details of the source. A comprehensive journal article describing the results of the source and how it advances the state of the art by several orders of magnitude was posted to the arXiv in January and finally published in Structural Dynamics in September [4].

Our most important result over the past year is the demonstration over the past year of the ability to record very small time-resolved laser-induced perturbation (i.e. pump-probe on a *logarithmic* scale) to the XUV photoelectron spectrum. This was a major technical goal of the ECRP proposal and we have shown this now both using the laser-assisted photoelectric effect (LAPE) and weak excitation of molecular films, in acquisition times of only a few minutes. Figures 1 and 2 show this for the cases of the laser-assisted photoeffect from bare Au (111) and a 10 monolayer film of C_{60} molecules on Au (111). C_{60} was chosen as a robust molecule with well characterized surface science suitable for first molecular pump/probe experiments. Since C_{60} is the most-used acceptor molecule in organic photovoltaics, the electron dynamics in C_{60} films are also of interest in their own right. The LAPE data is described in detail in [4] and the C_{60} is unpublished, preliminary data. We will continue with the C_{60} experiment after the electron analyzer and sample manipulator upgrades discussed below.

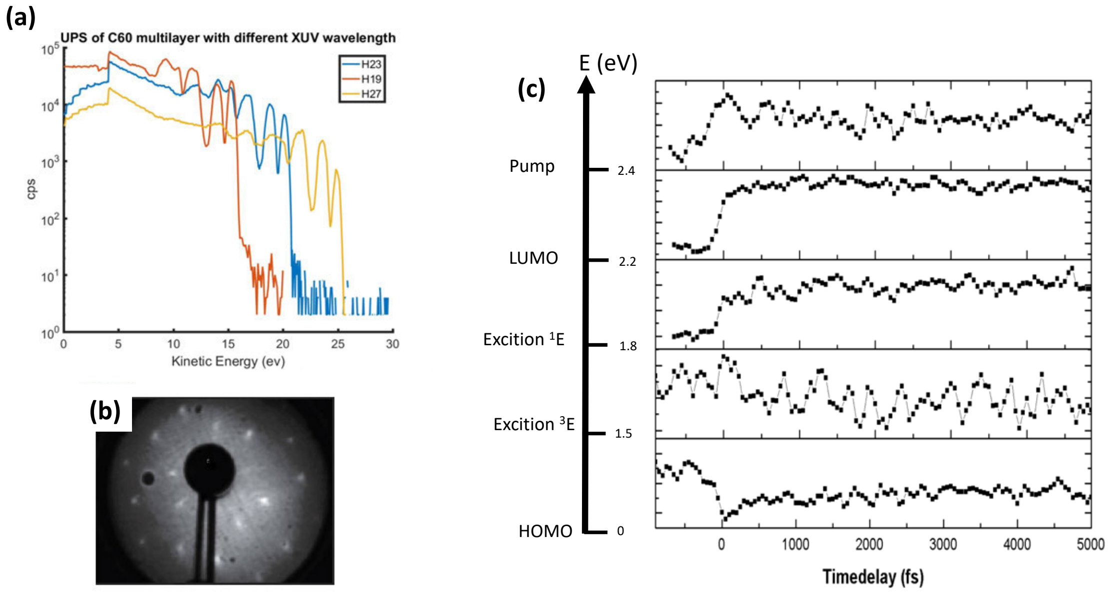

Figure 2: **Time-resolved photoelectron spectroscopy from ordered C_{60} films.** a) Photoelectron spectra of a 10 ML C_{60} film on Au (111) taken with different photon energies. The HOMO, HOMO-1 and HOMO-2 peaks are pronounced and in good agreement with previous work [6] b) LEED pattern of the 10 ML film showing crystalline order. c) Pump/probe traces at various electron energies (PRELIMINARY!). Pump wavelength is 515 nm ($h\nu = 2.4$ eV, slightly above resonant HOMO to LUMO excitation), and excitation level is approximately 10^{-3}.

Future Plans

Much of the past year has been spent preparing for the major upgrade of our electron energy analyzer and corresponding sample manipulator in collaboration with the Schönhense group at Johannes Gutenberg Universität in Mainz. This will improve our data rate by several orders of magnitude and also allow for angular resolution. The analyzer (and team from Mainz) are expected any day now and we have been modifying the surface science chamber to work with the new analyzer/manipulator, adding load/lock for fast sample exchange, and also adding additional differential pumping the the beamline to mitigate O_2/O_3 contamination/chemistry at the sample. We expect the endstation upgrades to be completed this fall and the first run experiments to produce data for several publications.

Peer-Reviewed Publications Resulting from this Project (2016-2018)

C. Corder, P. Zhao, J. Bakalis, X. L. Li, M. D. Kershis, A. R. Muraca, M. G. White, and T. K. Allison. Ultrafast extreme ultraviolet photoemission without space charge. *Structural Dynamics* **5**, 054301 (2018). DOI:10.1063/1.5045578

References

[1] D. N. Basov, Richard D. Averitt, Dirk van der Marel, Martin Dressel, and Kristjan Haule. Electrodynamics of correlated electron materials. *Rev. Mod. Phys.*, 83:471–541, Jun 2011.

[2] L.-P. Oloff, K. Hanff, A. Stange, G. Rohde, F. Diekmann, M. Bauer, and K. Rossnagel. Pump laser-induced space-charge effects in hhg-driven time- and angle-resolved photoelectron spectroscopy. *Journal of Applied Physics*, 119(22):225106, 2016.

[3] R Al-Obaidi, M Wilke, M Borgwardt, J Metje, A Moguilevski, N Engel, D Tolksdorf, A Raheem, T Kampen, S Mähl, I Yu Kiyan, and E F Aziz. Ultrafast photoelectron spectroscopy of solutions: space-charge effect. *New Journal of Physics*, 17(9):093016, 2015.

[4] Christopher Corder, Peng Zhao, Jin Bakalis, Xinlong Li, Matthew D. Kershis, Amanda R. Muraca, Michael G. White, and Thomas K. Allison. Ultrafast extreme ultraviolet photoemission without space charge. *Structural Dynamics*, 5(5):054301, 2018.

[5] Christopher Corder, Peng Zhao, Jin Bakalis, Xinlong Li, Matthew D. Kershis, Amanda R. Muraca, Michael G. White, and Thomas K. Allison. Development of a tunable high repetition rate xuv source for time-resolved photoemission studies of ultrafast dynamics at surfaces. *Proc.SPIE*, 10519:10519 – 10519 – 7, 2018.

[6] Petra Rudolf, Mark S Golden, and Paul A Brühwiler. Studies of fullerenes by the excitation, emission, and scattering of electrons. *Journal of Electron Spectroscopy and Related Phenomena*, 100(1):409 – 433, 1999.

Attosecond dynamics in molecules driven by ultrashort laser pulses

Principal Investigator: Andreas Becker

JILA and Department of Physics, University of Colorado at Boulder,
440 UCB, Boulder, CO 80309-0440

andreas.becker@colorado.edu

Project Scope

The application of high intensity laser systems has been closely linked to research in ultrafast science and the development of ultrafast optical techniques since laser pulses have been generated with shorter and shorter pulse durations. Substantial progress in the understanding and controlling of electron dynamics in the highly nonlinear process of harmonic generation throughout the last 15 years has been the gateway to the creation of the shortest pulse durations available today. These controlled electron dynamics over a sub-cycle of the driving laser pulse enables the emission of coherent light at extreme ultraviolet and soft X-ray wavelengths on a sub-optical cycle time scale, i.e. on a sub-femtosecond time scale. With this technological advance comes the ability to shift the frontier of temporal resolution of dynamical processes to the time scale of electron dynamics, which ultimately determines the structure of matter as well as the outcome of chemical reactions. The natural time scale of electron dynamics is given by the atomic unit of time, which is 24 attoseconds (1 as = 10^{-18} s). With our projects, we seek to provide theoretical support related to the establishment of ultrafast optical techniques as a tool to uncover new insights regarding the attosecond electron dynamics in atoms and molecules.

Our research plan is focused on two areas in attosecond and strong-field science. First, we perform theoretical studies on the application and interpretation of the attosecond streaking and other spectroscopic techniques which enable the retrieval of temporal information of ultrafast processes. Using ab-initio numerical solutions of the time-dependent Schrodinger equation as well as theoretical analysis we intend to study how temporal aspects of the electron dynamics and the coupling between electrons and nuclei can be retrieved from those measurements. This includes the task to establish strategies to identify contributions to the observed quantities during different steps of a process as well as to develop efficient analytical and numerical techniques for the calculations. In the second research thrust we aim to study and identify general features of strong field processes in the interaction of atoms and molecules with ultrashort laser pulses. This includes analysis of signatures of electron dynamics in excitation, ionization and high harmonic generation as well as more fundamental questions concerning the theoretical description of the interaction process.

Recent Progress

Recent developments undertaken and accomplishments completed in the research thrusts can be summarized as follows.

A. Application of Spectroscopic Techniques in the Attosecond Regime

A variety of spectroscopic techniques has been applied to temporally resolve dynamical processes on the attosecond time scale [DOE5]. Our previous efforts were mainly directed towards the analysis of the attosecond streaking method, in which a photoelectron, liberated into the continuum by an attosecond pulse, experiences a momentum shift due to the presence of a second near-infrared laser pulse. Since the magnitude of the shift depends on the vector potential at the time of ionization and the subsequent propagation of the electron wave packet, spectroscopic and timing information can be retrieved. While continuing these studies we have recently also started to explore the options to apply circularly and elliptically polarized isolated attosecond pulses, which have been demonstrated in experiment recently [1], to temporally resolve electron dynamics.

A.1 Time Delays

As reported previously, we have developed analytical formulas for streaking time delays obtained via single-photon absorption [DOE4] and resonant two-photon absorption [DOE7]. In view of the good agreement of the analytical predictions with results of numerical simulations and the efficiency to obtain predictions, the formulas have been applied to different situations. Besides studying effects such as the attochirp (see report of last year, [DOE6]) we have been able to analyze the role of the interaction of the photoelectron during the first half cycle of the streaking pulse, after the promotion in the continuum, on the observed time delay [2]. The results, obtained for a variety of streaking pulse wavelengths and XUV attosecond pulse frequencies, provided insights into the applicability of a recent related proposal [3], which has been put forward for the interpretation of RABBITT experiments.

Furthermore, we have shown how multiple resonances within the bandwidth of the ionizing pulse influence the time delay in model systems as well as simple atoms and molecules [2]. Specifically, comparison between ab-initio results and analytical predictions could reveal the interplay of contributions of several resonances on the total time delay. We have also observed additional features in the results of the time delay as a function of XUV central frequency, which we have attributed as due to the combined effect of the XUV attosecond pulse and the infrared streaking pulse. For example, the absorption or emission of an infrared photon can enhance the population of intermediate states which would otherwise be forbidden for a transition initiated by a single XUV photon.

A.2 Application of Elliptically Polarized Attosecond Pulses

The generation of isolated circularly and elliptically polarized attosecond pulses has recently been demonstrated experimentally [1]. Since this is a new development, the use of these pulses for applications in attosecond spectroscopy has not been thoroughly explored. We have studied the photoionization of atoms with isolated elliptically polarized attosecond pulses and demonstrated how the resulting photoelectron angular momentum distribution can be controlled via changing the ellipticity of the applied pulse [2]. Specifically, we identify a variation in angle of maximum emission as the ellipticity increases, which can be further verified by changing the helicity of the polarization. Besides the option of determine the ellipticity and helicity of the applied attosecond pulse, this observation may prove to be potentially useful for alternative ways to time resolve electron dynamics on a few-attosecond or even sub-attosecond time scale. For example, one may consider to relate the observed angle of maximum emission to a time of emission, similar as in the attoclock principle [4].

B. Excitation to Rydberg States in Strong Field Pulses

In the regime of strong-field physics it is common to use the single-active-electron approximation to a multielectron system, in which one electron responds to the influence of the external field while the rest of the electrons are considered as frozen. We have developed so-called single active electron potentials by fitting numerical pseudopotentials, based on DFT calculations (within the so-called Optimized Effective Potential (OEP) approximation), to a concise analytic expression, physically grounded in the structure of the exchange-correlation component of the full potential. In an application we have studied the excitation to Rydberg states in the interaction of an atom with a strong laser pulse [5]. Utilizing the solutions of the time-dependent Schrödinger equation we have found that the parity of the populated angular momentum distributions agrees with the selection rules for multiphoton resonant absorption at low intensities, as it has been previously established for monochromatic laser fields and pulses with a trapezoidal envelope.

Beyond the parity effect, we have observed that the population in certain low angular momentum states is suppressed. While these observations are in parts in agreement with an earlier explanation that these states are more likely depopulated by absorption of an additional photon [6], results for even parity processes exhibit patterns that do not comply with this mechanism. An alternative explanation has been put forward based on the assumption that resonant transitions to lower lying energy levels cause a trapping of population and a suppression of certain pathways in the excitation process. Signatures of the population in the excited states via the line emissions after the end of the pulse have been analyzed, which may enable the experimental verification of the theoretical predictions.

C. Role of Central Frequency in Light Induced Processes

We have analyzed the role of the difference between the central frequencies of the spectral distributions of the vector potential and the electric field of a short laser pulse. The frequency shift arises when the electric field is determined as the derivative of the vector potential to ensure that both quantities vanish at the beginning and end of the pulse [7], while the pulse is parametrized in the conventional way such that the peak intensity of the electric field remains constant when the frequency changes. The difference between these central frequencies is an electromagnetic effect, but it appears to be significant to understand its effects in light-induced processes, since in experiment typically the central frequency of the electric field is measured and reported, while in numerical calculations it is useful to define the laser pulse via the vector potential and the related central frequency

To analyze the effects on various light induced processes, such as excitation, ionization and high harmonic generation, we have derived an analytical estimate of the frequency shift and obtained solutions of the time-dependent Schrödinger equation, both numerically as well as within first-order perturbation theory [8]. For long pulses, the frequency shift is small, but it increases as pulse duration decreases. Both numerical results and perturbative predictions agree well with each other for linear processes, such as excitation and ionization, and confirm that the observables for processes involving few-cycle pulses with the same value for the two central frequencies do not agree. Furthermore, we have found that the frequency shift is also noticeable for nonlinear processes, such as two-photon excitation and high-order harmonic generation, and scales with the number of photons involved. Therefore, the shift should be taken into account when setting the central frequency of the vector potential in simulations to avoid potential misinterpretation of numerical results for processes induced by few-cycle pulses.

Future Plans

In the future, we plan to expand on our efforts concerning the theoretical studies of the physics and application of ultrafast spectroscopic techniques. Specifically, we want to further explore the options of using attosecond laser pulses with different polarization and the potential to identify ultrafast electron dynamics with these pulses in different set-ups. Furthermore, we plan to apply our development of analytical estimates for time delays for the analysis of the concept of an absorption time delay using other spectroscopic techniques, such as those based on the usage of attosecond pulse trains instead of isolated attosecond pulses. In the second thrust of our research program we plan to investigate the applicability of the proposed mechanism of suppression of excitation pathways via trapping of population in low-lying excited states by extending our analysis to other atoms, a broader range of frequencies as well as different polarization states of the applied ultrashort laser pulse.

References

[1] P.-C. Huang et al., Nat. Photon. **12**, 349 (2018).

[2] C. Goldsmith, PhD thesis (University of Colorado Boulder, August 2018).

[3] D. Kiesewetter et al., Nat. Physics **14**, 68 (2018).

[4] P. Eckle et al., Nat. Physics **4**, 565 (2008).

[5] J. Venzke, R. Reiff, Z. Xue, A. Jaron-Becker, and A. Becker, submitted for publication.

[6] Q. Li, X.-M. Tong, T. Morishita, C. Jin, H. Wei, and C.D. Lin, J. Phys. B **47**, 204019 (2014).

[7] S. Chelkowski and A.D. Bandrauk, Phys. Rev. A **65**, 061802 (2002).

[8] J. Venzke, T. Joyce, Z. Xue, A. Becker and A. Jaron-Becker, submitted for publication.

Peer-Reviewed Publications Resulting from this Project (2016-2018)

[DOE1] M.R. Miller, A. Jaron-Becker, and A. Becker, *High-harmonic spectroscopy of laser driven nonadiabatic electron dynamics in the hydrogen molecular ion,* Physical Review A **93**, 013406 (2016).

[DOE2] M.R. Miller, Y. Xia, A. Becker and A. Jaron-Becker, *Laser driven nonadiabatic electron dynamics in molecules,* Optica **3**, 259-269 (2016).

[DOE3] M.R. Miller, A. Jaron-Becker and A. Becker, *Signatures of transient electron localization in high-order harmonic generation*, Molecular Physics **115**, 1758 (2017).

[DOE4] C. Goldsmith, J. Su, A. Becker and A. Jaron-Becker, *Analytical estimates of attosecond streaking time delay in photoionization of atoms,* Physical Review A **96**, 053410 (2017).

[DOE5] A. Jaron-Becker and A. Becker, *Attosecond Spectroscopy,* Encyclopedia of Modern Optics (2nd Edition), edited by R. Guenther and D. Steel (Oxford: Elsevier, 2018) pp. 233-243.

[DOE6] C. Goldsmith, A. Jaron-Becker, and A. Becker, *Effect of attochirp on attosecond streaking time delay in photoionization of atoms,* Journal of Physics B: Atomic, Molecular and Optical Physics **51**, 025601 (2018).

[DOE7] C. Goldsmith, J. Su, A. Jaron-Becker, and A. Becker, *Analysis of absorption time delays in resonant and non-resonant two-photon ionization,* Journal of Physics B: Atomic, Molecular and Optical Physics **51**, 155602 (2018).

Molecular Dynamics Imaging from Within at the Femto- and Atto-Second Timescale using FELs

Nora Berrah
Physics Department, University of Connecticut, Storrs, CT 06268
e-mail:nora.berrah@uconn.edu

Project Scope

The goal of our research program is to investigate *fundamental interactions between ultrafast photons and molecular systems* to advance our quantitative understanding of electron correlations, charge transfer and many body phenomena. Our research investigations focus on probing, on femtosecond and attosecond time-scale, multi-electron interactions, and tracing nuclear motion in order to understand and ultimately control energy and charge transfer processes from electromagnetic radiation to matter. Most of our work is carried out in a strong partnership with theorists.

Our current interests include: **1)** Time-resolved molecular dynamics investigations using x-ray pump-x-ray probe techniques using free electron lasers (FELs), such as the ultrafast linac coherent light source (LCLS) x-ray FEL facility at the SLAC National Laboratory. Our experiments probe physical and chemical processes that happen on femto/atto second time scales. This is achieved by measuring and examining both electronic and nuclear dynamics subsequent to the interaction of molecules with LCLS pulses of various (4-20 fs) pulse duration and intensities. **2)** The study of non-linear and strong field phenomena, particularly in the soft and hard x-ray regime. **3)** Explore attosecond electron dynamics with the future new attosecond capability at LCLS. We use IR lasers and the ALS synchrotron to prepare our FELs experiments with the added benefit of comparing multi-photon ionization dynamics in the single and multiphoton IR and x-ray regimes. We present below results completed and in progress this past year and plans for the immediate future.

Recent Progress

1) LCLS In—Photon Out: Fluorescence Measurement of Neon using Femtosecond Soft X-Rays

Current ultrafast studies conducted with x-ray photons from the LCLS have focused on using electron and ion spectrometry to investigate non-linear processes and molecular dynamics. However, ion and electron yield spectroscopy provides only one side of the picture of the interaction with x-rays, while fluorescence provides a complementary view on the system undergoing transitions following specific selection rules. My group has built, in collaboration with LCLS scientists, a soft x-ray spectrometer to be used for gas-phase and solid systems. We tested the spectrometer to investigate the Ne produced fluorescence subsequent to ionization with soft x-rays of about 1200 eV [1]. The device consists of a variable line spacing (VLS) grating spectrometer to be used at the soft x-ray and AMO beamlines at LCLS. Irrespective of the low target density obtained using a capillary and the large focal area of the beam, the photon flux was sufficient enough to produce fluorescence count for a gas-phase system of ~1.2 photons/shot within the acceptance angle of the spectrometer. Three distinct peaks result for Ne following photoionization shake-off and Auger decay. Using the theory by Buth et al. [2] we provide the identification of the peaks resulting thereof. Our measurements confirm two of the peaks resulting from $1s^12s^22p^6 \rightarrow 1s^22s^22p^5$, and a combination of $1s^12s^22p^5 \rightarrow 1s^22s^22p^4$ and $1s^12s^12p^6 \rightarrow$

$1s^22s^12p^5$ transitions, identified in experiments measuring K emission spectrum of Ne [a]. We also identified the third peak originating from the fluorescence after a core ionization—Auger decay—core ionization (CAC) process, which is a two photon initiated channel [1] that cannot be accessed with a synchrotron source. Furthermore, we were able to use the theory to estimate the LCLS focal spot size of 7.30x7.30 μm^2 of the x-ray beam which is usually not known with most type of FEL experiments. All theoretical computations associated with this work are provided in our calculation in [2]. This successfully commissioned device on both solid and gas targets will be used in the future to investigate molecular dynamics. An instrumental paper will be written by my student Razib Obaid in the next few months.

2) Soft-X-Ray-Induced ionization and fragmentation dynamics of fullerenes investigated using an ion-ion-coincidence momentum-imaging technique

We have been preparing for LCLS-II based x-ray induced molecular studies using ion-ion coincidence momentum imaging technique using x-rays from the ALS paired with a similar instrument that will be available at LCLS-II. The planned high repetition rate of the future LCLS-II facility will be tested with the current high repletion rate of the ALS. The goal of the study is to understand in a large molecule like $Sc_3N@C_{80}$, energy transfer between a moiety (Sc_3N) and the cage (C_{80}) when we deposit energy in the Sc atom by ionizing its inner-shell. We targeted the Sc 2p shell of the encapsulated Sc_3N cluster and C 1s shell of the C_{80} cage, which lead to the molecule fragmentation through evaporation, release, fission, and Coulomb explosion mechanisms. The fragmentation processes are found to rely on the internal energy, which may be accumulated through electron-electron and electron-phonon couplings during the relaxation processes. Our analysis implies that charge transfer and redistribution play an important role in the fragmentation of the encaged cluster Sc_3N. Sequential release of two out of the three Sc atoms of the encaged molecule via fission in the form of Sc^+ or Sc-containing ions are found to be significant, while the probability of sequential release of all three encaged Sc atoms is much smaller. The resonant excitation of the Sc 2p-shell electrons significantly increased the yield of the parent $Sc_3N@C_{80}$ and its fragment ions, partially attributed to the collisional ionization by the energetic Auger electrons from the intermolecular Auger decay process that involves vacancies in the Sc site and electrons on the carbon cage [3]. Since synchrotron radiation allows only single photon ionization, we have tested future molecular work at LCLS-II by using an intense femtosecond near-infrared laser field. We observed that Ho^+ abundance associated with carbon cage opening dominates at an intensity of 1.1×10^{14} W/cm^2. As the intensity increases, the Ho^+ yield associated with multi-fragmentation of the carbon cage exceeds the prominence of Ho^+ associated with the gentler carbon cage opening. Moreover, the power law dependence of Ho^+ on laser intensity indicates that the transition of the most likely fragmentation mechanisms occurs around 2.0×10^{14} W/cm^2 [4].

3) The LAMP Instrument at the Linac Coherent Light Source Free-Electron Laser

My group built in collaboration with LCLS instrument scientists and commissioned with KSU faculty (D.R and A. R.) the LAMP instrument for soft x-ray imaging, non-linear physics, and ultrafast x-ray science experiments, available to users at the LCLS FEL. While the instrument resides in the Atomic, Molecular and Optical science hutch, its components can be used at any LCLS beamline. The end-station has a modular design that provides high flexibility in order to meet user-defined experimental requirements and specifications. The ultra-high-vacuum environment (10^{-10} T) supports different sample delivery systems, including pulsed and continuous atomic, molecular, and cluster jets; liquid and aerosols jets; and effusive metal vapor beams. It also houses movable, large-format, high-speed pnCCD x-ray detectors for detecting scattered and fluorescent photons. Multiple charged-particle spectrometer options are housed in the LAMP chamber, including a double-sided spectrometer for simultaneous and even coincident measurements of electrons, ions, and photons produced by the interaction of the high-intensity x-ray beam with the various samples [5]. This instrument will be used at LCLS-II to conduct e-ion ion coincidence experiments.

References

a. O. Keski-Rakhonen, Phys. Scr. **7** 173–6 (1973)

Future Plans.

The principal areas of investigation planned for the coming year are:
1) Finish and submit the manuscript for publication on time-resolved ionization dynamics of C_{60} induced by the LCLS since we now have the modeling finished by theorists Zoltan Jurek and Robin Santra. **2)** We were awarded beamtime to carry out, September 2018, at the FERMI FEL in Italy, an experiment to explore intermolecular interactions in weakly-bound systems, and specifically in molecular iodine solvated in small water clusters. **3)** We were awarded beamtime at the FLASH FEL in Hamburg, Germany to carry out an experiments on C_{60} resonances in the XUV range. **4)** We were awarded beamtime at FLASH FEL to carry out a time-resolved experiment on H-migration in alcohol samples. These three experiments will generate FEL-based data that will prepare and facilitate our future work we plan to carry out at LCLS-II, when it will be ready in 2020.

Peer-Reviewed Publications Resulting from this Project (2016-2018).

1. Razib Obaid Christian Buth, Georgi L. Dakovski, Randolf Beerwerth, Michael Holmes, J. Aldrich, Ming-Fu Lin, Michael Minitti , Timur Osipov, William Schlotter, Lorenz S. Cederbaum, Stephan Fritzsche, and Nora Berrah, “LCLS in - photon out: fluorescence measurement of neon using soft x-rays” J. Phys. B: At. Mol. Opt. Phys. **51**, 034003 (2018)
2. Buth Christian et al.,“Neon in ultrashort and intense x rays from free electron lasers", J. Phys. B **51**, 055602 (2018).
3. Hui Xiong, Razib Obaid, Li Fang, Cédric Bomme, Nora G. Kling, Utuq Ablikim, Vladimir Petrovic, Chelsea E. Liekhus-Schmaltz, Heng Li, Rene C. Bilodeau, Thomas Wolf, Timur Osipov, Daniel Rolles, and Nora Berrah, "Soft-x-ray-induced ionization and fragmentation dynamics of $Sc_3N@C_{80}$ investigated using an ion-ion-coincidence momentum-imaging technique", Phys. Rev. A. **96**, 033408 (2017).
4. Hui Xiong Li Fang, Timur Osipov, Nora G. Kling, Thomas J. A. Wolf, Emily Sistrunk, Razib Obaid, Markus Gühr, and Nora Berrah, “Fragmentation of endohedral fullerene $Ho_3N@C_{80}$ in an intense femtosecond near-infrared laser field”, Phys. Rev. A **97**, 023419 (2018).
5. Timur Osipov Christoph Bostedt, J-C Castagna, Ken R Ferguson, Maximilian Bucher, Sebastian C Montero, Michelle L Swiggers, Razib Obaid, Daniel Rolles, Artem Rudenko, John D Bozek, and Nora Berrah, “The LAMP Instrument at the Linac Coherent Light Source Free-Electron Laser”, Review of Scientific Instruments, Rev. of Sci. Instr., **89**(3), 035112 (2018). 'Editor's pick' section.
6. Kasra Amini et al., “ Photodissociation of aligned CH_3I and $C_6H_3F_2I$ molecules probed with time-resolved Coulomb explosion imaging”, Structural Dynamics, **5**, (2018) (in press)
7. N. Berrah, “Fullerene Dynamics with X-Ray Free-Electron Lasers” Book chapter in Fullerenes and Relative Materials, Edited by Natalia Kamanina, and Published by, IntechOpen. ISBN: 978-953-51-5591-1 (2018.
8. Li Fang Edwin Kukk, Nora Berrah,” book chapter in 'Advances in Optics: Reviews' Book Series, Vol. 2, e-ISBN: 978-84-697-9438-8, (2018).

9. I. Dumitri R. C. Bilodeau, T. W. Gorczyca, C. W. Walter, N. D. Gibson, D. Rolles, Z. D. Pešić, A. Aguilar and N. Berrah, “Inner-Shell Photodetachment from Ni^-: Giant Feshbach resonances“, Phys. Rev. A **96**, 023405 (2017).
10. Thomas J. A. Wolf, et al., “Observing femtosecond fragmentation using ultrafast x-ray induced Auger spectra “, Appl. Sci, **7**(7), 681 (2017).
11. Nora Berrah, “A Perspective for Investigating Photo-Induced Molecular Dynamics from Within with Femtosecond Free Electron Lasers” Phys. Chem. Chem. Phys., **19**, 19536 (2017).
12. T. J. A. Wolf, et al., “Probing ultrafast $\pi\pi^*/n\pi^*$ internal conversion in organic chromophores via K-edge resonant absorption”, Nature Communication, **8**, 29 (2017)
13. Carlo Callegari, et al., “Application of Matched-Filter Concepts to Unbiased Selection of Data in Pump-probe Experiments with Free Electron Lasers” Appl. Sci., **7**(6), 621; doi:10.3390/app7060621 (2017).
14. Kasra Amini, et al., “Alignment, Orientation, and Coulomb Explosion of Difluoroiodobenzene Studied with the Pixel Imaging Mass Spectrometry (PImMS) Camera” Journal of Chemical Physics **147**, 013933 (2017).
15. Evgeny Savelyev, et al., “Jitter-Correction for IR/UV-XUV Pump-Probe Experiments at the FLASH Free-Electron Laser” New Journal of Physics, **19**, 043009 (2017).
16. A. Sanchez-Gonzalez et al., “Accurate prediction of x-ray pulse properties from a free-electron laser using machine learning” Nature Comm. **8**, 15461 (2017).
17. Utuq Ablikim et al., “Isomer-dependent fragmentation dynamics of inner-shell photoionized difluoroiodobenzene, Physical Chemistry Chemical Physics **19**, 13419-13431 (2017).
18. Li Fang, Hui Xiong, Edwin Kukk and Nora Berrah “X-ray Pump–Probe Investigation of Charge and Dissociation Dynamics in Methyl Iodine Molecule“, Appl. Sci., **7**, 529 (2017).
19. Hui Xiong, Benoit Mignolet, Li Fang, Timur Osipov, Thomas J. A. Wolf, Emily Sistrunk, Markus Gühr, Francoise Remacle and Nora Berrah, “The Role of Super-Atom Molecular Orbitals in Doped Fullerenes in a Femtosecond Intense Laser Field” Scientific Reports (Nature) **7**, 121 (2017).
20. T. Takanashi et al.,“Time-Resolved Measurement of Interatomic Coulombic Decay Induced by Two-Photon Double Excitation of Ne_2”, Phys. Rev. Lett. **118**, 033202 (2017).
21. D. Iablonskyi et al., “Slow Interatomic Coulombic Decay of Multiply Excited Neon Clusters” Phys. Rev. Let. **117**, 276806 (2017).
22. Utuq Ablikim et al.,” Identification of absolute geometries of cis and trans molecular isomers by Coulomb Explosion Imaging” Scientific Reports **6**, 38202 (2016)
23. lberto A. Lutman, Timothy J. Maxwell, James P. MacArthur, Marc W. Guetg, Nora Berrah, Ryan N. Coffee, Yuantao Ding, Zhirong Huang, Agostino Marinelli, Stefan Moeller & Johann C. U. Zemella "Fresh-slice multicolour X-ray free-electron lasers" Nat. Photonics **10**, 745 (2016).
24. C. S. Lehmann et al., “Ultrafast measurements for molecular nuclear dynamics using two x-ray pulses”, Phys. Rev. A, **94**, 013426 (2016).
25. Nora Berrah Li Fang, Brendan F Murphy, Edwin Kukk, Timur Y. Osipov, Ryan Coffee, Ken R Ferguson, Hui Xiong, Jean-Charles Castagna, Vlad S Petrovic, Sebastian Carron Montero, and John D. Bozek, “A two mirrors x-ray pulse split and delay instrument for femtosecond time resolved investigations at the LCLS free electron laser facility” Optics Express **24** (11), 11768-11781 (2016).
26. A. Picon et al., “Hetero-site-specific ultrafast intramolecular dynamics”, Nature Comm. **7**, 11652 (2016).
27. Liu, Ji-Cai; Berrah, Nora; Cederbaum, Lorenz; Cryan, James; Glownia, James; Schafer, Kenneth; Buth, Christian “Rate equations for nitrogen molecules in ultrashort and intense x-ray pulses ” J. Phys. B: Atomic, Molecular and Optical Physics **49**, 075602 (2016).
28. Nora Berrah, “Molecular Dynamics Induced by Short and Intense X-rays Pulses from the LCLS” (Peer reviewed article based on an invited talk at the Nobel Symposium, Stigtuna, Stockholm, Sweden, June 15, 2015), Physica Scripta, T**169**, 014001 (2016).

Imaging Structural Dynamics in Isolated Molecules with Ultrafast Electron Diffraction

PI: Martin Centurion
Department of Physics and Astronomy, University of Nebraska, Lincoln, NE 68588-0299
martin.centurion@unl.edu

Program Scope or Definition

This project aims to investigate photochemical reactions at the molecular level by observing how the molecular structure changes upon light absorption. The project relies on ultrafast electron diffraction to image photo-induced reactions in isolated molecules with atomic resolution. A sample of molecules in the gas phase is excited by a femtosecond laser pulse, and the structure is probed by a femtosecond electron pulse. The scattering pattern of the probe electrons contains information on the structure of the molecule, and under certain conditions an image of the molecule can be retrieved with atomic resolution.

Introduction

In photo-induced molecular reactions light can be converted into chemical and kinetic energy on femtosecond time scales. Observing the motion of atoms and the resulting transient structures during these processes is essential to understand them. Diffraction methods are an ideal tool because they are directly sensitive to the spatial distribution of charge, and are thus complementary to spectroscopic methods that probe the energy landscape. We have implemented ultrafast electron diffraction (UED) with femtosecond temporal resolution to observe structural dynamics in isolated molecules.

A gas-phase diffraction experiment comprises four major parts: i) An electron gun that delivers short pulses on a target, ii) a laser that triggers both the electron gun and the photochemical reaction, iii) a sample delivery system that creates a gas jet target in a vacuum environment, and iv) a detection system. Two different systems will be used in this project. The first is the MeV electron gun at the ASTA test facility at SLAC National Lab. This RF photoelectron gun produces femtosecond electron pulses in an energy range between 2 MeV and 5 MeV, with a repetition rate of 120 Hz. We have designed and constructed an experimental chamber for gas phase diffraction experiments, in collaboration with the group of Xijie Wang at SLAC. The main advantage of using MeV electrons is that they are relativistic, which minimizes the velocity mismatch between laser and electrons and also the pulse spreading due to Coulomb forces. The velocity mismatch has been a major limitation in the temporal resolution of UED experiments with sub-relativistic pulses. Experiments will also be performed in the PI's lab at UNL using a photoelectron gun that combines a DC accelerator with an RF compression cavity. Electrons are accelerated to an energy of 90 keV and then temporally compressed at the target position by a small RF cavity, at a repetition rate of 5 kHz. This setup includes an optical system to deliver laser pulses with a tilted intensity front on the sample. The tilted pulses will serve to compensate the velocity mismatch of laser and electrons through the sample to reach femtosecond resolution. The setup at SLAC is expected to reach better temporal resolution due to the use of relativistic electron pulses, while the setup at UNL is expected to reach a better spatial resolution due to the higher average beam current that will allow for capturing the scattering at larger angles.

Recent Progress

Over the last year, we have made significant progress in analyzing the data from the relativistic UED experiments of 2017 and on preparing and carrying out new experiments this year. The data analysis was completed for two UED experiments on the photodissociation dynamics of CF_3I and $C_2F_4I_2$. The results on CF_3I have been published this year, while we are preparing a manuscript for submission based on the results on $C_2F_4I_2$. In both cases, the experimental results are supported by simulations from the group of Todd Martinez at Stanford. We have also performed the data analysis for the cis-trans isomerization of Stilbene, however, in this case we have determined that we do not have enough statistics to follow the reaction dynamics. In terms of new experiments, we spent a significant effort this year in improving the sample delivery system at the SLAC MeV UED setup. Currently we are carrying out experiments and have seen a significant improvement in the stability of the gas yet.

Data analysis

*UV-Photodissociation of CF_3I***.** **T**he absorption of a single UV photon leads to the dissociation through breaking of the CI (carbon-iodine) bond. Using UED, we have captured the photodissociation and a second reaction channel that is resonantly excited by two UV-photons into a Rydberg state. We were able to resolve the dynamics in both channels. In the dissociation channel, we have observed the recoil of the carbon atom when the bond breaks, and structure of the hot CF_3 fragment. In the second channel, we have observed the passage of a nuclear wavepacket through a conical intersection and the splitting of the wavepacket (Figure 1). The amplitude oscillations correspond to the wavepacket motion in the excited state, while the decrease in amplitude is due to dissociation.

*UV Photodissociation of $C_2F_4I_2$***.** The UV excitation of $C_2F_4I_2$ results in the sequential breaking of the two CI bonds: $C_2F_4I_2 \rightarrow C_2F_4I + I \rightarrow C_2F_4 + 2I$. In previous mass spectrometry experiments, the first reaction step takes has been measured to take place in approximately 200 fs, while the second step takes place on a time scale of approximately 20 ps, depending on the excitation wavelength. The C_2F_4I radical was found

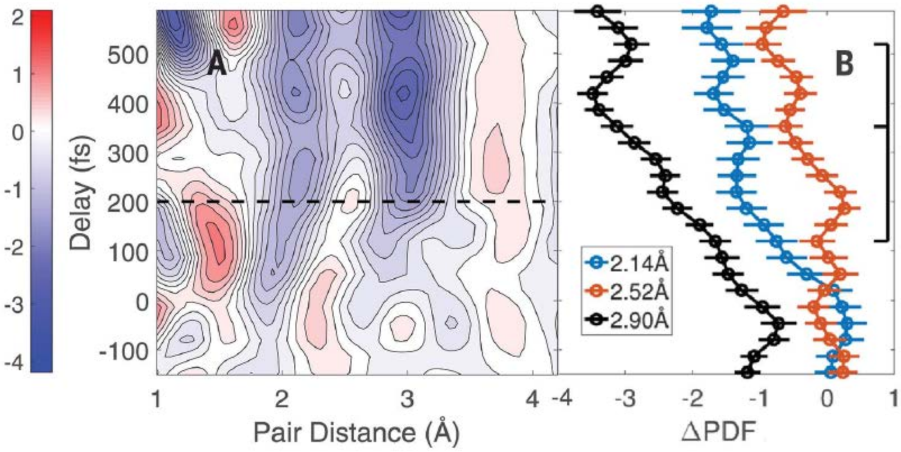

Figure 1. Photodissociation dynamics of CF_3I. (A) Change in the Pair Distribution Function (PDF) as a function of time delay. .The dashed line at 200 fs shows a rough separation between contributions from the one-photon and the two-photon channels. (B) Experimental time evolution of the difference PDF at 2.14, 2.52, and 2.90 Å, corresponding to different interatomic distances in the molecule.

to have a non-bridged structure by the Zewail group using UED with 5 picosecond time resolution [*H. Ihee et al, Science 291, 458 (2001)*]. Due to the limited time resolution, however, it was still unknown whether the bridged structure existed on a femtosecond timescale. We have used UED to capture the first reaction step with 150 femtosecond time resolution. Several new features of the reaction were revealed by our experiments, as shown in Figure 2. First, we were able to observe the motion of the dissociating iodine wavepacket, which was in good agreement with calculations performed by the group of Todd Martinez. This can be seen as the red streaks in Figure 2. The features are blurred out in the experiment due to the time resolution. The negative regions correspond to missing distances when one of the iodine atoms is removed. There is good agreement between experiment and theory on the major features. Second, we have determined that the classical structure forms within 200 fs, which corresponds to a single period in the C-I vibrational motion. Thus we can conclude that the bridged structure never forms. Third, we have observed coherent vibrations that take place in the electronic ground state of the radical. The nature of the vibrations was identified by comparing the experimental results with high level calculations.

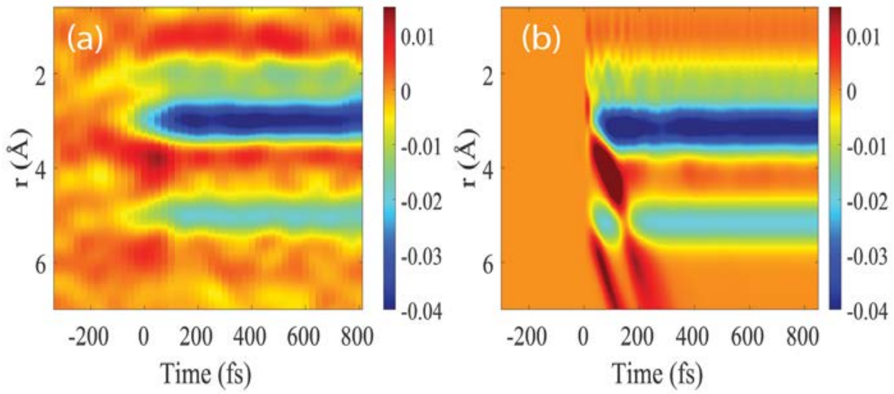

Figure 2. Photodissociation Dyanmics of C2F4I2. (a) Experimental difference PDF. (b) Theory difference PDF.

Improvements in the experimental setup

We have made significant improvements to the sample delivery at the SLAC MeV UED setup. One of the main challenges in previous experiments was to have stable delivery of the sample molecules for long periods of time (a day or more) to take data continuously. We have redesigned the existing setup to remove cold spots where the sample could condense along the line and optimized the temperature gradient between the sample holder and the nozzle. The initial results were very promising. We were able to run several experiments continuously for more than 24 hours, sometimes until the sample run out. However, we have also experienced difficulties with the new setup. Several samples that have low vapor pressure could not be delivered reliably, either because of a hot spot at some point along the line where the sample decomposed, or because the pressure of the carrier gas was not sufficient to move the sample molecules along the line. We have also designed and constructed a new sample delivery system that uses a continuous nozzle and can reach higher temperatures above 300 C (compared to 200 C for the pulsed nozzle). This setup will be useful for samples with very low vapor pressure. So far, the new setup was tested successfully in a static diffraction experiment over two hours, but has not yet been tested in extended operation during a full experiment.

Recent experiments

We have successfully recorded UED data on two reactions: The photoexcited dynamics of O-Nitrophenol and the dissociation of Iron Pentacarbonyl. The reaction of O-Nitrophenol involves a proton transfer and a rotation of the nitro group, followed by fragmentation. In the case of Iron Pentacarbonyl, we aim to capture the timescale for the photodissociation of one or more CO groups and the structure of the remaining Iron N-carbonyl. The experiments were completed in September of this year and we are just starting with the data analysis. Our group has also participated in setting up and taking data for several experiments lead by other groups.

Future plans

The future plans include the data analysis on the most recent UED experiments. We will also continue to make improvements to the sample delivery and start planning for the next round of experiments.

Peer-Reviewed Publications Resulting from this Project (2016-2018)

1. M. Centurion, "Ultrafast imaging of isolated molecules with electron diffraction (Topical Review)", *J. Phys. B*. 49, 062002 (2016).

2. J. Yang, M. Guehr, T. Vecchione, M. S. Robinson, R. Li, N. Hartmann, X. Shen, R. Coffee, J. Corbett, A. Fry, Ke. Gaffney, T. Gorkhover, C. Hast, K. Jobe, I. Makasyuk, A. Reid, J. Robinson, S. Vetter, F. Wang, S. Weathersby, C. Yoneda, M. Centurion, X. Wang, "Diffractive imaging of a rotational wavepacket in nitrogen molecules with femtosecond megaelectronvolt electron pulses" *Nature Commun*. 7, 11232 (2016).

3. J. Yang, M. Guehr, X. Shen, R. Li, T. Vecchione, R. Coffee, J. Corbett, A. Fry, N. Hartmann, C. Hast, K. Hegazy, K. Jobe, I. Makasyuk, J. Robinson, M. S. Robinson, S. Vetter, S. Weathersby, C. Yoneda, X. Wang, M. Centurion, "Diffractive Imaging of Coherent Nuclear Motion in Isolated Molecules" *Phys. Rev. Lett*. 117, 153002 (2016).

4. J. Yang, M. Guehr, T. Vecchione, M. S. Robinson, R. Li, N. Hartmann, X. Shen, R. Coffee, J. Corbett, A. Fry, Ke. Gaffney, T. Gorkhover, C. Hast, K. Jobe, I. Makasyuk, A. Reid, J. Robinson, S. Vetter, F. Wang, S. Weathersby, C. Yoneda, X. Wang, M. Centurion, "Femtosecond gas phase electron diffraction with MeV electrons" *Faraday Discuss* 194, 563 (2016).

5. O. Zandi, K. J. Wilkin, Y. Xiong, and M. Centurion, "High current table-top setup for femtosecond gas electron diffraction" *Structural Dynamics* 4, 044022 (2017).

6. J. Yang, X. Zhu, T. J.A. Wolf, Z. Li, J. P. F. Nunes, R. Coffee, J. P. Cryan, M. Gühr, K. Hegazy, T. F. Heinz, K. Jobe, R. Li, X. Shen, T. Veccione, S. Weathersby, K. J. Wilkin, C. Yoneda, Q. Zheng, T. J. Martinez, M. Centurion, X. Wang "Imaging CF3I conical intersection and photodissociation dynamics with ultrafast electron diffraction" *Science* 361, 64 (2018).

Capturing Ultrafast Electron Driven Chemical Reactions in Molecules

PI: Martin Centurion
Department of Physics and Astronomy, University of Nebraska, Lincoln, NE 68588-0299
martin.centurion@unl.edu

Program Scope or Definition

This project, which started on September 15, 2018, is in collaboration with the group of Daniel Slaughter at Lawrence Berkeley National Laboratory. The goal of the project is to perform time-resolved measurements of the dynamics in dissociative electron attachment (DEA) reactions. In this reaction, the attachment of a low energy electron to a molecule results in bond breaking and the fragmentation of the molecule. A new instrument will be designed and constructed to perform time resolved photoelectron spectroscopy and coincidence measurements of the photoelectron and the reaction fragments. The experiments proposed here will establish new tools to interrogate these dynamics on the fundamental timescales of the nuclear motion, by simultaneously probing the valence electronic structure and the fragmentation pathways.

Introduction

Low energy (few eV) electrons are readily generated in the interaction of radiation with matter, and these electrons can in turn interact with molecules and drive a large number of chemical processes in atmospheric, radiation and plasma chemistry. One of this processes is dissociative electron attachment, where a low energy electron attaches to a molecule and causes bond breaking and fragmentation. The transient anion system evolves from the electronic continuum, so dissociation competes with autodetachment of the electron. These reactions can take place on femtosecond time scales and exhibit strong coupling between electronic and nuclear motion. The breakdown of the Born-Oppenheimer approximation makes it challenging to accurately describe the dynamics with existing quantum chemistry models. It is also challenging to observe these reactions experimentally on the relevant timescale, due to the difficulty in delivering few-eV electron pulses on a sample to trigger the reaction with femtosecond resolution.

We are developing a new instrument to do kinematically complete time-resolved measurements of dissociative electron attachment reactions by combining two experimental methodologies: time resolved photoelectron spectroscopy and coincidence measurements of the photoelectron and the reaction fragments. The experiments proposed here will establish new tools to interrogate these dynamics on the fundamental timescales of the nuclear motion. Initial experiments will focus time resolved fragment momentum imaging, followed by time resolved photoelectron spectroscopic measurements of photodetached electrons. The next step will be to perform photoelectron and fragment measurements in coincidence. The coincidence measurements will allow us to assign the measured valence electron binding energies to specific fragmentation channels. The experiments will be supported by theoretical calculations of the electron attachment and dissociation processes.

Recent Progress

Nothing to report yet.

Future plans

The immediate future plans are to finish the design and start construction of the source chamber and ion beam optics. During the first year we expect to complete the construction of the source chamber and the design of the electron VMI detector and the fragment momentum imaging spectrometer.

Peer-Reviewed Publications Resulting from this Project (Project start date: 09/2018)

No publications to report.

Early Career: Probing Attosecond Bound Electron Dynamics Driven by Strong-Field Light Transients

Michael Chini
Department of Physics and CREOL, the College of Optics & Photonics
University of Central Florida, Orlando, FL 32816
e-mail: Michael.Chini@ucf.edu

Program Scope

The measurement and control of ultrafast dynamics in electronically-excited states of molecular systems have opened new frontiers in the study of internal energy conversion, charge transfer, and coupling of electronic and nuclear degrees of freedom. Recently, such control has been extended to the attosecond (1 attosecond = 10^{-18} seconds) regime, owing to the development of carrier-envelope phase-stabilized few-cycle lasers and isolated attosecond extreme ultraviolet (XUV) pulses. This project aims to use innovative laser techniques to reconstruct the time-dependent quantum mechanical wave packets initiated by strong-field excitation in bound electronic states of gas-phase atoms and molecules, and to control their dynamic evolution on attosecond to few-femtosecond (1 femtosecond = 10^{-15} seconds) timescales.

Recent Progress

Measurement and control of electronic motion requires time-resolved spectroscopic techniques with attosecond precision. In this project, coherent wave packet dynamics will be triggered using strong-field near-infrared light transients lasting only a single optical cycle. The dynamics will be followed using optical spectroscopies based on the interference of the coherence emission with an isolated attosecond pulse produced via high-order harmonic generation.

To support the project, we are developing a source of synchronized isolated attosecond pulses and single-cycle near-infrared pulses based on nonlinear compression of a Yb:KGW amplifier. While Yb-based laser technology offers significant advantages over other femtosecond laser platforms in terms of high average power, excellent power and pointing stability, and low thermal load, the long pulse durations (typically ~300 fs) have prevented their widespread application to attosecond science.

A schematic of the experimental setup is shown in Figure 1. Laser pulses from a carrier-envelope phase (CEP)-stablized 50 kHz Yb:KGW amplifier are to be spectrally broadened in long (>3 m) hollow-core fiber filled with Xe or other suitable gas, and compressed to single-cycle duration (<3.5 fs at 1030 nm central wavelength) in a two-channel light wave synthesizer. The spectrum, pulse duration, and CEP stability of the synthesized pulses will be characterized. The pulses will then be used to probe the dynamics of strong-field excitation, through time-domain measurements of perturbed XUV free-induction decay.

In our laboratory, we have recently explored pulse compression using both the multi-plate continuum[1] and hollow-core fiber[2] techniques. Multi-plate continuum resulted in a pulse duration of 18 fs; however the energy throughput was severely limited (~10%) due to both the requirement of a two-stage compressor and nonlinear beam distortion[3]. A Xe-filled fiber enabled compression to 15 fs, with substantially higher throughput (>50%) and good beam quality. We further observed a significant extension of the high-order harmonic cutoff when comparing between the uncompressed (280 fs) and compressed (15 fs) pulses[4]. Recently, we have been exploring the use of molecular gases for pulse compression[5], due to the high cost of Xe. In preliminary experiments, we have found that pulse compression in 1,1-difluoroethane ($C_2H_4F_2$, also known as R152a) works as well as, if not better than, Xe gas, resulting in a measured pulse duration of <13 fs (Fig. 2).

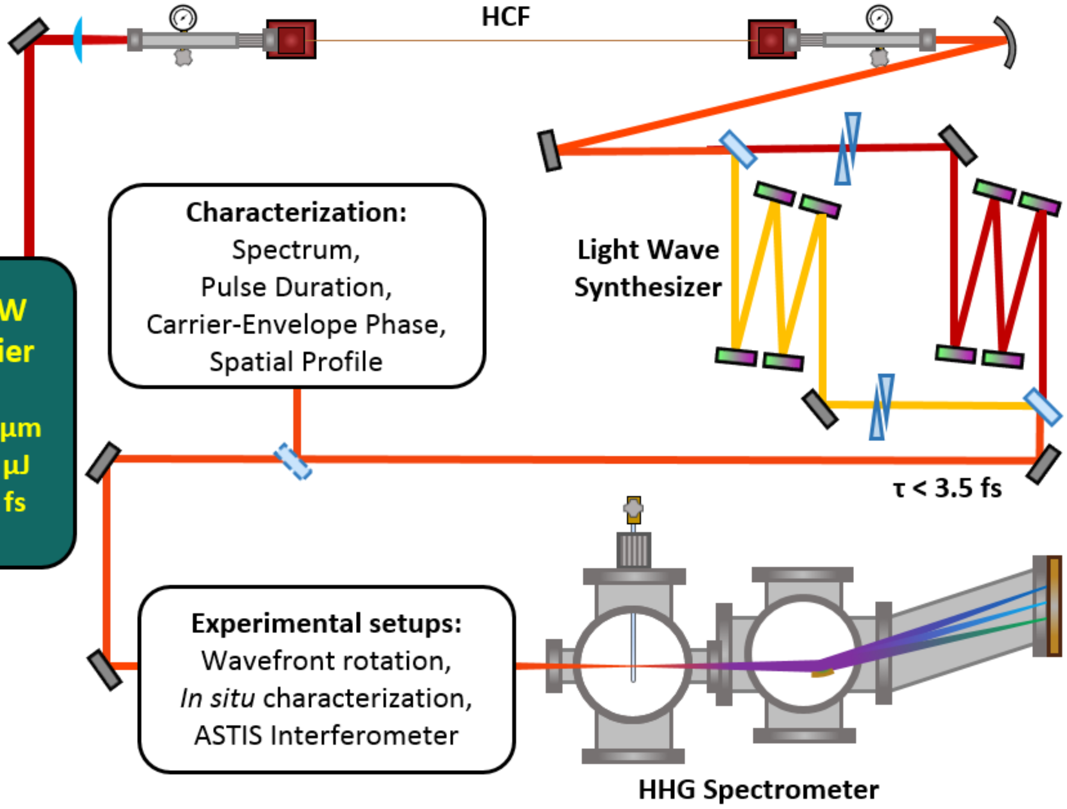

Figure 1: Schematic of the experimental setup.

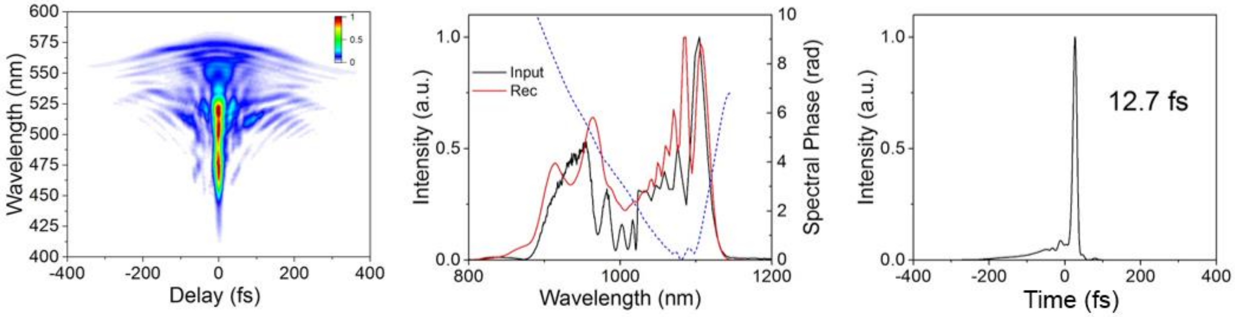

Figure 2: Characterization of pulses compressed in a 1,1-difluoroethane. *Left:* Experimentally measured FROG trace. *Center:* Comparison of the retrieved spectrum to an independently measured spectrum. *Right*: Reconstructed pulse with FWHM duration of 12.7 fs.

Future Plans

We are currently in the process of upgrading the 1.4-m hollow-core fiber compressor with a new 3.5-m fiber. The new fiber system will enable both higher throughput, due to an increase in the core diameter, and higher compression factor. Our calculations, supported by recent experimental results using a similar Yb:KGW laser amplifier[6], suggest that spectra supporting single-cycle field transients can be obtained in a single stage of compression. Chirped mirrors to compress the ultra-broadband spectrum are currently being evaluated. Following characterization of the pulse duration and CEP stability of the field transients, we will characterize the CEP-dependent spectrum of XUV free-induction decay for few- to single-cycle pulses.

References

1. C.-H. Lu, Y.-J. Tsou, H.-Y. Chen, B.-H. Chen, Y.-C. Cheng, S.-D. Yang, M.-C. Chen, C.-C. Hsu, and A. H. Kung, “Generation of intense supercontinuum in condensed media,” Optica **1**, 400-406 (2014).
2. M. Nisoli, S. D. Silvestri, and O. Svelto, "Generation of high energy 10 fs pulses by a new pulse compression technique," Appl. Phys. Lett. **68**, 2793-2795 (1996).
3. J. E. Beetar, S. Gholam-Mirzaei, and M. Chini, "Spectral broadening and pulse compression of a 400 μJ, 20 W Yb:KGW laser using a multi-plate medium," Applied Physics Letters **112**, 051102 (2018).
4. J. E. Beetar, F. Rivas, S. Gholam-Mirzaei, Y. Liu, and M. Chini, “Hollow-core fiber compression of a commercial Yb:KGW laser amplifier,” submitted to J. Opt. Soc. Am. B (2018)
5. E. Haddad, R. Safaei, A. Leblanc, R. Piccoli, Y.-g. Jeong, H. Ibrahim, B. E. Schmidt, R. Morandotti, L. Razzari, F. Légaré, and P. Lassonde, "Molecular gases for pulse compression in hollow core fibers," Opt. Express **26**, 25426-25436 (2018).
6. Y. G. Jeong, R. Piccoli, D. Ferachou, V. Cardin, M. Chini, S. Hadrich, J. Limpert, R. Morandotti, F. Legare, B. E. Schmidt, and L. Razzari, "Direct compression of 170-fs 50-cycle pulses down to 1.5 cycles with 70% transmission," Sci. Rep. **8**, 11794 (2018).

Peer-Reviewed Publications Resulting from this Project (Project start date: Sept. 1, 2018**)**
No publications to report.

Page is intentionally blank.

Atomic and Molecular Physics in Strong Fields

Shih-I Chu
Department of Chemistry, University of Kansas
Lawrence, Kansas 66045
E-mail: sichu@ku.edu

Program Scope

In this research program, we address the fundamental physics of the interaction of atoms and molecules with intense ultrashort laser fields. The main objectives are to develop new theoretical formalisms and accurate computational methods for *ab initio* nonperturbative investigations of multiphoton quantum dynamics and very high-order nonlinear optical processes of one-, two-, and many-electron quantum systems in intense laser fields. Particular attention will be paid to (i) the exploration of the effects of electron correlation and multi-electron response on high-harmonic generation (HHG) and multiphoton ionization (MPI) processes of atoms, and diatomic, and small polyatomic molecules; (ii) Development of new time-frequency transform to facilitate the exploration of dynamical origin of near- and below- threshold harmonic generation of atomic and molecular systems in mid-IR laser fields; and (iii) Coherent control of HHG processes for the generation of shorter and stronger linearly and circularly polarized attosecond laser pulses, etc.

Recent Progress

1. Coherent Control of the Generation of Single Ultrashort Attosecond Laser Pulse

The investigation of attosecond (*as*) physics in intense ultrashort laser fields is a forefront subject of much current interest and significance in ultrafast science and technology. Attosecond pulses can be produced by means of high-harmonic generation (HHG) of atoms or molecules in intense laser fields, and the time profile of the attosecond pulses can be controlled by tuning the laser pulse shape. The generation of ever-shorter attosecond pulses has continued to attract much interest. It has been demonstrated experimentally that, by superposing the supercontinuum harmonic spectrum, one can obtain a train of attosecond pulses (ATP) or an isolated pulse. The shortest isolated pulse being generated today is 43 attoseconds.

In the last few years, we have initiated a series of *ab initio* studies to explore new mechanisms for the coherent control of the quantum pathways for efficiently generating ultrashort attosecond (*as*) pulses. More recently, we have further presented an efficient *optimal control scheme* for the generation of the ultrabroad supercontinuum spectrum and an isolated ultrashort attosecond pulse in gases with a two-color mid-IR laser field [R1]. The optimal control scheme is implemented using a derivative-free unconstrained optimization algorithm called NEWUOA (NEW Unconstrained Optimization Algorithm). It is shown that the optimally shaped laser waveforms can greatly enhance and extend the HHG plateau and efficiently generate an isolated ultrashort attosecond pulse. Furthermore, the optimized pulse can produce a single ultrashort pulse that is not only much shorter but also more intense, by two orders of magnitude, than that produced by the initial un-optimized laser pulse. In another recent work in this direction, we have further found that optimally shaped *inhomogeneous* two-color mid-infrared laser fields can greatly enhance and extend the HHG plateau. Wavelet time-frequency analysis and classical simulations show that the superposition of resulting hydrogen HHG supercontinuum effectively gives rise to a robust isolated 5-*as* pulse [R2], the shortest *as* pulse ever simulated.

On a different route, we also pursue the exploration of the generation of isolated ultrashort attosecond pulses by coherent control of the population of excited states [1]. The population of the first two low-lying excited states of He^+ ions is selectively controlled by adding low intensity, high frequency laser pulses to a two color mid-IR laser field. Although the intensity of the added field is weak, its high frequency makes the subsequent ionization probability from excited states become much larger than for the case of many photons (mid-IR field), even though the intensity is smaller. We found that the intensity of the attosecond pulse generated by superposing a range of synchronized high harmonics is significantly enhanced by 20 orders of magnitude. Similar calculations have been performed for the neutral He atoms. We found that an intense and ultra-short isolated 18 *as* can be generated directly [1].

2. Dynamical Origin and Enhancement of Near- and Below-Threshold Harmonic Generation of in an Intense Mid-IR Laser Field

Near- and below- threshold harmonic generation provides a potential approach to achieve a high conversion efficiency of VUV and EUV sources for the advancement of spectroscopy [R3]. However, the dynamical origin of these lower harmonics is less understood and largely unexplored. Recently we perform an *ab initio* TDDFT quantum study of the near- and below- threshold harmonic generation (BTHG) of cesium (Cs) atoms in an intense 3,600-nm mid-infrared laser field [R4]. By means of the *synchrosqueezing transform* (SST) [R5] of the quantum time-frequency spectrum we have recently developed along with an extended semiclassical analysis, the roles of multiphoton and multiple rescattering trajectories on the near- and below- threshold harmonic generation processes are investigated in details. We find that the multiphoton-dominated trajectories only involve the electrons scattered off the higher part of the combined atom-field potential followed by the absorption of many photons in near- and below- threshold regime. Furthermore, only the near-resonant below-threshold harmonic is exclusive to exhibit phase locked features. Our results uncover the dynamical origin of near- and below- threshold harmonics as well as the role of multi-rescattering trajectories to the resonance-enhanced below-threshold harmonics for the first time. More recently, we have further extend the atomic study to probe multi-rescattering dynamics and electron quantum paths for below- and near-threshold harmonic generation for diatomic H_2^+ [2] and H_2 [3] systems.

Furthermore, in a different but related direction, we have explored the enhancement of VUV and EUV generation by field-controlled resonance structures of diatomic Molecules (CO and N_2) [4]. We find that with the use of different driving laser pulse shapes, one can control and enhance HHG through the excited-state resonance structures. Depending on the pulse shape, the enhancement can reach five to seven orders of magnitude as compared to the reference sine-squared laser pulse of the same duration. More recently, we propose an efficient method for the enhancement of BTHG by mid-infrared laser-driven excited states of atoms [5]. We found that the BTHG is significantly enhanced by two orders of magnitude compared with the case of the initial ground state. Furthermore, we find that a single VUV pulse can be generated by mid-IR laser-driven excited states by superposing several below-threshold harmonics of atoms. Our finding suggests that the generation of below-threshold harmonics by laser-driven excited states of an atom can provide a powerful methodology for the production of intense vacuum-ultraviolet pulses.

3. Controlling Electron Quantum Paths for the Generation of Circularly Polarized High-Order Harmonics

Recently, studies of bright circularly polarized high-harmonic beams from atoms in the soft-x-ray region as a source for x-ray magnetic circular dichroism measurement in a tabletop-scale setup have received considerable attention [R6]. In a recent work, we address the problem with molecular targets and perform a detailed quantum study of H_2^+, CO, and N_2 molecules in bichromatic counter-rotating circularly polarized laser fields [6] where we adopt wavelengths (1300 and 790 nm) and intensities (2×10^{14} W/cm^2) reported in a recent JILA experiment [R6]. Our treatment of multiphoton processes in homonuclear and heteronuclear diatomic molecules is nonperturbative and based on the time-dependent density-functional theory for multielectron systems. The calculated radiation spectrum contains doublets of left and right circularly polarized harmonics with high-energy photons in the XUV and soft-x-ray ranges. Our results reveal intriguing and substantially different nonlinear optical responses for homonuclear and heteronuclear diatomic molecules subject to circularly polarized intense laser fields. We study in detail the below- and above-threshold harmonic regions and analyze the ellipticity and phase of the generated harmonic peaks.

More recently, we further demonstrate the feasibility to control the electron recollisions giving three returns per one cycle of the fundamental frequency ω by using tailored bichromatic (ω, 2ω) counter-rotating circularly polarized laser fields with a molecular target [7]. The full control of the electronic pathway is first analyzed by a classical trajectory analysis and then extended to a detailed quantum study of H_2^+ molecules in bichromatic (ω, 2ω) counter-rotating circularly polarized laser fields. The radiation spectrum contains doublets of left- and right-circularly polarized harmonics in the XUV ranges. We study in detail the below-, near-, and above-threshold harmonic regions and describe how excited-state resonances alter the ellipticity and phase of the generated harmonic peaks [7].

4. Exploration of the Electron Multiple Recollision Dynamics in Intense Laser Fields

Recently it has been found that electron-nucleus multiple rescattering process plays a major role to the resonance-enhanced below-threshold harmonic generation [R3]. We initiate a study of electron multiple recollision dynamics under intense mid-infrared laser fields by means of the de Broglie–Bohm framework of Bohmian mechanics [8]. Bohmian trajectories contain all the information embedded in the time-dependent wave function. This makes the method suitable to investigate the coherent dynamic processes for which the phase information is crucial. In this study, the appearance of the subpeaks in the high-harmonic-generation time-frequency profiles and the asymmetric fine structures in the above-threshold ionization spectrum are analyzed by the comprehensive and intuitive picture provided by Bohmian mechanics. The time evolution of the individual electron trajectories is closely studied to address some of the major structural features of the photoelectron angular distributions.

More recently, we report a *self-interaction free* TDDFT study along with an extended semiclassical study for the nonperturbative probing of the multi-rescattering dynamics and electron quantum paths for below- and near-threshold harmonic generation of H_2 in an intense laser field [9]. We discover that short trajectories are multiphoton dominated and can have multiple returns for below-threshold harmonics, and excited-state resonances can have significant effects on the generation of neighboring below-threshold harmonics. Furthermore, we find that the electron dynamics for below-threshold long, short, and resonant trajectories differ greatly depending upon which hydrogen core (left or right) the electron was released from initially. An intuitive and appealing picture of near- and below-threshold harmonic generation discovered in our study can give guidance to future experiments in this forefront area of ultrafast atomic, molecular, and optical physics.

5. A New Graph-Theoretical Representation and Floquet Formulation for Probing Multiphoton Quantum Interference in Superconducting Quantum Circuits

We introduce a new graph-theoretical representation and Floquet formalism to study generic circuit quantum electrodynamics systems consisting of a two-level qubit coupled with a single-mode resonator in arbitrary coupling strength regimes beyond rotating-wave approximation [10]. We define colored-weighted graphs, and introduce different products between them to investigate the dynamics of superconducting qubits in transverse, longitudinal, and bidirectional coupling schemes. The intuitive and predictive picture provided by this method, and the simplicity of the mathematical construction, are demonstrated with some numerical studies of the multiphoton resonance processes and quantum interference phenomena for the superconducting qubit systems driven by intense ac fields.

More recently, we collaborate with the experimental group at Univ. of Kansas and report experimental observation of two distinct quantum interference patterns in the absorption spectra when a transmon superconducting qubit is subjected to a bichromatic microwave field with the same Rabi frequencies [11]. Within the two-mode Floquet formalism, we propose a graph-theoretical representation to model the interaction Hamiltonian for each of these observations. This theoretical framework provides a clear visual representation of various underlying physical processes in a systematic way beyond rotating-wave approximation. The presented approach is valuable to gain insights into the behavior of multichromatic field driven quantum two-level systems, such as two-level atoms and superconducting qubits. Each of the observed interference patterns is represented by appropriate graph products on the proposed color-weighted graphs. The underlying mechanisms and the characteristic features of the observed fine structures are identified by the transitions between the graph vertices, which represent the doubly dressed states of the system. The good agreement between the numerical simulation and experimental data confirms the validity of the theoretical method. Such multiphoton interference may be used in manipulating the quantum states and/or generate nonclassical microwave photons.

Future Research Plans

In addition to continuing the ongoing researches discussed above, we plan to initiate the following several new project directions: (a) Extension of the TDGPS method in momentum space [R7] to the study of HHG/ATI processes in intense free electron x-ray laser fields. (b) Further development of Bohmian mechanics approach [8] for the exploration of the electron quantum dynamics associated with HHG/MPI processes. (c) Extension of the new time-frequency method, the *synchrosqueezing transform* (SST) [R5], for the exploration of the novel quantum dynamics for below- and near- threshold harmonics of diatomic molecules. (d) Exploration of HHG dynamics of vibrating diatomic molecules [12]. (e) Development of new *non-adiabatic* time-dependent DFT [13,14], including the memory effect, for the treatment of novel strong-field AMO phenomena and phase transitions.

Publications acknowledging DOE Support (2016-2018):

[1] H.Z. Jooya, P.-C. Li, S.-L. Liao, and S.I. Chu, Generation of isolated ultra-short attosecond pulses by coherent control of the population of excited states, *Phys. Lett. A* **380**, 316 (2016).

[2] J. Heslar and S.I. Chu, Unravelling the dynamical origin of below- and near-threshold harmonic generation of H_2^+ in an intense NIR laser field, *Sci. Rep.* **6**, 37774 (2016).

[3] J. Heslar and S.I. Chu, Probing multi-rescattering dynamics and electron quantum paths for below- and near-threshold harmonic generation of H_2 in an intense laser field, *Phys. Rev. A* **95**, 043414 (2017).

[4] J. Heslar, D.A. Telnov, and S.I. Chu, Enhancement of VUV and EUV generation by field-controlled resonance structures of diatomic molecules, *Phys. Rev. A* **93**, 063401 (2016).

[5] Q.L. Guo, P.C. Li, X.X. Zhou, and S.I. Chu, Efficient enhancement of below-threshold harmonic generation by laser-driven excited states of Cs atom, *Optics Comm.* **410**, 262 (2018).

[6] J. Heslar, D.A. Telnov, and S.I. Chu, Generation of circularly polarized XUV and soft X-ray high-order harmonics by homonuclear and heteronuclear diatomic molecules subject to bichromatic counter-rotating circularly polarized intense laser fields, *Phys. Rev. A (Editors' suggestion paper)* **96**, 063404 (2017).

[7] J. Heslar, D.A. Telnov, and S.I. Chu, Controlling electron quantum paths for generation of circularly polarized high harmonics by H_2^+ subject to tailored (ω,2ω) counter-rotating laser fields, *Phys. Rev. A* **97**, 043419 (2018).

[8] H.Z. Jooya, D.A. Telnov, and S.I. Chu, Exploration of the electron multiple recollision dynamics in intense laser fields with Bohmian trajectories, *Phys. Rev. A* **93**, 063405 (2016).

[9] J. Heslar and S.I. Chu, Probing multirescattering dynamics and electron quantum paths for below- and near-threshold harmonic generation of H_2 in an intense laser field, *Phys. Rev. A* **95**, 043414 (2017).

[10] H.Z. Jooya, K. Reihani, and S.I. Chu, A graph-theoretical representation of multiphoton resonance processes in superconducting quantum circuits, *Sci. Rep.* **6**, 37544 (2016).

[11] J. Pan, H.Z. Jooya, G. Sun, Y. Fan, P. Wu, D.A. Telnov, S.I. Chu, and S. Han, Absorption spectra of superconducting qubits driven by bichromatic microwave fields, *Phys. Rev. B* **96**, 174518 (2017).

[12] D.A. Telnov, J. Heslar, and S.I. Chu, High harmonic generation of vibrating H_2^+ and D_2^+, *Phys. Rev. A* **95**, 043425 (2017).

[13] S. L. Liao, T.S. Ho, H. Rabitz, and S.I. Chu, Time-Local Equation for the Exact Optimized Effective Potential in Time-Dependent Density Functional Theory, *Phys. Rev. Lett.* **118**, 243001 (2017).

[14] S. L. Liao, T.S. Ho, H. Rabitz, and S.I. Chu, Exact-exchange optimized effective potential and memory effect in time-dependent density functional theory, *Eur. Phys. J. B* **91**, 147 (2018).

References:

[R1] Y. Chou, P.-C. Li, T.S. Ho, and S.I. Chu, Optimal control of high-order harmonics for the generation of an isolated ultrashort attosecond pulse with two-color midinfrared laser fields, *Phys. Rev. A* **91**, 063408 (2015).

[R2] Y. Chou, P.-C. Li, T.S. Ho, and S.I. Chu, Generation of an isolated few-attosecond pulse in optimized inhomogeneous two-color fields, *Phys. Rev. A* **92**, 023423 (2015).

[R3] M. Chini, X. Wang, Y. Cheng, H. Wang, Y. Wu, E. Cunningham, P.-C. Li, J. Heslar, D.A. Telnov, S.I. Chu, and Z. Chang, Coherent phase-matched VUV generation by field-controlled bound states, *Nat. Photonics* **8**,437(2014).

[R4] P.-C. Li, Y.L. Sheu, C. Laughlin, and S.I. Chu, Dynamical origin of near- and below-threshold harmonic generation of Cs in an intense mid-infrared laser field, *Nat. Commun.* **6**, 7178 (2015).

[R5] Y. L. Sheu, L.Y. Hsu, H.T. Wu, P. -C. Li, and S.I. Chu, A new time-frequency method to reveal quantum dynamics of H atoms in intense laser pulses: Synchrosqueezing transform, *AIP Advances* **4**, 117138 (2014).

[R6] T. Fan, *et. al.,* Bright circularly polarized soft X-ray high harmonics for X-ray magnetic circular dichroism**,** PNAS 112, 14206 (2015).

[R7] Z.Y. Zhou and S.I. Chu, Precision calculation of above-threshold multiphoton ionization in intense short-wavelength laser fields: The momentum-space approach and time-dependent generalized pseudospectral method, *Phys. Rev. A* **83**, 013405 (2011).

Optical Two-Dimensional Spectroscopy of Disordered Semiconductor Quantum Wells and Quantum Dots

Steven T. Cundiff
Department of Physics, University of Michigan, Ann Arbor, MI 48109
cundiff@umich.edu

October 2, 2018

Program Scope: The goal of this program has been to implement optical 2-dimensional coherent spectroscopy and apply it to electronic excitations, including excitons, in semiconductors. Specifically of interest are epitaxially grown quantum wells that exhibit disorder due to well width fluctuations and quantum dots. In both cases, 2-D spectroscopy provides information regarding coupling among excitonic localization sites.

Recent Progress: During the last year, we have continued our studies of colloidal quantum dots (CQDs), identifying signatures of non-Markovian coupling between excitons and LO-phonons and of finite size effects on acoustic phonons. We have studied an entirely new material, perovskite nanoparticles. We also competed and published work on using deconvolution algorithms used for deblurring images to extract the underlying physics from two-dimensional spectra.

Multidimensional coherent spectroscopy has become a powerful method in ultrafast optics that has largely replaced prior methods such as photon echo spectroscopy or transient absorption. However, it still suffers from the difficulty of interpreting the spectra, which are often daunting for the non-expert to understand. Furthermore, a theory-experiment comparison to probe the underlying physics, not the spectroscopy itself, requires calculations that capture both the physics and the spectroscopy. This requirement greatly limits the pool of theorists to those who understand both aspects.

To address this, we worked with a theorist, Marten Richter from the TU-Berlin, who proposed and demonstrated that it is possible to apply the same inversion algorithms used to "deblur" images to two-dimensional spectra to reveal the underlying dynamics free of the effects of the spectroscopy. As an example, we used two-dimensional coherent spectra of the exciton resonance in a quantum well taken as a function of the waiting time, T, between the second and third pulses. Spectral diffusion due to spatial migration and dynamic localization of excitons cause the 2D spectra to evolve during T. By using the inversion algorithm, it was possible to extract the Green's functions that described transfer process. This work was published in *Science Advances* this year, item 6 on the list of publications below.

In last year's abstract, we reported on using multidimensional spectroscopy to observe Rabi flopping of excitons in self-organized quantum dots (paper 3 below), which leveraged the ability of quantum dots to make a size resolved measurement in an ensemble of dots with size dispersion. During the last year, we extended this work by examining the detuning dependence of the Rabi flopping for both neutral excitons and trions.

We demonstrated coherent control over the entire frequency distribution for both neutral and charged QDs. The behavior of the trions' 2-level system appears symmetric with respect to the center energy of excitation laser. However, the exciton-biexciton 4-level system exhibits an asymmetric behavior. Although such a behavior is counter-intuitive, it reflects the asymmetric 4-level energy structure of the exciton-biexciton system. The experimental data is well reproduced by calculating 2-level and 4-level optical Bloch equations (OBEs) including detuning and excitation-induced dephasing (EID). We suggest one of the dominant EID sources is wetting layer carriers through temperature dependent measurements. This work was published as a Rapid Communication in *Physical Review B* (paper 5 in the list below, where is was selected as an "Editors Suggestion."

The comprehensive understanding of exciton dynamics required for CQD applications is hindered by complexities resulting from electronic states coupling to external degrees of freedom, such as vibrational modes or charge configurations. Fluctuations in the exciton resonance energy due to interactions with the local environment, called spectral diffusion, are not well understood. Though such fluctuations have been mitigated in other nanostructures, such as self-assembled dots, this is not true for CQDs. Spectral diffusion, which may be thought of as dynamic inhomogeneous broadening, is challenging to study via one-dimensional spectroscopic techniques since CQD ensembles possess inherent static inhomogeneous broadening due to dot size dispersion. However, elucidating the physical origins of energy gap fluctuations in CQDs is vital to opto-electronic applications of the material.

The interactions of excitons with their surroundings may be considered either Markovian (energy gap fluctuations are instantaneous and uncorrelated) or non- Markovian (timescales of the interactions and exciton dynamics are comparable, and energy gap fluctuations are highly correlated). In the Markovian regime, coherences dephase exponentially at a rate $1/T_2$ and the physical origins of the dephasing mechanisms are obscured. In the non-Markovian regime however, the physical nature of the dephasing interactions manifests as non-exponential dephasing of coherences. Though it is known that phonon coupling in semiconductors may induce non-Markovian dephasing, the μs temporal resolution limit of spectrally-resolved single dot studies exceeds the correlation time of the vibrational coupling in CQDs. Indeed, without access to exciton dynamics at timescales of the vibrational coupling itself, studies of CQDs and their optical properties have thus far assumed effective homogeneous broadening in the Markovian limit. A technique capable of circumventing inhomogeneous broadening in a CQD ensemble with femtosecond time-resolution is thus necessary to reveal signatures of non-Markovian dynamics in CQDs.

We applied multidimensional coherent spectroscopy at cryogenic temperatures to study coherent dynamics of a CdSe CQD ensemble on the femtosecond timescale. Spectrally separating third-order responses that involve intraband coherences from those that involve population states reveals differing temporal behaviors. Comparison to simulation provides further evidence that strong modification of exciton dephasing occurs via coupling to longitudinal-optical vibrational modes. Beyond simply increasing the transition homogeneous linewidth, we observe, for the first time, that LO-coupling induces highly non-Markovian dynamics that directly reflect the energy ga modulation by nuclear motion in the nanocrystal.

To date, two regimes of spectral diusion have been identified, on the seconds timescale and sub-μs timescale. Previous studies have focused on free surface charges and surface ligand rearrangement as possible causes for the band-edge Stark shift that leads to spectral diffusion (to be contrasted with spectral diffusion due to continuum scattering in higher dimensional systems). The above theories are not suffcient to explain our results, which clearly point to LO-phonon coupling as a major factor in spectral diffusion on femtosecond timescales. We propose the random environmental perturbations that cause energy gap fluctuations become less dominant when nuclear motion is initiated in the LO mode. The local fields induced by nuclear motion extend over many unit cells - effectively over the entire core volume of our CQDs. For CQDs grown with a shell structure, such as for our sample, it is reasonable to expect that surface charge dynamics are weak compared to Fröhlich coupling between the exciton and local fields that synchronizes the exciton motion with that of the CQD core lattice. The spectral diffusion dynamics may then approach timescales on the order of the LO phonon period $T_{LO} \approx 150$ fs, and highly non- Markovian evolution of coupled coherences could then occur. It was also found for 3 nm radius bare core (no shell) CQDs the anomalous dephasing dynamics largely disappear. This supports our theory, as removal of screening by a shell layer allows surface charge effects to take precedence over LO-phonon coupling. A detailed microscopic theory is needed to elucidate the exact mechanisms responsible. This work has been submitted for publication in *Physical Review Letters*.

A class of materials that has garnered tremendous interest is metal-halide perovskites, stimulated by meteoric increases in photovoltaic efficiencies of perovskite solar cells. In addition, many recent advances have been made in applying zero-dimensional perovskitenanocrystals in light-emitting devices. It was discovered recently that, for cesium lead-halide perovskite nanocrystals specifically, the cause underlying their unusually efficient light-emission is a unique excitonic fine-structure composed of three bright triplet states that form the band-edge. We used multidimensional coherent spectroscopy at cryogenic temperatures to reveal coherences involving triplet states of a $\mathrm{CsPbI_3}$ nanocrystal ensemble. The inter-triplet coherence lifetime is found to be on the picosecond timescale, and their quantum pathways exhibit strong polarization selectivity. Resolving the quantum pathways provides further information about the relative amplitudes and phases of the transition dipole moments bridging the ground and triplet states. This work gives insight into the fundamental properties of bright triplet states in lead-halide perovskite materials, and positions perovskite nanocrystals as a strong material candidate for coherent optoelectronic devices in quantum information applications.

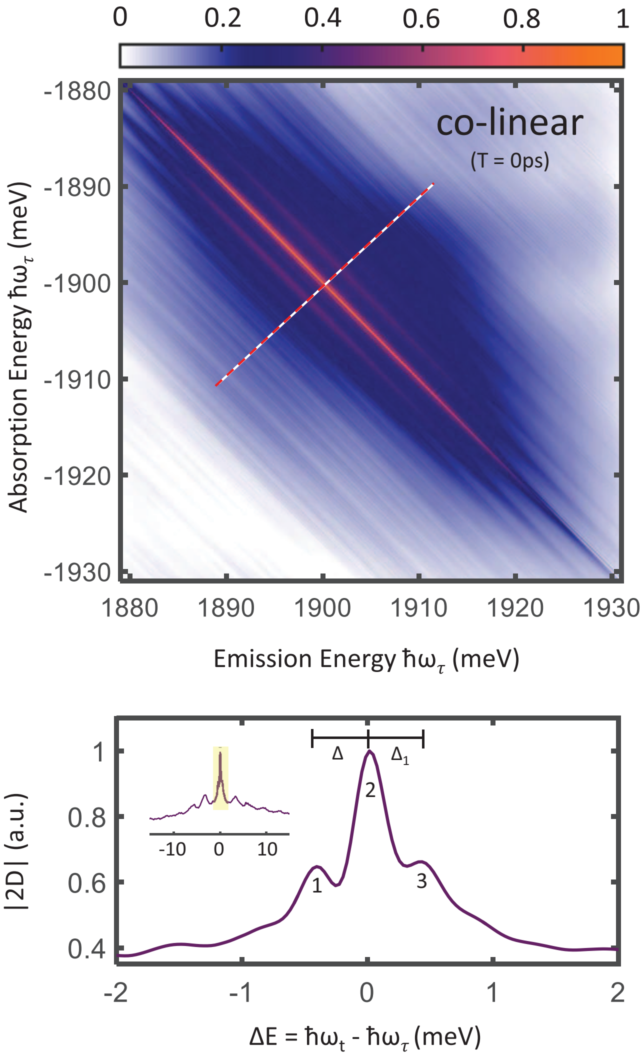

Figure 1: Triplet coherences in one-quantum two-dimensional spectra. Magnitude one-quantum spectrum at 4.6 K using co-linear excitation are shown at the top. The white/red dashed lines and solid black lines indicate the cross-slice locations and excitation/local oscillator pulse spectra respectively. Lower panel is cross-slice centered at $\hbar\omega_\tau = \hbar\omega_t = 1900\ \mathrm{meV}$ one-quantum spectrum. Numbers in lower panel indicate peaks arising from electronic interband coherences and populations.

One-quantum spectra were acquired at a temperature of 4.6 K with co-linear polarized excitation (shown in Fig. 1 top). Numerous peaks are evident that are elongated in the diagonal direction $\hbar\omega_\tau = \hbar\omega_t$, reflecting inhomogeneous broadening of the material response. By taking a cross-diagonal slice (indicated by the red/white dashed line) the ensemble-averaged homogeneous response of nanocrystals with a certain resonance energy is obtained. We plot a cross-diagonal slice of the one-quantum spectrum in the lower panel of Fig. 1. In the full slice (inset), asymmetric peaks are observed for $|\Delta E| > 4\ \mathrm{meV}$, which we attribute to electronic-vibrational coupling. The main plots of each slice section (high- lighted by the yellow boxes inset) show symmetric peaks, which are generated by triplet state coherences.

We have isolated both optical frequency triplet coherences and terahertz frequency inter-triplet coherences. From the coherence times extracted we find that both the triplet and inter-triplet coherence times are far from radiatively limited, indicating that much work remains in elucidating the physical processes responsible for dephasing in perovskite nanocrystals. As a material still in its infancy, perovskite nanocrystals show incredible promise towards applications in a variety of opto-electronic devices. Minimal thermal broadening was observed of the inter-triplet coherences, motivating their study and application above cryogenic temperatures. Furthermore, in a triplet-state analogue of valleytronics in transition metal dichalcogenide materials, extending the coherence time of inter-triplet coherences may allow for their coherent manipulation via terahertz radiation as information carriers. A manuscript describing these results is in preparation.

Future plans: During the next year, we plan to wrap our studies of the CdSe colloidal quantum dots. We are currently completing a manuscript on exciton-acoustic phonon coupling. The are are two messages. The first is that multidimensional coherent spectroscopy is the best tool for observing non-Markovian coupling to between excitons and acoustic phonons, evidenced as strong sidebands. The second point is that we can see the effects of acoustic phonon quantization in the CQDs. While this has been observed in single-dot studies, it has not been observed in ensembles. The strong acoustic-phonon sidebands make the quantization a prominent effect, whereas single QD studies are generally restricted to simple methods such as fluorescence, which do not show as prominent phonon sidebands.

We plan to continue our study of the perovskite nanocrystals. Beyond the interest in perovskite films for solar energy, these nanocrystals are generating interest on their own because they appear to emit light very efficiently. This feature appears to be due the lowest triplet states being bright, whereas in most colloidal nanocrystals, the lowest energy excited state is dark, trapping excitation.

Finally, we plan to study a new type of colloidal particle, provided by a collaborator in Korea, quantum shells. These particles have a low gap layer that forms a shell around a higher gap core, and then are encapsulated in a second higher gap shell. The lower gap shell is sufficiently thin to result in quantum confinement in the radial direction. We have just begun linear characterization of these samples, but already the look very interesting.

Peer-Reviewed Publications resulting from this project (2016-2018):

1. R. Singh, G.M. Moody, H. Li, M. Siemens and S.T. Cundiff, “Quantifying Spectral Diffusion by Direct Measurement of the Correlation Function for Excitons in Semiconductor Quantum Wells,” J. Opt. Soc. Am. B **33**, C137 (2016).
2. R. Singh, T. Suzuki, T. M. Autry, G. Moody, M. E. Siemens, and S. T. Cundiff, “Polarization Dependent Exciton Linewidth in Semiconductor Quantum Wells – a Consequence of Bosonic Nature of Excitons,” Phys. Rev. B **94**, 081304(R) (2016).
3. T. Suzuki, R. Singh, M. Bayer, A. Ludwig, A. D. Wieck, and S. T. Cundiff, “Coherent Control of the Exciton/Biexciton System in an InAs Self Assembled Quantum Dot Ensemble,” Phys. Rev. Lett. **117**, 157402 (2016).
4. R. Singh, M. Richter, G. Moody, M.E. Siemens, H. Li and S.T. Cundiff, “Localization dynamics of excitons in disordered semiconductor quantum wells,” Phys. Rev. B **95**, 235307 (2017).
5. T. Suzuki, R. Singh, M. Bayer, A. Ludwig, A. D. Wieck, and S. T. Cundiff, “Detuning dependence of Rabi oscillations in an InAs self-assembled quantum dot ensemble,” Phys. Rev. B **97** 161301(R), (2018).
6. M. Richter, R. Singh, M. Siemens, and S. T. Cundiff, “Deconvolution of optical multidimensional coherent spectra,” Sci. Adv. **4** , eaar7697 (2018).

SISGR: Understanding and Controlling Strong-Field Laser Interactions with Polyatomic Molecules

DOE Grant No. DE-SC0002325

Marcos Dantus, dantus@msu.edu
Department of Chemistry and Department of Physics and Astronomy, Michigan State University, East Lansing MI 48824

1. Program Scope

Advances made over the past two decades in our understanding of laser-matter interactions allow us to start thinking about strategies for not only observing, but also *controlling* the different processes and reactions that these interactions cause. Our program focuses on the chemical processes occurring in polyatomic molecules under intense laser excitation. Efforts on quantum control of electronic, vibrational, and rotational dynamics of molecules prior to and during strong-field interactions are in line with the Grand Challenge questions that have been proposed in recent DOE- and NSF-sponsored workshops. Recently, we have sharpened our focus towards better understanding and controlling of ultrafast hydrogen migration processes occurring in organic molecules under strong fields. These processes include the formation of neutral hydrogen molecules, and exotic chemical processes involving making and breaking of multiple chemical bonds that result in the formation of H_3^+, H_2O^+, H_3O^+, and CH_5^+. Our studies have provided the first evidence for roaming chemical reactions initiated by ion precursors. Our work, in collaboration with other groups within the DOE AMOS group, is improving the quantum mechanical descriptions of relatively unknown chemical reactions that involve roaming of neutral fragments.

2. Recent Progress

(a) Discovery of neutral H_2 roaming chemistry occurring under strong fields

N. Ekanayake, M. Nairat, B. Kaderiya, P. Feizollah, B. Jochim, T. Severt, B. Berry, K. Raju P., K. D. Carnes, S. Pathak, D. Rolles, A. Rudenko, I. Ben-Itzhak, C. A. Mancuso, B. S. Fales, J. E. Jackson, B. G. Levine, and M. Dantus "Mechanisms and time-resolved dynamics for trihydrogen cation (H_3^+) formation from organic molecules in strong laser fields," *Nature Scientific Reports*, 7, 4073 (2017)

Strong-field laser-matter interactions have been found to involve exotic chemical reactions. H_3^+ formation from organic molecules is one such case that requires multiple bonds to break and form. In this study, conducted in collaboration with the James R. Macdonald Laboratory at Kansas State University, we present evidence for the existence of two different reaction pathways for H_3^+ formation from organic molecules irradiated by a strong-field laser. The mechanistic details and timescales were experimentally determined by femtosecond time-resolved time-of-flight mass spectroscopy and photoion-photoion coincidence momentum measurements carried out on methanol isotopologues, ethylene glycol, and acetone. *Ab initio* molecular dynamics simulations suggest that H_3^+ formation occurs via a two-step mechanism in which a neutral H_2 molecule is formed, and then roams about the doubly-charged intermediate until it abstracts a proton from the remaining $CHOH^{2+}$ fragment. This reaction, proton abstraction by a roaming H_2 molecule, is reminiscent of the well-known Hogness and Lunn reaction for H_3^+ formation in the universe. These exotic chemical reaction mechanisms, involving roaming H_2 molecules, are found to occur in the ~100 fs timescale. Roaming molecule reactions may help to explain unlikely chemical processes, involving dissociation and formation of multiple chemical bonds, occurring under strong laser fields.

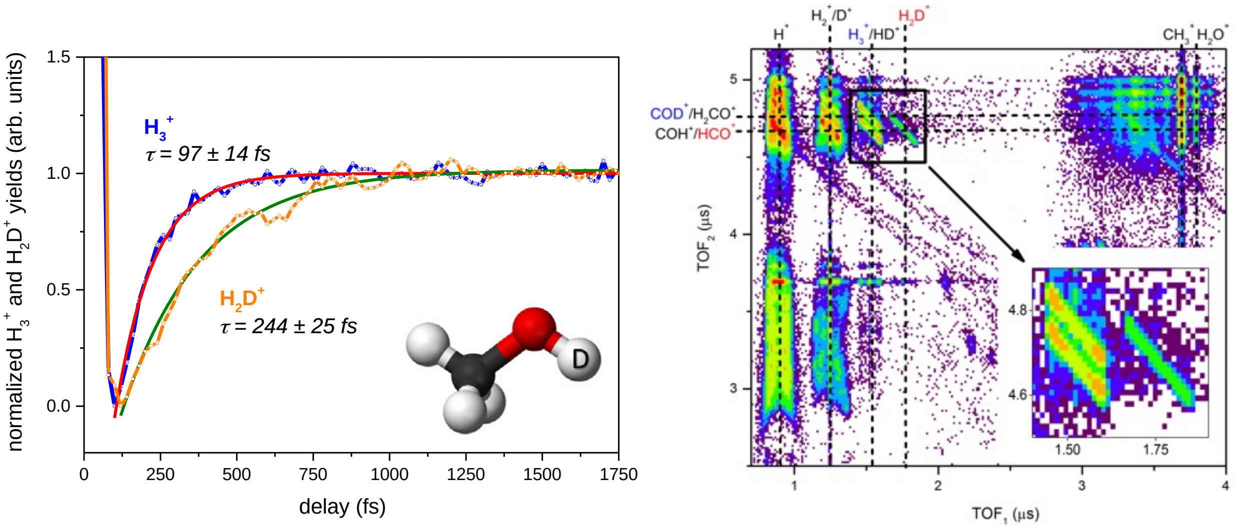

Fig. 1 (Left), Time resolved data used to determine the time for H_3^+ formation by two distinct pathways from CH_3OD. (Right) Photoion-photoion coincidence data from CH_3OD confirming the formation of H_3^+ and H_2D^+ via different pathways.

(b) H_2 roaming chemistry and the formation of H_3^+ from organic molecules in strong laser fields

N. Ekanayake, T. Severt, M. Nairat, N. P. Weingartz, B. M. Farris, B. Kaderiya, P. Feizollah, B. Jochim, F. Ziaee, K. Borne, K. Raju P., K. D. Carnes, D. Rolles, A. Rudenko, B. G. Levine, J. E. Jackson, I. Ben-Itzhak, and M. Dantus, *Nature Communications*. In Review after positive comments and revision (2018).

With the goal of understanding H_3^+ formation and enhancing its yield, we studied its formation from alcohols with different chain lengths. The mechanistic details and femtosecond time-resolved dynamics were obtained through a combination of strong-field laser excitation studies, photoion-photoion coincidence measurements, and *ab initio* molecular dynamics simulations. For small alcohols, four distinct pathways involving hydrogen migration and H_2 roaming prior to H_3^+ formation were uncovered. In principle, one might expect the yield would be proportional to the number of hydrogen atoms. However, we find that methanol has the highest efficiency while *tert*-butanol has the lowest. We explain the observed reaction timescales and yields with the aid of molecular dynamics simulations. Collaboration with JRML.

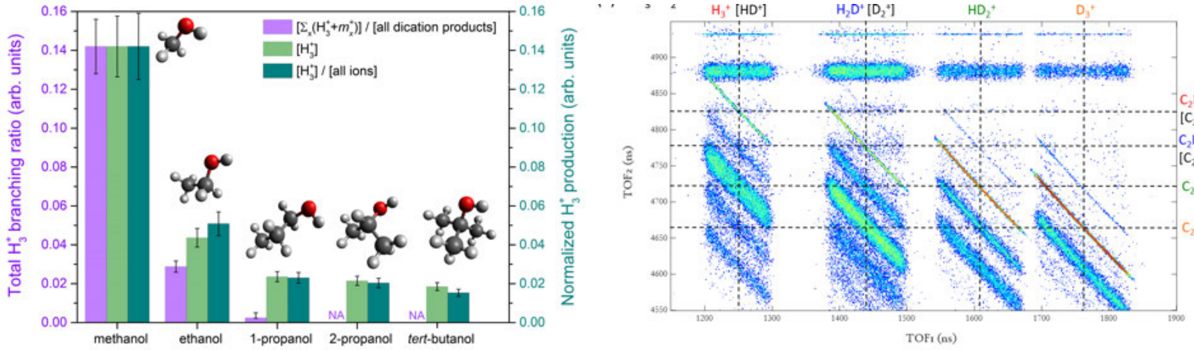

Fig. 2 (Left), Total H_3^+ branching ratios ($[\Sigma_x(H_3^+ + m_x^+)]/[\text{all dication products}]$) together with normalized H_3^+ ($[H_3^+]$), and fractional H_3^+ ($[H_3^+]/[\text{all ions}]$) production from dissociative ionization of methanol, ethanol, 1-propanol, 2-propanol, and tert-butanol in a linearly polarized laser field with a peak intensity of 2.0×10^{14} W/cm^2. The $[H_3^+]$ and $[H_3^+]/[\text{all ions}]$ yields were obtained through the time-of-flight technique, and each of them is normalized with respect to the corresponding branching ratio of methanol, $[(H_3^+ + HCO^+)] / [\text{all dication products}]$, determined by the coincidence time-of-flight (CTOF) method. Due to the complexity of quantitative analysis, CTOF measurements were not performed for large molecules (2-propanol and tert-butanol) and are indicated by 'NA' at the corresponding positions in the figure. (Right) Truncated CTOF maps focused only on H_3^+ production from dissociative ionization of CH_3CD_2OD in a linearly polarized laser pulse centered about 790 nm, 23-fs long with a peak intensity of 3.0×10^{14} W/cm^2. The labeled dashed lines indicate the two-body breakup ion pairs related to H_3^+ formation from the ethanol dication. The logarithmic color scale depicts the number of ion pairs recorded.

(c) Substituent effects on H_3^+ formation via H_2 roaming mechanisms under strong-field photodissociation of organic molecules

N. Ekanayake, M. Nairat, N. P. Weingartz, M. J. Michie, B. G. Levine, and M. Dantus, *Phys.Chem.Chem.Phys.* In Review (2018)

In this study, we investigate the photodissociation and H_3^+ formation from organosulfur compounds (thiols) and compare them with their alcohol counterparts. Thiols have a lower ionization potential and higher acidity relative to alcohols. Therefore, we expect thiols to produce a higher H_3^+ compared to alcohols. Contrary to expectations, the H_3^+ yield was found to be an order of magnitude lower for thiols compounds at certain laser field intensities. We present an in-depth analysis of experimental findings, supported by *ab initio* quantum mechanical calculations.

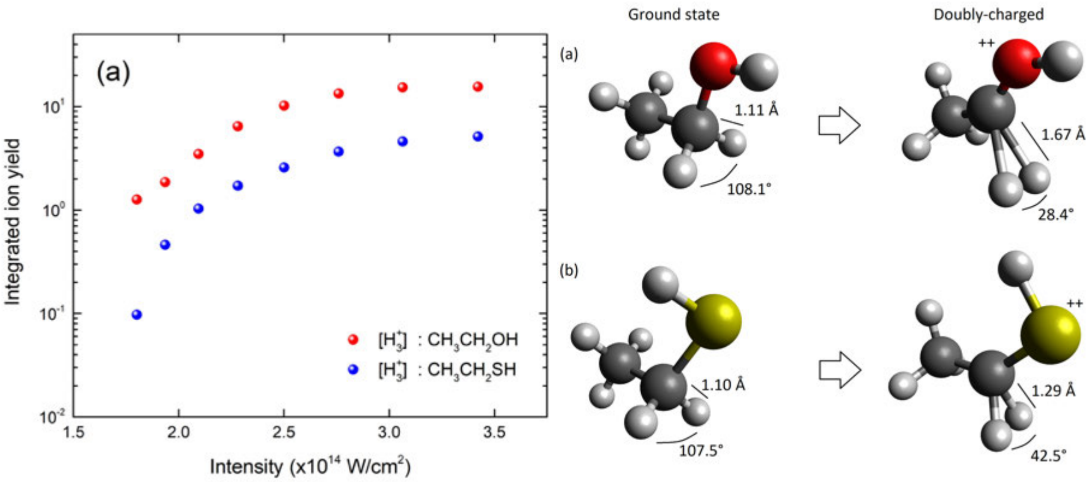

Fig. 3 (Left) Experimental photodissociation H_3^+ yields for CH_3CH_2OH are an order of magnitude greater than for CH_3CH_2SH, after ionization by an 800-nm 40-fs pulse. (Right) Neutral and doubly-charged structure minima for (a) ethanol and (b) ethanethiol carried out at the CCSD/aug-cc-pVDZ level of theory. Bond angles and bond lengths relevant to H_2 formation are shown. Doubly-charged ethanol shows longer αC–H bonds and smaller H–αC–H angles allowing H_2 ejection to be more efficient. In addition, unlike in ethanethiol, the hydroxy hydrogen in ethanol is pointing towards the nascent H_2.

(d) Quantum Coherent Control of H_3^+ Formation in Strong Fields

M. Michie, N. Ekanayake, N. P. Weingartz, J. Stamm, and M. Dantus. Manuscript to be submitted in October 2018.

Strong-field laser-matter interactions are well understood for isolated atoms and diatomic molecules, yet our understanding falls short when polyatomic molecules are involved. Similarly, quantum coherent control (QCC) of laser-matter interactions is well known for two- and three-photon resonant transitions, but not understood in cases with higher order transitions. Here, we consider the simplest approach to QCC, namely the use of a single spectral phase step, on a chemical process requiring strong-field double ionization. The goal is to determine if QCC can be used to control strong-field laser-matter interactions involving higher order 7- to 16-photon excitation. We find that indeed the spectral phase step provides a significant and unexpected method to control the yield of H_3^+ and its coincidence ion HCO^+ following the double ionization of methanol (see Fig. 4).

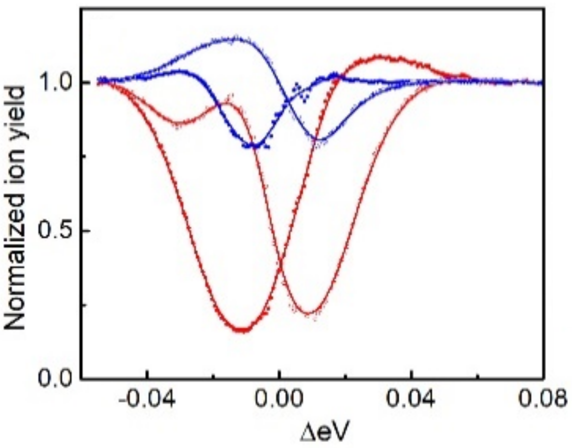

FIG. 4. The yield of H_3^+(red) and its coincidence ion HCO^+ (blue) detected as a function of scanning a positive or negative 3π/4 phase step phase across the spectrum. The ion yields are normalized to their value when TL pulses are used. Notice that in some cases the ion yield exceeds that obtained for TL pulses.

3. Future Plans

The proposed research addresses Grand Challenge questions related to quantum control of electrons in matter. We focus on coherent control of excited electronic states, optimal control, taking advantage of higher energies, broader bandwidth and shorter times afforded by shape femtosecond lasers. We plan to continue our work on elucidating and controlling hydrogen migration mechanisms occurring under strong-field excitation. We have a number of manuscripts in review, and to be submitted in a few weeks involving: thiols; quantum control of strong field H_3^+ formation from methane; formation of H_2O^+ and H_3O^+ from ethanol (collaboration with JRML); quantum control of H_3^+ formation from smaller molecules like methane and ethane (looking into controlling the re-scattering process likely responsible for double ionization); a project exploring direct probing of H_3^+ and H_2. We plan to write a comprehensive review about the lessons learned regarding hydrogen migration. Our findings are important because they include the first time-resolved roaming chemical processes, which happen to be the first roaming process recorded in ion chemistry. Understanding hydrogen atoms, their chemistry, and dynamics is important given that they make up the majority of atoms in the universe, therefore, the chemical dynamics we are observing teach us about timescales of fundamental chemical processes leading to hydrogen containing molecules in the universe. We will continue to take advantage of our expertise in pulse shaping, a new OPA that allows us to tune from 234 -2100 nm, and data from our PEPICO instrument.

5. Peer Reviewed Publications Resulting from this Project (2016-2018)

1. M. Nairat, J. Lantis, V. V. Lozovoy, and M. Dantus, "Order of Magnitude Dissociative Ionization Enhancement Observed for Pulses with High Order Dispersion", J. Phys. Chem. A **120**, 8529−8536 (2016)

2. Nagitha Ekanayake, Muath Nairat, Balram Kaderiya, Peyman Feizollah, Bethany Jochim, Travis Severt, Ben Berry, Kanaka Raju P., Kevin D. Carnes, Shashank Pathak[2], Daniel Rolles, Artem Rudenko, Itzik Ben-Itzhak, Christopher A. Mancuso, B. Scott Fales, James E. Jackson, Benjamin G. Levine, and Marcos Dantus "Mechanisms and time-resolved dynamics for trihydrogen cation (H_3^+) formation from organic molecules in strong laser fields," Nature Scientific Reports, 7, 4073 (2017)

3. Gennady Rasskazov, Muath Nairat, Ilias Magoulas, Vadim V. Lozovoy, Piotr Piecuch, Marcos Dantus, "Femtosecond real-time probing of reactions MMXVII: The predissociation of sodium iodide in the A 0+ state," Chem. Phys. Letters, 683, 127-127 (2017)

4. V. V. Lozovoy, M. Nairat, and M. Dantus, "Binary phase compression of stretched pulses," J. Optics 19, 105506 (2017)

PROGRAM TITLE: ATTOSECOND, IMAGING AND ULTRA-FAST X-RAY SCIENCE

PI: Louis F. DiMauro
Co-PI: Pierre Agostini, Emeritus
Co-PI: Terry A. Miller, Emeritus
Department of Physics
The Ohio State University
Columbus, OH 43210
dimauro.6@osu.edu
agostini@mps.ohio-state.edu
tamiller@chemistry.ohio-state.edu

1.1 PROJECT SCOPE

This grant aims at exploring the realm of ultrafast dynamics using different complementary tools. In one thrust, we explore and exploit fundamental aspects of generation and measurement of high harmonic and attosecond pulses to access fundamental atomic and molecular processes. A second thrust provides a natural link to our attosecond effort via the same underlying strong field physics, laboratory infrastructure and technical approach. The strong field driven "self-imaging" method uses elastic scattering of field-driven electron wave packets as an alternative route for spatial-temporal imaging in the gas phase. In 2011, the viability of this approach for achieving femtosecond timing and picometer spatial resolution was demonstrated in collaboration between OSU and KSU groups. A third scope is the implementation of an AMO science program using the ultra-fast, intense x-rays available at LCLS XFEL. The objective is the study of fundamental atomic processes involving multiple inner-shell ionization, x-ray nonlinear optics and the development of new methods for time-resolved x-ray physics. Our overall aim is advancing these methods as robust tools for imaging and probing electron dynamics thus producing the complete molecular movie.

Progress over the past year includes the completion of three projects: (1) dynamical spatial-temporal imaging of the C_{60} fullerene, (2) a general scheme for transferring OAM (optical angular momentum) to mid-infrared OPA pulses and (3) the measurement of the spectral phases near threshold for different inert gas atoms. One ongoing attosecond project uses a strong field simulator approach for studying rescattering physics. Two LCLS runs occurred in the Fall 2017 and Winter 2018: (1) real time streaking of the Auger decay in atoms and molecules and (2) diffractive imaging at the LCLS of pumped C_{60} fullerene. A third run is scheduled for the Fall 2018 for studying attosecond pulse generation using the LCLS.

1.2 RECENT PROGRESS: THE ATTOSECOND PROGRAM

The technical approach of the Ohio State University (OSU) group is the use of long wavelength ($\lambda >$ 1 μm) driving lasers for harmonic and attosecond generation, and imaging. Through support of this program, the long wavelength approach has been successful and adopted by many groups worldwide. Our program over the last several years has focused on using long wavelength generated harmonics for measurements, ultimately of dynamics. We are interested in addressing three basic questions related to attosecond physics. First, can high harmonic and attosecond spectroscopy extract atomic/molecular structure? Second, what is really being measured? Finally, can attosecond techniques simulate basic strong-field physics?

The Strong Field Simulator. In traditional strong field ionization experiments, a single high-intensity laser drives both the photoionization of an electron from its parent and the subsequent motion of that electron in the intense field. Electrons that return to interact with the parent ion are of particular interest due to the many physical phenomena attributed to them: elastic (LIED) and inelastic (NSDI, RESI) scattering or recombination (HHG). Here, we are interested in simulating these processes in

Helium and other systems. Helium provides an ideal platform for studying electron-electron interactions in strong-field processes since it is most accessible to theoretical investigation.

Usually a low-frequency strong field couples the ionization step, which dominantly occurs at phases near the peak of the field, to the recollision step, thus significantly constraining the ability to control these processes. To counter this, we employ the strong field simulator scheme, which replaces the tunnel ionization with photoionization by an attosecond XUV pulse (Fig. 1). The decoupling of ionization and propagation allows selection of any ionization phase, so that quantum trajectories not normally accessible are studied by controlling the time delay between the XUV pulse and the strong field. Tuning other properties of the XUV pulse may open additional avenues for investigation.

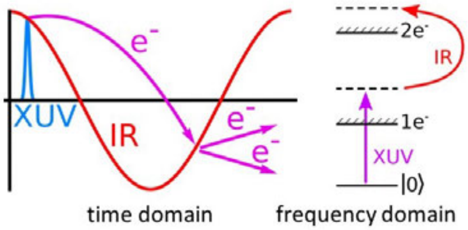

Figure 1: The strong field simulator conceptualized for (e,2e) process. In the time domain, a photoelectron is excited to the 1*e* helium threshold by an XUV attosecond pulse (see frequency domain). The electron accelerated by a phased locked low-frequency field can recollide with the He$^+$ core, freeing a second electron.

We have performed a set of preliminary measurements to demonstrate the strong field simulator approach. Using an existing attosecond beamline not optimize for this experiment, photoelectron spectra were collected as a function of the delay between the XUV and strong field pulses. The delay spectra exhibit an overall structure, which repeats with frequency 2ω, or twice each cycle of the strong field. There is also an energy dependence to the phase of this oscillation. As shown in Fig. 2, the total yield of the delay scan (XUV+MIR) is enhanced over the total yields of the two fields individually. This enhancement has its largest relative magnitude at lower strong field intensities, which predominantly comes from a broad energy region centered above zero (see Fig. 2(b). Our collaborators, Prof. Ken Schafer and Dr. Jens Egebjerg Bækhøj (LSU), are performing theoretical modelling of the strong field simulator scheme. Their work reproduces the primary features of our experimental results and provides guidance for further exploration.

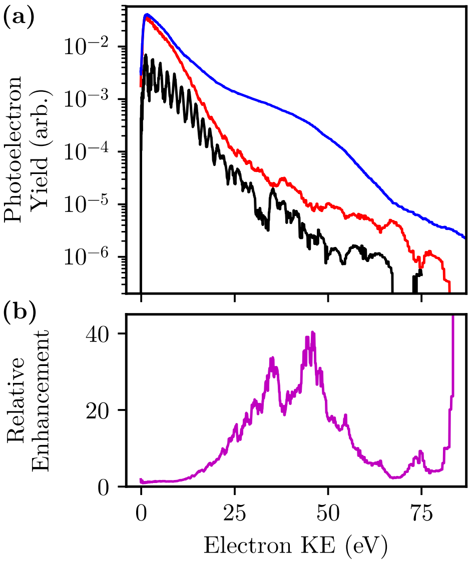

Figure 2: (a) Photoelectron yields from helium: XUV only (black), strong field only (red), and the average during a delay scan (blue). (b) The relative enhancement (ratio of delay scan average to strong field only). The wavelength is 1.3 µm and the strong field has $U_p \sim 8$ eV.

We are encouraged by the success of the proof-of-principle measurements and insights derived from theoretical input. Consequently, we are designing a new dedicated apparatus optimized to improve upon and extend the use of the strong field simulator scheme, with the ultimate goal of controlling the (e,2e) process in Helium. We are preparing a manuscript based on our initial results.

Probing Electronic Binding Potentials with Attosecond Photoelectron Wave Packets. In the field of attosecond physics, pump-probe techniques, such as Attosecond Streaking and Reconstruction of Attosecond Beating by Interference of Two-photon Transitions (RABBITT), employ short XUV radiation pulses synchronized with a near-infrared dressing field to clock electronic processes in atoms, molecules, and solids down to the exceptionally short timescales over which they occur. The Simpleman classical model provides the basic understanding of how the energy-transfer processes between the ionized electron and the dressing field yields a direct energy-to-time mapping. Many experiments exploit the simplicity of this model to uncover and understand the underlying physical processes from their results.

However, the Simpleman model assumes that the host atom has no influence on the outgoing photoionized electron, an approximation that ignores well-known spectroscopic features, such as auto-ionizing resonances and Cooper minima, and that becomes increasing worse as the electron's energy approaches zero. Removing the effects of this influence by the host in these measurements has been an active area of research, leading to an improved understanding of specific continuum features and intrinsic effects caused by the measurement technique itself. Working to apply this understanding to experimental results is difficult, requiring significant theoretical input that can be limited by the approximations required, notably, for our experiment, when the electron's energy is near zero.

We approached this problem from a different angle by experimentally extracting from the measured photoelectrons information about the host's effective potential, including multi-electron effects. We concentrate on the lowest-energy electrons, those most difficult to theoretically study, because they spend more time near the host's potential and therefore feel the largest effect. Using a simple, analytical reformulation of the Simpleman model applied to our experimental method, which we dub RABBITT+. The technique is a combination of a RABBITT phase measurement with additional amplitude information and an additional low-ionization-energy reference target (argon). We extract coarse information about the host's potential: the average effective potential and average slope of the effective potential experienced by slow-moving, low-energy electrons in the first 1.4 femtoseconds after ionization from helium and neon atoms.

We infer from our measurements that for helium a deep effective potential near the core with a rapid slope, a qualitatively expected result. The results for neon are considerably different, even though the ionization-energy is similar. Not only is the effective potential much shallower and less steep, but there is a change of sign in the average effective potential value as the electron energy changes. For slightly higher-energy electrons, the close-range effective potential becomes repulsive on average. These results are qualitatively comparable to a previous simulated experiment that used pseudopotentials for the atoms. The work is a collaboration with Prof. Bob Jones (UVa) and published in Nat. Phys. [7A].

1.3 RECENT PROGRESS: THE MOLECULAR IMAGING PROGRAM

Ultrafast dynamical imaging of C_{60} fullerene. The 1985 discovery of C_{60} by Kroto, Smalley and Curl marked the beginning of fullerene research in nanoscience. Fullerenes are the third allotrope of carbon next to graphite and diamond. Widespread in nature from soot to interstellar clouds, their world is comprised of a wide variety of nanoscale-size closed shapes from simple spheres to tubules, onions, rods, ribbons etc. each possessing interesting, specific and yet useful properties. Since its discovery, the soccer ball shaped C_{60} - the archetypical fullerene - remains the focus of ongoing scientific studies.

The interaction of C_{60} with strong femtosecond lasers has been the object of numerous studies which revealed that at photon energies comparable with the first excited state (~2.1 eV), the laser energy is efficient transferred into C_{60}'s internal degrees of freedom. This extra energy is subsequently "evaporated" via C-C pair "boil off" fragmenting the molecule. However, at lower photon energy (less than 2.1 eV/3) fragmentation is not observed and multiple ionization of the intact cage is possible even at high intensities (10^{14} W/cm^2).

Cage fragmentation suppression at long wavelengths (< 1.8 µm) does not imply a rigid molecule. Indeed, previous theoretical models have shown that collective effects lead to periodic cage deformations along the laser polarization, with $h_g(1)$ the dominant active mode. We have successfully extended the laser-driven self-imaging electron diffraction techniques for visualizing a C_{60} cage elongation of ~5% under irradiation with 80 TW/cm^2, 100 fs, 3.6 µm pulses. The observed deformation is verified by density functional theory (DFT) calculations of the nuclear dynamics on time-dependent adiabatic states. This result is the first step towards visualizing and studying the complex real time molecular dynamics of macromolecular structures. The work is a collaboration with Dr. Matthias Kling (LMU) and Prof. Hirohiko Kono (Tohoku U). A manuscript is under review at PRL.

1.4 RECENT PROGRESS: ULTRAFAST X-RAY SCIENCE

We conduct our x-ray campaigns utilizing the LCLS XFEL in team collaborations. A recent paper on "Femtosecond profiling of shaped X-ray pulses" that resulted from a previous LCLS on streaking is published in New J. Physics [8A]. The work was a collaboration with Dr. Adrian Cavalieri (Hamburg). We were awarded LCLS time at the end of September 2017 to perform dynamical x-ray imaging of C_{60}. The campaign was lead by Prof. Thomas Pfeiffer (Heidelberg). The results of this run are being analyzed. A second LCLS beam time was awarded in February 2018 for "Attosecond interrogation of relaxation dynamics in highly excited atoms and molecules". This is a continuation of our attempts to time-resolve Auger decay using a low-frequency streaking field with the LCLS x-ray beam. This campaign was successful and a manuscript is in preparation.

1.5 FUTURE PLANS

Strong field simulator: Based on the encouraging results described above, we decided to design a new attosecond beamline optimized for strong field simulator measurements. We completed the conceptual design in FY18. We are in the process of procuring the components and construction should begin before the end of 2018. The new beamline will represent a significant improvement in capability over the modified apparatus used above for collecting the preliminary results. Ken Schafer (LSU) will provide theory support for the program.

Imaging: The goal for FY19 is the application of LIED/FABLES to study ultrafast molecular dynamics using pump-probe geometries. (1) Work will continue on hydrocarbon chains. The initial investigations will time-resolve dissociation of the carbon chains following VIS/UV excitation; (2) extend the hydrocarbon studies to image aromatic compounds (benzene and its derivative); (iii) examine molecular grating effects in linear hydrocarbons; (iv) continue the work on fullerenes, including planning a second campaign in Barcelona for visualizing the breathing mode of C_{60}.

LCLS: We have been awarded beam time in November 2018 for the run "Time-resolving correlated continuum electron and core-excited state wavepackets by photoemission streaking". The run is lead by Dr. James Cryan (SLAC) and focused on the attosecond capabilities of the LCLS.

1.6 PUBLICATION RESULTING FROM THIS GRANT FROM 2016-2018

1A. *"Time-resolved molecular imaging"*, Junliang Xu, C. I. Blaga, P. Agostini and L. F. DiMauro, J. Phys. B **49**, 112001 (2016). doi:10.1088/0953-4075/49/11/112001.

2A. *"Synthesis and characterization of attosecond light vortices in the extreme ultraviolet",* R. Géneaux *et al.,* Nat. Comm. **7**, 12583 (2016). doi: 10.1038/ncomms12583.

3A. *"Precise access to the molecular-frame complex recombination dipole through high-harmonic spectroscopy"*, S. Schoun *et al.*, Physical Review Letters **118**, 033201 (2017).

4A. *"Radial index of Laguerre-Gaussian modes in high-order-harmonic generation"*, R. Geneaux *et al.*, Phys. Rev. A **95**, 051801 (2017). doi: 10.1103/PhysRevA.95.051801.

5A. *"Tunable orbital angular momentum in high-harmonic generation"*, D. Gauthier *et al.*, Nat. Comm. **8**, 14971 (2017). doi: 10.1038/ncomms14971.

6A. *"Tunable mid-infrared source of light carrying orbital angular momentum in the femtosecond regime"*, A. Camper et al., Opt. Lett. **42**, 3769 (2017). doi: https://doi.org/10.1364/OL.42.003769.

7A. *"Probing electronic binding potentials with attosecond photoelectron wavepackets"*, D. Kiesewetter *et al.*, Nat. Phys., **14**, 68 (2018). doi: 10.1038/NPHYS4279.

8A. *"Femtosecond profiling of shaped x-ray pulses"*, M. Hoffmann *et al.*, New J. Phys. **20**, 033008 (2018). doi: https://doi.org/10.1088/1367-2630/aab548.

Short-Time Electron Correlation and Tunneling

J. H. Eberly
Department of Physics and Astronomy
University of Rochester, Rochester, NY 14627
eberly@pas.rochester.edu

Project Scope

High-field effects of recent and current interest in AMO science are triggered by ultra-short (fs and sub-fs scale) laser pulses having intensities in the range near and above I = 0.1 PW/cm ^{2}. We believe it is important to improve understanding of the fundamental process whereby such laser pulses excite electrons in atoms and more complicated materials where electrons are the principal photon acceptors. These excitations lead to correlation effects ranging from multi-electron ejection to high-harmonic generation to the expanding zone of atto-science. The combination of phase-coherent character and short-time nature of laser irradiation creates substantial challenges to theoretical study in this high-field domain.

Our work, through the development of the virtual numerical detector (VND) method, has provided a unique avenue of theoretical access to still-mysterious features of ionization initiation. The perceived value of this work is indicated by the reception of our ISI Highly Cited invited review [1], the recent invitation to contribute to this year's special issue of Journal of Physics B coordinated by M. Vrakking (MPI-Erlangen) [2], and the invitation to deliver the opening plenary address [3] last year at the second International Conference on Matter and Radiation at Extremes, held in Beijing.

Recent Progress

Two avenues of *ab initio* evolution have enabled recent progress, and our calculations have followed both, leading in 2017 and 2018 to a PhD thesis and three peer-reviewed publications [2, 4, 5, 6].

The cooperation with the Barcelona-Heidelberg experimental teams [6] deals with the intriguing transition zone between non-sequential and sequential double ionization in multi-electron systems, previously largely overlooked. It takes an approach that is even partially analytical via extension of the "Simpleman" model, and the other two are substantially numerical. This provides an example of our ability to follow longer-than-optical wavelength experiments used to uncover new phenomena or enable more detailed studies.

A prominent example [5] is the incorporation of Coulomb effects that have captured attention in single-electron ionization experiments in the past 3-5 years. What has been missing is the ability to attend to the nature of electron behavior in the near neighborhood of the legendary (or mythical) "tunnel exit", which plays an important role in the standard tunneling-based "strong field approximation" (SFA). A need for attention to this point has existed since it was described a decade earlier by Ivanov, Spanner and Smirnova [7] where they said:

"Identifying the wavepacket dependence on v_x is much harder. The crucial difficulty stems from the fact that the laser field accelerates the electron while it tunnels out. The velocity distribution along the field is changed continuously during tunneling. ... Uncertainty in the moment of tunneling, which is responsible for the uncertainty in the initial velocity, also means that it is virtually impossible to separate the initial velocity distribution from the distortions caused by the electric field during this temporal uncertainty.”

Most recent work with the *ab initio* SENE approach (see [3, 4, 5]), shows that an outgoing wave packet will be accelerated and stretched in the direction of the laser field. In an adiabatic tunneling model, the electron cannot gain energy during the tunneling process. This assumption is correct for transverse momenta, but may reach misleading conclusions for longitudinal momentum distributions. For example, as we have shown, effects of temporal oscillations will be missed.

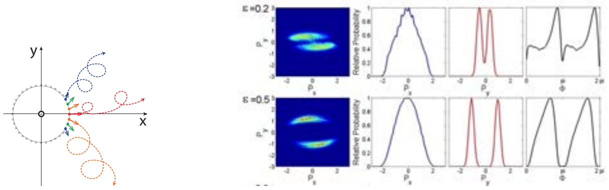

Figure 1: (left) Ionized electron momenta are sketched departing from the numerical detector ring. (right) Their TDNE evolution gives far-field electron momentum distributions consistent with data reported by Pfeiffer, et al. [9].

Future Plans

Ongoing and future work will be a competition between two different priorities. One is extension of our SENE application (see J. Tian, Ph.D. thesis [4]) of the Feuerstein-Thumm idea [8]. To summarize briefly: the SENE method solves the Schrödinger Equation (SE) numerically exactly in a small region near the ion. Then it makes “virtual” detection of the expanding quantum wave function of the electron by a purely numerical recording of its quantum phase over a sphere around the ion. In cases of elliptically polarized irradiation only a two-dimensional detector ring has been used. From this record a distribution of electron momenta is extracted from the gradient of the wave function’s phase at each point on the ring (or sphere). Then those momenta are used to initiate classical Newtonian Evolution (NE) into the far field, as shown in the left panel of Fig. 1. In the right panel we note the SE + NE = SENE result for $\varepsilon = 0.2$. Its asymmetry is consistent with the similar asymmetry in the experimental record on helium (see experimental Fig. 2b of Pfeiffer, et al. [9]).

The virtual numerical detector (VND), with the SENE method, has demonstrated attractive features. The successes to date of the two-staged SENE approach [5] mandate extended work. Current results have been satisfactory, but were obtained from detector ring radii in the neighborhood of 10 a_0 or larger. Several directions for improvement have been identified. One is to extend from a two-dimensional ring to a three-dimensional VND surface, and the two-dimensional detector ring could be improved itself, by allowing it to be placed closer to the ion. The ring is composed of a finite number of calculational cells and the cell-size discreteness interrupts the smoothness of the outgoing directional distribution of momenta, and compromises attempts to compare calculated momenta with experimental far-zone momenta. Thus our task continues to be to solve the directional smoothness issue. One approach is to replace the ring with an “onion” type detector that accepts information from more than one layer of cells.

The competition for time and effort will come from attention to a related issue having to do with timing, namely, is tunneling ionization instantaneous? Time scales of experimental practice will push deeper into the attosecond domain. Then the timing of electron emission will begin to

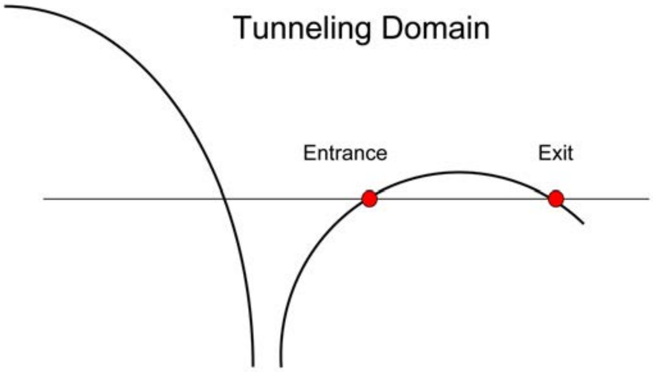

Figure 2: Illustration of tunneling entrance and tunneling exit in strong-field ionization. The black curve shows a tilted Coulomb potential in a laser electric field. The horizontal line shows the energy level of a bound state. The point of tunneling entrance and of tunneling exit can be well defined by the crossings of the energy level with the Coulomb potential barrier.

be questionable as different estimates and theoretical fudges are employed to obtain the tunneling "dwell time" in passage through the barrier. Of course, even the phrasing of such questions uses language that is quantum mechanically questionable.

Eckle, et al. [10], try to answer the question whether tunneling ionization is instantaneous. They retrieve the time difference between the peak of the laser electric field and the peak of tunneling ionization, which is known to be extremely sensitive to the electric field strength. Elliptically polarized laser pulses are used which have two properties to exploit: First, there are two clear field peaks each laser cycle so the time of laser field peak is well defined; second, electrons emitted at different times fly to different spatial angles due to the rotating feature of elliptical polarization. By measuring the angular distribution of the emitted electron and assuming the electron motion is classical after emission, the ionization time can be retrieved.

One sees that the interpretation provided by Eckle, et al., is largely based on classical mechanics. From the theoretical point of view, the first question to ask is probably: what quantity in quantum mechanics corresponds to the time delay between laser field peak and ionization?

Teeny, et al., [11, 12] use our VND concept and show that this time delay can be straightforwardly defined quantum mechanically . By putting a VND at the tunneling exit (as illustrated in Fig. 2), the VND records the electron probability current as a function of time, and a clear peak can be identified denoted as t_{exit}. The time delay that corresponds to the quantity retrieved by the experiment is $t_{delay} = t_{exit} - t_0$, where t_0 is the time of laser field peak. Teeny, et al., further show numerical results (see Fig. 4 of Ref. [12]) that this t_{delay} is not positive definite: it may vary between about ± 20 attoseconds depending on the laser electric field strength. This means that the electron may be emitted shortly (on the attosecond time scale) before or after the peak of the laser electric field. The numerical results are in good agreement with the conclusion of the experiment.

By putting another VND at the tunneling entrance (as illustrated in Fig. 2) and recording the electron probability current there, one finds the latter quantity peaks at time t_{in}. The time difference $t_{tunneling} = t_{exit} - t_{in}$ is, we believe, the most straightforward quantity that corresponds to our understanding of the time that the electron needs to tunnel through the potential barrier. Teeny, et al., show (see Fig. 4 of Ref. [12]) that this $t_{tunneling}$ is finite and positive definite, the precise value of which depends on the laser field strength. This work must be extended to both higher and lower field strengths, and test or confirm that the absolute value of the tunneling time is in the range 10 to 100 attoseconds for strong-field ionization.

Publications supported in recent grant periods are marked with * in the References listing.**

References

[1] ***W. Becker, X.J. Liu, P.J. Ho and J.H. Eberly, "Theories of Photo-Electron Correlation in Laser-Driven Multiple Atomic Ionization," *Rev. Mod. Phys.* **84**, 1011 (2012). [**ISI Highly Cited Paper**]

[2] ***Xu Wang, Justin Tian and J.H. Eberly, "Virtual Detector Theory for Strong-Filed Atomic Ionization", *J. Phys. B* **51**, 084002 (2018)

[3] *** J.H. Eberly, "Where Do the Electrons Come From?", Invited Plenary Lecture, International Conference on Matter and Radiation at Extremes (ICMRE), Beijing CHINA, June 26-30, 2017; and to be published.

[4] ***Justin Tian, "Theory of Strong-Field Atomic Ionizations", Ph.D. Dissertation, Department of Physics and Astronomy, University of Rochester (2017).

[5] ***J. Tian, X. Wang, and J.H. Eberly, "Numerical Detector Theory for the Longitudinal Momentum Distribution of the Electron in Strong Field Ionization," *Phys. Rev. Lett.* **118**, 213201 (2017).

[6] *** Michael G. Pullen, Benjamin Wolter, Xu Wang, Xiao-Min Tong, Michele Sclafani, Matthias Baudisch, Hugo Pires, Claus Dieter Schrter, Joachim Ullrich, Thomas Pfeifer, Robert Moshammer, J. H. Eberly and Jens Biegert, "Transition from nonsequential to sequential double ionization in many-electron systems", *Phys. Rev. A* **96**, 033401 (2017). DOI: 10.1103/PhysRevA.96.033401 .

[7] M. Y. Ivanov, M. Spanner, and O. Smirnova, *J. Mod. Opt.* **52**, 165 (2005).

[8] B. Feuerstein and U. Thumm, *J. Phys. B* **36**, 707 (2003).

[9] A.N. Pfeiffer, C. Cirelli, A.S. Landsman, M. Smolarski, D. Dimitrovski, L.B. Madsen and U. Keller, *Phys. Rev. Lett.* **109**, 083002 (2012).

[10] P. Eckle, A. N. Pfeiffer, C. Cirelli, A. Staudte, R.Dörner, H. G. Muller, M. Bütiker, and U. Keller, *Science* **322**, 1525 (2008).

[11] N. Teeny, E. Yakaboylu, H. Bauke, and C. H. Keitel, *Phys. Rev. Lett.* **116**, 063003 (2016).

[12] N. Teeny, C. H. Keitel, and H. Bauke, *Phys. Rev. A* **94**, 022104 (2016).

Peer-reviewed Publications Resulting from this Project (2016-2018)

"Virtual Detector Theory for Strong-Field Atomic Ionization", Xu Wang, Justin Tian and J.H. Eberly,
J. Phys. B **51**, 084002 (2018). https://doi.org/10.1088/1361-6455/aab5a4.

"Numerical Detector Theory for the Longitudinal Momentum Distribution of the Electron in Strong Field Ionization," J. Tian, X. Wang, and J.H. Eberly,
Phys. Rev. Lett. **118**, 213201 (2017). doi:10.1103/PhysRevLett.118.213201.

"Transition from nonsequential to sequential double ionization in many-electron systems", Michael G. Pullen, Benjamin Wolter, Xu Wang, Xiao-Min Tong, Michele Sclafani, Matthias Baudisch, Hugo Pires, Claus Dieter Schrter, Joachim Ullrich, Thomas Pfeifer, Robert Moshammer, J. H. Eberly and Jens Biegert,
Phys. Rev. A **96**, 033401 (2017). DOI: 10.1103/PhysRevA.96.033401 .

NONLINEAR X-RAY OPTICS

Matthias Fuchs[1] (PI), **David Reis**[2] (Co-PI)

[1]*Department of Physics and Astronomy, University of Nebraska - Lincoln, Lincoln, NE 68588, USA,*
mfuchs@unl.edu
[2]*Stanford PULSE Institute, SLAC National Accelerator Laboratory, Menlo Park, CA 94025, USA,*
dreis@stanford.edu

Project Scope

The scope of the project is the investigation of fundamental nonlinear X-ray - matter interactions. We are interested in studying the mechanism of coherent *non*-sequential multi-photon nonlinearities at X-ray wavelengths including novel effects and methods to increase their efficiency. X-ray free-electron lasers (XFELs) are capable of producing radiation with unprecedented properties. Specifically, their ultrashort coherent X-ray pulses can generate extreme peak intensities where ordinary rules of light-matter interaction may no longer apply and nonlinear processes start to become important. XFELs have made it possible to observe some of the most important coherent *non*-sequential nonlinearities, including X-ray - optical sum frequency generation (SFG)[1], X-ray second harmonic generation (XSHG)[2], nonlinear two-photon Compton scattering (2PCS)[3] and two-photon absorption (TPA)[4]. In particular, the 2PCS experiment has led to unexpected results, namely the observation of a substantial anomalous red shift in the energy of photons generated by nonlinear two-photon X-ray Compton scattering in beryllium. The energy shift is in addition to the predicted nonlinear Compton shift and was neither expected from extrapolations from linear X-ray interactions nor from nonlinear effects at optical wavelengths. Our results suggest a novel nonlinear scattering mechanism that can only be observed at high fields at X-ray wavelengths, where the photon energy is a significant fraction of the electron rest mass (and thus a significant momentum transfer to the electron occurs during the scattering) and where the interaction is not dominated by the quiver motion of the electron in the field (ponderomotive potential) as is usually the case at longer (optical) wavelengths.

Recent Progress

Nonlinear Two-Photon Compton Scattering

The first observation of nonlinear Compton scattering has resulted in an unexpected result: the energy of the generated photon from the simultaneously nonlinear scattering of two 9 keV X-ray photons in a beryllium target was measured to be significantly lower than expected. More specifically, the observed spectrum is redshifted from 18 keV by ~800 eV *in addition* to the expected nonlinear Compton shift. This energy shift is incompatible with the approximation of electrons interacting as quasi free in solids (impulse approximation) for hard X-ray – matter interactions far from atomic resonances. The experiment was performed at extremely high X-ray intensities of ~4x10^{20} W/cm^2.

In order to further investigate this effect and rule out trivial causes for the redshift we have performed a more detailed study. Part of the experiment was extending the measurement of the nonlinear signal into the forward scattering direction. In addition to the angular distribution, we were also able to extend the lower bound of the additional energy redshift to >2 keV by simultaneously investigating the effect for a wider photon energy range of the incoming beam.

Through linear Compton scattering spectroscopy, we were able to infer the temperature of the sample during the interaction. An additional redshift of 800 eV requires an extremely hot plasma temperature with an electronic temperature of kT > 320 eV. The spectrum of the linear Compton scattering does not show a significant broadening, which indicates that the there is no appreciable heating (kT < 10 eV) during the interaction. The unexpected small temperature can be explained by the X-ray interaction generating ~10 keV photoelectrons that propagate outside of the 100 nm focus before depositing most of their energy.

The experiment also included different target materials, namely a metal (Be) and dielectric (diamond). Although a nonlinear signal has been observed in the diamond, a quantitative comparison is limited by the statistics of the diamond data.

The observed emission pattern has a double-peaked shape with an asymmetry in intensity peaked at higher (backward) scattering angles. The asymmetry is increasing with increasing intensity. Although a quadrupole-like pattern is expected for a free-electron interaction, the position of the peaks and the minimum cannot be explained by a free-electron model.

An initial model of this process consists of a previously unobserved scattering mechanism that includes the whole atom in the process. In this model, the missing momentum and energy can be transferred to the third body. The process occurs through pA and A^2 scattering processes via a virtual intermediate electronic state, where p is the momentum operator and A the electromagnetic vector potential. However, the observed angular distribution can also not be explained by a simple model that uses the scattering from a virtual intermediate electronic state following photo-ionization.

In a very recent experiment performed at the SACLA free-electron laser, we have observed an extremely strong nonlinear signal by scattering photon with energy near the K absorption edge in iron. An initial analysis showed that the cross sections are approximately six orders of magnitude higher than what was expected from the LCLS experiment (far from atomic resonances) in Be. The cross section strongly increases as the photon energy is increased above the K edge. This is in contrast to Cu and Al targets where at the same photon energies (around 7.1 keV) the cross section were significantly smaller than in Fe and had varied only little as a function of with photon energy. This is additional support that the whole atom participates in the process rather than a free-electron interaction.

Despite this progress, the detailed mechanism of this fundamental scattering process is still not fully understood. The further investigate the process requires performing additional experiments including a complete measurement that has the ability to observe of not only the scattered photons but also the momentum distribution of the electrons and ions involved in the process.

Angularly-resolved X-ray Second Harmonic Generation

We have performed experiments to measure multiple Fourier components of X-ray second harmonic generation (XSHG) in order to further investigate the physics behind nonlinear X-ray – matter interactions. In particular, considering the results obtained from two-photon Compton scattering (TPCS), we are exploring any signs of a deviation from the quasi-free electron model. Since we are using a phase-matched geometry, the SHG signal can be observed at ~4 orders of magnitude lower intensities than the TPCS experiment. This will also allow us to explore a lower limit at which the impulse approximation breaks down and compare these findings to the TPCS results (in which case the impulse approximation has broken down). To this end we have performed experiments using highly intense beams at a photon energy of 9.8 keV generated by the LCLS XFEL. We have measured multiple Fourier components and the angle-dependence of the process with high statistics.

XSHG signals well above background have been observed for phase-matching conditions including the reflections from the [220], [111], [11-1], [00-4], [660], [113], [331] and [771] diamond lattice planes. For each reflection, we have measured the XSHG crystal rocking curve. In the quasi-free electron model, mainly two currents are contributing as source terms: one term that is due to the second order velocity caused by the $v \times B$ part of the Lorentz force, where v is the electron velocity and B the X-ray magnetic field (Lorentz term). The other term is due to the Doppler-shifted scattering of X-rays from electrons that are moving at the first order velocity due to the X-ray electric field (Doppler term). As these current terms have different emission pattern, the different phase-matching geometries allow us to investigate if there is any particular influence of either term. In particular from the emission at a scattering angle close to 90º (parallel to the FEL polarization) we expect that the emission is mainly governed by the Lorentz term of the nonlinear current and in case of more forward or backscattering geometries, it is mainly due to the Doppler term of the current. We have compared the experimental results to the quasi-free electron model. To do so, we have written a simulation that solves the wave equation and includes propagation and walk-off effects for different phase-matching geometries. The experimentally measured process efficiencies and intensity dependence agree reasonably well with the simulations. Only the width of the SHG crystal rocking curves wider than expected from simulations and tabulated Darwin widths. We measure that the widths and shapes of the rocking curves do not significantly change as a function of intensity. The increased width in the rocking curves is most likely due to the crystal quality as a broadened rocking curve is also seen for the fundamental diffraction peaks. The simulations also allow us to identify the leading contribution from the nonlinear source terms for each Fourier component. A quantitatively comparison of the signals for each of these different Fourier components shows no significant difference in terms of efficiencies and rocking curve width for these peaks. The data has been analyzed and a manuscript is in preparation.

Difference-frequency generation of optical radiation from two-color x-ray pulses

The goal of the experiment was the generation of optical radiation through difference-frequency generation of two hard X-ray photons. In the experiment, the full bandwidth LCLS beam around a photon energy of 9.5 keV is spectrally separated in a parts using a crystal- split-and-delay geometry and then combined under the appropriate crossing angle in a diamond crystal to generate an optical photon. We were not able to observe a clear signal of the process during the online analysis of the experimental data. The data is currently further processed and investigated.

Nuclear Nonlinear Optics: A Narrowband Mossbauer source driven by broadband x-ray pulses.

The goal of the experiment is the observation of nonlinear excitation of the 14.4 keV nuclear Mössbauer resonance in ^{57}Fe by two 7.2 keV photons. To that end, samples of enriched ^{57}Fe have been illuminated using the monochromatized LCLS beam. The expected signal consists of an incoherent fluorescence emission into 4 pi and a coherent emission into a narrow forward cone. As diagnostics for the signal we used fluorescence detection close to the sample and a spectrum analyzer in combination with a time-discriminating APD detector in order to observe the delayed coherent signal with a lifetime of 141 ns. The results of this experiment and a follow-up experiment at the SACLA XFEL strongly suggest the possibility of observing the effect. In particular during the run at SACLA using two-color operation at 7.1 keV + 7.3 keV showed some potential signal. The configuration allows a signal enhancement through the Fe K-shell resonance at 7.1 keV.

Hard X-Ray Transient Grating Spectroscopy

The goal of the experiment was to obtain a first critical step towards the investigation of higher-order nonlinear effects, namely four wave mixing (FWM). In particular, the experiment was aimed to use crossed X-ray beams to generate a transient grating on the sub-nanometer wavelength scale. To this end, the LCLS beam was split using a crystal split-and-delay setup and crossed in a Si target. The FEL third harmonic was used as a probe to diffract from the transient grating. Unfortunately, no clear signal could be observed as the many degrees of freedom of the split-and-delay, the recombination and the overlap of the third harmonic turned out to be too challenging for a single beamtime. However, we were able to gain invaluable information for a future implementation for future experiments.

Core-resonant Coherent Raman Scattering

The goal of the experiment was the observation of coherent anti-stokes Raman scattering (CARS) in the X-ray range. In order to enhance the signal, the core resonance of the Si L-edge was used. To this end, the LCLS was operated in two-color mode and the pulses were temporally and spatially combined at the suitable angles to satisfy the phase-matching condition using a split-and-delay in combination with a Laue and Bragg reflection (for one color). We have also taken an initial step in this direction performing a degenerate four-wave mixing experiment. Here two crossed X-ray pulses of the same color generate a transient grating from which an optical pulse gets diffracted. The experiments were performed only very recently and the data analysis is still going on.

Future Plans

In the future, we will expand on our observations of nonlinear effects at X-ray wavelengths. To this end, we will further investigate nonlinear Compton scattering and more specifically its wavelength dependence and core-resonant nonlinear Compton scattering. From this we expect to get invaluable insights into the process that are necessary to a theoretical description. We will also investigate the process in different states of matter, such as the gas phase and at higher X-ray intensities (beamtime proposal at the European XFEL pending). This will be a step towards performing a complete experiment that has the ability to observe of not only the scattered photons but also the momentum distribution of the electrons and ions involved in the process. We will further explore higher-order nonlinear processes and the possibility of imaging the local induced charge distribution. To this end we will perform an experiment to investigate second-order optical and X-ray mixing, which has been awarded beamtime at the SACLA XFEL in December 2018.

As nonlinear X-ray processes are typically weak, part of this research is the exploration of more efficient nonlinear X-ray processes by studying novel mechanisms including solid-state effects and the assistance of optical radiation. These experiments require extremely large X-ray field strengths, that can only be produced by XFELs. Nonlinear X-ray effects can lead to important applications in many research fields. For example, it could lead to instantaneous plasma diagnostics for materials in extreme conditions, as a method for combining atomic-scale structural sensitivity with chemical specificity, or as a probe of electron dynamics in solids on the attosecond (1 as = 10^{-18} s) time- and Ångstrom (10^{-10} m) length scales. We will investigate higher-order nonlinear effects, such as third-harmonic generation, self-phase modulation and self-focusing. We plan to investigate two-photon Compton scattering at different wavelength regimes and with a complete measurement that will allow us to measure the angular and momentum distribution of all scattered particles.

A detailed understanding of nonlinear X-ray matter interactions is crucial for understanding and extending the limits of structural determination at high intensity such as in serial femto-crystallography. If one can find a robust X-ray nonlinearity to exploit, the potential applications are numerous spanning from atomic physics, chemistry, materials science, to plasma physics and other disciplines. The results could have a profound impact on future light sources such as the LCLS-II.

References

[1] Glover, T.E., Fritz, D. M., Cammarata M., *et al.* X-ray and optical wave mixing. *Nature* **488**, 603–608 (2012).

[2] Shwartz, S., Fuchs, M., Hastings, J. B *et. al.* X-Ray Second Harmonic Generation. *Phys. Rev. Lett.* **112**, 163901 (2014).

[3] Fuchs, M., Trigo, M., Chen, J. *et. al.* Anomalous nonlinear X-ray Compton scattering. *Nat Phys* **11**, 964-970 (2015).

[4] Ghimire, S., Fuchs, M., Hastings, J., *et al.* Nonsequential Two-photon Absorption from the K-shell in Solid Zirconium. *Phys. Rev. A* **94** (2016).

Peer-Reviewed Publications Resulting from this Project (2016-2018)

No publications to report.

Studies of Autoionizing States Relevant to Dielectronic Recombination

T.F. Gallagher
Department of Physics
University of Virginia
P.O. Box 400714
Charlottesville, VA 22904-4714
tfg@virginia.edu

Project Scope

For most of its duration this research program has been focused on laser spectroscopy of doubly excited autoionizing states of alkaline earth atoms, with the goal of providing a better understanding of dielectronic recombination (DR), the recombination of an ion and an electron via an intermediate autoionizing Rydberg state.[1,2] DR is important in that it provides an efficient recombination mechanism for ions and electrons in astrophysical and laboratory plasmas.[3-5] In DR an electron colliding with a ground state ion excites the ion and is itself captured. If the resulting autoionizing state decays radiatively to a bound state, DR has occurred. The most important pathway for DR is through the autoionizing Rydberg states converging to the lowest lying excited states of the parent ion. Because Rydberg states are involved, DR rates are profoundly influenced by charged particle collisions and small electric and magnetic fields.[2,6-8]

We have taken two approaches to this problem. The first is the isolated core excitation (ICE) of bound Rydberg atoms to their autoionizing analogs.[9] An example of ICE is driving the Ba 6snd to 6pnd transition. In this excitation the nd Rydberg electron is a spectator while the Ba^+ ion core is excited.[10] ICE is precisely the inverse of DR, and we have used it to measure autoionization rates as a function of n and ℓ, the principal and angular momentum quantum numbers of the Rydberg electron. We have also measured the effects of static electric fields and microwave fields on these rates.[11] The static and microwave fields mimic the effects of the microscopic plasma fields due to ions and electrons. We have, in addition, used a second approach, which we term DR from a continuum of finite bandwidth.[12] The essential idea is as follows. The Ba $6p_{3/2}$ 11d state straddles the Ba^+ $6p_{1/2}$ ionization limit. If the laser driving the 6s11d to $6p_{3/2}$ 11d ICE transition is tuned below the $6p_{1/2}$ limit the 11d electron can deexctite the $6p_{3/2}$ core and be captured into a Rydberg state converging to the $6p_{1/2}$ limit. If this Rydberg state decays radiatively to a bound Rydberg state, DR has occurred. Experiments on DR from a continuum of finite bandwidth have shown explicitly that electric and magnetic fields increase DR rates. [8,12] The insights from this work have been directly applicable to zero kinetic energy (ZEKE) spectroscopy, which has been widely used to do molecular ion spectroscopy using neutral molecules. [13]

One of the most fascinating results from the DR from a continuum of finite bandwidth experiments is the observation that in the presence of a microwave field recombination can be observed even when the laser is tuned an integer multiple of the microwave frequency above the Ba^+ $6p_{1/2}$ ionization limit.[14] We have shown that recombination occurs when the laser excitation occurs at the phase of the microwave field at which energy is removed from the electron as it departs from the ion core.[15] Our experiments in which we excite

Rydberg atoms in the presence of a microwave field using a visible laser field are analogous to those in which a ground state atoms are excited by an attosecond pulse train (APT) of xuv pulses in the presence of an intense infrared (IR) field, a problem under investigation by several research groups.[16-20]

The singly charged ions of two valence electron atoms have optical transitions accessible to lasers and can be laser cooled. As a result, they are attractive candidates for optical atomic clocks. An important criterion for an atomic clock is the 300K black body shift of the clock transition. [21] The magnitude of the shift is proportional to the difference in the polarizabilities of the two clock states. It is, not surprisingly, difficult to measure the polarizability of an ion directly, but it is possible to measure its polarizability by measuring the energy intervals between the bound high angular momentum states of the neutral atom.[22,23]

Recent Progress

In earlier work we excited Li atoms to the vicinity of the ionization limit in the presence of 14 GHz microwave fields, using a narrowband laser amplitude modulated at 28 GHz, twice the microwave frequency.[15] We detected atoms which were bound after the laser excitation. With the laser tuned above the ionization limit we observed bound atoms when the excitation occurred at the phase of the microwave field such that energy was removed from the photoelectron as it began to leave the ion. With the laser tuned below the limit we observed ionization when the laser excitation occurred at the phase of the microwave field such that energy was given to the photoelectron.The amplitude modulation of the laser must be at twice the microwave frequency since the laser ejects photoelectrons in both the upfield and downfield directions, so the correct phase for recombining or ejecting the electrons occurs twice in a microwave cycle.

If the laser is modulated at the microwave frequency there is no dependence of the ionization on the phase of the microwave field at which excitation occurs, although there is a dependence of the angular distribution of the ejected electrons.[24] Applying a static field has the same effect as observing the electrons ejected in a specific direction. When the static field is parallel to the microwave field it destroys the forward-backward symmetry of the problem, and the two half cycles of the microwave field are no longer equivalent. As a result, there is a difference between laser excitation in the two half cycles. We have observed the phase dependent ionization in a 5 V/cm 16 GHz microwave field using static fields from 0 to 300 mV/cm. When the static field is applied perpendicular to the microwave field, it does not destroy the forward-backward symmetry of the microwave field, and, correspondingly, we do not observe a signal when the laser is amplitude modulated at the microwave frequency. Consider the case in which the laser is tuned 2 GHz above the ionization limit with the laser excitation at the microwave phase which results in the maximum number of bound atoms. At zero static field we observe no bound atoms. As the static field is raised from zero to 300 mV/cm we first observe an increase in the number of recombined atoms, as the symmetry is broken, then a decrease to zero as the static field begins to ionize all the atoms. When the laser is tuned below the zero field limit, by 14 or 30 GHz, we observe two interesting phenomena. First, with excitation at the same microwave phase as above, as the static field is raised from zero we first observe a decrease in the number of surviving bound atoms, followed by an increase, and finally a decrease to zero. Second, as the laser is tuned progressively further below the limit the minimum static field required to observe phase dependent ionization increases. Two dimensional classical simulations elucidate the origin of these phenomena. A report of the work has been submitted to Physical Review A.[25]

Raising the microwave frequency minimizes the effects of stray fields. For this reason we are generating the amplitude modulated optical beam by frequency modulating the laser beam using the same microwave source which generates the microwave field the atoms see. This approach allows the use of microwave frequencies up to 40 GHz. We use the two sidebands displaced from the optical carrier by plus or minus the microwave frequency to generate the amplitude modulated beam. We are presently using the frequency modulated optical beam to excite atomic states which are themselves frequency modulated by the microwave field, and we have made observations of the phase dependence of the production of bound states in excitation to the limit.

We have made microwave measurements of the intervals between the highly excited 6snℓ states of Yb. The high angular momentum bound Rydberg states of Yb are used for cold atom research, and Yb^+ is an atomic clock candidate. By microwave spectroscopy we have connected the 6sns, 6snd, 6sng, and 6snh series. We have completed the measurements of the 6sns and 6snd series, the latter of which is perturbed at n=26. After we had finished our analysis we discovered that the group at Laboratoire Aime Cotton in Orsay had done laser spectroscopy of the 6sns and 6snd series. We have written a joint paper, which has been submitted to Physical Review A.[26] We have, in addition, completed measurements of the Yb 6snd-6sng-6snh-6sni intervals. Since the 6snd quantum defects are now known absolutely, we can extract the Yb^+ polarizability from the quantum defects of the 6snh and 6sni states. Our measurement, $\alpha_d = 60.33(10)\ a_0^3$, is the first measurement of this polarizability, and we are completing a manuscript describing this work.

Future Plans

During the coming period we plan to use the new method of amplitude modulating the laser to do more refined experiments than those reported in ref. 15. We plan to finish the work on the Yb^+ polarizability and finish a study of forced autoionization of the perturbed Yb 6snd series..

References

1. A. Burgess, Astrophys. J. **139**, 776 (1964).
2. A. Burgess and H. P. Summers, Astrophysical Journal **157**, 1007 (1969).
3. A.L. Merts, R.D. Cowan, and N.H. Magee, Jr., Los Alamos Report No. LA-62200-MS (1976).
4. S. B. Kraemer, G. J. Ferland, and J. R. Gabel, Astrophys. J. **604** 556 (2004).
5. N. R. Badnell, M. G. O’Mullane, H. P. Summers, Z. Altun, M. A. Bautista, J. Colgan, T. W. Gorczyca, D. M. Mitnik, M. S. Pindzola, and O. Zatsarinny, Astronomy and Astrophysics, **406**, 1151 (2003).
6. V. L. Jacobs, J. L. Davis, and P. C. Kepple, Phys. Rev. Lett. **37**, 1390 (1976).
7. F. Robicheaux and M. S. Pindzola, Phys. Rev. Lett. **79**, 2237 (1997).

8. E. S. Shuman, Y. Wang, and T. F. Gallagher, Phys. Rev. A **76**, 031401 (2007).
9. W. E. Cooke, T. F. Gallagher, S. A. Edelstein, and R. M. Hill, Phys. Rev. Lett. **40**, 178 (1978).
10. N. H. Tran, P. Pillet, R. Kachru, and T. F. Gallagher, Phys. Rev. Lett. **29**, 2640 (1984).
11. S. M. Jaffe, R. Kachru, H. B. van Linden van den Heuvell, and T. F. Gallagher, Phys. Rev. A **32**, 1480 (1985).
12. J. G. Story, B. J. lyons, and T. F. Gallagher, Phys. Rev. A **51**, 2156 (1995).
13. W.A. chupka, J. Chem. Phys. **98**, 4520 (1993).
14. E. S. Shuman, R. R. Jones, and T. F. Gallagher, Phys. Rev. Lett. **101**, 263001 (2008).
15. V. Carrat, E. Magnuson, and T. F. Gallagher, Phys. Rev. A **92**, 063414 (2015).
16. P. Johnsson, R. Lopez-Martens, S. Kazamias, J. Mauritsson, C. Valentin, T. Remetter, K. Varju, M. B. Gaarde, Y. Mairesse, H. Wabnitz, P. Salieres, Ph. Balcou, K. J. Shafer, and A. L'Huillier, Phys. Rev. Lett. **95**, 013001 (2005).
17. P. Ranitovic, X. M. Tong, B. Gramkow, S. De, B. DePaola, K. P. Singh,. W. Cao, M. Magrakelidze, D. Ray, I. Bocharova, H. Mashiko, A. Sandhu, E. Gagnon, M. M. Murnane, H. C. Kapteyn, I. Litvinyuk, and C. L. Cocke, New J. Phys. **12**, 013008 (2010).
18. P. Johnsson, J. Mauritsson, T. Remetter, A. L'Huillier, and K. J. Schafer, Phys. Rev. Lett. **99**, 233001 (2007).
19. X. M. Tong, P. Ranitovic, C. L. Cocke, and N. Toshima, Phys. Rev. A **81**, 021404 (2010).
20. P. Riviere, O. Uhden, U. Saalmann, and J. M. Rost, New J. Phys. **11**, 053011 (2009).
21. C. W. Chou, D. B. Hume, J. C. J. Koelmeij, D. J. Wineland, and T. Rosenband, Phys. Rev. Lett. **104**, 070802 (2010).
22. J. E. Mayer and M. G. Mayer, Phys. Rev. **43**, 605 (1933).
23. J. H. Van Vleck and N. G. Whitelaw, Phys. Rev. **44**, 551 (1933).
24. C. Zhong and F. Robichaeux,, Phys. Rev. A **93**, 033410 (2016).
25. E. Magnuson and T. F. Gallagher, Phys. Rev. A (submitted)
26. H. Lehec, A. Zuliani, W. Maneult, E. Luc-Koenig, P. Pillet, P. Cheinet, F. Niyaz, and T. F. Gallagher, Phys. Rev. A (submitted).

Peer Reviewed Publications Resulting from this Project (2016-2018)

1. A. Arakelyan and T. F. Gallagher, "Resonant production of high lying states in the microwave ionization of Na," Phys. Rev. A **93**, 013411 (2016).
2. A. Arakelyan, J. Nunkaew, and T. F. Gallagher, "Ionization of Na Rydberg atoms by a 78 GHz microwave field," Phys. Rev. A **94**, 053416 (2016).

Physics of Correlated Systems

Chris H. Greene
Department of Physics & Astronomy, Purdue University, West Lafayette, IN 47907-2036
chgreene@purdue.edu

Project Scope

This research project is devoted to understanding systems where two or more degrees of freedom are nonperturbatively coupled owing to their interactions. The coupling of such degrees of freedom, which can be very general and arise in numerous different contexts, is also referred to in the literature as correlations between those degrees of freedom, or alternatively, as entanglement. Such correlations have vital importance in all forms of chemical reactivity and energy transfer. This is an active and challenging topic of study even in simple systems such as electron dynamics in a single atom or negative ion or small molecule, or in the coupling of electronic and dissociative degrees of freedom in molecules, because the starting point of the most frequently implemented theoretical descriptions is usually an uncorrelated approximation such as mean field theory or Hartree-Fock. While such methods can be improved to yield improved approximations, e.g. in the multiconfiguration variant of the Hartree-Fock method (MCHF), it is frequently desirable to tackle highly correlated phenomena using a method that builds in the key correlations from the very outset. The main thrust of this project is to develop such theoretical techniques and then apply them to problems where the coupling of multiple degrees of freedom has a controlling influence on the phenomenon or observable of interest. Some of our theoretical projects are aimed at interpreting experiments that have been carried out which have no satisfactory theoretical interpretation or understanding, while others are targeting new opportunities for intriguing and possibly useful quantum mechanical phenomena that are predicted and can hopefully be studied experimentally in the future, especially in the area of microscopic chemical transformations and energy transfer.

Recent Progress

(i) Extreme correlation in a regime of negative ion photodetachment

Atomic negative ions, even comparatively simple ones possessing just two valence electrons, have for many years served as prototypical systems for the observation of strong electron-electron correlations. One of the most dramatic regimes arises in processes where a negative ion absorbs a photon that excites two or more electrons to a high degree of excitation, after which the system decays by autodetachment, with one electron ejected and the remaining neutral atom left in a highly excited state. [1] An impressive series of experiments in such systems, specifically the alkali-metal negative ions, has been undertaken in recent years by the group of Dag Hanstorp in Gothenberg, Sweden. [See, e.g., Phys. Rev. Lett. 108, 033004 (2012); Eur. Phys. Lett. 106 (2014); Phys. Rev. A 88, 053410 (2013);] Some of their most striking experiments were carried out in the series of negative ions K^-, Na^-, and Cs^-, in which high double excitation and autodetachment are triggered by absorption of an ultraviolet photon.

One of the reasons this process is important is because it can serve as a prototype for using quantum control to steer atoms, via selective photoexcitation, into states with repulsive permanent and/or induced dispersion interactions. Such controlled creation of repulsive interactions is desirable because it then has the potential to minimize subsequent inelastic processes that are often detrimental. The experimental group of Hanstorp developed a simplified model that built in the long range induced dipole interaction between the photoelectron and the excited atomic state, but it omitted the electron interaction with the permanent electric dipole moment. Our analysis modifies that previous interpretation in a substantial, qualitatively crucial manner, because in fact, for the energy range where the experimental cross section is plotted, we find that the observed partial cross sections are dominated almost entirely by permanent rather than induced electron-dipole interactions.

These calculations carried out by the P.I. and graduate student Matt Eiles (who completed his PhD in May, 2018) required a significant enhancement of our two-electron R-matrix computer codes, in a number of ways.[1] First, to get more (and more accurate) radial basis states, which were needed to reach convergence in these larger box sizes and higher degrees of excitation, we switched over to a B-spline method to solve for the box-confined radial atomic eigenfunctions. This change allowed us to include up to 100 radial functions per partial wave, a major improvement. Second, we implemented an R-matrix propagation scheme to handle the very strong long-range couplings in the Hamiltonian outside the R-matrix box radius, where exchange could be neglected. This combination allowed us to obtain accurately converged results and quantitative agreement with experiment, even on the comparatively small and sensitive partial photodetachment cross sections that leave the residual atom in states of high energy and angular momentum, and also a detailed physical interpretation.

(ii) Few-body collisions in molecular physics and frame transformation theory

Indirect dissociative recombination is a seemingly simple problem, when the target of the incident electron is a small diatomic or triatomic molecular ion. But it is challenging for standard theoretical methods because there is no simple, direct dissociative pathway to visualize or compute, in contrast to ordinary dissociative recombination or attachment collisions that follow the Bates-type mechanism. One of the simplest yet prototype collision systems that requires a nontrivial level of sophistication in the theoretical description involves an electron colliding with the diatomic molecular ion HeH^+, especially at low energies where there is no identifiable direct pathway in the Born-Oppenheimer potential curves. Among the different possible outcomes of such a collision at low temperatures are rotational excitation of the molecule, vibrational excitation, or dissociative recombination. At higher energies, more complex processes such as dissociative ionization or ion-pair formation can also occur.

In an extended collaboration we have benchmarked the simplest version of the frame transformation theory of such collisions involving electron-nuclear correlations, by comparing a semi-realistic model of e-H_2^+ collisions with an essentially exact calculation.[2] This was useful to give a sense of the level of accuracy that can be expected from frame transformation calculations, which for some systems are the only option for a realistic theoretical treatment. The upshot of that study was that in the low energy range, extending over approximately 1 eV or thereabouts, the frame transformation theory combined with multichannel quantum defect theory does reasonably well in describing the complex resonance structures that an exact calculation produces in a dissociative recombination calculation. The most significant discrepancies are isolated occurrences of a low principal quantum number perturber that is sometimes located at a slightly shifted incorrect energy, and our current efforts following the publication of that article [2] are suggesting that this small shift can be remedied by an improved energy-dependent frame transformation treatment. In addition to the value of this study [2] in benchmarking the approximate frame transformation theory, it has at the same time provided the first estimate of the ungerade contribution to the H_2^+ dissociative recombination cross section.

In our 2017 article on the HeH^+ system [3], we implemented a new treatment of the low temperature collision regime, in order to test some conclusions published by another group (Takagi) which presented evidence that the computed cross sections for dissociative recombination depend (unphysically) on the choice one adopts for the origin of coordinates. Our results confirmed reassuringly that equivalent results could be obtained using different coordinate origins, but they also show that faster convergence in the electronic part of the calculation is obtained by choosing the origin to coincide with the center of charge of the molecular ion rather than the center of mass. Those calculations agreed reasonably well with older experiments. But an exciting development is that new results have been obtained for the first time with a very cold (<10K) ion storage ring experiment at the Cryogenic Storage Ring (CSR) in Heidelberg. This is expected to yield the sharpest test of theory yet, including low energy data with sufficient resolution to observe individual resonances. Our plan is to treat this using the new variant of the energy-dependent frame transformation theory that has recently been formulated and implemented in collaboration with the Prague research group of Roman Curik.

In another fundamental few-body reactive process, namely associative ionization following Rydberg state excitation, we have made some progress in understanding a class of experiments (both recent and somewhat older) that have been challenging to understand even qualitatively. A first theoretical treatment aimed at understanding experimental production of molecular ions such as Rb_2^+ in an associative ionization reaction was partially successful. That progress emerged from a collaboration between our theory group and the experimental group of Tilman Pfau in Stuttgart.[8] Specifically, the mechanism that forms these molecular ions turned out, surprisingly, to be triggered by the low energy $^3P^o$ electron-Rb scattering resonance that was shown in 2002 (independently by our group and by the Fabrikant group in Nebraska) to produce "butterfly molecule" potential curves that can accelerate a ground state atom inward towards the nucleus of a Rydberg atom. Such an implosion can drive the diatomic molecule into the autoionization region of the Born-Oppenheimer potential curves, and the resulting autoionization produces the molecular ions that are observed experimentally. However, attention in our group has become focused on a systematic set of discrepancies at high principal quantum numbers, and we have started to implement a modified version of our original picture, which includes contributions from a different set of pathways that can lead to molecular ion formation.

In other recent progress, the P.I. worked with former postdoctoral associate Jesus Perez-Rios to implement a classical Newtonian description of three-body recombination reactions between an ion and two neutral atoms, which can create molecular ions at a high rate. [7]

*(iii)*Fano resonances and short-pulse phase control

As one of our recent projects, we initiated some explorations in an attempt to find other scenarios in collision physics where Fano line shapes or even more complicated multichannel line shapes can be modified through ultrafast phase control. This study led to a first publication [4] that formulated and explored a model study of this phenomenon and pointed to its generality.

Future Plans

One major project that has been started and is expected to get finished within the coming year is a quantitative test of the rovibrational frame transformation theory. This will build on some of our preliminary evidence that a variant of the theory which incorporates the energy-dependence of the fixed nuclei scattering parameters can give improved cross sections for processes such as dissociative recombination and inelastic excitation over a broader energy range. While the simplest (energy-independent) variant of frame transformation theory has given excellent results over small energy ranges, in comparison with other theories as well as experiment, and permitted the solution of some highly challenging problems such as indirect dissociative recombination in diatomics and polyatomics with up to 5 atoms, its quantitative limitations are still not well understood.

While the rovibrational frame transformation can be viewed as a treatment of correlated electronic and nuclear motions, the correlation of an electron with the fields of two ions or one ion and one atom, e.g. in highly excited states of a diatomic molecule, is a purely electronic problem. With current postdoc Teri Price, we have formulated a first treatment of this class of correlations using the local frame transformation which involves a transformation between spherical and prolate spheroidal coordinates, and this should yield its first test applications during the coming year. In another direction related to ultrafast science, a recent theoretical treatment by the Dresden group of J.M. Rost has demonstrated that nonadiabatic turn-on and turn-off of a laser pulse can result in enhanced ionization. Our group has begun an exploration of this phenomenon to understand its wider applicability as well as its limitations.

Peer-Reviewed Publications Resulting from this Project (2016-2018)

[1] *Extreme correlation and repulsive interactions in highly excited atomic alkali anions,* M. Eiles and C H Greene, Phys. Rev. Lett. **121**, 133401-1 to -6 (2018); DOI: 10.1103/PhysRevLett.121.133401

[2] *Dissociative recombination by frame transformation to Siegert pseudostates: A comparison with a numerically solvable model,* D Hvizdoš, M Vána, K Houfek, C H Greene, T N Rescigno, C. W McCurdy, R Curík Phys. Rev. A **97**, 022704-1 to -12 (2018). DOI: 10.1103/PhysRevA.97.022704

[3] *Inelastic low-energy collisions of electrons with HeH$^+$: Rovibrational excitation and dissociative recombination,* R Čurík and C H Greene, J. Chem. Phys. **147**, 054307-1 to -11 (2017); DOI: 10.1063/1.4994921

[4] *Coupled-square-well model and Fano-phase correspondence,* Bin Yan and C H Greene, Phys. Rev. A **95**, 032706-1 to -7 (2017). DOI: 10.1103/PhysRevA.95.032706

[5] *Two-photon photoassociation spectroscopy of an ultracold heteronuclear molecule*, S Dutta, J Perez-Rios, D S Elliott, and Y P Chen, Phys. Rev. A 95, 013405-1 to -6 (2017) DOI: 10.1103/PhysRevA.95.013405

[6] *Universal few-body physics and cluster formation,* C H Greene, P. Giannakeas, and J. Pérez-Ríos, Rev. Mod. Phys. **89**, 035006-1 to -66 (2017). DOI: 10.1103/RevModPhys.89.035006

[7] *Energy Scaling of cold atom-atom-ion three-body recombination,* A. Kruekow, A. Mohammadi, A. Haerter, J. H. Denschlag, J Pérez-Ríos, and C H Greene, Phys. Rev. Lett. **116**, 193201-1 to -5 (2016).

[8] *Ultracold chemical reactions of a single Rydberg atom in a dense gas*, M. Schlagmueller, T. C. Liebisch, F. Engel, K. S. Kleinbach, F. Boettcher, U. Hermann, K. M. Westphal, A. Gaj, R. Loew, S. Hofferberth, T. Pfau, J Pérez-Ríos, and C H Greene, Phys. Rev. X **6**, 031020-1 to -14 (2016).

Manipulating and Probing Ultrafast Atomic and Molecular Dynamics

Robert R. Jones, Physics Department, University of Virginia
382 McCormick Road, P.O. Box 400714, Charlottesville, VA 22904-4714
bjones@virginia.edu

I. Project Scope

This project focuses on the exploration and control of dynamics in atoms, small molecules, and micro- or nano-structures driven by strong laser fields. Our goal is to exploit strong-field processes to implement novel ultrafast techniques for manipulating and probing coherent electronic and nuclear motion within atoms, molecules, and on surfaces. This motion occurs over attosecond to picosecond timescales. Ultimately, we hope to obtain a more complete picture of correlated multi-particle dynamics in molecules and other complex systems.

In our principal experiments, gas phase atoms and molecules are exposed to short pulses of electromagnetic radiation with frequencies ranging from THz into the XUV spectral regions, and with durations from picoseconds to attoseconds. The pulses coherently induce and/or probe dynamics in the electronic, vibrational, and rotational degrees of freedom of the targets. In one line of experiments, we will perform pump-probe measurements to clarify the roles of both electron correlation and coupled electronic-nuclear dynamics in directional multi-electron dissociative ionization of small molecules. In another, in collaboration with the DiMauro/Agostini group at Ohio State, we are developing novel techniques for directly probing the effective electronic potential experienced by an outgoing attosecond photoelectron wavepacket during the first femtosecond, or so, after its release. Lastly, we are exploiting large electric field enhancements near nano- and micro-structured metals to produce high-energy (up to 10 keV) electron bursts which might serve as fast probes of molecular structure and dynamics.

II. Recent Progress

A. Attosecond Photoelectron Probes

As noted above, in collaboration with the DiMauro/Agostini group, we are developing attosecond probes of the local environment experienced by outgoing electrons during photoionization. As an example, we recently showed that a technique, Reconstruction of Attosecond Beating By Interfering Two-photon Transitions (RABBITT), which was initially developed for characterizing XUV attosecond pulse trains through photoelectron spectroscopy in the presence of a weak IR dressing field [1], could be augmented to enable the direct extraction of specific, coarse-grained information about the electronic potential from which the ionized electron was released [a]. The revised method (which we call RABBITT+) takes advantage of the fact that both the maximum energy transfer to the departing electron, and the dressing-field phase (at the instant of ionization) for which the maximum energy transfer occurs, depend directly on the average momentum and acceleration of the electron during the first quarter-cycle of the dressing field after ionization. Accordingly, the average effective potential depth and its gradient as experienced by the electron during this quarter-cycle time window can be directly recovered from RABBITT+ interference measurements. Importantly, the extracted information includes the effects of both electron-ion and electron-electron interactions. We are currently exploring ways to obtain additional information from RABBITT+ measurements. Specifically, we are attempting to use the electron energy-dependence of the RABBITT+ interferograms to better understand how electron-electron correlations between the departing wave packet and the electrons remaining in the ion core evolve with increasing photoelectron momentum.

B. Electron Correlation and Coupled Electron-Nuclear Dynamics in Multi-Electron Dissociative Ionization

In another line of experiments we seek to probe the effects of electron correlation and coupled electronic-nuclear dynamics on directional dissociative ionization in small molecules. In previous work, we found that asymmetric bi-chromatic fields with durations of ~40 fs could induce strong directional fragmentation in a variety of molecular species [2]. We attributed this result to a well-known single electron effect, enhanced molecular ionization at a well-defined interatomic separation. Interestingly, the results of 2-color pump-probe experiments and corresponding calculations in I_2 provided strong evidence that electron correlation could also play a dominant role in the directional ionization [3]. However, analogous pump-probe measurements in N_2 using asymmetric few-cycle rather than bi-chromatic fields showed no evidence for directional ionization or the proposed electron correlation effects [4]. In an attempt to better understand these conflicting results, we intend to perform 2-color pump probe experiments in which the duration of the probe pulse can be varied from < 10 fs to > 30 fs. We wish to determine if the directional ionization, and perhaps the electron correlation effects that underlie them, require a minimum amount of time to develop in the asymmetric field. To enable the experiments, we have completed a major upgrade of our kHz Ti:Sapphire amplifier. The available output energy has been tripled to ~3.5 mJ, which should allow for the creation of sub-10 fs pump-probe pulse pairs with sufficient intensity to induce multi-electron dissociative ionization in small molecules.

III. Future Plans

With the filling of an open postdoctoral researcher position at the end of August, we plan to make rapid progress on two different fronts. First, we will measure the angular and temporal distributions of the high-energy electrons whose emission we have observed [b] from THz irradiated nano-tips. Our goal is to determine if these electrons might be useful as a time-resolved source of short electron bursts for initiating and probing molecular dynamics. Second, we hope to soon begin 2-color pump-probe directional ionization experiments in N_2, enabled by the laser upgrade (see above).

IV. References

[1] P.M. Paul, E.S. Thoma, P. Breger, G. Mullot, F. Auge, Ph. Balcou, H.G. Muller, and P. Agostini, "Observation of a Train of Attosecond Pulses from High Harmonic Generation," Science **292**, 1689 (2001).

[2] K. J. Betsch, D. W. Pinkham, and R. R. Jones, "Directional Emission of Multiply Charged Ions During Dissociative Ionization in Asymmetric Two-Color Laser Fields," Phys. Rev. Lett. **105**, 223002 (2010).

[3] V. Tagliamonti, H. Chen, and G. N. Gibson, "Multielectron Effects in Charge Asymmetric Molecules Induced by Asymmetric Laser Fields," Phys. Rev. Lett. **110**, 073002 (2013).

[4] X. Gong, M. Kunitski, K.J. Betsch, Q. Song, L. Ph. H. Schmidt, T. Jahnke, Nora G. Kling, O. Herrwerth, B. Bergues, A. Senftleben, J. Ullrich, R. Moshammer, G.G. Paulus, I. Ben-Itzhak, M. Lezius, M.F. Kling, H. Zeng, R.R. Jones, and J. Wu, "Multielectron Effects in Strong-field Dissociative Ionization of Molecules," Phys. Rev. A **89**, 043429 (2014).

V. Peer-Reviewed Publications Resulting from this Project (2016-2018)

Note: This project was on a required no-cost extension with very limited funds from 12/2015-12/2016

[a] D. Kiesewetter, R.R. Jones, A. Camper, S.B. Schoun, P. Agostini, and L.F. DiMauro, "Probing Electronic Binding Potentials with Attosecond Photoelectron Wavepackets," Nature Physics **14**, 68–73 (2018).

[b] S. Li and R.R. Jones, "High-Energy Electron Emission from Metallic Nano-tips Driven by Intense Single-Cycle Terahertz Pulses," Nat. Comm. 7, 13405 (2016).

Page is intentionally blank.

Real-time observation of multi-electron processes in atoms and diatomic molecules

Guillaume Marc Laurent (PI)
Department of Physics, Auburn University, Auburn, AL, 36849
Email: glaurent@auburn.edu

Project Scope:

The goal of this project is to implement a reliable experimental approach to observe, in real-time, electron dynamics in atoms and molecules at the attosecond time scale. Despite significant efforts that are underway, time-resolved studies at the attosecond time scale are still restricted to a few benchmark systems possessing an electronic structure sufficiently simple to make it possible to isolate a particular electronic process and univocally dissect its dynamic [1-7]. We plan to combine high-repetition-rate attosecond sources and sophisticated multi-particle imaging techniques, such as the well-established reaction microscope or COLTRIMS (Cold Target Recoil Ion Momentum Spectroscopy) [8,9] to investigate in kinematically complete experiments the correlated electron dynamics in atoms and small molecules. This new capability will offer promising possibilities to yield a deeper insight into atomic and molecular processes and ultimately to identify ways to control them. In addition, we expect that the multi-differential cross section measurements carried out in this project will foster the development of new theoretical models that are essential for a quantitative interpretation of experiments on complex systems.

Recent Progress:

The first milestone of this project is to develop a reliable experimental setup suitable for the proposed pump-probe experiments. Three main tasks were clearly identified, which includes (1) the generation and characterization of attosecond pulses of good contrast, (2) the implementation of the multi-coincidence momentum spectrometer and (3) the development of an EUV spectrometer for characterizing the spectrum of the attosecond pulse. Over the last year, we have successfully generated attosecond pulses of high brightness and completed the design of the EUV spectrometer.

1- Generation and characterization of attosecond pulses

Attosecond pulses with flux as high as 10^{8-9} photons per pulse have been generated using a variety of gas cell geometries and generation gas. The frequency components making up the pulses were determined from the energy-resolved photoelectron spectrum resulting from the photoionization of atoms by absorption of the pulse, that we corrected for the appropriate cross section. On the other hand, the spectral phases of the pulse were retrieved using the well-established RABITT technique [10]. Photoelectron spectra, in turn, were measured using a velocity-map imaging (VMI) system, which consists of projecting the electrons produced

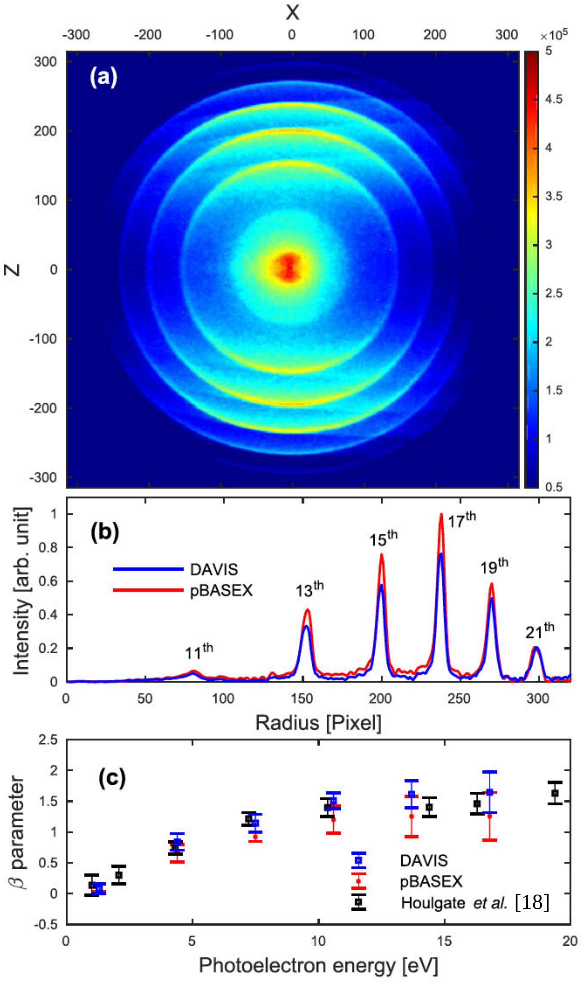

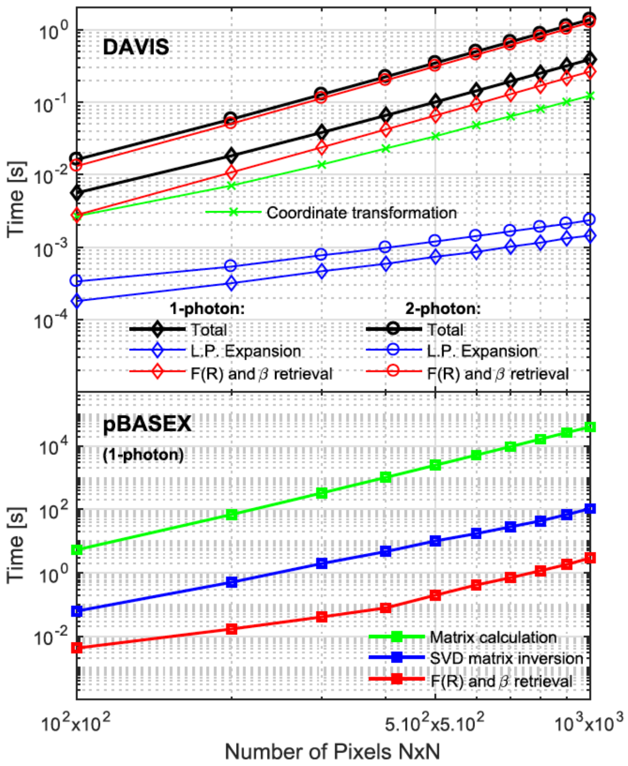

<u>Figure on the left</u>: (a) Image resulting from a one-photon ionization experiment on argon with a linearly polarized attosecond pulse train made of odd harmonics, (b) and (c) reconstructed radial distributions and asymmetry parameters obtained with DAVIS and pBASEX, respectively.
<u>Figure on the right</u>: Reconstruction times as a function of the image resolution using DAVIS and pBASEX.

through the light-target interaction onto a planar position sensitive detector by means of an electrostatic lens. In order to accurately retrieved the photoelectron spectra from the two-dimensional (2D) projected images, we have developed a new algorithm, named DAVIS, which has been recently published in the Journal of Chemical Physics [G.R. Harrison *et al.* J. Chem. Phys. **148**, 194101 (2018)]. We believe that such algorithm may be of interest for many groups in our community. Indeed, among the various techniques available to study the physics of the light-matter interaction, VMI systems has emerged as a first-choice option as they simultaneously give access to the angular and energy distributions of the particles (electrons or ions) produced during the interaction while retaining a high angular and energy resolution [11,12]. In addition, they also offer a large collection angle and a very high-count rate, which is adequate for many experiments performed with relatively unstable light sources like laser systems. On the basis of all these assets, VMI systems is extensively employed to study fundamental aspects of a variety of physical and chemical phenomena like photoionization, photo-detachment, and molecular photo-fragmentation dynamics. Despite the wealth of techniques already available [13-16], the inversion problem remains an ongoing subject of study as algorithms with improved accuracy, speed, and versatility are still highly desirable. Our method bears a similarity to the very popular pBASEX method [13]. Like pBASEX, our method consists of fitting the experimental data with the two-dimensional projection of a model 3D velocity distribution defined by the physics of the light-matter interaction. However, while pBASEX uses a numerical projection function, our method is based on a proper analytical representation of the projection, which is expanded as a sum of Legendre polynomials [17]. Both the velocity and velocity-dependent angular distributions are then directly retrieved from the resulting expansion coefficients by using an analytical inversion procedure. Our method offers two main advantages over pBASEX. First, it is less sensitive to noise and/or background as the meaningful angle-correlated information is extracted from the raw data by the Legendre polynomial expansion before inversion. Second, it is computationally much cheaper as the two-dimensional projection function is evaluated analytically rather than numerically and because the inversion procedure involves matrices of lower dimension compared to those embedded in pBASEX (see figure). Overall, our algorithm is simple, easy to implement, and fast, which allows for on-the-fly inversion of measured images. It is thus well-suited for experiments that require fast image-based feedback such as coherent-control or pump-probe experiments.

2- Development of an EUV spectrometer:

As described above, our current approach to measure the spectrum of the frequency components making up the attosecond pulses is based on the measurement of the energy-resolved photoelectron spectrum resulting from the photoionization of atoms by absorption of the pulse, that we corrected for the appropriate cross section. Due to the low photoionization cross-sections for atoms, each measurement generally takes a few minutes to be completed. As a consequence, fine-tuning the attosecond pulse's spectrum results to be time-consuming. To make this optimization process more convenient in a daily basis, we have designed and EUV spectrometer, which does not only offer a faster data collection (a few seconds per spectrum) but also allows to monitor the spectrum over the course of future experiments. The design of the spectrometer is already completed and we are currently waiting for the last mechanical parts to be produced. The spectrometer consists of a fixed toroidal grating and a microchannel plate/phosphor screen-based detector coupled to a CCD camera. By using the appropriate grating, the spectrometer covers the wavelength region from 10 to 170 nm (10 to 130 eV), with a spectral resolution of the order of 0.1 nm (2.10-4 eV).

Future Plans:

For the upcoming year, we plan to complete the assembling of the experimental setup which will be used to perform attosecond studies on atoms and diatomic molecules. In particular, our two main goals are (1) to assemble the EUV spectrometer and (2) to implement and calibrate the multi-coincidence particle's momentum spectrometer in the presence of EUV and IR pulses. As soon as the assembly of the apparatus will be completed, we will perform preliminary measurements of electron dynamics at the attosecond time scale.

References:

[1] M. Drescher et al., Nature 419, 803 (2002)
[2] E. Goulielmakis et al., Nature 466, 739 (2010)
[3] M. Schultze et al., 328, 1658 (2010)
[4] K. Klünder et al., Physical Review Letters 106, 143002 (2011)
[5] M. Uiberacker et al., Nature 446, 627 (2007)
[6] P. Eckle et al., Science 322, 1525 (2008)
[7] A. N. Pfeiffer et al., Nature Physics 7, 428 (2011)
[8] R. Dörner et al., Physics Reports 330, 95 (2000)
[9] J. Ullrich et al., Reports on Progress in Physics 66, 1463 (2003)
[10] P.M. Paul et al., Science 292, 1689 (2001)
[11] D. W. Chandler and P. L. Houston, J. Chem. Phys. 87, 1445 (1987).
[12] A. T. J. B. Eppink and D. H. Parker, Rev. Sci. Instrum. 68, 3477 (1997).
[13] M. J. J. Vrakking, Rev. Sci. Instrum. 72, 4084 (2001).
[14] G. A. Garcia et al., Rev. Sci. Instrum. 75, 4989 (2004).
[15] B. Dick, Phys. Chem. Chem. Phys. 16, 570 (2014).
[16] C. E. Rallis et al., Rev. Sci. Instrum. 85, 113105 (2014).
[17] G. M. Laurent, G. R. Harrison, arXiv preprint, arXiv:1711.00925 (2017)
[18] G. Houlgate, J. B.West, K. Codling, and G.V. Marr, J. Electron Spectrosc. Relat. Phenom. 9, 205 (1976).

Peer-Reviewed Publications Resulting from this Project (Project start date: 08/15/2017)

"DAVIS: A Direct Algorithm for Velocity-map Imaging System"
G. R. Harrison, J. C. Vaughan, B. Hidle, and G. M. Laurent
Journal of Chemical Physics, **148**, 194101 (2018)

Probing and Controlling Non-Equilibrium Multi-Electron Dynamics Towards Spatially and Temporally Resolving Chemical Reactivity in Molecules and Material

Wen Li, Wayne State University (wli@chem.wayne.edu)
Raphael Levine, University of California-Los Angeles (rafi@chem.ucla.edu)
Henry C. Kapteyn, University of Colorado at Boulder (Henry. Kaptyen@colorado.edu)
H. Bernhard Schlegel, Wayne State University (hbs@chem.wayne.edu)
Françoise Remacle, University of Liège, Belgium (FRemacle@uliege.be)
Margaret M. Murnane, University of Colorado at Boulder (Margaret.murnane@colorado.edu)

Program Scope

The main objective of this project is to achieve a long-standing goal of ultrafast science: probing and controlling multi-electron dynamics in molecules on their natural time scales. As the most fundamental character of molecular and condensed matter systems, multi-electron dynamics have been challenging to address both theoretically and experimentally. Three research thrusts are proposed to achieve this goal: 1. Probing attosecond multi-electron dynamics and their induced ultrafast nuclear dynamics. 2. Controlling electronic excitations and chemical reactions in neutral molecules using strong fields. 3. Developing advanced theory methods for quantum modeling of nuclear dynamics. In this funding period, our research teams have made significant progress in both theory and experiment in probing charge dynamics in small molecules and in the 2D material graphene. We summarize selected recent advances in the following.

Recent Progress

1. Disentangling strong field ionization/dissociation dynamics in CH_3I

In this joint work by the Li and Schlegel groups, the strong field single and double ionization dynamics of methyl iodide was studied using 3D two-electron angular streaking (*3D-2eAS*) implemented with a circularly polarized laser field. Orientation dependent ionization yield was obtained for the first time for this molecule (Fig. 1). It was found that the dissociative ionization channels leading to I^+ production mainly arise from HOMO-1 (σ-type orbital) ionization (72%)

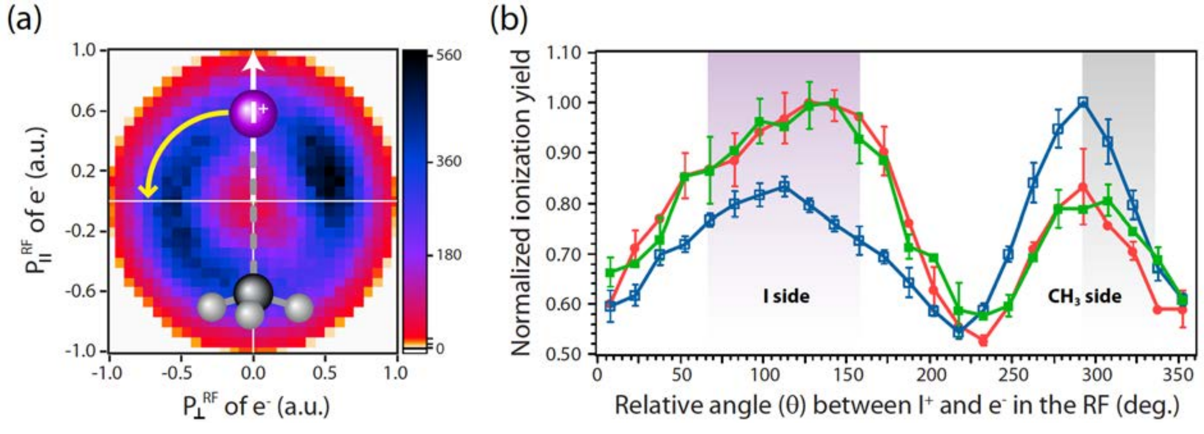

Fig. 1 (a) Recoil-frame electron momentum distribution obtained by coincidence measurements of electrons and I^+ for the dissociative single ionization of CH_3I. (b) RFPADs for dissociative single ionization (blue line) and dissociative double ionization measured with quadruple coincidence (green) and double coincidence (red line), respectively.

while HOMO (π-type) orbital ionization can also contribute by absorbing additional photons after ionization.

The dissociative double ionization dynamcis was studied by fully momentum resolved quadruple coincidence measurment. The angular dependent ionization yields of the first and second electron are plotted in a 2D graph, shown in Fig. 2(a). As far as we know this is the first presentation of such data and we call it a 2D photoionization spectrum. In this plot, the diagonal peaks represent the case of both electrons being ionized from the same site of the molecule while off-diagonal peaks are for sequential ionizations from two different sites. In Fig. 2(a), we see two peaks of each kind showing both cases are present in methyl iodide. However, the intensities of the peaks are quite different. The diagonal peak at (290°, 290°) is significantly weaker than the other peaks, which suggests that sequential ionizations from only CH_3 site is not favored. Considering that CH_3 site ionization is mainly from low-lying orbitals such as HOMO-1 and HOMO-2, this can be explained by the fact that ionization from two low-lying orbitals will produce highly excited dications which have lower ionization probability. On the other hand, the strongest diagonal feature at (120°, 120°) shows that it is highly favored that both electrons are ionized from the I site. From our calculation, we understand such a preference does not arise from ionization of two electrons from the same HOMO orbital. Instead this is due to the dominant double ionization channel HOMO (||) $\rightarrow \Pi_1$ cation→dication, in which each ionization step is dominated by ionizing electron from the I side. This work was recently published in the Journal of Physical Chemistry Letters and was featured on the cover.

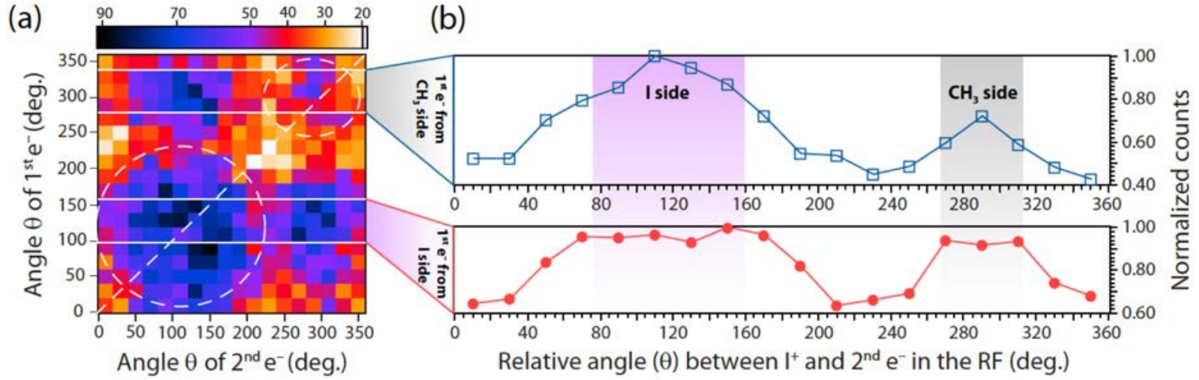

Fig. 2 (a) 2D electron-electron angular correlation in the recoil frame of the dissociative double ionization of CH_3I. The white dashed ovals indicate the two diagonal peaks. (b) Angular dependent ionization yields of the second electron in the recoil frame. The top panel corresponds to the case when the first electron is released from the I side, and the bottom panel corresponds to the case when the first electron is released from the peak in the CH_3 side (compare with Fig. 1(b)).

2. Uncover the excited states contribution in strong field dissociative double ionization dynamics of ethane

In this joint work by the Li, Schlegel and Remacle groups, the role of excited states in the strong field dissociative double ionization of ethane was revealed for the first time. In recent years, strong field dissociative double ionization of ethane has attracted considerable attention due to the high yield of H_3^+. It has been generally assumed that the dissociation dynamics take places on the ground state potential energy surface. Recent fully momentum-resolved coincidence experiments by the Li group show that the major dissociation channels are H_2+$C_2H_3^+$+H^+ and CH_3^++CH_3^+ and interestingly, the branching ratios changes as the ellipticity of the ionizing laser (Fig. 3). Dynamical calculations by the Remacle group suggest ground state alone cannot account for the production of high CH_3^+ and H_3^+ yield. The dissociation dynamics of different highly excited dication states were computed with surface hopping method and it was found that significant CH_3^+ production can be achieved. More interestingly, even though H_3^+ are exclusively produced in the ground state, it only happens after excited states internally convert to the ground state. This suggests significant vibrational energy on the ground states is needed to overcome the barrier for dissociation. Furthermore, different excited states are associated with different branching ratios (Table 1). The Schlegel group calculated the angle dependent ionization yields of the $1e_{g,u}$ and $3a_{1g}$ orbitals and found that the ionization yields are peaked at different angles in the molecular frame. This is used to explain the branching ratio variation with different laser ellipticity.

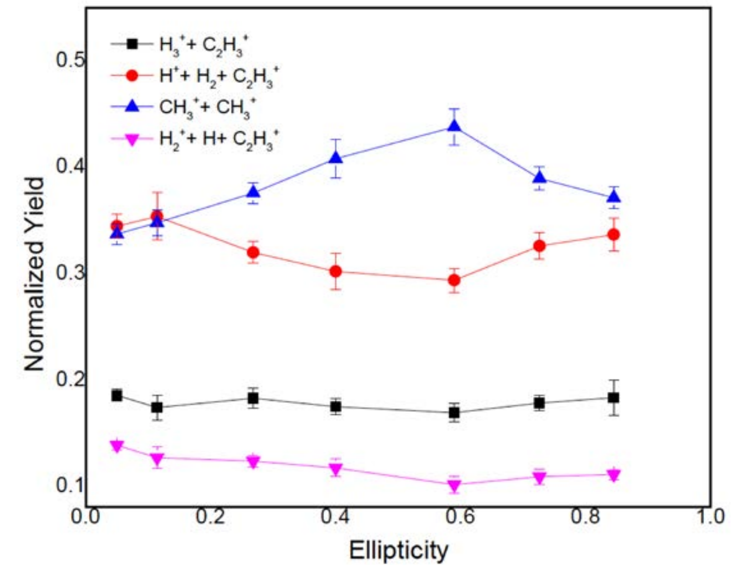

Fig. 3 The normalized yields of different dissociation pathways of ethane dication and their variation with the laser ellipticity.

Pathways States	H_3^++$C_2H_3^+$	H_2+$C_2H_3^+$+H^+	CH_3^++CH_3^+	H_2^++$C_2H_4^+$
D_0	0%	81%	7%	1%
D_3	3%	59%	18%	5%
D_4	14%	43%	25%	5%
D_6	13%	21%	41%	6%

Table 1. Computed branching ratios for different ethane dication states.

This work is the first complete dynamical study on strong field dissociative double ionization of ethane and the manuscript is currently in preparation.

3. Observing unprecedented slow carrier dynamics in graphene

The carrier decay lifetime in material upon photoexcitation is strongly dependent on multielectron interaction dynamics and is extremely important in determining the practicality of any optoelectrical material. In the past decade, there have been numerous studies on electron cooling dynamics in graphene. Graphene, once heralded as the miracle material, was basically written off as a good candidate for devices due to its extremely short carrier lifetime and a vanishing band gap. Previous measurements at room temperature have always yielded a few picoseconds or faster.

Recently, the Li group has carried out a study on the multi-electron decay dynamics of graphene carrier using a home-built TOF-based angular resolved photoelectron spectroscopy (ARPES) (Fig. 4). Our study suggests that at very low laser fluence (a few micro-Joules per square centimeters), there exists a significant decay channel for carriers that can have a much longer lifetime (a few hundred picoseconds). This has not been observed previously simply because that the low laser fluence requires an extremely high detection efficiency. This observation might rekindle the effort of making graphene-based optoelectrical device and we are interested in further studying the underlying mechanisms of this phenomenon. This work was published in the Journal of Physical Chemistry Letters.

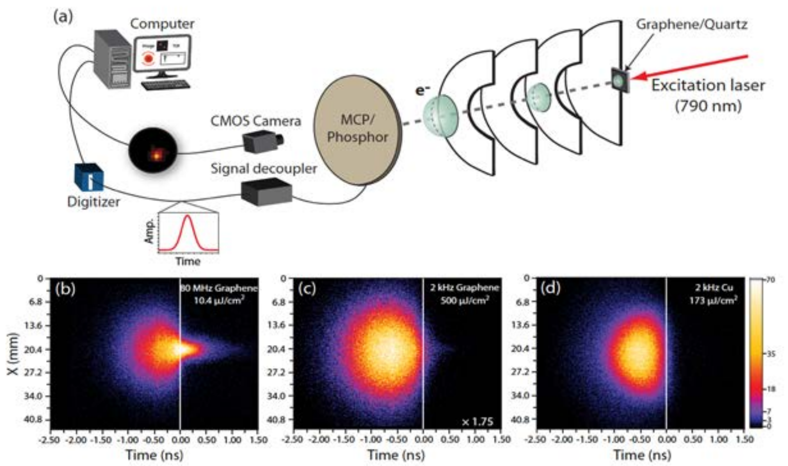

Fig. 4. new ARPES instrument and results of graphene carrier dynamics. (a) Schematic of the experiment setup. (b) (c) The 2D image of electrons from graphene at different laser fluencies. (d) Same as (b)(c) but for a Cu film for comparison. The electron arriving later after time zero can only be explained by delayed emission from long-lived carriers.

4. Role of the photoinduced multielectron dynamics on the large isotope effect in the photodissociation of N_2

We review the current status in the experimental/theoretical issue of the anomalously large isotope effect in the photodissociation of N_2. In 2011 the UCLA/ULiege suggested (PNAS 2011) that the extreme deviations of the isotopic branching on N atoms in the galaxy could be due to the wavelength dependence of the photodissociation of N_2. We suggested that the effect will be most dominant in those spectral regions where there are wide variations in state mixing of the valence and Rydberg states that are one-photon accessible from the ground state, most notably just below the excitation energy of 13.8eV. A direct experiment at the Berkeley advanced light source by Mark Thiemens and coworkers, UCSD, has verified this. To explore the mechanism, The UCLA/ULiege team has just published (PNAS 2018) a detailed theoretical discussion using a very short pulse to initiate the dissociation at time ‘zero’. At the same time the team of Thiemens *et al.* has measured the photodissociation over a wide spectral range. Their results are shown in the Fig. 5, which is superimposed on the fractional composition of the excited state of N_2 accessed at that wavelength.

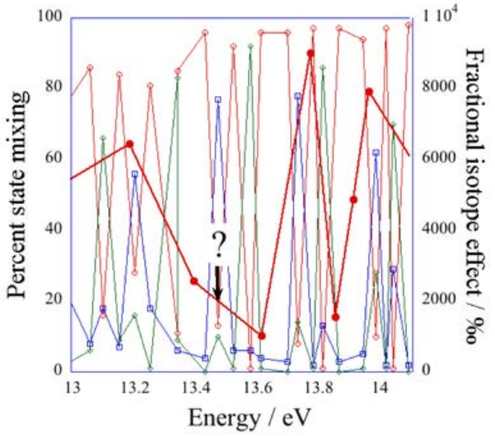

Fig. 5. Experimental fractional isotope effect in the photodissociation of N_2 vs. excitation wavelength. Measured at low temperature at the ALS light source by Thiemens et al. at UCSD, right ordinate. Such small effects are usually reported as parts per thousand. The left ordinate shows the extent of mixing of excited states at different wavelengths. The two more mixed states are the valence state b (red) and the Rydberg state c (green).

The mixing of states is due to there being three distinct excited state of N_2 that are one photon accessible from the ground state in the energy range of interest. An extensive mixing of the three states is clearly seen at the three wavelengths where the observed isotope effect is large. At other wavelengths the observed effect is far lower.

5. Photoinduced isomerization of norbornadiene to quadricyclane

The UCLA/ULiege team has developed the computational and visualization tools for designing control schemes of the multi-electron photoisomerization quantum dynamics of norbornadiene (open) to quadricyclane (closed) (C7H8) form, which implies controlling the electronic dynamics into making two new C-C bond, see Fig. 6c. We have selected 3 generalized nuclear coordinates (θ,γ,φ) suitable for simulating the coupled electronic-nuclear dynamics. 3-dimensional (3D) potential, transition dipole and non-adiabatic coupling (NAC) grids for a total of 65000 (25x26x100) geometries have been built at the SA(14)-CASSCF(4,8)//AUG-CC-PVDZ level of electronic structure using the quantum chemistry software MOLCAS for 14 interacting electronic states of the neutral. The 8 molecular orbitals (MO) of the active space include the Rydberg orbitals that play an essential role for describing accurately the high electronic excited states involved in the photoisomerization from the open and closed forms, Fig. 6a. The three nuclear coordinates have been selected to properly describe the conical intersection between the S1 and the S0 electronic state that plays a major role in the photoisomerization, Fig. 6b. In parallel, we have built the visualization tools that allow following the motion of populations and electronic coherences as function of time in 3D. Snapshots from these movies are plotted in Fig. 6d,e. We show snapshots of the localization of the wave packet on S0 and S1 in Fig. 6d and of the electronic coherence when the 3D wave packet crosses the S0/S1 conical intersection in Fig. 1e. The same simulation and

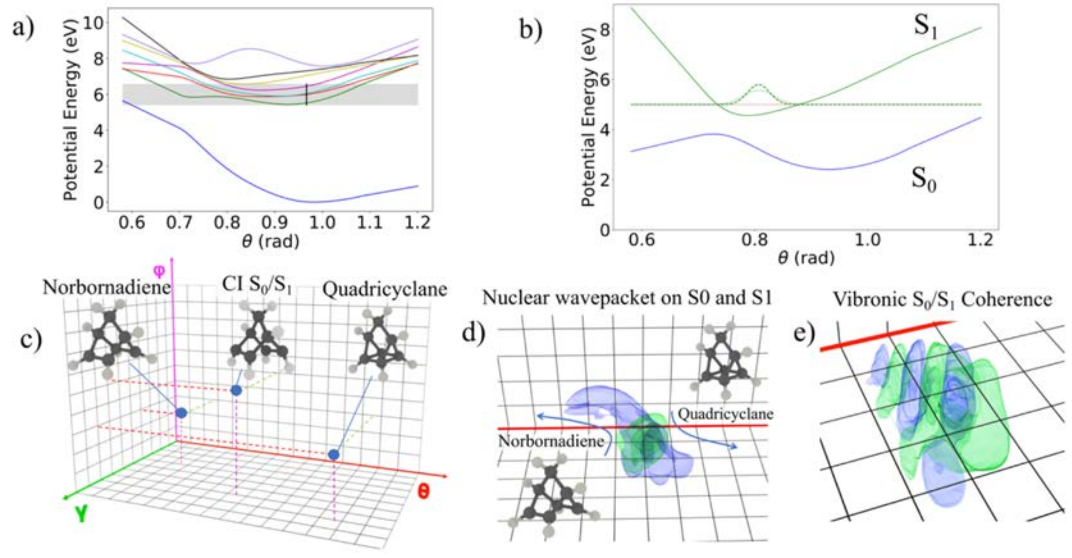

Fig. 6. Photoisomerization of norbornadiene to quadricyclane. (a) The 8 lowest electronic states along the θ coordinate. (b) The conical intersection (CI) between the S0 and the S1 states along the θ coordinate. (c) Location of the norbornadiene and the quadricyclane geometries, as well as the geometry at the S0/S1 CI in the 3 generalized coordinates θ,γ,φ. (d) Isocontours of the wave packets on the S0 (blue) and S1 (green) in the vicinity of the CI, plotted in (θ,γ,φ). (e) Isocontours of the wave packets on S0/S1 vibronic coherence in the vicinity of the CI, plotted in (θ,γ,φ), blue positive, green negative value of the isocontour.

visualization tools are currently also applied for simulating the 3D quantum dynamics of the photoisomerization of HCN, which is followed on 8 electronic states. These results were presented at the 'Strong Field Symposium' and at the 'From Potential Energy Surfaces to Dynamics & Kinetics' of the 256th ACS meeting in Boston.

6. Photoionization dynamics including nuclear motion

Simulating the quantum dynamics of photoionization coupled to nuclear motion requires the computation of dense grids of photoionization matrix elements (discretization of the continua states) for each grid point of nuclear coordinates. Therefore, simulations of the quantum dynamics become rapidly untractable as the number of nuclear degrees of freedom increases. On the other hand, understanding and controlling the coupling between photoionization and nuclear motion is essential for implementing control schemes based on the excitation of the neutral through Raman-like strong field processes induced by the recollision of the electronic wave packet with the cation. In order to reduce both the computer time and storage requirements of such quantum dynamics simulations, the ULiege/UCLA team has developed a new algorithm for computing the photoionization matrix elements and the Dyson orbitals, based on using the analytical expressions of the atomic orbitals (AO) for deriving the analytical expressions of the dipoles of the Dyson orbitals using a basis set of plane waves for the continua states. This fully analytical approach was benchmarked on LiH. These results were presented at the 'Strong Field Symposium' of the 256th ACS meeting in Boston. Work is in progress with the Wayne State team (Schlegel) for including both the photoionization and strong field ionization processes (using the TDCI-CAP approach) which contribute to the ionization process in the 3D-2eAS experiments. In parallel, computation of the potential energy, non-adiabatic coupling and photoionization matrix elements of the three lowest states of the CH_4 cation including the Jahn-Teller process are under way.

7. Quantum simulation of 3D-2eAS for probing electronic dynamics

In collaboration with the Wayne state team, the ULiege/UCLA team designed a 3D-2eAS scheme for probing electronic dynamics in neutral excited states of LiH using a Negative-Neutral-Positive) NeNePo photoexcitation scheme. In the two-electron angular streaking experiment represented in Fig. 7, the laser pulse doubly ionizes the LiH anion to the cation. By using a linearly polarized few-cycle IR pulse, it is possible to correlate the ionization time of the first electron (from the anion to the neutral) with the ionization time of the second electron (from the neutral to the cation), Fig. 7d. The heatmap of the streaking spectrum in the laser polarization direction reflects the ionization time of the two electrons (Fig. 7d) while the spectra in the perpendicular directions reflect the electronic dynamics occurring in the neutral states. For aligned molecules, the electronic dynamics strongly depends on the laser polarization. For a laser polarized along z, the molecular axis, only Σ states are accessed and the photoelectron angular distributions along x and y are isotropic. For a laser polarized along x or y, both Σ and Π states are accessed, which triggers a motion of the electronic density in the z-x/y plane that is reflected by an anisotropic distribution along z as shown in Fig. 7e.

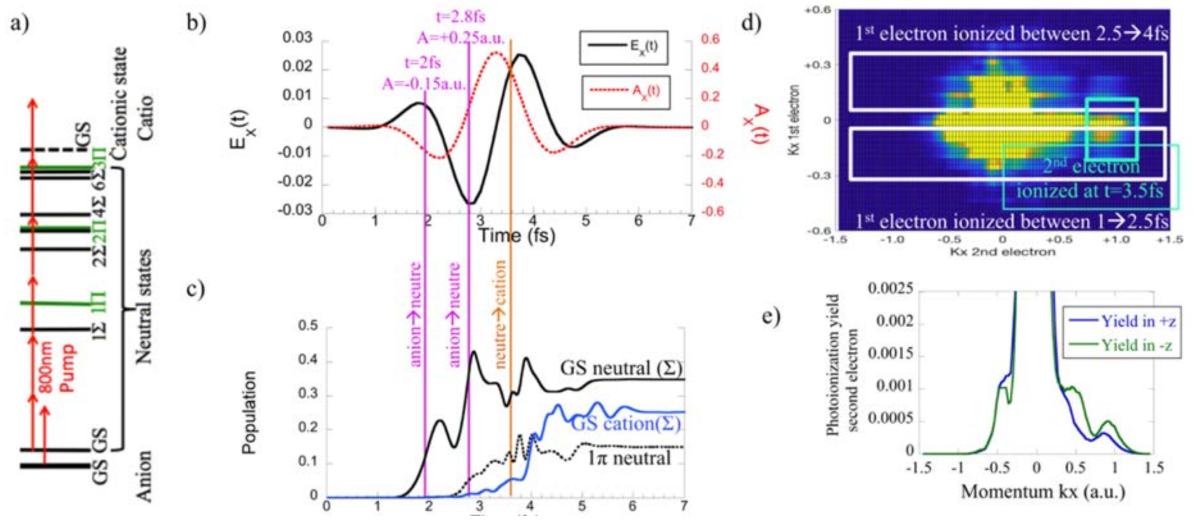

Fig. 7 (a) Scheme of the NeNePo streaking experiment using an ultrashort few-cycle laser pulse polarized perpendicularly to the molecular axis (2.8fs 800nm IR pulse). (b) Time profile of the electric field (E) and its vector potential (A) of the pulse (ω=0.057 a.u., Gaussian envelope, σ=50 a.u., polarization along *x*, field strength=0.03 a.u.) (c) Evolution of the anionic, neutral (only the GS(Σ) and 1Π states are showed) and cationic states. (d) Heatmap of the ioinization yield of the second photoelectron plotted as a function of the momentum along the x direction (perpendicular to the molecular axis) between the first and second ionized electron. (e) Computed anisotropy along the z direction of the yield of the second electron that reflects the beating dynamics of the coherent superposition of the GS and Π state of the neutral.

Future Plans

We are working on producing few-cycle laser pulses that allow us to access the dynamics that takes place in the first few femtoseconds after ionization. This will be combined with *3D-2eAS* and we will use timed sequential double ionization to study charge migration and ultrafast nuclear dynamics that involves hydrogen atoms such as CH_4^+ nuclear arrangement.

We are working on fully elucidate the mechanism of the isotope effect we propose to compute the ultrafast ionization of the excited N_2 as a function of the delay time between the pump and the probe. This will also allow us to explore recollision, in a realistic setting. We will continue developing the algebraic approach to quantum dynamics that allows for extending the ‘on the fly’ grid method based on the finite difference algorithm to larger systems.

Work is in progress for the simulation of a full isomerization process pump and probed by short UV/IR pulses. Implementing the finite difference algorithm for running the dynamics in 3D is a preliminary step for developing the on the fly approach.

We are computing the vibronic photo and strong field ionization dynamics in LiH, HCN and CH_4. This step is essential for being able to simulate the probing of ultrafast electronic and nuclear dynamics using the 3D-2eAS streaking experiments. We will develop scheme using circularly polarized pulses and include the motion of the nuclei using the progress aforementioned.

We are developing a 3D virtual detector to monitor the direction and momentum of electrons ejected from polyatomic molecules as a function of the direction of linearly and elliptically polarized, ultrashort, intense laser pulses.

We will seek opportunities in organizing conferences and symposia to promote interactions among peer scientists and student learning, continuing our recent success in organizing the ACS Strong Field Chemistry symposium.

Peer-Reviewed Publications Resulting from this Project (2016-2018) with Institutional Contribution

1. J. S. Ajay, K. G. Komarova, F. Remacle, R. D. Levine, "Time-Dependent View of an Isotope Effect in Electron-Nuclear Nonequilibrium Dynamics with Applications to N_2". *Proc. Natl. Acad. Sci,* 115, 5890 **2018** DOI 10.1073/pnas.1804455115 (**UCLA-ULiege**)
2. A. H. Winney, G. Basnayake, D. A. Debrah, Y. F. Lin, S. K. Lee, P. Hoerner, Q. Liao, H. B. Schlegel and W. Li, "Disentangling strong field multi-electron dynamics with angular streaking", *J. Phys. Chem. Lett.*, 9, 2539 (2018) (**WSU**)
3. L. Fan, S. K. Lee, P. Y. Chen and W. Li, "Observation of nanosecond hot carrier decay dynamics in graphene", *J. Phys. Chem. Lett.,* 9, 1485 (2018) (**WSU**)
4. T. C. Jenks, M. D. Bailey, J. L. Hovey, S. Fernando, G. Basnayake, M. E. Cross, W. Li and M. Allen, "First use of a divalent lanthanide for visible-light-promoted photoredox catalysis", *Chem. Sci.* 9, 1273 (2018) (**WSU**)
5. K. G. Komarova, F. Remacle, R. D. Levine, "Propagation of Nonstationary Electronic and Nuclear States: Attosecond Dynamics in LiF", *Mol. Phys.,* 116, 2524 (2018) **(UCLA-ULiege)**
6. K. G. Komarova, F. Remacle, R. D. Levine, "On the Fly Quantum Dynamics of Electronic and Nuclear Wave Packets". *Chem. Phys. Lett.,* 699, 155 (2018) **(UCLA-ULiege**)
7. Jayantha, S. A.; Komarova, K. G.; Wildenberg, S. v. d.; Remacle, F.; Levine, R. D., Attophotochemistry: Coherent Electronic Dynamics and Nuclear Motion. In *Attosecond Molecular Dynamics*, Vrakking, M. J. J.; Lepine, F., Eds. Royal Society of Chemistry: Cambridge, 2018; Vol. 13, 308-347 (**UCLA-ULiege**).
8. Levine, R. D., "Photochemistry of Highly Excited States" *Proc. Natl. Acad. Sci.,* 114, 13594, (2017) (**UCLA**)
9. W. K. Peters, D. E. Couch, B. Mignolet, X. Shi, Q. L. Nguyen, R. C. Fortenberry, H. B. Schlegel, F. Remacle, H. C. Kapteyn, M. M. Murnane and W. Li, "Ultrafast 25 fs relaxation in highly excited states of methyl azide mediated by strong nonadiabatic coupling", *Proc. Natl. Acad. Sci.,* 114, E11072 (2017) (**CU-WSU-ULiege**)
10. J. Hollett and W. Li, "The relative alignment of electron momenta in atoms and molecules and the effect of a static electric field", *J. Phys. Chem. A*, **121**, 8026 (2017) (**WSU**)
11. L. Fan, S. K. Lee, Y. J. Tu, B. Mignolet, D. Couch, K. Dorney, Q. Nguyen, L. Wooldridge, M. Murnane, F. Remacle, H. B. Schlegel, W. Li, "A new electron-ion coincidence 3D momentum-imaging method and its applications in probing strong field dynamics of PENNA", *J. Chem. Phys.,* **147**, 013920 (2017) **(WSU-ULiege-CU)**
12. S. Sun, B. Mignolet, L. Fan, W. Li, R. D. Levine, F. Remacle, "Nuclear motion driven ultrafast photodissociative charge transfer of PENNA cation", *J. Phys. Chem. A*, **121**, 1442 (2017) **(ULiege-UCLA-WSU)**
13. A. Winney, S. Lee, Y. Lin, P. Adhikari, G. Basnayake, Q. Liao, H. Schlegel, W. Li, "Attosecond electron correlation dynamics in double ionization of benzene probed with two-electron angular streaking", *Phys. Rev. Lett.* **119**, 123201 (2017) **(WSU)**
14. Q. B. Zhang, G. Basnayake, A. Winney, Y. F. Lin, D. Debrah, S. K. Lee, W. Li, "Orbital-resolved nonadiabatic tunneling ionization", *Phys. Rev. A,* **96**, 023422 (2017**) (WSU)**
15. D. E. Couch, H. C. Kapteyn, M. M. Murnane, William K. Peters, "Uncovering highly-excited state mixing with in acetone ultrafast VUV pulses and coincidence imaging techniques", *J. Phys. Chem. A,* **121**, 2361 (2017) **(CU)**

16. A. Nikodem, R. D. Levine, and F. Remacle, "Spatial and temporal control of populations, branching ratios, and electronic coherences in LiH by a single one-cycle infrared pulse", *Phys. Rev. A,* **95**, 053404 (2017) **(UCLA-ULiege)**
17. V. Schwanen, F. Remacle, "Photoinduced Ultrafast Charge Transfer and Charge Migration in Small Gold Clusters Passivated by a Chromophoric Ligand", *Nano Letters*, *in press*, 10.1021/acs.nanolett.7b02568 **(ULiege)**
18. S. van den Wildenberg, B. Mignolet, R. Levine, and F. Remacle, "Pumping and probing vibrational modulated coupled electronic coherence in HCN using short UV fs laser pulses: a 2D quantum nuclear dynamical study", *Phys. Chem. Chem. Phys.,* **19**, 19837 (2017) **(UCLA-ULiege)**
19. H. Xiong, B. Mignolet, L. Fang, T. Osipov, T. Wolf, E. Sistrunk, M. Gühr, F. Remacle, N. Berrah, "The Role of Super-Atom Molecular Orbitals in Doped Fullerenes in a fs Intense Laser Field", Sci. Rep. **7**, 121 (2017). **(ULiege)**
20. X. Shi. W. Li, H. B. Schlegel, "Computational Simulations of Hydrogen Circular Migration in Protonated Acetylene Induced by Circularly Polarized Light", *J. Chem. Phys*., **145**, 084309 (2016) **(WSU)**
21. Q. Liao, W. Li, H. Schlegel, "Angle-Dependent Strong Field Ionization of Triple Bonded Systems Calculated by Time-Dependent Configuration Interaction, with an Absorbing Potential", *Can. J. Chem.,* **94**, 989, (2016) **(WSU)**
22. X. Shi, B. Thapa, W. Li, H. B. Schlegel, "Controlling chemical reactions by short, intense mid-infrared laser pulses: comparison of linear and circularly polarized light in simulations of $ClCHO^+$ fragmentation", *J. Phys. Chem. A*, **120**, 1120 (2016) **(WSU)**
23. Ajay, J. Šmydke, F. Remacle, and R. D. Levine, "Probing in Space and Time the Nuclear Motion Driven by Non-equilibrium Electronic Dynamics in Ultrafast Pumped N_2", *J. Phys. Chem. A*, **120**, 3335 (2016) **(UCLA-ULiege)**
24. H. Li, B. Mignolet, Z. Wang, K. J. Betsch, K. D. Carnes, I. Ben-Itzhak, C. L. Cocke, F. Remacle, and M. F. Kling, "Transition from SAMO to Rydberg State Ionization in C_{60} in Femtosecond Laser Fields", *J. Phys. Chem. Lett.* **7**, 4677 (2016) **(ULiege)**
25. A. Nikodem, R. D. Levine, and F. Remacle, "Quantum Nuclear Dynamics Pumped and Probed by Ultrafast Polarization Controlled Steering of a Coherent Electronic State in LiH", *J. Phys. Chem. A*, **120**, 3343 (2016). **(UCLA-ULiege)**

Page is intentionally blank.

Early Career: First-Principles Tools for Nonadiabatic Attosecond Dynamics in Materials

Kenneth Lopata

Department of Chemistry, Center for Computation and Technology,
Louisiana State University, Baton Rouge, LA 70803
klopata@lsu.edu

Project Scope

The sub-femtosecond response of materials to intense and/or high energy light underpins a range of processes such as light harvesting and radiation damage, and forms the basis for time-resolved measurements of dynamics at light sources. At the atomistic level many of the underlying mechanisms are poorly understood, especially concerning the sub-femtosecond electron dynamics immediately following excitation, as well as subsequent femtosecond-scale electron/lattice motion such as and photochemistry-like processes around dopants and defects. The overarching goal of this project is to develop quantum chemistry techniques for simulating attosecond electron dynamics and femtosecond electron/lattice in solid state materials with an emphasis on X-ray driven and/or probed processes. These tools will be validated against ultrafast experiments and help interpret and motivate new directions. In addition, all software will be released as part of the free/open source NWChem package, where it is expected to be broadly applicable to ongoing ultrafast efforts spanning molecular and materials systems.

Recent Progress

During the first year of this project, our efforts were focused on developing a framework of time-dependent density functional theory (TDDFT) tools necessary for simulating attosecond electron dynamics in materials. The initial emphasis is on ultrafast X-ray probes, i.e., extending quantum chemistry techniques to capture transient X-ray absorption near dopants and defects. We have made recent progress in three inter-related directions: (I) covalently embedded bulk-mimicking clusters for simulating excitations near dopants in semiconductors, (II) development of a relativistic TDDFT code (necessary when X-ray spectra involve spin-orbit split transitions), and (III) development of a massively parallel electrodynamics code for electrodynamical embedding and beyond dipole interactions. Emphasis has been, up to this point, on validation via weak intensity (linear response) X-ray spectra, with extension to strong-fields and attosecond dynamics in the coming year. These three sub-projects are outlined below.

(I) X-Ray Absorption in Transition Metal Oxides

Simulating X-ray driven processes in solids using TDDFT is challenging for various reasons, including: basis set inadequacies (e.g., planewaves typically require pseudopotentials), failures of traditional DFT functionals for electron dynamics, and difficulty in treating defects and dopants. Bulk-mimicking finite clusters with atom-centered basis sets offer a good alternative to periodic methods as they are naturally all electron (including core states), hybrid DFT functionals are efficient to evaluate, and dopants can be captured without requiring prohibitively large supercells. While cluster models are somewhat well-developed technique for spectroscopy simulations [1], however, their validity for electronic dynamics remains relatively unexplored.

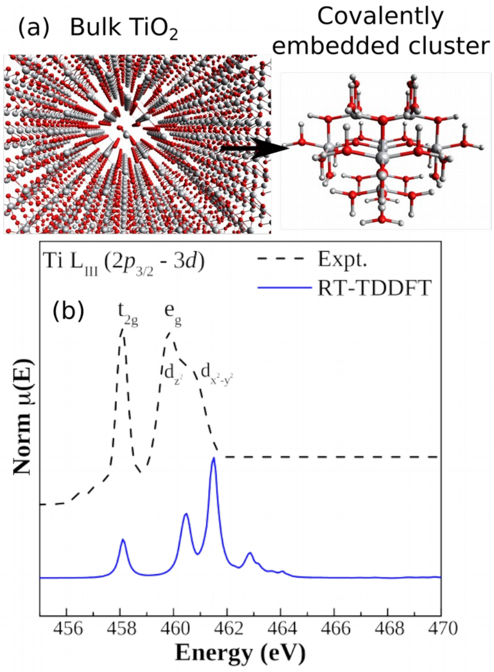

Figure 1: (a) Bulk-mimicking cluster constructed by capping the dangling oxygens with partially charged H atoms. (b) The resulting TDDFT spectrum captures the main features of the Ti L_3 XANES features.

To address this, we have begun implementing these approaches for transient X-ray absorption in semiconductors and insulators. Before tacking dynamics, we first validated cluster models for the case of linear response X-ray absorption. Recently, in collaboration with James Dorman (LSU Chemical Engineering) we have successfully adapted a covalent quasi-atom capping technique to capture X-ray near-edge (XANES) features of metal oxides (titania, nickel oxide). In a nutshell, this approach consists of passivating the boundary oxygen atoms with partially charged hydrogen atoms, with the O-H bond length chosen to ensure each atom the cluster has the same atomic charge. For the case of the titanium XANES, one central "absorbing center" titanium atom is described with a very large uncontracted basis set. Our results agree qualitatively well with experiment (Fig. 1), but somewhat overestimate the peak splittings, likely due to either a basis set or cluster geometry issue. Here, hybrid DFT (PBE0 in this case) seems adequate to capture the spectral response, but additional functionals are being explored, including optimally tuned range-separated hybrids.

Due to the relatively large system sizes, computation of spectra (and X-ray transients in the future) initially required simulations spanning many days on an HPC systems. This is largely due to slow convergence of the Fourier transform (FT) with simulation time which would make transient XAS simulations prohibitively inefficient. To overcome this, we adapted our acceleration technique [2] where the time-dependent dipole is decomposed into transition dipoles between occupied and virtual orbitals, each of which is transformed via a Padé approximant to the FT. Since spectra in these large clusters involve tens of thousands of transitions, this post-processing required extensive optimization, including Toeplitz-specific matrix inversion and parallelization over the transition dipoles. As an example, for a large TiO_2 cluster this method reduced simulation time from two weeks to approximately two days simulation followed by a few hours of post-processing. A manuscript detailing the cluster and acceleration results is currently under preparation. Looking forward, we are extending the cluster and Padé acceleration techniques to transient X-ray absorption.

(II) Real-time Spin-Orbit Time-Dependent Density Functional Theory

Spin-orbit effects play an important role in the X-ray response of solid state materials. Soft and tender X-ray spectra of 3rd row and transition metal elements, for example, involve spin-orbit splittings (~1 eV) comparable to the splittings between spectra features and can result in "overlapping" L_2 and L_3 branches. Simulating transient processes in these systems, e.g., X-ray triggered dynamics and/or X-ray probes, thus requires a relativistic electronic structure method. To address these issues, in collaboration with Dr. Niri Govind (PNNL), we have implemented relativistic real-time TDDFT in the massively parallel free/open source NWChem software package.

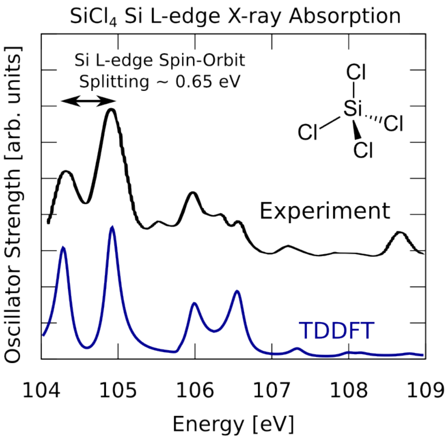

Figure 2: Simulated Si-L edge X-ray absorption of the SiCl4 molecule using spin-orbit real-time TDDFT. SO-RTDDFT accurately captures SO split features in the experimental near-edge absorption [5].

Our approach is based on zeroth-order regular approximation (ZORA) with spin-orbit model potentials constructed from four component atomic densities [3]. The time evolution then involves propagating a two-component density matrix under a complex two-component Fock matrix (effective Hamiltonian).

To check the implementation, we are currently validating against literature four-component simulations [4] as well as experimental X-ray and UV/Visible absorption in a range of molecular systems. To compute these spectra, we use a delta-function (broadband) excitation, decomposition of the time-dependent dipole moment into occupied/virtual pairs of spin-orbitals, and Pade approximants to the Fourier transform of the dipole contributions [2]. This significantly reduces the required simulation time and allows us to determine which spin-orbitals contribute to each transition. Fig. 2 shows our TDDFT spectrum for the $SiCl_4$ molecule Si L-edge X-ray absorption (shifted by 4.7 eV to line up with experiment) computed using the aug-cc-CPVTZ basis and PBE0 functional. Our computed spectrum correctly captures the spin-orbit split features near the absorption edge (~104 eV), their relative oscillator strengths, as well as higher energy transitions. Additional validation cases likewise show good agreement with experiment. A manuscript detailing this work is currently being prepared. Critically, since this approach is based real-time propagation, it is readily applied to electron dynamics problems where spin-orbit effects are important, such as: transient X-ray absorption, strong-field ionization, and charge migration in systems containing heavy elements. Work in these directions is ongoing.

(III) Massively Parallel Electrodynamics for Dynamical Embedding

Finally, extending finite cluster simulations to attosecond simulations requires some method of embedding beyond electrostatics (point charges) or simple covalent capping. Instead, a dynamical approach necessary, such as where the quantum region (cluster) is embedded in a background with the correct frequency-dependent response. To this end, we are currently developing a coupled TDDFT/electrodynamics scheme where the QM bulk-mimicking clusters are embedded in time-evolving classical electric and magnetic fields propagated using the finite-difference time-domain (FDTD) method. This technique potentially allows for improved excitation energies, less unphysical finite cluster sizes effects, simulation of long-range propagation through the medium, and beyond dipole (nonuniform) electric field coupling.

As a first step in this direction, we have developed a massively parallel 3D FDTD code in the NWChem package, which is based on the Global Arrays distributed memory architecture. Here, the electric and magnetic fields are discretized in space and partitioned into sub-regions, each of which is assigned to a compute node. The both speeds up the calculation of the curls via finite differences, and also allows for simulations with significantly more grid points, since the fields are distributed in memory across multiple compute nodes. As finite-differences are nonlocal operations, communication is required between regions. This is accomplished with "ghost" cells that border the domains (see Fig. 3) Currently, we have a functional 3D vacuum propagation code that has been validated and scales on both single node and high performance computing facilities. In addition to being a general-purpose FDTD code (e.g., suitable for nanoplasmonics modeling), what makes this implementation unique is the integration with the electronic structure modules of NWChem, specifically the real-time TDDFT one. This will allow for seamlessly coupled highly parallelized Maxwell/Schrodinger simulations on a large scale, which opens the door to future extensions such as electrodynamical embedding and beyond dipole coupling in the quantum Hamiltonian.

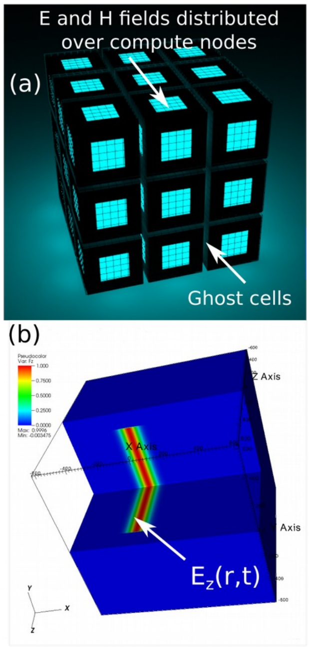

Figure 3: (a) Schematic of the FDTD parallelization via decomposition into sub-domains, with finite-differences done using ghost cells. (b) Snapshot of a simulated z-polarized laser pulse traveling through vacuum.

Future Plans

In the coming year, efforts will pivot from spectra to focus primarily on two directions: attosecond electron dynamics in insulators, and electrodynamics embedding. The electron dynamics future work includes:

- Development of Padé-based schemes for accelerating computation of transient absorption spectra. This will be validated against simple atomic systems including hydrogen, argon, and xenon.
- Validation of TDDFT for intense off-resonant electronic response of solids using finite clusters. This will focus on simple, well-characterized materials such as SiO_2, TiO_2, diamond, and silicon.
- X-ray pump/X-ray probe simulations where the initial state is created via "sudden" creation of a core-hole [6], potentially involving coherences between spin-orbit split states. Sudden ionization offers a way to sidestep issues with TDDFT resonant excitation, which is known to have issues for adiabatic (local-in-time) functionals.

For the electrodynamics thrust future plans include:

- Implement lossy dispersive materials into FDTD code, release as part of NWChem trunk.
- Couple TDDFT/FDTD via quantum sub-regions that allow for energy sharing between the classical and quantum sub-regions [7].
- Incorporate spatial-dependent fields into TDDFT via FDTD. This will enable beyond dipole coupling, which is vital for hard X-rays which have wavelengths on the order of bonds or shorter. Results will be validated against linear-response hard X-ray XANES for molecules and materials.

References

[1] R. G. Fernando, M. C. Balhoff, and K. Lopata, "X-ray absorption in insulators with non-Hermitian real-time time-dependent density functional theory", *J. Chem. Theory Comput.* **11**, 646 (2015).

[2] A. Bruner, D. LaMaster, and K. Lopata, "Accelerated broadband spectra using transition dipole decomposition and Pade Approximants", *J. Chem. Theory Comput.* **12**, 3741 (2016).

[3] C. van Wullen and C. Michauk, "Accurate and efficient treatment of two-electron contributions in quasirelativistic high-order Douglas-Kroll density-functional calculations", *J. Chem. Phys.* **123**, 204113 (2005).

[4] T. Fransson, D. Burdakova, and P. Norman, "K- and L-edge X-ray absorption spectrum calculations of closed-shell carbon, silicon, germanium, and sulfur compounds using damped four-component density functional response theory", *Phys. Chem. Chem. Phys.* **18**, 13591 (2016).

[5] R. Püttner, M. Domke, and G. Kaindl, "Comparative study of Si−2p core-excitation spectra in the tetrahedral molecules SiX_4", *Phys. Rev. A* **57**, 297 (1998).

[6] A. Bruner, S. Hernandez, F. Mauger, P. M. Abanador, D. J. LaMaster, M. B. Gaarde, K. J. Schafer, and K. Lopata, "Attosecond charge migration with TDDFT: Accurate dynamics from a well-defined initial state", *J. Phys. Chem. Lett.* **8**, 3991 (2017).

[7] H. T. Smith, T. E. Karam, L. H. Haber, and K. Lopata, "Capturing plasmon-molecule dynamics in dye monolayers on metal nanoparticles using classical electrodynamics with quantum embedding", *J. Phys. Chem. C* **121**, 16932 (2017).

Peer-Reviewed Publications Resulting from this Project (Project start date: 09/2017)

None yet.

Complexity and Correlated Motion of Electrons in Free and Confined Atomic Systems

Steven T. Manson, Principal Investigator
Department of Physics and Astronomy, Georgia State University, Atlanta, Georgia 30303
(smanson@gsu.edu)

Project Scope

The goals of this research program are: to further our understanding of the interaction of radiation with matter; to provide theoretical support to, and collaboration with, various experimental programs that employ latest generation light sources, particularly ALS, APS and LCLS; and to study the properties (especially photoemission) of confined atoms and ions. Specifically, calculations are performed using and upgrading state-of-the-art theoretical methods to help understand the essential physics of the experimental results; to suggest future experimental investigations; and seek out new phenomenology, especially in the areas of attosecond time delay in photoemission (including negative ion photodetachment), outer-shell photoemission in the vicinity of inner-shell thresholds and confined systems. The primary areas of programmatic focus are: nondipole and relativistic effects in photoionization; photoabsorption of inner and outer shells of atoms and atomic ions (positive and negative); dynamical properties of atoms endrohedrally confined in buckyballs, primarily C_{60}; studies of Wigner time delay on the attosecond scale in photoemission of free and confined atomic systems. Flexibility is maintained to respond to opportunities as they arise.

Recent Progress

A number of aspects of attosecond motion of electrons in the photoemission process, as revealed by Wigner time delay [1,2] were explored. Time delay of photoemission from valence subshells of noble-gas atoms were theoretically scrutinized within the framework of the dipole relativistic random phase approximation [3] with a focus on the variation of time delay in the vicinity of the Cooper minima where the corresponding dipole matrix element changes its sign while passing through a node. It was found that the presence of the Cooper minimum in one photoionization channel has a strong effect on time delay in other channels owing to interchannel coupling, and that relativistic effects strongly affect the time delay in regions of Cooper minima; it is likely that relativistic effects will be even more important as one goes to heavier and heavier elements. A study of Wigner time delay in Mn photoionization in the region of the $3p\rightarrow3d$ giant resonance showed the dramatic effect of the resonance on the time delay of photoemission from the $3d$ and $4s$ valence subshells of the Mn atom [4]. Similar features are expected to emerge in photoionization time delays of other transition-metal and rare-earth atoms with half-filled subshells that possess giant autoionization resonances as well. It was shown that photoionization time delay in the autoionizing resonance region is explicitly associated with the resonance lifetime, which can, thus, be directly measured in attosecond time-delay experiments. We also conducted a systematic study of the dipole phase and the Wigner time delay in inner-shell photoionization of noble gas atoms from Ne to Xe [5] using both the relativistic and the nonrelativistic versions of the random-phase approximation and found that the time delay, as a function of photoelectron energy, follows more or less a universal shape. And the angular distribution of Wigner time delay was investigated and it was found that strong angular anisotropy of the time delay in photoemission occurs near Cooper minima while the spin-orbit splitting affects the time delay near threshold [6]. It has also been found that in the vicinity of autoionizing resonances, the time delay spectrum can become quite complicated, exhibiting both positive and negative delays across the resonance profile [7]. A model was introduced that indicated that the shape of the time-delay spectrum is related to the Fano *q* parameter [8]. And aside from the complex energy dependence of Wigner time delay across a resonance profile, our preliminary calculations indicate that the angular distribution is also quite complex, even to the point that at certain energies, the time delay can be positive in one direction of photoemission, and negative in another direction, a most peculiar result from a physical point of view.

Multielectron correlations in the form of interchannel coupling have been found to crucial determinants of time delay for outer subshells in the neighborhood of inner thresholds [9]; this suggests that time delay measurements can be used as a sensitive indicator of many-body interactions. Since Wigner time delay near the photoionization threshold is dominated by the long-range Coulomb interaction between the photoelectron and residual ion [5-7], we have initiated studies of attosecond time delay in negative ion photodetachment in Cl^-, Br^-, I^- and Tm^- (which are isoelectronic to Ar, Kr, Xe and Yb, respectively) where the long-range Coulomb interaction is obviated and the effects of near-threshold shape resonances are emphasized in the time-delay spectrum [10]. And we have also initiated investigations of valence photodetachment near inner-shell thresholds. Preliminary results indicate multielectron correlation effects owing to interchannel coupling are much stronger and more energy-dependent than the counterparts in neutral atom photoionization [9].

It has also been found that confinement resonances in the photoionization of endohedral atoms induce rather significant resonances in the attosecond time delay of photoelectron emission [11], which suggests that time-domain spectroscopy might be efficacious in studying endohedral systems and clusters. And in high-Z atoms, it was found that spin-orbit induced confinement resonances [12] also induce rather significant structures in the Wigner time delay, in the vicinity of these induced resonances, another domain that is ripe for experimental investigations. Also, a study of the angular-dependence of Wigner time delay has been performed on the 4d subshell of $Xe@C_{60}$ and various new phenomena have been uncovered including a new kind of Cooper-like minima in certain of the photoionization channels which can lead to huge time delays and great sensitivity to the details of the confinement [13]; confined Xe 4d was chosen because its cross section has already been studied experimentally [14], thereby suggesting the possibility of experimental study of the Wigner time delay of $Xe@C_{60}$.

Investigation of confined atoms is a rapidly growing field. Theoretical investigations of various atoms endohedrally confined in C_{60} [15,16] abound, but experimental studies are sparse [14]. Our theoretical program is aimed at mapping out the properties of such systems, especially photoionization, to guide experiment and uncover new phenomena. Among our major results, we have found that a huge transfer of oscillator strength from the C_{60} shell, in the neighborhood of the giant plasmon resonance, to the encapsulated atom for both $Ar@C_{60}$ [17] and $Mg@C_{60}$ [18]. And confinement resonances [19], oscillations in the photoionization cross section of an endohedral atom due to interferences of the photoelectron wave function for direct emission with those scattered from the surrounding carbon shell, were predicted in a broad range of cases; and their existence has been confirmed experimentally [14]. Further, in the photoionization of endohedral atoms within nested fullerenes, as a result of the multi-walled confinement, the confinement resonances become considerably more complicated [20]. In addition, spin-orbit induced confinement resonances in photoionization have been found owing to interchannel coupling between inner-shell spin-orbit split channels in high-Z endohedral atoms [12], an effect which occurs solely owing to relativistic interactions. We have also explored the interatomic Coulomb decay (ICD) phenomenon in confined atoms and found, owing to hibridization between atomic and shell orbitals, that ICD occurs both ways, from atom to shell and shell to atom, and the rates (widths) are often much larger than the ordinary Auger rates [11-14]; the widths of these resonances makes them excellent candidates for experimental study of endohedral atoms.

Future Plans

We will continue investigating attosecond time delay in photoemission that has been found in various experiments, including a focus on how electron-electron correlation effects become important in the vicinity of inner-shell thresholds (interchannel coupling), particularly in negative-ion photodetachment, and we will work to further our understanding of how confinement might affects Wigner time delay. To provide a "road map" for experimental investigations at various synchrotron facilities, we will perform exploratory calculations of atomic photoionization at high energies (tens of keV) to predict where many-body interactions alter the simple behavior of cross sections that is the present conventional wisdom; preliminary indications are that this can be very significant ph. In addition, the search for cases where nondipole effects are important, as a guide for experiment, and quadrupole Cooper minima, will continue. In the area of confined atoms, expand on our studies of interatomic Coulomb decay (ICD) of resonances. We will also work on ways to enhance the time-dependent local-density approximation to make it more accurate in our calculations of confined atoms. In addition, we shall work towards upgrading our theory to include relativistic interactions to be able to deal with heavy endohedrals with quantitative accuracy. In addition, we shall focus upon calculations taking into account the full molecular symmetry of free and endohedral C_{60} to understand the limits of utility of simple potential models representing the C_{60} cage, and to deal with off-center endohedral confinement in a realistic manner. And we shall respond to new experimental capabilities as they are developed and new experimental results as they come up.

Peer-Reviewed Publications Resulting from this Project (2016-2018)

- "Coherence of Auger and inter-Coulombic decay processes in the photoionization of Ar@C_{60} versus Kr@C_{60}," M. Magrakvelidze, R. De, M. H. Javani, M. E. Madjet, S. T. Manson, and H. S. Chakraborty, Eur. Phys. J. D **70**, 96-1-7 (2016).
- "Correlation Study of Endohedrally Confined Alkali Earth Atoms (A@C_{60})," M. F. Hasoğlu, H.-L. Zhou, and S. T. Manson, Phys. Rev. A **93**, 022512-1-5 (2016).
- "First prediction of inter-Coulombic decay of C_{60} inner vacancies through the continuum of confined atoms," R. De, M. Magrakvelidze, M. E. Madjet, S. T. Manson and H. S. Chakraborty, J. Phys. B **49**, 11LT01-1-5 (2016).

- "Relativistic calculations of angular dependent photoemission time delay," A. Kheifets, A. Mandal, P. C. Deshmukh, V. K. Dolmatov, D. A. Keating and S. T. Manson, Phys. Rev. A **94**, 013423-1-7 (2016).
- "Wigner photoemission time delays from endohedral anions," A. Kumar, H. R. Varma, P. C. Deshmukh, S. T. Manson, V. K. Dolmatov and A. S. Kheifets, Phys. Rev. A **94**, 043401-1-9 (2016).
- "Wigner time delay and spin-orbit-activated confinement resonances," D. A. Keating, P. C. Deshmukh and S. T. Manson, J. Phys. B **50**, 175001-1-9 (2017).
- "Photoionization of atomic barium subshells in the 4*d* threshold region using the relativistic multi-configuration Tamm-Dancoff approximation," A. Ganesan, P. C. Deshmukh, and S. T. Manson, Phys. Rev. A **95**, 033417-1-8 (2017).
- "Wigner-Eisenbud-Smith photoionization time delay due to autoionization resonances," Pranawa C. Deshmukh, Ashish Kumar, Hari R. Varma, Sourav Banerjee, Steven T. Manson, Valeriy K. Dolmatov and Anatoli Kheifets, J. Phys. B **51**, 065108-1-8 (2018).
- "Angle resolved Wigner time delay in atomic photoionization: the 4d subshell of free and confined Xe," A. Mandal, P. C. Deshmukh, A. S. Kheifets, V. K. Dolmatov and S. T. Manson, Phys. Rev. A **96**, 053407-1-9 (2017).
- "Intershell-correlation-induced time delay in atomic photoionization," D. A. Keating, S. T. Manson, V. K. Dolmatov, A. Mandal, P. C. Deshmukh, Faiza Naseem and A. S. Kheifets, Phys. Rev. A **98**, 013420-1-10 (2018).
- "Interference in electron-molecule elastic scattering," A. S. Baltenkov, S. T. Manson and A. Z. Msezane, J. Phys. B, in press (2018).

References

[1] E. P. Wigner, Phys. Rev. **98**, 145 (1955).
[2] R. Pazourek, S. Nagele and J. Burgdörfer, Rev. Mod. Phys. **87**, 765 (2015) and references therein.
[3] S. Saha, A. Mandal, J. Jose, H. R. Varma, P. C. Deshmukh, A. S. Kheifets, V. K. Dolmatov and S. T. Manson, Phys. Rev. A **90**, 053406 (2014).
[4] V. K. Dolmatov, A. S. Kheifets, P. C. Deshmukh and S. T. Manson, Phys. Rev. A **91**, 053415 (2015).
[5] A. S. Kheifets, S. Saha, P. C. Deshmukh, D. A. Keating, and S. T. Manson, Phys. Rev. A **92**, 063422 (2015).
[6] A. Kheifets, A. Mandal, P. C. Deshmukh, V. K. Dolmatov, D. A. Keating and S. T. Manson, Phys. Rev. A **94**, 013423 (2016).
[7] P. C. Deshmukh, A. Kumar, H. R. Varma, S. Banerjee, S. T. Manson, V. K. Dolmatov and A. Kheifets, J. Phys. B **51**, 065108 (2018).
[8] U. Fano, Phys. Rev. **124**, 1866 (1961).
[9] D. A. Keating, S. T. Manson, V. K. Dolmatov, A. Mandal, P. C. Deshmukh, F. Naseem and A. S. Kheifets, Phys. Rev. A **98**, 013420 (2018).
[10] S. Saha, A. Mandal, P. C. Deshmukh. V. K. Dolmatov, A. Kheifets and S. T. Manson, Bull. Am. Phys. Soc. **63**(5), 190 (2018).
[11] P. C. Deshmukh, A. Mandal, S. Saha, A. S. Kheifets, V. K. Dolmatov and S T Manson, Phys. Rev. A **89**, 053424 (2014).
[12] D. A. Keating, P. C. Deshmukh and S. T. Manson, J. Phys. B **50**, 175001-1-9 (2017).
[13] A. Mandal, P. C. Deshmukh, A. S. Kheifets, V. K. Dolmatov and S. T. Manson, Phys. Rev. A **96**, 053407 (2017).
[14] R. A. Phaneuf, A. L. D. Kilcoyne, N. B. Aryal, K. K. Baral, D. A. Esteves-Macaluso, C. M. Thomas, J. Hellhund, R. Lomsadze, T. W. Gorczyca, C. P. Ballance, S. T. Manson, M. F. Hasoglu, S. Schippers, and A. Müller, Phys. Rev. A **88**, 053402-1-7 (2013) and references therein
[15] V. K. Dolmatov, A. S. Baltenkov, J.-P. Connerade and S. T. Manson, Radiation Phys. Chem. **70**, 417 (2004) and references therein.
[16] V. K. Dolmatov, Advances in Quantum Chemistry, **58**, 13 (2009) and references therein.
[17] M. E. Madjet, H. S. Chakraborty and S. T. Manson, Phys. Rev. Letters **99**, 243003 (2007).
[18] M. E. Madjet, H. S. Chakraborty, J. M. Rost and S. T. Manson, Phys. Rev. A **78**, 013201 (2008).
[19] V. K. Dolmatov and S. T. Manson, J. Phys. B **41**, 165001 (2008).
[20] V. K. Dolmatov and S. T. Manson, J. Phys. Rev. A **78**, 013415 (2008).
[21] R. De, M. Magrakvelidze, M. E. Madjet, S. T. Manson and H. S. Chakraborty, J. Phys. B **49**, 11LT01 (2016) and references therein.

ELECTRON/PHOTON INTERACTIONS WITH ATOMS/IONS

Alfred Z. Msezane (email: amsezane@cau.edu)

Clark Atlanta University, Department of Physics and CTSPS, Atlanta, Georgia 30314

PROJECT SCOPE

The project's primary objective is to gain a fundamental understanding of the near-threshold electron attachment mechanism in low energy electron elastic scattering from complex heavy systems through the calculation of integral and differential cross sections. The complex angular momentum (CAM) methodology, wherein is fully embedded the crucial electron-electron correlations and the core polarization interaction, is used for the investigations. Regge trajectories allow us to probe electron attachment at the fundamental level near threshold, thereby uncovering new manifestations, including the mechanism of nanocatalysis, and determine reliable electron affinities (EAs). The recently revealed characteristic correlation and polarization induced dramatically sharp resonances manifesting long-lived metastable negative ion formation in fullerenes are explored. These are important in nanocatalysis, organic solar cells and chemical sensor technology. The time-dependent-density-functional theory is utilized to investigate the photoabsorption spectra of encapsulated atoms, focusing on the confinement resonances. Standard codes are used to generate sophisticated wave functions for investigating CI mixing and relativistic effects in atomic ions. The wave functions are also used to explore correlation effects in dipole and non-dipole studies as well as in R-matrix calculations of photoionization of inner-shell Cl.

RECENT PROGRESS

Recently, a theoretical breakthrough was achieved in low-energy electron scattering from complex heavy systems through our robust Regge pole methodology. Entirely new in the field of electron-cluster/fullerene collisions, the Regge pole methodology was benchmarked on the measured electron affinities of the C_{60} and C_{70}. Consequently, the current report focuses mainly on the unprecedented accomplishments of the Regge pole methodology in the investigation of negative ion formation in low-energy electron elastic scattering from complex heavy systems such as fullerene molecules and actinide atoms. From the sharp peaks in the calculated electron cross sections, the anionic binding energies (BEs) are extracted; for ground state scattering these BEs yield the theoretically challenging to calculate EAs. This theoretical feat has never been accomplished before and the Regge pole methodology requires no assistance whatsoever from either experiment or other theory to achieve the impressive presented results.

OVERVIEW

One of the most challenging problems in atomic and molecular physics, when exploring negative ion formation in complex heavy systems and to date still continues to plague both experiments and theory, is the determination of accurate and reliable values of the important electron affinity (EA) of the relevant atoms and molecules. Accurate and reliable atomic and molecular affinities are essential for understanding chemical reactions involving negative ions, whose importance and vast utility in terrestrial and stellar atmospheres as well as in device fabrication, drug delivery and organic solar cells are well-documented. In the lanthanide and actinide atoms the presence of two or more open d- and f- subshell electrons results in enormous numbers of complicated and diverse electron configurations that characterize low-energy electron interactions in these systems. These present formidable computational complexity when using conventional theoretical methods that renders obtaining accurate and reliable EAs very difficult, if not impossible. Thus the published literature abounds in incorrect EAs for the lanthanide and actinide atoms. These reflect the difficulties in the theoretical understanding of the fundamental mechanism responsible for low-energy electron attachment in these systems leading to stable negative ion formation. The following are our accomplishments during the period covered by this report.

Negative ion formation in fullerenes and complex heavy atoms

Regge poles are generalized bound states. Our robust Regge pole methodology is used to investigate negative ion formation in low-energy electron elastic scattering from the fullerenes C_n (n=24, 28, 44, 60, 70, 74, 82, 94, 100 and 140) and the lanthanide (Gd and Dy) and actinide (Pa and U) atoms through the elastic total cross sections (TCSs) calculations. All the TCSs are found to be characterized by Ramsauer-Townsend (R-T) minima, shape resonances and dramatically sharp resonances manifesting stable ground and metastable negative ion formation during the collisions. Our ground states anionic binding energies (BEs) for C_n^- (n=24, 28, 44, 60, 70, 82) match excellently the measured EAs. The thus benchmarked Regge pole methodology on the ground states anionic BEs for these fullerenes, is then used to calculate the ground and the metastable elastic TCSs for the fullerenes and the heavy atoms wherefrom their anionic BEs are extracted and compared with the measured EAs where they are available.

Surprisingly, the C_{74} fullerene has the largest anionic ground state BE value among the investigated fullerenes in this paper and the ground state of the C_{140}^- anion has a large BE as well. Many of these fullerenes could be useful in nanocatalysis, sensor technology and organic solar cells through their ground and metastable anionic BEs. For the heavy atoms the extracted ground and metastable anionic BEs are compared with the measured and calculated EAs. These results particularly the ground states anionic BEs of the fullerenes and the complex atoms are expected to inspire and guide the long overdue experimental and theoretical explorations of electron attachment in low-energy electron scattering in these and related systems. Notably, conventional theoretical calculations are still struggling to go beyond the simple C_{60}.

Low-energy electron scattering from atomic Th, Pa, U, Np and Pu: Negative ion formation

Here we investigate ground and metastable negative ion formation in low-energy electron collisions with the actinide atoms Th, Pa, U, Np and Pu through the elastic total cross sections (TCSs) calculations. For these atoms, the presence of two or more open d- and f- subshell electrons presents a formidable computational task for conventional theoretical methods, making it difficult to interpret the calculated results. Our robust Regge pole methodology which embeds the crucial electron correlations and the vital core-polarization interaction is used for the calculations. These are the major physical effects mostly responsible for stable negative ion formation in low-energy electron scattering from complex heavy systems. We find that the TCSs are characterized generally by R-T minima, shape resonances and dramatically sharp resonances manifesting ground and metastable negative ion formation during the collisions. The extracted from the ground states TCSs anionic binding energies (BEs) are found to be 3.09 eV, 2.98 eV, 3.03 eV, 3.06 eV and 3.25 eV for Th, Pa, U, Np and Pu, respectively. Interestingly, an additional polarization-induced metastable TCS with anionic BE value of 1.22 eV is created in Pu due to the size effect. We also found that our excited states anionic BEs for several of these atoms compare well with the existing theoretical electron affinities including those calculated using the relativistic configuration-interaction method. We conclude that the existing theoretical calculations tend to identify incorrectly the BEs of the resultant excited anionic states with the EAs of the investigated actinide atoms. This has led to the proliferation of incorrect EAs for complex heavy systems in the published literature, suggesting a need for an unambiguous definition of the EA.

Novel mechanism for creating long-lived metastable atomic negative ions

A novel mechanism is proposed for creating long-lived metastable atomic negative ions in complex atoms, such as the lanthanides. It exploits the orbital collapse of the 5d orbital in Gd (Z= 64) into the 4f orbital of Tb (Z= 65). In the region of collapse the properties of the 5d and 4f orbitals are quite sensitive to the changes in the effective potential. Consequently the collapse phenomenon impacts the core-polarization interaction significantly in the relevant atom, namely Tb inducing a new excited Tb^- anion. The mechanism is demonstrated in the lanthanide atoms Tb and Dy through the appearance of long-lived Tb^- and Dy^- anions in the Regge pole calculated electron elastic total cross sections. Ground and long-lived metastable negative ion formation occurs at the second Ramsauer -Townsend minima. More recently, the effect of the orbital collapse mechanism impacting the polarization interaction has been realized in the actinide atoms Th and Pa. This has been used to understand the significant difference in the metastable and excited anionic BEs in Th and Pa. For instance, the 6d orbital collapse to the 5f when transitioning from Th ($5f^06d^27s^2$) to Pa ($5f^26d^17s^2$) impacts the polarization interaction reducing the anionic BE value of the first excited state of Th from 0.549 to 0.395 eV in Pa. This value of 0.395 eV is further reduced to 0.220 eV in U ($5f^36d^17s^2$) since the effect of the 6d orbital collapse lingers on through U as was discussed for the lanthanide atoms.

The Regge pole methodology, benchmarked on the measured EAs of C_{60}, C_{70}, C_{76}, C_{82} and C_{92} through their ground states anionic BEs obtained from the calculated electron elastic TCSs, has also been used to explore polarization-induced long-lived metastable negative ion formation in these fullerenes. Indeed, the calculated TCSs for these fullerenes have been found to behave very much like those of their corresponding ground states. Namely, they are characterized generally by R-T minima, shape resonances and dramatically sharp resonances manifesting long-lived metastable negative ion formation at 1.86 eV, 1.77 eV, 2.20 eV, 1.72 eV and 2.35 eV for C_{60}^-, C_{70}^-, C_{76}^-, C_{82}^- and C_{92}^-, respectively. The polarization-induced TCSs with their metastable anionic BEs given above and located at their second R-T minima close to those of their respective ground states, demonstrate the importance of identifying and delineating the resonance structures in low-energy electron scattering from fullerenes.

Conundrum in Measured Electron Affinities of Complex Heavy Atoms

Low-energy electron scattering from the lanthanide atoms Eu, Tb, Tm, Gd, and Nd including Nb has been investigated through calculated electron elastic total cross sections using our robust Regge-pole methodology. The extracted binding energies of the resultant ground and metastable anions formed during the collisions have been contrasted with the measured electron affinities. It has been concluded that the measured EAs for these atoms require reinterpretation and new recommended values have been presented. Indeed, calculated electron affinities of atoms and molecules provide a stringent test of theoretical methods when the results are compared with those from reliable measurements. And our revolutionary Regge pole methodology will certainly provide reliable and definitive EAs for complex heavy systems without the experimental and/or other theoretical assistance.

FUTURE PLANS

We continue with the theoretical investigations of negative ion formation in low-energy electron scattering from complex heavy systems, such as the actinide and lanthanide atoms, including fullerene molecules. The main objective is to determine accurate and reliable anionic BEs for the resultant anions formed during the collisions, particularly those of the ground states since they yield the desired EAs. The resultant resonance structures in the characteristic TCSs, unique to each complex heavy system, provide an important signature for each system that can be used for their detection and/or functionalization in nanocatalysis, chemical sensors and organic solar cell materials. Notably, once the anionic ground, metastable and excited states of the complex heavy systems have been determined reliably as has been accomplished using our robust Regge pole methodology, then sophisticated elaborate CI wave functions can be generated using standard structure types methods, suitable in R-matrix calculations.

Our TCSs for the actinide atoms Th, Pa, U, Np and Pu, rich in ground, metastable and excited states negative ion formation, yield the anionic ground states BE values of 3.09 eV, 2.98 eV, 3.03 eV, 3.06 eV and 3.25 eV for Th, Pa, U, Np and Pu, respectively. These should be considered as the EAs of the investigated actinide atoms and suggest the use of low-energy electron scattering for determining unambiguously the EAs of complex heavy systems such as the actinide atoms. Our immediate objective is to similarly investigate negative ion formation in the remaining actinide atoms and extract their EAs.

Additionally, the exploration of negative ion formation in low-energy electron scattering from complex heavy atoms and empty fullerene molecules is expected to lead to a better understanding and interpretation of the resonance structures observed in electron scattering and photoionization cross sections of the endohedral $A@C_n$ (C_n = fullerene molecule) systems. Photoabsorption of endohedral fullerenes, strongly correlated systems and atomic structure energy levels are currently being investigated. Sophisticated and elaborate wave functions will be constructed for fullerenes for use in R-matrix calculations. New accurate and reliable EAs for complex heavy systems such as large fullerenes will be obtained and nanocatalysts for various chemical reactions will be investigated and identified as well.

PEER-REVIEWED PUBLICATIONS RESULTING FROM THIS PROJECT (2016-2018)

1. “Simple method to calculate binding energies of fullerene negative ions”, Z. Felfli and A.Z. Msezane, Euro Phys. J. D **72**, 78 (2018)
2. “Low-energy electron scattering from fullerenes and heavy complex atoms: Negative ions formation”, Alfred Z. Msezane and Zineb Felfli, Euro Phys. J. D, At Press (2018)
3. “Conundrum in Measured Electron Affinities of Complex Heavy Atoms”, Zineb Felfli and Alfred Z. Msezane, Journal of Atomic, Molecular, Condensate & Nano Physics**,** Vol. 5, No. 2, pp. 1–8 (2018). DOI: 10.26713/jamcnp.v5i2.1093
4. “New insights in low-energy electron-fullerene interactions”, A.Z. Msezane and Z. Felfli, Chem. Phys. **503**, 50 (2018)
5. “Universal Behavior of Quantum Spin Liquid and Optical Conductivity in the Insulator Herbertsmithite”, V. R. Shaginyan, A. Z. Msezane, V. A. Stephanovich, K. G. Popov, G. S. Japaridze, J Low Temp Phys **191**:4–13 (2018)
6. “Asymmetric Tunneling Conductance and the non-Fermi Liquid Behavior of Strongly Correlated Fermi Systems”, V.R. Shaginyan, A. Z. Msezane, G. S. Japaridze, V.A. Stephanovich, Y. S. Leevik, ISSN 0021-3640, JETP Letters (2018). doi.org/10.1134/S0021364018170010
7. “New State of Matter: Heavy Fermion Systems, Quantum Spin Liquids, Quasicrystals, Cold Gases, and High-Temperature Superconductors”, V. R. Shaginyan, V. A. Stephanovich, A. Z. Msezane, P. Schuck, J. W. Clark, M. Ya. Amusia, G. S. Japaridze, K. G. Popov, and E. V. Kirichenko, J. Low Temp. Phys.; DOI: 10.1007/s10909-017-1801-3 (2017)
8. “The influence of topological phase transition on the superfluid density of overdoped copper oxides”, Vasily R. Shaginyan, Vladimir A. Stephanovich, Alfred Z Msezane, George Japaridze and Konstantin Popov, Phys. Chem. Chem. Phys**. 19,** 21964 (2017)
9. “Huygens-Fresnel picture for electron-molecule elastic scattering”, Arkadiy S. Baltenkov and Alfred Z. Msezane, Eur. Phys. J. D **71**, 305 (2017)
10. “ANIONIC FORMATION IN LOW-ENERGY ELECTRON SCATTERING FROM LARGE FULLERENES: THEIR MULTIPLE FUNCTIONALIZATION”, Msezane A. Z, Felfli Z, Shaginyan V. and Amusia M. Ya., International Journal of Current Advanced Research **6**(12) 8503-8509 (2017)
11. “Scaling behavior of the thermopower of the archetypal heavy-fermion metal YbRh2Si2,” V. R. Shaginyan, A.Z. Msezane, G.S. Japaridze, K.G. Popov and V.A. Khodel, Front. Phys. **11**, 117101 (2016).
12. “Strongly correlated Fermi systems as a new state of matter,” V. R. Shaginyan, A. Z. Msezane, G. S. Japaridze, K. G. Popov, and V. A. Khodel, Front. Phys. **11**(5), 117103 (2016).
13. “Electronic Quantum Confinement in Cylindrical Potential Well,” A. S. Baltenkov and A. Z. Msezane, Euro Phys. J. D **70**, 81 (2016).
14. “Interference in electron-molecule elastic scattering", Arkadiy Baltenkov; Steven Manson; Alfred Z Msezane, J. Phys. B, At Press (2018).

Theory and Simulation of Nonlinear X-ray Spectroscopy of Molecules

Shaul Mukamel
University of California, Irvine, CA 92697
smukamel@uci.edu
Progress Report August 2018
DOE DE-FG02-04ER15571

Program Scope

Nonlinear X-ray spectroscopy experiments which use sequences of coherent broadband X-ray pulses are made possible by new ultrafast X-ray free electron laser (XFEL) and high harmonic generation (HHG) sources. These techniques provide unique windows into the motions of electrons and nuclei in molecules and materials and offer novel probes for electron and energy transfer in molecular complexes. This program is aimed at the design of X-ray pulse sequences for probing core and valence electronic excitations, and the development of effective simulation protocols for describing multiple-core excited state energetics and dynamics. Applications are made to time-resolved photoelectron spectroscopy, and detecting strongly coupled electron-nuclear dynamics in molecules through electronic coherence observed in multidimensional broadband stimulated X-ray Raman signals.

Recent Progress

Direct imaging of ultrafast electron dynamics by X-Ray sum frequency generation. X-ray diffraction from molecules in the ground state produces an image of their charge density, and time-resolved X-ray diffraction can thus monitor the motion of the nuclei. However, it is hard to monitor the density change of excited valence electrons upon optical excitation with regular diffraction techniques due to the overwhelming background contribution of the core electrons. We proposed a nonlinear X-ray technique which provides a spatial electron density image of valence electron excitations. The technique, sum frequency generation carried out with a visible pump and a broadband X-ray diffraction pulse (Fig 1), yields snapshots of the *transition charge densities*, which represent the electron density variations upon optical excitation. The technique was illustrated by ab initio simulations of transition charge density imaging of the optically induced electronic dynamics in a donor/acceptor substituted stilbene. Simulations were further carried out for formyl fluoride, which is nonchiral in the ground state and evolves into a chiral nonplanar structure in the first excited state upon excitation by a circularly polarized UV pump. A coherently controlled elliptically polarized pump is used to prepare the molecule in a selected enantiomer and the chiral interconversion dynamics is then monitored by the probe diffraction. The simulations are presented in Fig 2.

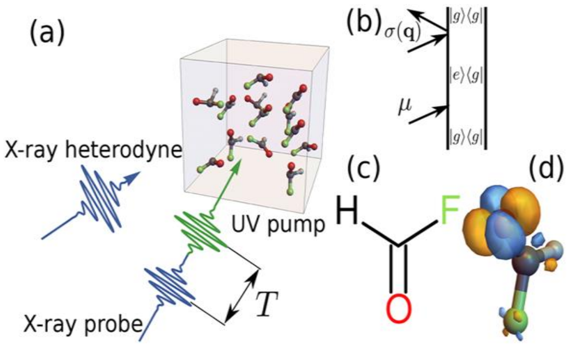

***Figure 1**. (a) SFG experimental setup. Excited-state dynamics is launched by a UV pump pulse, and after a delay T, an X-ray pulse is diffracted by an ensemble of randomly oriented molecules. (b) Diagram representing the stimulated SFG signal, (c) Lewis structure of formyl fluoride. (d) Transition charge density between the ground and first excited states for the planar configuration.*

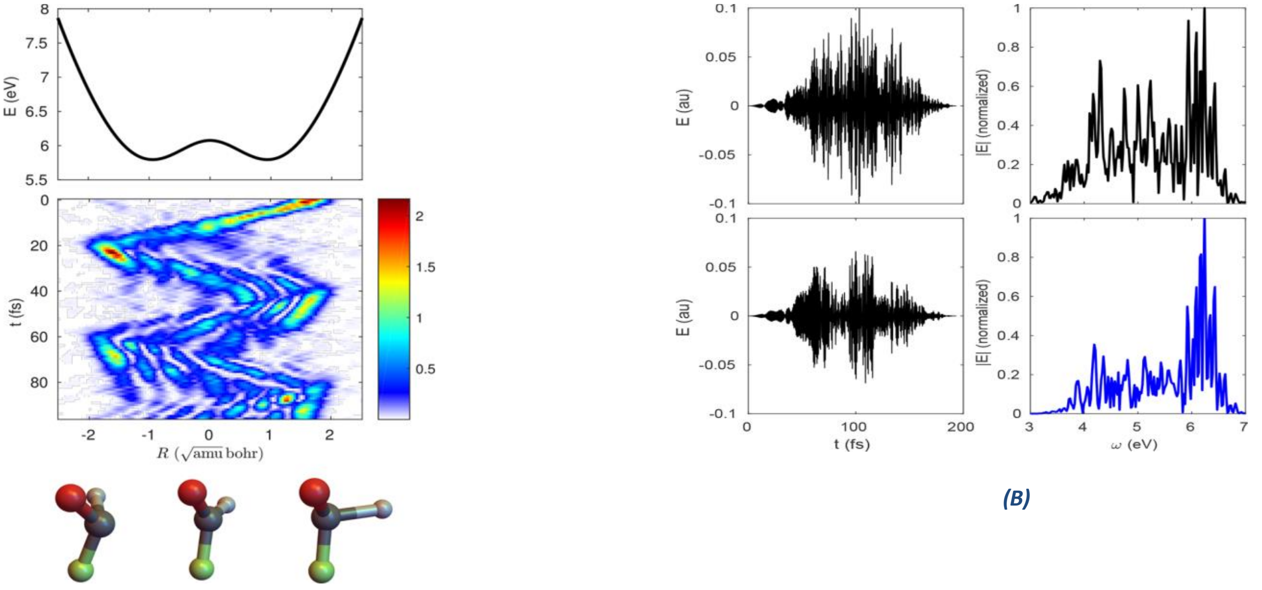

(B)

(A)

Figure 2 (A) *Enantiomeric interconversion dynamics in formyl fluoride after interaction with an elliptically polarized shaped pump pulse that selects a single enantiomer. R is the out-of-plane bending nuclear coordinates of the molecule. Upper panel: first excited-state potential. Lower panel: time evolution of the nuclear wave packet in the electronic excited state* $(|\Psi e(t)|2)$ *following the pump pulse excitation. The molecular configurations corresponding to the normal coordinates are shown at the bottom.* ***(B)*** *Components of the elliptical polarized coherently controlled pump field that create the localized wave packet. The left column shows the electric fields in the time domain, and the right column shows the electric fields in the frequency domain. The upper and lower rows are the x and the y components, respectively.*

A phase cycling real-time time-dependent density functional theory (RT-TDDFT) simulation protocol was developed for nonlinear XUV and X-ray Molecular Spectroscopy. The technique provides a practical algorithm for propagating a many-electron system driven by external laser fields. The fields are included nonperturbatively in the propagation, and the molecular reduced single-electron density operator and various spectroscopic and diffraction signals can be computed directly, avoiding the expensive calculation of many-body states. Nonlinear optical signals contain contributions of multiple pathways. A phase cycling protocol was implemented in order to separate these pathways. Simulations of XUV four-wave mixing signals in the CO molecule (Fig 3) agree with exact, much more expensive, ab initio sum-over-states calculations.

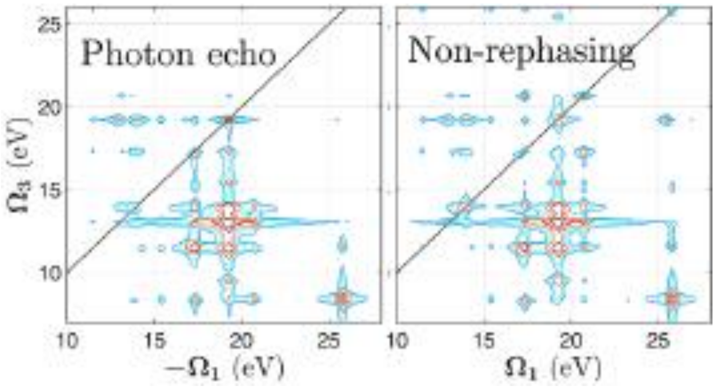

Figure 3: *RT-TDDFT four-wave mixing signals of CO*

Another application was made to attosecond X-ray diffraction triggered by core or valence ionization. We employed the RT-TDDFT method to simulate the electronic dynamics after an impulse core or valence ionization in the glycine−phenylalanine (GF) dipeptide. The time-evolving dipole moment, the charge density, and the time-resolved X-ray diffraction signals were calculated. The charge oscillation is calculated for 7 fs for valence ionization and 500 as for core ionization is slightly longer than that found in a phenylalanine monomer (4 fs) because of the elongated glycine chain. Following valence ionization, the charge migration is mediated by the delocalized lone-pair orbitals of oxygen and nitrogen of the electron-rich amide group. The temporal Fourier transform of the dipole moment provides detailed information on the charge migration dynamics and the molecular orbitals involved. Simulation techniques for coherent multidimensional spectroscopy of nonadiabatic molecular processes at conical intersections, spanning the infrared to the x-ray regime were developed.

Future Plans

So far, our simulations of signatures of conical intersections in x-ray diffraction and nonlinear spectroscopy involved exact calculations of nonadiabatic dynamics treating the nuclei on a numerical grid. These were limited to small model systems with 2 nuclear degrees of freedom. We plan to develop approximate, less expensive, protocols that could be applied to larger molecules and include the coupling to bath degrees of freedom. By including additional nuclear coordinates, our approach may be used to predict signatures of conical intersections in polyatomic molecules. The ring opening reaction of cyclohexadiene (CHD) will be used as test case. Photoelectron based techniques, such as time resolved photoelectron spectroscopy with streaking will be calculated.

Experimental signals based on electronic coherence will be used to test the validity of existing simulation protocols for nonadiabatic dynamics such as surface hopping. More elaborate sequences of stimulated Raman pulses will be studied. X-ray signals will be calculated using a quantum description of the field and photon counting and coincidence protocols will be studied.

We will explore new families of signals that provide structural information on chirality. The SFG X-ray diffraction signal can monitor time-evolving transition charge densities in oriented samples. Diffraction of circularly polarized pulses will be considered. We will examine Raman optical activity signals in the X-ray regime by calculating the diffraction intensity difference between a left and right polarized X-ray pulse.

Peer-Reviewed Publications Resulting from the Project (2016-2018)

1. *Pump-probe spectroscopy using quantum light with two-photon coincidence detection",Frank Schlawin, Konstantin E. Dorfman, and Shaul Mukamel. Physical Review A. 93, 023807 (2016)*
2. *"Time-and-frequency gated photon coincidence counting; a novel multidimensional spectroscopy tool", K. E. Dorfman and S. Mukamel. Phys. Scr.. 91, 083004 (2016)*
3. *"Multidimensional Resonant Nonlinear Spectroscopy with Coherent Broadband X-ray Pulses", K. Bennett, Y. Zhang, M. Kowalewski, W. Hua, and S. Mukamel. 2016 Phys. Scr. 91 083004 doi:10.1088/0031-8949/91/8/083004*
4. *"Non-local real space analysis of chiral optical signals ", J. Rouxel, V. Y. Chernyak, and S. Mukamel. Chem. Sci., 2016, Advance Article DOI: 10.1039/C6SC01743F*
5. *"Study of double core hole excitations in molecules by X-ray double-quantum coherence signals: a multi-configurational simulation", W. Hua, K. Bennett, Y. Zhang, Y. Luo, and S. Mukamel. Chemical Science, 2016, DOI: 10.1039/C6SC01571A*
6. *" Monitoring conical intersections in the ring opening of furan by Attosecond Stimulated X-ray Raman Spectroscopy", W. Hua , S. Oesterling , J. Biggs , Y. Zhang , H. Ando , R. De Vivie-Riedle , B. Fingerhut, S. Mukamel. Structural Dynamics. 3, 023601 (2016)*
7. *"Multiple decay mechanisms and 2D-UV spectroscopic fingerprints of singlet excited solvated adenine-uracil monophosphate", Q. Li, A. Giussani, J. Segarra-Martí, A. Nenov, I. Rivalta, A. A. Voityuk, S. Mukamel, D. Roca-Sanjuán, M. Garavelli and L. Blancafort, Chem EurJ. (2016) DOI: 10.1002/chem.201505086*
8. *"Two-dimensional infrared spectroscopy of vibrational polaritons of molecules in an optical cavity", JCP, 144,*

124115 (2016)

9. *"Wigner-Lindbald equations for quantum friction", D. I. Bondar, R. Cabrera, A. Campos, S. Mukamel, and H. Rabitz. JPC Letters, 7, 1632-1637 (2016)*
10. *"Tunabale photonic cavity coupled to voltage-biased double quantum dot system: Diagrammatic NEGF approach", B. Kumar Agarwalla, M. Kulkarni, S. Mukamel, and D. Segal. Mesoscale and Nanoscale Physics-Cond-mat-mes-hall (2016) http://arxiv.org/abs/1604.01811*
11. *"Cavity femtochemistry; Manipulating nonadiabatic dynamics at avoided crossings", M. Kowalewski, K. Bennett, and S. Mukamel. J. Phys. Chem. Lett ,2016, 7, 2050-2054*
12. *"Novel Photochemistry of Molecular Polaritons in Optical Cavities", K. Bennett, M. Kowalewski, and S. Mukamel. Faraday Discussions, 2016, DOI: 10.1039/*
13. *"Monitoring nonadiabatic electron-nuclear dynamics in molecules by attosecond streaking of photoelectrons", M. Kowalewski, K. Bennett, J. Rouxel, and S. Mukamel. Phys. Rev. Lett. 117, 043201 (2016)*
14. *"Current vs charge density contributions to nonlinear x-ray spectroscopy", J. Rouxel, M. Kowalewski, and S. Mukamel* J. Chem. Theory Comput.*, 2016, DOI: 10.1021/acs.jctc.6b00279*
15. *"Photoinduced molecular chirality probed by ultrafast resonant X-ray spectroscopy". J. R. Rouxel, M. Kowalewski, and S. Mukamel. Structural Dynamics. 4, 044006 (2017)*
16. *"Manipulating Impulsive Stimulated Raman Spectroscopy With a Chirped Probe Pulse" Monacelli, L; Batignani, G; Fumero, G; Ferrante, C; Mukamel, S; Scopigno, T. Journal of Physical Chemistry Letters, 8, 966-974 (2017)*
17. *"Monitoring Nonadiabatic Avoided Crossing Dynamics in Molecules by Ultrafast X-Ray Diffraction", M. Kowalewski, K. Bennett, and S. Mukamel. Structural Dynamics, 4, 054101 (2017)*
18. *Comment on "Self-Referenced Coherent Diffraction X-ray Movie of Angstrom-and Femtosecond-Scale Atomic Motion", K. Bennett, M. Kowalewski, and S. Mukamel. PRL, 119, 069301(2017)*
19. *"Discriminating Cascading Processes in Nonlinear Optics; A QED Analysis Based on Their Molecular and Geometric Origin", Kochise Bennett, Vladimir Y. Chernyak, and Shaul Mukamel. PRA, 95, 033840 (2017)*
20. *"X-ray Circular Dichroism Signals: A Unique Probe of Local Molecular Chirality", Y. Zhang, J. R. Rouxel, J. Autschbach, N. Govind and S. Mukamel. Chemical Science, 2017, DOI: 10.1039/C7SC01347G*
21. *"Using Coherence to Enhance Function in Chemical and Biophysical Systems", G. D. Scholes, G. R. Fleming, L. X. Chen, A. Aspuru-Guzik, A. Buchleitner, D. F. Coker, G. S. Engel, R. van Grondelle, A. Ishizaki, D. M. Jonas, J. S. Lundeen, J. K. McCusker, S. Mukamel et al. Nature (2017). DOI 10.1038/nature21425*
22. *"Simulating Coherent Multidimensional Spectroscopy of Nonadiabatic Molecular Processes; from the Infrared to the X-ray Regime", M. Kowalewski, B. Fingerhut, K. Dorfman, K. Bennett and S. Mukamel. Chem. Rev., 2017. DOI: 10.1021/acs.chemrev.7b00081*
23. *"Linear and nonlinear frequency- and time-domain spectroscopy with multiple frequency combs", K. Bennett, J. Rouxel, and S. Mukamel. JCP, 147, 094304 (2017)*
24. *"Utilizing Microcavities to Suppress Third-Order Cascades in Fifth-Order Raman Spectra", Zhang, Z; Bennett, K; Chernyak, V; Mukamel, S. Journal of Physical Chemistry Letters (2017), DOI: 10.1021/acs.jpclett.7b01129*
25. *"Translational and rotational averaging of nonlocal response tensors for nano-shaped light", J. R. Rouxel, V. Y. Chernyak, and S. Mukamel. Journal of Physics B, 51, 034004 (2018)*
26. *"Multidimensional Nonlinear X-ray Spectroscopy of Molecules", Shaul Mukamel. J. Phys. B: At. Mol. Opt. Phys. 51 (2018) 032003 Roadmap of Ultrafast X-ray Atomic and Molecular Physics, Linda Young, Editor.*
27. *"X-Ray sum frequency generation; direct imaging of ultrafast electron dynamics", J. R. Rouxel, M. Kowalewski, K. Bennett, S. Mukamel. Phys. Rev. Lett. (2018) DOI: 10.1103/PhysRevLett.120.243902*
28. *"Attosecond X-ray diffraction triggered by core or valence ionization of a dipeptide", Cho, D; Rouxel, J; Kowalewski, M; Lee, J. Y.; Mukamel, S. Journal of Chemical Theory and Computation. 14,0329-338 (2018)*
29. *"Monitoring molecular nonadiabatic dynamics with femtosecond X-ray diffraction", K. Bennett, M. Kowalewski, J. Rouxel and S. Mukamel. PNAS (2018) DOI: 10.1073/pnas.1805335115*
30. *" Comprehensive Experimental and Computational Spectroscopic Study of Hexacyanoferrate Complexes in Water: from Infrared to X-ray Wavelengths", Ross, M; Andersen, A; Fox, Z; Zhang, Y; Hong, K; Lee, J; Cordones, A; March, A; Doumy, G; Southworth, S; Marcus, M; Schoenlein, R; Mukamel, S; Govind, N; Khalil, M. The Journal of Physical Chemistry B, (2018) DOI: 10.1021/acs.jpcb.7b12532*
31. *"Phase Cycling RT-TDDFT Simulation Protocol for Nonlinear XUV and X-ray Molecular Spectroscopy", D. Cho, J. Rouxel, M. Kowalewski, P. Saurabh, J. Y. Lee, and S. Mukamel. JPCL, 9, 1072-1078 (2018)*
32. *"Diffraction-detected sum frequency generation; novel ultrafast x-ray probe of molecular dynamics", J. Rouxel, M.Kowalewski, and S. Mukamel. JPCL, 9, 3392-3396 (2018)*

Theory and Simulation of Ultrafast Multidimensional Nonlinear X-ray Spectroscopy of Molecules

Shaul Mukamel, University of California, Irvine, (Principle Investigator)
Sergei Tretiak, Los Alamos National Laboratory (Co-PI)
Niranjan Govind, Pacific Northwest National Laboratory (Co-PI)
Marco Garavelli, University of Bologna (Co-PI)

Progress Report September 2018
DOE Proposal # 0000241178

Program Scope

Emerging X-ray free electron laser (XFEL) beam sources offer new types of probes of matter with unprecedented spatial and temporal resolutions. Robust theoretical and computational tools that provide predictive modeling capacity of the underlining electronic and structural dynamics must meet these experimental advances. The latter will be essential for the design of sophisticated multi-pulse experiments and for their interpretation. The research effort will focus on developing cutting- edge practical simulation tools for nonlinear multidimensional X-ray/optical spectroscopies.

Future Plans

XFEL multidimensional nonlinear techniques, which combine sequences of X-ray and possibly optical pulses, provide a unique experimental toolbox for probing the dynamics of core and valence electronic excitations, as well as material structure. Predictive modeling of these dynamical processes requires the combination of analytical theory for nonlinear interactions of light and matter, robust quantum-chemical methodologies for the accurate description of electronic structure of various materials, and multiscale *ab initio* electron and nuclear dynamics techniques operating beyond Born-Oppenheimer approximation. These challenges will be addressed with three research thrusts (i) Develop and implement theoretical apparatus for modeling a broad range of multidimensional spectroscopic techniques enabled by present and upcoming XFEL facilities. This thrust also includes the incorporation of a computational module in the DOE supported open-source NWChem computational chemistry package as well as the development of other open-source codes ready for dissemination across a broad user base; (ii) Propose and design new multi-pulse experiments that make use of the capabilities of the incoming LCLS-II facility; (iii) Perform selected applications to specific molecular systems that can be carried out at LCLS-II and demonstrate how these X-ray sources may be used to study nonadiabatic dynamics through conical interactions, electronic correlations in multi-core excitons, and charge transfer/energy transfer processes.

The Spectron code, developed by Mukamel and co-workers, implements several simulation protocols of nonlinear signals. It allows for the low-cost inclusion of bath modes and can handle complex line shapes. This code will be interfaced with existing computational chemistry capabilities, offering methods from low to high accuracy that can target a broad range of system sizes and will be further refined extended to the x-ray regime and implemented in NWChem.

Real-time time developed density functional theory (RT-TDDFT) will be augmented with relativistic spin-orbit corrections. We will extend the existing module in NWChem for fast electron dynamics to include spin-orbit (SO) and relativistic effects, allowing the treatment of heavier metals (for example, transition metal, lanthanide and actinide) complexes and the description of spin-forbidden transitions. On-the-fly modeling of nonlinear spectroscopy techniques will be carried out. These include multiple pulse stimulated X-ray Raman, time resolved diffraction, monitoring nonadiabatic dynamics in molecules at conical intersections via electronic coherences and resonant x-ray four-wave mixing. Applications include excited state dynamics in conjugated organic and mixed-valence chromophores as shown in Fig 1, excitation energy transfer and charge transfer, and electronic dynamics in transition metal and heavy element molecular complexes.

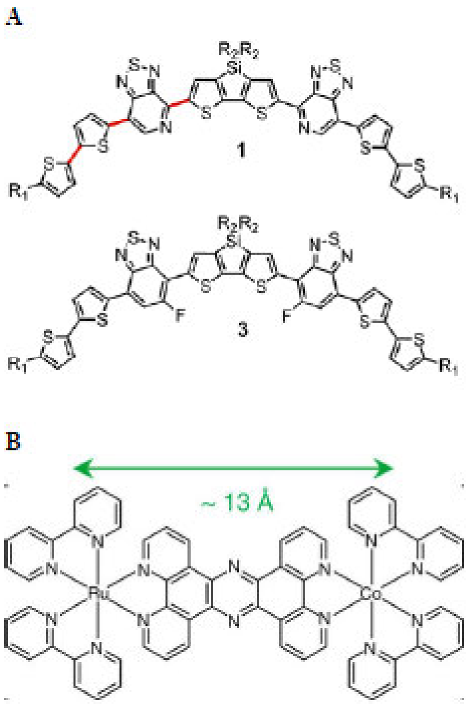

Figure 1. **(A)** p- DTS(PTTh2)2 molecular donor exhibiting the world-record performance for organic solar cells based on small molecules. **(B)** The molecular structure of mixed-valence complex showing ultrafast charge transfer resolved by XFEL experiments

Peer-Reviewed Publications Resulting from this Project (Project start date: Sept. 1, 2018**)**
No publications to report.

Quantum Dynamics Probed by Coherent Soft X-Rays

Margaret M. Murnane and Henry C. Kapteyn
JILA and Department of Physics, University of Colorado at Boulder
Phone: (303) 210-0396; E-mail: Margaret.Murnane@colorado.edu

Project Scope

The goal of this work is to develop novel short wavelength quantum light sources, and use them to to understand the dynamic response of quantum systems (atoms, molecules and nanosystems) to short wavelength and strong laser fields. We made exciting advances in several areas since 2016, with 14 peer-reviewed publications. Recent highlights include –

Recent Progress

Tabletop EUV and X-ray Spectroscopy [1,10]: Tabletop high harmonic generation driven by mid-infrared lasers produces highly coherent, ultra-broad bandwidth, femtosecond-to-attosecond soft X-ray supercontinua that are opening up new capabilities for probing atomic, molecular, material and energy systems. In this work, we demonstrated the first high-quality near- and extended-edge soft x-ray absorption spectroscopy at the K- and L-absorption edges of solids using high harmonic (HHG) sources. Ultrafast coherent high harmonic soft X-ray sources are ideal for capturing the fastest charge and spin dynamics in molecular and materials systems, with characteristic time and length scales from attoseconds and picometers on up. X-rays have advantages over visible light because they can penetrate opaque samples. Moreover, the absorption of X-ray light in a material is influenced by the position of nearest-neighbor atoms and the chemical/magnetic state, providing a powerful probe of the instantaneous structure and dynamics within a material.

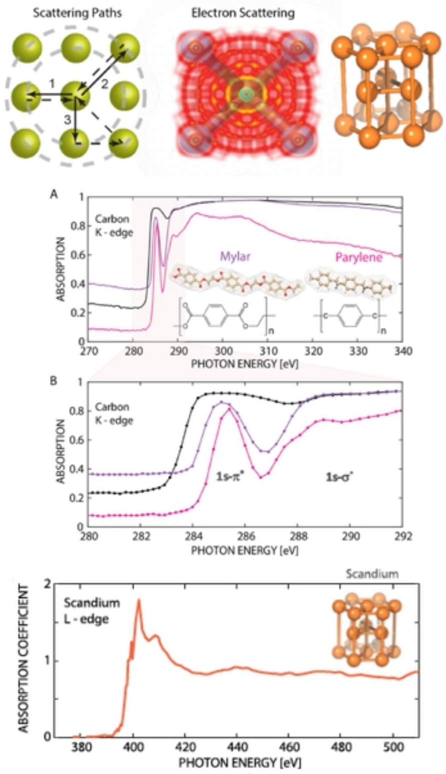

Figure 1: Photoelectron scattering and interference of an electron-wave packet in a 2D planar lattice, which give rise to a modulated x-ray absorption spectra that are characteristic for each material.

Polarization Control of Attosecond HHG Waveforms [2,5,9,14]: High harmonic generation driven by femtosecond lasers makes it possible to capture the fastest dynamics in molecules and materials. However, thus far the shortest isolated attosecond pulses have only been produced with linear polarization, which limits the range of physics that can be explored. In work that emerged from theoretical calculations and experimental work joint between JILA, the Colorado School of Mines, and with international partners from Salamanca, we proposed the first two schemes for generating isolated attosecond pulses of pure circular polarization. Both schemes generate circularly polarized HHG by crossing two circularly polarized counter-rotating pulses in a noncollinear geometry. Our results show that isolation of a single attosecond pulse can be achieved either by restricting the driver pulse duration to a few cycles, or by temporally delaying the two crossed driver pulses. In recent work, our predictions were confirmed experimentally in joint work with our collaborators from Taiwan. We demonstrated robust polarization control of isolated EUV pulses by exploiting non-collinear high harmonic generation driven by two counter-rotating few-cycle laser beams. The circularly polarized supercontinuum is produced at a photon energy of 33 eV with 190 attoseconds transform limit and a predicted linear chirp of 330 attoseconds. Furthermore, by adjusting the ellipticity of the two counter-rotating driving pulses simultaneously, we control the polarization state of isolated high harmonic pulses - from circular through elliptical to linear polarization without sacrificing conversion efficiency. Access to purely circularly polarized supercontinuum, combined with full helicity and ellipticity control paves the way towards attosecond metrology of circular dichroism in molecular and materials systems.

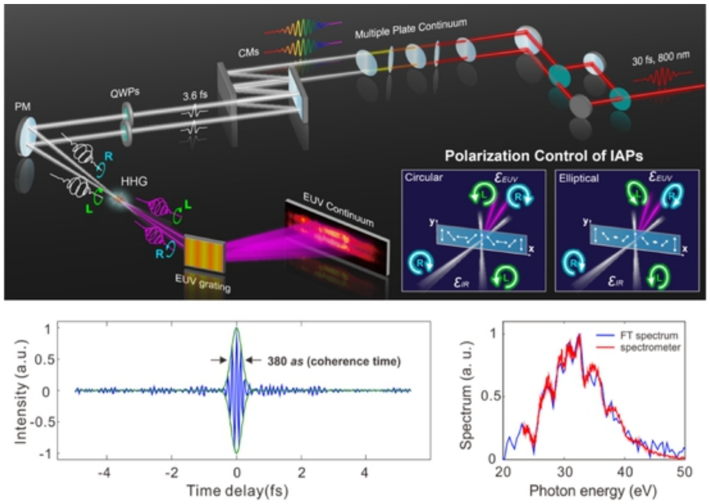

Figure 2. Generating arbitrarily-polarized isolated attosecond pulses using few-cycle driving lasers. (top) Insets show the laser electric fields at the focal plane. Controlling the ellipticity of the driving lasers results in control of the amplitude and phase of the linearly polarized HHG fields, resulting in polarization control of the HHG beams in the far field. (bottom) Field auto-correlation trace of circularly-polarized HHG. Circularly-polarized EUV spectrum measured by a spectrometer (red) and compared with the Fourier-transform of the field autocorrelation (blue).

<u>High Harmonics with Spatially-Varying Ellipticity [3]</u>: We developed a new method to produce ultrashort pulses of circularly polarized extreme ultraviolet (EUV) light through high-harmonic generation. HHG is a powerful tool to generate bright laser-like beams of EUV and soft x-ray light with ultrashort pulse durations, which are important for many spectroscopic and imaging applications in materials, chemical, and nano sciences. Historically HHG was restricted to linear polarization; however, recent advances we made are making it possible to precisely control the polarization state of the emitted light simply by adjusting the driving laser beams and geometry. In this work, we gain polarization control by combining two spatially separated and orthogonally linearly polarized HHG sources to produce a far-field beam with a uniform intensity distribution but with a spatially varying ellipticity—ranging from linearly to fully circularly polarized. This spatially varying ellipticity was characterized using

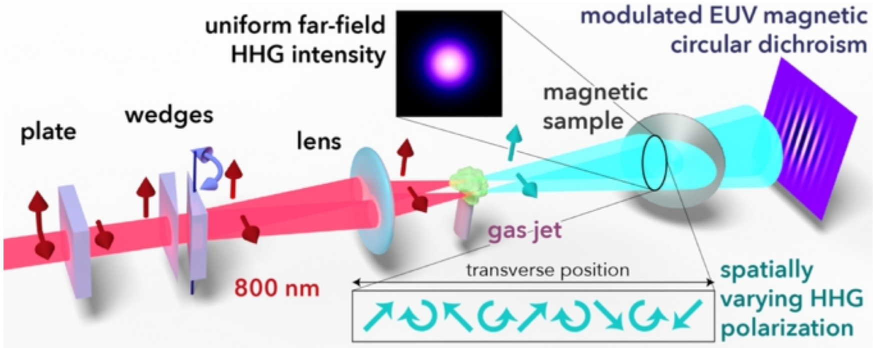

Figure 3: Experimental setup for generating HHG beams with spatially-varying ellipticity. A common-path interferometer creates two orthogonally polarized and angularly separated laser beams, which are focused to two spatially separated focal spots. Each independently drive the HHG process yielding two orthogonally polarized HHG beams, which diverge to overlap in the far field and thereby produce a far-field distribution with a spatially varying ellipticity (SVE-HHG). This ellipticity distribution is measured using the extreme ultraviolet magnetic circular dichroism (EUV MCD) response of a cobalt thin film.

EUV magnetic circular dichroism, which demonstrates that a high degree of circularity is achieved, reaching almost 100 % near the magnetic M-edge of cobalt. The spatial modulation of the polarization facilitates measurements of circular dichroism, enabling us to measure spectrally resolved magnetic circular dichroism without the use of an EUV spectrometer, thereby avoiding the associated losses in both flux and spatial resolution, which could enable hyperspectral imaging of chiral systems. Through numerical simulations, we also show the generality of this scheme, which can be applied with both discrete harmonic orders generated by many-cycle pulses, or high-harmonic supercontinua generated by few-cycle driving laser pulses. Therefore, this technique provides a promising route for the production of bright isolated attosecond pulses with circular polarization that can probe ultrafast spin dynamics in molecular and materials systems.

Atomic and Molecular Dynamics Probed using HHG and Strong Laser Fields [4,6,7,8,11,12,13]: Understanding electron-electron correlations in matter ranging from atoms to solids represents a grand challenge for both experiment and theory. These correlations can occur on attosecond time scales and have only recently become experimentally accessible. In the case of highly excited systems, the task of understanding and probing correlated interactions is even greater. In this work, we combined state-of-the-art light sources and advanced detection techniques with ab-initio calculations to unravel the role of electron-electron correlation in D_2 photoionization by mapping the dissociation of a highly excited D_2^+ molecule. Correlations between the two electrons dictate the pathways along which the molecule dissociates and lead to a superposition of excited ionic states.

Future work

We will extend polarization-shaped high harmonics from the EUV into the soft x-ray regions and use them to probe dynamics in molecular, nano and materials systems. Ultra-broad bandwidth, ultrafast HHG will be used implement dynamic x-ray spectroscopies in gas, solid and liquid-phase samples excited using mid-IR – UV light. We will also capture orbital dynamics in molecules and nanosystems using photoelectron spectroscopies.

Peer-Reviewed Publications Resulting from this Project (2016-2018)

1. D. Popmintchev, B. Galloway, M.C. Chen, F. Dolar, C. Mancuso, L. Miaja-Avila, G. O’Neil, J. Shaw, G. Fan, S. Ališauskas, G. Andriukaitis, T. Balčiunas, O. Mücke, A. Pugzlys, A. Baltuška, H. Kapteyn, T. Popmintchev, M. Murnane, “Near and extended edge X-ray absorption fine structure spectroscopy using ultrafast coherent high harmonic supercontinua”, Physical Review Letters **120**, 093002 (2018). *Also featured in Physics, https://physics.aps.org/synopsis-for/10.1103/PhysRevLett.120.093002*

2. P-C. Huang, J. Huang, C. Hernández-García, B. Huang, C. Lu, L. Rego, D. Hickstein, J. Ellis, A. Jaron-Becker, A. Becker, S. Yang, C. Durfee, L. Plaja, H. Kapteyn, M. Murnane, A. Kung, M.-C. Chen, “Polarization Control of Isolated Attosecond Pulses,” Nature Photonics **12**, 349 (2018). doi:10.1038/s41566-018-0145-0

3. J. Ellis, K. Dorney, D. Hickstein, N. Brooks, C. Gentry, C. Hernandez-Garcia, D. Zusin, J. Shaw, Q. Nguyen, C. Mancuso, S. Witte, H. Kapteyn, M. Murnane, “High harmonics with spatially varying ellipticity”, Optica **5**, 479 (2018).

4. L. Martin, R. Bello, C. Hogle, A. Palacios, X. Tong, J. Sanz-Vicario, T. Jahnke, M. Schöffler, R. Dörner, T. Weber, F. Martín, H. Kapteyn, M. Murnane, P. Ranitovic, “Revealing the Role of Electron-Electron Correlations by Mapping Dissociation of Highly Excited D_2^+ using Attosecond XUV Pulses,” Physical Review A **97**, 062508 (2018).
5. K. Dorney, J. Ellis, C. Hernández-García, D. Hickstein, C.A. Mancuso, N. Brooks, T. Fan, G. Fan, P. Grychtol, D. Zusin, C. Gentry, H. Kapteyn, M. Murnane, “Helicity-selective enhancement and polarization control of attosecond high harmonic waveforms driven by bichromatic circularly polarized laser fields”, Physical Review Letters **119**, 063201 (2017).
6. C. Mancuso, K. Dorney, D. Hickstein, J. Chaloupka, X-M. Tong, J. Ellis, H. Kapteyn, M. Murnane, “Observation of ionization enhancement in two-color circularly polarized laser fields,” Physical Review A **96**, 023402 (2017). DOI: 10.1103/PhysRevA.96.023402
7. W. Peters, D. Couch, R. Fortenberry, H. Kapteyn, M. Murnane, “Uncovering highly-excited state mixing in acetone using ultrafast VUV pulses and coincidence imaging techniques,” J. Phys. Chem. A, **121**, 2361–2366 (2017). 10.1021/acs.jpca.7b01112
8. D. Couch, G. Buckingham, J. Baraban, J. Porterfield, L. Wooldridge, G.B. Ellison, H. Kapteyn, M. Murnane, W. Peters, “Tabletop Femtosecond VUV Photoionization and PEPICO Detection of Microreactor Pyrolysis Products,” J. Phys. Chem. **121**, 5280 (2017).
9. J. Ellis, K. Dorney, C. Durfee, C. Hernandez-Garcia, F. Dollar, C. Mancuso, T. Fan, P. Grychtol, D. Zusin, C. Gentry, H. Kapteyn, M. Murnane, D. Hickstein, “Phase Matching of Noncollinear Sum and Difference Frequency High-Harmonic Generation,” Optics Express **25**(9), 10126-10144 (2017).
10. J. Hernandez-Charpak, K. Hoogeboom-Pot, Q. Li, T. Frazer, J. Knobloch, M. Tripp, S. King, E. Anderson, W. Chao, M. Murnane, H. Kapteyn, D. Nardi, “Full characterization of the mechanical properties of 11-50nm ultrathin films: influence of bond coordination on the Poisson’s ratio”, Nano Letters **17**, 2178 (2017).
11. J. Ellis, D. Hickstein, W. Xiong, F. Dollar, B. Palm, K. Keister, K. Dorney, C. Ding, T. Fan, M. Wilker, K. Schnitzenbaumer, G. Dukovic, J. Jimenez, H. Kapteyn, M. Murnane, "Materials Properties and Solvated Electron Dynamics of Isolated Nanoparticles and Nanodroplets Probed with Ultrafast EUV Beams”, J. Phys. Chem. Lett. **7**, 609 (2016).
12. C. Mancuso, K. Dorney, J. Chaloupka, J. Ellis, F. Dollar, R. Knut, P. Grychtol, D. Zusin, C. Gentry, H. Kapteyn, D. Hickstein, M. Murnane, “Controlling nonsequential double ionization in two-color circularly polarized femtosecond laser fields,” Physical Review Letters **117**, 133201 (2016).
13. C.A. Mancuso, D.D. Hickstein, K.M. Dorney, J.L. Ellis, E. Hasovic, R. Knut, P. Grychtol, C. Gentry, M. Gopalakrishnan, D. Zusin, F.J. Dollar, X.M. Tong, D.B. Milosevic, W. Becker, H.C. Kapteyn, M.M. Murnane, “Controlling electron-ion rescattering in two-color circularly polarized femtosecond laser fields”, Physical Review A **93** (5), 053406 (2016). *Also selected as an Editor’s Suggestion.*
14. C. Hern´andez-Garcıa, C.G. Durfee, D. Hickstein, T. Popmintchev, A. Meier, M. M. Murnane, H. C. Kapteyn, I. J. Sola, A. Jaron-Becker, A. Becker, “Schemes for generation of isolated attosecond pulses of pure circular polarization”, Physical Review A **93**, 043855 (2016). *Also selected as an Editor’s Suggestion.*

Revealing Nanoscale Energy Flow Using Ultrafast THz to X-ray Beams

Keith A. Nelson
Department of Chemistry, Massachusetts Institute of Technology
Cambridge, MA 02139
Email: kanelson@mit.edu

Margaret M. Murnane
JILA, University of Colorado and National Institutes of Technology
Boulder, CO 80309
E-mail: murnane@jila.colorado.edu

Program Scope

We are developing novel spectroscopic methods and making use of them to study energy flow and material properties on nanometer length scales and ultrafast time scales. Access to short length scales is provided through the use of light beams with short wavelengths (EUV through hard x-ray spectral ranges) and/or fabricated structural elements with nanometer dimensions. Recent advances in tabletop high harmonic generation of extreme ultraviolet (EUV) pulses are exploited to measure thermal transport and acoustic vibrations using time-resolved diffraction from photoexcited periodic nanostructures, revealing new physics that arises at length scales of tens to hundreds of nm. The tabletop EUV sources as well as the FERMI free electron laser at FERMI-Elettra in Trieste can be used to generate as well as measure nanoscale thermoelastic responses without the need for patterned nanostructures, with the short length scale coming from optical interference patterns formed by crossing pairs of beams in transient grating experiments. We also use EUV and optical sources to excite and monitor ultrahigh-frequency acoustic waves (coherent phonons) at ultraflat interfaces and multilayer structures, extending our recent measurements of the highest-frequency coherent acoustic waves observed to date. Our measurements of acoustic properties allow direct calculation of thermal conductivities which can be compared with our measurements of thermal transport and with first-principles calculations. Terahertz-frequency acoustic measurements can also be used to reveal complex relaxation dynamics in glass-forming liquids and partially disordered solids. Acoustic measurements are also used to investigate the confinement effect in ultrathin liquid layers and to characterize mechanical properties of ultrathin solid layers. The methods we develop have broad fundamental applications and may also enable new practical metrology for use in nanoelectronics, just as earlier methods we developed have found commercial applications in microelectronics metrology.

Recent Progress

Experiments at LCLS: time-resolved phonon spectroscopy with hard x-rays

Coherent phonon excitation in an x-ray split-and-delay experiment

A very exciting recent development at LCLS is the split-and-delay capability for hard x-rays. In December 2017, PI Nelson, in collaboration with D. Reis of SLAC, conducted the first user experiment on this newly developed setup. The sample was irradiated by two 30 fs x-ray pulses at 9.8 keV photon energy, separated by a variable time delay, and the diffuse x-ray scattering was monitored by an area detector. In $SrTiO_3$ and $KTaO_3$ samples we observed an unexpectedly intense modulation of the diffuse scattering intensity (see Fig. 1), comparable to the static thermal diffuse scattering background. Further investigation revealed oscillations of the diffuse scattering intensity at the longitudinal acoustic phonon frequencies up to ~0.5 THz. Our analysis indicates that we are exciting coherent LA phonons at every reciprocal space point up to a wavevector below ~0.06 nm^{-1}. This finding is totally unexpected since there is no apparent mechanism for the generation of a broad spectrum of coherent phonons by spatially uniform irradiation. Our hypothesis is that the x-ray excitation creates a spatially inhomogeneous concentration of photoexcited carriers, resulting in the generation of both acoustic phonons and a "quasistatic" strain pattern reflecting the carrier concentration distribution. We believe that these experiments provide fundamentally important information on the interaction of hard x-rays with dielectric crystals. Further analysis of the results is currently underway.

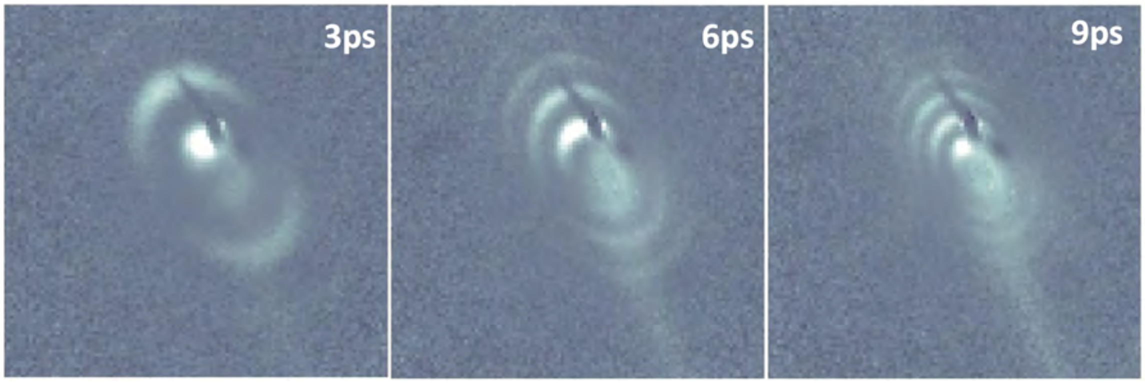

Fig. 1. X-ray pump-probe measurements on $SrTiO_3$ at 9.8 keV: modulation of diffuse x-ray scattering intensity on the detector as a function time delay. The fringes are due to LA phonons excited by the first x-ray pulse.

Phonon spectroscopy of SiGe with time-resolved x-ray scattering by squeezed thermal phonons

In another very recent experiment at LCLS we used the new phonon spectroscopy technique developed by D. Reis and colleagues, based on x-ray diffuse scattering by squeezed thermal phonon populations created by an optical excitation, to study transverse acoustic phonons in a $Si_{0.1}Ge_{0.9}$ alloy across the entire BZ. SiGe in an important thermoelectric material and there has been a lot of recent interest in SiGe in the context of nanoscale thermal transport. The objective of our experiment was to measure thermal phonon lifetimes in SiGe and to probe high-wavevector phonons near the BZ boundary. Some preliminary results are shown in Fig. 2. We were able to measure TA phonons across the entire BZ in the Γ-L direction of the reciprocal lattice; however, in the Γ-X direction the dispersion curve peters out near the BZ boundary. This suggests that we may be reaching the Ioffe-Regel limit, i.e. phonons near the X point no longer exist as plane waves. In the same experimental run, we measured the evolution of the TDS intensity pattern from GaAs and found that the acoustic phonon population remains out of thermal equilibrium within 30 ps following laser excitation. We also observed peculiar oscillations of TDS intensity in the vicinity of Bragg rods. Further analysis of the results of this experiment is currently underway.

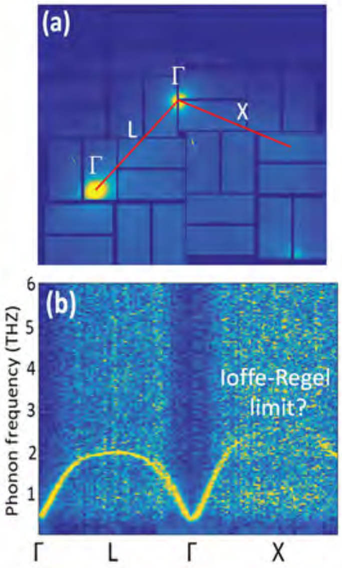

Fig. 2. (a) Diffuse scattering pattern from the $Si_{0.1}Ge_{0.9}$ alloy and (b) TA phonon dispersion along the red lines in (a).

Direct measurement of THz phonon mean free path in GaN

In parallel with phonon lifetime measurements at LCLS, we continued to pursue an alternative approach to measuring phonon lifetime and mean free path (MFP) using a laser pump-probe technique in which semiconductor superlattices are used for optical excitation and detection of THz acoustic phonon wavepackets. Earlier in the current funding period, in a joined study with C-K Sun's group at the National Taiwan University [1], we used two InGaN superlattice structures separated by a 2 µm-thick GaN layer to make the first observation of the propagation of acoustic wavepackets above 1 THz at room temperature. However, we were unable to accurately measure the phonon lifetime because the apparent attenuation was dominated by extrinsic factors such as nonuniformity of the GaN layer thickness within the laser spot. In a new series of experiments, we used temperature dependence of the intrinsic phonon lifetime dominated by anharmonic phonon-phonon scattering to separate it from extrinsic contributions. The measurements yielded room temperature intrinsic phonon MFPs of 5.4 μm at 1 THz and 3.8 μm at 1.4 THz, in good agreement with ab-initio calculations by our collaborator L. Lindsay of Oak Ridge. This is the first measurement of THz phonon MFPs in a high thermal conductivity material (traditional techniques such as inelastic neutron and x-ray scattering were only measure low thermal conductivity materials in which the phonon MFP is very short, such as PbTe, due to the limited instrumental resolution). This is also the first time that ab-initio calculations of acoustic phonon MFPs was confirmed by experiment. The long-MFP THz phonons we studied are especially important for micro- and nano-scale thermal transport, as they determine the distance scale at which the bulk κ value can no longer be used to describe heat conduction. The paper (T.-H. Chou et al., "Long mean free paths (>5 μm) of THz acoustic phonons in a high thermal conductivity material at room temperature") has been prepared for publication, preprint available.

Controlling nanoscale thermal transport: size- and spacing-dependent cooling of nanostructures

At JILA, in addition to participating in the experiments at the Fermi XFEL, we further explored nanoscale thermal transport because of its relevance both to fundamental materials behavior and also to high efficiency thermoelectric devices and nanoscience. Direct experimental measurements of heat flow in nanoscale systems are challenging, and first principle models of real geometries are not yet computationally feasible. In past work we used ultrafast pulses of short wavelength light to uncover a surprising new regime of nanoscale thermal transport that occurs when the width and separation of heat sources are comparable to the mean free paths of the dominant heat carrying phonons in the substrate. In recent work, to show that we could predict the nanoscale transport properties in this new regime, we systematically compared thermal transport from gratings of metallic nanolines with different periodicities, on both silicon and fused silica substrates. By monitoring the surface profile dynamics with sub-Å sensitivity, we directly measured thermal transport from the nanolines into the substrate [1,2]. This allows us to quantify how the nanoline period significantly impacts thermal transport into the substrate, and thereby confirm the surprising prediction that closely spaced nanoscale heat sources can cool more quickly than when far apart, at early times. These findings are important for benchmarking new theories that go beyond the Fourier model of heat diffusion, and for informed design of nanoengineered systems. Finally, we are working with several theory groups to compare our measurements to the Boltzmann transport equation (BTE), hydrodynamic and super-diffusive views of the BTE, including phononic effects that can modify the thermal transport in nanostructured systems, even at room temperature.

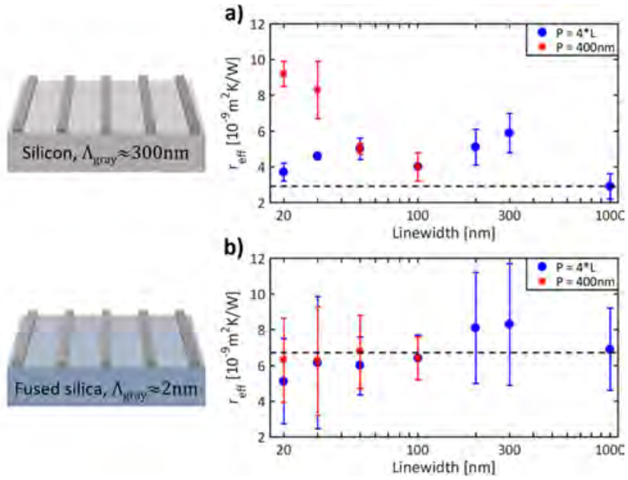

Fig. 3. Best fit effective thermal boundary resistivity for nanolines on silicon and fused silica. (a) For Si, as the linewidth is reduced below 50 nm, the effective resistivity of the constant 25% duty cycle gratings (blue points) decreases, which is a return towards the diffusive prediction. In contrast, the constant 400 nm period gratings' resistivities increase as the linewidth is reduced (red stars). The dotted line shows the 1000 nm grating effective resistivity to highlight the deviations of the smaller linewidth gratings. (b) For fused silica, the resistivities of constant duty cycle (blue points) and 400 nm period (red stars) gratings all agree within error bars. This indicates that there is no non-diffusive transport, as expected.

Future Plans

We continue to focus on the development of short-wavelength transient grating (TG) spectroscopy. While we do not have beamtime at the FERMI FEL this year (our proposal submitted in the fall 2017 was approved, but the beamtime was allocated in July 2019), our collaborators at FERMI (F. Bencivenga, C.

Macchiovecio and colleagues) continued experiments with the all-EUV TG setup started during our beamtime in April 2017 and demonstrated TG measurements with 13.3 nm excitation and probe and a TG period of 28 nm. This opens exciting prospects for probing transport phenomena in materials at ~10 nm spatial scale during our scheduled beamtime in 2019. Furthermore, the recent addition of the 20.8 nm probe wavelength to the EUV TG setup at FERMI will permit probing magnetic circular dichroism at the absorption M-edge of Co and thus enable TG studies of ultrafast magnetic phenomena on the ~10 nm spatial scale. Designing EUV TG experiments to study ultrafast magnetism is currently underway. At the same time, we are working to extend the optical TG setup at MIT extending into the UV range (200 nm wavelengths) to shorten the TG period down to almost 100 nm (further progress will be made using "solid immersion" prism couplers to shorten the wavelength by a factor of the prism refractive index). We are also working with collaborators at SLAC (D. Reis, J. Hastings) and at Paul Scherrer Institute in Switzerland (C. Svetina) to attempt preliminary TG measurements using hard x-rays. A proposal for a demonstration experiment using x-ray excitation and optical probing at SwissFEL has just been submitted. The SLAC and SwissFEL collaborative efforts will open the door to wide-ranging x-ray four-wave mixing measurements.

References

[1] J. Hernandez-Charpak, T. Frazer, J. Knobloch, K. Hoogeboom-Pot, D. Nardi, W. Chao, L. Jiang, M. Tripp, S. King, H. Kapteyn, and M. Murnane, "Reliable characterization of materials and nanostructured systems <<50nm using coherent EUV beams," SPIE Advanced Lithography, 9778, 97780I (2016).

[2] T. Frazer, J. Knobloch, K. Hoogeboom-Pot, D. Nardi, W. Chao, R. Falcone , M. Murnane, H. Kapteyn, J. Hernandez-Charpak, "Engineering nanoscale thermal transport: Size- and spacing-dependent cooling of nanostructures," submitted (2018).

Peer-Reviewed Publications Resulting from this Project (2016-2018)

1. A. A. Maznev, et al., "Propagation of THz acoustic wave packets in GaN at room temperature," Appl. Phys. Lett. 112, 061903 (2018).
2. T. Hecksher, et al., "Direct Test of Supercooled Liquid Scaling Relations," PNAS 114, 8710 (2017).
3. I. Chaban, et al., "Time-domain Brillouin scattering for the determination of laser-induced temperature gradients in liquids," Rev. Sci. Instrum. 88, 074904 (2017).
4. F. Bencivenga et al., "Four-wave-mixing experiments with seeded free electron lasers," Faraday Discuss., 194, 283 (2016).
5. V. V. Temnov, et al., "Towards the nonlinear acousto-magnetoplasmonics," J. Opt. 18, 093002 (2016).
6. J. Hernandez-Charpak, K. Hoogeboom-Pot, Q. Li, T. Frazer, J. Knobloch, M. Tripp, S. King, E. Anderson, W. Chao, M. Murnane, H. Kapteyn, D. Nardi, "Full characterization of the mechanical properties of 11-50nm ultrathin films: influence of bond coordination on the Poisson's ratio," Nano Letters 17, 2178–2183 (2017).
7. A. Vega-Flick, R. A. Duncan, S. P. Wallen, N. Boechler, C. Stelling, M. Retsch, J. J. Alvarado-Gil, K. A. Nelson, and A. A. Maznev, "Vibrational dynamics of a two-dimensional micro-granular crystal," Phys. Rev. B 96, 024303 (2017).
8. A. Vega-Flick, R. A. Duncan, S. P. Wallen, N. Boechler, C. Stelling, M. Retsch, J. J. Alvarado-Gil, K. A. Nelson, and A. A. Maznev, "Contact-based and spheroidal vibrational modes of a hexagonal monolayer of microspheres on a substrate," Wave Motion 76, 122 (2018).
9. P. H. Otsuka, S. Mezil, O. Matsuda, M. Tomoda, A. A. Maznev, T. Gan, N. Fang, N. Boechler, V. E. Gusev and O. B. Wright, "Time-domain imaging of GHz surface waves on an acoustic metamaterial," New J. Phys. 20 013026 (2018).
10. A.A. Maznev and A.G. Every, "Bound acoustic modes in the radiation continuum in isotropic material systems without periodic structures," Phys. Rev. B 97, 014108 (2018).
11. A. G. Every and A. A. Maznev, "Fano line shapes of leaky surface acoustic waves extending from supersonic surface wave points," Wave Motion 79, 1-9 (2018).
12. J. Pudell, A. A. Maznev, M. Herzog, M. Kronseder, C. Back, G. Malinowski, A. von Reppert, and M. Bargheer, "Layer specific observation of the slow thermal equilibration in ultrathin metallic nanostructures by femtosecond x-ray diffraction," Nature Commun. 9, 3335 (2018).

"Low-Energy Electron Interactions with Complex Molecules and Biological Targets"

Thomas M. Orlando
School of Chemistry and Biochemistry and School of Physics,
Georgia Institute of Technology, Atlanta, GA 30332-0400
Thomas.Orlando@chemistry.gatech.edu, Phone: (404) 894-4012, FAX: (404) 894-7452

Project Scope: The primary objectives of this program are to investigate the fundamental physics and chemistry involved in low-energy (1-250 eV) electron and soft x-ray interactions with complex molecules and biological targets. There is a particular emphasis on understanding correlated electron interactions and energy exchange in the deep valence and shallow core regions of the polyatomic collision targets. Our investigations should help determine the roles of hole exchange via inter-atomic and inter-molecular Coulomb decay (ICD), electron transfer mediated decay (ETMD) and energy exchange via localized shape and Feshbach resonances in the non-thermal damage of weakly interacting molecules at heterogeneous interfaces. We are focusing our studies on RNA and DNA nucleotides in addition to well-defined sequences of RNA and DNA oligomers. The intent is to understand the primary mechanisms of secondary electron induced damage. We are also developing a beam source of cold biomolecules for atto-second ionization and time resolved dissociative attachment studies. These will complement our present energy resolved efforts.

Recent Progress: We have investigated the inter-atomic coulomb decay (ICD) at weakly interacting interfaces involving mixed rare gases[1], and small hydrocarbons adsorbed on Ar multilayers. The bulk of our efforts were spent carrying out X-ray and low-energy electron induced damage of DNA and RNA nucleotides adsorbed on 50 nm thick Au coated doped silica [2] and graphene coated Cu surfaces[3]. We have preliminary data on the development of laser induced acoustic desorption (LIAD) as a useful method of producing cold molecular beams of nucleotides for attosecond ionization dynamics studies.

Task 1. Investigating intermolecular Coulomb decay (ICD) at weakly interacting interfaces.

We have continued studies of intermolecular Coulomb decay (ICD) on or within condensed interfaces composed of weakly interacting rare gases and/or polyatomic molecules. Specifically, we probe ICD in rare gas (Ar or Xe) samples condensed at 25 K on graphite surfaces by monitoring the ejected cation masses and kinetic energies as a function of incident electron energy.[1] The low-energy electron-induced thresholds for the formation and desorption of Ar^+ and Ar_2^+ ions and mixed dimer ($ArXe^+$) ions correlate with ionization of the Ar 3s level. We extended this by examining ICD of ethane and acetylene adsorbed on Ar multilayers. We are also working on the ICD of acetylene co-adsorbed with water since this system involves an ultrafast proton transfer channel which complicates the simple Coulomb ejection process.

Task 2. X-ray induced damage of DNA and RNA nucleotides.

We have continued our collaboration on X-ray induced damage of adsorbed DNA[2-6] and completed a third set of experiments at the Advanced Photon Source at Argonne National Laboratory. Specifically, we examined the cross sections and rates of secondary electron induced damage of 2'-deoxyadenosine 5'-monophosphate (dAMP), adenosine 5'-monophosphate (rAMP), 2'-deoxycytidine 5'-monophosphate (dCMP) and cytidine 5'-monophosphate (rCMP) using tunable X-rays. As shown in Figure 1, a 950 eV synchrotron x-ray beam was used to collect XPS data for the O 1s transition as a function of secondary electron fluence. Similar data was obtained for the C 1s transitions of all four nucleotide samples. The O 1s spectra can be fit with three components associated with specific bonding motifs: i) C-O-C, C-OH and C-O-P, ii) P-O$^-$, P=O, P-OH and C=O and iii) adsorbed H_2O. The reduction of components i and iii and growth of component ii for the oxygen indicate breakage and/or loss of C-O bonds and water with corresponding formation of P-O bonds. Additionally, the lack of growth features in the C 1s and N 1s spectra indicate minimal base and sugar damage. Instead, the primary damage pathway either involves direct capture by the phosphate or initial electron capture by the base, transfer through the sugar and eventual localization on the sugar phosphate bond. Water likely contributes to the damage, possibly via formation of compound dissociative electron attachment resonances. Modeling the O 1s radiolysis series as a single-term exponential decay yields dAMP, rAMP, dCMP, and rCMP C-O-P damage cross sections of 2.3 ±0.3 × 10^{-17}, 2.5 ±0.3 × 10^{-17}, 3.3 ±1.0 × 10^{-17} and 4.3±0.4 × 10^{-17} cm^2, respectively. There are no measurable effects due to the identity of the sugar (2'-deoxyribose or ribose). However, CMP nucleotides show a statistically valid increase in sugar-phosphate bond breakage and rate of water damage/removal compared to AMP nucleotides. This synergy is consistent with the hypothesis that despite DEA resonances being the initial entrance channel, the actual damage likely involves compound states that undergo autodetachment and the formation of two reactive radicals.[2,7]

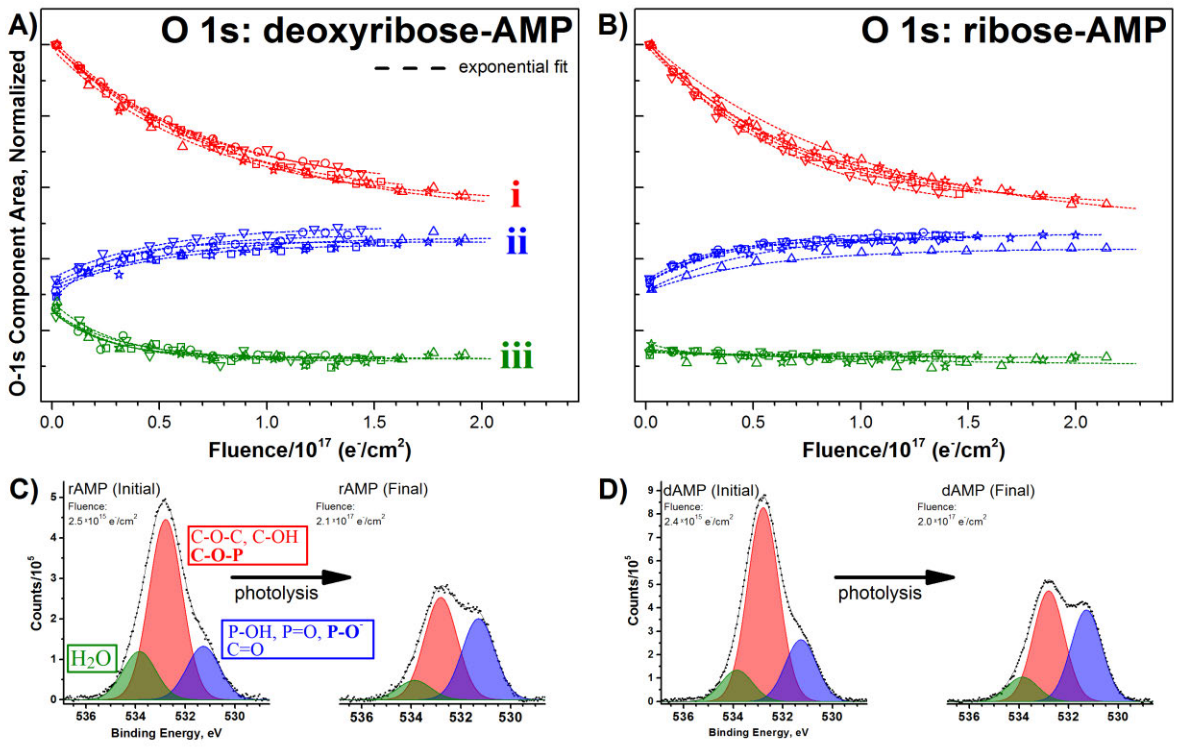

Figure 1. XPS data for O 1s components of dAMP and rAMP adsorbed on an Au thin-film, as a function of electron fluence, clearly showing x-ray induced damage. Peak 1 decay: Loss of C–O–P or C–O–C and Peak 2 rise: Formation of P-O bonds which correpsonds to breaking the sugar-phosphate bond. This is formally a single strand break in a DNA or RNA oligomer.

Task 3. Developing a cold molecular beam source for attosecond ionization of biomolecules.

A technique known as laser induced acoustic desorption (LIAD) has been exploited to introduce liable biomolecules into the gas-phase for ultrafast ionization dynamics studies. Though the acronym implies that acoustic waves drive the desorption event, this is somewhat misleading. We are unraveling the physics of this desorption process using state-resolved laser detection schemes. We are also exploiting this technique using different substrates, such as graphene, to produced well defined molecular beams of nucleotides, nucleosides and short oligomers for attosecond ionization dynamics studies. Initial work using microplasmas under ambient atmospheric conditions proved the viability of this approach.[8]

Future Plans.

We will complete the ICD studies of mixed rare gas overlayers as well as water clusters adsorbed on weakly coupled molecular solids such as C_2H_6, C_2H_2, and/or HCHO. This series has been chosen since it spans the regime of essentially no coupling (C_2H_6), to weak π-interactions (C_2H_2), and hydrogen bonding (HCHO).

- Low energy electron induce damage dAMP, rAMP, dCMP, and rCMP adsorbed on graphene coated substrates that have been functionalized with amino acids will be examined using Raman micro-spectroscopy and atomic force microscopy. This information will ultimately be valuable to ongoing studies regarding targeted treatment of cancer using radiotherapies and nanoparticles.

- We plan to screen LIAD active substrates such as graphene for use in generating cold molecuelar beams of biomolecules such as nucleobases, nucleotides and short oligomers of DNA and RNA. If viable, collaborative studies on attosecond ionization and DEA of nucleotides will be carried out.

- Apply for additional beam-time at APS/ANL to carry out spin-resolved DEA studies of nucleotide films.

References:

1. M. Schiiable, S. Kindu, B. Jones, and T. M. Orlando, “Intermolecular Coulomb Decay in Mixed Rare Gas Overlayers” (in preparation, *Chem. Phys. Lett.*)
2. A. D. McKee, M. Schiable, S. Kundu, R. Rosenberg and T. M. Orlando, “The role of water and negative ion resonances in X-ray induced damage of dAMP, rAMP, dCMP and rCMP adsorbed on Au coated Si”, (in preparation, *J. Chem. Phys.*)
3. S. Kundu, M. Schiable, A. McKee, R. Rosenberg and T. M. Orlando, “Energy resolved low-energy induced damage of dAMP, rAMP, dCMP and rCMP adsorbed on graphene:Cu substrates”, (in preparation, *J. Phys. Chem. Lett.*)
4. R. A. Rosenberg, J. M. Symonds, K. Vjayalakshmi, D. Mishra, T. M. Orlando, and R. Naaman, “The relationship between interfacial bonding and radiation damage of adsorbed DNA”, *Phys. Chem. Chem. Phys.* **16**, 15319-15325 (2014).
5. R. A. Rosenberg, J. M. Symonds, V. Kalyanaraman, T. Z. Markus, T. M. Orlando, R. Naaman, E. a. Medina, F. A. Lopez and V. Muijca, “Kinetic Energy Dependence of Spin Filtering of Electrons Transmitted through Organized Layers of DNA”, *J. Phys. Chem. C.* **117,** 22307-22313, (2013).

6. R. Rosenberg, J. M. Symonds, T. Z. Markus, T. M. Orlando and R. Naaman, “The lack of spin selectivity in low-energy electron induced damage of DNA films”, *J. Phys. Chem. C.* 117(43), 22307-22313 (2013).
7. E. Alizadeh, T. M. Orlando and L. Sanche, “Biomolecular damage induced by ionizing radiation; The direct and indirect effects of low-energy electrons on DNA”, *Ann. Rev. of Phys. Chem*. 66, 379-98 (2015).
8. K. Benham, R. Hodyss, F. Fernandez, and T. M. Orlando, “Laser-Induced Acoustic Desorption Atmospheric Pressure Photoionization via VUV-Generating Microplasmas”, *J. of Amer. Soc. for Mass Spectrom.* 27 (11), 1805-1812 (2016).

Peer-Reviewed Publications Resulting from this Project (2016-2018)

1. A. N. Sidorov and T. M. Orlando, Correction to “Monolayer Graphene Platform for the Study of DNA Damage by Low-Energy Electrons” *J. Phys. Chem. Lett.* 7, 2168, (2016).

Presentations acknowledging support from this program

1. T. M. Orlando, “Very low energy (<5 eV) electron induced damage of DNA and RNA nucleotides”, Argonne National Laboratory Colloquium, May 1, 2018.
2. T. M. Orlando, “Very low energy (<5 eV) electron induced damage of complex biomolecules”, “Miller Conference on Radiation Chemistry”, Oct. 7- 11, Sicily 2017.
3. T. M. Orlando, “Low-energy electron interactions with complex targets”, Dept. of Energy, Atomic, Molecular and Optical Physics Meeting, Oct.23-26, 2016.

SISGR - Structure from Fleeting Illumination of Faint Spinning Objects in Flight

A. Ourmazd
Dept. of Physics, University of Wisconsin Milwaukee
3135 N. Maryland Ave, Milwaukee, WI 53211
ourmazd@uwm.edu

Project Scope

The advent of intense, ultrashort pulses of X-rays and electrons has made it possible to obtain two-dimensional snapshots of molecular machines performing their native function. We are developing a new generation of data-analytical algorithms to recover three-dimensional structure and dynamics from noisy snapshots of molecular machines viewed at highly uncertain time points. Combining concepts from machine learning, differential geometry, general relativity, graph theory, and diffraction physics, these techniques promise to revolutionize our understanding of molecular function at the atomic level.

Recent Progress

The binding of a so-called ligand to a molecular machine is the lynchpin of a wide range of important functional and regulatory processes (*1*). Despite sustained experimental and theoretical scrutiny for decades, the mechanisms by which ligands bind to molecular machines (*2, 3*) remain the subject of intense debate (see, e.g., (*1, 4, 5*)). Broadly speaking, even the nature and sequence of events are controversial. In addition to fundamental scientific interest, these issues have important implications for our ability to understand, and ultimately control molecular machines (*6*).

Experimentally determined multidimensional landscapes specifying the free energies of the conformations relevant to molecular function offer a powerful framework for elucidating mechanisms (*7, 8*), but have remained largely inaccessible. Using experimental single-particle snapshots, we have succeeded in mapping the multidimensional energy landscapes of a molecular machine involved in ligand binding (Fig. 1).

These energy landscapes reveal multiple routes to ligand binding with comparable branching ratios. Three-dimensional movies along these routes identify the continuous conformational changes associated with ligand binding at near-atomic level, both overall and at specific binding sites. The approach can be used to elucidate the conformational changes enabling function in a wide range of systems. More generally, our work establishes that single-particle study of systems *in equilibrium* offers access to into processes hitherto thought accessible only by *non-equilibrium, time-resolved* experiments.

We have validated our approach with reference to the ryanodine receptor (RyR1), a fourfold-symmetric (C4) ion channel. This molecular machine is a calcium-activated calcium channel critical to excitation/contraction coupling in a wide range of systems.

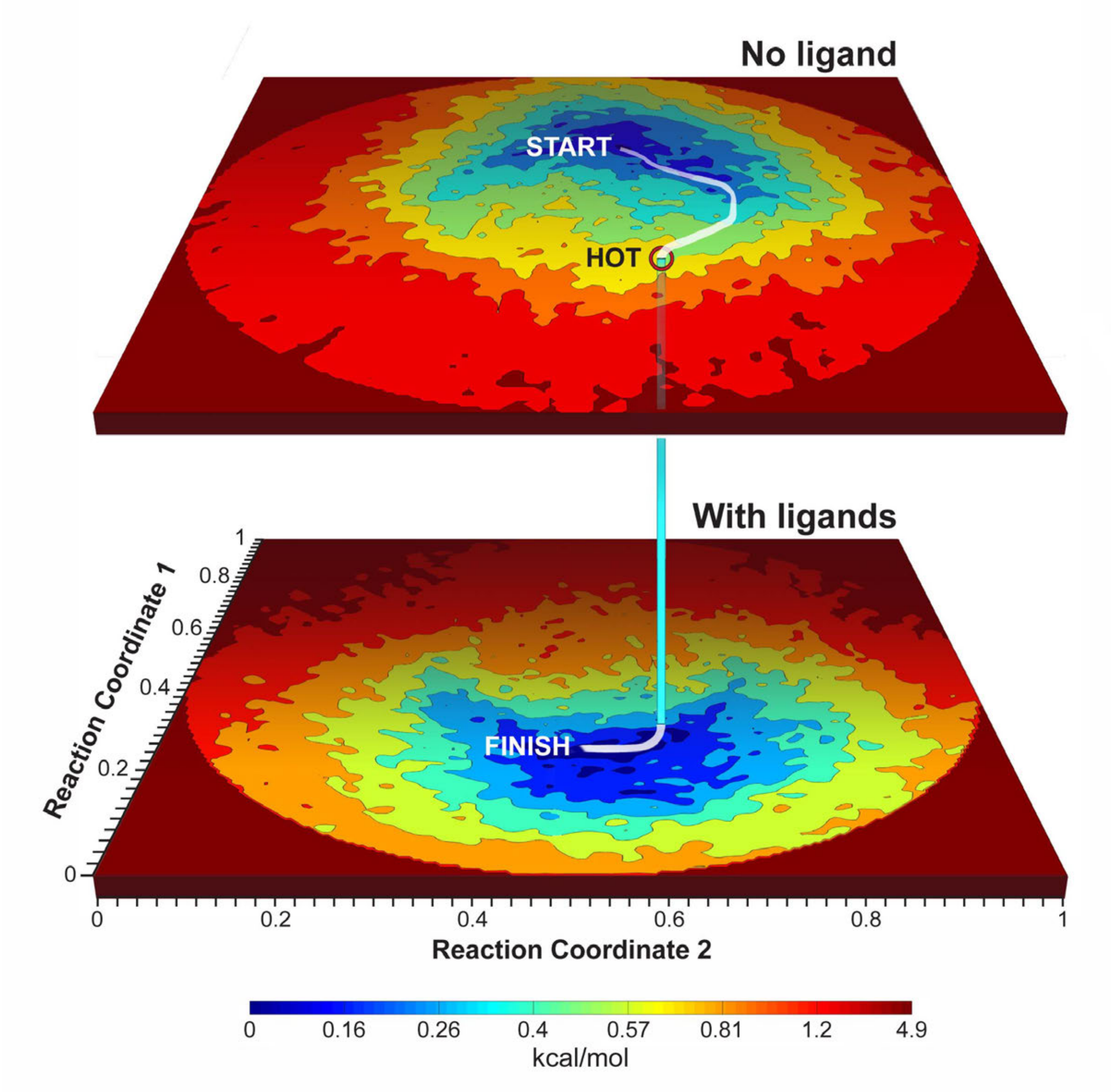

Figure 1. Data-analytically determined energy landscapes for the molecular machine RyR1, without and with ligands (Ca^{++}, ATP, and caffeine). The landscapes are described in terms of the most important two of a common set of orthogonal conformational coordinates. The curved path represents the least-action (i.e., high-probability route) to the binding of ligands. This path starts at the minimum-energy molecular conformation without ligands ("START"), follows the conduit of least-action to a point with a high probability of transition to the with-ligands energy landscape ("HOT"), and terminates at the minimum-energy conformation with ligands ("FINISH"). (With A. Dashti, A. des George & J. Frank, unpublished.)

Several recent cryo-EM studies have revealed, in exquisite detail, the many conformations assumed by the closed channel (*9-11*), with activation and gating of the channel upon ligand binding changing the nature of the conformational states (*12*). But the plethora of discrete conformations revealed by maximum likelihood classification (*13*) provides scant guidance on the *sequence* of conformational changes involved in ligand binding, the responsible *reaction coordinates*, the *energy landscapes*, or the *routes* to ligand binding and channel gating. Such information is essential for a deep understanding of molecular machines, and the thermodynamics of molecular function in general.

Using geometric machine learning, a transparent, mathematically rigorous, unsupervised data-analytical approach (*14-16*), we have previously demonstrated that experimental snapshots of single molecular machines idling in equilibrium can be used to determine their energy landscapes in terms of orthogonal coordinates describing *continuous* conformational changes relevant to translation (*16*). Such landscapes reveal all conformations with energies up to an upper limit set by the vanishing occupation probability of high-energy states. The key point is that thermal fluctuations in *equilibrium* lead to sightings of all states up to a limit set by the number of snapshots in the dataset.

A key feature of our most recent study is the pooling of single-particle snapshots from two experiments. In one, the molecular machines were in equilibrium with a thermal bath. In the other, the machines were in equilibrium with a thermal bath *and* a ligand reservoir (*12*). This pooling of data has two important consequences. First, both species (with and without ligands, henceforth ±ligand) are described in terms of the same set of conformational reaction coordinates. Second, this approach reveals the heavily populated conformational conduits connecting the two species, thus identifying the least-action routes relevant to ligand binding (Fig. 1).

The approach outlined above has enabled us to determine the ±ligand energy landscapes for RyR1 in terms of the same binding-relevant reaction coordinates. Subject to reasonable assumptions, Fermi's Golden Rule is then used to estimate the transition probability between the two landscapes, with "hotspots" identifying the most probable transition points between the with- and without-ligand landscapes. Using the least-action conduits on each landscape, we are thus able to compile, for the first time, three-dimensional functional movies of ligand binding in a molecular machine. Importantly, the course of conformational motions associated with ligand binding differs in crucial ways from that obtained by discrete clustering techniques (*12*).

Future Plans

An experimental observation entails projecting all system variables onto the (small) subset of variables actually measured. Thus, one records only a small fraction of the information needed for a full understanding and control of the system under study. For example, XFEL-based serial femtosecond crystallographic datasets are ~ 99% incomplete.

We plan to extend our data-analytical approach to cases of extreme data incompleteness, with particular emphasis on ultrafast structure-dynamical measurements. This would constitute a data-driven (i.e., unbiased) route to understanding, and ultimately controlling the dynamics of key processes at near-atomic level.

References

1. E. Di Cera, *Biophys Chem* **186**, 1 (2014).
2. J. Koshland, D. E. , *Proc Natl Acad Sci U S A* **44**, 98 (1958).
3. J. Monod, J. Wyman, J. P. Changeux, *J Mol Biol* **12**, 88 (1965).
4. J. P. Changeux, S. Edelstein, *F1000 Biol Rep* **3**, 19 (2011).
5. T. R. Weikl, F. Paul, *Protein Sci* **23**, 1508 (2014).
6. F. Feixas, S. Lindert, W. Sinko, J. A. McCammon, *Biophys Chem* **186**, 31 (2014).
7. D. Wales, *Energy Landscapes: Applications to Clusters, Biomolecules and Glasses*. (Cambridge University Press, Cambridge, 2003), pp. 681.
8. X. Deupi, B. K. Kobilka, *Physiology (Bethesda)* **25**, 293 (2010).
9. Z. Yan *et al.*, *Nature* **517**, 50 (2015).
10. R. Zalk *et al.*, *Nature* **517**, 44 (2015).
11. R. G. Efremov, A. Leitner, R. Aebersold, S. Raunser, *Nature* **517**, 39 (2015).
12. A. des Georges *et al.*, *Cell* **167**, 145 (2016).
13. S. H. Scheres, *J Mol Biol* **415**, 406 (2012).
14. R. Coifman, S. Lafon, *Appl. Comput. Harmon. Anal.* **21**, 5 (2006).
15. D. Giannakis, A. J. Majda, *Proc Natl Acad Sci U S A* **109**, 2222 (2012).
16. A. Dashti *et al.*, *Proc Natl Acad Sci U S A* **111**, 17492 (2014).

Peer-reviewed Publications Resulting from this Project (2016-2018)

1. Enzyme intermediates captured “on the fly” by mix-and-inject serial crystallography, J.D. Olmos Jr. et al., **BMC Biology 16**, 59 (2018).
2. Free-electron laser data for multiple-particle fluctuation scattering analysis, K. Pande et al. **Scientific Data** (accepted).
3. Conformational landscape of a virus by single-particle X-ray scattering, A. Hosseinizadeh, G. Mashayekhi, J. Copperman, P. Schwander, A. Dashti, R. Sepehr, R. Fung, M. Schmidt, C.H. Yoon, B.G. Hogue, G. Williams, A. Aquila, and A. Ourmazd, **Nature Methods 14**, 878 (2017).
4. Machine-learning routes to dynamics, thermodynamics, and work cycles of biological nanomachines, **X-Ray Free Electron Lasers: Applications in Materials, Chemistry, and Biology; Energy & Environment Series** (eds U. Bergmann, V. Yachandra, & J. Yano) Ch. 22, 418 (Royal Society of Chemistry, 2017)
5. Laser control over the ultrafast Coulomb explosion of N_2^{2+} after Auger decay: A quantum mechanical investigation, A.M. Hanna, O. Vendrell, A. Ourmazd, and R. Santra, **Physical Review A 95**, 043419 (2017).
6. Structural enzymology using X-ray free electron lasers, C. Kupitz et al., **Structural Dynamics 4**, 044003 (2017).
7. Femtosecond structural dynamics drives the trans/cis isomerization in photoactive yellow protein, K. Pande et al., **Science 352**, 725 (2016).
8. Coherent soft X-ray diffraction imaging of the coliphage PR772 at the Linac Coherent Light Source, H.K.N. Reddy et al., **Scientific Data 4**, 170079 (2017).
9. Coherent diffraction of single Rice Dwarf virus particles using hard X-rays at the Linac Coherent Light Source, A. Munke et al., **Scientific Data 3**, 160064 (2016).
10. Dynamics from noisy data with extreme timing uncertainty, R. Fung, A.M. Hanna, O. Vendrell, S. Ramakrishna, T. Seideman, R. Santra, and A. Ourmazd, **Nature 532**, 471 (2016).

Control of Molecular Dynamics: Algorithms for Design and Implementation

Herschel Rabitz and Tak-San Ho
Princeton University, Frick Laboratory, Princeton, NJ 08540
hrabitz@princeton.edu, tsho@princeton.edu

A. Program Scope:

Advances in ultrafast laser technology along with flexible pulse shaping capabilities has enabled a rapidly rising number of successes in the control of broad varieties of quantum phenomena. The subject is now open for advanced development, and the major goal of this research project aims to address several key topics in this regard. The primary focus is on developing theoretical concepts and practical algorithms for their transfer into the laboratory to enhance the quality of the experiments as well as to extract greater information from these endeavors. The collective planned studies aim at exploring a number of issues at the foundation of laser control over quantum phenomenon

B. Recent Progress:

During the current DOE grant period, from October 2017 to September 2018, a broad variety of research topics were pursued in the general area of understanding and controlling quantum dynamics phenomena. A summary of these accomplishments is provided below:

[1] Gaining Mechanistic Insight with Control Pulse Slicing: Application to the Dissociative Ionization of CH_2BrI: In this study we successfully employed, without the need for modeling, a new easy-to-implement experimental analysis tool - the Control Pulse Slicing (CPS) - directly in the laboratory to gain mechanistic insights about control experiments. Specifically, we applied the CPS to dissociative ionization of CH_2BrI with mass spectral detection, where two pulses with similar intensities were investigated,with each capable of distinctively controlling the ratio of Br^+/CH_2Br^+. By comparing the dynamical evolution of the observed multiple fragment ion yields upon slicing scans of the two distinct pulses, we were able to reveal insights about the control mechanism for manipulating the objective ratio.

[2] Analytic Solutions to Coherent Control of the Dirac Equation: In this work we developed a simple framework of relativistic dynamical inversion (RDI), opening up a new route to coherent control for the Dirac dynamics. We analytically designed electromagnetic fields, obeying Maxwell's equations, to yield a desired evolution. In particular, we showed how to achieve coherent rotation and translation of wave packets. To this end, a scalar interaction coupled to the mass was incorporated into RDI. This opens up prospects for quantum technologies in new realms of physics and may further expand the scope of control landscape analysis.

[3] The roles of drift and control field constraints upon quantum control speed limits: In this work we obtained a lower bound for the minimum time required to implement a target unitary transformation through a classical time-dependent field in a closed quantum system. The bound depends on the target gate, the strength of the internal Hamiltonian, and the highest permitted control field amplitude. In particular, for fully controllable systems, we identified a lower bound for the time at which all unitary gates become reachable. Moreover, in the single qubit case, our analytical findings describe the relationship between the highest control field amplitude and the minimum evolution time remarkably well.

[4] Dependence of the quantum speed limit on system size and control complexity: In this study we derived a lower bound for the minimum time necessary to implement a unitary transformation on a generic, closed quantum system with an arbitrary number of classical control fields. This bound was explicitly analyzed for a specific N-level system of interest in quantum control for quantum computation. The value of the bound, determined numerically, and an estimate of the true minimum gate time were systematically compared for a range of system dimensions and number of controls. It was shown that the bound captures the scaling of the minimum time well for the systems studied, and is quantitatively correct in the order of magnitude.

[5] Optimal control of orientation and entanglement for two dipole-dipole coupled quantum planar rotors: In this study we successfully performed optimal control simulations for orientation and entanglement of two dipole-dipole coupled identical quantum rotors. We found that the maximally oriented state (MOS) of the two rotors is readily attainable at all rotor separations. Whereas, the maximally entangled state (MES) is most conveniently attainable at small separations. The peak orientation expectation value attained by the MOS at large separations exhibits a longtime revival pattern. Moreover, the peak entanglement entropy value attained by the MES remains largely unchanged as the two rotors are transported to large separations after turning off the control field. Finally, optimal control transition dynamics reveals the intricate interplay between orientation and entanglement.

[6] Exact-exchange optimized effective potential and memory effect in time-dependent density functional theory (TDDFT): In this study, we carried out non-adiabatic calculations for a one-dimensional two-electron Helium model in a triplet state using the recently formulated Sturm-Liouville-type time-local equation for the time-dependent optimized effective potential (TDOEP) with the exact exchange functional, and it was found that the results agree with the exact time-dependent Schrödinger equation solutions. It was also found that the non-adiabatic and memory-dependent terms in the time-local TDOEP equation correctly describe the time-dependent structure of the exchange-correlation potential and yield the probability density evolution. These findings should provide important insights toward future studies on memory effects in TDDFT.

[7] Control landscapes for a classof non-linear dynamical systems: sufficient conditions for the absence of traps: In this work we established three tractable, jointly sufficient conditions for the control landscapes of non-linear dynamical systems to be trap free. These results extended prior research primarily regarding the Schrödinger equation to a broader class of non-linear control problems encompassing both quantum and other dynamical systems. Importantly, it was demonstrated that the new general results encompass end-point objectives for a general class of non-linear control systems having the form of a linear time invariant term with an additional state dependent non-linear term. Within this large class of non-linear control problems, it was shown that each of the three sufficient conditions holds for all but a null set of cases. A detailed numerical investigation using the D-MOPRH gradient control optimization algorithm was presented for a particular example amongst this family of systems.

[8] Hamiltonian amplification: The speed-up of quantum dynamics is of paramount importance for quantum technology. However, in finite dimensions and without full knowledge of the dynamics, it can be easily shown that the speed-up is impossible. In this work, we showed that via the novel concept of Hamiltonian amplification through local squeezing, many continuous variable systems can be sped-up without full knowledge of the dynamics. To this end, we have thoroughly investigated the performance, physical realizations and robustness of Hamiltonian amplification. In particular, by combining amplification with dynamical decoupling, we showed it is possible to achieve amplifiers that are free from environmental noise. Moreover, a significant reduction in gate times of cavity resonator qubits was possible due to the viability of Hamiltonian amplification.

[9] <u>Why is Successful Control of Quantum and Classical Phenomena so Prevalent: the surprising ease of finding optimal solutions for complex systems</u>: In this work we gave a perspective on the observed relative ease of achieving optimal control of quantum mechanical, and more generally described nonlinear, phenomena. The circumstances involved are wide-ranging, including manipulation of atomic scale processes, maximization of chemical and material synthesis yields, and Nature's optimization of species' populations through survival of the fittest. The empirical observations on the ease of achieving control in these diverse domains naturally raises the question of why this occurs despite the generally inherent complexity of the systems in each scenario. The key to addressing the question posed here lies in the associated control landscape. Quantum mechanical simulations provide extensive evidence and some experiments furnish specific confirmation for the structure of control landscape, while other more complex scenarios (*i.e.*, in chemistry and evolution) have limited reliable simulations, but generally supporting direct experimental landscape evidence on the ease of achieving optimization. In all circumstances, understanding the structure of the control landscape depends on satisfaction of three assumptions: (i) the existence of an optimal solution, (ii) the ability to freely move locally on the landscape, and (iii) the required control resources are available. Upon satisfaction of the assumptions, the associated control landscape may be shown to be free of traps that could halt a search from reaching the optimal outcome. A conjecture, based on our findings, is that controlling phenomena, of possibly even broader character than considered here, may be unified through consideration of control landscapes with the same common set of three underlying assumptions. The full scope and significance of this unifying control principle must await the outcome of future studies.

C. Future Plans:

In the coming year, we plan to expand our studies on controlling quantum dynamics phenomena, with a particular emphasis on obtaining a deeper understanding of the topology of the underlying control landscapes. The nature of these landscapes has a dominant influence on whether optimal control of quantum phenomena is even achievable, and whether such a control can be found with relative ease. A special focus will be given to understanding the tetrad of cases where the system and control are either drawn from classical or quantum resources. All of these cases have their own practical significance as well as fundamental importance. These collective studies are especially important for informing about which algorithms should be most effective, both in simulations and in the laboratory for seeking the best quantum control performance. We also plan to exploit the toolkit to accelerate the discovery of controls for complex systems described by quantum dynamics, but in the case of polyatomic molecules with many atoms, the dimension of the underlying Hilbert space is far too large to simply exploit the toolkit alone. Thus, this plan will combine the toolkit with a special form Hartree technique (and at an advanced stage, Hartree-multiconfiguration). Finally, although the primary focus of the research is on quantum control, extensive experimental evidence exists that a common control principle is operative when seeking optimal performance in various domains of science. Further evidence will be gathered in this regard, aiming to lay out foundations for a fundamental principle linking optimal control in various scientific domains at a basic (i.e., topological) level.

D. Peer-Reviewed Publications Resulting from this Project (2016-2018)

1] The role of dissociation channels of excited electronic states in quantum optimal control of ozone isomerization: A three-state dynamical model, Y. Kurosaki, T.-S. Ho, H. Rabitz, Chem. Phys. **115**, 469 (2016).

[2] On choosing the form of the objective functional for optimal control of molecules, C. Joe-Wong, T.-S. Ho, H. Rabitz, J. Math. Chem. **54**, 1 (2016).

[3] Wigner-Lindblad Equations for Quantum Friction, D. I. Bondar, R. Cabrera, A. Campos, S. Mukamel, H. Rabitz, J. Phys. Chem. Lett. **7**, 1632 (2016).
[4] Frequency domain quantum optimal control under multiple constraints, C.-C. Shu, T.-S. Ho, X. Xing, H. Rabitz, Phys. Rev. A **93**, 033417 (2016).
[5] Identifying a cooperative control mechanism between an applied field and the environment of open quantum systems, F. Gao, R. Rey-de-Castro, Y. Wang, H. Rabitz, F. Shuang, Phys. Rev. A **93**, 053407 (2016).
[6] Monotonic convergent quantum optimal control method with exact equality constraints on the optimized control fields, C.-C. Shu, T.-S. Ho, H. Rabitz, Phys. Rev. A **93**, 053418 (2016).
[7] Efficient computations of quantum canonical Gibbs state in phase space, D. I. Bondar, A. Campos, R. Cabrera, H. Rabitz, Phys. Rev. E **93**, 063304 (2016).
[8] Conductance and Activation Energy for Electron Transport in Series and Parallel Intramolecular Circuits, L.-Y. Hsu, N. Wu, H. Rabitz, PCCP **18**, 32087 (2016).
[9] Theory of molecular conductance using a modular approach, L.-Y. Hsu and H. Rabitz, J. Chem. Phys. **145**, 234702 (2016).
[10] Dirac open-quantum-system dynamics: Formulations and simulations, R. Cabrera, A. G. Campos, D. I. Bondar, H. Rabitz, Phys. Rev. A **94**, 052111 (2016).
[11] How to Make Distinct Dynamical Systems Appear Spectrally Identical, A. G. Campos, D. I. Bondar, R. Cabrera, H. Rabitz, Phys. Rev. Lett. **118**, 083201 (2017).
[12] Pareto-front shape in multiobservable quantum control, Q. Sun, R.-B. Wu, H. Rabitz, Phys. Rev. A **95**, 032319 (2017).
[13] Control landscapes are almost always trap free: a geometric assessment, B. Russell, H. Rabitz, R.-B. Wu, J. Phys. A. Theor. **50**, 205302 (2017).
[14] Searching for an optimal control in the presence of saddles on the quantum-mechanical observable landscape, G. Riviello, R.-B. Wu, Q. Sun, H. Rabitz, Phys. Rev. A **95**, 063418 (2017).
[15] Time-Local Equation for the Exact Optimized Effective Potential in Time-Dependent Density Functional Theory, S.-L. Liao, T.-S. Ho, S.-I Chu, H. Rabitz, Phys. Rev. Lett. **118**, 243001 (2017).
[16] Relationship between sensitivity indices defined by variance- and covariance-based methods, G.Li and H. Rabitz, Reliability Engineering and System Safety **167**, 136 (2017).
[17] Gaining Mechanistic Insight with Control Pulse Slicing: Application to the Dissociative Ionization of CH_2BrI, X. Xing, R. Rey-de-Castro, H. Rabitz. J. Phys. Chem. A121, 8632 (2017).
[18] Analytic Solutions to Coherent Control of the Dirac Equation, A. Campos, R. Cabrera, H. Rabitz, D. Bondar, Phys. Rev. Lett. 119, 173203 (2017).
[19] The roles of drift and control field constraints upon quantum control speed limits, C. Arenz, B. Russell, D. Burgarth, H. Rabitz, New J. Phys. 19, 103015
[20] Dependence of the quantum speed limit on system size and control complexity, J. Lee, C. Arenz, H. Rabitz, B. Russell, New J. Phys. 20, 063002 (2018)
[21] Optimal control of orientation and entanglement for two dipole-dipole coupled quantumplanar rotors, H. Yu, T.-S. Ho, H. Rabitz, PCCP, 20, 13008 (2018).
[22] Exact-exchange optimized effective potential and memory effect in time-dependent density functional theory**,** S.-L. Liao, T.-S. Ho, H. Rabitz, S.-I Chu, Eur. Phys. J. B 91, 147 (2018)
[23] High efficiency classification of children with autism spectrum disorder, G. Li, O. Lee, H. Rabitz, PLoS ONE 13(2):e0192867, February 15, 2018
[24] Control landscapes for a classof non-linear dynamical systems: sufficient conditions for the absence of traps, B. Russell, S. Vuglar, H. Rabitz, J. Phys. A: Math. Theor. in print (2018).

“Atoms and Ions Interacting with Particles and Fields”

F. Robicheaux
Purdue University, Department of Physics and Astronomy,
525 Northwestern Ave, West Lafayette IN 47907
(robichf@purdue.edu)

Program Scope

This theory project focuses on the time evolution of systems subjected to either coherent or incoherent interactions represented by fields and particles, respectively. This study is divided into three categories: (1) coherent evolution of highly excited quantum states, (2) incoherent evolution of highly excited quantum states, and (3) the interplay between ultra-cold plasmas and Rydberg atoms. Some of the techniques we developed have been used to study collision processes in ions, atoms and molecules. In particular, we have used these techniques to study the correlation between two (or more) continuum electrons and electron impact ionization of small molecules.

Recent Progress (Publications 10/2017-9/2018)

Two electron physics: In Ref. [9], we showed the simulated results of using fast single-cycle pulses to detect the properties of double Rydberg wave packets. Fully quantum and classical calculations were performed for a helium atom with two excited, radially localized Rydberg wave packets. The differences between the classical and quantum methods were compared for a wide range of principal quantum numbers to study the validity of the classical method for low-lying states. The effects of fast terahertz single-cycle pulses on an atomic system with one or two Rydberg wave packets were also studied using classical equations of motion. These results suggested that single-cycle pulses can be used as time-resolved probes to detect motion of the wave packets and to investigate autoionization properties. In Ref. [10], we investigated the post-collision interaction in Auger processes where the photoelectron energy is near or below the ionization threshold. To predict the properties of this process, we numerically solved the time dependent Schrodinger equation. To interpret the results, we performed classical calculations. When the photoelectron is more deeply bound, interference patterns can be seen in the angular and photoelectron energy distributions from the quantum calculation but are not present in the classical calculations. A semiclassical analysis using actions from two-path trajectories gives the relative locations of the interference maxima very close to those from the full quantum calculations. The two paths that leave the photoelectron with the same final energy and relative direction are: 1) a photoelectron moving outward scatters the Auger electron and 2) a photoelectron moving inward more strongly scatters the Auger electron.

Finally, this program has several projects that are strongly numerical but only require knowledge of classical mechanics. This combination is ideal for starting undergraduates on publication quality research. Since 2004, thirty-five undergraduates have participated in research projects in my group. Most of these students have completed projects published in peer reviewed journals. Two undergraduates, Michael Wall in 2006 and Patrick Donnan in 2012, were one of the 5 undergraduates invited to give a talk on their research at the undergraduate session of the DAMOP meeting. One publication during the past three years had an undergraduate supported by DOE as first author or coauthor.

Future Plans

Basic scattering theory: We will further apply the developments in Refs. [6] to perform precision studies of Stark states. Previously, the local-frame-transformation theory gives qualitative agreement with measurements but allows an intuitive method for including the effects from strong fields. We will extend our recent developments to perform calculations for actual atoms including the strong fields, spin-orbit interactions, etc. A successful implementation will confirm that the GLFT can be used both as an intuitive method and as a spectroscopically accurate technique.

Two electron physics: The graduate student Xiao Wang will lead the study of time dependent two electron systems. We will focus on the cases where two electrons are launched successively into Rydberg wave packets as in the joint experiment/calculation with R.R. Jones in 2013. The first studies will probe where the classical and quantum correspondence breaks down. If we can make rapid progress, we will also investigate whether stable wave packet states can be formed by this technique and, if they can, we will study their generic properties. We will also investigate the properties of the recaptured electron when the photo-electron is launched near threshold.

Benchmarking Strong Field Programs: Jens Svensmark and Brett Esry proposed a test problem to benchmark the programs used for calculating the strong laser-atom ionization at 800 nm. They organized this project involving many different theory groups around the world. The goal is to compare the performance of the many different methods being used in the strong field community. The test case they chose was the angular momentum distribution at 0.1 Up and 10 Up for H with the laser at a particular strength and frequency. The calculation was done blind by the different groups and the results sent to Svensmark and Esry to be compared and organized. A paper will be written comparing the different methods.

Peer-Reviewed Publications Resulting from this Project (2016-2018)

[1] C. Zhong and F. Robicheaux, “Coherence and quasistable states in a strong infrared field,” Phys. Rev. A **93**, 033410 (2016).

[2] B.C. Yang and F. Robicheaux, “Closed-orbit theory for photodetachment in a time-dependent electric field,” Phys. Rev. A **93**, 053413 (2016).

[3] H.-C. Shao and F. Robicheaux, “Photodetachment of H^- from intense, short, high-frequency pulses,” Phys. Rev. A **93**, 053414 (2016).

[4] M.S. Pindzola, J. Colgan, F. Robicheaux, T.G. Lee, M.F. Ciappina, M. Foster, J.A. Ludlow, and Sh.A. Abdel-Naby, “Time-dependent close-coupling calculations for ion-impact ionization of atoms and molecules,” Adv. At. Mol. Opt. Phys. **65**, 291 (2016).

[5] S. Cohen, M. M. Harb, A. Ollagnier, F. Robicheaux, M. J. J. Vrakking, T. Barillot, F. Lepine, and C. Bordas, “Photoionization microscopy of the lithium atom: Wave-function imaging of quasibound and continuum Stark states,” Phys. Rev. A **94**, 013414 (2016).

[6] P. Giannakeas, Chris H. Greene, and F. Robicheaux, “Generalized local-frame-transformation theory for excited species in external fields,” Phys. Rev. A **94**, 013419 (2016).

[7] H.-C. Shao and A.F. Starace, “Imaging population transfer in atoms with ultrafast electron pulses,” Phys. Rev. A **94**, 030702(R) (2016).

[8] E. Moufarej, M. Vielle-Grosjean, G. Khalili, A.J. McCulloch, F. Robicheaux, Y.J. Picard, and D. Comparat, “Forced field ionization of Rydberg states for the production of monochromatic beams,” Phys. Rev. A **95**, 043409 (2017).

[9] X. Wang and F. Robicheaux, “Probing double Rydberg wave packets in a helium atom with fast single-cycle pulses,” Phys. Rev. A **96**, 043409 (2017).
[10] X. Wang and F. Robicheaux, “Interference patterns from post-collision interaction in below-threshold photoexcitation Auger processes,” Phys. Rev. A **98**, 013421 (2018).

Page is intentionally blank.

Generation of Bright Soft X-ray Laser Beams

Jorge J. Rocca
Department of Electrical and Computer Engineering and Department of Physics
Colorado State University, Fort Collins, CO 80523-1373,
jorge.rocca@colostate.edu

Project Scope

The great interest in the use of high intensity coherent soft x-ray and x-ray light motivates the development of compact sources of intense coherent short wavelength light that can be readily accessible. The project goals are to explore amplification from the radiation from atomic transitions in plasma regimes leading to compact soft x-ray lasers emitting energy laser pulses at high repetition rates. This research builds on recent progress in the generation of bright soft x-ray laser beams on a table-top that demonstrated operation at 100 Hz repetition rate, producing a record 0.1 mW average power at 13.9 nm. The combination of an increased pumping efficiency with a further increase in repetition rate can be expected to yield soft x-ray laser beams with an unprecedented average power on a table-top for applications demanding a high photon flux. Recent results from this project include the demonstration of 18.9 nm soft x-ray laser operation at 400 Hz repetition rate, the highest reported today for a soft x-ray laser, and the extension of repetitive gain-saturated plasma-based table-top x-ray lasers to the shortest wavelength to date: 6.85 nm *(Optica, **5**, 257, (2018))*. Laser amplification was also observed at wavelengths as short at 5.8 nm by isolectronic scaling in Ni-like lanthanide ions. The work conducted under this program also includes the use of compact plasma-based soft x-ray lasers in applications to problems of chemical interest. Recent results include isotopic composition mapping of micron-size U particles with nanoscale resolution, and nanoscale depth profiling analysis of a CoNCN-coated electrodes for water oxidation catalysis.

Recent Progress

Realization of a Gain-saturated plasma based X-ray lasers down to 6.8 nm and gain at lower wavelengths. During this report period we have completed the development of gain saturated repetitive x-ray lasers with wavelengths down to 6.85 nm in Ni-like Gd. These lanthanide Ni ion-based collisionally pumped lasers generate μJ pulses which will enable for example sequential single-shot imaging of ultrafast nano-scale phenomena using sub-7 nm light. Furthermore, in the same series of experiments we have observed gain at wavelengths as short s 5.8 nm in Ni-like Dy. These results are published in *Optica, **5**, 257, (2018))*.

The results were obtained creating line focus plasmas using a sequence of two 800 nm laser pulses consisting of a normal-incidence pre-pulse followed by a main sub-picosecond pulse impinging at selected grazing incidence angles in a traveling wave configuration. The results were modeled and analyzed with hydrodynamic/atomic physics simulations with the code Radex. A post processor ray tracing code was used to model the soft x-ray laser beam propagation along the plasma column. This allowed us to compute the gain saturation behavior, the role of refraction, the x-ray laser output pulse energy, and the beam divergence. To compute the small signal gain, the Ni-like ions were modeled with 287 levels including inner and outer shell levels. Other ions in vicinity of the Ni-like were modeled using 300 single and doubly excited levels using atomic data and collisional rates from the code HULLAC. Ions far from the Ni-like state were modeled with just the lowest energy outer shell configuration plus the lowest inner shell and double excited levels. The atomic model was run self- consistently with the hydrocode including up to 3000 levels. We observed that the computed gain decreases as the complexity of the atomic model and the number of levels is increased until the resulting gain becomes practically insensitive to a further increase in the number of levels. The dashed curve in Fig. 1(a) is the result of the model simulations of the Gd 6.85 nm laser for the pump conditions used in the experiment assuming the width of the gain region in the direction parallel to the target is 10 μm. Good agreement with the experimental results is observed. The model predicts a beam divergence of 2.4 mrad in the directions parallel to the target, in good agreement with the measured value (see Fig. 1(b)). The agreement with the experimental results allows us to use the simulations to further understand the operation of this x-ray laser amplifier. Fig. 2 shows the computed spatial distribution of the beam intensity as a function of plasma column length. The model simulations show that in the case of the higher Z-ions refraction shifts the maximum gain to the lower density region where the electron density is (4 - 5) x 10^{20} cm^{-3}. At this density the saturation intensity is computed to be 1.2×10^{10} W cm^{-2}. Simulations show this intensity is reached after the rays travel ~ 6 mm along the plasma column axis. The output intensity is computed to exceed the saturation intensity by > 3× at the exit of the amplifier. Refraction is observed to shift the amplified beam progressively away from the target , decreasing the output pulse energy. The demonstration of a gain-saturated tabletop laser at λ= 6.85 nm in Ni-like Gd at this reduced pump energy also opens the prospect for bright high-repetition-rate plasma-based lasers at shorter wavelengths. In progress toward this goal we used isoelectronic scaling along elements of the lanthanide series to obtain lasing in several other shorter wavelengths transitions from Ni-like ions at wavelengths as short as 5.8 nm in Ni-like Dy.

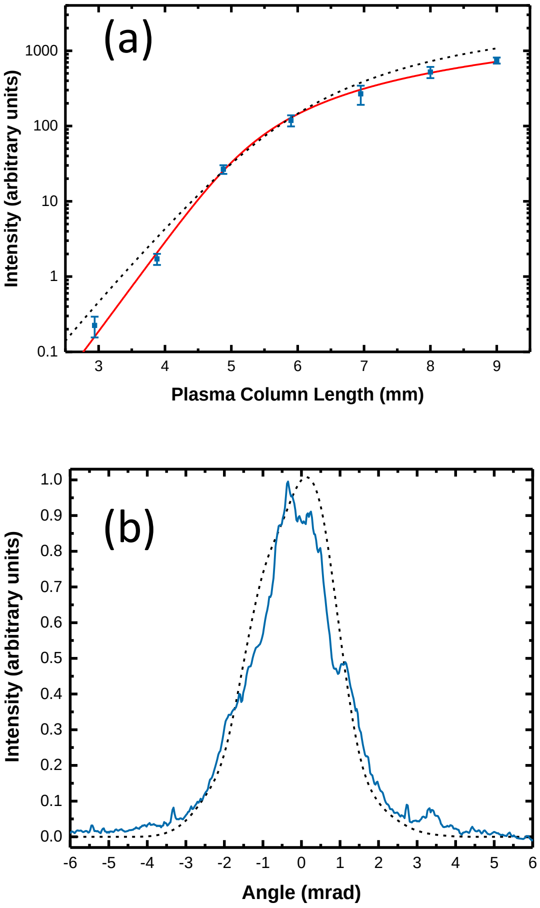

Fig. 1 (a) Intensity of the λ= 6.85 nm laser line as a function of the plasma-column length. The solid red line is a fit of the data that yields a gain-length product of 16.2.. The black dashed line is the result of atomic physics/hydrodynamic simulation. **(b)** Measured (blue trace) and simulated (black dashed) Ni-like Gd laser far field beam intensity profile in the direction parallel to the target surface. The FWHM beam divergence is ~ 2.4 mrad.

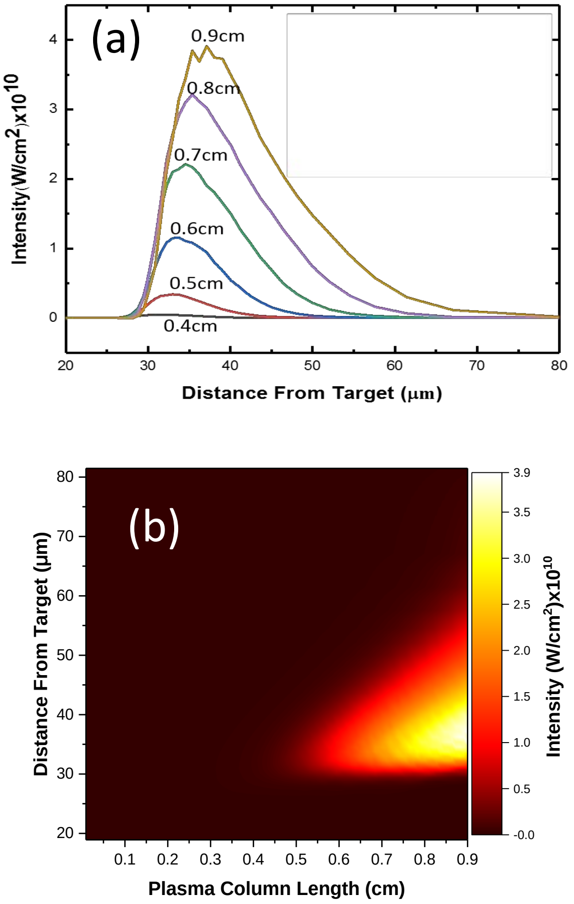

Fig. 2. Computed evolution of the intensity distribution of the 6.85 nm x-ray laser beam in Ni-like Gd as function of plasma column length. (a) Intensity vs distance to the target for increasing plasma column lengths between 0.4 and 0.9 cm. (b) Pseudocolor map of the laser line intensity as a function of distance to the target and plasma column length.

Depth profile analysis of CoNCN for water oxidation catalyst by nano-ablation mass spectrometry with a compact extreme ultraviolet laser.

The implementation of renewable hydrogen sources relies on the development of efficient catalysts for photo-and electrocatalytic water splitting. The bottleneck of the overall efficiency is considered to be the thermodynamically demanding four-electron oxidation of water to molecular oxygen. Earth-abundant heterogeneous transition metal electro-catalysts improve the oxygen formation kinetics and are leading candidates for affordable large scale water electrolysis, both for the classical alkaline electrolyzers and direct photo-electrocatalytic approaches. In order to allow targeted catalyst design and rational development the catalytic mechanisms, reactive species and structure-activity relationships remain to be elucidated. For electrochemical water oxidation catalysts based on transition metals the formation of oxides or hydroxides on the electrode surface under turnover conditions is frequently debated and still a major concern. Even a monolayer of surface species can significantly alter the reaction processes that take place at the electrode-electrolyte interface. Among the relatively abundant transition metals, cobalt shows catalytic activity in various forms of oxides and hydroxides. We used extreme ultraviolet (XUV) laser ablation time-of-flight mass spectrometry to conduct nano-scale depth resolution profiling analysis of a CoNCN-coated electrode for water oxidation catalysis. This method allowed us to distinguish different composite components of the catalyst-Nafion blend, used to modify a screen-printed carbon electrode surface. Chemical information was extracted by fragment assignment and relative amplitude analysis of the mass spectrometry peaks. Pure Nafion and the exposed carbon substrate were compared as references. Material specific non-overlapping fragments were clearly identified by the detected mass-to-charge peaks of Nafion and CoNCN. 3D mapping of relevant mass peak amplitudes was used to determine the lateral distribution and to generate depth profiles from consecutive laser pulses (Fig.3). Evaluating the profiles of pristine electrodes gave insight into fragmentation behavior of the catalyst in a functional matrix.

Time-of-flight mass (TOF) spectra of XUV-laser ablated pre- and post-catalytic CoNCN coated screen-printed electrodes for water oxidation revealed significant chemical depth profiling information. It was shown that the mass-to-charge peaks corresponding to N^+ as well as the ones correlated to the fragmentation of CoNCN ($CoCN^+$ and Co_2CN^+) and Nafion (CF^+, CF_3^+ and $C_3F_5^+$) are practically absent from the averaged mass spectra of the selected post-catalytic sample spots. Together with the increase in C_2^+ amplitude the results may indicate that these spots are devoid of a catalyst layer. On the other hand

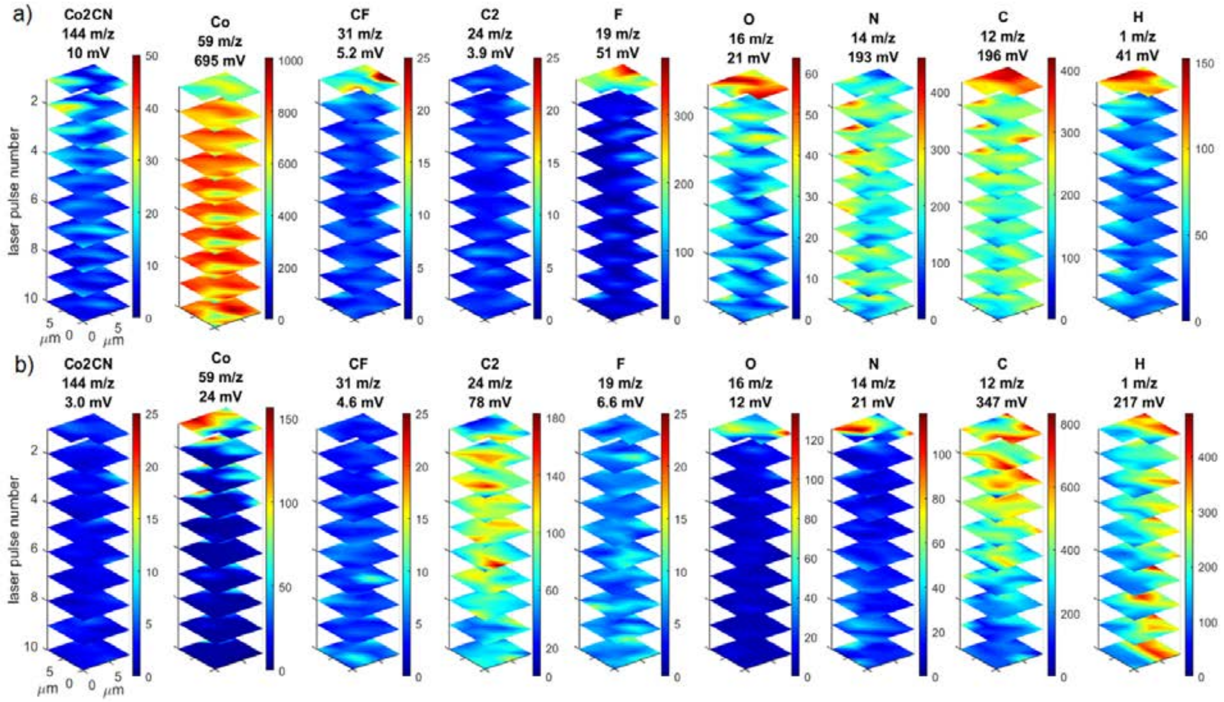

Fig 3: Depth profile representation of mass fragment peak areas by stacked 2D maps for a) pre-catalytic and b) post-catalytic CoNCN@Nafion coated SPEs. Below the peak assignment the rounded nominal mass and the average peak area is noted. The peak area magnitude is represented by color and is normalized to the corresponding signal maximum and set to 1 mV×ns for lower signals. Note the significant decrease of peak area and the adjusted scale for N^+, F^+ and Co^+ in the post catalytic sample.

Co^+ and N^+ are clearly detected on the first pulse, which shows that even small amounts of superficial catalyst remains above the substrate background. The confirmed localized absence of Nafion after electrocatalysis provides valuable information to address possible layer-degradation and redeposition processes in a targeted way. Understanding the cause and process of electrode transformations is essential for the progress in catalyst development, especially for technological applications. To this end, also investigation of reference materials of different types and the impact of morphology and mixed materials requires additional attention. Overall, the sensitivity and spatial resolution we obtained fulfilled the required high demands of micro- to nanoscale electrode surface characterization, paving the way for a wider use of tabletop XUV laser TOFMS on chemistry applications beyond the field of electrocatalysis.

Future Plans. We plan to continue expanding compact plasma-driven soft x-ray lasers to shorter wavelengths using transient collisional excitation of atomic transitions in highly ionized, aiming also to shorter pulse duration, and increased average power. We plan to study approaches to obtain amplification in lanthanide ions at sub- 6 nm wavelengths, and to investigate plasma gain media with increased bandwidth to allow the amplification of bright soft x-ray pulses of femtosecond duration. In addition we plan to continue taking advantage of the large energy per pulse, and short wavelength of soft x-ray lasers to study chemistry and material science problems.

Peer-Reviewed Publications Resulting from this Project (2016-2018)

1. A. Rockwood, Y. Wang, S. Wang, M. Berrill, V.N. Shlyaptsev, and J.J. Rocca, "Compact gain-saturated x-ray lasers down to 6.85 nm and amplification down to 5.85 nm". Optica. **5**, 257, (2018).
2. R. Muller, I. Kuznetsov, Y. Arbelo, M. Trottman, C.S.Menoni, J.J. Rocca, G.R. Patzke, D. Bleiner, “Depth-Profiling Microanalysis of CoNCN Water-Oxidation Catalyst Using a lambda=46.9 nm Plasma Laser for Nano-Ionization Mass Spectrometry,” Analytical Chemistry, **90**, 9234, (2018).
3. V. Vozda, T. Durian, J. Chalupsky, V. Dedic, V. Hajkova, P. Hlidek, L. Juha, M. Kozlova,. M. Kraus, J. Kunc, M. Rejjan, L.Vysin, J.J. Rocca and J. Franc. “Micro-Raman mapping of surface changes induced by XUV laser radiation in cadmium telluride,” J. Alloys and Compounds, **763**, 662 (2018).
4. L. Vysin, T. Burian, E.Ukraintsev, M.Davidkowva, M. Grisham, S. Heinbuch, J.J. Rocca, and L. Juha. “Dose-rate effects in breaking DNA strands by short pulses of extreme ultraviolet radiation”, Radiation Research, **189**, 466, (2018)
5. T. Green et al , “Characterization of extreme ultraviolet laser ablation mass spectrometry for actinide trace analysis and nanoscale isotopic imaging**”,** Journal of Analytical Atomic Spectrometry**, 32,** 1092-1100 (2017).
6. C. Baumgarten, M. Pedicone, H. Bravo, H.C. Wang, L. Yin, C.S. Menoni, J.J. Rocca, B.A. Reagan, “1 J, 0.5 kHz repetition rate picosecond laser”, Optics Letters **41**, 3339 (2016).
7. V. Aslanyan, I. Kuznetsov, H. Bravo, M. R. Woolston, A. K. Rossall, C. S. Menoni, J. J. Rocca, and G. J. Tallents, “Ablation and transmission of thin solid targets irradiated by intense extreme ultraviolet laser radiation”, Applied Physics Letters Photonics, **1,** 066101 (2016).

Investigating charge transfer and charge migration on the few- to sub-femtosecond time scale

Artem Rudenko, Daniel Rolles, Loren Greenman
J. R. Macdonald Laboratory, Department of Physics, Kansas State University, 116 Cardwell Hall, Manhattan, KS 66506
rudenko@phys.ksu.edu, rolles@phys.ksu.edu, lgreenman@phys.ksu.edu
Robin Santra, *Center for Free-Electron Laser Science, Deutsches Elektronen-Synchrotron DESY, 22607 Hamburg, Germany* robin.santra@cfel.de

Program Scope: The main goal of this project is to study ultrafast charge transfer and charge migration phenomena in gas-phase molecules utilizing unique novel capabilities provided by the LCLS-II. This includes time-resolved, multi-particle coincidence experiments investigating charge dynamics triggered by valence and inner-shell photoabsorption, detailed theoretical modelling of these experiments, and further development of theoretical tools required for the adequate description of the core-ionized states at the proper level of electronic correlation. A particular focus will be placed on visualizing and understanding electronic motion within the first femtosecond after the photoabsorption employing attosecond X-ray pulses developed at LCLS. These studies, which are based on single-photon probing of time-dependent charge density distribution, will complement our efforts within the JRML program aimed to understand electronic and nuclear dynamics driven by extreme multiphoton absorption at ultrahigh X-ray intensities.

Background and Future Plans: Intramolecular motion of electronic charge is one of the most important primary events in all photo-induced processes in chemistry and biology, and is critical for technological applications related to energy conversion and storage. Understanding charge dynamics at the microscopic level is essential for fundamental insights into the key steps in photosynthesis and metabolism, oxidation and reduction reactions, light-driven charge transfer in metal complexes, as well as for improving applications relying on charge motion and separation, from artificial photosynthesis and molecular electronics to photocatalytic and photovoltaic devices.

Currently, a generally accepted picture of the photo-induced charge dynamics includes purely electronic *charge migration* driven by the electronic coherence, and *charge transfer* driven by and correlated with the motion of the atomic nuclei. The development of attosecond science sparked particular interest in the charge migration, which is often expected to precede nuclear motion. However, despite intense experimental and theoretical investigations (see [1,2] for recent reviews), the underlying charge dynamics are far from being understood. The distinction between the "migration" and "transfer" processes, and the understanding to which extent observables used to characterize electronic dynamics are influenced by the nuclear motion [3,4], remains particularly challenging.

Our understanding of ultrafast electronic dynamics and the ability to disentangle signatures of different contributing processes are, to a large extent, limited by the experimental techniques employed. Since it also remains difficult to accurately describe both nuclear and electronic dynamics and their coupling theoretically [5], much more robust and comprehensive experimental data are needed to understand the differing roles of charge migration, charge transfer and the coupling between electron and nuclear motion, and to determine the validity of various theoretical models. Ultrafast X-rays represent a promising tool for probing such correlated electronic and nuclear dynamics, mainly because of their sensitivity to the local charge density. This program is focused on investigating such dynamics in gas-phase molecules employing ultrashort XFEL pulses at high repetition rate as a probe. Planned combined experimental and theoretical analysis is expected to yield comprehensive information on the evolution of charge density and nuclear geometry following core-shell or valence-shell photoionization. Our efforts to achieve this general goal will concentrate on three major themes outlined below.

1. X-ray pump – X-ray probe experiments

Recent developments of novel short pulse generation schemes and X-ray pulse pairs at LCLS make pump-probe experiments with two attosecond pulses (and, thus, with sub-fs temporal resolution) a realistic possibility. Sub-fs, single-spike pulses have been generated and characterized in the hard X-ray domain [6], and the development and testing of attosecond capabilities in the soft X-ray regime is currently underway (within the so-called XLEAP initiative). Meanwhile, several schemes delivering pairs of few-fs pulses in single-color or two-color modes have been demonstrated and can be routinely applied for experiments [7]. We plan to exploit these novel LCLS capabilities to study ultrafast charge dynamics following X-ray core-shell photoabsorption.

Several recent calculations [8,9] suggested that the inner-shell ionization of polyatomic molecules triggers sub-fs oscillatory charge migration continuing until the core hole decays via Auger process. Initial simulations for nitrogen 1s ionization in the nitrosobenzene molecule were followed by similar predictions for oxygen 1s ionization of the carbonyl sulfide (OCS), pointing towards the universal nature of such attosecond electronic response. We plan to explore the predicted ultrafast charge migration following core-shell ionization using a pair of sub-fs soft X-ray pulses, generated either by the XLEAP configuration, which is currently being tested at the LCLS-I, or by an alternative attosecond pulse generation scheme available at the LCLS II. A sketch of such experiment is shown in Fig. 1a. The key point for the successful observation of the signatures of the charge migration in the scheme we plan to employ is reliable identification of the photoelectrons resulting from the probe step, which we plan to achieve by employing photoion-photoelectron coincident measurements.

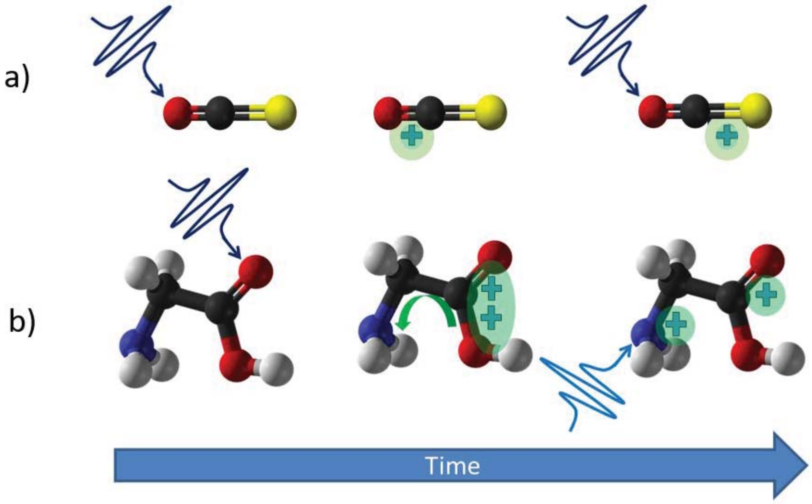

Figure 1: Schematic illustration of the two types of proposed X-ray pump – X-ray probe experiments. a) A single-color pump-probe measurement aimed at studying charge migration in OCS molecules. Oxygen 1s ionization triggers sub-fs dynamics in the valence shell of the OCS^+, and the temporal evolution of the created hole density is probed by the second ionization at the same site with the same photon energy. b) Two-color pump-probe experiments on glycine aimed at studying charge transfer after the Auger decay. Here a pump pulse, tuned just above the oxygen 1s shell of glycine, ionizes one of the oxygen atoms creating a double valence vacancy after Auger, which moves across the molecule. A second, delayed probe pulse at slightly lower photon energy core-ionizes the nitrogen atom in the glycine dication, triggering a second Auger decay that will probe the evolving electronic structure of the molecule.

We plan to complement the studies employing sub-fs X-ray pulses with experiments relying on a hetero-site-specific X-ray pump-probe scheme combined with time-resolved Auger spectroscopy. This approach appears to be a promising tool for investigating nuclear-motion-driven charge transfer unfolding on a few fs time scale. It was recently found that after oxygen K-shell ionization and subsequent Auger decay in the glycine molecule, the created double hole can be transferred within 3 to 4 fs between both functional ends of the glycine molecule, driven solely by specific nuclear displacements and non-Born-Oppenheimer effects [10]. An experimental scheme to study these dynamics is illustrated in Fig. 1b. Here, a pump pulse, tuned just above the oxygen 1*s* shell of glycine, ionizes one of the oxygen atoms creating a double valence vacancy after Auger, which moves across the molecule. A second, delayed probe pulse at slightly lower photon energy core-ionizes the nitrogen atom in the glycine dication, triggering a second Auger decay. We plan to employ time-resolved Auger electron spectroscopy to map the time-dependent, site-specific electronic structure of the glycine dication.

2. UV pump – X-ray probe experiments

While X-ray driven processes induced by core-shell interactions discussed in the previous section represent attractive test grounds for studies of ultrafast charge dynamics, it is the electronic motion upon valence-shell photoabsorption (in particular, photo-induced electron transfer) that is of more general interest for chemical or biological applications. It would be therefore beneficial for a multidisciplinary community interested in ultrafast photochemical reactions to employ such efficient probing tool as ultrashort, intense X-ray pulses at high repetition rate of LCLS-II to map electron motion triggered by the interaction with visible, UV or XUV light. However, the temporal resolution for studies involving valence interactions at LCLS is much worse than that for X-ray pump – X-ray probe experiment. It is typically restricted by the optical pulse duration, which lies in the range of 30 to 50 fs (FWHM) for infrared 800 nm Ti:Sa pulses, and is considerably longer for the UV light (e.g., 3rd harmonic of

800 nm light at 266 nm). Correspondingly, the temporal resolution of typical experiments involving 266 nm pump pulses was above 100 fs (see e.g., [11,12]). To address this problem, we will, in close interaction with the LCLS laser group and instrument scientists, develop a dedicated compact UV source capable of delivering 15-20 fs pulses at several UV wavelengths. We will then employ this source for to investigate different aspects of charge transfer processes. This includes (i) time-resolved studies of UV-driven charge transfer dynamics in several prototypical molecular systems employing coincident photoelectron-photoion spectroscopy to probe the evolving charge density, and (ii) experiments aimed at mapping internuclear distance dependence of charge transfer probability between two sites of a laser-dissociated molecule [12,13].

3. Theory development

An essential part of the planned effort is the development and application of advanced theory that will be developed by the participating groups at CFEL/DESY and at Kansas State University. While a significant body of theoretical work is available on the topic of ultrafast, correlation-driven charge migration *preceding* nuclear motion (see [1,2]) and some recent studies have investigated the occurrence of charge migration and ultrafast valence charge transfer after inner-shell ionization [8-10], a complete theory describing both, coherent electronic and nuclear dynamics and, in particular, the role of nuclear motion as a cause of a dephasing of the electronic dynamics [3,4], has yet to be constructed.

The main objective of the theoretical work is twofold. First, we will employ an advanced machinery developed at CFEL over the recent years to describe X-ray-matter interactions for detailed simulations of the experimental pump-probe studies proposed here. Second, we will work on further elaboration of these approaches and on the development of theoretical tools required for better description of valence- and core-ionized states at the proper level of electronic correlation and including the explicit coupling to the nuclear motion. Theory will provide a quantitative description of the interaction of the ultra-intense X-rays with the molecules that will be employed as the pump or the probe step in the experiment. These simulations will be based on the XMOLECULE [14,15] and XMDYN [16] packages developed at DESY, which has been successfully employed by this collaboration to describe previous experiments at LCLS [17,18]. Furthermore, a self-adapting grid method [19] that is currently being developed at Kansas State University can be incorporated in order to increase the accuracy of these calculations, which currently use a single-center approximation to describe the photoionization and Auger processes. Self-adapting overset grids, pictured in Figure 2, are comprised of multiple spherical grids centered at each atomic nucleus in a molecule. They therefore provide a natural description of the geometry of complex molecules [19]. Since the overset grid is currently already implemented in the scattering package *ePolyScat*, the use of overset grids as representations for the molecular continuum states combined with the XMOLECULE code is straightforward.

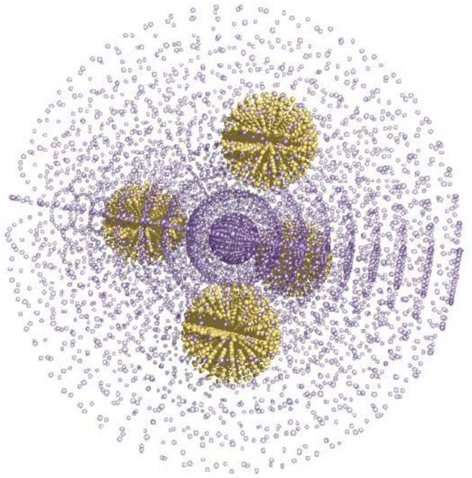

Figure 2: *Three-dimensional schematic representation of an overset grid for CF_4.*

References

[1] M. Nisoli, P. Decleva, F. Calegari, A. Palacios, F. Martin, *“Attosecond Electron Dynamics in Molecules*”, Chem, Rev. **117**, 10760 (2017).

[2] H. J. Wörner et al., *“Charge migration and charge transfer in molecular systems”*, Structural Dynamics **4**, 061508 (2017).

[3] M. Vacher, M. J. Bearpark, M.A. Robb, and J. P. Malhado, *“Electron dynamics upon Ionization of Polyatomic Molecules: Coupling to Quantum Nuclear Motion and Decoherence”*, Phys. Rev. Lett. **118**, 083001 (2017).

[4] C. Arnold, O. Vendrell, and R. Santra, *“Electronic decoherence following photoionization: Full quantum-dynamical treatment of the influence of nuclear motion”*, Phys. Rev. A **95**, 033425 (2017).

[5] B. F. E. Curchod, T. J. Martinez, *“Ab Initio Nonadiabatic Quantum Molecular Dynamics”*, Chem. Rev. **118**, 3305 (2018).

[6] S. Huang et al., *Generating Single-Spike Hard X-Ray Pulses with Nonlinear Bunch Compression in Free-Electron Lasers”*, Phys. Rev. Lett. **119**, 154801 (2017).

[7] A. A. Lutman et. al.*“Experimental Demonstration of Femtosecond Two-Color X-Ray Free-Electron Lasers”*, Phys. Rev. Lett. **110**, 134801 (2013).

[8] A. I. Kuleff, N. V. Kryzhevoi, M. Pernpointner, and L. S. Cederbaum, "*Core Ionization Initiates Subfemtosecond Charge Migration in the Valence Shell of Molecules*", Phys. Rev. Lett. **117**, 093002 (2016).

[9] A. Bruner et. al., *"Attosecond Charge Migration with TDDFT: Accurate Dynamics from a Well-Defined Initial State"*, J. Phys. Chem. Lett. **8**, 3991 (2017).

[10] Z. Li, O. Vendrell, R Santra, *"Ultrafast Charge Transfer of a Valence Double Hole in Glycine Driven Exclusively by Nuclear Motion*", Phys. Rev. Lett. **115**, 143002 (2015).

[11] B. K. McFarland et. al, *"Ultrafast X-ray Auger probing of photoexcited molecular dynamics"*, Nature Communications **5**, 4235 (2014).

[12] R. Boll et. al., *"Charge transfer in dissociating iodomethane and fluoromethane molecules ionized by intense femtosecond X-ray pulses"*, Structural Dynamics **3**, 043207 (2016).

[13] B. Erk et. al., *"Imaging charge transfer in iodomethane upon x-ray photoabsorption*", Science **345**, 288 (2014).

[14] Y. Hao, L. Inhester, K. Hanasaki, S.-K. Son, R. Santra, *"Efficient electronic structure calculation for molecular ionization dynamics at high x-ray intensity"*, Struct. Dyn. **2**, 041707 (2015).

[15] L. Inhester, K. Hanasaki, Y. Hao, S.-K. Son, R. Santra, *"X-ray multiphoton ionization dynamics of a water molecule irradiated by an X-ray free-electron laser pulse",* Phys. Rev. A **94**, 023422 (2016).

[16] Z. Jurek, S.-K. Son, B. Ziaja, R. Santra, *"XMDYN and XATOM: versatile simulation tools for quantitative modeling of X-ray free-electron laser induced dynamics of matter"*, J. Appl. Cryst. **49**, 1048–1056 (2016).

[17] B. F. Murphy et. al., *"Femtosecond X-ray-induced explosion of C60 at extreme intensity"*, Nature Communications **5**, 4281 (2014).

[18] A. Rudenko et al., *"Femtosecond response of polyatomic molecules to ultra-intense hard X-rays"*, Nature **546**, 129-132 (2017).

[19] L. Greenman, R. R. Lucchese, and C. W. McCurdy, *"Variational treatment of electron-polyatomic molecule scattering calculations using adaptive overset grids,"* Phys. Rev. A **96**, 052706 (2017).

Peer-Reviewed Publications Resulting from this Project (Project Start Date: 09/2018)
None to report.

Light-induced modification of electronic interactions and electron-nuclear couplings

PI: Arvinder Sandhu
Department of Physics and College of Optical Sciences
The University of Arizona
Tucson AZ 85721
asandhu@email.arizona.edu

Project Scope

Electron-nuclear couplings and electronic correlations play a central role in determining how the charge and energy get distributed inside molecules and materials. For example, immediately following an excitation event, an electron or a hole can migrate across a molecule on attosecond to few-femtosecond timescales, driven by electronic correlations[1,2]. Concurrently, the coupling between electronic and nuclear degrees of freedom[3] leads to exchange of energy, and eventual transfer of the charge between molecular moieties or across an interface. Important examples of such many-body interaction mediated, ultrafast charge and energy transfer dynamics lie in light harvesting, photo-catalysis, interfacial energy storage, DNA stability etc.

Attosecond spectroscopy forms an ideal tool to study correlation and coupling driven electron dynamics in molecules and materials. Using ultrafast XUV-NIR spectroscopy, PI and coworkers have conducted a number of studies[4–9] to investigate atomic and molecular dynamics using Attosecond Transient Absorption Spectroscopy (ATAS) and Velocity Map Imaging (VMI) techniques. However, typical attosecond spectroscopy schemes employ attosecond extreme-ultraviolet (XUV) pulses in combination with strong near-infrared (NIR) laser pulses to extract the pertinent information. In such measurements, understanding and disentangling the role of strong-field modification is crucial for uncovering the dynamics of interest. We aim to characterize the strong-field electronic couplings, and use them as a tool to tune the interactions that drive electron dynamics in molecules.

Specifically, we will use a tunable multi-pulse pump-probe schemes to study electronic processes, where attosecond XUV excitation will be implemented along with a wavelength-tunable femtosecond infrared (0.6-1.4 eV) pulse for dressing or control. We plan to conduct two main types of experiments: 1) Study of light-induced couplings and electronic interactions 2) Light-induced modification of electron-nuclear couplings. The first topic will study of how light-induced couplings manifest in the attosecond transient absorption and how they could be used to alter the fast dynamics stemming from interaction between electrons, e.g. in atomic and molecular autoionization. The second topic concerns the light-induced modification of electron-nuclear coupling driven dynamics in small polyatomics, e.g. near conical intersections. We will mainly use electron and ion imaging in the latter studies. In this program, the application of tunable IR fields for systematic study of resonant and non-resonant electronic couplings will also lead to new strategies for control over the electron dynamics governed by many-body interactions.

Recent Progress

We made substantial progress on the first topic of our project, i.e. control of dynamics responsible for attosecond transient absorption lineshapes and four-wave-mixing emissions by using tunable

IR light fields. In a recent publication[10], we demonstrated a transient absorption scheme that uses a fixed-spectrum attosecond pulse train in conjunction with a tunable IR probe laser to access a wide range of nonlinear light-atom interactions. We exhibited control over the time-dependent Autler-Townes (AT) splitting of the 1s4p absorption line in helium, and studied its evolution from a resonant doublet to a light-induced sideband with changing probe wavelength. The novelty of these studies is that non-commensurate probe allows for the background-free study of two-IR-photon mediated Four-Wave-Mixing (FWM) emission in a collinear geometry. Using this capability, we observed two different XUV emission pathways with non-trivial delay dependence, one prompt and the other delayed. The peculiar spectral and temporal structure of emission results from contributions from several excited states (e.g. 3s, 3p, 4p). We identified the nonlinear processes underlying these non-intuitive FWM pathways by comparing the experimental results to time-dependent Schrödinger equation based calculations conducted in collaboration with the group of Ken Schafer and Mette Gaarde at Louisiana State University.

The comparison of experimental and theoretical results on the temporal and spectral structure of XUV emissions is shown in the figure 2. Within the framework of the restricted excitation model, specific states can be made ‘invisible’ to the XUV field, so that the coupling to that state from the ground state is set to zero, while still contributing to the IR induced dynamics and to the time-dependent dipole moment. When the 3p state is made XUV-invisible, we refer to the corresponding model as the ‘4p model’ [see panel (c) in Fig. 2], since the population initially promoted to the 4p

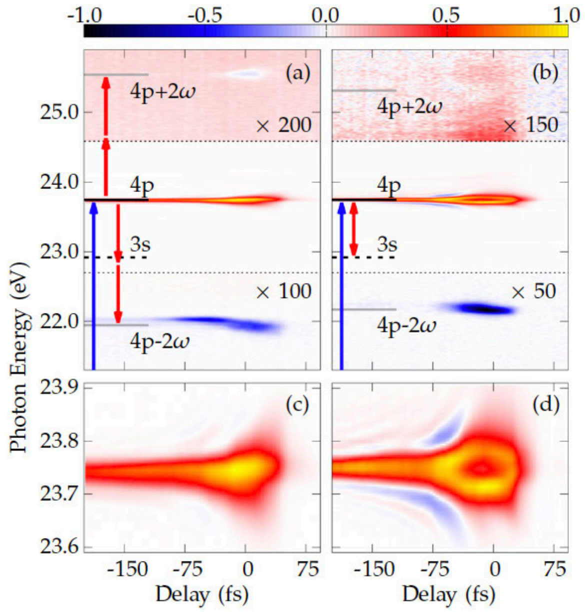

Fig 1. Experimentally obtained delay-dependent transient absorption spectra using a 1380 nm (a,c) or a 1580 nm (b,d) IR probe. Panels (c) and (d) show close-ups of the 4p absorption feature for the two wavelengths. In panel (d) the Autler-Townes (AT) splitting feature is clearly visible. The Four-Wave-Mixing (FWM) emission feature is seen at ~22 eV in panels (a) and (b). In the left side of panel (a) [(b)] a sketch of the light couplings responsible for the FWM [AT] process is shown.

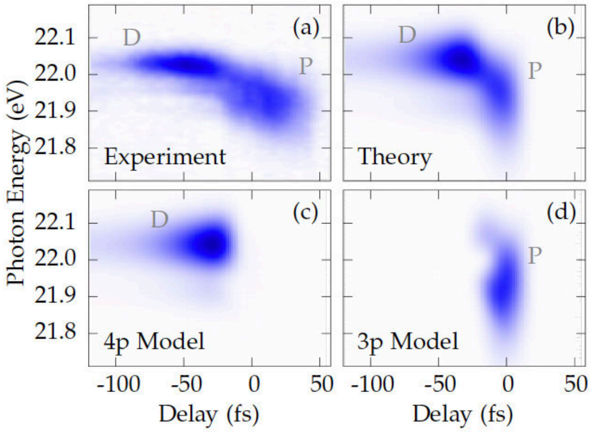

Fig. 2. Experimentally (a) and theoretically (b) obtained delay-dependent transient absorption spectra at 1380 nm showing the FWM emission features. The prompt emission feature centered around zero delay is labeled ’P’ while the delayed feature at -50fs is labeled ’D’. Panels (c) and (d) show spectra calculated in models in which the role of specific states can be identified.

state by the XUV pulse dominates the dynamics of the system in this case. In the same way, the model in which the 4p state is made XUV-invisible is referred to as the '3p model' [see panel (d) in Fig. 2]. It is clear from panels (c) and (d) in Fig. 2 that the delayed feature 'D' is almost uniquely a result of the population initially promoted to the 4p state, while the prompt feature 'P' is almost uniquely a result of the population initially promoted to the 3p state. It is surprising that the 3p state plays any role in the observed dynamics as there is no XUV flux at the 3p energy, and the 3p state is therefore only transiently populated by the XUV field, i.e., no population is left in the 3p state after the XUV pulse is over. This discovery gives us some insight into the delay dependence of the sidebands. Since the feature 'P' depends on the transient population of the 3p state it only appears when the IR and XUV pulses overlap, close to zero delay. The non-transient nature of the 4p population allows the feature 'D' to be located at larger negative delays, while destructive interference during the XUV pulse prevents this feature from appearing close to zero delay.

Future Plans

The tunable IR, and non-commensurate XUV+IR geometry has opened the door for investigation of the effects of laser dressing vis-à-vis the static electronic resonances, without the complication of interferences between various excitation paths stemming from different high harmonics. We are conducting additional experiments to gain insight into the non-linear mechanisms responsible for the fast energy exchange between the multi-electronic systems and the light fields. In the near term, we are focusing on the dynamics of autotionizing states in atoms and molecules, including the optically dark states, which can be accessed with multi-pulse, tunable IR experiments.

The tunable, background-free ATAS spectroscopy technique developed will enhance the attosecond science toolkit by providing new control knobs. We envision that this approach will offer significant advantages in disentangling of the ultrafast dynamics of electrons along the complex manifold of molecular potential energy surfaces, and could also provide information on the lifetimes and coupling strengths for optically dark states. We are also setting up a coincidence detection based VMI system to look at the effects of light-induced couplings on the conical intersection dynamics. These results are expected to shed light on the light-induced modification of relaxation and fragmentation pathways in polyatomics.

The broader goal here is to study if the IR laser induced modification, and the resulting changes in transient absorption line shapes, can be used to characterize the unknown electronic properties of a fast evolving atomic or molecular system. Systematic and focused investigations, aimed at the light-induced modification of correlated and coupled electron dynamics, will provide means for benchmarking the theoretical calculations, and guide the design of next generation of experiments. The research proposed here will also provide strategies for controlling the charge and energy redistribution in molecules, which can in-turn enable the development of transformative solutions for light harvesting, energy conversion, and catalysis – topics that are clearly of immense importance to the society.

References Cited

(1) Kuleff, A. I.; Cederbaum, L. S. Ultrafast correlation-driven electron dynamics. *J. Phys. B-Atomic Mol. Opt. Phys.* **2014**, *47* (12), 124002.

(2) Sansone, G.; Pfeifer, T.; Simeonidis, K.; Kuleff, A. I. Electron Correlation in Real Time. *ChemPhysChem* **2012**, *13* (3), 661–680.

(3) Li, Z.; Vendrell, O.; Santra, R. Ultrafast Charge Transfer of a Valence Double Hole in Glycine Driven Exclusively by Nuclear Motion. *Phys. Rev. Lett.* **2015**, *115* (14), 143002.
(4) Shivaram, N.; Timmers, H.; Tong, X. M.; Sandhu, A. Attosecond-resolved evolution of a laser-dressed helium atom: Interfering excitation paths and quantum phases. *Phys. Rev. Lett.* **2012**, *108* (19), 193002.
(5) Timmers, H.; Shivaram, N.; Sandhu, A. Ultrafast dynamics of neutral superexcited Oxygen: A direct measurement of the competition between autoionization and predissociation. *Phys. Rev. Lett.* **2012**, *109*, 173001.
(6) Timmers, H.; Li, Z.; Shivaram, N.; Santra, R.; Vendrell, O.; Sandhu, A. Coherent Electron Hole Dynamics Near a Conical Intersection. *Phys. Rev. Lett.* **2014**, *113* (11), 113003.
(7) Liao, C.-T.; Sandhu, A.; Camp, S.; Schafer, K. J.; Gaarde, M. B. Beyond the Single-Atom Response in Absorption Line Shapes: Probing a Dense, Laser-Dressed Helium Gas with Attosecond Pulse Trains. *Phys. Rev. Lett.* **2015**, *114* (14), 143002.
(8) Liao, C. T.; Sandhu, A.; Camp, S.; Schafer, K. J.; Gaarde, M. B. Attosecond transient absorption in dense gases: Exploring the interplay between resonant pulse propagation and laser-induced line-shape control. *Phys. Rev. A* **2016**, *93* (3), 033405.
(9) Liao, C. T.; Li, X.; Haxton, D. J.; Rescigno, T. N.; Lucchese, R. R.; McCurdy, C. W.; Sandhu, A. Probing autoionizing states of molecular oxygen with XUV transient absorption: Electronic-symmetry-dependent lineshapes and laser-induced modifications. *Phys. Rev. A* **2017**, *95*, 043427.
(10) Harkema, N.; Bækhøj, J. E.; Liao, C.-T.; Gaarde, M. B.; Schafer, K. J.; Sandhu, A. Controlling attosecond transient absorption with tunable, non-commensurate light fields. *Opt. Lett.* **2018**.

Peer-Reviewed Publications Resulting from this Project (Project Start Date: 08/2017)

1) Nathan Harkema, Jens Baekhoj, Chen-Ting Liao, Mette Gaarde, Ken Schafer, Arvinder Sandhu, "Controlling attosecond transient absorption with tunable, non-commensurate light fields", *Optics Letters* **43**, 3357-3360 (2018).

Transient Absorption and Reshaping of Ultrafast Radiation

DE-SC0010431

Kenneth J. Schafer (schafer@phys.lsu.edu)
Mette B. Gaarde (gaarde@phys.lsu.edu)

Department of Physics and Astronomy, Louisiana State University
Baton Rouge, LA 70803

September 2018

Project Scope

Our program is centered around the theoretical study of transient absorption of ultrafast extreme ultraviolet (XUV) radiation by atoms and materials interacting with a precisely synchronized near-to-mid infrared (IR) laser pulse, and emphasizes both fundamental theoretical research and a close connection with experimental groups doing attosecond physics. Transient absorption spectroscopy can in principle provide high spectral resolution and high (attosecond) time resolution simultaneously, by spectrally resolving the light transmitted through a sample as a function of delay between the dressing laser pulse and the broadband attosecond EUV probe. As in all transient absorption scenarios, one of the main challenges we confront is the extraction of time-dependent dynamics from delay-dependent information. In addition, we must also account for the reshaping of the broadband XUV light in the macroscopic medium. We study attosecond transient absorption (ATA) using a versatile theoretical treatment that takes account of both the laser-matter interaction at the atomic level via the time-dependent Schrödinger equation (TDSE), as well as propagation of the emitted radiation in the non-linear medium via the Maxwell wave equation (MWE), often in the single-active electron (SAE) approximation [1]. We have also extended our TDSE/MWE treatment in atoms to fully-active two electron calculations in helium, in both full and reduced dimensions [2]. More recently we have also started considering attosecond transient absorption and reflection in condensed phase systems.

Recent Progress

We have completed a number of research projects, several of them in collaboration with experimental groups carrying out ATA measurements, see [R1-R5] and [2–4]. We have also recently published an *Topical Review* in *Journal of Physics B* [R3] that summarizes and places in context many of the ATA results obtained in the course of our work on this topic. In this abstract we focus on our two most recent collaborations:

(1) Transient grating spectroscopy involving light-induced resonances in helium: In collaboration with the Leone/Neumark experimental group at UC Berkeley we have studied ultrafast transient grating spectroscopy in a helium gas interacting with an XUV beam and two IR beams intersecting the XUV beam at small angles. This leads to a number of four- six- and higher-order-wave mixing processes that appear as emission signals off axis in the far field, at energies corresponding to the 1snp resonances as well as those of light-induced states (LIS) (see Fig. 1(a,b)). We have in particular studied the higher-order mixing processes located approximately one IR photon below the 1s3d dark (non-dipole allowed) state, i.e. the 3d- LIS. A well-known alternative picture of the four- and higher-order wave mixing processes is that they represent the first and higher-order side peaks diffracted from a transient grating formed in the medium by the XUV and the crossed IR beams.

In this work we have shown, for the first time to the best of our knowledge, an intrinsic delay between the different diffraction orders, for both the 1snp and the LIS features. For example, theory shows directly that the third order LIS peak appears about 3 fs later than the first order peak (Fig. 1(e)). In the experiment, this is manifested as a 3 fs difference in the delay-dependence of these two peaks (Fig. 1(d)), and an order-dependent AC Stark shift of the LIS peaks in the frequency domain (Fig. 1(a)). The order-dependent shift

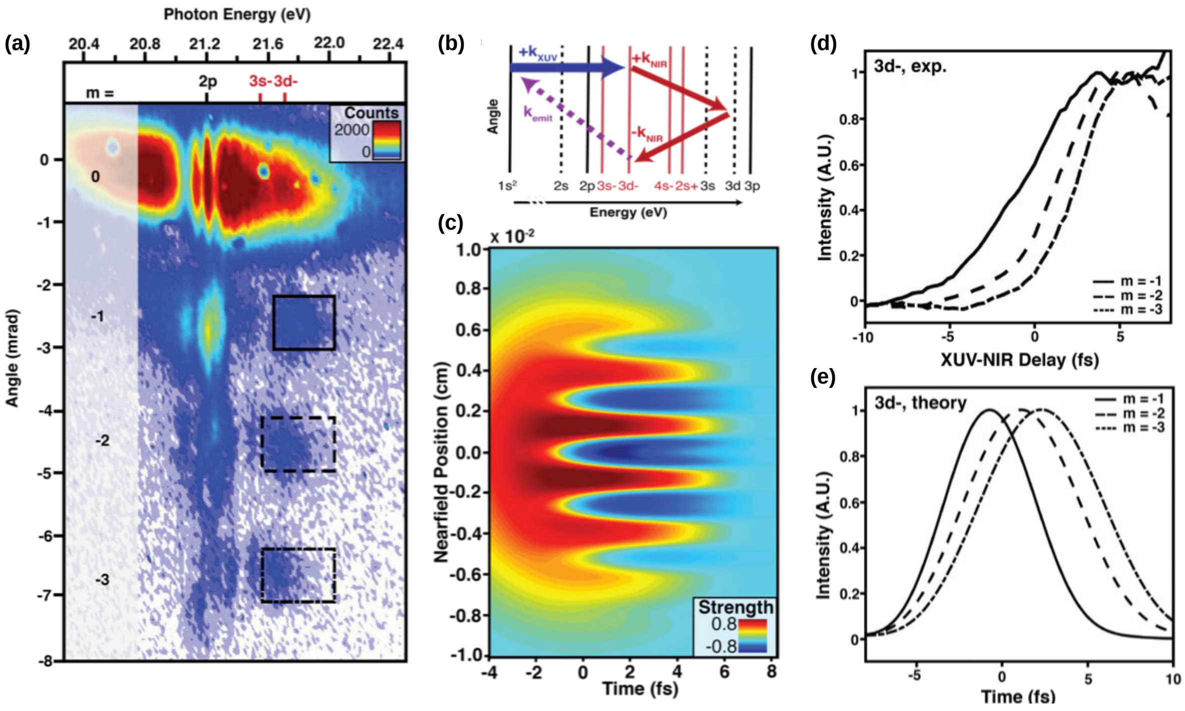

Figure 1: (a) XUV spatiospectral emission profile after interacting with He gas dressed by two crossed IR beams. On axis the XUV light is absorbed, but off axis three higher-order emission peaks are visible near the 2p and the 3d- energies, marked as m=-1 to -3. The 3d- peaks are blue-shifted relative to the field-free 3d- energy marked on the top axis and the blue shift decreases with increasing order. (b) Wave-mixing picture of the process leading to the m=-1 peak, involving two IR photons. (c) The space- and time-dependent AC Stark shift leads to a phase accumulation in the time-dependent dipole moment which causes a grating-modulation of the 3d- emission amplitude illustrated here. The depth of the modulation increases with time as the phase is accumulated. (d,e) Delay (d) and time (e) dependence of the different order 3d- peaks as measured in the experiment (d) or calculated by theory (e). The difference is appearance time can be understood by considering the build-up of the grating in (c): a weak grating scatters only the low orders, whereas a more strongly modulated grating will scatter the higher orders as well. Adapted from [3].

is a direct consequence of the delayed appearance of the higher orders, which means that their effective interaction time with the IR field (which controls the accumulation of the AC Stark phase) is reduced. We have also found that the order dependence of the appearance time can be understood using a simple phase-grating idea: the crossed IR beams means that the XUV-excited atoms accumulate an AC Stark phase in the form of a grating in the transverse direction. The phase grating leads to a modulation of the amplitude of the emitted light (Fig. 1(c)). The depth of this modulation (amplitude grating) controls the relative efficiency of the different diffraction orders in the far field, so that a weakly modulated grating predominantly scatters into the zeroth and first orders, whereas a better-defined grating also scatters into the higher orders. This work is currently under review [3].

(ii) **ATA spectroscopy with a variable-wavelength IR control field:** In collaboration with the Sandhu experimental group at U Arizona (see also [R2]), we studied ATA spectroscopy in which the dressing laser field is tunable, in the mid-IR region between 1300 and 1600 nm. The XUV field was an attosecond pulse train (APT), synthesized from a few harmonics of an 800nm laser field, and the target He gas thus interacted with non-commensurate XUV and IR frequencies. This scenario is interesting for several reasons: (a) The variable IR wavelength controls whether pairs of excited states are in or out of resonance with each other, and (b) It allows for background free detection of IR-induced signals. This work in particular focused on the evolution of the laser dressed 1s4p line in He, from a symmetric Autler-Townes doublet on resonance (with the lower-lying 1s3s state) to a light-induced sideband as the wavelength was varied. This work has been published in Optics Letters [R5].

Future Plans

Several projects are in progress or planned for the near future:

(i) *Influence of resonant pulse propagation in transient grating spectroscopy:* Continuing the work in [3], we are interested in the effects of resonant pulse propagation (RPP) on the transient grating build-up discussed above. RPP refers to temporal and spectral reshaping of an ultrafast pulse propagating through a medium with a long-lived resonance, and has in particular been studied near the strong 2p resonance in helium (see e.g. [R5]). We are interested in the extent to which RPP influences the 3d- emission, either on its own or through the strong reshaping of the nearby 2p emission.

(ii) *Signature of excitons in condensed phase attosecond transient reflection:* Also in collaboration with the Leone group, we consider ultrafast electron dynamics in a condensed phase system interacting with a dressing IR pulse, using attosecond transient reflectivity. We are interested in the signatures of excitonic states in the vicinity of the band gap, in particular whether there is evidence of light-induced couplings between bright and dark excitonic states, similar to those seen in atomic and molecular systems.

(iii) *Probing nonlinear Stark shifts with opto-optical phase modulation:* Continuing the work in [R4], we have investigated spatial manifestions of bound-state linear and nonlinear AC Stark shifts via opto-optical modulation (OOM). We find that for some dressing-laser parameters, the Stark shift of the 1s2p state is highly nonlinear, and that this behavior can be traced by to a two-IR-photon resonance between the 1s2p state and high-lying 1snf states.

Peer-Reviewed Publications Resulting from this Project (2016-2018)

R1 X. Li, D. J. Haxton, M. B. Gaarde, K. J. Schafer, and C. W. McCurdy, *Direct extraction of intense-field-induced polarization in the continuum on the attosecond time scale from transient absorption*, **Phys. Rev. A** 93, 023401 (2016).

R2 C.-T. Liao, A. Sandhu, S. Camp, K. J. Schafer, and M. B. Gaarde, *Attosecond Transient Absorption in Dense Gases: Exploring the Interplay between Resonant Pulse Propagation and Laser-Induced Line Shape Control*, **Phys. Rev. A** 93, 033405 (2016).

R3 M. Wu, S. Chen, S. Camp, K. J. Schafer, and M. B. Gaarde, *Topical Review: Theory of strong-field attosecond transient absorption*, **J. Phys. B** 49, 062003 (2016).

R4 S. Bengtsson, E. W. Larsen, D. Kroon, S. Camp, M. Miranda, C. L. Arnold, A. L'Huillier, K. J. Schafer, M. B. Gaarde, L. Rippe, and J. Mauritsson, *Controlled free-induction decay in the extreme ultraviolet*, **Nature Photonics**, 11, 252 (2017).

R5 N. Harkema, J. E. Bækhøj, C.-T. Liao, M. B. Gaarde, K. J. Schafer, and A. Sandhu, *Controlling attosecond transient absorption with tunable, non-commensurate light fields*, Opt.Lett. **43**, 3357 (2018).

References

[1] Mette B. Gaarde, Christian Buth, Jennifer L. Tate, and Kenneth J. Schafer. Transient absorption and reshaping of ultrafast XUV light by laser-dressed helium. *Phys. Rev. A*, 83(1):013419, January 2011.

[2] X. Guan, M. Wu, M. B. Gaarde, and K. J. Schafer. Correlated attosecond transient absorption in helium atoms above the first ionization threshold. In preparation, 2018.

[3] A. P. Fidler, S. J. Camp, E. R. Warrick, E. Bloch, H. J. B. Marroux, D. M. Neumark, K. J. Schafer, M. B. Gaarde, and S. R. Leone. Nonlinear XUV Signal Generation Probed by Attosecond Transient Grating Spectroscopy. Submitted, 2018.

[4] E. Simpson, S. Bengtsson, S. J. Camp, M. B. Gaarde, K. J. Schafer, and J. Mauritsson. Probing nonlinear Stark shifts with opto-optical phase modulation. In preparation, 2018.

Page is intentionally blank.

Coherent Probes of Charge Migration

Science Using Ultrafast Probes: DE-SC0012462

Kenneth Schafer[1,*], Mette Gaarde[1], Kenneth Lopata[2],
Louis DiMauro[3], Pierre Agostini[3], Robert Jones[4]
1) Department of Physics and Astronomy, Louisiana State University, Baton Rouge, LA
2) Department of Chemistry, Louisiana State University, Baton Rouge, LA
3) Department of Physics, The Ohio State University, Columbus, OH
4) Department of Physics, University of Virginia, Charlottesville, VA

*schafer@phys.lsu.edu

Project Scope

When forced out of equilibrium, electrons in matter can respond exceedingly fast, on time-scales approaching the attosecond. At this time scale, the dynamics are inherently quantum, and they are not yet impacted by the weaker coupling to a system "bath" that involves large numbers of additional degrees of freedom. This potentially complex quantum evolution can expose correlations between electrons and holes that are otherwise hidden in the static properties of the system. These correlations, and the dynamics they evoke, are of great importance as they can impact fundamental processes, such as charge transport and photoelectric energy conversion. From the perspective of furthering basic science or a desire to optically manipulate the outcome of a reaction, one needs to understand how and when attosecond electron-hole dynamics initiate, drive, or steer physical or chemical processes, which typically occur on much longer time scales. For example, in chemical reactions involving polyatomic molecules, are such attosecond charge migration dynamics relevant, or are they simply averaged over during the slower nuclear motion on which the reactions usually depend [Remacle 2006, Stolow 2013, Lépine 2014]?

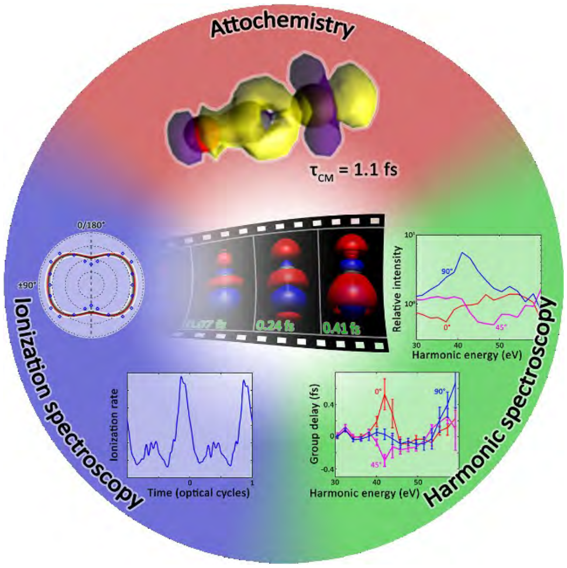

Figure 1: The ATTO-CM network is organized around three main thrusts: (i) Attochemistry, (ii) high harmonic spectroscopy, and (iii) frequency-matched ionization spectroscopy. In the figure we illustrate these thrusts with recent experiments and theory on OCS molecules: (top) Calculations of charge migration modes, (right) measurements of the amplitude and phase of harmonics from aligned OCS, and (left) measurements and calculations of ionization from aligned OCS.

The ATTO-CM team is focused on developing and applying coherent probes to directly characterize correlation-driven ultrafast charge migration dynamics that are initiated by different means across molecular families. In this context, charge migration refers to the rapid movement (femtosecond or faster) of positively charged holes in a molecule following localized excitation or ionization. Understanding the mechanisms of this migration, and developing experimental tools for observing it, is crucial to advancing ultrafast science and potential applications across disciplines. The objective of the ATTO-CM team is to advance ultrafast science in the US, both at small- and large-scale facilities, using a concerted effort of theorists and experimentalists, as illustrated in Figure 1. Enabled by an integrated relationship between theory and experiment, our emphasis is on the implementation of high-harmonic spectroscopy and frequency-matched ionization spectroscopy as coherent probes of charge migration dynamics in chemical systems. Our ultimate goal is to develop experimental probes that can provide direct access to specific time-resolved information in a manner that does not require sophisticated modeling for interpretation. For practical implementation, part of our focus has been to identify parameters to probe and control those dynamics, *e.g.*, molecular alignment and/or functionalization of the target. The initial experiments are laboratory based but experiments on large-scale facilities, like LCLS, are envisioned for the future.

Recent Progress

As illustrated in Figure 1, in our effort to understand and observe charge migration with strong laser fields we have identified three main thrusts on which we have focused our efforts: "Attochemistry picture of charge migration", "High-harmonic spectroscopy (HHS)", and "Frequency-matched Ionization spectroscopy (FIS)". As demonstrated in what follows, all three nodes of the ATTO-CM network are closely involved in each of the three thrusts defining our program. In brief, our key recent results are:

1. Thrust 1: Attochemistry picture of charge migration – We have validated TDDFT as a means to simulate attosecond charge migration and constructed the necessary tools to quantify and characterize the migration dynamics [Bruner 2017]. We have developed an algorithm to identify relevant charge-migration modes, developed metrics to characterize these modes, and found a universal ≈ 2 bond per femtosecond speed for that migration in conjugated molecules [Bruner 2018].
2. Thrust 2: High-harmonic spectroscopy (HHS) – We have demonstrated HHG as a spectroscopic tool to access target-specific information, both in the spectral amplitude and phase, in unaligned [Scarborough 2018] and aligned [Gorman 2018] molecules. We have developed models, both at the ab-initio (TDDFT) and the conceptual levels to reproduce and interpret experimental results.
3. Thrust 3: Frequency-matched ionization spectroscopy (FIS) – We have obtained intensity- and angle-dependent ionization yields for a range of molecules, with matching experimental and theoretical results [Sándor 2018a, Sándor 2018b]. Numerically, we have established alignment-controlled strong-field ionization as a means to initiate and control electron-hole localization in molecules following strong-field ionization. We have established THz-field enhancement using micro-structured metals [Khatri 2018], with possible applications for molecular orientation.

Thrust 1: Attochemistry picture of charge migration

Thrust 1 of the ATTO-CM network focuses on the chemical mechanisms that support charge migration in molecules, which we shorthand as "attochemistry". Briefly, using first-principles methods, we have simulated attosecond charge migration in a cyclic molecule and demonstrated that TDDFT can capture charge migration dynamics [Bruner 2017] by comparison to benchmark results in the literature. Following this, we developed an algorithm to identify the relevant charge-migration modes from the dynamics and found a "universal" ≈2 bonds per femtosecond speed for the migration in a range of conjugated molecules. A joint manuscript between all nodes of the ATTO-CM network describing these results will be submitted soon [Bruner 2018]. Our attochemistry developments are informed and guided by experimental efforts on high-harmonic (Thrust 2) and frequency-matched (Thrust 3) spectroscopies discussed in the following sections.

Time-dependent density-functional theory (TDDFT) offers a good tradeoff between accuracy and computational efficiency, as found in many studies of spectral properties. The accuracy of TDDFT for correlation-driven electron dynamics is less well documented. Here a fundamental limitation may arise when using an adiabatic (local-in-time) approximation for the exchange-correlation functional. To address this issue, we recently validated TDDFT for the case of X-ray triggered valence charge migration [Bruner 2017], using Gaussian basis sets and hybrid exchange-correlation functionals. From a simulation standpoint, core-electron-hole initial states are simpler to prepare than valence holes, as they can be constructed from knowledge of a single orbital. This offers a simple test for the accuracy of the TDDFT method for describing charge migration without ambiguities related to the choice of initial state. In [Bruner 2017] we showed that TDDFT with a hybrid functional (PBE0) gives excellent agreement with benchmark fourth-order algebraic diagrammatic construction (ADC(4)) results, whereas generalized gradient approximation functionals (*e.g.*, PBE) qualitatively fail.

After this first validation of TDDFT for attochemistry, we performed similar computations in a range of molecules. As an important first step towards predicting which molecules can support charge migration, we have developed tools for identifying and characterizing charge-migration modes from within the complete manifold of excitations of a rapidly ionized molecule [Bruner 2018]. In a numerical simulation, sudden ionization (core-hole, strong-field ionization, etc.), acts as a broadband pump and typically creates multiple modes of electron dynamics. The charge migration mode analysis algorithm allowed us to (i) separate these modes in frequency, and (ii) sort out "interesting" charge-migration modes in space, which involve particle-like movement of a localized hole from one end of the molecule to another, from less-interesting localized excitations, which typically also occur at higher frequencies.

The algorithm to disentangle charge-migration modes, and distinguish between migration and non-migration ones, is based on spatial Fourier analysis of the hole motion. In essence, it involves four steps: (i) triggering dynamics with a rapid ionization that reflects a particular process (*e.g.*, orbital populations extracted from a strong-field ionization calculation), (ii) propagating the density over a few periods of motion, (iii) Fourier transforming the hole density to identify the modes, and (iv) constructing hole migration maps for each observed mode. These migration maps correspond to the Fourier transform of the hole density at the relevant charge-migration frequency. They show the spatial extent of the hole at the two extremes of the migration process – purple and yellow volumes, respectively, in the right column of Figure 2. In this representation, charge migration corresponds to maps with two separated hole (+) and electron (-) regions with significant populations. In the time domain, the charge then periodically migrates from the negative to positive region and back. On the other hand, maps with several small hole regions and a large electron region are indicative of a non-migrating, localized excitation.

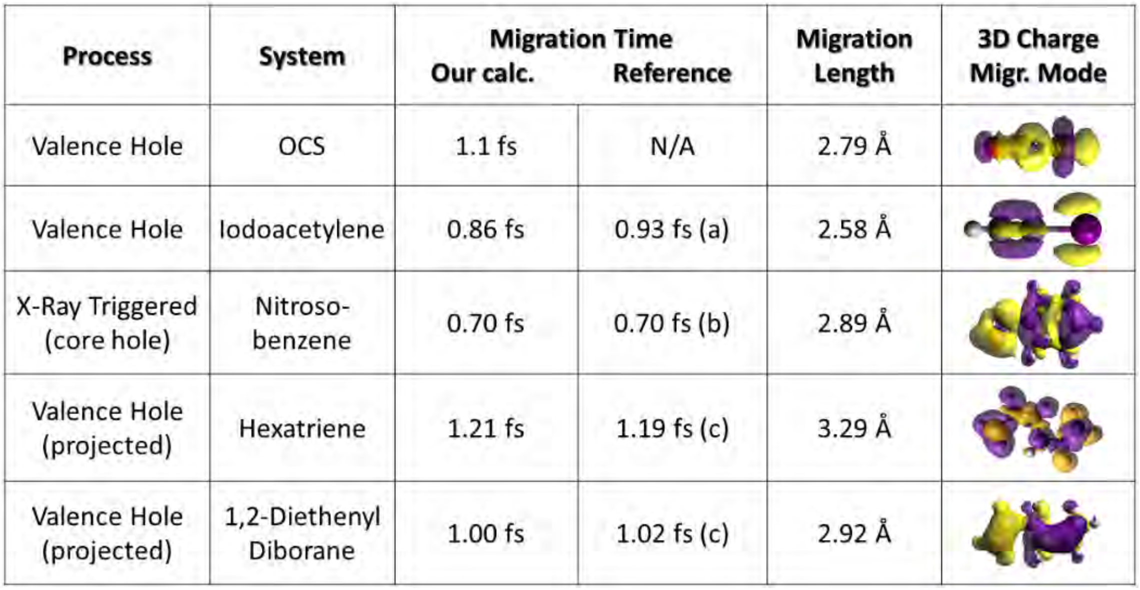

Process	System	Migration Time Our calc.	 Reference	Migration Length	3D Charge Migr. Mode
Valence Hole	OCS	1.1 fs	N/A	2.79 Å	
Valence Hole	Iodoacetylene	0.86 fs	0.93 fs (a)	2.58 Å	
X-Ray Triggered (core hole)	Nitroso-benzene	0.70 fs	0.70 fs (b)	2.89 Å	
Valence Hole (projected)	Hexatriene	1.21 fs	1.19 fs (c)	3.29 Å	
Valence Hole (projected)	1,2-Diethenyl Diborane	1.00 fs	1.02 fs (c)	2.92 Å	

Figure 2: Charge migration modes for a selection of molecules and ionization processes. Our calculated migration times (TD-PBE0) agree well with experimental – (a) [Kraus 2015] – and computed values – (b) [Kuleff 2016], (c) [Dutoi 2011]. The 3D migration maps show the spatial extent of the hole at the two extremes of the charge migration process. For example, in iodoacetylene the hole starts on iodine (yellow; shaped like a p-orbital) and moves to the C≡C (purple, π-like) after ≈0.9 fs.

From the spatial (migration map) and spectral (frequency) information, we also defined a set of metrics that are relevant to measuring charge migration [Bruner 2018]. These include

- Migration time: The time scale for a hole to move across a molecule dictates the coherent probe necessary to observe the dynamics in harmonic and ionization spectroscopies (*e.g.*, the harmonic order, choice of driving wavelength, etc. – see Thrusts 2 and 3 below).
- Migration length: Larger distances are likely to yield better resolved signatures for the different molecular sites visited by a given migrating mode. These would then be more easily tagged in time-resolved spectroscopy (see, *e.g.*, the discussion in Thrust 2 below).

- Hole localization: Along a similar idea, a localized hole is more particle-like and likely easier to observe. It would yield strong target-site sensitivity, compared to a delocalized hole with averaged contribution from several active regions of the molecule.

In Figure 2, we compare these metrics for various molecular targets. Wherever experimental or theoretical reference is available, our computed migration times are in excellent agreement with the literature (see caption). Moreover, we observe a roughly universal hole travel speed of ≈2 bonds per femtosecond in conjugated molecules.

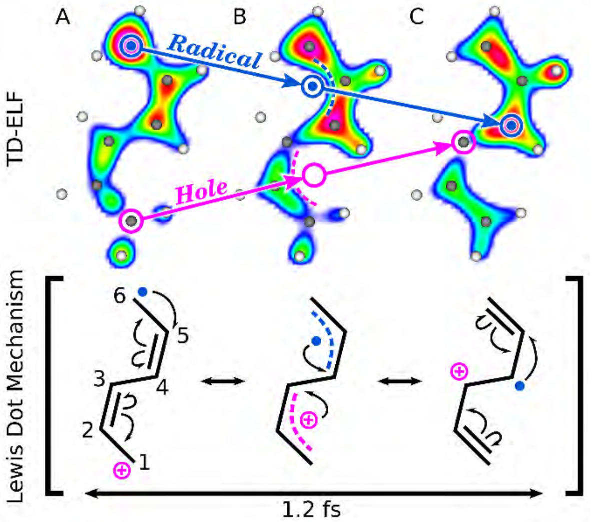

Figure 3: Snapshots of hole dynamics following ionization from the bottom π-orbital of hexatriene. The electron localization function from the TDDFT simulation (top) and the corresponding Lewis-dot resonance structures (bottom) show the mechanism of hole migration [Bruner 2018].

In the attochemistry framework, and building on our finding of a universal migration speed, we have developed a mechanistic picture of charge migration. For instance, narrow-pass filtering the dynamics around a charge-migration mode frequency allows us to directly observe the time-evolution of the corresponding mode. This includes calculating both the hole density, as well as the electron localization function (TDELF), which can be used to interpret the dynamics in terms of the shuffling of bonds and lone pairs [Bruner 2017]. This picture offers the potential for predicting promising candidates for charge-migration investigations based on simple chemical principles, *e.g.*, using the electron-pushing mechanisms familiar from organic chemistry. For example, from our work in nitrosobenzene [Bruner 2017] and hexatriene [Bruner 2018], we know that the charge migration occurs via a shuffling of the double bonds in the system (see Figure 3). This suggests that conjugation can facilitate charge migration, analogous to molecular conductivity. Generalizing this, chemical modification (*e.g.*, breaking the conjugation) or functionalization with electron/hole acceptors/donors can potentially be used to control the migration.

Thrust 2: High-harmonic spectroscopy (HHS)

As illustrated in Figure 1, Thrust 2 of the ATTO-CM network focuses on HHG as a spectroscopic tool for probing charge migration. With our ability to extract target-specific information [Scarborough 2018], we have performed high-resolution angularly-resolved HHS of three linear molecules – CO_2, N_2O and OCS. For each target, we characterized the spectral amplitude and phase in the vicinity of the two-center interference, both in OSU measurements and LSU computations. A joint manuscript, between all nodes of the network, is in preparation [Gorman 2018] and a second joint paper, with more details on the new theoretical methods we have developed for calculating HHS signals, is being prepared. The close contact between the nodes, through frequent Skype meetings and emails, has been instrumental in combining experimental and theoretical efforts.

Building on the attochemistry picture of charge migration as the shuffling of electron/hole across the molecule (Thrust 1 above), *e.g.*, between two ends with possibly different atomic properties, a requirement for successful implementation of HHS is the identification of well-understood features that can be tagged to each such center. While the charge migration dynamics unfolds, each tag would then encode the time-dependence with site-specificity within the target. To this end, we have developed methods which remove the dominant generic component – the "attochirp" – from our HHS phase (group delay) measurements. Applied to CH_3Cl, we demonstrated full characterization of a molecular Cooper minimum [Cooper 1962], both in spectral amplitude and phase in a publication including all three nodes of the ATTO-CM network [Scarborough 2018]. We found that the Cooper minimum feature is dominantly a result of the Cl contribution to the HOMO of CH_3Cl and that it can be identified as one such "tag" that can be used to study charge migration via HHS.

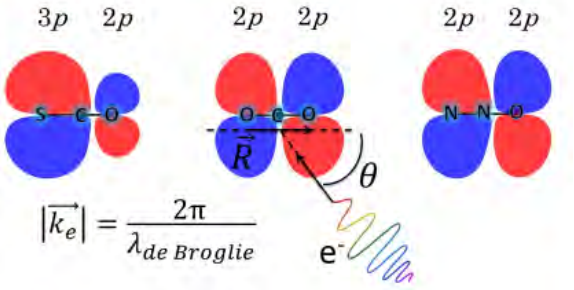

Figure 4: Two-center interference of a recolliding electron with de Broglie wavelength λ_e in OCS, CO_2 and N_2O. Compared to the other two targets, the 3p-like structure of OCS HOMO, on the S site, imprints unique features to the outgoing HHG signal.

Next, we investigated interference between the contributions of different spatially-separated tagged sites visited by a migrating charge. This type of interference is typically referred to as two- or multiple-center interference. In a charge migration context, the interferometric condition is controlled by time. To begin, here we focus on static – time-independent – two-center interference in the recombination dipole and use molecular alignment (with respect to the laser polarization) to modulate the interference condition. In this framework, ignoring the recombination amplitudes, destructive interference of a recolliding electron with wavevector magnitude $|\boldsymbol{k}_e| = 2\pi/\lambda_e$ (λ_e is the de Broglie wavelength) on the two centers separated by distance R, and molecular alignment angle θ, is given by [Etches 2011]

$$|\boldsymbol{k}_e|R\cos\theta + \varphi_2(\theta,\boldsymbol{k}_e) - \varphi_1(\theta,\boldsymbol{k}_e) = (2m+1)\pi \tag{1}$$

for m integer, see Figure 4. Here $\varphi_2 - \varphi_1$ is interpreted as the recombination dipole phase difference between the two centers.

Concerted theory-experiment two-center interference investigations were carried out in OCS and CO_2. In the experiments, N_2O was also used as a control to rule out effects from the permanent dipole of OCS. As shown in Figure 4, all three targets have similar HOMO structure, consisting largely of atomic 2p and 3p character. In the context of Eq. (1), $\varphi_2 - \varphi_1$ is the phase difference between these two atomic contributions. The choice of OCS as a target was motivated by ionization spectroscopy measurements discussed in Thrust 3 below.

Experimental results from the two-center HHS studies are shown in Figure 5. Harmonic spectra (upper row) and group delay (lower) were measured for all three molecules as a function of the time delay of the alignment pulse and the HHG pulse; this is equivalent to a measurement at different molecular rotation angles relative to the laser polarization. While the CO_2 and N_2O results are similar in both the spectral intensities and group delays (both showing negative group delays at all alignment angles), OCS is an outlier in several ways. In the unaligned sample, represented here in OCS by HHG-alignment delay times less than 41 ps, the spectrum of OCS drops sharply by 40 eV, and remains weak up through the cutoff near 60 eV. In the aligned OCS samples (≈43 ps), the deepest minima in the spectra do not occur at 0°, as in the case of CO_2 and N_2O. Finally, the angle-dependent group delays of OCS change sign with varying angles. Because the two centers in CO_2 and N_2O are comprised of very similar 2p atomic contributions, we attribute both

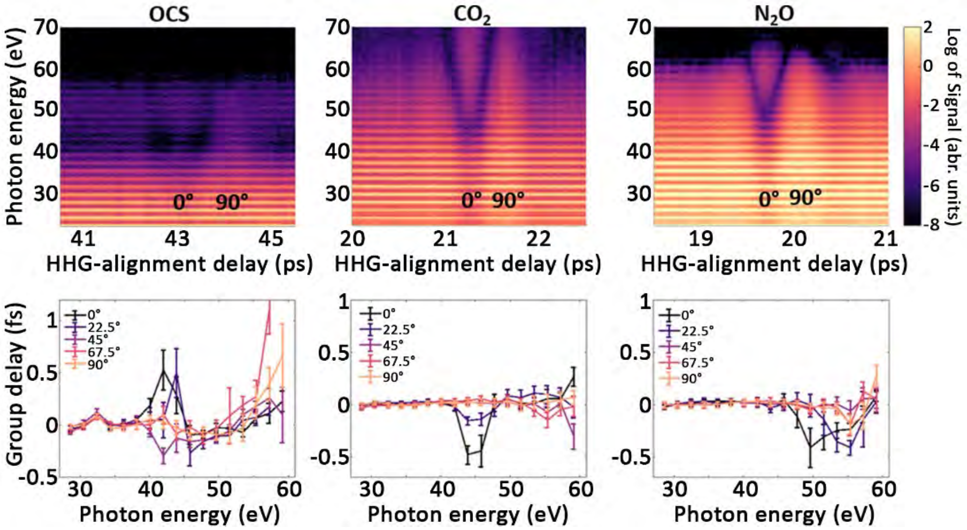

Figure 5: Two-center interferences of OCS, CO_2, and N_2O. The interferences between lobes of the HOMO orbitals of OCS, CO_2, and N_2O produce minima in the harmonic spectra (upper row) at different angles; these minima are associated with structures in the group delays (lower row).

the spectral and group delay features in these molecules to be indicative of the geometric contribution $|\boldsymbol{k}_e| R \cos\theta$ to the phase of the two-center interference. Deviations from these trends in OCS are attributed to the site-specific contribution from the 3p orbital of S.

On the theory side, LSU has performed calculations both at the ab-initio and the conceptual level to reproduce and interpret the OSU experimental results. A challenge for all single-molecule computations of HHG is the inherent interference between multiple quantum-path contributions to the HHG process [Lewenstein 1995]. This is, in particular, an issue when one is attempting to extract structural and/or dynamical information from the spectral amplitude and phase. To this end we have developed and implemented a range of signal isolation and processing techniques, to be detailed in a future paper.

In a top-down approach, we have performed ab-initio TDDFT calculations using the Octopus package [Andrade 2015] to calculate the angle-dependent harmonic spectra in CO_2 and OCS. We use a 1500 nm, 6×10^{13} W/cm^2 laser field in combination with a weak attosecond pulse train (APT) consisting of harmonics 9-17 of the mid-infrared (MIR) laser. The APT dominates the ionization step in the HHG process, which strongly enhances the short quantum-path contribution, thereby suppressing sub-cycle interference effects [Schafer 2004]. In addition, we consider the HHG response only in the first half-cycle after the MIR field has been ramped up to its peak value. The resulting angle dependent spectral yields (Figure 6) show clear evidence of a destructive interference feature that shifts upward in energy with increasing angle, in good agreement with the expectation from the molecular geometry.

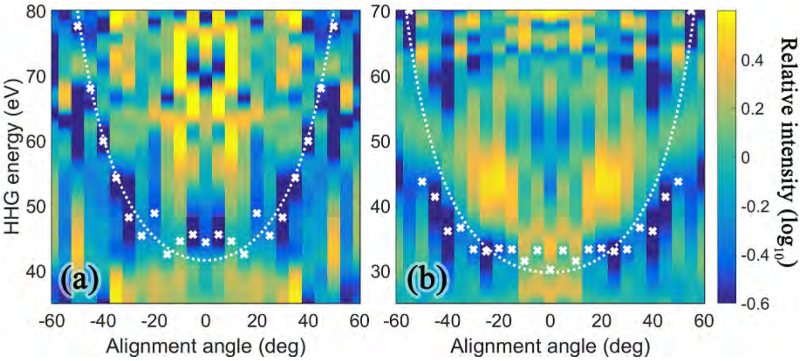

Figure 6: Angle-dependent spectral yields in (a) CO_2 and (b) OCS, normalized by intensity average over shown angles. Dashed, white lines show the geometric expectation for the location of the two-center minimum, given 0° values of (a) 42 eV and (b) 30 eV. Crosses mark the angle-dependent location of the local spectral minimum closest to the white line.

To extract the spectral phase, we additionally employ either time-frequency reassignment (TFR) [Auger 2013], which allows us to directly read the group delay of the TDDFT-calculated signal, or a quantitative rescattering (QRS) approach [Lin 2010] including a reference computation, from which we can extract the molecule-specific spectral amplitude and phase. Both techniques are limited by our ability to (i) generate clean signals where short trajectories have been selected by the APT seed, and (ii) filter out other unwanted contributions that clutter the signal of interest. Overall, we have made good progress in our ability to isolate such target-specific spectral information, as illustrated in Figure 6.

Alternatively, in a bottom-up approach, we have developed a conceptual two-center model to explain the main features of the OSU measurements. For CO_2 and N_2O, we build a model harmonic spectrum with a feature in amplitude and phase that moves upward in energy with molecular orientation angle. The width and depth of the amplitude minimum and the phase rotation at 0° are taken from experiment. This gives good qualitative agreement with experimental results at other angles. To model the S-site 3p contribution in OCS, we add an angle-independent feature to the model, similarly using parameters from the experiment, and again we find qualitative agreement with OSU measurements. Beyond the three targets considered here, we expect such conceptual models to shed light on and guide our understanding of how charge-migration dynamics imprints itself into HHG spectra.

Thrust 3: Frequency-matched ionization spectroscopy (FIS)

Frequency-matched ionization spectroscopy (FIS) refers to the notion of using multiple ionization for coherently probing hole dynamics induced by single ionization. More generally, work under Thrust 3 of the ATTO-CM network addresses strong-field single and multiple ionization from aligned and oriented molecules. Strong-field ionization is at the core of all the research within the network, both as the first step in HHG and as a potential means for inducing and probing charge migration dynamics. In this context, we have extracted intensity- and angle-dependent ionization yields for different molecules, both from UVa measurements and LSU computations. A joint manuscript on OCS, involving all nodes of the network, has been accepted for publication [Sándor 2018a]. A second joint manuscript, investigating the role of functionalization in the CH_3X (X halogen) family, is currently in preparation [Sándor 2018b]. The UVa node is also exploring field-enhancement for THz-induced molecular orientation. Encouraging results, using micro-structured metals, have been found and are being summarized in a manuscript [Khatri 2018].

Accurate measurements of angle-dependent ionization rates serve as important tests of the theory which, in turn, can guide future HHS and FIS measurements and their interpretation by providing insights into aspects of the dynamics that are not readily obtained from experiment. Interactions between all three nodes have been essential for progress in Thrust 3 and for its impact on the other two thrusts and the overall goals of the network. For example, the optimal molecular species to be studied in ionization measurements at UVa were determined through numerous discussions with the LSU and OSU personnel, based on previous experience and prospects for future calculations and HHS measurements. After verification of our TDDFT approach through comparison with angle-resolved ionization measurements performed at UVa, the LSU node has been able to predict, with confidence, that molecular alignment plays a key role in the degree of localization of a hole produced through strong field ionization. In addition, the alignment/orientation expertise developed at UVa can better contribute to aspects of molecular-frame HHS measurements at OSU (see Thrust 2 above).

The LSU node has also made substantial progress towards using TDDFT to simulate the strong field ionization process. These simulations are a first step towards reliably predicting the channels involved in strong field ionization, and ultimately what the charge migration dynamics is. Our TDDFT ionization computations use Gaussian basis sets, complex absorbing potentials, and optimally tuned range-separated functionals. Critically for strong-field ionization, these functionals give accurate ionization potentials and have reduced self-interaction errors, without requiring any input from experiment. Comparison with experiment allows for validation of TDDFT algorithms for ionization across a wide range of laser intensities and polarizations (see Figure 7).

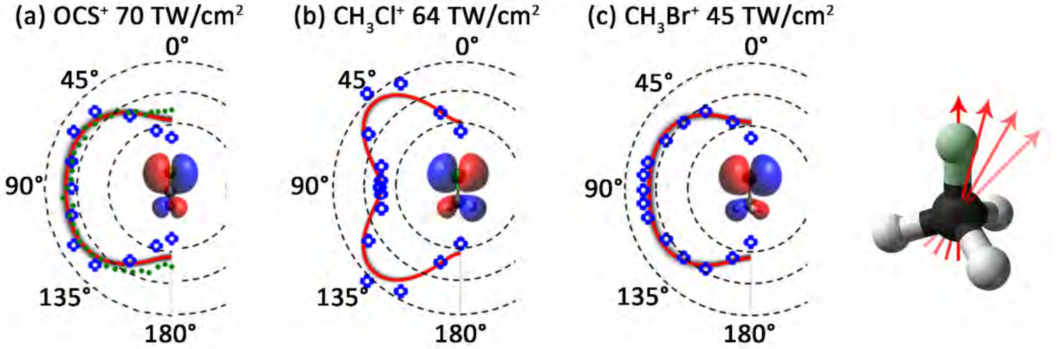

Figure 7: Measured (solid red curves and grey shading uncertainties) and calculated (blue flowers) angle-dependent strong-field ionization yields for OCS, CH_3Cl, and CH_3Br. The green dots in a) show the measured yields obtained from [Hansen 2012]. The inset in each angular distribution shows the structure of the HOMO. As illustrated in the cartoon on the right, θ represents the angle between the laser polarization and the molecular axis. Molecules are aligned, not oriented, so the distributions are implicitly (experiment) and explicitly (theory) symmetrized about $\theta = 90°$.

Experimentally, the UVa node has developed the ability to extract accurate angle-dependent strong-field ionization yields as tests of the TDDFT calculations. Specifically, ionization yields are measured as a function of delay between non-ionizing "alignment" and more intense "ionization" pulses. The delay-dependent yields are then fit using moments of the delay-dependent rotational distributions (which can be calculated with high accuracy), with the coefficients of those moments and key experimental parameters (*e.g.*, laser intensity and rotational temperature) determined from the fits [Makhija 2016, Marceau 2017]. A manuscript describing our combined theoretical and experimental results for OCS has been accepted for publication in Phys. Rev. A [Sándor 2018a].

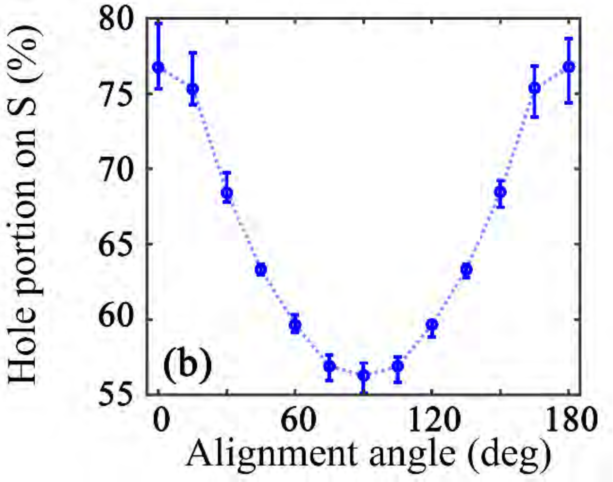

Figure 8: Cycle-average hole localization on the S end of the OCS cation following strong-field ionization [Sándor 2018a]. The hole localization is extracted from the sub-cycle TDDFT one-body density.

More recently, we have obtained similar results in a family of methyl-halide molecules (CH_3X) [Sándor 2018b]. Figure 7 shows a comparison of the measured and calculated angle-dependent strong-field ionization yields for OCS, CH_3Cl, and CH_3Br. In each case, the calculated and measured yields are in impressive agreement with each other, suggesting that the theory accurately captures the underlying strong-field dynamics. Perhaps the most interesting feature of the results in Figure 7 is that despite the strong similarity of the structure of the HOMO in all three molecules, there is a striking difference in the angular distribution for ionization of CH_3Cl as compared to CH_3Br and OCS. The TDDFT method makes it possible to assign these differences to molecule-dependent contributions to ionization from more tightly bound orbitals, presumably influencing the characteristics of the remaining hole in the cation. Preliminary results suggest this can be understood in terms of multi-channel ionization in CH_3Cl versus single channel ionization for CH_3Br.

After experimental validation of LSU TDDFT simulations, we performed a sub-cycle analysis of our results to shed light on the localization of the hole in OCS following ionization [Sándor 2018a]. In a two-center model of strong-field ionization, we computed time-dependent charges on the two ends – S and CO – of the molecule. After filtering out the part of the signal associated with the neutral component, we identify a laser-cycle-average localization of the electron hole on either end of the molecule. As shown in Figure 8, we find a strong sensitivity of the hole localization with the alignment angle, with maximum hole localization (on S) when the laser polarization is parallel to the molecule. Since hole localization is expected to be a necessary condition for charge migration, these results demonstrate how future TDDFT ionization simulations will be instrumental in identifying potential molecules for charge migration studies, both for simulations (Thrust 1) as well as experimental coherent probes (Thrusts 2, 3). Similarly, we are currently preforming hole localization and sub-cycle (orientation-dependent) analyses in the CH_3X family, in conjunction with experiments at UVa mentioned above.

The ability to make measurements on dipole-oriented, not just aligned, molecules will be critical, both for initiating specific charge-migration dynamics through strong-field ionization and for implementing HHS and FIS measurements to probe those dynamics. As a result, the UVa node is continuing to explore methods for improving the degree of field-free orientation that can be achieved. Whereas ionization appears to be a substantial drawback for two-color optical orientation methods [Znakovskaya 2014], THz-based schemes are currently limited only by the strength of the THz fields that can be applied [Machholm 2001, Fleischer 2011, Kitano 2013, Egodapitiya 2014]. To that end, we have been exploring the use of micro-structured metals as a means for enhancing the available THz field throughout a substantial fraction of the focal volume of an intense laser. As a first step, we have employed THz-enhanced surface

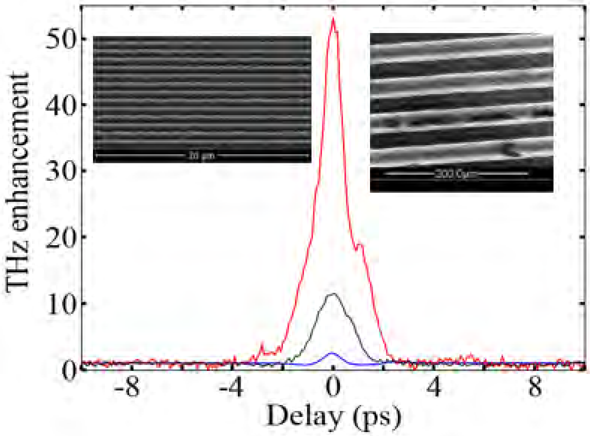

Figure 9: THz-enhancement of the SSH yield from different surfaces as a function of delay between a 100-fs, 800-nm laser pulse and a single-cycle THz pulse at grazing incidence to a gold mirror (blue), a gold reflection grating (black), and a coarse stainless-steel grating (red). Left and right insets show SEM images of the gold and steel grating surfaces, respectively.

second harmonic (SSH) generation as a local probe to characterize the THz field enhancement at the surface of metals with different structures.

Figure 9 shows some preliminary results, comparing the ratio of the SSH yield, with:without THz for several different surfaces, as a function of delay between a 100-fs, 800-nm laser pulse and a 2-ps single-cycle, 50 kV/cm, THz field. In the cases shown, the laser and THz pulses strike the surfaces at grazing incidence with linear polarizations approximately parallel to the surface normal. To our knowledge, this is the first observation of THz enhanced SSH generation. The SSH yield enhancement is roughly proportional to the applied THz field. While an optically flat gold surface shows a maximum enhancement factor of approximately 3, the periodically etched gold surface ($\approx 1\ \mu$m period) results in an enhancement greater than 10. Coarser (50 μm period) structures in stainless steel result in an even greater THz enhancement factor, over 50, but similar enhancements in stainless steel are also observed for rough surfaces without a periodic structure. In general, the results of these measurements are very encouraging in the context of enhancing THz fields for improved orientation measurements. We are now preparing a manuscript reporting our observation of THz enhanced SSH generation and its dependence on surface texture [Khatri 2018].

Cross-training and interactions between the partners

We have successfully built and maintained a network, ATTO-CM, that provides an environment where theorists and experimentalist work cooperatively on problems relevant to charge migration. It has been nurtured by cross-training visits between nodes, and a variety of continuous communication channels across the nodes. These communication channels include:

- Monthly Skype meetings between all partners, together with frequent, internode email, phone, and Skype communications between smaller working groups that target specific tasks.
- An intranet website (with content access restricted to members of the ATTO-CM network), featuring results of common interest, all meeting notes, and many relevant papers. The network also has a cloud storage facility to share, archive and back up data.
- Extended visits between the partners. For most visits, all nodes are represented to maximize coordination and information sharing between them. These visits are extremely beneficial for:
    - Cross training between the two experimental nodes, on each-other's apparatus and techniques related to alignment/orientation studies including the RABBITT beamline at OSU and angle resolved ionization measurements at UVa.
    - Training of the experimental nodes on theoretical and numerical methods and capabilities from LSU.
    - Training of the theoretical node in the basics of OSU and UVa experimental apparatus and capabilities, the resolution of measurements, and how raw data are processed to extract physical information.
- Writing of the present grant application renewal. In a concerted effort between all ATTO-CM personnel, we have reaffirmed and revised what we believed to be the best approaches moving forward, given our experience and results from the previous funding period.

These active exchanges have resulted in building a strong collaborative community among the PIs, students and postdocs. Results of the ATTO-CM network were showcased in numerous international conferences. These conferences also provided additional opportunities for in-person discussions and interactions when members of more than one node were present.

Future Plans

Overall, we believe that the continued interactions and cross-training between the three nodes of the ATTO-CM network is a cornerstone to our success. We fully intend to continue our current interactions, with regular communication (Skype, phone, emails) and exchange visits between the nodes. Building upon the results in our Recent Progress section, for each thrust area we intend to focus our efforts as follows:

- Thrust 1: Utilize the attochemistry picture to initiate and control charge migration. This will both incorporate lessons learned from, and serve as input for developments of, Thrusts 2 and 3.
- Thrust 2: Pursue and develop HHS as a probe of charge migration, refining both experimental and theoretical methods and exploring charge migration signatures.

- Thrust 3: Initiate FIS experiments and refine strong-field-ionization computational methods. Pursue and characterize molecular orientation with bi-chromatic and/or THz fields. With maturation, these techniques would be transferred to molecular-frame HHS (Thrust 2).

Below we briefly explain the main avenues we intend to pursue to advance our chances of observing charge migration with strong laser fields.

CONTROL OF CHARGE MIGRATION: The electronic configuration in which the molecular cation is left following the removal of one, or several, electron(s) determines how its dynamics subsequently unfolds (see Thrust 1). The alignment/orientation of the molecules, which can be achieved using optical and/or THz fields (Thrust 3), is an important control knob for inducing and probing charge migration, both in HHS (Thrust 2) and FIS (Thrust 3). Orientation/alignment of the molecules in space allows control over which ionization channels contribute to electron-hole motion, so that selection rules, in combination with the laser polarization, can be used to selectively couple cation states and to control the charge migration. Conversely, once electron dynamics are initiated, the molecular alignment/orientation influences field-driven recombination or further ionization, which we hope to exploit as coherent, time-resolved probes.

The importance of molecular-site-specific properties in HHS – through two-center interference (Thrust 2) – and functionalization – CH_3X family (Thrust 3) – is currently under investigation in close theory-experiment collaboration in the ATTO-CM network. These results will help refine the most relevant attochemistry metrics and/or properties for experimental purpose (Thrust 1). LSU is currently moving to systematic studies of charge migration in organic molecules, including varying the length of the molecules, conjugated/unconjugated, electron/hole acceptor/donor systems, branched molecules, etc. We will use the result of these studies, together with the experimental feedback, to select candidates for our next campaigns.

PROBING CHARGE MIGRATION THROUGH FIS: Following a recent upgrade of the kHz Ti:Sapphire amplifier at UVa, we are preparing for experiments which will directly compare, in the same apparatus and with the same molecules (*e.g.*, OCS and CH_3X), the degree of field- and ionization-free orientation that can be achieved with bichromatic laser and THz techniques, respectively. The optimum orientation approach will then be employed to explore ionization of oriented molecules using bichromatic pulses that have a pronounced (and known) directional field asymmetry. Through such measurements, we will test TDDFT predictions from the LSU node for the dependence of the molecular ionization rate vs orientation relative to the ionizing field. Using calculations for the time-scales for principal charge migration modes in different species (Thrust 1, Figure 2), we will prepare for FIS measurements by experimentally characterizing dissociative and non-dissociative ionization in aligned and/or oriented candidate molecules.

In the context of FIS, we are pursuing multiple avenues to improve TDDFT methodology. Despite the excellent agreement near the saturation intensity, computing lower intensity rates remains a challenge for basis-set TDDFT due to "leakage" from the ground state related to our implementation of complex absorbing potentials. We are currently remedying this problem using molecular-orbital based (rather than spatial) complex absorbing potentials. Another challenge is double ionization, where TDDFT has two major deficiencies: separating the single and double ionization contributions from the time-dependent norm (a problem in all mean-field theories), and inaccuracies in the DFT functional when multiple electrons are removed. We are working towards tackling double ionization in two ways: (i) computing yields from cations prepared with hole population in particular orbitals (*i.e.*, bypass pitfalls of TDDFT, but only valid for sequential double ionization), and (ii) using multi-IP tuned range-separated hybrids to ensure proper straight-line behavior (reduced delocalization error) for norms ranging from [N, N-2]. Additionally, we are working towards simulating orientation-dependent and two-color coherent double ionization via sub-cycle analysis of the norm, akin to the hole-localization analysis of OCS discussed previously.

PROBING CHARGE MIGRATION THROUGH HHS: As the ATTO-CM network efforts move towards bigger, more complex targets, an experimental difficulty for HHS campaigns is the general trend of room-temperature vapor pressure plummeting with molecular size, because high pressures are necessary for HHG. The OSU node is presently investigating multiple paths toward combating this issue. (i) Using the molecule of interest as a target, rather than generator, of HHG radiation. OSU is currently performing experiments to determine the feasibility of this approach within their experimental setup. (ii) A setup capable of delivering molecules, normally with low vapor pressures, into HHG at high pressure. This is achieved with a customized heat bath at high temperatures, as demonstrated in [Marangos 2016]. Additionally, OSU is exploring the use of their two-source apparatus as a means to measure the phase of the harmonic emission as a function of an excitation parameter. Since it is highly stable, the two-source apparatus is able to reveal small phase variations induced by low-efficiency processes like molecular dissociation and/or charge migration. Finally, OSU is also nearing the completion of an amplified MIR source capable of generating ~6 mJ pulses at a 2.5 μm fundamental wavelength. This new source will greatly extend the energetic span of their harmonic spectra since the cutoff scales as λ^2. With a period of 8.4 fs – about the time for charge migration to go through 17 molecular bonds per Thrust 1 predictions – the new source should prove useful to charge migration studies.

LSU will take a multi-pronged approach toward characterizing charge migration using HHS. (i) We will continue to refine signal processing efforts to extract more detailed information from the large-scale TDDFT computations. In particular, we are exploring how to optimize the ionization seed that helps to isolate the short-path contribution to the spectrum, both in terms of maximizing its path-selectivity and minimizing its influence on the subsequent electron dynamics. (ii) We are working on building a purely theory-based bottom-up model in which all ionization, propagation, and recombination steps will be parametrized using output from ab-initio calculations (TDDFT and ePOLYSCAT). The LSU node is in the process of hiring a new postdoc who will be primarily responsible for this. (iii) We are working towards combining the knowledge gained in Thrust 1 (controlling initial conditions to induce charge migration and being able to follow it with TDDFT calculations) with large-scale TDDFT calculations and signal processing of harmonic spectra. This should allow LSU to do a TDDFT calculation of an HHG process taking place alongside charge migration and might give a first look at how it is imprinted on the HHG spectral amplitude and phase. A long-term goal is to compare such results to those of the bottom-up models in which one can independently control the charge migration through choice of parameters.

References

[Andrade 2015] X. Andrade *et al.*, “Real-space grids and the Octopus code as tools for the development of new simulation approaches for electronic systems,” Phys. Chem. Chem. Phys. 17, 31371 (2015).

[Auger 2013] F. Auger *et al.*, “Time-Frequency Reassignment and Synchrosqueezing,” IEEE Signal Process. Mag. 30, 32 (2013).

[Bruner 2018] A. Bruner *et al.*, “A Chemical Picture of Charge Migration,” in preparation.

[Cooper 1962] J.W. Cooper, “Photoionization from Outer Atomic Subshells. A Model Study,” Phys. Rev. 128, 681 (1962).

[Dutoi 2011] A.D. Dutoi *et al.*, “Ultrafast charge separation driven by differential particle and hole mobilities,” J. Chem. Phys. 134, 024303 (2011).

[Egodapitiya 2014] K. N. Egodapitiya *et al.*, “Terahertz-Induced Field-Free Orientation of Rotationally Excited Molecules,” Phys. Rev. Lett. 112, 103002 (2014).

[Etches 2011] A. Etches *et al.*, “Two-center minima in harmonic spectra from aligned polar molecules,” Phys. Rev. A84, 023418 (2011).

[Fleischer 2011] S. Fleischer *et al.*, “Molecular Orientation and Alignment by Intense Single-Cycle THz Pulses,” Phys. Rev. Lett. 107, 163603 (2011).

[Gorman 2018] T.T. Gorman *et al.*, “Molecular-frame Interference of Distinct Recombination Dipoles via Two-Center Interference in OCS,” in preparation.

[Hansen 2012] J.L. Hansen *et al.*, “Orientation-dependent ionization yields from strong-field ionization of fixed-in-space linear and asymmetric top molecules,” J. Phys. B 45, 015101 (2012).

[Khatri 2018] S. Khatri *et al.*, “THz-enhanced surface second harmonic generation,” in preparation.

[Kitano 2013] K. Kitano *et al.*, “Orientation of jet-cooled polar molecules with an intense single-cycle THz pulse,” Phys. Rev. A 88, 061405(R) (2013).

[Kraus 2015] P.M. Kraus *et al.*, “Measurement and Laser Control of Attosecond Charge Migration in Ionized Iodoacetylene,” Science 350, 6262 (2015).

[Kuleff 2016] A.I. Kuleff *et al.*, “Core ionization initiates subfemtosecond charge migration in the valence shell of molecules,” Phys. Rev. Lett. 117, 093002 (2016).

[Lépine 2014] F. Lépine *et al.*, “Attosecond molecular dynamics: fact or fiction?,” Nat. Phot. 8, 195 (2014).

[Lewenstein 1995] M. Lewenstein *et al.*, “Phase of the atomic polarization in high-order harmonic generation,” Phys. Rev. A 52, 4747 (1995).

[Lin 2010] C.D Lin *et al.*, “Strong-field rescattering physics – self-imaging of a molecule by its own electrons,” J. Phys. B 43, 122001 (2010).

[Machholm 2001] M. Machholm *et al.*, “Field-Free Orientation of Molecules,” Phys. Rev. Lett. 87, 193001 (2001).

[Makhija 2016] V. Makhija *et al.* "Orientation Resolution through Rotational Coherence Spectroscopy," arXiv:1611.06476v2 (2016).

[Marangos 2016] J.P. Marangos, "Development of high harmonic generation spectroscopy of organic molecules and biomolecules," J. Phys. B 49, 132001 (2016).

[Marceau 2017] C. Marceau *et al.*, "Molecular Frame Reconstruction Using Time-Domain Photoionization Interferometry," Phys. Rev. Lett. 119, 083401 (2017).

[Remacle 2006] F. Remacle *et al.*, "An electronic time scale in chemistry," PNAS 103, 6793 (2006).

[Sándor 2018b] P. Sándor *et al*, "Angle-dependent Strong-Field Ionization of Methyl Chloride and Methyl Bromide," in preparation.

[Schafer 2004] K.J. Schafer *et al.*, "Strong Field Quantum Path Control Using Attosecond Pulse Trains," Phys. Rev. Lett. 92, 023003 (2004).

[Stolow 2013] A. Stolow, "The three pillars of photo-initiated quantum molecular dynamics," Faraday Discuss. 163, 9 (2013).

[Znakovskaya 2014] I. Znakovskaya *et al.*, "Transition between Mechanisms of Laser-Induced Field-Free Molecular Orientation," Phys. Rev. Lett. 112, 113005 (2014).

Peer-Reviewed Publications Resulting from this Project (2016-2018)

[Abanador 2018] P.M. Abanador, F. Mauger, K. Lopata, M.B. Gaarde, and K.J. Schafer, "Wavelength and intensity dependence of recollision-enhanced multielectron effects in high-harmonic generation," Phys. Rev. A 97, 043414 (2018).

[Kiesewetter 2018] D. Kiesewetter, R.R. Jones, A. Camper, S.B. Schoun, P. Agostini, and L.F. DiMauro, "Probing Electronic Binding Potentials with Attosecond Photoelectron Wavepackets," Nat. Phys. 14, 68 (2018).

[Mauger 2018] F. Mauger, P.M. Abanador, A. Bruner, A. Sissay, M.B. Gaarde, K. Lopata, and K.J. Schafer, "Signature of charge migration in modulation of double ionization," Phys. Rev. A 97, 043407 (2018).

[Scarborough 2018] T.D. Scarborough, T.T. Gorman, F. Mauger, P. Sándor, S. Khatri, M.B. Gaarde, K.J. Schafer, P. Agostini, and L.F. DiMauro, "Full Characterization of a Molecular Cooper Minimum Using High-Harmonic Spectroscopy," Appl. Sc. 8, 1129 (2018).

[Sándor 2018a] P. Sándor, A. Sissay, F. Mauger, P.M. Abanador, T.T. Gorman, T.D. Scarborough, M.B. Gaarde, K. Lopata, K.J. Schafer and R.R. Jones, "Angle-dependence of Strong-Field Single- and Double-Ionization of Carbonyl Sulfide," Phys. Rev. A, accepted for publication (2018).

[Abanador 2017] P.M. Abanador, F. Mauger, K. Lopata, M.B. Gaarde, and K.J. Schafer, "Semiclassical modeling of high-order harmonic generation driven by an elliptically polarized laser field: the role of recolliding periodic orbits," J. Phys. B 50, 035601 (2017).

[Bruner 2017] A. Bruner, S. Hernandez, F. Mauger, P.M. Abanador, D.J. LaMaster, M.B. Gaarde, K.J. Schafer, and Kenneth Lopata, "Attosecond Charge Migration with TDDFT: Accurate Dynamics from a Well-Defined Initial State," J. Phys. Chem. Lett. 8, 3991 (2017).

[Geneaux 2017] R. Géneaux, C. Chappuis, T. Auguste, S. Beaulieu, T.T. Gorman, F. Lepetit, L.F. DiMauro, and T. Ruchon, "Radial index of Laguerre-Gaussian modes in high-order harmonic generation," Phys. Rev. A 95, 051801 (2017).

[Li 2016] S. Li and R.R. Jones, "High-Energy Electron Emission from Metallic Nano-tips Driven by Intense Single-Cycle Terahertz Pulses," Nat. Comm. 7, 13405 (2016).

[Mauger 2016] F. Mauger, P.M. Abanador, K. Lopata, K.J. Schafer, and M.B. Gaarde, "Semiclassical-wave-function perspective on high-harmonic generation," Phys. Rev. A 93, 043815 (2016).

[Sissay 2016] A. Sissay, P. Abanador, F. Mauger, M. Gaarde, K.J. Schafer, and K. Lopata, "Angle-dependent strong-field molecular ionization rates with tuned range-separated time-dependent density functional theory," J. Chem. Phys. 145, 094105 (2016).

DYNAMICS OF FEW-BODY ATOMIC PROCESSES

Anthony F. Starace, P.I.
The University of Nebraska, Department of Physics and Astronomy
855 North 16th Street, 208 Jorgensen Hall, Lincoln, NE 68588-0299
Email: astarace1@unl.edu

PROGRAM SCOPE

The goals of this project are to understand, describe, control, and image processes involving energy transfers from intense electromagnetic radiation to matter as well as the time-dependent dynamics of interacting few-body, quantum systems. Investigations of current interest are in the areas of strong field (intense laser) physics, attosecond physics, high energy density physics, and multiphoton ionization processes. Nearly all proposed projects require large-scale numerical computations, involving, e.g., the direct solution of the full-dimensional time-dependent or time-independent Schrödinger equation for two-electron (or multi-electron) systems interacting with electromagnetic radiation. In some cases our studies are supportive of and/or have been stimulated by experimental work carried out by other investigators funded by the DOE AMOS physics program. Principal benefits and outcomes of this research are improved understanding of how to control atomic and molecular processes with electromagnetic radiation and how to transfer energy optimally from electromagnetic radiation to matter.

RECENT PROGRESS

A. *Multi-start Spiral Electron Vortices in Ionization by Circularly Polarized UV Pulses*

Multi-start spiral vortex patterns have been predicted for the electron momentum distributions in the polarization plane following ionization of the He atom by two time-delayed circularly polarized ultrashort laser pulses. For two ultraviolet (UV) pulses having the same frequency (such that two photons are required for ionization), single-color two-photon interferometry with co-rotating or counter-rotating time-delayed pulses was found to lead respectively to zero-start or four-start spiral vortex patterns in the ionized electron momentum distributions in the polarization plane. In contrast, two-color one-photon plus two-photon interferometry with time-delayed co-rotating or counter-rotating UV pulses was found to lead respectively to one-start or three-start spiral vortex patterns. These predicted multi-start electron vortex patterns were found to be sensitive to the carrier frequencies, handedness, time delay, and relative phase of the two pulses. Our numerical predictions are obtained by solving the six-dimensional two-electron time-dependent Schrödinger equation (TDSE). They are explained analytically using perturbation theory (PT). Comparison of our TDSE and PT results for single-color two-photon processes probes the role played by the time-delay-dependent ionization cross channels in which one photon is absorbed from each pulse. These cross channels can be controlled by means of the parameters of the fields and the ionized electron detection geometries. (*See publication [P1] the list of project publications below*.)

B. *Discontinuities in the electromagnetic fields of vortex beams in the complex source-sink model*

Laser beams that carry orbital angular momentum (OAM) provide a novel means of investigation into laser-matter interactions. Multiple nonparaxial analytic representations have been developed to model tightly-focused beams having nonzero OAM. A leading model is the so-called *complex source-sink model* [1] for solving the scalar Helmholtz equation analytically. From that solution, termed the phasor, the laser electric and magnetic fields can be calculated. However, we discovered an analytical discontinuity in what was thought to be the discontinuity-free exact nonparaxial vortex beam phasor obtained within the complex source-sink model [P2]. This discontinuity appears for all odd values of the orbital angular momentum mode. Such discontinuities in the phasor lead to nonphysical discontinuities in the real electromagnetic field components. We identified the source of the discontinuities, and provided both analytic and graphical evidence of the discontinuous real electric fields for the first and third orbital angular momentum modes. We then presented a simple means of avoiding these discontinuities. (*See publication [P2] in the list of project publications below.*)

C. Kinematical Vortices in Double Photoionization of Helium by Attosecond Pulses

Two-armed helical vortex structures are predicted in the two-electron momentum distributions produced in double photoionization (DPI) of the He atom by a pair of time-delayed elliptically polarized attosecond pulses with opposite helicities. These predictions are based upon both a first-order perturbation theory analysis and numerical solutions of the two-electron, time-dependent Schrödinger equation in six spatial dimensions. The helical vortex structures originate from Ramsey interference of a pair of ionized two-electron wave packets, each having a total angular momentum of unity, and appear in the six-fold differential DPI probability distribution for any energy partitioning between the two electrons. The vortex structures are exquisitely sensitive to the time delay between the two pulses, their relative phase, their ellipticity, and their handedness; moreover, they occur in a variety of electron detection geometries. However, the vortex structures only occur when the angular separation β between the electron momenta $\mathbf{p}_1$ and $\mathbf{p}_2$ is held fixed. The vortex structures can also be observed in the four-fold differential DPI probability distribution obtained by averaging the six-fold differential probability over the emission angles of one electron. Such kinematical vortices are a general phenomenon that may occur in any ionization process, initiated by two time-delayed short pulses with opposite ellipticities, for particular detection geometries. (*See publication [P3] in the list of project publications below.*)

D. Doubly-Excited State Effects on Two-Photon Double Ionization of Helium by Time-Delayed, Oppositely Circularly-Polarized Attosecond Pulses

We have studied two-photon double ionization (TPDI) of helium by a pair of time-delayed (non-overlapping), oppositely circularly-polarized attosecond pulses whose carrier frequencies are resonant with $^1P^o$ doubly-excited states. All of our TPDI results are obtained by numerical solution of the two-electron time-dependent Schrödinger equation for the six-dimensional case of circularly-polarized attosecond pulses, and they are analyzed using perturbation theory (PT). As compared with the corresponding non-resonant TPDI process, we find that the doubly-excited states change the character of vortex patterns in the two-electron momentum distributions for the case of back-to-back (BTB) detection of the two ionized electrons in the polarization plane. The doubly-excited states also completely change the structure of fixed-energy, two-electron angular distributions. Moreover, both the fixed-energy and energy-integrated *angular* distributions, as well as the two-electron *energy* distributions, exhibit a periodicity with time delay τ between the two attosecond pulses of about 69 as, *i.e.*, the beat period between the $(2s2p)^1P^o$ doubly-excited state and the He ground state. Using PT we derive an expression for an angle-integrated *energy* distribution that is sensitive to the slower beat period ~1.2 fs between different doubly-excited states as well as to the long timescale ~17 fs of autoionization lifetimes. (*See publication [P4] in the list of project publications below.*)

E. Perturbative Representation of Ultrashort Nonparaxial Elegant Laguerre-Gaussian Fields

We have been investigating the use of radially-polarized, non-zero Laguerre-Gaussian (LG) radial mode laser pulses for vacuum acceleration of electrons. Currently, the most effective vacuum acceleration schemes for creating electron bunches involve a high power radially-polarized Gaussian laser beam (the zero LG radial mode) incident on a diffuse gas target [2]. In order to describe such structured electromagnetic fields in a tight laser focus, we have developed an analytical method for calculating the fields of a nonparaxial elegant Laguerre-Gaussian (LG) vortex beam for arbitrary pulse duration, spot size, and LG mode [P5]. This perturbative approach, using the perturbative phasor of Bandres and Gutiérrez-Vega [3], provides a numerically tractable model for the calculation of arbitrarily high radial and azimuthal LG modes in the nonparaxial regime, without requiring integral representations of the fields. A key feature of this perturbative model is its use of a Poisson-like frequency spectrum, which allows for the proper description of pulses of arbitrarily short duration. This model is thus appropriate for simulating laser-matter interactions, including those involving short laser pulses. (*See publication [P5] in the list of project publications below*.)

FUTURE PLANS

Our group is currently carrying out research on the following additional projects:

- We are studying *electron momentum vortices in single-photon double ionization of H_2* by time-delayed, counter-rotating, elliptically-polarized attosecond pulses propagating either parallel or perpendicular to the molecular axis **R**. For propagation parallel to **R**, *kinematical vortices* occur similar to those found for He [P3]. For propagation perpendicular to **R**, however, we find *dynamical vortex structures* originating from an ellipticity-dependent interplay of $^1\Sigma_u^+$ and $^1\Pi_u^+$ continuum amplitudes. Combining these ellipticity-dependent electron momentum distributions with information from the two-electron angular distributions, we are able to propose a *complete experiment* for determining the magnitudes and relative phase of the $^1\Sigma_u^+$ and $^1\Pi_u^+$ amplitudes by varying the pulse ellipticities and their time delays. This work has been submitted for publication.

- We are studying the use of an elliptically-polarized attosecond pulse to induce and control a novel dichroic effect in single-photon double ionization of a fixed-in-space H_2 molecule. This phenomenon, which we term a *molecular-symmetry-induced dichroism (MSID)*, is predicted to occur in the doubly-ionized electron momentum and angular distributions. It stems from a strong mixing of comparable $^1\Pi^+$ and $^1\Sigma^+$ ionization amplitudes. MSID is found to occur for any laser configuration, except the one in which the light propagates along the molecular axis **R**. We show how MSID can be measured directly by choosing particular detection geometries in which atomic dichroism effects vanish.

- We are developing a *generalized description of a perturbative nonparaxial elegant Laguerre-Gaussian phasor* for describing ultrashort pulses in the time domain. This generalization of our results in [P5] allows one to calculate the time-domain phasor to arbitrarily high perturbation order as a non-recursive, closed-form expression. This generalization eliminates the need for explicit calculations of Fourier integrals, which would be prohibitively difficult to calculate individually for arbitrarily many orders of perturbation. Instead, the electromagnetic fields can be calculated immediately from simple derivatives of the generalized time-domain phasor.

- We are investigating a number of extensions of our prior harmonic generation works [4, 5] with the aim of understanding the conditions under which one can produce *a harmonic generation plateau in the multiphoton regime* when doubly-excited or singly-excited states are on resonance with the driving laser field. These extensions include study of the sensitivity to the initial state, the use of chirped driving laser fields, and the use of elliptically-polarized driving laser fields. Our preliminary findings are that the multiphoton regime harmonic generation plateau occurs when singly-excited states are on resonance with the driving laser field.

REFERENCES

[1] Z. Ulanowski and I.K. Ludlow, "Scalar field of nonparaxial Gaussian beams," *Opt. Lett.* **25**, 1792 (2000).

[2] C. Varin, V. Marceau, P. Hogan-Lamarre, T. Fennel, M. Piché, and T. Brabec, "MeV femtosecond electron pulses from direct-field acceleration in low density atomic gases," *J. Phys. B* **49**, 024001 (2016).

[3] M.A. Bandres and J. C. Gutiérrez-Vega, "Higher-order complex source for elegant Laguerre–Gaussian waves," *Opt. Lett.* **29**, 2213 (2004).

[4] J.M. Ngoko Djiokap and A.F. Starace, "Evidence of the 2s2p(^{1}P) Doubly Excited State in the Harmonic Generation Spectrum of He," *Phys. Rev. A* **84**, 013404 (2011).

[5] J.M. Ngoko Djiokap and A.F. Starace, "Resonant Enhancement of the Harmonic Generation Spectrum of Beryllium," *Phys. Rev. A* **88**, 053412 (2013).

PEER-REVIEWED PUBLICATIONS RESULTING FROM THIS PROJECT (2016 – 2018)

[P1] J.M. Ngoko Djiokap, A.V. Meremianin, N.L. Manakov, S.X. Hu, L.B. Madsen, and A.F. Starace, "Multistart Spiral Electron Vortices in Ionization by Circularly Polarized UV Pulses," *Phys. Rev. A* **94**, 013408 (2016).

[P2] A. Vikartofsky, L.-W. Pi, and A.F. Starace, "Discontinuities in the Electromagnetic Fields of Vortex Beams in the Complex Source-Sink Model," *Phys. Rev. A* **95**, 053826 (2017).

[P3] J.M. Ngoko Djiokap, A.V. Meremianin, N.L. Manakov, S.X. Hu, L.B. Madsen, and A.F. Starace, "Kinematical Vortices in Double Photoionization of Helium by Attosecond Pulses," *Phys. Rev. A* **96**, 013405 (2017).

[P4] J.M. Ngoko Djiokap and A.F. Starace, "Doubly-Excited State Effects on Two-Photon Double Ionization of Helium by Time-Delayed, Oppositely Circularly-Polarized Attosecond Pulses," *J. Optics* **19**, 124003 (2017) (DOI: https://doi.org/10.1088/2040-8986/aa8fc0). *This is an invited contribution to a special issue on emerging attosecond technologies*.

[P5] A. Vikartofsky, A. F. Starace, and L.-W. Pi, "Perturbative Representation of Ultrashort Nonparaxial Elegant Laguerre-Gaussian Fields," *Phys. Rev. A* (accepted 21 September 2018; in press).

FEMTOSECOND AND ATTOSECOND LASER-PULSE ENERGY TRANSFORMATION AND CONCENTRATION IN NANOSTRUCTURED SYSTEMS

DOE Grant No. DE-FG02-01ER15213

Mark I. Stockman (PI) and Vadym Apalkov (co-PI)

Department of Physics and Astronomy, Georgia State University, Atlanta, GA 30303

E-mail: mstockman@gsu.edu

1 Program Scope

The program is aimed at theoretical investigations of a wide range of phenomena induced by ultrafast laser-light excitation of nanostructured or nanosize systems, in particular, metal/semiconductor/dielectric nanocomposites and nanoclusters. Among the primary phenomena are femtosecond and attosecond processes of energy transformation, generation, transfer, and localization on the nanoscale and control of such phenomena.

2 Recent Progress and Publications

The recent progress is illustrated below by selected peer-reviewed articles that we consider most significant. All peer-reviewed publications resulting from this DOE Grant and acknowledging this DOE support during the period of 2016-2018 are: [1-11]. Among these publications, the following articles acknowledging this Grant's major support have been published: [2, 5-7, 9-11]. The following articles have received, as acknowledged, supplementary support of this grant during the Grant: [1, 3, 4, 8].

2.1 Femtosecond valley polarization and topological resonances in transition metal dichalcogenides [10]

We have theoretically introduced the fundamentally fastest induction of a significant population and valley polarization in a monolayer of a transition metal dichalcogenide (i.e., MoS2 and WS2). This may be extended to other two-dimensional materials with the same symmetry. This valley polarization can be written and read out by a pulse consisting of just a single optical oscillation with a duration of a few femtoseconds and an amplitude of ~0.25 V/Å. Under these conditions, we predict an effect of topological resonance, which is due to the Bloch motion of electrons in the reciprocal space where electron population textures are formed due to non-Abelian Berry curvature. The predicted phenomena can be applied for information storage and processing in PHz-band optoelectronics.

2.2 Fundamentally fastest optical processes at the surface of a topological insulator [9]

We have predicted that a single oscillation of a strong optical pulse can significantly populate the surface conduction band of a three-dimensional topological insulator, Bi2Se3. Both linearly- and circularly-polarized pulses generate chiral textures of interference fringes of population in the surface Brillouin zone. These fringes constitute a self-referenced electron hologram carrying information on the topology of the surface Bloch bands, in particular, on the effect of the warping term of the low-energy Hamiltonian. These electron-interference phenomena are in a sharp contrast to graphene where there are no chiral textures for a linearly-polarized pulse and no interference fringes for circularly-polarized pulse. These predicted reciprocal space electron-population textures can be measured experimentally by time resolved angle resolved photoelectron spectroscopy (TR-ARPES) to gain direct access to non-Abelian Berry curvature at topological insulator surfaces.

2.3 Attosecond nanoscale near-field sampling [1]

The promise of ultrafast light-field-driven electronic nanocircuits has stimulated the development of the new fundamental research field of attosecond nanophysics. An essential prerequisite for advancing this new area is the ability to characterize optical near fields from light interaction with nanostructures, with sub-cycle resolution. In this article [1], we demonstrate attosecond near-field retrieval for a tapered gold nanowire. By comparison of the results to those obtained from noble gas experiments and the corresponding theory, the spectral response of the nanotaper near field arising from laser excitation can be extracted.

Photoemission from solids is one of the most fundamental and long-studied electron phenomena in nature. Related photon–electron interactions form the basis for modern optoelectronics, where light can trigger electron transfer, amplification and emission; vice versa, electron injection and excitation can result in the emission of light. Attosecond nanoscale near-field sampling (ANNS), proposed by us in 2007 has been shown to provide sub-cycle resolution of optical near-field dynamics in nanostructured materials. The ANNS relies on the emission of photoelectrons with high initial momentum by an attosecond extreme ultraviolet (XUV) pulse, and subsequent acceleration of the photoelectrons in the near fields. In this work, we perform ANNS measurements and develop the corresponding theory for a nanotaper at near-infrared (NIR) intensities well below the onset of non-linear effects. Using the gold nanotaper sample geometry, we show that through theoretical analysis of field homogeneity and streaking electron trajectories, a meaningful attosecond characterization of near fields can be performed.

2.4 Graphene superlattices in strong circularly polarized fields: Chirality, Berry Phase, and attosecond dynamics [6]

Topological properties of quantum-mechanical Hilbert space have had pronounced influence on physics as a whole and condensed matter physics in particular. Nontrivial topological properties of graphene in the reciprocal **k**-space are due to the presence of nonzero Berry, which is a geometric counterpart of a magnetic field localized at the Dirac points. In this work, we propose an approach to directly observe the Berry phase without a magnetic field. The idea is to use a superlattice superimposed on graphene to cause electron diffraction (Bragg reflection) in the reciprocal space. This diffraction from the superlattice creates a “which way” quantum-mechanical uncertainty causing interference of the electron wave with itself and making the Berry phase directly visible in discontinuities of the self-referenced electron interferogram, which can be experimentally observed using the time-resolved angle-resolved electron photoemission (TR-ARPES) method.

2.5 Interaction of crystalline topological insulator with an ultrashort laser pulse [7]

We theoretically study the interaction of crystalline topological insulator (CTIs), characterized by surface quadratic gapless bands, with an ultrashort (few-femtosecond) optical pulse. The electron dynamics in such an optical pulse is determined by a strong lattice-momentum dependence of the interband dipole coupling, which is anisotropic and singular at the degeneracy point. The interband mixing induced by the ultrashort pulse results in a finite conduction band population, the distribution of which in the reciprocal space is correlated with the profile of the interband dipole matrix elements and has a high contrast. The number of such high-contrast regions depends on the polarization direction of the optical pulse. The ultrashort pulse also causes an electrical current and a net charge transfer through the system in the direction of the maximum field. These findings open up routs to ultrafast optical-field control of the CTIs and petahertz-band optoelectronics.

2.6 Semimetallization of dielectrics in strong optical fields [5]

At the heart of ever growing demands for faster signal processing is ultrafast charge transport and control by electromagnetic fields in semiconductors. Intense optical fields have opened fascinating avenues for new phenomena and applications in solids. Because the period of optical fields is on the order of a femtosecond, the current switching and its control by an optical field may pave a way to petahertz optoelectronic devices. Lately, a reversible semimetallization in fused silica on a femtosecond time scale by using a few-cycle strong field (~1 V/Å) is manifested. The strong Wannier-Stark localization and Zener-type tunneling were expected to drive this ultrafast semimetallization. Wider spread of this technology demands better understanding of whether the strong field behavior is universally similar for different dielectrics. In this publication [5], we develop theory of the universal semimetallization; experimentally, we employ a carrier-envelope-phase stabilized, few-cycle strong optical field to drive the semimetallization in sapphire, calcium fluoride and quartz and to compare this phenomenon and show its remarkable similarity between them. The similarity in response of these materials, despite the distinguishable differences in their physical properties, suggests the universality of the physical picture explained by the localization of Wannier-Stark states. Our results elucidate fundamental limit on optical field-induced processes in solids and may blaze a trail to PHz-rate optoelectronics.

3 Future Plans

We will develop the present success in the optics of ultrastrong and ultrafast fields on the nanoscale. We will extend the existing theory focusing on modern two-dimensional solids such as graphene, transitional metal dichalcogenides, boron nitride, and topological insulators. We will extend theory to describe photoelectron emission caused by the strong ultrashort pulses and probe attosecond XUV pulses in in the two-dimensional materials. In addition to ultrafast angular-resolved photoelectron emission spectroscopy (TR-ARPES) from two-dimensional materials and topological insulators, we will describe a plethora of optical and electric phenomena due to ultrafast valley- and spin-selective ultrafast excitation of the conduction band. Among them, currents during and after the pulse, edge currents in topological edge states and emission of THz radiation due to these currents. We will also describe induced ultrafast light reflection and absorption by such systems. Of particular interest is the study of effects of the Bloch band topology.

4 Peer-Reviewed Publications Resulting from this Project (2016-2018)

1. B. Förg, J. Schötz, F. Süßmann, M. Förster, M. Krüger, B. Ahn, W. Okell, K. Wintersperger, S. Zherebtsov, A. Guggenmos, V. Pervak, A. Kessel, S. Trushin, A. Azzeer, M. Stockman, D. E. Kim, F. Krausz, P. Hommelhoff, and M. Kling, *Attosecond Nanoscale near-Field Sampling*, Nat. Commun. **7**, 11717-1-7 (2016).
2. Y. Abate, D. Seidlitz, A. Fali, S. Gamage, V. E. Babicheva, V. S. Yakovlev, M. I. Stockman, R. Collazo, D. E. Alden, and N. Dietz, *Nanoscopy of Phase Separation in In$_x$ga$_{1-X}$n Alloys*, ACS Appl Mater Inter **8**, 23160−23166 (2016).
3. M. H. Javani and M. I. Stockman, *Real and Imaginary Properties of Epsilon-near-Zero Materials*, Phys. Rev. Lett. **117**, 107404-1-6 (2016).
4. H. K. Kelardeh, V. Apalkov, and M. I. Stockman, *Attosecond Strong-Field Interferometry in Graphene: Chirality, Singularity, and {Berry} Phase*, Phys. Rev. B **93**, 155434-1-7 (2016).
5. O. Kwon, T. Paasch-Colberg, V. Apalkov, B.-K. Kim, J.-J. Kim, M. I. Stockman, and D. E. Kim, *Semimetallization of Dielectrics in Strong Optical Fields*, Sci. Rep. **6**, 21272-1-9 (2016).
6. H. Koochaki Kelardeh, V. Apalkov, and M. I. Stockman, *Graphene Superlattices in Strong Circularly Polarized Fields: Chirality, {Berry} Phase, and Attosecond Dynamics*, Phys. Rev. B **96**, 075409-1-8 (2017).
7. S. A. Oliaei Motlagh, V. Apalkov, and M. I. Stockman, *Interaction of Crystalline Topological Insulator with an Ultrashort Laser Pulse*, Phys. Rev. B **95**, 085438-1-8 (2017).
8. J. Schötz, B. Förg, M. Förster, W. A. Okell, M. I. Stockman, F. Krausz, P. Hommelhoff, and M. F. Kling, *Reconstruction of Nanoscale near Fields by Attosecond Streaking*, IEEE J. Sel. Top. Quant. Elec. **23**, 1-11 (2017).
9. S. A. O. Motlagh, J.-S. Wu, V. Apalkov, and M. I. Stockman, *Fundamentally Fastest Optical Processes at the Surface of a Topological Insulator*, arXiv:1807.02139 [cond-mat.mes-hall]; Phys. Rev. B (In Print), 1-10 (2018).
10. S. A. Oliaei Motlagh, J.-S. Wu, V. Apalkov, and M. I. Stockman, *Femtosecond Valley Polarization and Topological Resonances in Transition Metal Dichalcogenides*, Phys. Rev. B **98**, 081406(R)-1-6 (2018).
11. F. Nematollahi, V. Apalkov, and M. I. Stockman, *Phosphorene in Ultrafast Laser Field*, Phys. Rev. B **97**, 035407-1-6 (2018).

Page is intentionally blank.

Complete spectroscopy in the attosecond regime

Carlos A. Trallero
Department of Physics, University of Connecticut, Storrs, CT 06268
`carlos.trallero@uconn.edu`

1 Project Scope

The main scope of my research is to perform coherent measurements of the time dependent molecular structure with femto and attosecond time resolution.

2 Recent progress

2.1 Characterization of Bessel beams and application to high-harmonic generation

In a recent publication (Summers, et.al., Opt. Exp. 2017) we examined the profiles of Bessel-like beams generated with the combination of a lens and an axicon by controlling the focal length of the lens (f) and the distance between the lens and the axicon (L). We use two laser sources, a continuous-wave (CW) HeNe laser and a femtosecond laser.

One of the main findings is that for certain combinations of lens and axicon, the central core of the beam remains at or above 50% of the peak intensity over distances that are more than 20 times longer than a Gaussian beam with a similar spot diameter. Therefore, proper manipulation of Bessel-like beams can produce tight focuses while maintaining long work distances, a very important property for many optics experiments.

2.1.1 Generation of higher-order harmonics with Bessel beams

Since the Bessel beams can be controlled so dynamicall and also the center part of the field vanishes in the far field, they could provide an ideal tool for the generation of XUV and attosecond pulses through high harmonic generation (HHG). One main question however is whereas the harmonics generated this way are collimated or not in the far field, since the fundamental has a ring shape.

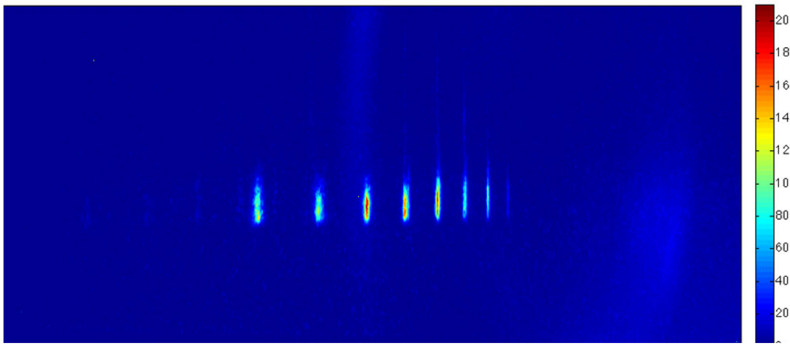

Figure 1: Raw image of the harmonics 11 (left most) to 25 (right most) generated with a lens-axicon system. The detector was placed more than a meter from the interaction region. From the figure it is clear that the harmonics are collimated in the far field.

Figure 1 shows a raw picture of the harmonics generated with a lens-axicon system showing that in the far field it is indeed possible to obtain collimated XUV and attosecond pulses while having a spatially-self-filtering fundamental. We still need to explore the different phase matching conditions for this new set of beams as well as the possible generation of attosecond pulses.

The pulse duration of the Bessel-like beam was not measured in this study. However, it is not expected to significantly differ from pulse durations achievable using a standard transmissive lens. We believe this is particularly so for the case of a shallow axicon like the one used in this study. However, since we were able to generate harmonics with this combination we know that the pulses can not be very long.

3 Future work

In the Fall of 2018 we will install a new laser in our lab. The laser will be able to generate 20 mJ of energy per pulse with 16-35 fs duration, at 1 kHz repetition rate. It can be used to seed a dual high energy OPA that can produce two signals and idlers that are all coherent relative to each other. Since the laser can produce

16 fs, thanks to a pulse shaper before the amplification, we will explore the generation of few-cycle pulses in the idler, directly from the OPA. This approach has the benefit of not needing a hollow core fiber for the generation of broadband pulses and thus should be more stable when use for HHG and attosecond pulse generation. Another improvement of the laser is that it uses BiBO (BiB_3O_6) crystals to generate wavelengths as far as 2.7 μm while still providing hundreds of μJ of energy per pulse. In combination with the pulse shaper mentioned above we should be able to generate attosecond pulses with photon energies in excess of 300 eV.

In addition to this laser we are building, in collaboration with a company a 20 kHz repetition rate with 6 mJ of energy per pulse and 6fs of pulse duration laser. This laser is being purchased through a Defense University Research Infrastructure (DURIP) grant but will be used for some of our studies under this program. In particular, we plan to use it in collaboration with the COLTRIMS of Prof. Nora Berrah for strong field-attosecond resolved experiments. The ultimate goal is to generate isolated attosecond pulses that can be combined with an IR probe for molecular dynamics. Since the center wavelength of the laser is at 1030 nm, the pulses are few-cycle in nature and also will have a high energy cutoff when used for HHG.

We will continue to develop our recently developed attosecond interferometer. In particular we are interested in studying the phase evolution during ionization of molecular isomers. We will employ our newly acquired Even-Lavie valve to generate cold molecular targets when possible for impulsive alignment of such molecular isomers. In these studies, a pump pulse will either align or excite a molecular target and through an attosecond interferometer we will follow the evolution of the phase. Because we will employ an SLM we will have access to two time scales. The first one is the femtosecond regime and is accessible by delaying the pump beam respect to the harmonic generating probe. The second time scale is in the attosecond regime and is accessible by controlling the optical phase of the fundamental with the SLM and will provide insight on the phase evolution during ionization of excited and/or aligned molecules.

Finally, we are studying the possibility of extending our interferometric technique to a transient absorption method. This will remove the constrain of having to generate harmonics from the molecules under study (in-situ HHG spectroscopy), which often limits the amount of harmonics over which spectroscopic information can be extracted. The goal is to use two Bessel beams to generate XUV pulses through HHG and control the relative optical phase of such pulses. The XUV pulses are then passed through the target sample which in turn can be excited and/or aligned. Just as in the case of the interferometer above we will have access to two time scales (atto and femto seconds) while also providing information about the phase. To date we have shown that is indeed possible to generate two Bessel beams whose phase can be controlled with an SLM. We have also shown that the field-free region of the Bessel beams in the far field does not change when the relative phase changes.

Peer-Reviewed Publications Resulting from this Project (Project Start Date: 08/16/2018)
No publications to report.

Laser-Produced Coherent X-Ray Sources

Donald Umstadter
Physics and Astronomy Department
500 Stadium Drive,101 Behlen Laboratory
University of Nebraska, Lincoln, NE 68588-0207
donald.umstadter@unl.edu

Program Scope

Sources of femtosecond-duration pulses of three different types of radiation—infrared light, electrons and x-rays—are under development for the investigation of ultrafast photo-induced atomic and electronic processes. All three are generated by a single high-peak-power laser system at the Extreme Light Laboratory of the University of Nebraska-Lincoln. Near absolute synchronization allows any combination of these pulses to be overlapped in space and in time with micron resolution. The optical pulse can be focused to a high intensity, corresponding to high electromagnetic field strength and photon density. With atomic-scale temporal and spatial resolution, the evolution of matter under highly non-equilibrium conditions can be probed. The research is relevant not only to the Chemical Sciences Division, but several other areas that are also of interest to the Department of Energy, including controlled thermonuclear fusion energy, high-energy-density physics, materials in extreme environments, and non-equilibrium processes. Moreover, the experimental test facility is small enough to fit in a university laboratory and operated by graduate students and postdocs.

Recent Progress

Laser-wakefield electron accelerators have ultrahigh acceleration gradients (GeV/cm) and produce electrons that have femtosecond pulse duration and picocoulomb charge. Being inherently synchronized with the laser beam, such electron pulses are also ideal for time-resolved dynamical studies. They also serve as the driver for a novel x-ray source light based on inverse-Compton scattering, which was developed and is currently in operation at the Extreme Light Laboratory of the University of Nebraska-Lincoln [2].

Up until now, the pulse duration of these electron beams has been characterized by indirect methods, such as coherent transition radiation. We are in the process of using inverse-Compton scattering in a 90-degree interaction geometry to characterize the duration of the electron pulse as well as its space and time structure.

Critical for use in experiments or as drivers for x-ray light sources is the quality of the electron beams in terms of their emittance, charge and energy spread. The output parameters of the accelerated beam are defined by the initial properties of electrons injected into wakefields, such as the phase-space area they occupy, as well as their energy spread, and transverse momentum. Finding a reliable and easily controllable way to inject electrons into a wake is critical for high quality electron beam generation. Optical injection promises great controllability over electron trapping via manipulating multiple involved laser pulses. We recently demonstrated a new optical injection method [1].

The experiments were performed with the Diocles Ti:Sapphire laser system. The drive beam (1.2 J max., 36 fs), which drove the accelerating wake, was focused by a f/14 parabolic mirror to a 20-um (FWHM) focal spot. The injector beam (0.9 J, 34 fs), which was used to inject electrons into the accelerating wake, was focused by an f/2 parabolic mirror to a 2.8-um (FWHM) Gaussian focal spot. The drive and injector beams were polarized in the horizontal plane and intersected at a 155° angle inside a 2-mm gas jet. Both beams drove their own plasma wakes. The electron-beam energy spectrum was measured using a double-screen magnetic spectrometer. The setup is shown in Figure 1.

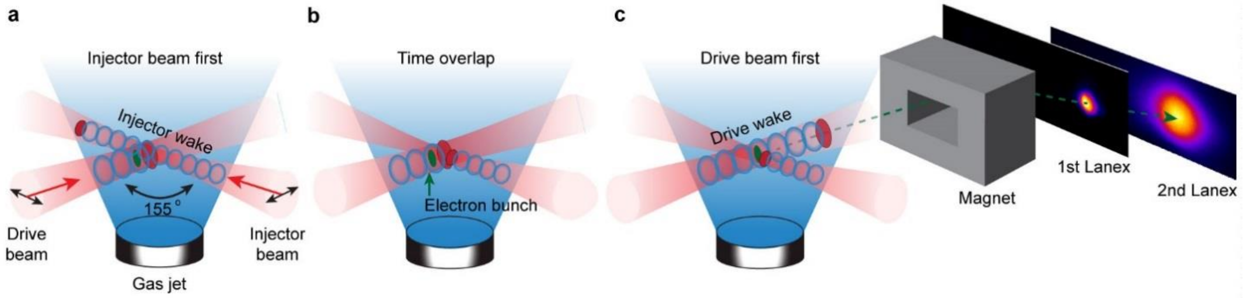

Figure 1. Schematic of the preliminary experiments on optical injection. Based on the time delay between the beams, there are three possible scenarios a) injector beam comes to the intersection point before the drive, and the drive beam interacts with the injector wake. b) Both beams arrive at the intersection point simultaneously. c) The drive beam arrives at the intersection before the injector, and the injector beam interacts with the drive wake.

Varying time delay between the laser pulses, we studied three scenarios: a) drive beam is delayed and interacts with the injector beam wake, b) temporal overlap, and c) injector beam is delayed and interacts with the drive beam wake (see Figure 2a, b, and c). The robust injection was observed up to delay of ±1 ps (±30 plasma periods) resulting in stable quasi-monoenergetic electron beams. The charge and energy of the beams are shown in Figure 2. We did two time-delay scans: a course one, with a step size larger than plasma period (67 fs vs. 35 fs, Figure 2a), and a fine one, with a step size smaller than plasma period (6 fs vs. 40 fs, Figure 2b).

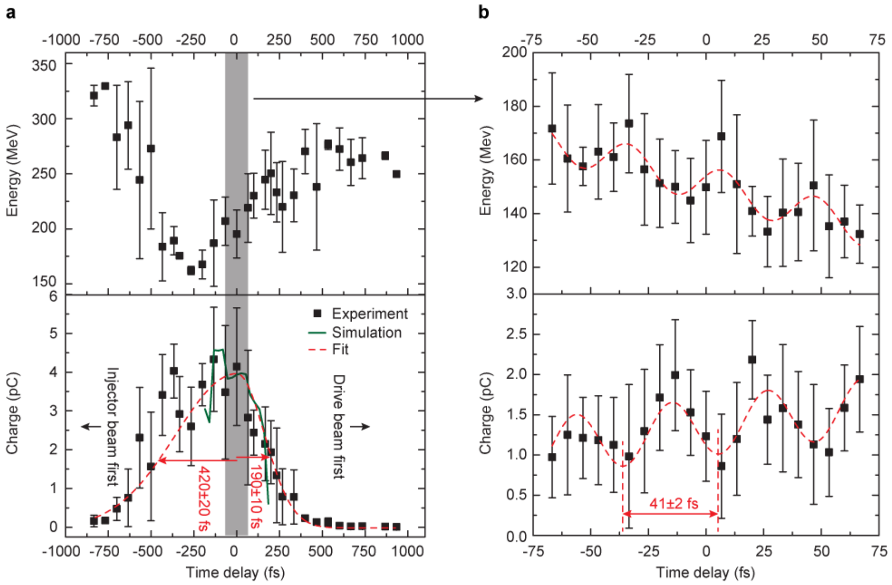

Figure 2. Dependence of electron beam properties on time delay between the injection and drive laser pulses. a) Course time scan. The plasma density is 1.0×10^{19} cm^{-3}, plasma period (calculated based on plasma density) is 35 fs. b) Fine time scan. The plasma density is 7.6×10^{18} cm^{-3}, plasma period (calculated based on plasma density) is 40 fs. The red dashed lines show data fits with a) bi-Gaussian function (red numbers show half-width-at-half-maximum lifetimes of the wakes, calculated from the fit); b) with sums of sine and linear functions (red numbers show a period of the plasma wave, calculated from the fit).

Results of preliminary PIC-simulations of the experiment allowed us to identify contributions from several different injection mechanisms, each playing an important role at varying time delays.

The first mechanism is injection due to the laser-wake collision, or ponderomotive injection. In this case, the ponderomotive force of a strong injector pulse gives background electrons momentum and phase required to become trapped by the drive wake. This type of injection was first theoretically discussed in but never observed experimentally.

Another mechanism observed is injection due to the wake-wake collision. Some background electrons, oscillating in the fields of both drive and injector wakes, were injected into the drive wake even though they experienced neither drive- nor injector-laser-beam fields.

A unique feature of the novel optical injection mechanisms is its ability to initiate injection at a precise position within an accelerating wake by changing the position at which the injector laser pulse overlaps the drive wake. This allows electrons to be controllably injected into different buckets of the wake (Figure 2a) and even more precise into a different phase of a wake within a single bucket (Figure 2b).

Plans

As the first step towards using our electron source for femtosecond time-resolved dynamics study, we will use the inverse-Compton x-ray scattering to study the electron-beam temporal profile. We will then utilize the characterized ultrafast electron beam for ultrafast time-resolved dynamic studies. A new inverse-Compton scattering beam line with a 90-degree interaction geometry is shown in Fig. 3. This will permit measurement of the electron beam pulse duration with femtosecond resolution.

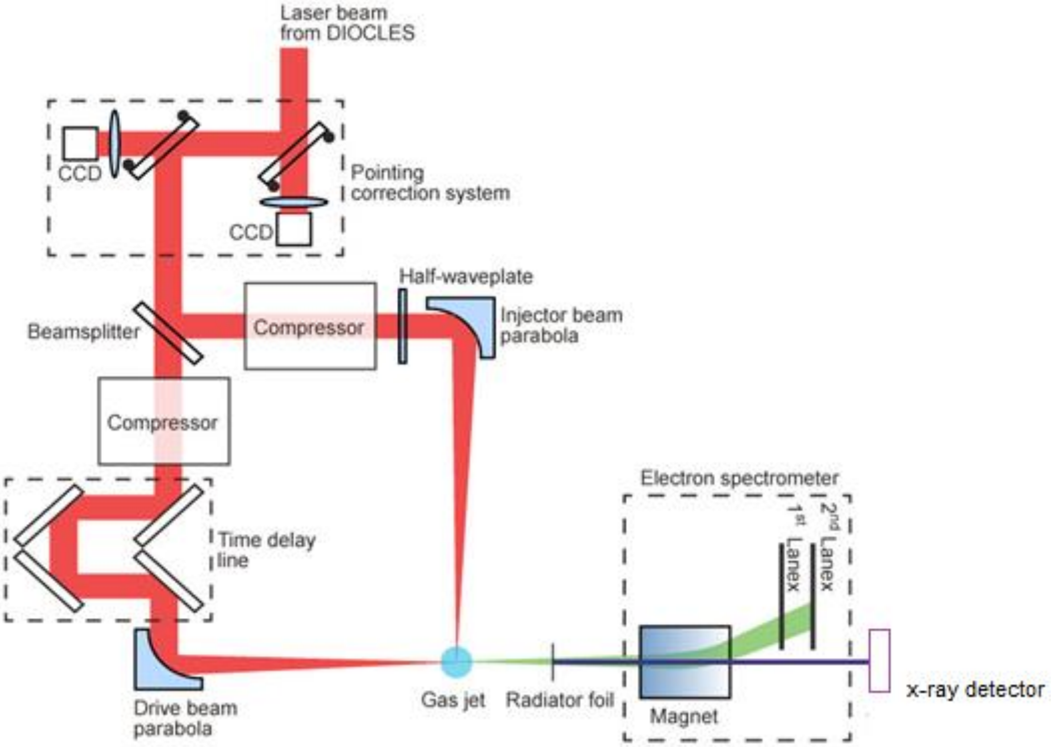

Figure 3: Experiment setup for electron temporal structure measurement using inverse-Compton scattering.

Peer-reviewed Publications (2016-2018)

1. G. Golovin, W. Yan, J. Luo, C. Fruhling, D. Haden, B. Zhao, C. Liu, M. Chen, S. Chen, P. Zhang, S. Banerjee and D. Umstadter, “Electron Trapping from Interactions between Laser-Driven Relativistic Plasma Waves,” Physical Review Letters **121**, 104801 (2018). doi: 10.1103/PhysRevLett.121.104801.
2. W. Yan, C. Fruhling, G. Golovin, D. Haden, J. Luo, P. Zhang, B. Zhao, J. Zhang, C. Liu, M. Chen, S. Chen, S. Banerjee, and D. Umstadter, “High-order multiphoton Thomson scattering.” Nature Photonics **11** 514-520 (2017). doi:10.1038/nphoton.2017.100
3. G. Golovin, S. Banerjee, C. Liu, S. Chen, J. Zhang, B. Zhao, P. Zhang, M. Veale, M. Wilson, P. Seller, and D. Umstadter, "Intrinsic beam emittance of laser-accelerated electrons measured by x-ray spectroscopic imaging," Scientific Reports **6,** 24622 (2016). doi:10.1038/srep24622.
4. G. Golovin, S. Banerjee, S. Chen, N. Powers, C. Liu, W. Yan, J. Zhang, P. Zhang, B. Zhao, and D. Umstadter, "Control and optimization of a staged laser-wakefield accelerator," Nuclear Instruments and Methods in Physics Research Section A **830**, 375-380 (2016). doi:10.1016/j.nima.2016.06.022.
5. S. Chen, G. Golovin, C. Miller, D. Haden, S. Banerjee, P. Zhang, C. Liu, J. Zhang, B. Zhao, S. Clarke, S. Pozzi, and D. Umstadter, “Shielded radiography with a laser-driven MeV-energy X-ray source, " Nuclear Instruments and Methods in Physics Research Section B **366**, 217-223 (2016). doi.org/10.1016/j.nimb.2015.11.007

Structural Molecular Dynamics Using Ultrafast Gas X-Ray Scattering

Peter M. Weber
Department of Chemistry
Brown University, Providence, Rhode Island 02912
Peter_Weber@brown.edu

I. Project Scope

Understanding the structures and chemical dynamics of molecules in their excited states is of great importance for basic energy science and myriad applications within and outside of Chemistry and Physics. This project develops two experimental tools and applies them to explore both the *nuclear dynamics*, i.e. the geometrical arrangement of atomic nuclei in molecules, and *electron dynamics*, i.e. the time evolution of electron probability density distributions during chemical reactions. The experimental approach focuses on ultrafast time resolved gas X-ray scattering, which is pursued at the LCLS light source at SLAC National Accelerator Laboratory. The X-ray scattering experiments are complemented by time-resolved Rydberg fingerprint spectroscopy experiments, which are conducted at Brown University. Both methods are sensitive to the structures of molecules in excited states with a time resolution of <100 fs. Because the experimental methods are complementary, their coordinated application to the same systems provides deeper insights into the molecular dynamics than each technique would give in isolation.

The experiments explore molecular phenomena associated with the nuclear and electron structural dynamics of molecules during reactions. This includes the motions through conical intersections, charge delocalization, the fracture of chemical bonds, vibrational motions and the propagation and spreading of wave packets. Model systems for those investigations include medium-sized organic systems: cyclohexadiene, trimethyl amine, N-methylmorpholine, quadricyclane, N,N-dimethylpiperazine, heterocyclic tetrazoles, and 1,2-dithiane. Those systems were deliberately chosen to broaden the investigations beyond standard prototypes. By focusing on structurally well-defined molecules, the project will advance our knowledge of molecules in excited electronic states and their chemical reaction dynamics. This will aid numerous applications and will also be valuable to the continued development of computational methods.

II. Recent Progress

We were fortunate to be awarded two beam times, LO92 in October 2017 and LR83 in March 2018. In these beam runs we perfected our experimental procedure to measure molecular movies, i.e. movies of structural motions of molecules on femtosecond time scales. This work rests on the first time-resolved molecular movie of the ring-opening reaction of cyclohexadiene, which we published a couple of years ago [1].

In the experiment, an ultrashort laser pulse initiates the dynamic motions by exciting the target molecules to an excited electronic state. The time-delayed X-ray pulse intersects the sample and is scattered off the excited-state molecules, Figure 1. The molecular movie is, conceptually, obtained by stitching together the structural measurements for a sequence of time delays.

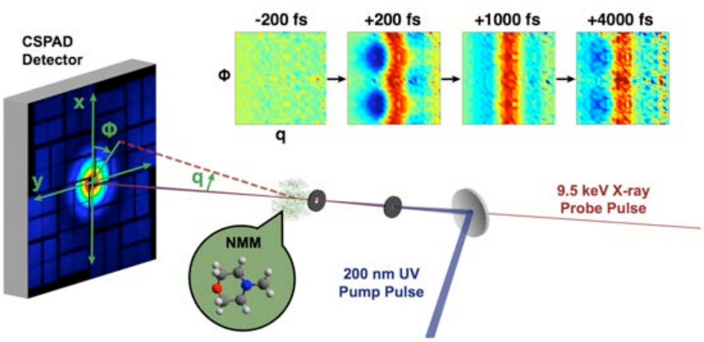

Figure 1: Experimental scheme: The molecules in the interaction region are intercepted by a linearly polarized UV laser (blue) and, at some time delay, by the X-ray pulse (red). Absorption of the UV pump pulse launches the structural molecular response. The X-ray probe is variably delayed (Δt_P) with respect to the UV pump pulse to image the time dependent dynamics. Scattering signals are captured by the CSPAD detector.

Several technical advances were implemented in the recent beam runs. The most important one was a separate, shot-to-shot intensity measurement of the X-ray pulse intensity. We tested two methods and found that a straightforward photodiode measurement of the X-ray pulse emerging from the vacuum and passing through air yields a measurement of sufficient quality. The approach, which was suggested by S. Boutet, allows us to correct each scattering image for the fluctuating X-ray intensity, thereby reducing the overall noise of the measurement.

The beam runs were tremendously successful and we harvested 100's of TB of data on multiple molecular systems. The analysis of this data requires extracting the molecular motions from this large amount of information. Importantly, since no standard way to analyze such data exists, we are developing the algorithm for capturing molecular motions as we analyze the data. These efforts are now bearing fruit, as will be described in the following on one of the target molecules, N-methyl morpholine (NMM). This particular system was chosen because it displays a transition from coherent to incoherent dynamics, and because structural coherence is found to survive the transition through a conical intersection that leads from the initially excited 3p to the lower 3s state.[2,3]

In the NMM experiment, the molecules are prepared in the 3p electronic state by a 200 nm laser pulse. Rapid internal conversion on the 100 fs time scale brings the molecule to 3s. More apparent in the scattering signal is the structural motion, in particular the umbrella motion, which is launched by the optical excitation. Several of the time frames are included in Figure 1 for illustration.

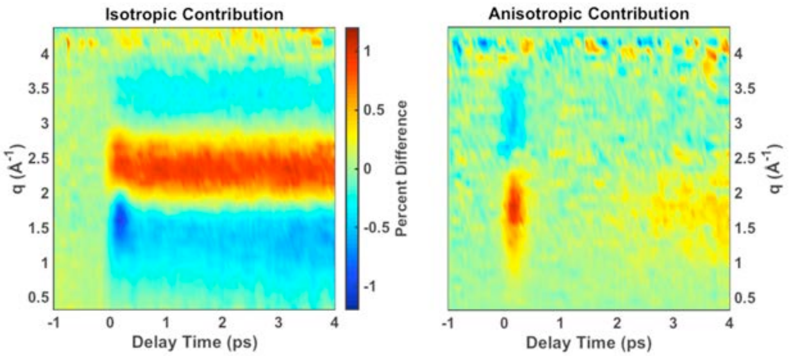

Figure 2: The time-dependent scattering signals of NMM upon excitation to the 3p state with 200 nm pulses. The isotropic signal, left, reveals most sensitively the structural time evolution of the molecule. The anisotropic signal, right, relates to the angular orientation of the time-dependent structures.

Figure 2 shows the time-dependent response of the molecular system. Shown is the change in the scattering

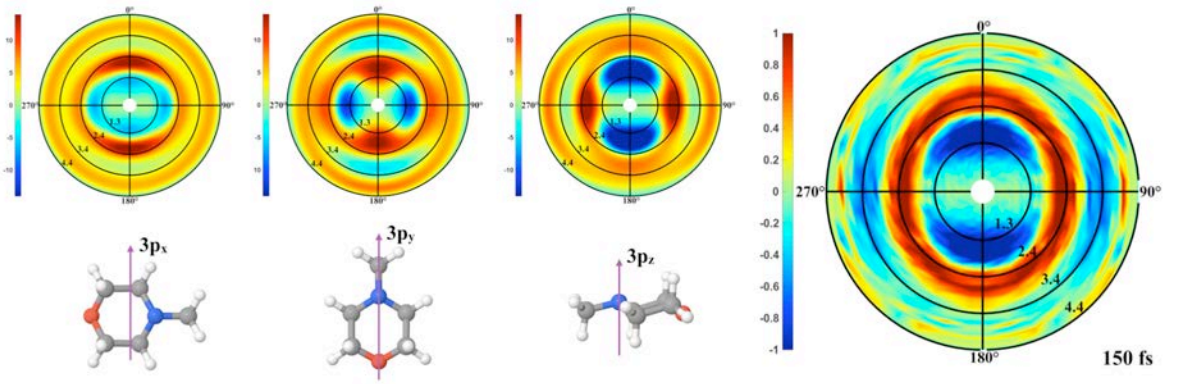

Figure 3: The calculated scattering signals of NMM upon excitation to the three possible 3p state with 200 nm pulses (three left-most panels). The anisotropy of the signals stems from the alignment of the excited state molecules by the polarized laser pulse on account of the orientation of the transition dipole moment. The experimental result, right, matches only the right-most pattern, and therefore clearly identifies the $3p_z$ state as the one that is optically accessed.

signal upon excitation, as a function of delay time. The change of the scattering signal is given as a percentage, i.e. (laser-on signal – laser-off signal)/(laser-off signal) x 100.

The isotropic signal reveals the structural motions of the molecule upon optical excitation. The anisotropic contribution to the signal stems from the angular orientation of the time-evolving molecular structures. We note that in our experiments, the molecules are excited by a weak laser pulse, which avoids undesired multi-photon processes. The pump-probe signals are therefore very small. But as is evident from Figure 2, we are now able to measure changes in the scattering signals below the 0.1% level.

A great deal of information is contained in the time-dependent pump-probe scattering signals. The anisotropic part arises because the linearly polarized laser pulse preferentially selects those molecules whose transition dipole moment is aligned with the laser polarization. The structural dynamics alters the molecular structure, which then imprints the pump-probe scattering signal onto the spatial alignment of the molecules. Before rotational dephasing destroys this alignment, the scattering signal therefore shows the structural image of the molecules in the laboratory frame, with the transition dipole moments aligned with the laser polarization.

This effect allowed us to identify the orientation of the transition dipole moment, and thereby the nature of the excited state (which, in this molecule, had been in question). Figure 3 shows the result of a computational simulation for the three possible orientations of the dipole moments. The experimental results, also shown in Figure 3, clearly identify the $3p_z$ state as the one that is optically excited.

The isotropic signals, see Figure 2, most directly reflect the structural evolution of the molecule. However, the X-ray scattering signal is, fundamentally, a scattering from the electron cloud in the molecule. Optical excitation changes the electron density distribution, and therefore the scattering signal, even when no structural time evolution is present.

Since only one out of 56 electrons is affected by optical excitation in NMM, the effect of electron density distributions might be deemed small. However, most of the atom-atom distances also don't change, so that the structural signal is also small. Consequently, before the time-dependent structure of the molecule can be extracted and the molecular movie assembled, one must consider and subtract out the contribution from electronic excitation.

Figure 4 shows the relative magnitudes of the effects from the change in electron density distribution and the structural change. Depending on the scattering angle, the two are of nearly comparable magnitude.

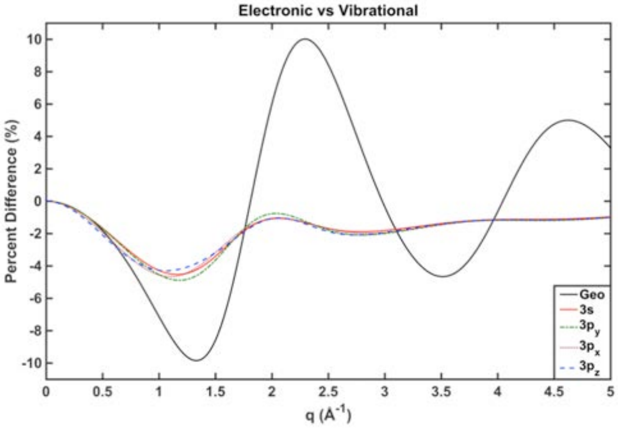

Figure 4: The calculated contributions to the pump-probe scattering signals of NMM upon excitation to the 3p state with 200 nm pulses. The dashed lines show the effect from the changing electron density distribution for excitation to different excited electronic states. Electron densities were obtained from a CAS(2,5)/6-311+g* calculation. The solid line results from the geometrical change in the molecular structure. To extract the latter from the experimental data, the electron density contribution must be considered.

The ongoing data analysis seeks to account for the different contributions of electron density and structural motions. In NMM, the contribution from the electron densities of excited states appears to be an additive term. Consequently, it can be subtracted out without requiring knowledge of the dependence of electron density distributions on molecular structure. The results of these investigations will be communicated at a future time.

III. Future Plans

With LCLS currently under construction, our efforts in the coming year will be to prepare for a new generation of experiments with LCLS-II. This includes, in particular, methods to read out scattering images that utilize the high repetition rate pulse sequences. Additional efforts will include designing a scattering apparatus for cold molecules, which should reduce the thermal broadening of molecular structures.

Several data sets of other molecular systems remain to be analyzed. This includes dithiane, N,N-dimethyl piperazine, trimethyl amine and CHD with excitation at higher energies than previously done. The algorithms developed for the analysis of NMM will be refined, with an eye toward determining the distribution of molecular structures over multiple forms.

IV. References

[1] “Imaging Molecular Motion: Femtosecond X-Ray Scattering of the Ring Opening in 1,3-Cyclohexadiene,” M.P. Minitti, J.M. Budarz, A. Kirrander, J.S. Robinson, D. Ratner, T.J. Lane, D. Zhu, J.M. Glownia, M. Kozina, H. T. Lemke, M. Sikorski, Y. Feng, S. Nelson, K. Saita, B. Stankus, T. Northey, J.B. Hastings & P.M. Weber, *Phys. Rev. Lett.* 114, 255501 (**2015**).

[2] “Coherence in Nonradiative Transitions: Internal Conversion in Rydberg-Excited N-Methyl and N-Ethyl Morpholine,” Yao Zhang, Hannes Jónsson, Peter M. Weber, *Physical Chemistry Chemical Physics*, **2017**, DOI: 10.1039/C7CP05244H.

[3] “Observation of Structural Wavepacket Motion: The Umbrella Mode in Rydberg-Excited N‑Methyl Morpholine,” Yao Zhang, Sanghamitra Deb, Hannes Jónsson, Peter M. Weber, *J. Phys. Chem. Lett.* **2017**, 8, 3740 – 3744, DOI: 10.1021/acs.jpclett.7b01274.

V. Peer-Reviewed Publications resulting from this Project

“Putting the Disulfide Bridge at Risk - How UVC Radiation Leads to Ultrafast Rupture of the S-S bond” Martin A.B. Larsen, Anders B. Skov, Christian M. Clausen, Jennifer Ruddock, Brian Stankus, Peter M. Weber and Theis I. Sølling, ChemPhysChem **2018** *19*, DOI 10.1002/cphc.201800610.

Combining High Level *Ab Initio* Calculations with Laser Control of Molecular Dynamics

Thomas Weinacht
Department of Physics and Astronomy
Stony Brook University
Stony Brook, NY
thomas.weinacht@stonybrook.edu

and

Spiridoula Matsika
Department of Chemistry
Temple University
Philadelphia, PA
smatsika@temple.edu

1 Project Scope

We use intense, shaped, ultrafast laser pulses to follow and control molecular dynamics and high level *ab initio* calculations to interpret the dynamics and guide the control.

2 Recent Progress

Our scientific focus over the past year has been on coupled electron-nuclear dynamics and correlated electron dynamics in small organic molecules. Over the past year we have made a number of improvements to our apparatus, carried out several new measurements and calculations and interpreted their results. A brief summary of our activities includes: We have integrated the Timepix camera into our coincidence VMI apparatus, and are currently doing so with our UV/VUV apparatus, which was recently upgraded to include velocity map imaging in the detection of ions and electrons. We have carried out electronic structure and trajectory surface hopping calculations for a number of molecules, in order to directly compare time resolved photoelectron spectroscopy measurements with a calculated observable. Finally, we have carried out measurements at two different national facilities (ultrafast electron diffraction at SLAC in Palo Alto, CA and time resolved photoelectron spectroscopy at the National Research Council in Ottawa Canada) in order to compare different measurement approaches. More details on specific major advances are described below.

2.1 UV pump VUV probe measurements and surface hopping calculations of excited state dynamics

We performed time-resolved UV pump (4.77 eV) and VUV probe (7.94 eV) measurements. We have made several advances using the new UV/VUV pump-probe apparatus. We studied the relaxation dynamics of several systems using the 8 eV pulse either as a pump or a probe. The development of this weak field probe motivated us to move in a couple of different directions.

One direction focused on conjugated systems. In the past we performed time-resolved UV/VUV pump-probe measurements of internal conversion of 1,3-cyclohexadiene (CHD). Our measurements revealed a substantial ionization of the hot ground state following internal conversion despite the fact that our probe photon energy is below the ionization potential (8.21 eV). We contrasted our measurements in CHD with another similar molecule, cis,cis-1,3-cyclooctadiene (cis,cis-COD), for which we did not see the effect. We are currently extending this work, focusing on excited state dynamics in conjugated systems more generally. We would like to broaden our understanding of photoinitiated non-adiabatic dynamics in these molecules. We are performing trajectory surface hopping calculations exploring the non-adiabatic dynamics of COD in more detail, exploring the competition between photophysics (i.e. relaxation back to the ground state), isomerization, and photochemistry. We are exploring a variety of electronic structure approaches (specifically CASSCF and MRCI methods with a variety of active spaces) in order to find their effect on the dynamics.

2.2 Strong and weak-field ionization in pump-probe spectroscopy

Another very important area that we have focused on is a comparison between strong and weak field ionization as a probe of excited state dynamics in polyatomic molecules. In previous work we

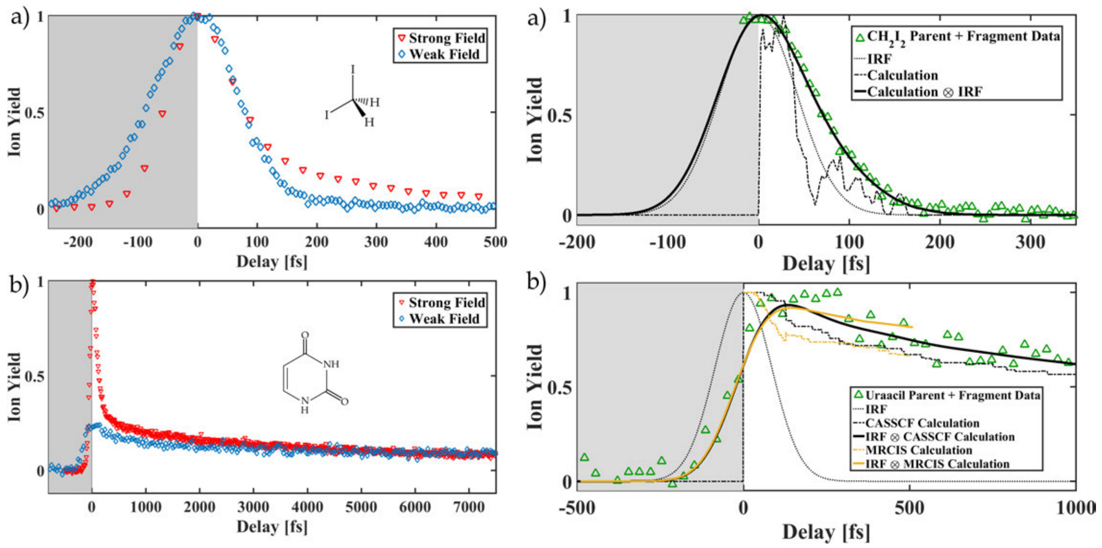

Figure 1: *Left: a) Weak-field UV-VUV and strong-field UV-IR total ion yield pump-probe measurement on (a) diiodomethane and (b) uracil. Right: (a) CH_2I_2 WFI UV-VUV pump-probe total ion yield data (green triangle), CASPT2 dynamics with Dyson norms calculation on CH_2I_2 (dotted-dashed line), IRF of our apparatus (dotted line), and convolution of the calculation and the IRF of the system (solid line). (b) Uracil WFI UV-VUV pump-probe total ion yield data (upward facing green triangle), CASSCF calculation for uracil (black dotted-dashed line), impulse response function (IRF) of our apparatus (black dotted line), convolution of the CASSCF calculation and the IRF of the system (solid black line), MRCIS calculation for uracil (gold dotted-dashed line), and convolution of the MRCIS calculation and the IRF of the system (solid gold line).*

developed and made use of both weak and strong field ionization as a probe of these dynamics. The availability of both approaches gives us the opportunity to compare the results, and determine whether the different probes provide similar or complementary information about the excited state dynamics. Theoretical studies using electronic structure and non-adiabatic dynamics have interpreted these results. Strong field ionization is advantageous because it uses wavelengths that are relatively easy to generate, and one can always ionize the molecule with sufficient intensity. However, for strong field ionization it is difficult to calculate observables, such as the time-dependent ion yield, since the calculation of the ionization dynamics including multi-photon processes is computationally expensive, and difficult to carry out for many molecular geometries. Weak field ionization has the advantage that calculations of observables are tractable. However, the generation and implementation of the appropriate wavelengths (photon energies) can be challenging, and the fixed energy of the probe can lead to technical complications in following the dynamics from excited states back down to the ground state. We performed a quantitative comparison of the two approaches for following the excited state dynamics of two molecules, CH_2I_2 and uracil. Our work indicates that while strong and weak field ionization provide qualitatively similar information about the excited state dynamics, only weak field results can be compared quantitatively with calculations. Figure 1 shows the comparison between theory and experiment for uracil.

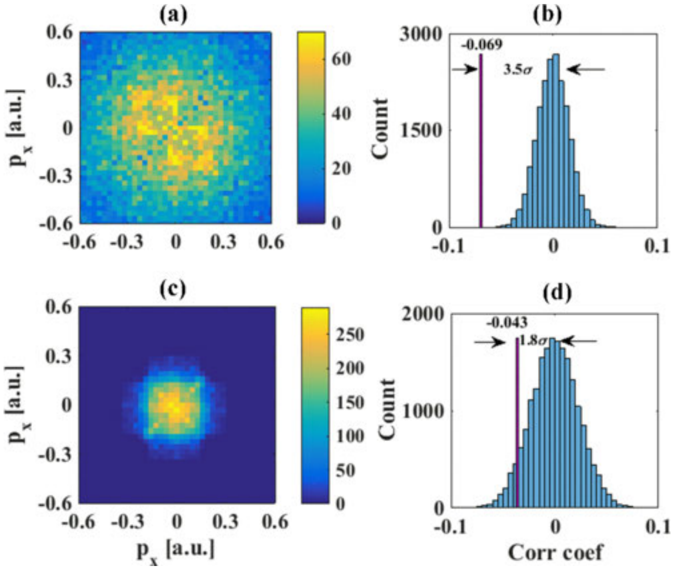

Figure 2: *Comparison of electron joint momentum distributions (EJMDs) from two molecules: (a)* C_6H_8 *and (c)* CH_2IBr*. By randomizing the pairing of the two electrons, we can generate histograms (b)* C_6H_8 *and (d)* CH_2IBr*, showing the statistical significance of the anticorrelation quantified by the* r_P *(corr coef). The y axis labels the number of random pairings. Fitting the histogram with a Gaussian distribution, the observed correlation coefficient in* C_6H_8 *is 3.5* σ *away from the mean 0, with a p value of 0.0003. In contrast, we see a smaller correlation in the EJMD for* CH_2IBr*, with a p value of just over 0.05.*

2.3 Quadruple coincidence measurement of electron correlation in strong field molecular double ionization

We have studied strong-field dissociative molecular double ionization with momentum-resolved quadruple coincidence measurements, measuring the two electrons and two ionic fragments produced with a coincidence velocity map imaging apparatus. We contrasted measurements for two different molecules. In one case, our measurements reveal anticorrelation in the momentum for the two electrons, while in the other, we find no anticorrelation, indicating differences between the two molecules in the underlying ionization dynamics (see Figure 2).

3 Future Plans

We have several goals for the immediate future:

1. We plan on implementing the Timepix camera in the UV pump VUV probe experiments.
2. We plan on completing our analysis of the ultrafast electron diffraction data acquired at SLAC and comparing it directly with time resolved photoelectron spectroscopy measurements for the same system.
3. We plan on extending and further interpreting through electronic structure calculations our quadruple coincidence measurements of molecular double ionization.
4. We plan on extending our excited state dynamics calculations in conjugated systems in order to establish systematic trends in the dynamics and associate features in the photoelectron spectra with specific trajectories.

5. We plan on comparing the performance of different electronic structure methods on the description of nonadiabatic dynamics through trajectory surface hopping calculations.

4 Peer-Reviewed Publications Resulting from this Project (2016-2018)

- "Surface hopping investigation of the relaxation dynamics in radical cations", Mariana Assmann, Thomas Weinacht, and Spiridoula Matsika, *J. Chem. Phys.*, **144**, 034301 (2016)

- "Molecular Double Ionization using Strong Field Few Cycle Laser Pulses", Arthur Zhao, Péter Sándor, Vincent Tagliamonti, Thomas Weinacht, and Spiridoula Matsika, *J. Phys. Chem. A*, **120**, pp 3233 - 3240, (2016)

- "Ultrafast Internal Conversion Dynamics of Highly Excited Pyrrole Studied with VUV/UV Pump Probe Spectroscopy", Spencer L. Horton, Yusong Liu, Pratip Chakraborty, Spiridoula Matsika, and Thomas Weinacht, *J. Chem. Phys.*, **146**, 064306 (2017)

- "Controlling Photorelaxation in Uracil with Shaped Laser Pulses: A Theoretical Assessment", Daniel Keefer, Sebastian Thallmair, Spiridoula Matsika, Regina de Vivie-Riedle, *J.Am. Chem. Soc.*, **139**, 5061 - 5066, (2017)

- "Vibrationally Assisted Below Threshold Ionization", Spencer L. Horton, Yusong Liu, Pratip Chakraborty, Spiridoula Matsika, and Thomas Weinacht, *Phys. Rev. A*, **95**, 063413, (2017)

- "Coincidence velocity map imaging using Tpx3Cam, a time stamping optical camera with 1.5 ns time resolution", Arthur Zhao, Martin van Beuzekom, Bram Bouwens, Dmitry Byelov, Irakli Chakaberia, Chuan Cheng, Erik Maddox, Andrei Nomerotski, Peter Svihra, Jan Visser, Vaclav Vrba, and Thomas Weinacht, *Review of Scientific Instruments*, **88**, 113104 (2017)

- "Quadruple coincidence measurement of electron correlation in strong-field molecular double ionization", Arthur Zhao, Chuan Cheng, Spiridoula Matsika and Thomas Weinacht, *Phys. Rev. A*, **97**,043412, (2018)

- "Strong-Field vs Weak-Field Ionization Pump-Probe Spectroscopy", Spencer Horton, Yusong Liu, Pratip Chakraborty, Philipp Marquetand,Tamas Rozgonyi, Spiridoula Matsika, and Thomas Weinacht, *Phys. Rev. A*, in press (2018)

- "Real-Time Adjustable, 11 Microsecond FWHM, > 5 KHz Piezo Electric Actuated Pulsed Atomic Beam Source", Anthony Catanese, Spencer Horton, Yusong Liu and Thomas Weinacht, *Review of Scientific Instruments*, in press (2018)

PARTICIPANT LIST

2018 Atomic, Molecular and Optical Sciences Research PI Meeting

October 22 – 24, 2018

Thomas Allison
Stony Brook University
thomas.allison@stonybrook.edu

Andreas Becker
University of Colorado, Boulder
andreas.becker@colorado.edu

Itzhak Ben-Itzhak
Kansas State University
ibi@phys.ksu.edu

Nora Berrah
University of Connecticut
nora.berrah@uconn.edu

Cosmin Blaga
Kansas State University
blaga@phys.ksu.edu

Philip Bucksbaum
Stanford University/SLAC
phb@slac.stanford.edu

Martin Centurion
University of Nebraska, Lincoln
martin.centurion@unl.edu

Michael Chini
University of Central Florida
michael.chini@ucf.edu

Shih-I Chu
University of Kansas
sichu@ku.edu

Amy Cordones-Hahn
SLAC National Accelerator Laboratory
acordon@slac.stanford.edu

Alex Cronin
National Science Foundation
acronin@nsf.gov

James Cryan
Stanford PULSE Institute
jcryan@slac.stanford.edu

Steven Cundiff
University of Michigan
cundiff@umich.edu

Marcos Dantus
Michigan State University
dantus@msu.edu

Louis DiMauro
Ohio State University
dimauro.6@osu.edu

Gilles Doumy
Argonne National Laboratory
gdoumy@aps.anl.gov

Joseph Eberly
University of Rochester
eberly@pas.rochester.edu

Brett Esry
Kansas State University
esry@phys.ksu.edu

Roger Falcone
University of California, Berkeley
rwf@berkeley.edu

Matthias Fuchs
University of Nebraska
mfuchs@unl.edu

Mette Gaarde
Louisiana State University
gaarde@phys.lsu.edu

Kelly Gaffney
SLAC National Accelerator Laboratory
kgaffney@slac.stanford.edu

Thomas Gallagher
University of Virginia
tfg@virginia.edu

Bruce Garrett
U.S. Department of Energy/BES
Bruce.Garrett@science.doe.gov

Oliver Gessner
Lawrence Berkeley National Laboratory
ogessner@lbl.gov

Shambhu Ghimire
SLAC/Stanford University
shambhu@slac.stanford.edu

Taisia Gorkhover
SLAC National Accelerator Laboratory
taisgork@slac.stanford.edu

Chris Greene
Purdue University
chgreene@purdue.edu

Loren Greenman
Kansas State University
lgreenman@phys.ksu.edu

Martin Head-Gordon
University of California, Berkeley
mhg@cchem.berkeley.edu

Tony Heinz
SLAC National Accelerator Laboratory
tony.heinz@stanford.edu

Phay Ho
Argonne National Laboratory
pho@anl.gov

Cynthia Jenks
Argonne National Labortory
cjenks@anl.gov

Robert Jones
University of Virginia
rrj3c@virginia.edu

Henry Kapteyn
JILA, University of Colorado
Henry.Kapteyn@colorado.edu

Jeffrey Krause
U.S. Department of Energy/BES
jeff.krause@science.doe.gov

Vinod Kumarappan
Kansas State University
vinod@phys.ksu.edu

Guillaume Marc Laurent
Auburn University
glaurent@auburn.edu

Stephen Leone
University of California, Berkeley
srl@berkeley.edu

Raphael Levine
University of California, Los Angeles
rafi@chem.ucla.edu

Wen Li
Wayne State University
wli@chem.wayne.edu

Kenneth Lopata
Louisiana State University
klopata@lsu.edu

Robert Lucchese
Lawrence Berkeley National Laboratory
rlucchese@lbl.gov

Steven Manson
Georgia State University
smanson@gsu.edu

Anne Marie March
Argonne National Laboratory
amarch@anl.gov

Todd Martinez
SLAC National Accelerator Laboratory
Todd.Martinez@stanford.edu

Spiridoula Matsika
Temple University
smatsika@temple.edu

C. William McCurdy
Lawrence Berkeley National Laboratory
cwmccurdy@lbl.gov

Alfred Z. Msezane
Clark Atlanta University
amsezane@cau.edu

Shaul Mukamel
University of California, Irvine
smukamel@uci.edu

Margaret Murnane
JILA, University of Colorado
Margaret.Murnane@colorado.edu

Adi Natan
SLAC National Accelerator Laboratory
natan@slac.stanford.edu

Keith Nelson
Massachusetts Institue of Technology
kanelson@mit.edu

Daniel Neumark
University of California
dneumark@berkeley.edu

Thomas Orlando
Georgia Institute of Technology
thomas.orlando@chemistry.gatech.edu

Abbas Ourmazd
University of Wisconsin, Milwaukee
ourmazd@uwm.edu

Herschel Rabitz
Princeton University
hrabitz@princeton.edu

David Reis
University of California
dreis@stanford.edu

Francoise Remacle
University of Liege
fremacle@uliege.be

Francis Robicheaux
Purdue University
robichf@purdue.edu

Jorge Rocca
Colorado State University
jorgerocca9@gmail.com

Daniel Rolles
Kansas State University
rolles@phys.ksu.edu

Artem Rudenko
Kansas State University
rudenko@phys.ksu.edu

Arvinder Sandhu
University of Arizona
asandhu@email.arizona.edu

Kenneth Schafer
Louisiana State University
schafer@rouge.phys.lsu.edu

H. Bernhard Schlegel
Wayne State University
hbs@chem.wayne.edu

Robert Schoenlein
SLAC National Accelerator Laboratory
rwschoen@slac.stanford.edu

Thomas Settersten
U.S. Department of Energy/BES
thomas.settersten@science.doe.gov

Daniel Slaughter
Lawrence Berkeley National Laboratory
DSSlaughter@lbl.gov

Stephen Southworth
Argonne National Laboratory
southworth@anl.gov

Anthony F. Starace
University of Nebraska
astarace1@unl.edu

Mark Stockman
Georgia State University
mstockman@gsu.edu

Uwe Thumm
Kansas State University
thumm@phys.ksu.edu

Carlos Trallero
University of Connecticut
carlos.trallero@uconn.edu

Donald Umstadter
University of Nebraska, Lincoln
donald.umstadter@unl.edu

Peter Walter
SLAC National Accelerator Laboratory
pwalter@slac.stanford.edu

Thorsten Weber
Lawrence Berkeley National Laboratory
TWeber@lbl.gov

Peter Weber
Brown University
peter_weber@brown.edu

Thomas Weinacht
Stony Brook University
thomas.weinacht@stonybrook.edu

Thomas Wolf
SLAC National Accelerator Laboratory
thomas.wolf@slac.stanford.edu

Linda Young
Argonne National Laboratory
young@anl.gov

Page is intentionally blank.